U.S. Department
of Commerce

Volume 103
Number 2
April 2005

Fishery Bulletin

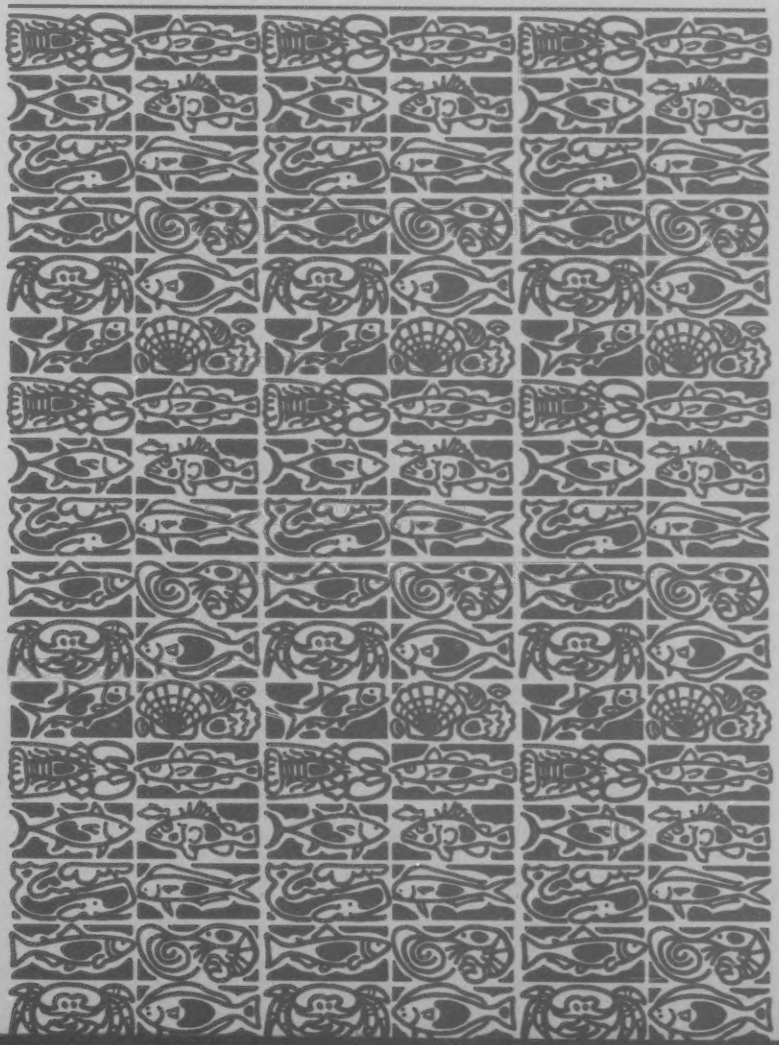

U.S. Department of Commerce
Carlos M. Gutierrez
Secretary

National Oceanic and Atmospheric Administration
Vice Admiral
Conrad C. Lautenbacher Jr., USN (ret.)
Under Secretary for Oceans and Atmosphere

National Marine Fisheries Service
William T. Hogarth
Assistant Administrator for Fisheries

The *Fishery Bulletin* (ISSN 0090-0656) is published quarterly by the Scientific Publications Office, National Marine Fisheries Service, NOAA, 7600 Sand Point Way NE, BIN C15700, Seattle, WA 98115-0070. Periodicals postage is paid at Seattle, WA, and at additional mailing offices. POSTMASTER: Send address changes for subscriptions to Fishery Bulletin, Superintendent of Documents, Attn.: Chief, Mail List Branch, Mail Stop SSOM, Washington, DC 20402-9373.

Although the contents of this publication have not been copyrighted and may be reprinted entirely, reference to source is appreciated.

The Secretary of Commerce has determined that the publication of this periodical is necessary according to law for the transaction of public business of this Department. Use of funds for printing of this periodical has been approved by the Director of the Office of Management and Budget.

For sale by the Superintendent of Documents, U.S. Government Printing Office, Washington, DC 20402. Subscription price per year: $55.00 domestic and $68.75 foreign. Cost per single issue: $28.00 domestic and $35.00 foreign. **See back for order form.**

Fishery Bulletin

Scientific Editor
Norman Bartoo, Ph.D.

Associate Editor
Sarah Shoffler

National Marine Fisheries Service, NOAA
8604 La Jolla Shores Drive
La Jolla, California 92037

Managing Editor
Sharyn Matriotti

National Marine Fisheries Service
Scientific Publications Office
7600 Sand Point Way NE, BIN C15700
Seattle, Washington 98115-0070

Editorial Committee

Harlyn O. Halvorson, Ph.D.	University of Massachusetts, Boston
Ronald W. Hardy, Ph.D.	University of Idaho, Hagerman
Richard D. Methot, Ph.D.	National Marine Fisheries Service
Theodore W. Pietsch, Ph.D.	University of Washington, Seattle
Joseph E. Powers, Ph.D.	National Marine Fisheries Service
Harald Rosenthal, Ph.D.	Universität Kiel, Germany
Fredric M. Serchuk, Ph.D.	National Marine Fisheries Service
George Watters, Ph.D.	National Marine Fisheries Service

***Fishery Bulletin* web site: www.fishbull.noaa.gov**

The *Fishery Bulletin* carries original research reports and technical notes on investigations in fishery science, engineering, and economics. It began as the Bulletin of the United States Fish Commission in 1881; it became the Bulletin of the Bureau of Fisheries in 1904 and the *Fishery Bulletin* of the Fish and Wildlife Service in 1941. Separates were issued as documents through volume 46; the last document was No. 1103. Beginning with volume 47 in 1931 and continuing through volume 62 in 1963, each separate appeared as a numbered bulletin. A new system began in 1963 with volume 63 in which papers are bound together in a single issue of the bulletin. Beginning with volume 70, number 1, January 1972, the *Fishery Bulletin* became a periodical, issued quarterly. In this form, it is available by subscription from the Superintendent of Documents, U.S. Government Printing Office, Washington, DC 20402. It is also available free in limited numbers to libraries, research institutions, State and Federal agencies, and in exchange for other scientific publications.

U.S. Department of Commerce
Seattle, Washington

Volume 103
Number 2
April 2005

Fishery Bulletin

Contents

Articles

229–245 **Alonzo, Suzanne H., and Marc Mangel**
Sex-change rules, stock dynamics, and the performance of spawning-per-recruit measures in protogynous stocks

246–257 **Brandon, Elisif A. A., Donald G. Calkins, Thomas R. Loughlin, and Randall W. Davis**
Neonatal growth of Steller sea lion (*Eumetopias jubatus*) pups in Alaska

258–269 **Brouwer, Stephen L., and Marc H. Griffiths**
Reproductive biology of carpenter seabream (*Argyrozona argyrozona*) (Pisces: Sparidae) in a marine protected area

270–279 **Burn, Douglas M., and Angela M. Doroff**
Decline in sea otter (*Enhydra lutris*) populations along the Alaska Peninsula, 1986–2001

280–291 **Carlson, John K., and Ivy E. Baremore**
Growth dynamics of the spinner shark (*Carcharhinus brevipinna*) off the United States southeast and Gulf of Mexico coasts: a comparison of methods

292–306 **Domeier, Michael L., Dale Kiefer, Nicole Nasby-Lucas, Adam Wagschal, and Frank O'Brien**
Tracking Pacific bluefin tuna (*Thunnus thynnus orientalis*) in the northeastern Pacific with an automated algorithm that estimates latitude by matching sea-surface-temperature data from satellites with temperature data from tags on fish

307–319 **Fischer, Andrew J., M. Scott Baker Jr., Charles A Wilson, and David L. Nieland**
Age, growth, mortality, and radiometric age validation of gray snapper (*Lutjanus griseus*) from Louisiana

320–330 **Grabowski, Robert C., Thomas Windholz, and Yong Chen**
Estimating exploitable stock biomass for the Maine green sea urchin (*Strongylocentrotus droebachiensis*) fishery using a spatial statistics approach

The conclusions and opinions expressed in *Fishery Bulletin* are solely those of the authors and do not represent the official position of the National Marine Fisheries Service (NOAA) or any other agency or institution.

The National Marine Fisheries Service (NMFS) does not approve, recommend, or endorse any proprietary product or proprietary material mentioned in this publication. No reference shall be made to NMFS, or to this publication furnished by NMFS, in any advertising or sales promotion which would indicate or imply that NMFS approves, recommends, or endorses any proprietary product or proprietary material mentioned herein, or which has as its purpose an intent to cause directly or indirectly the advertised product to be used or purchased because of this NMFS publication.

331–343 **Lowry, Mark S., and Karin A. Forney**
Abundance and distribution of California sea lions (*Zalophus californianus*) in central and northern California during 1998 and summer 1999

344–354 **Mackie, Michael C., Paul D. Lewis, Daniel J. Gaughan, and Stephen J. Newman**
Variability in spawning frequency and reproductive development of the narrow-barred Spanish mackerel (*Scomberomorus commerson*) along the west coast of Australia

355–370 **Ruggerone, Gregory T., Ed Farley, Jennifer Nielson, and Peter Hagen**
Seasonal marine growth of Bristol Bay sockeye salmon (*Oncorhynchus nerka*) in relation to competition with Asian pink salmon (*O. gorbuscha*) and the 1977 ocean regime shift

371–379 **Shoji, Jun, and Masaru Tanaka**
Distribution, feeding condition, and growth of Japanese Spanish mackerel (*Scomberomorus niphonius*) larvae in the Seto Inland Sea

380–391 **Wang, You-Gan, and Nick Ellis**
Maximum likelihood estimation of mortality and growth with individual variability from multiple length-frequency data

392–403 **Williams, Erik H., and Kyle W. Shertzer**
Effects of fishing on growth traits: a simulation analysis

Notes

404–406 **Burton, Michael L., Kenneth J. Brennan, Roldan C. Muñoz, and Richard O. Parker Jr.**
Preliminary evidence of increased spawning aggregations of mutton snapper (*Lutjanus analis*) at Riley's Hump two years after establishment of the Tortugas South Ecological Reserve

411–416 **Carpentieri, Paolo, Francesco Colloca, Massimiliano Cardinale, Andrea Belluscio, and Giandomenico D. Ardizzone**
Feeding habits of European hake (*Merluccius merluccius*) in the central Mediterranean Sea

417–425 **Gobert, Bertrand, Alain Guillou, Peter Murray, Patrick Berthou, Maria D. Oqueli Turcios, Ester Lopez, Pascal Lorance, Jérôme Huet, Nicolas Diaz, and Paul Gervain**
Biology of the queen snapper (*Etelis oculatus*: Lutjanidae) in the Caribbean

426–432 **Graham, Rachel T., and Daniel W. Castellanos**
Courtship and spawning behaviors of carangid species in Belize

433–437 **Hewitt, David A., and John M. Hoenig**
Comparison of two approaches for estimating natural mortality based on longevity

438–444 **Lindquist, David C., and Richard F. Shaw**
Effects of current speed and turbidity on stationary light-trap catches of larval and juvenile fishes

445–452 **Macchi, Gustavo J., Marcelo Pájaro, and Adrián Madirolas**
Can a change in spawning pattern of Argentine hake (*Merluccius hubbsi*) affect its recruitment?

453–460 **Raymundo-Huizar, Alma R., Horacio Pérez-España, Maite Mascaró, and Xavier Chiappa-Carrara**
Feeding habits of the dwarf weakfish (*Cynoscion nannus*) off the coasts of Jalisco and Colima, Mexico

461–466 **Wood, Anthony D.**
Using bone measurements to estimate the original sizes of bluefish (*Pomatomus saltatrix*) from digested remains

467 **Subscription form**

Sex-change rules, stock dynamics, and the performance of spawning-per-recruit measures in protogynous stocks

Suzanne H. Alonzo

Institute of Marine Sciences and the Center for Stock Assessment Research (CSTAR)
University of California Santa Cruz
1156 High Street
Santa Cruz, California 95064
Present address: Department of Ecology and Evolutionary Biology
Yale University
165 Prospect St., OML 427
New Haven, Connecticut 06511
E-mail address: Suzanne.Alonzo@yale.edu

Marc Mangel

Department of Applied Mathematics and Statistics
Jack Baskin School of Engineering and the Center for Stock Assessment Research (CSTAR)
University of California Santa Cruz
1156 High Street
Santa Cruz Calilfornia 95064

Abstract—Predicting and understanding the dynamics of a population requires knowledge of vital rates such as survival, growth, and reproduction. However, these variables are influenced by individual behavior, and when managing exploited populations, it is now generally realized that knowledge of a species' behavior and life history strategies is required. However, predicting and understanding a response to novel conditions—such as increased fishing-induced mortality, changes in environmental conditions, or specific management strategies—also require knowing the endogenous or exogenous cues that induce phenotypic changes and knowing whether these behaviors and life history patterns are plastic. Although a wide variety of patterns of sex change have been observed in the wild, it is not known how the specific sex-change rule and cues that induce sex change affect stock dynamics. Using an individual based model, we examined the effect of the sex-change rule on the predicted stock dynamics, the effect of mating group size, and the performance of traditional spawning-per-recruit (SPR) measures in a protogynous stock. We considered four different patterns of sex change in which the probability of sex change is determined by 1) the absolute size of the individual, 2) the relative length of individuals at the mating site, 3) the frequency of smaller individuals at the mating site, and 4) expected reproductive success. All four patterns of sex change have distinct stock dynamics. Although each sex-change rule leads to the prediction that the stock will be sensitive to the size-selective fishing pattern and may crash if too many reproductive size classes are fished, the performance of traditional spawning-per-recruit measures, the fishing pattern that leads to the greatest yield, and the effect of mating group size all differ distinctly for the four sex-change rules. These results indicate that the management of individual species requires knowledge of whether sex change occurs, as well as an understanding of the endogenous or exogenous cues that induce sex change.

Manuscript submitted 22 September 2003 to the Scientific Editor's Office.

Manuscript approved for publication 20 December 2004 by the Scientific Editor.

Fish. Bull. 103:229–245 (2005).

Growth, survival, and reproduction all affect the dynamics of a population and its response to fishing and management (Quinn and Deriso, 1999; Haddon, 2001). However, these three key variables are influenced by many aspects of a species' biology, environment, and evolutionary history. There is an increasing realization that the management of populations requires an understanding of their behavior, life history strategies, and reproductive patterns (Sutherland, 1990; Huntsman and Schaaf, 1994; Collins et al., 1996; Greene et al., 1998; Sutherland, 1998; Beets and Friedlander, 1999; Coleman et al., 1999; Fulton et al., 1999; Kruuk et al., 1999; Constable et al., 2000; Cowen et al., 2000; Koeller et al., 2000; Fu et al., 2001; Apostolaki et al., 2002; Levin and Grimes, 2002). Although it is important to document the normal patterns of behavior and reproduction within a population, predicting and understanding a stock's response to novel conditions also requires knowledge of the degree of plasticity in behaviors that affect growth, survival, and reproduction, and the cues that induce phenotypic changes. Numerous examples exist of context- and condition-dependent behavior in fish (e.g., Metcalfe et al., 1989; Snyder and Dingle, 1990; Schultz and Warner, 1991; Wainwright et al., 1991; Mittelbach et al., 1992; Nishibori and Kawata, 1993; Ridgeway and Shuter, 1994; Breden et al., 1995), and this kind of plasticity has the potential to affect the dynamics of a stock. For example, many commercially important species of fish change sex from female to male. Researchers have argued that this life history pattern will lead to different population dynamics and responses to fishing and management strategies than will the life history pattern of dioecious (separate-sex) species (e.g., Snyder and Dingle, 1990; Schultz and Warner, 1991; Wainwright et al., 1991; Nishibori and Kawata, 1993; Ridgeway and Shuter, 1994; Alonzo and Mangel, 2004). However, it is important to consider not only whether sex change occurs, but also how it occurs; whether plasticity in sex change exists and what cues determine sex change in an individual species.

A variety of patterns of sex change have been observed in the wild (Warner and Lejeune, 1985; Charnov, 1986; Shapiro, 1987; Charnov and Bull, 1989; Iwasa, 1990; Warner and Swearer, 1991; Lutnesky, 1994, 1996;

Kuwamura and Nakashima, 1998; Koeller et al., 2000; Nakashima et al., 2000). At one extreme, sex change may occur at a fixed size or age threshold. However, sex change is known in many species to be mediated by local factors such as population density, reproductive skew, sex ratio, and size distribution (Warner and Lejeune, 1985; Warner and Swearer, 1991; Lutnesky, 1994, 1996; Kuwamura and Nakashima, 1998; Koeller et al., 2000; Nakashima et al., 2000). In many sex-changing species, overlap exists between the sexes in size and age and this overlap indicates that sex change may also depend on individual experience and local conditions (Munoz and Warner, 2003). The pattern of sex change may have important implications for a species' response to fishing. For example, if the size at sex change is fixed, then the population sex ratio may be affected by size-selective fishing of males, resulting in sperm limitation and decreased larval production (Alonzo and Mangel, 2004). In contrast, if sex change is mediated at the level of the spawning group in single-male harems and mating group size remains the same, sex ratios are maintained if the largest female always changes sex. In such a case, larval production will be reduced only because of the decreased size distribution of the population due to fishing. However, if sex change is controlled by the reproductive skew in the group (e.g., the expected potential for reproduction as a male versus present fecundity as a female), then the largest individual might not change sex and the spawning group could be without a male (Munoz and Warner, 2003). This result would clearly lead to a much greater effect on the productivity of the stock. A detailed understanding of the factors determining sex change and the cascading effects on sperm production, fecundity, and sex ratio can be critical to predicting stock dynamics. Furthermore, most animals have "rules-of-thumb" which determine their behavior and reproduction. Although these rules will have evolved under normal conditions, in the presence of fishing or other human-induced disturbances, animals are likely to continue to use these behavioral rules on ecological time scales even if they no longer function to maximize reproduction.

Although previous fisheries models have examined sex change, a consensus does not exist regarding how sex change is predicted to affect stock dynamics. Some research has suggested that sex-changing stocks will be more sensitive to fishing and cannot be managed as if they were identical to separate-sex stocks (Bannerot et al., 1987; Punt et al., 1993; Huntsman and Schaaf, 1994; Coleman et al., 1996; Beets and Friedlander, 1999; Brule et al., 1999; Coleman et al., 1999; Armsworth, 2001; Fu et al., 2001). However, it has also been argued that, in the absence of sperm limitation, protogynous stocks should be less sensitive to size-selective fishing because female biomass and thus population fecundity should not decrease as much as in a dioecious population, making traditional management and theory conservative when applied to these species. In general, protogynous stocks have been predicted to be at risk of population crashes because of their potential for nonlinear population dynamics in the presence of exploitation, yet there is no consensus regarding the importance of the exact pattern of sex change. For example, Armsworth (2001) examined protogynous stock dynamics when the probability of sex change was a fixed function of individual age and when the probability of sex change depended on the mean age of individuals in the population. He found that these two patterns of sex change had similar general dynamics and argued that management of a protogynous stock might not require knowledge of the precise pattern of sex change. In contrast, Huntsman and Schaaf (1994) and Coleman et al (1999) have argued that a consideration of the pattern of sex change can be important to managing stocks. But, past theory has generally focused on comparing fixed patterns of sex change with fully compensating reproductive patterns that maintain a fixed sex ratio or ratio of female to male biomass. However, a variety of patterns of sex change exist and there is no reason to believe that all species have evolved to exhibit full compensation under natural conditions, let alone under new situations. Thus, it is important to consider how specific sex change rules will affect the dynamics and management of protogynous stocks and whether knowledge of the cues that determine sex change will be important.

We (Alonzo and Mangel, 2004) developed a general modeling approach for examining the impact of reproductive behavior and life history pattern on stock dynamics. Using this approach, we then compared the dynamics of a protogynous population with fixed size at sex change and an otherwise identical dioecious species (Alonzo and Mangel, 2004). These analyses showed that although dioecious and protogynous stocks clearly have distinct dynamics, simple statements arguing that one life history pattern is more or less sensitive to fishing cannot be made. Protogynous stocks with fixed patterns of sex change were predicted to experience sperm limitation and lowered larval recruitment at high fishing pressure, whereas the dioecious stock was predicted to show a large drop in mean population size even at low fishing mortality, but was not predicted to experience lowered fertilization rates due to size-selective fishing. Both stocks were predicted to be sensitive to fishing pattern, but a fixed pattern of sex change was predicted to put a population at risk of crashing if all male size classes were fished even at relatively low fishing mortality. Finally, classic spawning-per-recruit (SPR) measures were not predicted to be good indicators of changes in the mean population size of protogynous stocks because they cannot indicate whether a population is experiencing sperm limitation and whether this limitation may lead to decreased population size or cause the stock to crash with small changes in fishing mortality. Although we found that whether or not a stock changes sex was important, that knowledge alone was not sufficient to understand and predict the response of the stock to fishing or management. We also found that sperm production and mating system were important variables affecting the probability that a population

would experience sperm limitation and would affect the performance of traditional spawning-per-recruit measures. However, we did not consider the possibility that size at sex change may be plastic and depend on local social conditions or relative rather than absolute size. Plastic sex change may allow a protogynous species to compensate for any effect of size-selective fishing on the sex ratio of the population, rendering its dynamics identical to the dynamics of a dioecious species. However, as described above, a wide variety of patterns of sex change have been observed in the wild and have been proposed to occur. Therefore, the exact pattern of sex change and cue driving phenotypic changes may lead to unique stock dynamics. In this study we apply the same general method we used previously (Alonzo and Mangel, 2004) to examine the effect of four different patterns of sex change (one fixed and three plastic) on the stock dynamics of a protogynous species.

Methods

We applied the same general method and individual-based population dynamic model as our previous study (Alonzo and Mangel, 2004). However, we now included the effect of four different patterns of sex change on the stock dynamics and performance of spawning-per-recruit measures in a protogynous species. Individuals vary in age, size, sex, and location (i.e. mating site). We assumed annual time periods and determined individual survival, size, and reproduction as described below. We simulated 100 years prior to examining the impact of fishing on stock dynamics and then simulated 100 more years in the presence of fishing with a constant mean fishing-induced mortality. This allowed the population to reach a stable age, sex, and size distribution prior to fishing which is independent of initial conditions. Because a number of elements of the model are stochastic, we examined 20 simulations for each scenario and set of parameter values, which was more than sufficient in all cases to lead to low variability in the key measures of interest.

Fishing and adult survival

We assume age and size do not affect natural adult mortality, μ_A, and that adult mortality is density-independent. The fishery is size selective; if L represents fish size, F annual fishing mortality, L_f the size at which there is 50% chance an individual of that size will be taken, and r the steepness of the selectivity pattern, the fishing selectivity per size class $s(L)$ is given by

$$s(L) = \frac{1}{1+\exp\left(-r(L-L_f)\right)} \tag{1}$$

and adult annual survival is

$$\sigma(L) = \exp\left(-\mu_A - Fs(L)\right). \tag{2}$$

Population dynamics

The number of larvae that enter the population is determined by larval survival and the total production of fertilized eggs $P(t)$, which is determined by total fecundity and fertility within each mating site as described below. Larval survival is assumed to have both density-independent and density-dependent components (e.g., Cowen et al., 2000; Sale, 2002), and we use a Beverton-Holt recruitment function (Quinn and Deriso, 1999; Jennings et al., 2001) to calculate larval survival . The number of larvae surviving to recruit in any year t, $N_0(t)$, is given by

$$\begin{aligned} N_0(t) &= \left(\alpha P(t)\right)/\left(1+\beta P(t)\right) \\ &\text{if } \left(\alpha P(t)\right)/\left(1+\beta P(t)\right) + \sum_{a=1} N_a(t) \le N_{\max} \\ N_0(t) &= \max\left(0, N_{\max} - \sum_{a=1} N_a(t)\right) \\ &\text{if } \left(\alpha P(t)\right)/\left(1+\beta P(t)\right) + \sum_{a=1} N_a(t) > N_{\max}, \end{aligned} \tag{3}$$

where α gives density-independent survival, β determines the strength of the density-dependence in the larval phase, and N_{max} represents the maximum population size. We assume that the population is open between mating sites, a single larval pool exists, larval recruitment is random among mating sites, and there is no emigration to or immigration from outside populations.

Growth dynamics

Larvae that survive to recruit begin at size L_0 and growth is assumed to be deterministic and independent of sex or reproductive status. We calculate growth between age classes using a discrete time version of the von Bertalanffy growth equation (Beverton, 1987, 1992) where $L_{\inf}$ represents the asymptotic size and k is the growth rate. Then an individual of length $L(t)$ at time t will grow in the next time period to size $L(t+1)$:

$$L(t+1) = L_{\inf}\left(1-\exp(-k)\right) + L(t)\exp(-k). \tag{4}$$

Mating system

As in our previous model, we assume that reproduction occurs at the level of the mating group, and we examine the effect of varying mating group size and the number of mating sites. Juveniles and adults are assumed to exhibit site fidelity and larvae settle randomly among mating sites. The carrying capacity of the population is split equally among the mating sites and the total capacity of all mating sites exceeds the maximum population size in the absence of fishing as determined by

adult mortality and the recruitment function. As before (Alonzo and Mangel, 2004), we examine the following three cases: 1) the entire population mates at one site (1 mating site with up to 1000 individuals); 2) a few large mating groups exist (10 sites with a maximum of 100 individuals per site); and 3) many small mating aggregations exist (20 mating sites with a maximum of 50 individuals per site). We assume that within a mating site, individuals mate in proportion to their fertility and fecundity and that males that are large enough to change sex have a chance of reproducing that is proportional to their fertility and thus a large male reproductive advantage exists. This is equivalent to assuming that females exhibit a mate choice threshold (Janetos, 1980) that has evolved with the size at pattern of sex change and that male fertilization success is proportional to fertility.

Reproduction

We assume female fecundity $E(L)$ and male sperm production $S(L)$ can be represented by the allometric relationships $E(L)=aL^b$ and $S(L)=cL^b$ respectively where a, b and c are constants. We assume that at any body length males produce 1000 times more sperm than females produce eggs. This leads to the realistic pattern that (in the absence of fishing) fertilization rates are high and that multiple males are needed to fertilize all the eggs produced by females. We calculate the average expected fertilization rate per mating site based on the total production of sperm and eggs at the site, where S represents the number of sperm released (in millions) and E the number of eggs released at each mating site. The proportion of eggs fertilized per mating site p_F is given by

$$P_F = \frac{S}{1+(\kappa E+\chi)S}, \tag{5}$$

where κ and χ are constants fitted to data. The proportion of eggs fertilized (p_F) depends on both total sperm production (S) and egg production (E). If sperm production is very high in relation to egg production, fertilization rates will be at or near 100%. However, if total sperm production (S) decreases and egg production remains the same, fertilization rates will decrease. Similarly, as egg production (E) increases in relation to total sperm production (S) fertilization rates will decrease (see Fig. 2, Alonzo and Mangel, 2004). The number of eggs fertilized per group is $p_F E$ and the total production of fertilized eggs $P(t)$ is the sum of the number of eggs fertilized in all mating groups. For more details on the fertilization function and individual sperm production see Alonzo and Mangel (2004).

Patterns of sex change

We examine four possible patterns of sex change, determined by absolute or relative size of the individual. Although a variety of other possibilities exist, these examples represent four plausible patterns that differ in the cues or mechanisms that induce sex change, the degree of compensation or plasticity assumed, and encompass the diversity that has been observed and hypothesized for a variety of sex-changing fish populations (Helfman, 1997).

Rule 1: Fixed For the first sex-change rule, we assume that the probability of sex change $p_C(L)$ is determined by the absolute length of the individual and is

$$p_c(L) = \frac{1}{1+\exp\left(-\rho(L-L_c)\right)}, \tag{6}$$

where L_C represents the size at which 50% of mature females change sex and ρ is a constant that determines the steepness of the probability function. With this sex change rule, we also assume that the probability an individual matures $p_M(L)$ is determined by absolute size. Once an individual matures, she remains female until sex change. L_M represents the length at which 50% of juveniles are expected to mature.

$$p_M(L) = \frac{1}{1+\exp\left(-q(L-L_M)\right)}, \tag{7}$$

where q determines the steepness of the probability function and where $L_C > L_M$.

Rule 2: Relative size For the second sex change rule, the mean size of all individuals in the mating group determines the probability of sex change for an individual. First, we find the mean size of all individuals at each mating site. We let L_i represent the mean size in the mating site i. Then the probability of sex change for an individual of length L is

$$p_c(L) = \frac{1}{1+\exp\left(-\rho\left(L-(L_i+\Delta L_c)\right)\right)}, \tag{8}$$

where ΔL_C represents the difference from the mean at which the probability of sex change is 0.5. For these analyses, we also assumed that the probability an individual matures also depends on the mean size of individuals at the mating site. Then the probability of maturity is

$$p_M(L) = \frac{1}{1+\exp\left(-q\left(L-(L_i+\Delta L_M)\right)\right)}, \tag{9}$$

where ΔL_M represents the difference from the population mean at which the probability an individual will mature is 0.5.

Rule 3: Relative frequency Sex change may also be induced by the social conditions at the mating site. For example, sex change may depend on the frequency of

other mature individuals or the frequency of smaller individuals. We examine the case where sex change depends on the frequency of smaller mature individuals. For each mature female, we find the frequency of mature individuals at the same mating site that are smaller. We let F_i represent the frequency of mature individuals that are smaller than the mature female and F_C represents the frequency at which 50% of the individuals are expected to change sex. Then the probability of sex change is

$$p_c(L) = \frac{1}{1+\exp\left(-\rho(F_i - F_c)\right)}. \quad (10)$$

The probability of maturing depends on the frequency of smaller individuals. We let f_i represent the frequency of all smaller individuals at mating site i and f_M represent the frequency at which there is a 50% probability of an individual maturing. Then the probability of maturing is

$$p_M(L) = \frac{1}{1+\exp\left(-q(f_i - f_M)\right)}. \quad (11)$$

Rule 4: Reproductive success Finally, we consider the case where sex change occurs when an individual's size-dependent expected reproductive success is greater as a male than as a female (Charnov, 1982). This pattern of sex change has been proposed to explain the observation that individual variation exists in size at sex change and that it is not always the largest individual in a group that changes sex (Munoz and Warner, 2003). We assume that a fish will change sex when its expected egg production at its current length ($E(L)=aL^b$ as given above) is exceeded by its expected paternity at the mating site which is given by the total egg production of all other females at the site multiplied by the focal individual's relative sperm production. This value is given by expected fertility $S(L)$ divided by the total sperm production (by all males at the site plus their own expected fertility) at the same mating site. We further assume that sex change occurs once a year in rank order from the largest to smallest female at the site. (For this scenario we assumed that the probability of maturing depends on absolute size as in Equation 7.) However, we still assume that individuals can only change sex once during their lifetime and only mature females can change sex. Thus, mature females change sex when their current expected fertilization success as a male is greater than their current expected fecundity as a female.

Measures of spawning stock biomass per recruit

We examine the same spawning-per-recruit measures as in our previous paper (Alonzo and Mangel, 2004) and compare the results of the patterns of sex change considered here with one another and with a hypothetical dioecious species, where sex is determined stochastically at birth and the primary sex ratio is fixed. We compute the total spawning stock biomass per recruit starting from the beginning of fishing for the next 50 years. We use the generally recognized pattern that fish wet weight tends to be approximately proportional to the cube of fish length (Gunderson, 1997) to convert fish length, L, into relative biomass, $B(L)\sim L^3$. Then we calculate total, female, and male spawning stock biomass per recruit (SSBR). We also keep track of the total fecundity (egg production per recruit), fertility (sperm production per recruit), and eggs fertilized per recruit.

Parameter values

We use parameters based on previous research (Warner, 1975; Cowen, 1985; Cowen, 1990) on California sheephead (Labridae, *Semicossyphus pulcher*), a commercially important sex-changing fish, to provide evolutionarily and ecologically reasonable parameters for the model. Although the growth, survival, and reproduction of this species have been studied, less is known about the factors that induce sex change and mating behavior. In this species, sex change occurs at approximately 30 cm, although the exact pattern varies among populations (Warner, 1975; Cowen, 1990). It is not known whether sex change is fixed or socially mediated. For the first sex-change rule, we assume that individuals have a 50% chance of maturing (L_m) at 20 cm (the mean size of maturity observed in natural populations) and of changing sex at (L_c) 30 cm. This leads to a sex ratio of 2/3 mature females to 1/3 males on average and a mean length of 20 cm in the absence of fishing as is observed in the wild. For consistency, we also assume for the second sex-change rule, that individuals have a 50% chance of changing sex at 10cm (ΔL_c=10) above the mean size and have a 50% chance of maturing at the mean size in the mating site (ΔL_m=0). Similarly, for the third rule, the frequency of smaller mature individuals at which there is a 50% of sex change is assumed to be 0.67 and when 50% of all individuals are smaller, an individual will have a 0.5 probability of maturing. Therefore in the absence of fishing all four sex change rules lead to the same maturity and sex-change patterns as a function of age and size. For more information on the parameter values considered here, see Table 1.

Individual-based simulations are computationally very intensive. As a result, it was not feasible to explore a wide range of values for all parameters. Furthermore, because growth, mortality, reproduction, maturity, and sex change are coevolved characters within any species, it does not make sense in this context to vary them independently. Instead, we used estimates from California sheephead for as many parameters as possible (mortality, growth, fecundity, size at maturity, and sex change) and when necessary from a closely related species (fertilization rate). We then focused on exploring the effect, for this species, of varying the sex-change rule and fishing pattern while all other parameters remained the same. Our focus was on determining the impact of the sex change rule on the predicted stock

Table 1

The parameter values used in the model were based on available data for California sheephead (*Semicossyphus pulcher*). See text for details.

Parameter	Parameter values	Definition and source
Growth		
k	0.05	Growth rate (based on Cowen, 1990)
L_{inf}	90 cm	Asymptotic size (based on Cowen, 1990)
L_0	8 cm	Larval size at recruitment
Population		
N_{max}	1000	Maximum population size
μ_A	0.35	Adult mortality (based on Cowen, 1990)
α	0.0001	Density-independent larval mortality
β	$\alpha/(1-\exp(-\mu_A))\,N_{max}$ (3.33×10^{-7})	Larval recruitment function parameter (see text)
Fishing		
r	1 (0.1)	Steepness of selectivity curve
L_f	30 (25, 35)	Length at which 50% chance a fish will be removed
F	0–3	Fishing mortality
Reproduction		
a	7.04	Constant in the fecundity relationship (Warner, 1975)
b	2.95	Exponent in the allometric relationship (Warner, 1975)
c	$10^{-3}a$	Constant in the sperm production function (measured in millions of sperm)
κ	0.000003	Slope of fertilization function parameter
χ	0.09	Intercept of fertilization function parameter (based on Peterson et al., 2001) see text for details
Rule 1		
L_c	30 cm	Length at which 50% of fish change sex
ρ	1	Shape parameter in the sex-change function
L_m	20 cm	Length at which 50% of fish mature
q	1	Shape parameter in the maturity function
Rule 2		
ΔL_c	10 cm	Difference from the mean size at which $p_c(L)= 0.5$
ρ	1	Shape parameter in the sex change function
ΔL_m	0 cm	Difference from the mean size at which $p_M(L)= 0.5$
q	1	Shape parameter in the maturity function
Rule 3		
F_c	0.67	Frequency of smaller mature individuals where $p_c(L)=0.5$
ρ	50	Shape parameter in the sex-change function
F_m	0.50	Frequency of smaller individuals at which $p_M(L)=0.5$
q	50	Shape parameter in the maturity function
Rule 4		No additional parameters required

dynamics rather than on exploring all possible parameter combinations. However, it would certainly be useful in the future to examine the same question using parameter estimates based on other commercially exploited species that change sex.

Results

We present the average across simulations of the mean population measures of the last 50 years for each simulation. The variation around the mean in all measures considered is hundredths of a percent of the mean or less. For the spawning-per-recruit (SPR) measures we give the mean value across the first 50 years of fishing to ensure that the entire cohort under consideration had died before the end of the simulation. Parameter values used are given in Table 1

General dynamics

In all cases, size-selective fishing is predicted to decrease population size and decrease the mean length of fish in the population. Although all scenarios are predicted to lead to the same change in average fish length, the effect of fishing on predicted population size and the mechanisms leading to changes in population size differ between the four sex-change rules (Figs. 1 and 2, Table 2). The largest differences occur between the fixed rule and the three plastic patterns of sex change. How-

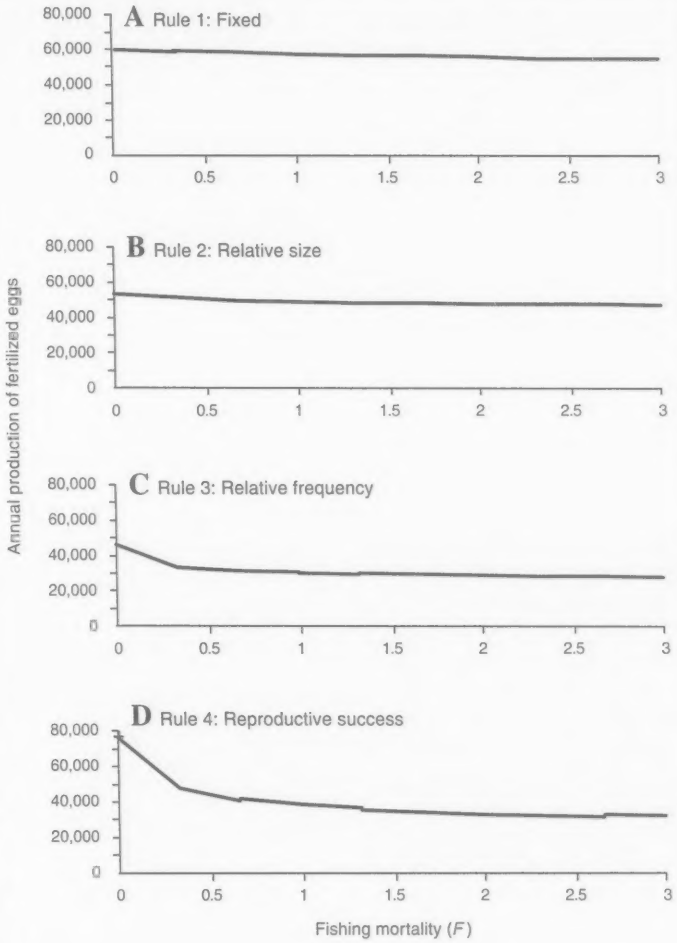

Figure 1

The predicted effect of fishing mortality on the production of fertilized eggs. Results are shown for the case where one mating group exists and the fishing selectivity is characterized by L_f=30 and r=1. The same basic pattern is predicted for multiple mating sites as well.

ever, the exact pattern of sex change has an important and qualitative effect on the predicted stock dynamics (Table 2). All three plastic patterns of sex change are predicted to show lower sperm limitation and higher fertilization rates in the presence of fishing than the fixed pattern of sex change (Table 2). However, associated with plastic sex change is also a greater predicted drop in egg production (total and fertilized) and mean population size than when the effect of size on the probability of sex change is fixed (Fig. 1, Table 2). This drop in egg production and mean population size occurs because female biomass is predicted to decrease as a result of the combination of fishing on larger individuals and smaller sizes at sex change (Fig. 2). The basic patterns are the same for the case with multiple mating sites. Most of the significant reductions in stock size are predicted at high fishing mortality. However, it is important to remember that we have assumed that the stock is very resilient (Table 1), and our focus is on the differences among sex-change rules and fishing patterns rather than on absolute fishing mortality.

The effect of mating group size

Although mating group size is predicted to have an effect in most cases on the stock dynamics of the population,

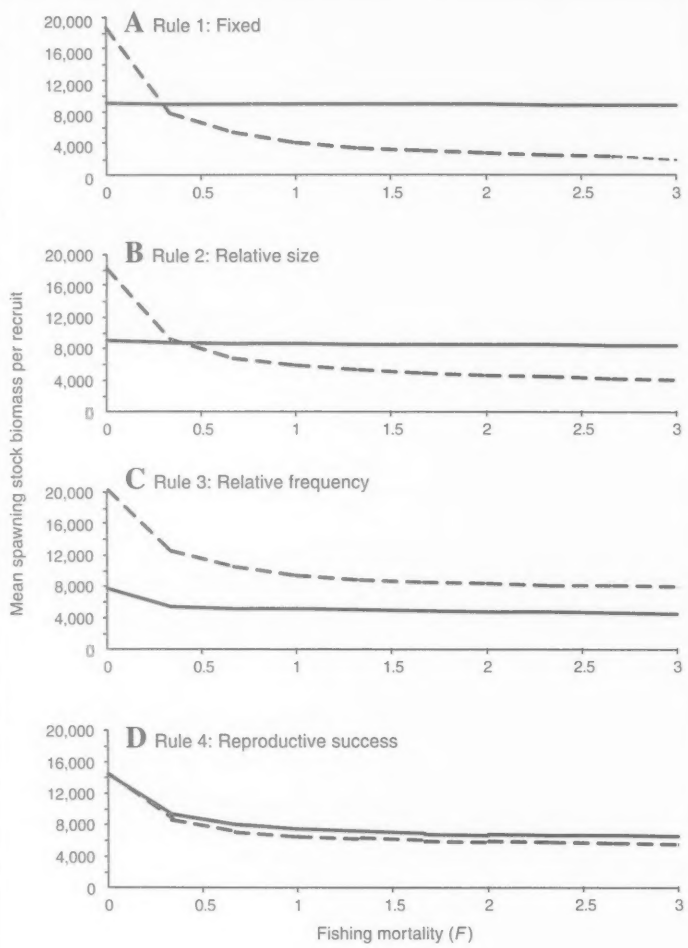

Figure 2

The predicted effect of fishing mortality on the spawning stock biomass per male recruit (dashed lines) and per female recruit (solid lines) for all four patterns of sex change. Results are shown for the case of one mating group and the fishing selectivity is characterized by L_f=30 and r=1. The same basic pattern is predicted for multiple mating sites as well.

the strongest effect is predicted when size at sex change is fixed or determined by the frequency of small fish in the population (Fig. 3, A and C). When the size at sex change is fixed, populations are predicted to crash when mating sites are very small (Fig. 3A). In the case where size at sex change is determined by expected reproductive success, group size is predicted to have no effect on the relative production of eggs and mean population size (Fig. 3D). However, for all the other rules of sex change considered, smaller mating sites are predicted to experience sperm limitation in the presence of fishing, leading to a decrease in the relative production of fertilized eggs and a decrease in mean population size (Fig. 3). However, unlike in the case of fixed size at sex change, the smaller mating groups (20 mating sites with up to 50 individuals per site) are stable both in the presence and absence of fishing and are not predicted to collapse for most fishing patterns.

Sensitivity to fishing pattern

Rule 1 The size-selective pattern of the fishery has a large effect on the predicted stock dynamics when the size at sex change is fixed. When the selectivity of the

Table 2

A comparison of stock dynamics for four sex-change rules. Results are reported for the situation where the fishing selectivity pattern and the probability of sex change are both centered at the same size (L_f=30). These results assume a near knife-edge selectivity (r=1) and that one mating site exists. Numbers given are for the predicted relative change as a result of fishing (when F=3 compared to F=0). SSBR = spawning stock biomass per recruit.

	Rule 1: Fixed	Rule 2: Relative size	Rule 3: Relative frequency	Rule 4: Reproductive success
Mean population size	90%	90%	73%	72%
Total SSBR	40%	45%	44%	39%
Male SSBR	11%	22%	39%	39%
Female SSBR	98%	92%	58%	39%
Sex ratio	0.67 → 0.92	0.67 → 0.84	No change	0.8 → 0.66
Mean size	88%	88%	88%	88%
Sperm production	11%	23%	40%	40%
Egg production	98%	93%	59%	41%
Fertilized egg production	88%	86%	59%	41%

fishery is centered below the mean size at sex change (L_f=25, r=1), the stock was predicted to crash at high fishing mortality ($F \geq 1$, Fig. 4A). Furthermore, when the selectivity pattern was not steep (L_f=30, r=0.1), the population was always predicted to crash even at low fishing mortality (and thus this case is not shown in Figs. 4A–6A). When the steepness of the fishery's selectivity changes, the size range over which fish are targeted also changes. Thus, smaller and younger fish are removed by the fishery when r=0.1 and hence a greater number of age classes are affected by fishing. At an extreme, fishing mortality could be high enough that all of the individuals in any size classes targeted by the fishery are removed. As a result, although the steepness of the selectivity function only affects the spread of the function mathematically, it has the biological effect of decreasing the size at which fish experience fishing mortality and can have a large effect on the size and age distribution of the population. In contrast, when the fishery's selectivity is steep (r=1) and only fish at or above the mean size at sex change ($L_f \geq 30$) are targeted, the effect of fishing on the population is predicted to be much less (Fig. 4A). Independent of the selectivity pattern, the population sex ratio is predicted to be more female-biased in the presence of fishing than in the absence of fishing. The lower the mean size removed by the fishery, the greater the predicted change in population sex ratio as a result of fishing (Fig. 5A). For situations in which the stock is not predicted to crash (i.e., $L_f \geq 30$ and r=1), yield is predicted to increase with diminishing returns with fishing mortality (Fig. 6A), catch is not predicted to decline with increased fishing mortality (at least up to F=3), and steep size-selective fishing patterns with lower size thresholds are predicted to lead to more yield (Fig. 6A).

Rule 2 When sex change is determined by the mean size of individuals in the mating site and the size-selectivity is weak (r=0.1), the population is predicted to crash when $F \geq 1.67$ (Fig. 4B). This crash occurs because individuals do not escape fishing mortality even at small sizes. However, unlike when sex change is fixed (Fig. 4A), the population is predicted not to crash when the size selected by the fishery is less than the mean size at sex change in the absence of fishing (L_f=25, Fig. 4B). The larger the mean size selected by the fishery, the smaller the predicted effect of fishing on the mean population size and the population sex ratio (Figs. 4B and 5B). Although catch is predicted to increase with diminishing returns as fishing mortality increases from zero to three, the difference between the size-selectivity patterns is predicted to decrease and yield will be greater annually if larger fish are targeted (Fig. 6B).

Rule 3 As above, when the probability of sex change depends on the relative frequency of smaller mature individuals, the population is predicted to crash whenever size-selectivity is weak because fish do not escape fishing even when small (r=0.1, Fig. 4C). Although the population is predicted not to crash when the size targeted by the fishery is less than the mean size at sex change in the absence of fishing (L_f=25, Fig. 4C), this fishing pattern is predicted to lead to a large decrease in mean population size and a marked decrease in population sex ratio (Figs. 4C and 5C). In contrast fishing selectivity that is centered at or above the mean size of sex change in the absence of fishing (L_f=30 and L_f=35) is predicted to lead to a weaker effect on mean population size and to almost no effect on the population sex ratio (Figs. 4C and 5C). However, in contrast to the two scenarios described above this pattern of sex change leads to the prediction that targeting fish at or larger than the normal mean size of sex change (L_f=30 and r=1) will lead to the greatest annual yield over time for most fishing mortalities (Fig. 6C).

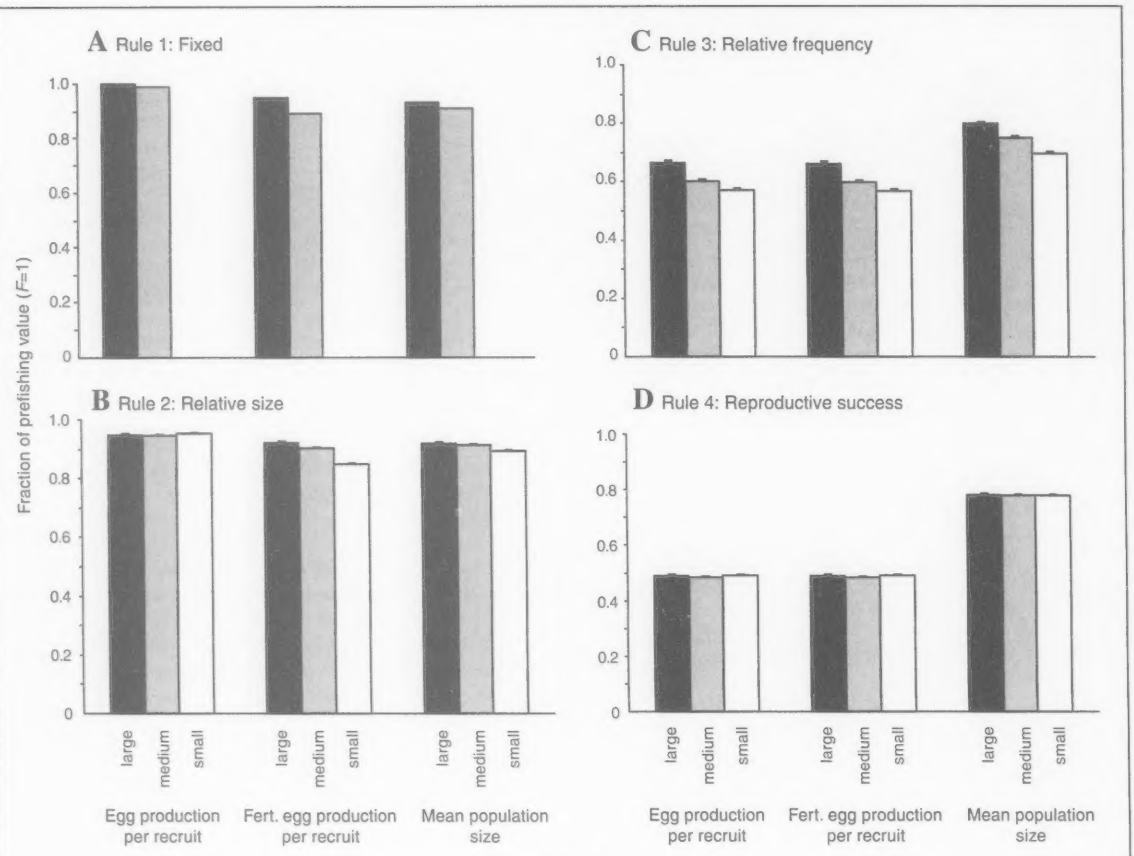

Figure 3

Effects of mating group size on the response of egg production per recruit, fertilized egg production per recruit, and mean population size to fishing pressure. Large (one large mating aggregation), medium (10 medium-sized mating aggregations) and small (20 small mating aggregations) situations are compared. Percent change in the presence of fishing (from F=0 to F=1) is given. Total population fecundity and mean body size are lower for smaller mating aggregations as well. Results are shown for L_f=30 and r=1. No bars are shown for small mating groups with fixed size at sex change because these populations are predicted to crash.

Rule 4 As with all of the other patterns of sex change, populations with sex change based on expected reproductive success are predicted to crash whenever small fish experience fishing mortality (r=0.1, Fig. 4D). Furthermore, as with the other two plastic sex change rules, populations are predicted not to crash when fish below the normal mean size at sex change are included in the fishery because the population can compensate with smaller sizes at sex change in the presence of fishing (Fig. 4D). Although only small differences among fishing patterns are predicted in the mean population sex ratio, the effect on the population size is predicted to be greatest when many size classes are fished, and large differences are predicted between the fishing patterns in mean population size (Fig. 5D). Finally, in the scenario of sex change based on expected reproductive success, the fishing pattern predicted to lead to the greatest catch is to target only fish above the normal mean size at sex change (L_f=35, Fig. 6D).

In summary, fishing is always predicted to decrease total production of fertilized eggs and mean population size. However, the strength of the effect depends both on fishing selectivity and the pattern of sex change (see above and Figs. 4–6). Although populations with fixed patterns of sex change are predicted to crash in the presence of fishing below the mean size at sex change, plastic patterns of sex change are predicted to lead to more resilience since these populations can compensate for the removal of large males more effectively. However, all scenarios are predicted to crash in the presence of fishing across a broad range of size classes (when r=0.1) even in completely compensatory patterns of sex change.

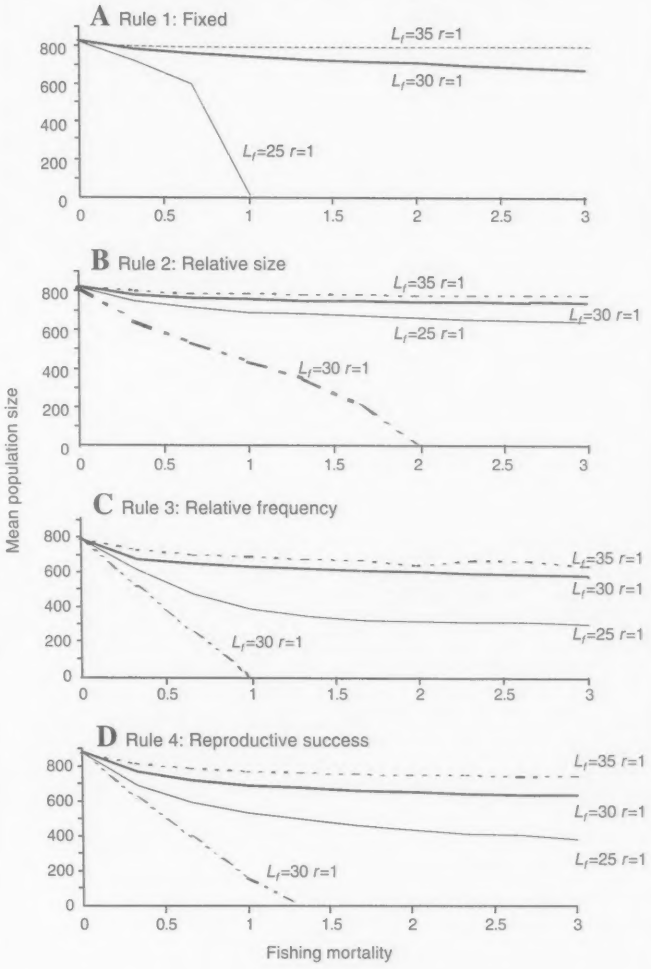

Figure 4

The effect of size-selective fishing on the predicted mean population size for all four patterns of sex change. We present results for a sex-changing stock with one mating site. Means across 20 simulations are given. For details see text. The same basic patterns are predicted with multiple mating sites. A line is not shown in panel A (when sex change is fixed) where L_f=30 and r=0.1 because the population is predicted to crash at any fishing mortality in this scenario.

Yet, the exact response depends greatly on the specific pattern of sex change. For example, the population sex ratio is not predicted to change much in the presence of fishing when sex change is based on expected reproductive success and fishing pattern has little effect on the sex ratio (Fig. 5). However, when sex change is based on expected reproductive success, the annual yield is greater for fishing patterns with larger size thresholds (Fig. 6). In contrast, when sex change is determined by the mean size of individuals at the mating site, sex ratio is predicted to increase with fishing and increase more when smaller size classes are fished. However, for this pattern of sex change, the smallest size threshold is also predicted to lead to the largest yield of the fishery, although as fishing mortality increases the difference between fishing patterns with differing size thresholds decreases. Therefore, the fishing pattern that will produce optimal yield will depend on the exact pattern of sex change (Fig. 6).

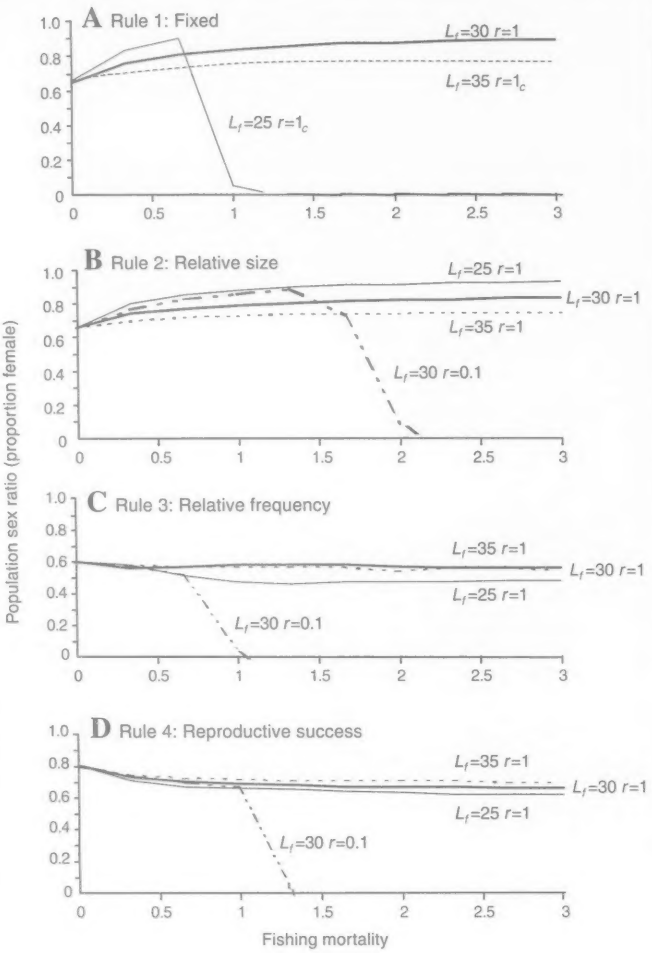

Figure 5

The effect of size-selective fishing on the predicted population sex ratio for all four patterns of sex change. We present results for a sex-changing stock with one mating site. Means across 20 simulations are given. For details see text. The same basic patterns are predicted with multiple mating sites. A line is not shown in panel A (when sex change is fixed) where L_f=30 and r=0.1 because the population is predicted to crash at any fishing mortality in this scenario.

Spawning-per-recruit (SPR) measures and a comparison of protogynous and dioecious stocks

Our previous results (Alonzo and Mangel, 2004) have shown that whether species change sex or are dioecious is predicted to have dramatic effects on both the stock dynamics and performance of classic SPR measures. However, our results show that the exact pattern of sex change, and not just whether the pattern is plastic or fixed, can have a strong effect on these measures as well (Fig. 7). Because of the population dynamics of the model, all the scenarios represented in the present study show a great resiliency to fishing. Hence, the predicted changes in stock size are all above the common threshold of allowing a reduction of spawning per recruit measures to 40% of their values in the unfished condition. However, our aim is not determine if this population is overfished. Instead, it is to determine whether classic

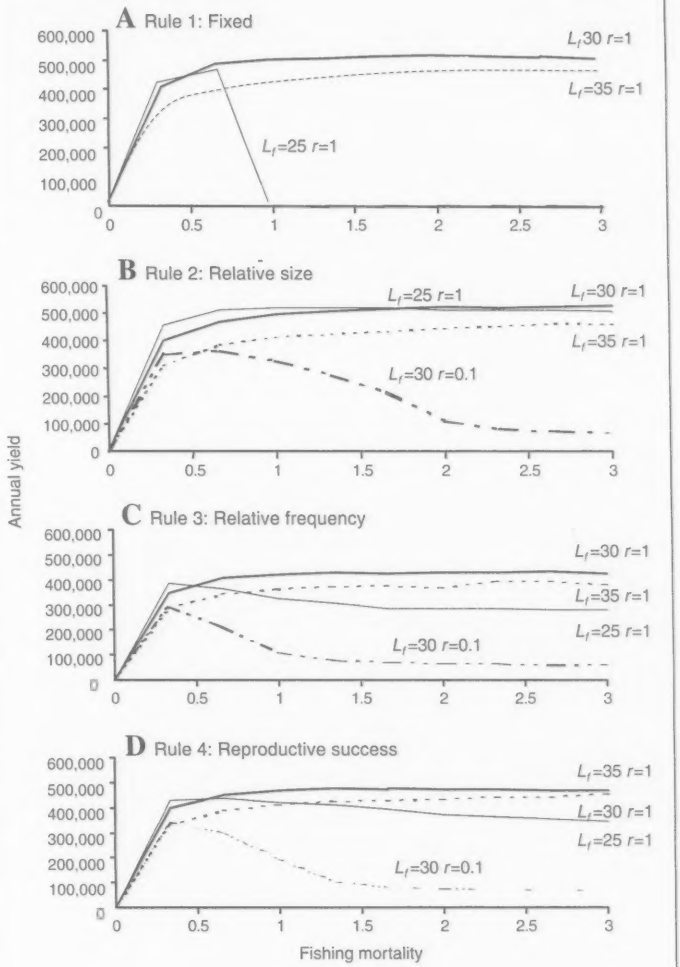

Figure 6

The effect of size-selective fishing on the predicted annual yield for all four patterns of sex change. We present results for a sex-changing stock with one mating site. Means across 20 simulations are given. For details see text. The same basic patterns are predicted with multiple mating sites. A line is not shown in panel A (when sex change is fixed) where L_f=30 and r=0.1 because the population is predicted to crash at any fishing mortality in this scenario.

spawning per recruit measures based on egg production or fecundity could accurately assess the status of sex-changing stocks. Although the fixed pattern of sex change is predicted to show the greatest difference between egg production per recruit and fertilized eggs produced per recruit, each population shows deviations between egg production and the production of fertilized eggs. Thus egg production alone cannot tell us how the population is being affected by fishing and classic SPR measures based on population fecundity may be misleading for sex-changing stocks in cases where the sex-change rule is not completely compensatory (rules 1–3). It is also interesting to ask whether consistent differences exist (as has been suggested) in the resiliency of sex-changing stocks, compared to stocks with separate sexes. Our results indicate that sex change based on expected reproductive success is predicted to have very similar dynamics to the dioecious population,

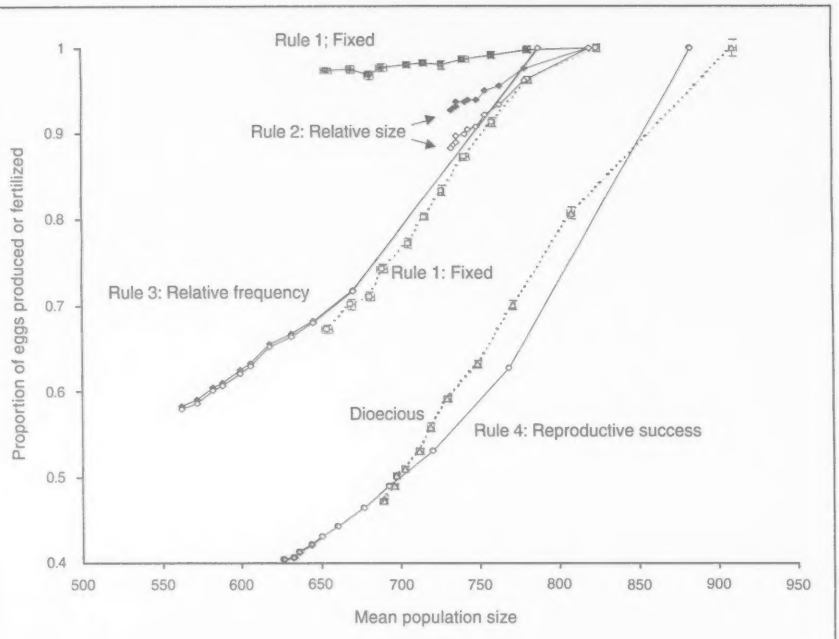

Figure 7

Spawning-per-recruit (SPR) measures for all four patterns of sex change and an otherwise identical dioecious stock: mean egg production per recruit (filled) and mean fertilized eggs per recruit (open) are shown for a population with one large mating group when L_f=30 and r=1. The same basic patterns are predicted for multiple mating sites. Each line represents the same range of fishing mortalities, and each point represents fishing mortality increasing from 0 to 3 in increments of 1/3 moving from the right to the left. For the fourth rule (expected reproductive success), the two lines (eggs produced per recruit and eggs fertilized per recruit) overlap.

whereas sex change based on relative size or the relative frequency of individuals in a mating site is predicted to have similar dynamics to those for the fixed pattern of sex change. Thus, it is not possible to say that sex-changing stocks tend to be more or less resilient to fishing than are dioecious populations. However, the sex change rule clearly affects the predicted relationship between fishing mortality and the response of the stock to fishing.

Discussion

We apply a general approach using individual-based simulation models to determine the predicted effect of the pattern of sex change on the stock dynamics of a protogynous species. Although the model structure and parameter values considered will not apply to all commercially important protogynous species, it is important to realize that all the scenarios considered are identical except for the pattern of sex change. As a result, any predicted differences that arise between these situations are a result of the sex-change rule and indicate that knowing simply that a species exhibits sex change but not what the behavioral rule of sex change is will lead to an incomplete ability to understand and predict the dynamics of the stock and its response to fishing or management strategies.

Independent of the sex-change rule, the protogynous stocks are always predicted to be sensitive to the size-selective fishing pattern. Mean population size is always predicted to decrease as fishing mortality increases, despite the fact that we have assumed that recruitment is strongly density dependent and that the species is very productive. Stocks are predicted to crash even at low fishing mortality when the size-selective fishing pattern targets all reproductive size classes and for the fixed sex change rule whenever all male sizes sizes are targeted by the fishery. It will be necessary but not sufficient to avoid overfishing at spawning aggregations. Our results indicate that it will also be important to allow smaller and nonreproductive individuals to escape fishing as well. These results indicate that independent of the exact pattern of sex change, management strategies for all protogynous stocks need to be sensitive to the size-selectivity of

the fishing pattern in relation to size at maturity and size at sex change observed in the population, and a failure to do so can lead to a sudden and unexpected collapse of the fishery—a collapse from which it may be difficult to recover.

We assume in all cases that the same cues determine both the probability of maturity and the probability of sex change within a species. For example, when sex change was affected by the relative size of individuals at the mating site, we assume that this same cue affected the probability of maturing. This assumption has a large effect on the predicted dynamics of the stock. Alternatives exist. For example, the size at which fish mature could be determined by endogenous rather than exogenous factors even in a population where the probability of sex change is affected by external cues. If this were the case, the population can easily be fished into a situation where it cannot compensate for size-selective fishing and is predicted to crash for any fishing pattern that targets reproductive individuals. For example, when L_f=30 and r=1, populations with plastic size at maturity and sex change were not predicted to crash independent of fishing mortality. In contrast, simulations where populations were assumed to have fixed size at maturity rules (L_m=20) but plastic patterns of sex change crashed at most fishing mortalities with L_f=30 and r=1. Hence, knowledge of the cues determining both maturity and sex change will be important in predicting and understanding larval production and the effect of fishing on a population.

It is possible to argue that a protogynous species with fixed patterns of sex change may have very different dynamics than dioecious stocks, but the compensatory patterns of sex change will be less sensitive to fishing and exhibit dynamics very similar to their dioecious counterparts. However, our results indicate that even stocks with plastic patterns of sex change are predicted to have dynamics distinctly different from otherwise identical dioecious populations. For example, sperm limitation is predicted to occur for all sex change rules, except for the pattern where sex change is determined by expected reproductive success (rule 4). However, even a stock exhibiting the reproductive sucess rule has dynamics that are distinctly different from those of a dioecious species because a change in the size distribution of the population due to size-selective fishing is predicted to have a large effect on the productivity and sex ratio of the protogynous population. Similarly, mating group size is predicted to affect the stock dynamics in all cases except for the reproductive success rule. Therefore, although knowing the pattern of sex change is predicted to be important in understanding stock dynamics, it is also clear that the pattern of sex change must be considered in the context of the mating system of the stock, as well as in the context of the basic biology of the stock.

Protogynous stocks are thus predicted to be sensitive to the fishing pattern, and nonlinear stock dynamics are possible when fishing operations target a wide range of fish sizes. However, each stock is also predicted to have a unique response to the same fishing pattern (Figs. 4–6) and to have different relationships between traditional spawning-per-recruit measures and changes in mean population size with fishing mortality (Figs. 1, 2, and 7). As a result, monitoring changes in spawning stock biomass per recruit or egg production per recruit alone will not make it possible to determine the relationship between these measures and mean population size or to know whether the population is at risk for large and sudden declines in population size. Our results indicate that although it is important to know whether sex change occurs when managing a stock, it will also be important to know what endogenous or exogenous cues induce sex change and how behavioral patterns and life history strategies affect the demographic rates of the stock.

Plasticity is not predicted to yield populations that have stock dynamics that are identical to those of dioecious species, and the performance of spawning-per-recruit measures and the relationship between egg production and population size differed greatly between all four patterns of sex change, despite the fact that the basic patterns of growth, survival, and fecundity where identical between all the scenarios considered. Because sperm limitation is more common with the fixed and relative size rules of sex change, these situations are predicted to have the greatest difference between classic SPR measures and the production of fertilized eggs. Clearly it is not just whether a population changes sex or not, but also how sex change is induced, that determines the population's predicted response to fishing and the performance of spawning-per-recruit measures in predicting and indicating the effect of fishing on the population.

Although it is important to know what life history strategy and behavioral patterns are observed in a species, these alone will not always be sufficient to predict expected changes in population size and productivity under new conditions. Instead, knowledge of the plasticity of behavioral and life history patterns, as well as information about the internal and external cues that induce phenotypic changes, may also be necessary. Phenotypic plasticity is often expressed as a threshold response (such as sex change) to a continuous endogenous or exogenous cue. Therefore, as predicted by our model, plasticity can generate nonlinear changes in important demographic characters. An understanding of the natural variation in behavior and life history combined with knowledge of fish vital rates and environmental conditions will lead to a better understanding of and ability to predict the response of a stock to fishing mortality, environmental changes, and specific management strategies.

Acknowledgments

This research was supported by National Science Foundation grant IBN-0110506 to Suzanne Alonzo and the Center for Stock Assessment Research (CSTAR).

Literature cited

Alonzo, S. H., and M. Mangel.
2004. Size-selective fisheries, sperm limitation and spawning per recruit in sex changing fish. Fish. Bull. 102:1–13.

Apostolaki, P., E. J. Milner-Gulland, M. K. McAllister, and G. P. Kirkwood.
2002. Modelling the effects of establishing a marine reserve for mobile fish species. Can. J. Fish. Aquat. Sci. 59:405–415.

Armsworth, P. R.
2001. Effects of fishing on a protogynous hermaphrodite. Can. J. Fish. Aquat. Sci. 58:568–578.

Bannerot, S., W. F. Fox, and J. E. Powers.
1987. Reproductive strategies and the management of snappers and groupers in the gulf of Mexico and Caribbean. *In* Tropical snappers and groupers: biology and fisheries management. (J. J. Polovina and S. Ralston, eds.), p. 561–603. Westview Press, Boulder, CO.

Beets, J., and A. Friedlander.
1999. Evaluation of a conservation strategy: a spawning aggregation closure for red hind, *Epinephelus guttatus*, in the U.S. Virgin Islands. Environ. Biol. Fish. 55:91–98.

Beverton, R. J. H.
1987. Longevity in fish: some ecological and evolutionary considerations. *In* Evolution of longevity in animals. (A. D. Woodhead and K.H. Thompson, eds.) p. 161–185. Plenum Press, New York, NY.

Beverton, R. J. H.
1992. Patterns of reproductive strategy parameters in some marine teleost fishes. J. Fish Biol. 41 (Suppl. B) 41:137–160.

Breden, F., D. Novinger, and A. Schubert.
1995. The effect of experience on mate choice in the Trinidad guppy, *Poecilia reticulata*. Environ. Biol. Fish. 42:323–328.

Brule, T., C. Deniel, T. Colas-Marrufo, and M. Sanchez-Crespo.
1999. Red grouper reproduction in the southern Gulf of Mexico. Trans. Am. Fish. Soc. 128:385–402.

Charnov, E. L.
1982. The theory of sex allocation, 355 p. Princeton Univ. Press, Princeton, NJ.
1986. Size advantage may not always favor sex change. J. Theor. Biol. 119:283–285.

Charnov, E. L., and J. J. Bull.
1989. Non-Fisherian sex ratios with sex change and environmental sex determination. Nature 338:148–150.

Coleman, F. C., A. Eklund, and C. B. Grimes.
1999. Management and conservation of temperate reef fishes in the grouper-snapper complex of the southeastern United States. Am. Fish. Soc. Sym. 23:233–242.

Coleman, F. C., C. C. Koenig, and L. A. Collins.
1996. Reproductive styles of shallow-water groupers (Pisces: Serranidae) in the eastern Gulf of Mexico and the consequences of fishing spawning aggregations. Environ. Biol. Fish. 47:129–141.

Collins, L. A., A. G. Johnson, and C. P. Keim.
1996. Spawning and annual fecundity of the red snapper (*Lutjanus campechanus*) from the northeastern Gulf of Mexico. *In* Biology, fisheries, and culture of tropical groupers and snappers (F. Arreguin-Sanchez, J. L. Munro, M. C. Balgos, and D. Pauly, eds.) p. 174–188. ICLARM (International Center for Living Aquatic Resources Management) conference proceedings 48, ICLARM, Makati City, Philippines.

Constable, A. J., W. K. de la Mare, D. J. Agnew, I. Everson, and D. Miller.
2000. Managing fisheries to conserve the Antarctic marine ecosystem: practical implementation of the convention on the conservation of Antarctic marine living resources (CCAMLR). ICES J. Mar. Sci. 57:778–791.

Cowen, R. K.
1985. Large-scale pattern of recruitment by the labrid, *Semicossyphus pulcher*: causes and implications. J. Mar. Res. 43:719–742.
1990. Sex change and life history patterns of the labrid, *Semicossyphus pulcher*, across an environmental gradient. Copeia 1990:787–795.

Cowen, R. K., K. M. M. Lwiza, S. Sponaugle, C. B. Paris, and D. B. Olson.
2000. Connectivity of marine populations: open or closed? Science 287:857–859.

Fu, C., T. J. Quinn, II, and T. C. Shirley.
2001. The role of sex change, growth and mortality in *Pandalus* population dynamics and management. ICES J. Mar. Sci. 58:607–621.

Fulton, E., D. Kault, B. Mapstone, and M. Sheaves.
1999. Spawning season influences on commercial catch rates: computer simulations and *Plectropomus leopardus*, a case in point. Can. J. Fish. Aquat. Sci. 56:1096–1108.

Greene, C., J. Umbanhowar, M. Mangel, and T. Caro.
1998. Animal breeding systems, hunter selectivity, and consumptive use in wildlife conservation. *In* Behavioral ecology and conservation biology (T. Caro, ed.) p. 271–305. Oxford Univ. Press, New York, NY.

Gunderson, D. R.
1997. Trade-off between reproductive effort and adult survival in oviparous and viviparous fishes. Can. J. Fish. Aquat. Sci. 54:990–998.

Haddon, M.
2001. Modelling and quantitative methods in fisheries, 406 p. Chapman and Hall, Boca Raton, FL.

Helfman, G. S.
1997. The diversity of fishes, 528 p. Blackwell Science, Malden, MA.

Huntsman, G. R., and W. E. Schaaf.
1994. Simulation of the impact of fishing on reproduction of a protogynous grouper, the graysby. No. Am. J. Fish. Manag. 14:41–52.

Iwasa, Y.
1990. Sex change evolution and cost of reproduction. Behav. Ecol. 2:56–68.

Janetos, A. C.
1980. Strategies of female mate choice: a theoretical analysis. Behav. Ecol. Sociobiol. 7:107–112.

Jennings, S., M. J. Kaiser, and J. D. Reynolds.
2001. Marine fisheries ecology, 417 p. Blackwell Science, Oxford, UK.

Koeller, P., R. Mohn, and M. Etter.
2000. Density dependant sex change in northern shrimp, *Pandalus borealis*, on the Scotian Shelf. J. No. Atl. Fish. Sci. 27:107–118.

Kruuk, L. E. B., T. H. Clutton-Brock, S. D. Albon, J. M. Pemberton, and F. E. Guinness.
1999. Population density affects sex ratio variation in red deer. Nature 399:459–461.

Kuwamura, T., and Y. Nakashima.
1998. New aspects of sex change among reef fishes: Recent studies in Japan. Environ. Biol. Fish. 52:125–135.

Levin, P. F., and C. B. Grimes.
2002. Reef fish ecology and grouper conservation and management. *In* Coral reef fishes: dynamics and diversity in a complex ecosystem (P. F. Sale, ed.) p. 377–390. Academic Press, Amsterdam, The Netherlands.

Lutnesky, M. M. F.
1994. Density-dependent protogynous sex change in territorial-haremic fishes: models and evidence. Behav. Ecol. 5:375–383.
1996. Size-dependent rate of protogynous sex change in the pomacanthid angelfish, *Centropyge potteri*. Copeia 1996:209–212.

Metcalfe, N. B., F. A. Huntingford, W. D. Graham, and J. E. Thorpe.
1989. Early social status and the development of life-history strategies in Atlantic salmon. Proc. Roy. Soc. Lond. B 236:7–19.

Mittelbach, G. G., C. W. Osenberg, and P. C. Wainwright.
1992. Variation in resource abundance affects diet and feeding morphology in the pumpkinseed sunfish (*Lepmis gibbosus*). Oecologia 90:8–13.

Munoz, R. C., and R. R. Warner.
2003. A new version of the size-advantage hypothesis for sex change: Incorporating sperm competition and size-fecundity skew. Am.Naturalist 161:749–761.

Nakashima, Y., Y. Sakai, K. Karino, and T. Kuwamura.
2000. Female-female spawning and sex change in a haremic coral-reef fish, *Labroides dimidiatus*. Zool. Sci. 17:967–970.

Nishibori, M., and M. Kawata.
1993. The effect of visual density on the fecundity of the guppy, *Poecilia reticulata*. Environ. Biol. Fish. 37:213–217.

Petersen, C. W., R. R. Warner, D. Y. Shapiro, and A. Marconato.
2001. Components of fertilization success in the bluehead wrasse, *Thalassoma bifasciatum*. Behav. Ecol. 12:237–245.

Punt, A. E., P. A. Garratt, and A. Govender.
1993. On an approach for applying per-recruit measures to a protogynous hermaphrodite, with an illustration for the slinger *Chrysoblephus puniceus* (Pisces: Sparidae). S. Afr. J. Mar. Sci. 12:109–119.

Quinn, T. J., and R. B. Deriso.
1999. Quantitative fish dynamics, 542 p. Oxford Univ. Press, New York, NY.

Ridgeway, M. S., and B. J. Shuter.
1994. The effects of supplemental food on reproduction in parental male smallmouth bass. Environ. Biol. Fish. 39:201–207.

Sale, P. F.
2002. The science we need to develop more effective management. *In* Coral reef fishes: dynamics and diversity in a complex ecosystem (P. F. Sale, ed.), p. 361–376. Academic Press, Amsterdam, The Netherlands.

Schultz, E. T., and R. R. Warner.
1991. Phenotypic plasticity in life-history traits of female *Thalassoma bifasciatum* (Pisces: Labridae): 2. Correlation of fecundity and growth rate in comparative studies. Environ. Biol. Fish. 30:333–344.

Shapiro, D. Y.
1987. Reproduction in groupers. *In* Tropical snappers and groupers: biology and fisheries management (J. J. Polvina and S. Ralston, eds.), p. 295–328. Westview Press, Boulder, CO.

Snyder, R. J., and H. Dingle.
1990. Effects of freshwater and marine overwintering environments on life histories of threespine sticklebacks: evidence for adaptive variation between anadromous and resident freshwater populations. Oecologia 84:386–390.

Sutherland, W. J.
1990. Evolution and fisheries. Nature 344:814–815.
1998. The importance of behavioural studies in conservation biology. Anim. Behav. 56:801–809.

Wainwright, P. C., C. W. Osenberg, and G. G. Mittelbach.
1991. Trophic polymorphism in the pumpkinseed sunfish (*Lepomis gibbosus* Linnaeus): effects of environment on ontogeny. Funct. Ecol. 5:40–55.

Warner, R. R.
1975. The reproductive biology of the protogynous hermaphrodite *Pimelometopon pulchrum* (Pisces: Labridae). Fish. Bull. 73:262–283.

Warner, R. R., and P. Lejeune.
1985. Sex change limited by paternal care: A test using four Mediterranean labrid fishes, genus *Symphodus*. Mar. Biol. 87:89–100.

Warner, R. R., and S. E. Swearer.
1991. Social control of sex change in the bluehead wrasse, *Thalassoma bifasciatum* (Pisces: Labridae). Biol. Bull. 181:199–204.

Neonatal growth of Steller sea lion (*Eumetopias jubatus*) pups in Alaska

Elisif A. A. Brandon
Department of Marine Biology
Texas A&M University at Galveston
5007 Avenue U
Galveston, Texas 77551
Present address: 97A Lowell Ave.
Newton, Massachusetts 02460

Donald G. Calkins
Alaska SeaLife Center
P.O. Box 1329
Seward, Alaska 99664

Thomas R. Loughlin
National Marine Mammal Laboratory
Alaska Fisheries Science Center, NMFS
7600 Sand Point Way, NE
Seattle, Washington 98115

Randall W. Davis
Department of Marine Biology
Texas A&M University at Galveston
5007 Avenue U
Galveston, Texas 77551
E-mail address (for R. W. Davis, contact author): davisr@tamug.edu

Abstract—The growth rate of Steller sea lion (*Eumetopias jubatus*) pups was studied in southeast Alaska, the Gulf of Alaska, and the Aleutian Islands during the first six weeks after birth. The Steller sea lion population is currently stable in southeast Alaska but is declining in the Aleutian Islands and parts of the Gulf of Alaska. Male pups (22.6 kg [±2.21 SD]) were significantly heavier than female pups (19.6 kg [±1.80 SD]) at 1–5 days of age, but there were no significant differences among rookeries. Male and female pups grew (in mass, standard length, and axillary girth) at the same rate. Body mass and standard length increased at a faster rate for pups in the Aleutian Islands and the western Gulf of Alaska (0.45–0.48 kg/day and 0.47–0.53 cm/day, respectively) than in southeast Alaska (0.23 kg/day and 0.20 cm/day). Additionally, axillary girth increased at a faster rate for pups in the Aleutian Islands (0.59 cm/day) than for pups in southeast Alaska v(0.25 cm/day). Our results indicate a greater maternal investment in male pups during gestation, but not during early lactation. Although differences in pup growth rate occurred among rookeries, there was no evidence that female sea lions and their pups were nutritionally stressed in the area of population decline.

Manuscript submitted 26 April 2004 to the Scientific Editor's Office.
Manuscript approved for publication 2 December 2004 by the Scientific Editor.
Fish. Bull. 103:246–257 (2005).

Sea lion (order Carnivora, family Otariidae) pups depend entirely on milk for neonatal growth (Bonner, 1984). Studies of sea lions and fur seals have shown that if a pup does not obtain enough milk from its mother, it will exhibit poor body condition (i.e., reduced lean mass and total lipid mass for a given age or standard length) and a reduced growth rate (Trillmich and Limberger, 1985; Ono et al., 1987). Poor body condition and reduced growth rate, in turn, may have lifelong consequences because neonatal growth is an important factor in determining adult size and survival (Bryden, 1968; Innes et al., 1981; Calambokidis and Gentry, 1985; Albon et al., 1992; Baker and Fowler, 1992; Gaillard et al., 1997; Boltnev et al., 1998; Tveraa et al., 1998; Burns, 1999). Because of their large size, aggressive behavior, sensitivity to disturbance, and the remote location of their rookeries, less is known about the early growth of Steller sea lions (SSL) than of most other pinniped (seals, sea lions, and walrus) species. Higgins et al. (1988) measured body mass of SSL pups on Año Nuevo Island in California but only reweighed five pups to measure growth rates. Merrick et al. (1995) weighed SSL pups at a number of locations throughout the Gulf of Alaska and the Aleutian Islands but did not reweigh them to assess individual growth rates.

Genetic studies show that there are distinct eastern and western populations of SSL (Bickham et al., 1996, 1998) (Fig. 1). The eastern population comprises animals in California, Oregon, British Columbia, and southeast Alaska. The western population comprises animals in the Gulf of Alaska, the Aleutian Islands, the Bering Sea, the Commander Islands, Kamchatka, and the Kuril Islands. A severe popu-

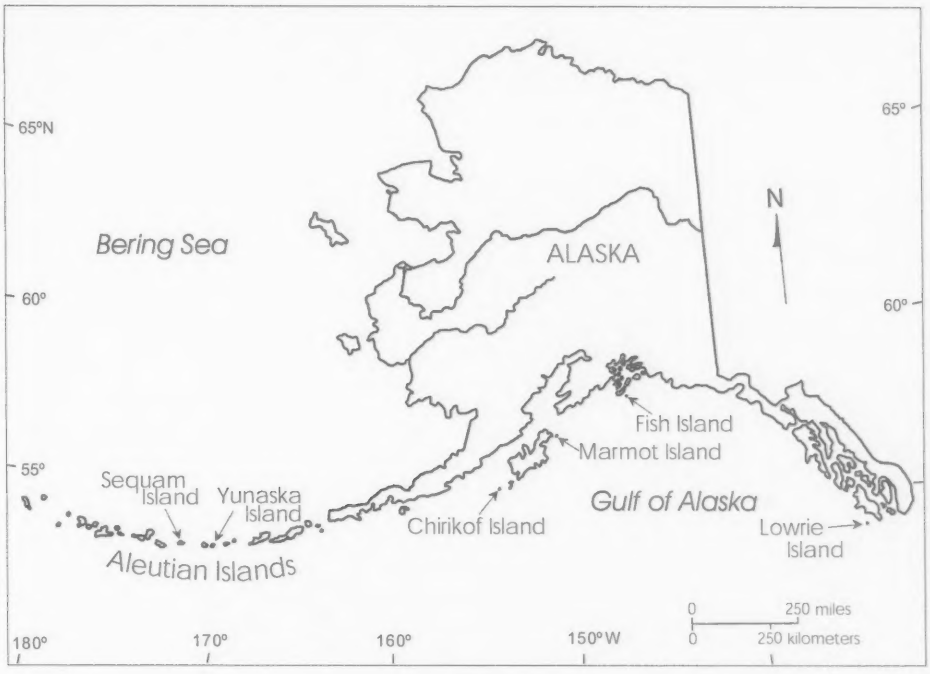

Figure 1

Study sites for Steller sea lions (*Eumetopias jubatus*) in Alaska. The Lowrie Island rookery in southeast Alaska has a stable population but rookeries at Fish, Marmot and Chirikof Islands in the Gulf of Alaska and Yunaska and Seguam Islands in the Aleutian Islands are areas where the population of Steller sea lions has declined.

lation decline (>80%) occurred in the western population between the 1970s and the 1990s. In 1997, these population changes led to the reclassification of the western population from "threatened" to "endangered" and a classification of the eastern population as "threatened" under the Endangered Species Act (U.S. Federal Register 62:24345–24355).

One hypothesis for the decline in population of SSLs is a decrease in food availability or quality in the Gulf of Alaska and the Aleutian Islands (Pascual and Adkison, 1994; York, 1994; Calkins et al., 1999; NMFS[1,2]). If females are unsuccessful in obtaining sufficient food, pups will develop more slowly or die because of a decrease in milk supply. To examine the potential effects of food availability on pup development, we measured growth rates of male and female pups from stable and declining populations of SSL in Alaska from 1990 to 1997. Our null hypothesis was that there was no difference in pup growth rates among rookeries in southeast Alaska, the Gulf of Alaska, and the Aleutian Islands. The alternative hypothesis was that pups grew at a faster rate in southeast Alaska, the area of stable population. However, our results showed that pups grew faster in the area of declining population during the first six weeks after birth. In addition, females invested more energy in male pups at all locations during gestation, but not during early lactation.

Materials and methods

Animals and study sites

From 1990 to 1997, SSL pups were studied at locations in southeast Alaska, the Gulf of Alaska, and the Aleutian Islands (Fig. 1 and Table 1). At Lowrie Island (54°51′N, 133°32′W) in southeast Alaska, measurements were made in 1993, 1994, and 1997. The rookery at Lowrie Island is in the area of the stable population (Calkins et al., 1999). In the Gulf of Alaska, measure-

[1] NMFS (National Marine Fisheries Service). 1992. Recovery plan for the Steller sea lion (*Eumetopias jubatus*), 92 p. Prepared by the Steller Sea Lion Recovery Team for the National Marine Fisheries Service, Silver Spring, MD. [Available from the National Marine Mammal Laboratory, 7600 Sandpoint Way, NE, Seattle, Washington 98115.]

[2] NMFS (National Marine Fisheries Service). 1995. Status review of the United States Steller sea lion (*Eumetopias jubatus*) population, 61 p. Prepared by the National Marine Mammal Laboratory, Alaska Fisheries Science Center. [Available from the National Marine Mammal Laboratory, 7600 Sandpoint Way, NE, Seattle, Washington 98115.]

Table 1

Locations, dates, and the number of Steller sea lion (*Eumetopias jubatus*) pups captured (*n*).

	Location	Dates	*n*
Stable population	Lowrie Island (1993)	26 May–5 June	25
		15–19 June	5
		3 July	1
	Lowrie Island (1994)	15–22 June	28
		24–30 June	9
		13–14 July	3
	Lowrie Island (1997)	5–12 June	25
		16–29 June	11
Declining population	Fish Island (1995)	9–10 June	20
		24–26 June	13
		13–14 July	12
	Marmot Island (1990)	27 June	8
	Marmot Island (1991)	30 June	11
	Marmot Island (1994)	27 June	21[1]
		15 July	11[2]
	Chirikof Island (1993)	11–17 June	20
		27–28 June	14
		7 July	11
		18 July	4
	Yunaska and Seguam Islands (1997)	8–16 June	16
		22–24 June	12
		4 July	5

[1] Nine known-age pups.
[2] Six known-age pups.

ments were made in 1990, 1991, and 1994 on Marmot Island (58°12′N, 151°50′W), in 1993 on Chirikof Island (55°10′N, 155°8′W) and in 1995 on Fish Island (59°53′N, 147°20′W). On the Aleutian Islands of Seguam (52°30′N, 172°30′W) and Yunaska (52°45′N, 170°45′W), pups were studied in 1997. Data from Seguam and Yunaska Islands were combined because the islands are geographically close and can be considered part of one rookery complex. Rookeries in the Gulf of Alaska and the Aleutian Islands are in the area of declining population, although the rookery on Fish Island has not shown as precipitous a decline. Samples could not be obtained from all rookeries in all years because of logistical constraints and the need to minimize disturbance to rookeries. However, concurrent data were obtained from the declining and stable populations in 1993, 1994, and 1997.

Only pups that had an attached umbilical cord or an unhealed umbilicus were selected for study. The freshness of the umbilical cord was used as a rough estimate of age between 1 and 5 days (Davis and Brandon[3]). Choosing only pups with fresh umbilical cords minimized the age bias (Trites, 1993) that occurs when pups are captured at different times and rookeries (Table 1).

Although pups were not selected by sex, sex was noted and used as a factor in analyses. Body mass (BM), standard length (SL), axillary girth (AG) (Am. Soc. Mammalogists, 1967) and body composition were measured for each pup. BM was measured to the nearest kilogram with a mechanical spring scale (Chatillon 160, Ametek, FL) on Marmot Island in 1990 and 1991 and on Lowrie Island in 1993. Body mass of pups at all other sites and years was measured to the nearest tenth of a kilogram by using an electronic scale (Rice Lake Weighing Systems, Rice Lake, WI; Ohaus I-20W, Ohaus, Pine Brook, NJ). Standard length was measured as a straight line from tip-of-nose to tip-of-tail, ventral surface down. Pups were restrained by hand and marked for later identification with hair bleach (Lady Clairol Maxi Blond, Clairol, Inc.) and with flipper tags attached in the axillary area of the fore-flippers.

Body composition was measured by using the labeled water method (Nagy 1975; Nagy and Costa, 1980; Costa, 1987; Bowen and Iverson, 1998). In this study, water labeled with a stable isotope of hydrogen (deuterium)

[3] Davis, R. W, and A. A. Brandon. Unpubl. data. [Data are on file at Texas A&M University, 5007 Avenue U, Galveston, Texas 77551.]

was used to estimate total body water (TBW in kg and %TBW as a percentage of BM). Background concentration of deuterium was determined from blood samples taken from pups that were subsequently injected intramuscularly with 10 mL deuterium oxide (D_2O) (99% enriched, Cambridge Isotope Laboratories, Andover, MA). After a two-hour equilibration period (Costa, 1987), blood samples were taken to determine the dilution of injected deuterium in total body water.

Pups were recaptured at approximately two-week intervals over periods ranging in length from 18 to 38 days (average measurement period was 29.6 days) (Table 1) and were weighed, measured, and a blood sample was taken from each pup. Similar protocols were used at all rookeries, except Marmot Island in 1990 and 1991, when only BM and SL were measured, and the age of pups was not estimated. Therefore, no growth rates were obtained from these data.

Labeled water sample analysis

Blood samples were centrifuged in the field in serum separator tubes, and the serum was transferred to cryovials that were frozen at –20°C until analysis. Isotope-ratio mass spectrometry was used to determine the ratio of deuterium (^2H) to hydrogen (H) (Laboratory of Biochemical and Environmental Studies at University of California, Los Angeles, CA). The hydrogen-isotope dilution space was calculated from this ratio by using Equation 3 in Schoeller et al. (1980). However, the hydrogen-isotope dilution space has been shown to underestimate TBW in a number of pinniped species (Reilly and Fedak, 1990; Arnould et al., 1996b), leading Bowen and Iverson (1998) to develop a single predictive equation to estimate %TBW from hydrogen-isotope dilution space in pinnipeds for which data on the accuracy of the hydrogen-isotope method are lacking. The equation

$$\%TBW = 0.003 + 0.968\ H\text{-}dilution\ space \quad (1)$$

was used in the present study to correct the overestimated *%TBW* by 3.3% (Bowen and Iverson, 1998, Eq. 5). Percent total body lipid (*%TBL*, as a percentage of BM) was calculated by using predictive equations derived from the relationship between *%TBW* and *%TBL* for Antarctic fur seals (Arnould et al., 1996b):

$$\%TBL = 66.562 - 0.845\ \%TBW. \quad (2)$$

%TBL was then compared between male and female pups and among rookeries.

Statistical analyses

Statistics were performed by using Systat (version 11, SPSS, Inc, Chicago, IL), and by first treating each study site and year as a separate "location," then combining data for multiple years at a location (e.g., Marmot Island and Lowrie Island) when no significant interannual differences were found. Significance was determined at $P \leq 0.05$. Data were examined for heteroscedasticity (unequal variances) before analysis (Zar, 1984). All *post hoc* pairwise comparisons were made with the Tukey multiple comparison test. Data from the first capture (1–5 days of age) were analyzed for comparison by location and sex by using two-way ANOVA. Pup growth rate was estimated by performing a linear regression for each pup and extrapolating to $t = 0$ to estimate birth mass. Differences among means of pup growth rate and birth mass were then analyzed by using two-way ANOVA to determine differences by location and sex.

Results

Neonatal size

There were no significant differences by rookery in pup mass at 1–5 days of age (Table 2) and no significant interaction between rookery and sex. The only significant difference in SL of 1–5 day old pups was that both genders were significantly longer on Seguam and Yunaska Islands than on Fish Island ($P=0.0395$). Pups on Chirikof Island had significantly smaller AG than pups on Lowrie, Fish, and Seguam and Yunaska Islands ($P<0.02$). Male and female pups were significantly different for all three morphometric measurements. Overall, male pups averaged 22.6 kg (±2.21 SD, $n=71$) and female pups averaged 19.6 kg (±1.80 SD, $n=74$) at first capture (1–5 days of age).

There was no significant difference by rookery or sex and no significant interaction between rookery and sex in %TBW or %TBL of pups at first capture. When all pups at all rookeries were combined ($n=116$), %TBW was 72.1% of BM (±3.17 SD) and %TBL was 5.6% of BM (±2.68 SD). Male pups had a significantly greater absolute TBW than female pups ($P<0.0001$), as would be expected because of the difference in BM at birth. There was a significant correlation between TBW and BM (Pearson $r=0.945$, $P<0.001$, $n=116$; TBW (kg)=0.6895 × BM + 0.6618).

Neonatal growth

Growth rates were treated as linear over the period monitored; there were not enough data to determine if growth was nonlinear. Male and female pups on the same rookery grew at the same rate (in BM, SL, and AG) during the first six weeks after birth (Fig. 2). When compared by rookery, BM increased at a faster rate for pups on Chirikof Island ($P=0.0005$) and on Seguam and Yunaska Islands ($P=0.0002$) than on Lowrie Island (Fig. 3 and Table 3). The increase in BM for pups on Fish Island did not differ significantly from that at other rookeries. Marmot Island pups grew significantly more slowly than pups on Seguam and Yunaska Islands ($P=0.0382$) but did not differ significantly from growth of pups at other rookeries.

Standard length increased at a faster rate for pups on Chirikof Island ($P=0.0068$) and Seguam and Yu-

naska Islands (P=0.0050) than it did for pups on Lowrie Island (Table 3). Growth in SL was also faster on Chirikof (P=0.0383) and Seguam and Yunaska Islands (P=0.0230) than on Fish Island, whereas the increase in SL on Marmot Island did not differ significantly from the other rookeries. The increase in AG was significantly greater on Seguam and Yunaska Islands (P=0.0021) and Marmot Island (P=0.0364) than on Lowrie Island. There was no significant interaction between rookery and sex in the growth rate of BM, SL, and AG.

Body mass at birth extrapolated to t = 0 from growth rates did not differ by rookery. There was no significant interaction between rookery and sex, but extrapolated birth mass did differ by sex (P<0.0001). Male pups at all rookeries averaged 22.4 kg (±2.36 SD, n=39), whereas female pups averaged 18.7 kg (±2.08 SD, n=35). These extrapolated birth masses were similar to the average BM measured on the rookery for male (22.6 kg) and female (19.6) pups 1–5 days old. There was no correlation between extrapolated birth mass and growth rate (Pearson r=–0.09, P=0.45).

Table 2

Body mass (BM), standard length (SL), and axillary girth (AG) of neonatal (1–5 day old) Steller sea lion (*Eumetopias jubatus*) pups in the stable (Lowrie Island) and declining (Fish Is., Marmot Is., Chirikof Is., Seguam Is., Yunaska Is.) populations (mean ±SD). An asterisk (*) indicates significant differences from all other sites, and † indicates a significant difference between two sites. Standard length from Fish Is. was significantly different from SL on Seguam and Yunaska Is. Axillary girth on Chirikof Is. was significantly different from AG at all other sites. In all cases, males were significantly larger than females. There were no significant interannual differences; therefore data from all years at Lowrie Is. were combined.

		BM (kg)		SL (cm)		AG (cm)	
Location	n	male	female	male	female	male	female
Lowrie Is. (1993–97)	39M	22.1	19.5	98.3	94.1	64.9	64.3
	41F	±2.20	±1.67	±4.56	±3.96	±3.33	±5.01
Fish Is. (1995)	11M	22.6	19.2	96.2†	93.3†	68.5	64.0
	9F	±1.69	±2.39	±26.76	±6.39	±2.96	±4.00
Marmot Is. (1994)	3M	21.7	20.2	101.7	97.4	65.5	61.8
	6F	±1.80	±2.42	±1.53	±2.67	±2.78	±5.38
Chirikof Is. (1993)	11M	23.21	19.02	99.1	94.9	62.7*	60.1*
	9F	±2.59	±1.05	±5.24	±2.40	±3.52	±2.15
Aleutian Is. (Seguam and Yunaska Is.) (1997)	7M	24.2	20.5	101.4†	96.3†	67.7	63.9
	9F	±1.97	±1.88	±4.29	±2.55	±3.50	±3.66

Table 3

Steller sea lion (*Eumetopias jubatus*) pup growth from 0 to 40 days of age (mean ±SD). There were no significant differences between male and female pups. BM=body mass; SL = standard length; AG=axillary girth. Underlining indicates that there were no significant differences within an underlined grouping (e.g., for body mass growth rate, C was significantly different from L, and A was significantly different from M and L).

Location	n	BM growth rate (kg/day)	SL growth rate (cm/day)	AG growth rate (cm/day)
Lowrie Is. (L)	26	0.23 ±0.176	0.20 ±0.322	0.25 ±0.244
Fish Is. (F)	13	0.35 ±0.171	0.22 ±0.183	0.41 ±0.235
Marmot Is. (M)	6	0.28 ±0.141	0.22 ±0.287	0.59 ±0.510
Chirikof Is. (C)	17	0.45 ±0.126	0.47 ±0.171	0.47 ±0.187
Aleutian Is. (A) (Seguam and Yunaska Is.)	12	0.48 ±0.168	0.53 ±0.163	0.59 ±0.257
ANOVA results		L M F C A	L F M C A	L F C M A

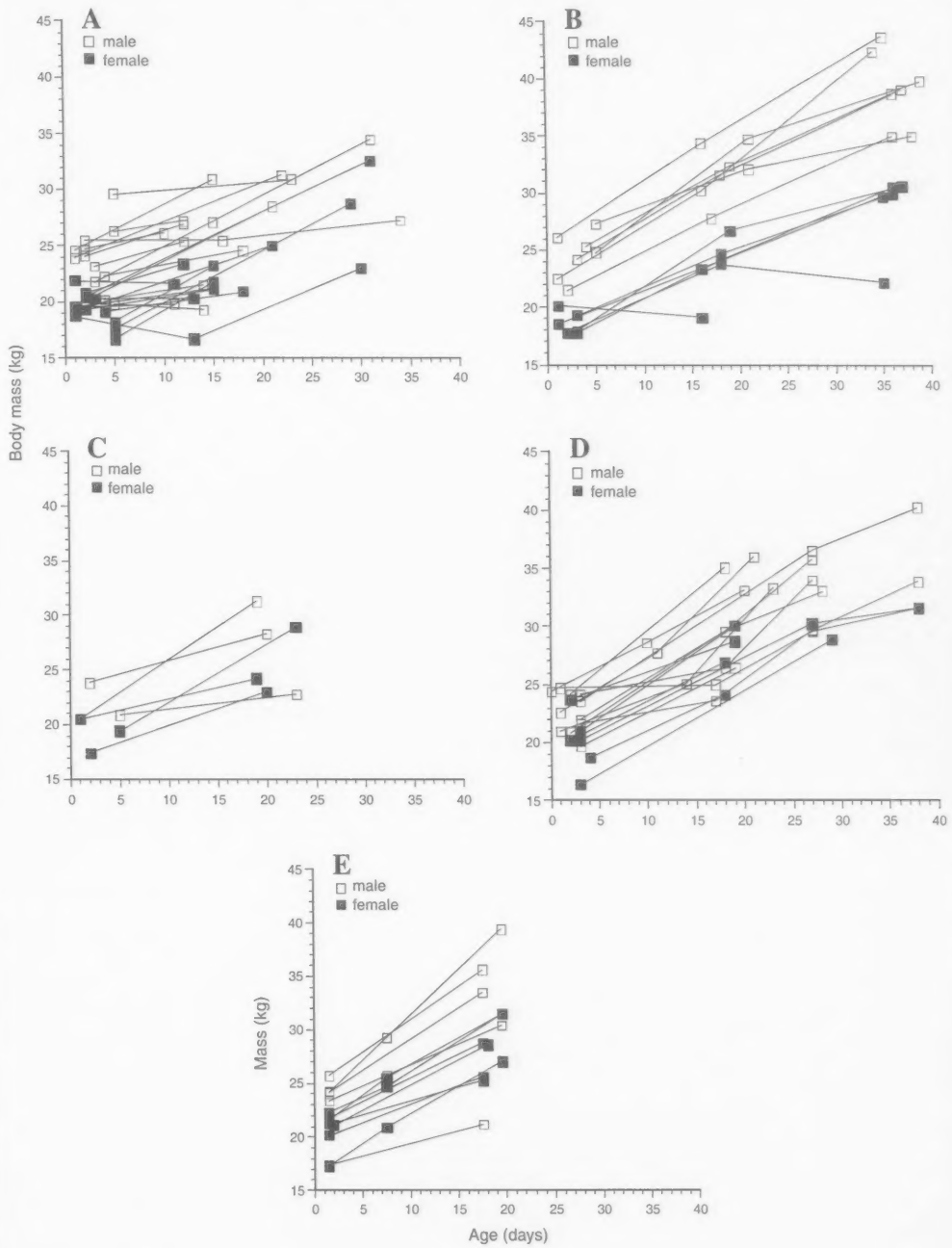

Figure 2

Change in body mass of individual Steller sea lion (*Eumetopias jubatus*) pups captured on (**A**) Lowrie Island in 1993, 1994, and 1997, (**B**) Fish Island in 1995, (**C**) Marmot Island in 1994, (**D**) Chirikof Island in 1993, and (**E**) Yunaska and Seguam Islands in 1997.

Discussion

Compared to other species of sea lions and fur seals, SSL pups are large, although this species produces smaller pups in relation to adult size than do smaller otariids (Kovacs and Lavigne, 1992; McLaren, 1993). In the present study, male pups averaged 22.6 kg and female pups averaged 19.6 kg at 1–5 days of age, which is in the range of birth masses reported in the literature. Two studies conducted before the recent population decline reported 17 kg for male pups at birth (Scheffer, 1945) and a range of 9.1–21.8 kg for male and female pups (Mathisen et al., 1962). Late in the population decline, studies reported a range of 16–23 kg for pups at birth in Alaska (Calkins and Pitcher, 1982) and an extrapolated birth mass of 17.9 kg for five pups for which growth rates were measured in California (Higgins et al., 1988).

This is the first, large-scale (in terms of sample size and geographic area) longitudinal study of growth in Steller sea lion pups. Growth rates reported in our study are the highest absolute growth rates reported for any sea lion or fur seal. This is to be expected because adult SSLs are the largest otariids (Kovacs and Lavigne, 1992). The growth rate of 0.38 kg/day measured for five SSL pups at Año Nuevo Island in California (Higgins et al., 1988) falls within the range of average growth rates measured in the present study (0.23–0.48 kg/day). The only other measurement of pup growth in SSLs was conducted on captive pups that were already several months old. In terms of growth rate in relation to size at birth, SSL pups gained 1–2.3% of their birth weight per day (Lowrie Island and Seguam and Yunaska Islands, respectively, based on an average birth mass of 21.1 kg), which was faster than the relative growth rates reported for other otariid species (Kovacs and Lavigne, 1992, calculated from Table 1), except for northern fur seals. In contrast, seals (order Carnivora, family Phocidae) exhibit faster growth rates (1.3–5.6 kg/day or 8–26% birth weight per day) (Stewart and Lavigne, 1980; Bowen et al., 1985; Kovacs and Lavigne, 1985; Bowen et al., 1987; Bowen et al., 1992; Campagna et al., 1992). Although adult SSLs are larger than many species of phocid seals, phocids have much shorter lactation periods and their pups grow at a more accelerated rate than do otariids.

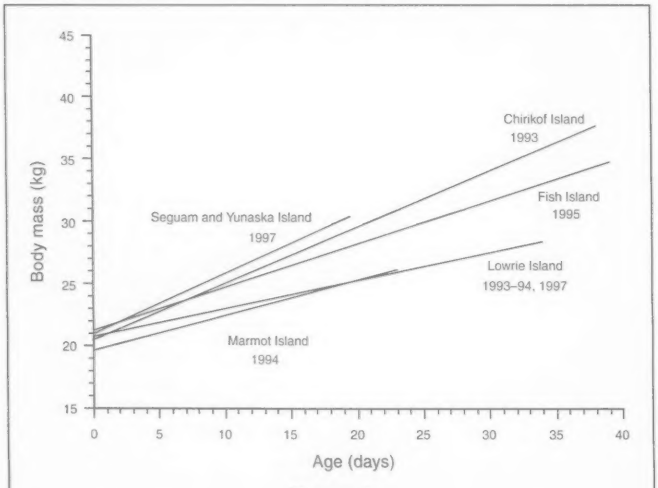

Figure 3

Summary of Steller sea lion (*Eumetopias jubatus*) pup growth (body mass) during the first six weeks after birth for all five rookeries. The length of each line indicates the length of the study period at that location. Pups from Seguam, Yunaska, and Chirikof Islands, in the declining population, grew significantly faster than pups from Lowrie Island, in the stable population. Pups from Seguam and Yunaska Islands also grew significantly faster than pups from Marmot Island.

Male-female differences

Male pups weighed 15% more than females at birth, indicating a difference in maternal investment during gestation, which has been found in other otariids including Antarctic fur seals (Doidge et al., 1984; Lunn and Boyd, 1993; Goldsworthy, 1995; Boyd, 1996), South American fur seals (*Arctocephalus australis*) (Lima and Páez, 1995), California sea lions (Ono and Boness, 1996), and southern sea lions (*Otaria byronia*) (Cappozzo et al., 1991). These results are consistent with the predictions of Maynard-Smith's (1980) theory on sexual investment. Steller sea lion adults are extremely sexually dimorphic: females weigh 263 kg on average (maximum of approximately 350 kg); males weigh more than twice as much (average of 566 kg, maximum of approximately 1120 kg) (Calkins and Pitcher, 1982). In view of this dimorphism and the fact that size is more important to male fitness than to female fitness in a polygynous species (McCann, 1981) such as the SSL, theory predicts that males would be heavier than females at birth. Northern fur seal females with male fetuses are in poorer condition than mothers with female fetuses (Trites, 1992), and male fetuses grow at a faster rate than female fetuses (Trites, 1991), indicating that mothers invest more in male offspring during gestation.

However, there were no male-female differences in neonatal growth (BM, SL, and AG) rate in SSL during the first six weeks after birth. In a species as sexually dimorphic as SSL, one would expect males to grow at a faster rate than females during development. However, this difference may not occur until the animals are older. There is some evidence that male otariids undergo a sharp increase in growth rate near sexual maturity (McLaren, 1993; Bester and Van Jaarsveld, 1994), after females have already reached sexual maturity and their growth has slowed.

Conflicting results have been reported in other growth studies of otariids. Several studies reported that male pups grew faster than female pups (Antarctic fur seals: Payne, 1979; Doidge et al., 1984; Antarctic and Subantarctic fur seals: Kerley, 1985; New Zealand fur seals: Mattlin 1981). However, cross-sectional data on growth rate were used in these studies. Conversely, longitudinal data, considered to be more accurate, demonstrate no differences in neonatal growth rate between male and female Antarctic fur seal pups (Doidge and Croxall, 1989; Lunn et al., 1993; Lunn and Arnould, 1997); Goldsworthy (1995), however, is the exception. Ono and Boness (1996) collected longitudinal growth data on California sea lion pups and found that males grew faster than females, but they found no other evidence of differential maternal investment. In phocids, most studies have found no difference in neonatal male and female growth rates, regardless of whether the data were longitudinal or cross sectional (Stewart and Lavigne, 1980; Innes et al., 1981; Bowen et al., 1992). This is true for species with extreme sexual dimorphism such as elephant seals (McCann et al., 1989; Campagna et al., 1992). The only other study where growth rates for SSL pups were measured did not have a large enough sample size for a comparison between males and females (Higgins et al., 1988). No differences between male and female pups were found for suckling behavior or maternal attendance behavior (Higgins et al., 1988).

Total body lipid

Average %TBL of neonatal pups was low (5.6% BM). Steller sea pups are born with small energy stores and normally fast for short periods (about one day) while their mothers make foraging trips to sea. There have been few measurements of lipid content in otariid neonates. Jonker and Trites (2000) found a blubber content of 9.7% BM in five SSL pups in the first month after birth. However, this measurement does not correspond directly to body fat content because they measured blubber content by weighing the sculp (skin plus blubber) and then calculating the fraction of sculp that was blubber by measuring skin and blubber thicknesses. Using the same labeled water method as in the present study, Arnould et al. (1996b) found a %TBL of 9.4% BM in four Antarctic fur seal pups in the first month after birth. In a similar study of one-day-old Antarctic fur seal pups, Arnould et al. (1996a) found a %TBL of 7.0% BM for female pups and 4.9% BM for male pups. Also using labeled water, Oftedal et al. (1987a) found an average %TBL of 5% BM for neonatal California sea lion pups.

Arnould et al. (1996b) suggested two explanations for the higher lipid content that they found in Antarctic fur seal pups in comparison to California sea lion pups (Oftedal et al. 1987b). First, in colder habitats, a larger subcutaneous lipid store may be necessary for thermoregulation. The data here do not support that explanation. SSL live in a colder habitat than California sea lions, but have a similar %TBL. The more likely explanation is that larger lipid stores are found in species in which pups normally fast longer while their mothers are foraging. Steller sea lion pups have the smallest lipid stores and shortest fasting periods (Brandon, 2000) of the three species.

Differences in pup size among rookeries

Although male and female pups differed significantly in size, there were no significant differences in pup size at birth among the rookeries studied. Rookery location should have less influence on pup size at birth than on neonatal growth because maternal foraging range is much greater during gestation than during lactation (Merrick and Loughlin, 1997). This greater maternal foraging range during gestation reduces, among rookeries, variation in maternal size and feeding conditions (quantity and quality of prey available) during gestation, both of which have been shown to influence pup birth mass in pinnipeds (Calambokidis and Gentry, 1985; Kovacs and Lavigne, 1986; Trites, 1991; Trites 1992). The lack of a difference in pup BM at birth among rookeries could also be explained by the fact that females that are "successful" (i.e., carry their fetuses to term) have a significantly better body condition than females that do not carry their fetuses to term (Pitcher et al., 1998). As a consequence of our study design, only those females that were successful were used, and therefore our sample was biased toward females in the population with better body condition. In addition, gestation is less energetically expensive than early lactation; therefore differences in food availability would have less of an effect during gestation (Robbins and Robbins, 1979; Albon et al., 1983; Oftedal, 1984).

Although most pup morphometrics at first capture did not differ among rookeries, growth parameters differed significantly (Table 3). Growth rates of pups on Seguam and Yunaska Islands (0.48 kg/day) and on Lowrie Island (0.23 kg/day) represented the extremes, whereas growth rates of pups on Chirikof, Marmot, and Fish Islands fell between these two extremes. In general, faster growth rates occurred in the west and slower growth rates in the east. In terms of mass, Seguam and Yunaska Islands and Chirikof Island pups grew twice as fast as Lowrie Island pups. A concurrent study of the attendance patterns of lactating females (Brandon, 2000) showed that foraging trip duration decreased from east (25.6 hours on Lowrie Island) to west (an average of 9.4 hours on Chirikof and Seguam Islands). Therefore, it is possible that the higher growth rates in SSL pups in the western Gulf of Alaska and Aleutian Islands resulted from shorter periods of fasting while females were foraging at sea (Arnould et al., 1996a; Goldsworthy, 1995).

Is food limiting growth in Steller sea lion pups in the area of population decline?

If the cause of the population decline were decreased food availability, which is one of the leading hypotheses

(Pascual and Adkison, 1994; York, 1994; NMFS[2]), one might expect the animals in the declining population to show signs of nutritional stress compared to those in the stable population. The results for pup size and growth give no indication of food stress during early lactation. In fact, pups from the declining population on Seguam, Yunaska, and Chirikof Islands grew faster than pups from the stable population on Lowrie Island during the first six weeks. Similar results were also found in a study of pup BM (Merrick et al., 1995), in which pups were weighed on rookeries from Oregon to the Aleutian Islands in late June and early July from 1987 to 1994. Although the pups' ages were unknown, weighing date was used as a covariate in the analysis. Merrick et al. (1995) found a continuous increase in pup BM from Oregon to southeast Alaska and to the Aleutian Islands. These investigators also concluded that pup BM was on average greater in the declining population.

In most other studies of declining populations or differences among rookeries, such contradictory results have not been seen. A study of California sea lion pups during an ENSO (El Niño Southern Oscilliation) event revealed lower pup growth during the period of food stress (Boness et al., 1991). Trillmich and Limberger (1985) have also seen clear effects of low food availability during an ENSO in Galapagos fur seals and sea lions. Antarctic fur seals are affected in predictable ways (increased pup mortality and increased female foraging time) during times of decreased food availability (Costa et al., 1989). Hood and Ono (1997) found that in the declining California population of SSLs, pups spent less time suckling when adult females made longer foraging trips in 1992 than in 1973 when the population was larger. The longer foraging trips suggested less abundant food resources.

Considering the results for SSL pup growth in light of the population decline, we suggest three alternative hypotheses: 1) food availability was never a factor in the population decline; 2) food availability caused the overall decline, but lactating females and their pups were not affected during early lactation; or 3) our study was conducted when pups and lactating females were no longer experiencing decreased food availability.

Faster rates of pup growth may be normal for the Aleutian Islands and western Gulf of Alaska despite the population decline. The declining and stable populations are genetically distinct (Bickham et al., 1996), and perhaps the differences seen in our study are normal differences between the two populations. It is impossible to determine if growth and foraging behavior have changed over time because historical data on maternal investment are sparse. Juveniles rather than neonates may be the affected age class in the declining population (Merrick et al., 1988), whereas lactating females are feeding on either different prey or age classes and not experiencing decreased food availability. York (1994) constructed a population model for SSLs in Alaska and concluded that the current population decline could be accounted for by increased juvenile mortality.

Alternatively, because our study was performed late in the decline, the higher growth rates could be the result of lower population density and less competition for food in the declining population. Trites and Bigg (1992) reported larger body sizes in northern fur seal populations during a period of decline. The northern fur seal population in the Pribilof Islands in the Bering Sea increased from the early 1900s to the 1950s. During this period, adult body size decreased. From 1950 to the 1970s the population declined and there was a concurrent increase in individual body size (Trites and Bigg, 1992). Scheffer (1955) hypothesized that increased body size was due to decreased competition for food, which in turn would be due to the lower population density. It is possible that the same density-dependent effects are occurring in the declining SSL population because our study was performed late in the decline, after the original cause may have abated. More information will be needed to determine the cause of the SSL decline and whether it is related to availability of food, especially for different age classes, and to different times of the year.

Acknowledgments

We thank T. Adams, R. Andrews , D. Bradley, J. Burns, M. Castellini, J. K. Chumbley, W. and S. Cunningham, J. Davis, F. Gulland, D. Gummeson, B. Heath, D. Johnson, S. Kanatous, D. Lidgard, R. Lindeman, R. Merrick, D. McAllister, L. Milette, K. Ono, L. Polasek, T. Porter, D. Rosen, J. Sease, T. Spraker, U. Swain, W. Taylor, A. Trites, D. van den Bosch, T. Williams, and the captain and crew of the RV *Medeia* for assistance in the field. We thank K. Andrews for the map and D. Brandon for assistance in data collection and analysis. G. Worthy, A. Trites, T. Lacher, D. Owens, and M. Reynolds reviewed an early version of this manuscript. Funding and logistical support in the field were provided by the Alaska Department of Fish and Game, the National Marine Fisheries Service/National Marine Mammal Laboratory, Texas A&M University, and the Texas Institute of Oceanography. This research was conducted under Marine Mammal permit no. 846 and 963.

Literature cited

Albon, S. D., T. H. Clutton-Brock, and R. Langvatn.
1992. Cohort variation in reproduction and survival: implications for population demography. *In* The biology of deer (R. D. Brown, ed.), p. 15–21. Springer-Verlag, New York, NY.

Albon, S. D., F. E. Guinness, and T. H. Clutton-Brock.
1983. The influence of climatic variation on the birth weights of red deer (*Cervus elaphus*). J. Zool. (Lond.) 203:295–298.

American Society of Mammalogists.
1967. Standard measurements of seals. J. Mammal. 48:459–462.

Arnould, J. P. Y., I. L. Boyd, and D. G. Socha.
1996a. Milk consumption and growth efficiency in Ant-

arctic fur seal (*Arctocephalus gazella*) pups. Can. J. Zool. 74:254–266.

Arnould, J. P. Y., L. L. Boyd, and J. R. Speakman.
1996b. Measuring the body composition of Antarctic fur seals (*Arctocephalus gazella*): validation of hydrogen isotope dilution. Physiol. Zool. 69:93–116.

Baker, J. D., and C. W. Fowler.
1992. Pup weight and survival of northern fur seals *Callorhinus ursinus*. J. Zool. (Lond.) 227:231–238.

Bester, M. N., and A. S. Van Jaarsveld.
1994. Sex-specific and latitudinal variance in postnatal growth of the Subantarctic fur seal (*Arctocephalus tropicalis*). Can. J. Zool. 72:1126–1133.

Bickham, J. W., T. R. Loughlin, J. R. Wickliffe, and V. N. Burkanov.
1998. Geographic variation in the mitochondrial DNA of Steller sea lions: haplotype diversity and endemism in the Kuril Islands. Biosphere Conservation, 1: 107–117

Bickham, J. W., J. C. Patton, and T. R. Loughlin.
1996. High variability for control-region sequences in a marine mammal: implications for conservation and biogeography of Steller sea lions (*Eumetopias jubatus*). J. Mammal. 77:95–108.

Boltnev, A. I., A. E. York, and G. A. Antonelis.
1998. Northern fur seal young: interrelationships among birth size, growth, and survival. Can. J. Zool. 76: 843–854.

Boness, D. J., O. T. Oftedal, and K. A. Ono.
1991. The effect of El Niño on pup development in the California sea lion (*Zalophus californianus*) I. Early postnatal growth. *In* Pinnipeds and El Niño: responses to environmental stress (F. Trillmich and K. Ono, eds.), p. 173–184. Springer-Verlag, Berlin.

Bonner, W. N.
1984. Lactation strategies in Pinnipeds: problems for a marine mammalian group. Symp. Zool. Soc. Lond. 51:253–272.

Bowen, W. D., and S. J. Iverson.
1998. Estimation of total body water in pinnipeds using hydrogen-isotope dilution. Physiol. Zool. 71:329–332.

Bowen, D., D. J. Boness, and O. T. Oftedal.
1985. Birth to weaning in 4 days: remarkable growth in the hooded seal, *Cystophora cristata*. Can. J. Zool. 63:2841–2846.
1987. Mass transfer from mother to pup and subsequent mass loss by the weaned pup in the hooded seal, *Cystophora cristata*. Can. J. Zool. 65:1–8.

Bowen, W.D., W. T. Stobo, and S. J. Smith.
1992. Mass changes of grey seal *Halichoerus grypus* pups on Sable Island: differential maternal investment reconsidered. J. Zool. (Lond.) 227:607–622.

Boyd, I. L.
1996. Individual variation in the duration of pregnancy and birth date in Antarctic fur seals: the role of environment, age, and sex of fetus. J. Mammal. 77:124–133.

Brandon, E. A. A.
2000. Maternal investment in Steller sea lions in Alaska. Ph.D. diss., 137 p. Texas A&M University, Galveston, TX.

Bryden, M. M.
1968. Control of growth in two populations of elephant seals. Nature 217:1106–1108.

Burns, J. M.
1999. The development of diving behavior in juvenile Weddell seals: pushing physiological limits in order survive. Can. J. Zool. 77:737–747.

Calambokidis, J., and R. Gentry.
1985. Mortality of northern fur seal pups in relation to growth and birth weights. J. Wildl. Dis. 21:327–330.

Calkins, D. G., D. C. McAllister, K. W. Pitcher, and G. W. Pendleton.
1999. Steller sea lion status and trend in Southeast Alaska: 1979–1997. Mar. Mammal Sci. 15:462–477.

Calkins, D. G., and K. W. Pitcher.
1982. Population assessment, ecology and trophic relationships of Steller sea lions in the Gulf of Alaska, 140 p. Final report to Outer Continental Shelf Environment Assessment Program, contract 03-5-022-69. Alaska Department of Fish and Game, Anchorage, AK.

Campagna, C., B. J. Le Boeuf, M. Lewis, and C. Bisioli.
1992. Equal investment in male and female offspring in southern elephant seals. J. Zool. (Lond.) 226:551–561.

Cappozzo, H. L., C. Campagna, and J. Monserrat.
1991. Sexual dimorphism in newborn Southern sea lions. Mar. Mamm. Sci. 7:385–394.

Costa, D. P.
1987. Isotopic methods for quantifying material and energy intake of free-ranging marine mammals. *In* Marine mammal energetics (A. C. Huntley, D. P. Costa, G. A.J. Worthy, and M. A. Castellini, eds.), p. 43–66. Soc. Mar. Mammal. Special Publ. 1. Allen Press, Lawrence, KS.

Costa, D. P., J. P. Croxall, and C. D. Duck.
1989. Foraging energetics of Antarctic fur seals in relation to changes in prey availability. Ecology 70:596–606.

Doidge, D. W., and J. P. Croxall.
1989. Factors affecting weaning weight in Antarctic fur seals *Arctocephalus gazella* at South Georgia. Polar Biol. 9:155–160.

Doidge, D. W., J. P. Croxall, and C. Ricketts.
1984. Growth rates of Antarctic fur seal *Arctocephalus gazella* pups at South Georgia. J. Zool. (Lond.) 203:87–93.

Gaillard, J.-M., J.-M. Boutin, D. Delorme, G. Van Laere, P. Duncan, and J.-D. Lebreton.
1997. Early survival in roe deer: causes and consequences of cohort variation in two contrasted populations. Oecologia 112:502–513.

Goldsworthy, S. D.
1995. Differential expenditure of maternal resources in Antarctic fur seals, *Arctocephalus gazella*, and Heard Island, southern Indian Ocean. Behav. Ecol. 6:218–228.

Higgins, L.V., C. P. Costa, A. C. Huntley, and B. J. Le Boeuf.
1988. Behavioral and physiological measurements of maternal investment in the Steller sea lion, *Eumetopias jubatus*. Mar. Mammal Sci. 4:44–58.

Hood, W. R., and K. A. Ono.
1997. Variation in maternal attendance patterns and pup behaviour in a declining population of Steller sea lions (*Eumetopias jubatus*). Can. J. Zool. 75:1241–1246.

Innes, S., R. E. A. Stewart, and D. M. Lavigne.
1981. Growth in Northwest Atlantic harp seals *Phoca groenlandica*. J. Zool. (Lond.) 194:11–24.

Jonker, R. A. H., and A. W. Trites.
2000. The reliability of skinfold-calipers for measuring blubber thickness of Steller sea lion pups (*Eumetopias jubatus*). Mar. Mamm. Sci. 16:757–766.

Kerley, G. I. H.
1985. Pup growth in the fur seals *Arctocephalus tropicalis* and *A. gazella* on Marion Island. J. Zool. (Lond.) 205:315–324.

Kovacs, K. M., and D. M. Lavigne.
1985. Neonatal growth and organ allometry of Northwest Atlantic harp seals (*Phoca groenlandica*). Can. J. Zool. 63:2793–2799.
1986. Maternal investment and neonatal growth in phocid seals. J. Anim. Ecol. 55:1035–1051.
1992. Maternal investment in otariid seals and walruses. Can. J. Zool. 70:1953–1964.

Lima, M., and E. Páez.
1995. Growth and reproductive patterns in the South American fur seal. J. Mammal. 76:1249–1255.

Lunn, N. J., and J. P. Y. Arnould.
1997. Maternal investment in Antarctic fur seals: evidence for equality in the sexes? Behav. Ecol. Sociobiol. 40:351–362.

Lunn, N. J., and I. L. Boyd.
1993. Effects of maternal age and condition on parturition and the perinatal period of Antarctic fur seals. J. Zool. (Lond.) 229:55–67.

Lunn, N. J., I. L. Boyd, T. Barton, and J. P. Croxall.
1993. Factors affecting the growth rate and mass at weaning of Antarctic fur seals at Bird Island, South Georgia. J. Mammal. 74:908–919.

Mathisen, O. A., R. T. Baade, and R. J. Lopp.
1962. Breeding habits, growth and stomach contents of the Steller sea lion in Alaska. J. Mammal. 43:469–477.

Mattlin, R. H.
1981. Pup growth of the New Zealand fur seal *Arctocephalus forsteri* on the Open Bay Islands, New Zealand. J. Zool. (Lond.) 193:305–314.

Maynard-Smith, J.
1980. A new theory of sexual investment. Behav. Ecol. Sociobiol. 7:247–251.

McCann, T. S.
1981. Aggression and sexual activity of male Southern elephant seals, *Mirounga leonina*. J. Zool. (Lond.) 195:295–310.

McCann, T. S., M. A. Fedak, and J. Harwood.
1989. Parental investment in southern elephant seals, *Mirounga leonina*. Behav. Ecol. Sociobiol. 25:81–87.

McLaren, I. A.
1993. Growth in pinnipeds. Biol. Rev. 68:1–79.

Merrick, R. L., R. Brown, D. G. Calkins, and T. R. Loughlin.
1995. A comparison of Steller sea lion, *Eumetopias jubatus*, pup masses between rookeries with increasing and decreasing populations. Fish. Bull. 93:753–758.

Merrick, R., P. Gearin, S. Osmet, and D. Withrow.
1988. Field studies of northern sea lions at Ugamak Island, Alaska, during the 1985 and 1986 breeding seasons. NOAA Tech. Memo. NMFS F/NWC-43, 60 p.

Merrick, R. L., and T. R. Loughlin.
1997. Foraging behavior of adult female and young-of-the-year Steller sea lions in Alaskan waters. Can. J. Zool. 75:776–786.

Nagy, K. A.
1975. Water and energy budgets of free-living animals: measurement using isotopically labeled water. *In* Environmental physiology of desert organisms (N. Hadley, ed.), p. 227–245. Dowden, Hutchinson, and Ross, Stroudsburg, PA.

Nagy, K. A., and D. P. Costa.
1980. Water flux in animals: analysis of potential errors in the tritiated water method. Am. J. Physiol. 238: R454–R465.

Oftedal, O. T.
1984. Body size and reproductive strategy as correlates of milk energy output in lactating mammals. Acta Zoologica Fennica 171:183–186.

Oftedal, O.T., S. J. Iverson, and D. J. Boness.
1987a. Milk and energy intakes of suckling California sea lion *Zalophus californianus* pups in relation to sex, growth, and predicted maintenance requirements. Physiol. Zool. 60:560–575.

Oftedal, O. T., D. J. Boness, and R. A. Tedman.
1987b. The behavior, physiology, and anatomy of lactation in the Pinnipedia. Curr. Mammal. 1:175–245.

Ono, K. A., and D. J. Boness.
1996. Sexual dimorphism in sea lion pups: differential maternal investment, or sex-specific differences in energy allocation? Behav. Ecol. Sociobiol. 38:31–41.

Ono, K. A., D. J. Boness, and O. T. Oftedal.
1987a. The effect of a natural environmental disturbance on maternal investment and pup behavior in the California sea lion. Behav. Ecol. Sociobiol. 21:109–118.

Pascual, M.A., and M. D. Adkison.
1994. The decline of the Steller sea lion in the Northeast Pacific: demography, harvest, or environment? Ecol. Appl. 4:393–403.

Payne, M. R.
1979. Growth in the Antarctic fur seal *Arctocephalus gazella*. J. Zool. (Lond.) 187:1–20.

Pitcher, K. W., D. G. Calkins, and G. W. Pendleton.
1998. Reproductive performance of female Steller sea lions: an energetics-based reproductive strategy. Can. J. Zool. 76:2075.

Reilly, J., and M. A. Fedak.
1990. Measurement of body composition in living gray seals by hydrogen isotope dilution. J. Appl. Physiol. 69:885–891.

Robbins, C. H., and B. L. Robbins.
1979. Fetal and neonatal growth patterns and maternal reproductive efforts in ungulates and subungulates. Am. Nat. 114:101–116.

Scheffer, V. B.
1945. Growth and behavior of young sea lions. J. Mammal. 26:390–392.
1955. Body size with relation to population density in mammals. J. Mammal. 39:493–515.

Schoeller, D. A., E. van Santen, D. W. Peterson, W. Dietz, J. Jaspan, and P. D. Klein.
1980. Total body water measurement in humans with 18O and D2 labeled water. Am. J. Clin. Nutr. 33:2686–2693.

Stewart, R. E. A., and D. M. Lavigne.
1980. Neonatal growth of Northwest Atlantic harp seals, *Pagophilus groenlandicus*. J. Mammal. 61:670–680.

Trillmich, F., and D. Limberger.
1985. Drastic effects of El Niño on Galapagos pinnipeds. Oecologia, 67:19–22.

Trites, A. W.
1991. Fetal growth of northern fur seals: life-history strategy and sources of variation. Can. J. Zool. 69:2608–2617.
1992. Fetal growth and the condition of pregnant northern fur seals off western North America from 1958 to 1972. Can. J. Zool. 70:2125–2131.
1993. Biased estimates of fur seal pup mass: origins and implications. J. Zool. (Lond.) 229:515–525.

Trites, A. W., and M. A. Bigg.
1992. Changes in body growth of northern fur seals

from 1958 to 1974: density effects or changes in the ecosystem? Fish. Oceanog. 1:127–136.

Tveraa, T., B.-E. Sæther, R. Aanes, and K. E. Erikstad.
1998. Body mass and parental decisions in the Antarctic petrel *Thalassioca antarctica*: how long should the parents guard the chick? Behav. Ecol. Sociobiol. 43:73–79.

York, A. E.
1994. The population dynamics of Northern sea lions, 1975–1985. Mar. Mammal Sci. 10:38–51.

Zar, J. H.
1984. Biostatistical analysis, 718 p. Prentice-Hall, Englewood Cliffs, NJ.

Reproductive biology of carpenter seabream (*Argyrozona argyrozona*) (Pisces: Sparidae) in a marine protected area

Stephen L. Brouwer

Marc. H. Griffiths

Department of Marine and Coastal Management
Private Bag X2
Rogge Bay 8012, South Africa

E-mail (for S. L. Brouwer): sbrouwer@deat.gov.za.

Abstract—The carpenter seabream (*Argyrozona argyrozona*) is an endemic South African sparid that comprises an important part of the handline fishery. A three-year study (1998–2000) into its reproductive biology within the Tsitsikamma National Park revealed that these fishes are serial spawning late gonochorists. The size at 50% maturity (L_{50}) was estimated at 292 and 297 mm FL for both females and males, respectively. A likelihood ratio test revealed that there was no significant difference between male and female L_{50} ($P>0.5$). Both monthly gonadosomatic indices and macroscopically determined ovarian stages strongly indicate that *A. argyrozona* within the Tsitsikamma National Park spawn in the astral summer between November and April. The presence of postovulatory follicles (POFs) confirmed a six-month spawning season, and monthly proportions of early (0–6 hour old) POFs showed that spawning frequency was highest (once every 1–2 days) from December to March. Although spawning season was more highly correlated to photoperiod ($r=0.859$) than temperature ($r=-0.161$), the daily proportion of spawning fish was strongly correlated ($r=0.93$) to ambient temperature over the range 9–22°C. These results indicate that short-term upwelling events, a strong feature in the Tsitsikamma National Park during summer, may negatively affect carpenter fecundity. Both spawning frequency and duration (i.e., length of spawning season) increased with fish length. As a result of the allometric relationship between annual fecundity and fish mass a 3-kg fish was calculated to produce fivefold more eggs per kilogram of body weight than a fish of 1 kg. In addition to producing more eggs per unit of weight each year, larger fish also produce significantly larger eggs.

Manuscript submitted 22 September 2003 to the Scientific Editor's Office.

Manuscript approved for publication 30 August 2004 by the Scientific Editor.

Fish. Bull. 103:258–269 (2005).

The carpenter seabream (*Argyrozona argyrozona*), known as "carpenter" regionally, is an endemic South African sparid found between St Helena Bay and KwaZulu-Natal (Fig.1) (Smith and Heemstra, 1986). Although the third most important species in the line-fishery in terms of landed mass, catch per unit of effort (CPUE) on traditional fishing grounds, declined by 95% during the twentieth century (Griffiths, 2000). Despite the importance of this resource, little research attention has been given to this species. The only previous study on the reproductive biology of carpenter was based on specimens collected towards the western extreme of the distribution range (west of Cape Agulhas), where most of the fish examined were reproductively inactive (Nepgen, 1977). As a result spawning seasonality was not accurately delineated and sizes at 50% maturity were not calculated. Assuming carpenter to be determinate spawners, Nepgen (1977) overestimated batch fecundity by counting immature oocytes.

The objective of the present study was to provide information on spawning seasonality, size at maturity, and annual fecundity of carpenter in the Tsitsikamma National Park (TNP), a 75-km no-take marine protected area (MPA) that has existed for 38 years (Fig. 1). It was envisaged that in conjunction with other studies on carpenter (Brouwer and Griffiths[1]) in exploited areas this information would assist in determining the affects of fishing on the life history of carpenter.

Materials and methods

Fish were caught from a research vessel at depths between 20 and 90 m by using handlines with baited hooks of 2/o–6/o in size. An attempt was made to sample 60 fish per month between March 1996 and June 1999, although weather conditions did not always allow this number. Sampling involved measuring total and fork length (FL) (mm), whole mass (g), gutted mass (g), determining the sex of fish, and removing the gonads. Gonads were staged macroscopically according to a seven-stage maturity index (Table 1) and weighed to the nearest 0.1 g. The whole gonads were preserved in 10% neutrally buffered formalin or alternatively fixed in Bouin's solution for 48 hours and then stored in 60% ethanol. Preserved samples were processed for histological analysis according to the techniques described by Osborne et al. (1999).

Length at maturity was modelled by using a 2-parameter logistic ogive of the form

$$p_i = \frac{1}{1+\exp^{-(L_i-L_{50})/a}},$$

where p_i = the proportion of mature fish in size class i, sampled during the spawning season (November to April);

[1] Brouwer, S. L., and M. H. Griffiths. In prep. Stock separation and life history of *Argyrozona argyrozona* (Pisces: Sparidae) on the South African east coast.

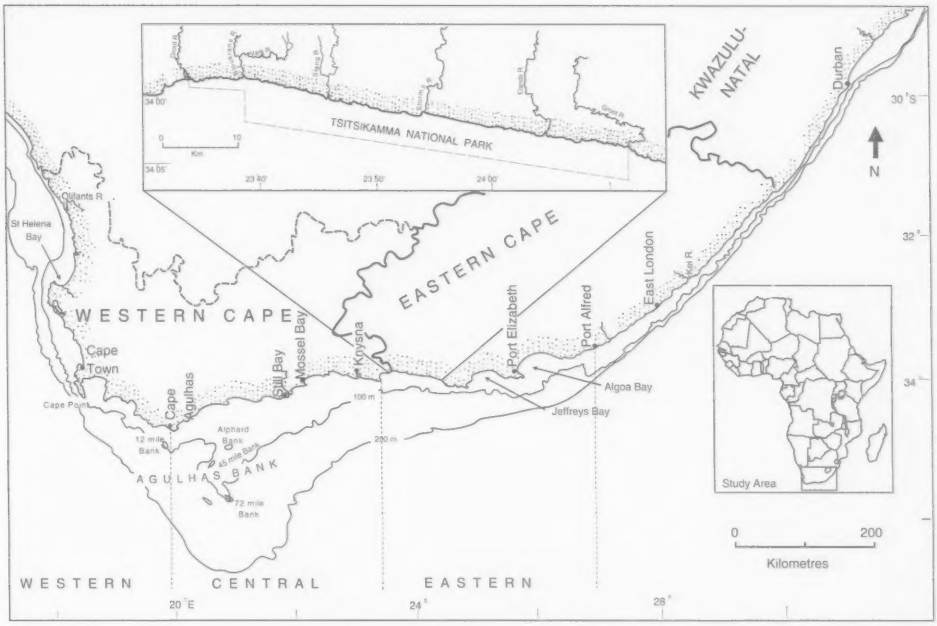

Figure 1

Map of the study area showing the position of the Agulhas Bank, Tsitsikamma National Park, 100- and 200-m isobaths and the places mentioned in the text.

Table 1

Classification and descriptions of macroscopic and microscopic ovary and testis stages of carpenter (*Argyrozona argyrozona*) sampled in the Tsitsikamma National Park.

Stage	Macroscopic	Microscopic
1 Juvenile female	Ovotestis appears as a thin transparent vessel.	Both ovarian and testicular tissues are present in equal proportions; however in the later stages ovarian tissue becomes dominant.
1 Juvenile male	Ovotestis appears as a thin transparent vessel.	Both ovarian and testicular tissue present in equal proportions; however in the later stages ovarian tissue becomes dominant.
2 Immature, resting female	Translucent orange tubes, no eggs visible to naked eye.	Cells in the perinucleolus stage have a large nucleus containing 8–15 nucleoli located along the periphery of the nucleus. There may be remnants of the testes on the periphery of the ovary.
2 Immature, resting male	Testes thin white and flaccid but larger than those in stage 1, no sperm in tissue.	No sperm cells are noticeable and the seminiferous tubules appear to be empty. Remnants of ovarian tissue may be present in the centre of the testes.
3 Active female	Oocytes visible to naked eye as tiny granules in gelatinous orange matrix; little increase in diameter of ovary.	Vitellogenesis begins in the oocytes, which become more rounded and begin to accumulate yolk (yolk vesicles). Yolk appears as a narrow ring of small yolk vesicles in the periphery of the cytoplasm.

continued

L_i = length of size class i;
L_{50} = the length at which 50% of the fish are sexually mature (stage 4+); and
A = the width of the ogive.

The ogive was fitted by minimizing the negative log-likelihood. Differences in male and female L_{50} and a were tested by using a ratio test that minimizes the binomial log-likelihood of the form

$$-L = -\sum_{i=1}^{n}\left[m_i \times \ln\left(\frac{p_i}{1-p_i}\right) + n_i \times \ln(1-p_i) + \ln\binom{n_i}{m_i}\right],$$

where n = the number of samples in size class i; and
m_i = the number of mature fish in size class i.

Spawning frequency was estimated by using daily proportions of ovaries containing early postovulatory follicles (POFs), hereafter referred to as the spawn-

Table 1 (continued)

Stage	Macroscopic	Microscopic
3 Active male	Testes wider and triangular in cross section.	The seminal vesicles expand and become filled with spermatogonia.
4 Developing female	Ovary larger and orange-yellow in color. Eggs clearly discernible. Veins and arteries large and plentiful.	Yolk vesicles are common and primary yolk oocytes begin to appear, which are characterized by the formation of small spherical yolk granules.
4 Developing male	Testes wider and deeper, creamy white in colour, obvious presence of sperm in main sperm duct.	The seminiferous tubules of the testes are filled with spermatozoa, which are also present in the primary sperm duct.
5 Ripe female	Ovaries are large in diameter, may have a few hydrated eggs. Yellow oocytes take up all the space. Veins and arteries large and plentiful.	Tertiary yolk oocytes, characteriszed by large yolk plates, appear along with primary yolk and yolk vesicles. The nucleus becomes irregular in shape and smaller in size. The nucleus migrates to the animal pole of the cell after which hydration begins, resulting in increased transparency of the cells and an increase in cell size.
5 Ripe male	Sperm present in main sperm duct and in tissue. Gonad soft and breaks when lightly pinched.	The seminiferous tubules expand with copious amounts of spermatozoa that fill the lumen of the primary sperm duct.
6 Ripe, running female	Ovary amber in colour. Large with substantial proportion of gonad with hydrated eggs, which fill the lumen. Veins and arteries large and plentiful.	Filled with hydrated oocytes. Due to dehydration during the histological preparation, these oocytes appear as collapsed bags. Hydrated oocytes may squash and reshape the immature oocytes that surround them.
6 Ripe, running male	Free-flowing sperm extruded from fish when the abdomen is lightly squeezed. Testes very delicate and break easily when handled. Copious amounts of sperm present in main sperm duct and in tissue.	The seminiferous tubules of the testes appear distended and are filled with mature spermatozoa as is the lumen of the primary sperm duct.
7 Spent female	Ovary reduced in size similar to stage-2 flaccid ovary. Few yolked oocytes remaining. Ovary bloodshot.	Cells in various stages of atresia, and some hydrated and mature oocytes may be present in the tissue.
7 Spent male	Testes white in color, small shrivelled, and bloodshot.	The seminiferous tubules are no longer distended and have thicker walls than stage-6 tubules. They contain few spermatozoa, which are present in the lumen of the primary sperm duct. Large blood vessels are apparent in the tissue.

ing fraction (Hunter and Macewicz, 1985). POFs were aged by comparing them with known age POFs from spawning females under captive conditions. Female carpenter were held in a flow-through system at ambient sea temperature (mean 16°C, range 9.5–20°C) in 5000-liter circular tanks, were stimulated to ovulate with a commercially available GnRH-analogue (Davis, 1996). Three fish were sacrificed immediately after ovulation and then three fish every six hours over the following 48-hour period. Histological analysis of ovaries revealed three clearly defined POF stages (Fig. 2). The proportions of wild-caught fish with stage-1 POFs (the spawning fraction) were inverted to produce an estimate of spawning frequency (Wilson and Nieland, 1994).

Batch fecundity was estimated from counts of hydrated oocytes from ovaries without POFs or atretic oocytes (Hunter and Macewicz, 1985). A ±1.00-g section was removed from the middle of the right ovary. This was weighed to the nearest 0.01 g and the hydrated oocytes were separated according to the method described by Lowerre-Barbieri and Barbieri (1993). Hydrated oocytes were suspended in water and counted at 8–10 times magnification in a Bokkeroff tray and measured to 0.1 mm with an ocular micrometer along the longest diameter.

Annual fecundity was calculated as follows:

$$Af_t = \left(\frac{ls_j}{sf_j}\right) \times fb_t,$$

where Af_t = the annual fecundity for fish t;
ls = the length of the spawning season (days) for fish of size class j;
sf = the spawning frequency (days) for fish of size class j (all months combined); and
fb_t = the batch fecundity of fish t.

Spawning season was established by calculating the monthly proportions of macroscopic gonad stages and mean monthly gonodosomatic index (GSI) for fish larger than L_{50}:

$$GSI = \left(\frac{m_g}{m_s}\right) \times 100,$$

where m_g = the gonad mass (g); and
m_s = the somatic mass (g) (minus gonad and stomach mass).

In order to investigate the relationship between spawning and temperature, temperature data were collected at the sampling site with a Seamon Mini (Hugrun, Iceland) recorder stationed at at a depth of 35 m on the reef from which the biological samples were collected. A thermistor array consisting of four underwater temperature recorders (UTRs) at depths of 12 m, 19 m, 27 m, and 35 m recorded the temperature every minute

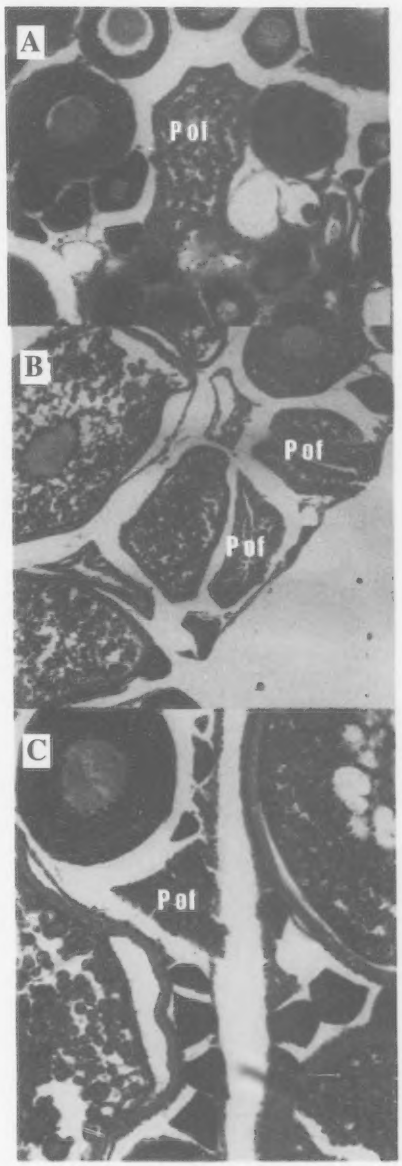

Figure 2

Postovulatory follicle (POF) stages determined from carpenter (*Argyrozona argyrozona*) chemically induced to spawn in an open circulating system housed at the Tsitsikamma National Park. (**A**) = stage 1 (0–6 hours), (**B**) = stage 2 (7–24) hours and (**C**) = stage 3 (25–48) hours.

and stored an hourly average (Roberts[2]). Photoperiod data were downloaded from the South African Astronomical Observatory database.[3] Pearson Rank correlation was used to measure the correlation between GSI and temperature, and GSI and photoperiod trends.

Results

Histological examination of the gonads revealed that although juveniles possess both testicular and ovarian tissue simultaneously (i.e., as hermaphrodites) they mature as either a male or female (Table 1) and are therefore late gonochorists (rudimentary hermaphrodites). Gametogenesis was similar to that described for other late gonochoristic sparids e.g., *Pterogymnus laniarius* (Booth and Hecht, 1997). The size at 50% maturity was estimated at 292 and 297 mm FL for females and males, respectively (Fig. 3), and in both cases is equivalent to an age of about five years (Brouwer and Griffiths 2004). A likelihood ratio test revealed that there was no significant difference between male and female L_{50} ($P>0.5$) or a ($P>0.1$). Complete (100%) maturity for both sexes occurred at 480 mm FL, an age of about 15 years (Brouwer and Griffiths 2004). The sex ratio was 1F:1.3M ($n=1776$); a chi-square test with Yates' correction factor revealed that this sex ratio was a significant difference from unity ($P<0.01$).

Three age-related POF stages were identified within the ovaries of captive spawned carpenter (Fig. 2). Stage-1 POFs (0–6 hours) were very loosely arranged and appeared as a long convoluted string with a large clearly defined lumen. The granulosa cells were clearly visible and widely spaced and had clearly visible nuclei (Melo, 1994). Stage-2 POFs (7–24 hours) are smaller and more densely packed but still have a visible lumen. The granulosa cells are closely packed and dense. Stage-3 POFs (25–48 hours) are small and densely packed. There is no lumen and the granulosa cells are closely arranged and no longer distinguishable from one another. After 48 hours at 16°C, POFs were no longer detectable.

Mean GSI and the proportions of ripe (stage-5) and ripe, running (stage-6) fish increased in November and remained high until April (Figs. 4 and 5), indicating that carpenter are summer spawners. The presence of early POFs from November to March (sample numbers being too low for April) supported the macroscopically determined spawning season. The monthly spawning fraction did, however, reveal that spawning frequency was highest in January and February when the fish spawned at two-day intervals and lowest in November and April when they were found to spawn every 2–3 days (Table 2).

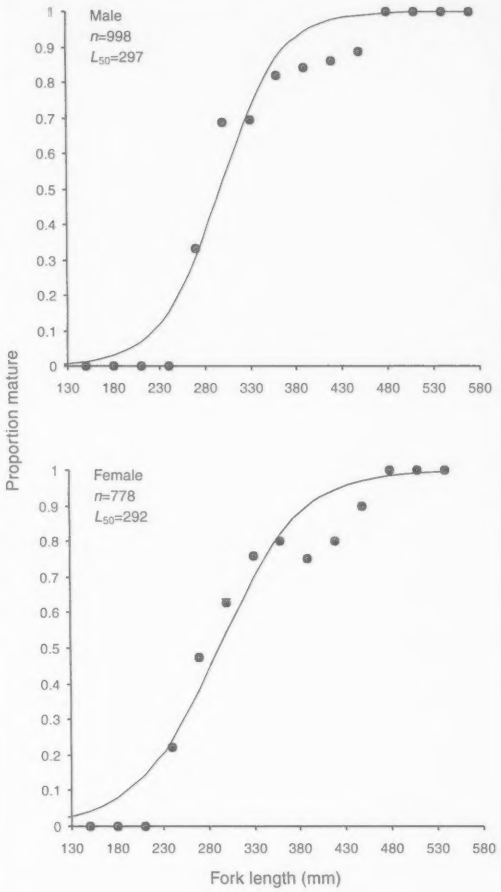

Figure 3

The proportion of mature carpenter (*Argyrozona argyrozona*) in length classes sampled in the Tsitsikamma National Park. The curves were fitted with a 2-parameter logistic ogive.

Batch fecundity was positively correlated with both fish mass ($r=0.71$) and fork length ($r=0.71$). No correlation was found between fish length and relative batch fecundity (eggs/fish somatic mass) (Fig. 6). The proportion of fish with stage-1 POFs revealed that spawning frequency and length of the spawning season increased with fish length (Table 3). Accounting for size-related patterns in spawning season (Fig. 7) and frequency, we found that annual fecundity increased allometrically with mass (Fig. 8) and age (Table 4). Hydrated egg size was significantly smaller and more variable (average 1.0 mm ±0.16) in fish below the length at 100% maturity (480 mm FL) than those above this length (1.1 mm ±0.09) (t-test, $P<0.005$).

[2] Roberts, M. J. 1999. CD-ROM, Tsitsikamma National Park oceanographic data, version 1.0. Marine and coastal management, Private Bag X2, Rogge Bay 8012, South Africa.

[3] http://www.saao.ac.za [Accessed August 2000].

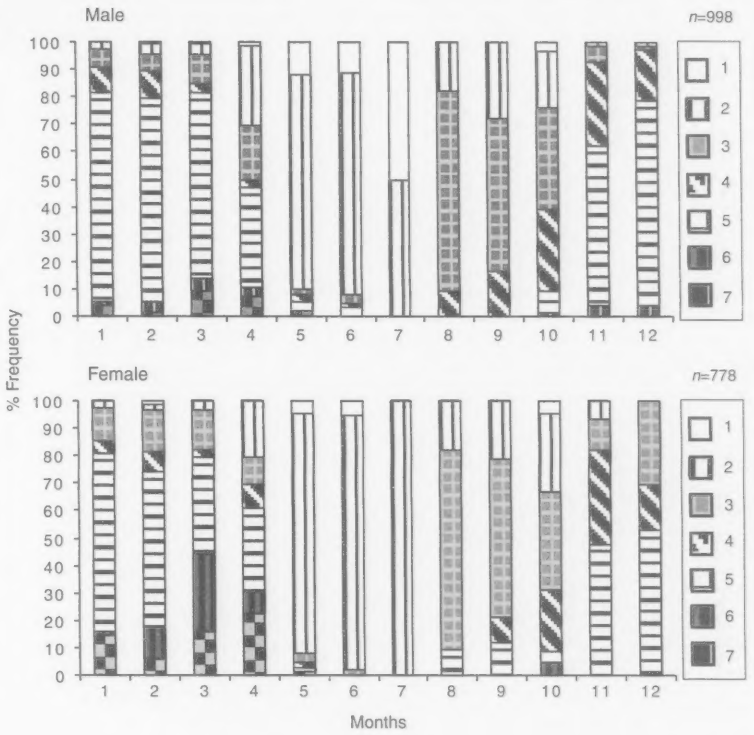

Figure 4

Monthly variation in the proportion of macroscopic gonad stages of carpenter (*Argyrozona argyrozona*) >L_{50} caught in the Tsitsikamma National Park (March 1996–July 1999). Numbers in the legend refer to the gonad stages in Table 1. 1 = juvenile, 2 = immature, 3 = active, 4 = developing, 5 = ripe, 6 = ripe, running, and 7 = spent.

Table 2

Spawning frequency determined for carpenter (*A. argyrozona*) from the proportion of ovaries with stage-1 POFs or macroscopically determined from hydrated oocytes.

Month	Spawning frequency (days)		% ovaries with hydrated oocytes	% ovaries with stage-1 POFs
	Macroscopic	POFs		
November	2.1 (44)	4.6 (23)	48	22
December	1.9 (53)	3.5 (21)	53	28
January	1.5 (119)	1.6 (5)	66	60
February	1.5 (160)	1.5 (35)	68	66
March	1.6 (99)	—	64	Not enough data
April	2.6 (49)	—	39	Not enough data

A positive relationship between temperature at the time of spawning (back-calculated from stage-1 POFs, assuming a delay of 6 hours) and the proportion of ovaries with stage-1 POFs indicated that spawning events were positively correlated with temperature (r=0.93) over the range 9°C and 22°C (Fig. 9). GSI was how-

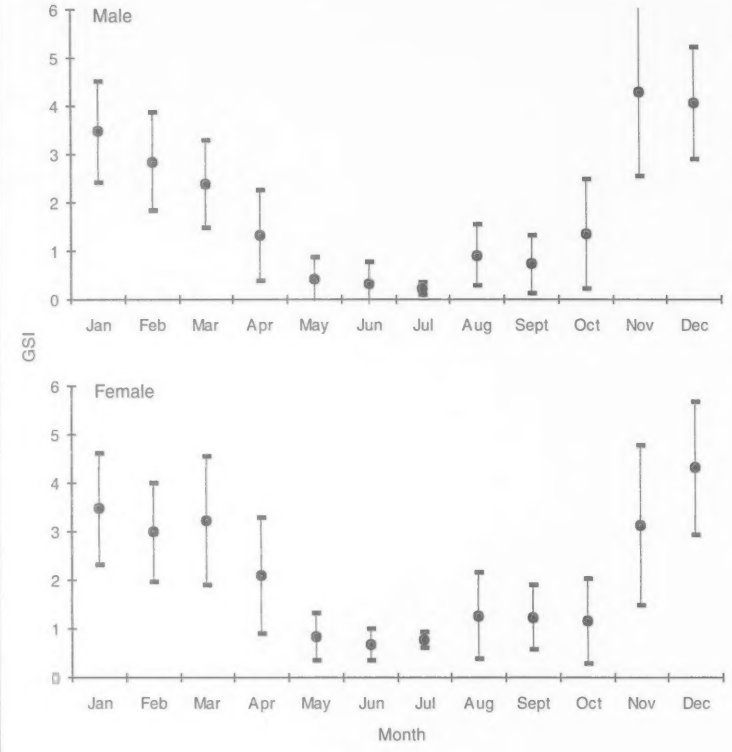

Figure 5

Seasonal variation of the standard deviation in the gonadosomatic index (GSI) and mean values (●) for male and female carpenter (*Argyrozona argyrozona*) sampled in the Tsitsikamma National Park.

ever strongly correlated (r=0.86) with photoperiod but exhibited a weak negatively relationship with seasonal temperature (Fig. 10).

Discussion

Late gonochorism, protandry, protogyny, and hermaphroditism are the recognized reproductive styles of sparids (Smale, 1988; Buxton and Garratt, 1990). Although carpenter were previously described as gonochoristic (Nepgen, 1977), microscopic examination of the gonads revealed that they are late gonochorists. The sex ratio calculated during this study (1 female:1.3 male) was typical for those observed for other late gonochorists (Griffiths et al., 2002).

Upon reviewing 90 species of reef fish, Sadovy (1996) concluded that although GSIs reflect the gonad maturity patterns for a species, they are poor indicators of peak spawning times. By way of example, in red hind grouper (*Epinephelis guttatus*) yolked oocytes are present in the ovaries for four months of the year but actual spawning is limited to a period of 10 days (Sadovy, 1996). In the case of carpenter, however, the presence of POFs from November to April supports the six-month spawning season indicated by macroscopic methods (although in some larger individuals [>480 mm FL] hydrated

Table 3

Spawning frequency (averaged over all months) and length of the spawning season calculated from the presence of stage-1 POFs in carpenter (*Argyrozona argyrozona*) ovaries in three size classes.

Size class (mm)	Average spawning frequency (days)	Spawning season (months)
250–339	9	6
340–479	4	7
480+	3.9	9

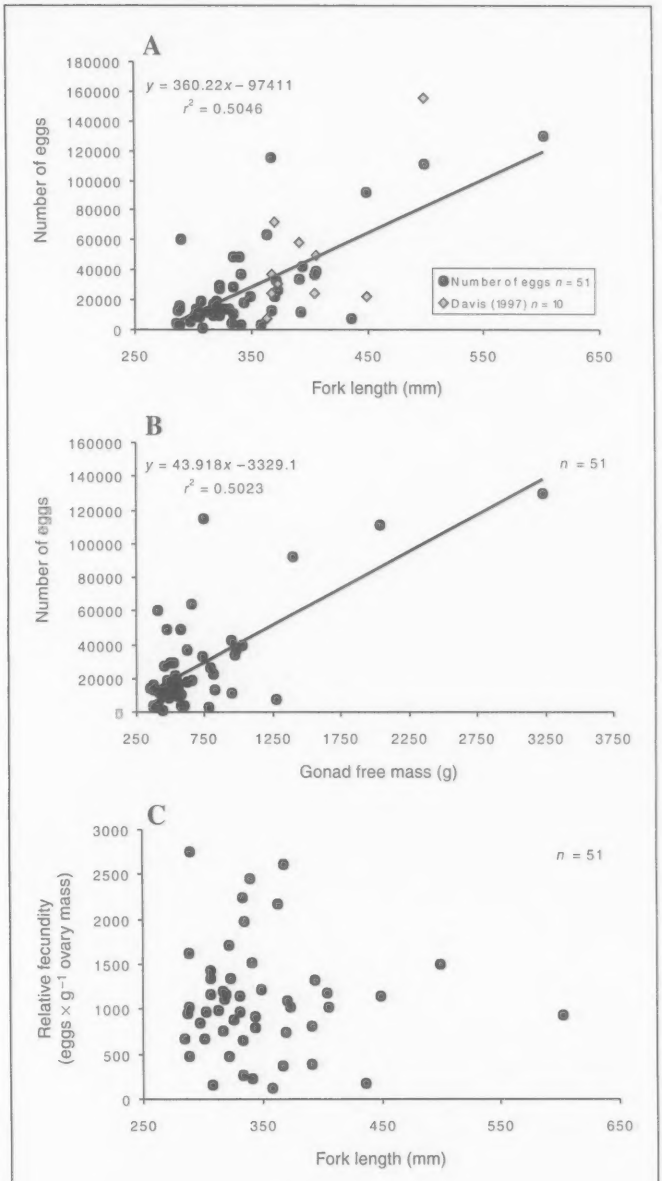

Figure 6

The relationships for carpenter (*Argyrozona argyrozona*) between (**A**) fish length and batch fecundity including data from fish spawned artificially in a previous study (Davis, 1996), (**B**) fish mass and batch fecundity and (**C**) fish length and relative batch fecundity.

oocytes and POFs were found from October to May). Monthly spawning fraction and percentage of ovaries with hydrated oocytes nevertheless reached a peak during January and February (Table 2); these trends were not detected in the monthly GSIs. But given that the macroscopic determinations of stage followed trends in the proportions of POFs that were present, we conclude that expensive and time-consuming histological analysis is not necessary for determining spawning peaks for this species.

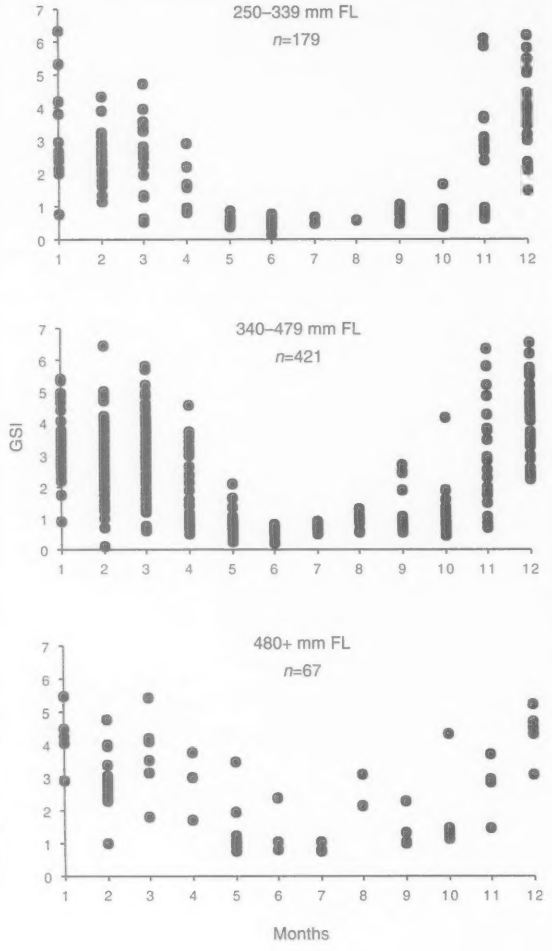

Figure 7

Seasonal variation in the gonadosomatic index (GSI) for female carpenter (*Argyrozona argyrozona*) from three size classes sampled in the Tsitsikamma National Park.

Apart from being indicators of spawning seasonality, GSI trends can provide insight into the mating patterns of a species (Sadovy, 1996). Pair-spawning sparids such as *Chrysoblephus laticeps* have low male GSI (±10% of female) during the spawning season (Buxton, 1990). Although the spawning behavior of carpenter has not been documented, the GSI of males (average 3.0 ±1.4) was similar to that of females (average 3.3 ±1.4) during the spawning season (Fig. 4). The large testes size suggests that carpenter are group spawners and that sperm competition is high (Sadovy, 1996). Further evidence for group spawning is the lack of sexual dimorphism in this species (Smale, 1988; Mann and Buxton, 1998; Griffiths et al., 2002).

Like many other South African sparids, carpenter are summer spawners (Buxton and Clarke, 1986; Buxton and Clarke, 1991; Buxton, 1993). Although various environmental cues have been suggested for this seasonal spawning, it is probably a combination of events that leads to gonad maturation and spawning. Smale (1988) and Garratt (1985) speculated that increases in gonad activity of *Petrus rupestris* and *Chrysoblephus puniceus* were attributed to an increase in photoperiod and water temperature respectively; Scott and Pankhurst (1992),

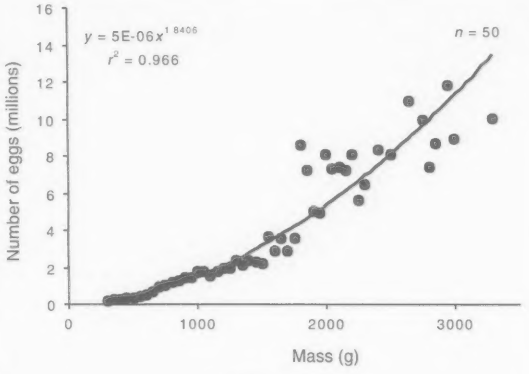

Figure 8

The relationship between annual fecundity and fish weight for carpenter (*Argyrozona argyrozona*) in the Tsitsikamma National Park.

Table 4

Age-based annual fecundity of carpenter (*Argyrozona argyrozona*) in the Tsitsikamma National Park.

Age (yr)	Number of eggs (millions)
1	0
2	0
3	0
4	0.143
5	0.288
6	0.367
7	0.441
8	0.870
9	1.014
10	1.228
11	1.498
12	1.706
13	1.763
14	2.260
15	2.233
16	2.427
17	3.132
18	3.175
19	5.363
20	6.308
21	6.308
22	7.815
23	7.430
24	6.480
25	7.421
26	8.363
27	8.363
28	8.064
29	10.397
30	11.808

however, showed that seasonal temperature regulated gonad development for *Pagrus aratus*. Based on the data collected during our study, photoperiod appears to be responsible for the onset of gonad maturation in carpenter; when day length increases (but water temperature is variable) in September and October, and their gonads begin to develop (Fig. 10). Photoperiod was also highly correlated with GSI (r=0.86), whereas temperature showed a weakly negative relationship (r=−0.16).

Nepgen (1977) calculated spawning frequency for this species with an oocyte-size-frequency analysis of inactive females. Finding only one peak in the oocyte-size-frequency distribution, he assumed that carpenter spawned only once a year. In our study POFs and various yolk stage oocytes were found to occur simultaneously, proving that carpenter are serial spawners. Accounting for monthly trends in spawning frequency and the length of the spawning season, carpenter in the Tsitsikamma National Park are estimated to spawn at least 30 times per year. This spawning frequency is similar to other predatory reef fishes, e.g., *Mycteroperca microlepis* (30–40 times per year) (Collins et al., 1998). Nevertheless, as with other species (Danilowicz, 1995), spawning fraction in carpenter during the spawning season was highly correlated with water temperature (r=0.931) (Fig. 9), indicating that short-term cold water upwellings, a common feature of the TNP during summer (Schumann et al., 1982), may negatively impact annual carpenter fecundity in this area.

Although fecundity in fishes is highly variable between individuals (Sadovy 1996), absolute fecundity increases with size (Hunter et al., 1985; Davis and West, 1993; Wilson and Nieland, 1994; Collins et al., 1998). In our study absolute annual fecundity increased markedly with fish size (Table 4) and spawning season was longer for large fish (Fig. 7) (Table 3). The positive correlation of batch fecundity and fish size (r=0.71), coupled with the increased length of the spawning season for the older fish, greatly increases the absolute annual fecundity of larger fishes (Fig. 8). Sadovy (1996) noted that for red snapper (*Lutjanus compechanus*) one large female (601 mm FL) will produce as many eggs as 212 small (420 mm FL) females. Similarly, one large female carpenter of 3.3 kg will produce as many eggs as 72 small ones of 0.3 kg. In addition to higher fecundity, the larger fish produce significantly larger eggs and presumably more viable larvae (Ojanguren et al., 1996; Pepin and Anderson, 1997).

Exploited populations were traditionally managed to maximize growth (Griffiths, 1997). However it is imperative to maintain sufficient numbers of reproduc-

tive adults to ensure egg production and avoid recruitment failure. To address proper management of line-caught fish in South Africa, spawner biomass per recruit models have been used (Griffiths, 1997). One assumption of this approach is that fecundity is linearly related to spawning biomass, regardless of individual size (Buxton, 1992). Because our study has shown that fecundity in carpenter is allometrically related to individual mass, egg-per-recruit models would be more appropriate for future stock assessment of this species.

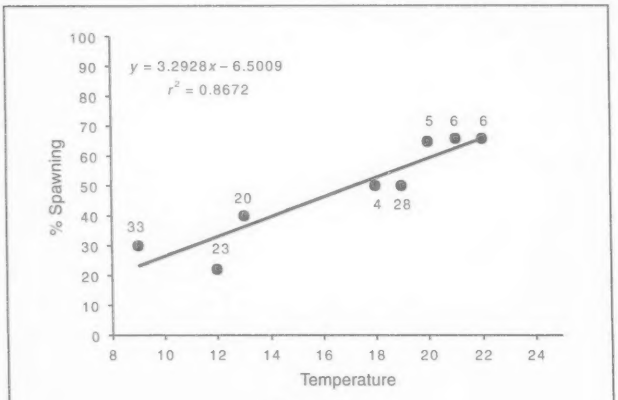

Figure 9

The relationship between proportion of carpenter (*Argyrozona argyrozona*) spawning (back calculated from stage-1 POFs, 0–6 hours) and temperature in the Tsitsikamma National Park. Numbers above symbols refer to number of fish sampled with POFs.

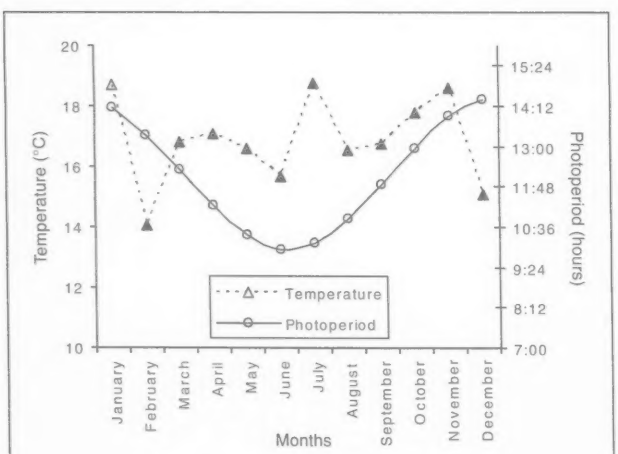

Figure 10

Monthly average temperature and photoperiod for the Tsitsikamma National Park.

Acknowledgments

We thank the staff at South African National Parks, for accommodation at the Tsitsikamma National Park and for use of their vessel. John Allen and Karoels Piterse are thanked for many hours at sea. Yolande Melo is thanked for her assistance with histological preparation and interpretation and Jeanine Van der Pol for assistance in laboratory and Tony Booth and two anonymous referees for constructive comments on this manuscript. This research was funded by the Marine Living Resources Fund.

Literature cited

Booth, A. J., and T. Hecht.
1997. A description of gametogenesis in the panga *Pterogymnus laniarius* (Pisces: Sparidae) with comments on changes in maturity patterns over the past two decades. S. Afr. J. Zool. 32(2):49–53.

Brouwer, S. L., and M. H. Griffiths.
2004. Age and growth of *Argyrozona argyrozona* (Pisces: Sparidae) in a Marine Protected Area: an evaluation of methods based on whole otoliths, sectioned otoliths and mark recapture. Fish. Res. 61:1–12.

Buxton, C. D.
1990. The reproductive biology of *Chrysoblephus laticeps* and *C. cristiceps* (Teleostei: Sparidae). J. Zool. Lond. 220:497–511.
1992. The application of yield-per-recruit models to two South African sparid reef species, with special consideration to sex change. Fish. Res. 15:1–16.
1993. Life-history changes in exploited reef fishes on the east coast of South Africa. Environ. Biol. Fish. 36: 47–63.

Buxton, C. D., and J. R. Clarke.
1986. Age growth and feeding of the blue hottentot *Pachymetopon aeneum* (Teleostei: Sparidae) with notes on reproductive biology. S. Afr. J. Zool. 21:33–38.
1991. The biology of the white musselcracker *Sparodon durbanensis* (Pisces: Sparidae) on the Eastern Cape coast, South Africa. S. Afr. J. Mar. Sci. 10:285–296.

Buxton, C. D., and P. A. Garratt.
1990. Alternative reproductive styles in seabreams (Pisces: Sparidae). Environ. Biol. Fish. 28:113–124.

Collins, L. A., A. G. Johnson, C. C. Koenig, and M. S. Baker.
1998. Reproductive patterns, sex ratio, and fecundity in gag, *Mycteroperca microlepis* (Serranidae), a protogynous grouper from the northeastern Gulf of Mexico. Fish. Bull. 96:415–427.

Danilowicz, B. S.
1995. The role of temperature in spawning of damselfish *Dascyllus albisella*. Bull. Mar. Sci. 57(3): 624–636.

Davis, J. A.
1996. Investigations into the larval rearing of

two South African sparid species. M.S. thesis, 138 p. Rhodes Univ., Grahamstown, Eastern Cape, South Africa.

Davis, T. L. O., and G. J. West.
1993. Maturation, reproductive seasonality, fecundity, and spawning frequency in *Lutjanus vittus* (Quoy and Gaimard) from the North West shelf of Australia. Fish. Bull. 91:224–236.

Garratt, P. A.
1985. The offshore linefishery of Natal. II: Reproductive biology of the sparids *Chrysoblephus puniceus* and *Cheimerius nufar*. Invest. Rep. Oceanogr. Res. Inst. 63:1–21.

Griffiths, M.H.
1997. The application of per-recruit models to *Argyrosomus inodorus*, an important South African sciaenid fish. Fish. Res. 30:103–115.
2000. Long-term trends in the catch and effort of commercial linefish off South Africa's Cape Province: snapshots of the 20th century. S. Afr. J. Mar. Sci. 22:81–110.

Griffiths, M. H., C. Wilke, A. J. Penny, and Y. Melo.
2002. Life history of white stumpnose *Rhabdosargus globiceps* (Pisces: Sparidae) off South Africa. S. Afr. J. Mar. Sci. 281–300.

Hunter, J. R., N. C. H. Lo, and R. J. H. Leong.
1985. Batch fecundity and multiple spawning in fishes. *In* An egg production method for estimating spawner biomass of pelagic fish: application to the northern anchovy, *Engraulis mordax* (R. Lasker, ed.), 67–77. NOAA Tech. Rep. NMFS 36.

Hunter, J. R., and B. J. Macewicz.
1985. Rates of atresia in the ovary of captive and wild northern anchovy *Engraulis mordax*. Fish. Bull. 83(2): 119–136.

Lowerre-Barbieri, S. K., and L. R. Barbieri.
1993. A new method of oocyte separation and preservation for fish reproduction studies. Fish. Bull. 91: 165–170.

Mann, B. Q., and C. D. Buxton.
1998. The reproductive biology of *Diplodus sargus capensis* and *D. cervinus hottentotus* (Sparidae) off the South-East Cape coast, South Africa. Cybium 22(1):31–47.

Melo, Y. C.
1994. Spawning frequency of the anchovy *Engraulis capensis*. S. Afr. J. Mar. Sci. 14:321–331.

Nepgen, C. S. V.
1977. The biology of the hottentot *Pachymetopon blochii* (Val.) and the silverfish *Argyrozona argyrozona* (Val.) along the cape south-west coast. Investl. Rep. Div. Sea Fish. Rep. S. Afr. 105:1–35.

Ojanguren, A. F., and F. G. Reyes-Gavilan F. Brana.
1996. Effects of egg size on offspring development and fitness in brown trout, *Salmo trutta* L. Aquaculture 147(1–2):9–20.

Osborne, R. F., Y. C. Melo, M. D. Hofmeyer, and D. W. Japp.
1999. Serial spawning and batch fecundity of *Merluccius capensis* and *M. paradoxus*. S. Afr. J. Mar. Sci. 21:2111–216.

Pepin, D., C. Orr, and J. T. Anderson.
1997. Time to hatch and larval size in relation to temperature and egg size in Atlantic cod (*Gadus morhua*). Can. J. Fish. Aquat. Sci. 54 (suppl. 1):2–10.

Sadovy, Y. J.
1996. Reproduction of reef fish species. *In* Reef fisheries (N. V. C. Polunin and C. M. Roberts, eds.), p. 15–59. Chapman and Hall, London.

Schumann, E. H., L.-A. Perrins, and I. T. Hunter.
1982. Upwelling along the South Coast of the Cape province, South Africa. S. Afr. J. Sci. 78:238–242.

Scott, S. G., and N. W. Pankhurst.
1992. Interannual variation in the reproductive cycle of the New Zealand snapper *Pagrus aratus* (Bloch & Schneider) (Sparidae). J. Fish Biol. 41:685–696.

Smale, M. J.
1988. Distribution and reproduction of the reef fish *Petrus rupestris* (Pisces: Sparidae) off the coast of South Africa. A. Afr. J. Zool. 1988. 23(4):272–287.

Smith, M. M., and P. C. Heemstra.
1986. Smiths Sea fishes, 1047 p. Southern Book Publishers, Johannesburg, South Africa.

Wilson, C. A., and D. L. Nieland.
1994. Reproductive biology of red drum, *Sciaenops ocellatus*, from the neritic waters of the northern Gulf of Mexico. Fish. Bull. 92:841–850.

Decline in sea otter (*Enhydra lutris*) populations along the Alaska Peninsula, 1986–2001

Douglas M. Burn
Angela M. Doroff
Marine Mammals Management Office
U.S. Fish and Wildlife Service
1011 East Tudor Road
Anchorage, Alaska 99503
E-mail address (for D. M. Burn): douglas_burn@fws.gov

Abstract—During the 1990s, sea otter (*Enhydra lutris*) counts in the Aleutian archipelago decreased by 70% throughout the archipelago between 1992 and 2000. Recent aerial surveys in the Aleutians did not identify the eastward extent of the decline; therefore we conducted an aerial survey along the Alaska Peninsula for comparison with baseline information. Since 1986, abundance estimates in offshore habitat have declined by 27–49% and 93–94% in northern and southern Alaska Peninsula study areas, respectively. During this same time period, sea otter density has declined by 63% along the island coastlines within the south Alaska Peninsula study area. Between 1989 and 2001, sea otter density along the southern coastline of the Alaska Peninsula declined by 35% to the west of Castle Cape but density increased by 4% to the east, which may indicate an eastward extent of the decline. In all study areas, sea otters were primarily concentrated in bays and lagoon, whereas historically, large rafts of otters had been distributed offshore. The population declines observed along the Alaska Peninsula occurred at roughly the same time as declines in the Aleutian islands to the east and the Kodiak archipelago to the west. Since the mid-1980s, the sea otter population throughout southwest Alaska has declined overall by an estimated 56–68%, and the decline may be one of the most significant sea otter conservation issues in our time.

Manuscript submitted 2 September 2003 to the Scientific Editor's Office.
Manuscript approved for publication 30 August 2004 by the Scientific Editor.
Fish. Bull. 103:270–279 (2005).

During the 1990s, the sea otter (*Enhydra lutris*) population in the Aleutian archipelago declined at a rate of 17.5%/yr and, overall, counts decreased by 70% throughout the archipelago between 1992 and 2000 (Doroff et al., 2003). By modeling population trends back to the mid-1980s, Burn et al. (2003) estimated the population in the Aleutian Island chain decreased by 65,000 sea otters and was at about 10% of its carrying capacity in 2000. The 2000 aerial survey of Doroff et al. (2003) did not identify an eastward extent of the population decline however; therefore additional sea otter surveys along the Alaska Peninsula were needed.

Historic information on population status and trends is sparse for sea otters along the Alaska Peninsula. Sea otters were exploited to near extinction in the commercial fur trades (1742–1911) and were removed from large portions of their historic range worldwide (Kenyon, 1969; Lensink, 1962). At the time of their protection in 1911 by an international fur seal treaty, there were 13 remnant populations remaining worldwide, 11 of which persisted and grew to recolonize much of the former range of this species (Kenyon, 1969). Studies of both remnant native and translocated sea otter populations have indicated a pattern of colonization with high population growth rates up to 20% per year, and an expansion into adjacent, unoccupied habitat (Estes, 1990).

One remnant population survived on the north side of the Alaska Peninsula near Unimak Island (Kenyon, 1969; Schneider, 1976). Sea otter habitat in this area is unique in that shallow water (less than 100 m) extends up to 50 km offshore, covering more than 10,000 km of open water. The remnant population in this area likely numbered fewer than 100 sea otters in 1911 (Kenyon, 1969). This population grew steadily and expanded its range to the northeast along the Peninsula until 1970, when extreme sea ice conditions temporarily reduced the range and likely the size of the population (Schneider and Faro, 1975). By 1976, most of the sea otters in this area were concentrated between Cape Mordvinof and Cape Leontovich (Schneider, 1976).

In addition to the remnant population on the north side of Unimak Island, there were also two remnant populations of sea otters located to the south of the Alaska Peninsula in the Sandman Reefs and the outer Shumagin Islands (Kenyon, 1969). Sea otter habitat along the southern Alaska Peninsula differs from the northern side and comprises primarily rocky, mixed substrate, and extensive offshore reefs (Brueggeman et al.[1]). In the Sandman Reefs a small number of sea otters were sighted in

[1] Brueggeman, J. J., G. A. Green, R. A. Grotefendt, and D. G. Chapman. 1988. Aerial surveys of sea otters in the northwestern Gulf of Alaska and the southeastern Bering Sea. Minerals Management Service and NOAA final report, 87 p. Minerals Management Service, Anchorage, AK. [Contract no. 85-ABCV-00093.]

1922, and by 1962 the population had grown to an estimated 1625 sea otters (Lensink, 1962; Kenyon, 1969). Around the same time, the population in the Shumagin Islands was estimated to be 2724 sea otters (Kenyon, 1969).

The first systematic surveys of sea otter abundance along the north side of the Alaska Peninsula were conducted in the mid-1970s (Schneider, 1976), followed by surveys in 1982 and 1983 by Cimberg et al.[2] Brueggeman et al.[1] conducted quarterly surveys of both the northern and southern Peninsula in 1986 to assess sea otter abundance and seasonal distribution. The surveys conducted in 1986 provided seasonal estimates of abundance during a single, ice-free year, and a clear picture of habitat use in the mid-1980s along the Alaska Peninsula (Brueggeman et al.[1]).

The sea otter surveys described above were concentrated along the western end of the Alaska Peninsula where remnant populations existed and appeared to have recovered. By the late 1980s, sea otters had also returned to the nearshore waters of the entire peninsula as far east as Cape Douglas (DeGange et al.[3]). Prior to this survey in 1989, little was known about sea otter distribution and abundance on the Alaska Peninsula east of Kupreanof Point.

The objectives of our study were 1) to assess current sea otter distribution and abundance along the northern and southern Alaska Peninsula, 2) to contrast our results with prior surveys conducted in 1986 and 1989, and 3) to relate these data to the observed sea otter population declines observed elsewhere in southwest Alaska. We repeated the aerial survey methods developed by Brueggeman et al.[1] for sea otter habitat along the Alaska Peninsula which consisted of a combination of strip transects in offshore habitat (to the 70-m isobath) and coastline surveys (≤1 km of shore) of island groups within the study area. We also repeated the coastline surveys of DeGange et al.[2] to determine the eastward extent of the decline.

Materials and methods

Offshore survey areas

The north Alaska Peninsula (NAP) study area ranged from Cape Mordvinof on Unimak Island in the west to Cape Seniavin in the east. This area was further subdivided into two subunits (NAPa and NAPb), and a line at 162°W longitude divided the two subunits (Brueggeman et al.[1]). The south Alaska Peninsula (SAP) study area ranged from the Ikatan Peninsula in the west to the Shumagin Islands in the east. The seaward extent of both the NAP and SAP study areas was the approximate 70-m depth contour (Fig. 1A).

The strip transect method developed by Brueggeman et al.[1] consisted of a series of transects oriented north-south which were spaced every three minutes of longitude throughout the study area. In 1986, surveys were flown in a DeHavilland Twin Otter aircraft equipped with bubble windows at an altitude of 92 m and an airspeed of 185 km/h. Two observers, one on each side of the aircraft, relayed sea otter sighting information to a data recorder seated in the aft section of the aircraft. Sea otter sightings were grouped into three distance intervals spaced at right angles to the transect line: 0.0–0.23 km, 0.23–0.46 km, and 0.46–0.93 km. These distance zones were determined by using a clinometer to place marks on the inside of the bubble windows. Environmental information on sea state, visibility, and glare was recorded throughout the survey.

In May 2000 and April 2001, we repeated the survey conducted by Brueggeman et al.[1] using similar methods, with the exception that our survey aircraft was an Aero Commander equipped with bubble windows and we grouped sea otter sightings into five distance intervals: 0.0–0.115 km, 0.115–0.23 km, 0.23–0.345 km, 0.345–0.46 km, and 0.46–0.575 km.

Coastline survey areas

In 1986, Brueggeman et al.[1] also surveyed the coastlines of 22 islands on the south side of the Alaska Peninsula quarterly at a distance of 0.46 km from shore, using the same aircraft, altitude, and airspeed as in the offshore area surveys (Fig. 1B). In 1989, DeGange et al.[2] surveyed the coastlines of these same islands and the Alaska Peninsula from False Pass to Cape Douglas (Fig. 1C). The 1989 survey was conducted from Bell 206 and Hughes 500 helicopters at a distance of 0.2 km from shore at an altitude of 92 m and an airspeed of 130 km/h. We used similar methods (0.23 km from shore, altitude 92 m, airspeed 185 km/h) to survey the coastlines of these 22 islands and the Alaska Peninsula in April and May 2001. The area of the offshore surveys was adjacent to, but did not overlap, the area of the coastline surveys. Coastline surveys were not conducted in the NAP study area.

Offshore survey analyses

Prior to the analysis of the 2000-01 offshore survey data, we tested several assumptions made in the 1986 analysis regarding the detectability of sea otters as a function of 1) survey strip width, 2) survey conditions, and 3) time of day. We examined the distribution of sea otter sightings by distance zone using a chi-square analysis to determine the appropriate survey strip width to use

[2] Cimberg, R. L., D. P. Costa, and P. A. Fishman. 1984. Ecological characterization of shallow subtidal habitats in the north Aleutian Shelf. OCSEAP Final Rep. no. 4197, 99 p. U.S. Dept. of Commerce, National Oceanographic and Atmospheric Administration, Anchorage, Alaska 99501.

[3] DeGange, A. R., D. C. Douglas, D. H. Monson and C. M. Robbins. 1994. Surveys of sea otters in the Gulf of Alaska in response to the *Exxon Valdez* oil spill. Final report to the Exxon Valdez Oil Spill Trustee Council, Marine Mammal Study 6-7, 11 p. U.S. Fish and Wildlife Service, Anchorage, Alaska 99503.

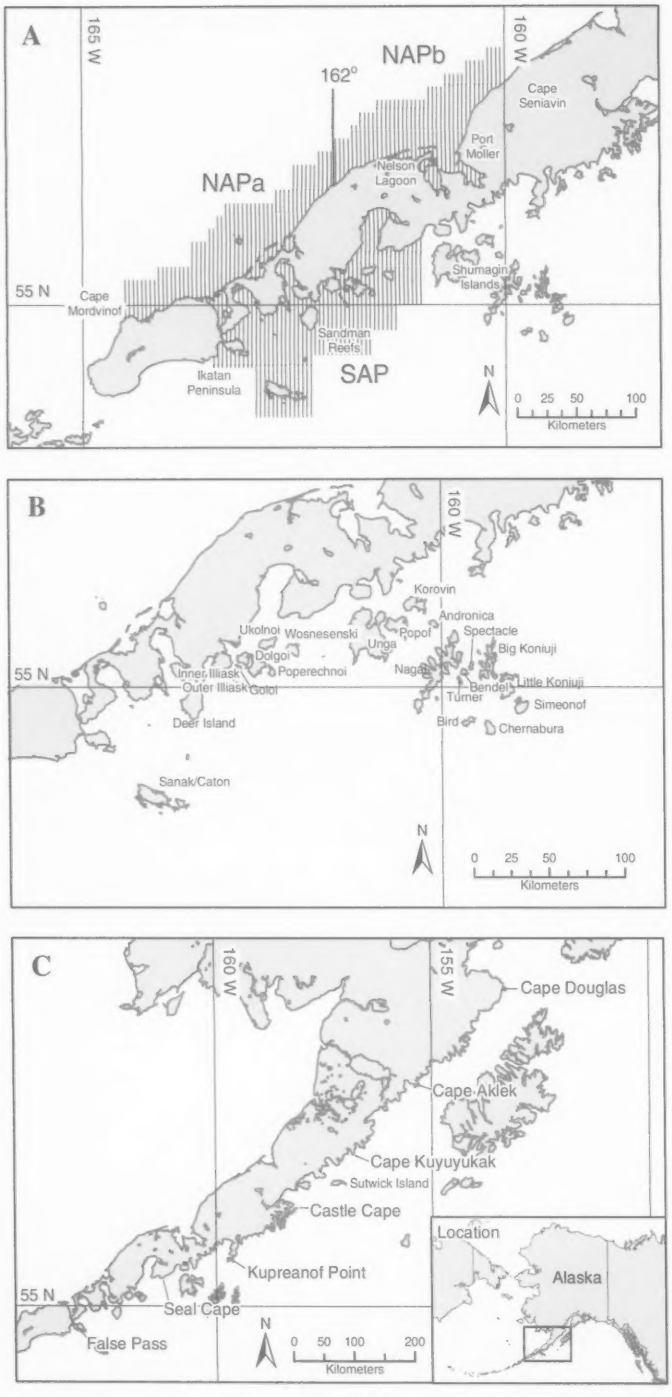

Figure 1

Sea otter (*Enhydra lutris*) survey areas along the Alaska Peninsula. (**A**) Offshore areas. (**B**) South Alaska Peninsula Islands. (**C**) Alaska Peninsula coastline. Surveyed areas in (B) and (C) include a 0.46-km zone adjacent to shore.

for estimating abundance. We calculated an encounter rate as the number of sea otter groups per km of survey effort and used this rate to examine the effects of time of day and environmental conditions (wave height, and visibility) on detectability of sea otters.

At the time of the surveys in 1986, researchers had documented a core resting period for sea otters which occurs about mid-day (Garshelis and Garshelis, 1984; Estes, 1977). As a result, Brueggeman et al.[1] subset the 1986 data using only effort and observations recorded between 0830 and 1430 hours local sun time for their abundance estimates. Recent studies indicate activity patterns for sea otters are strongly linked to sex, age, weather condition, season, and time of day (Gelatt et al., 2002). We tested the assumption that sea otters were more visible during the core resting period using a *t*-test of the encounter rate for each transect during presumed rest and nonrest periods for the 1986 and the 2000–01 data.

We measured the area of the NAP and SAP study areas using a geographic information system (Arc/Info). Our measurements differed from those of Brueggeman et al.,[1] presumably because the original researchers had not used an equal-area map projection in their calculations. Like Brueggeman et al.,[1] we estimated abundance of sea otters in the Alaska Peninsula offshore areas using the modified ratio of means estimator (method I) of Estes and Gilbert (1978). Noting computational errors in the original analysis, we recalculated abundance estimates from the original 1986 data of Brueggeman et al.[1] The proportion of sea otters within the survey swath that went undetected by observers was not estimated in either our survey or the surveys of Brueggeman et al.[1]; therefore all abundance estimates were biased low to an unknown degree. We computed the proportional change in abundance between survey periods ($(N_{t2}-N_{t1})/N_{t1}$) as a range, using the minimum and maximum estimates from 1986 as a baseline and assuming no significant difference in the proportion of sea otters detected between surveys.

Coastline survey analyses

We calculated the area surveyed as the product of the coastline length and the survey strip width and calculated the density of sea otters per km^2 surveyed. Once

again assuming no significant difference in the proportion of sea otters detected between surveys, we computed the proportional change in density between survey periods ($(D_{t2}-D_{t1})/D_{t1}$) of sea otter density at each island within the study area between 2001 and 1986 (Brueggeman et al.[1]) and each Alaska Peninsula coastline segment between 2001 and 1989 (DeGange et al.[2]).

Results

Offshore surveys

In 1986, Brueggeman et al.[1] flew four surveys and an average of 3676 km of transect effort per survey. The majority (59%) of the 1986 survey effort was conducted in Beaufort sea state 2 (wind less than 7.4–11.1 km/h, no whitecaps) or less; and 95% of the survey effort was conducted with visibility categorized as good or better. In May 2000 and April 2001, we flew 6334 km of transects and 56% of our effort was conducted in Beaufort sea state 2 or less; 97% of our effort was conducted in visibility categorized as good or better.

In 1986, sea otter detection probability was not uniform between sighting zones (χ^2=1796, df=2, P<0.0001) and substantially more sea otters were observed than expected in the 0.0–0.23 km distance zone (Fig. 2A). As a result, Brueggeman et al. (1988) used only this zone in their calculation of sea otter abundance. In our 2000–01 surveys, sea otter detection probability was also not uniform (χ^2=217, df=5, P<0.0001). The observed frequency of sea otter sightings exceeded the expected value in our second (0.115–0.230 km) and third zones (0.230–0.345 km) but in the first zone (0.0–0.115 km) we recorded only half as many sea otter sightings as in the second zone (Fig. 2B). Therefore, only sightings from the second and third zones were used in our calculation of sea otter abundance. As a result, the overall width of the survey strip was the same for the 1986 and the 2000–01 surveys (0.46 km), but our strip was offset by 0.115 km from the trackline. The proportion of all sea otter sightings was similar between the usable zones in 1986 (62.8%) and 2000–01 (62.4%).

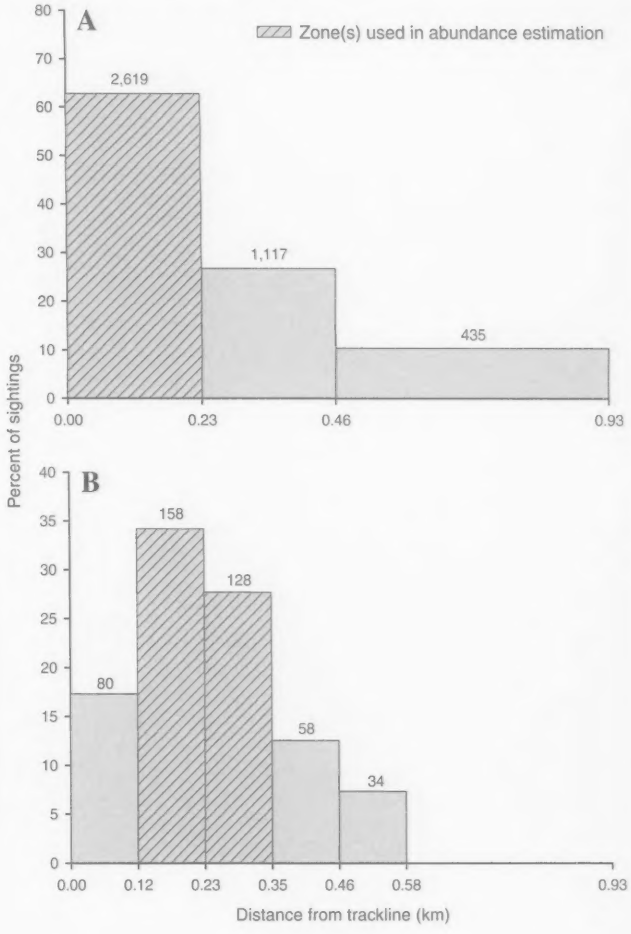

Figure 2

Distribution of sea otter (*Enhydra lutris*) sightings in offshore areas grouped according to perpendicular distance from the survey trackline. (**A**) 1986 data from Brueggeman et al.[1] (**B**) 2000–01 data from this study. Values above bars represent total number of sightings in each zone.

Sea otter encounter rate (otter groups/km) decreased as wave height increased and visibility conditions became worse in both the 1986 and 2000–01 surveys. As noted by Kenyon (1969), wave height has a profound influence on the ability of observers to detect sea otters. Prior to calculating abundance estimates for both 1986 and 2001, we subset both data sets to include only those transects where Beaufort sea state was ≤2 and visibility was categorized as good or excellent for counting sea otters. This procedure reduced the 1986 usable survey effort by 42%, and the 2000–01 survey efforts by 44%.

Sea otter encounter rates did not differ significantly between rest and nonrest periods in the 1986 data (t=1.63, df=79, P<0.1064). Likewise, there was no difference in encounter rates for rest and nonrest periods in 2000–01 (t=–0.79, df=71.6, P<0.4327). As a result, we did not exclude any survey effort and sea otter sightings based on time of day.

Table 1

Sea otter (*Enhydra lutris*) population estimates for Alaska Peninsula offshore study areas. Study areas: north Alaska Peninsula a [NAPa] = 6257 km^2; and b [NAPb] = 5531 km^2; south Alaska Peninsula [SAP] = 9469 km^2.

Survey area	Survey date	Total number of transects	Area sampled (km^2)	Number of otter groups	Density (groups/km^2)	Group abundance	Mean group size	Estimated abundance	95% confidence interval
NAPa	March 1986	35	446.2	243	0.545	3408	2.082	7096	±2558
	Late June–early July 1986	39	398.8	124	0.311	1945	2.177	4236	±1818
	August 1986	31	421.7	225	0.534	3338	2.169	7240	±2978
	October 1986	36	511.6	274	0.536	3351	1.982	6642	±2050
	May 2000	40	552.3	18	0.033	204	1.833	374	±318
NAPb	Late June–early July 1986	29	469.5	98	0.209	1155	1.939	2238	±840
	August 1986	6	120.4	23	0.191	1056	1.870	1975	±2212
	October 1986	14	314.3	42	0.134	739	1.214	897	±467
	May 2000	40	443.3	184	0.415	2296	1.897	4354	±3007
SAP	March 1986	26	358.3	254	0.709	6712	2.071	13,900	±6456
	Late June–early July 1986	33	424.8	227	0.534	5060	2.775	14,042	±5178
	October 1986	33	442.6	418	0.944	8943	1.957	17,500	±5768
	April 2001	38	631.2	22	0.035	330	3.045	1005	±1597

The estimated abundance of sea otters decreased by 91–94% in the NAPa study area, which ranged from 4236–7240 in 1986 to 374 in 2000 (Table 1). Estimated abundance increased by 95–385% in the NAPb study area, which ranged from 897 to 2238 in 1986 to 4354 in 2001. Overall, abundance estimates in the NAP study area declined by 27–49% between 1986 and 2000. Within the NAP area, sea otters were distributed primarily near the coast rather than further offshore as was observed in 1986 (Fig. 3). In May 2000, the majority of sightings occurred in the Port Moller and Nelson Lagoon areas, which had contained few otters during the 1986 surveys. Estimated abundance within the SAP study area declined by 93–94%, from 13,900–17,500 in 1986 to 1005 in 2001. Similar to the NAP results, areas that had previously supported dense aggregations of sea otters were largely vacant in 2001 and the areas of highest concentrations were in bays and lagoons.

Coastline survey analyses

Between 1986 and 1989 there was considerable variability in sea otter counts at islands in the south Alaska Peninsula study area (Table 2). Some areas had increased (Sanak, Caton, and the Pavlof Islands) while others decreased (Deer Island, Shumagin Islands). However by 2001, sea otter counts and density had decreased at nearly all islands and net losses of over 100 otters occurred at Deer, Dolgoi, Goloi, Unga, and Nagai islands. Overall, sea otter counts at these islands declined from 2174 in 1986 to 402 in 2001—a 63% decline in density.

In April and May 2001 we surveyed approximately 3800 km of coastline from Cape Douglas to False Pass (Table 3). Sea otter density in 2001 was 35% lower than in 1989 for the three westernmost coastline segments from False Pass to Castle Cape (1782 km of coastline). To the east of Castle Cape, sea otter density was 4% greater in 2001 than in 1989 (2018 km of coastline). These results indicate that an eastward extent of the decline along the Alaska Peninsula may occur in the area of Castle Cape. Overall, sea otter density declined by 12.4% along the coastline of the Alaska Peninsula from False Pass to Cape Douglas between 1989 and 2001.

Discussion

When compared to surveys conducted in 1986, our results indicated that sea otter abundance has declined severely in the SAP and NAPa study areas along the Alaska Peninsula, whereas sea otter abundance increased in the NAPb study area (specifically Port Moller) and east of Castle Cape along the south side of the Peninsula. To determine the geographic extent and magnitude of the sea otter population decline, current data were needed to assess population abundance and trends along the Alaska Peninsula.

Variations in survey methods limited our ability to assess population trends for the Alaska Peninsula prior to 1986. In 1976, the sea otter population along the NAP was estimated to be 17,000 and continued range expansion was expected (Schneider, 1976). In 1982–83, seasonal estimates of sea otter abundance in the NAP study area varied between March (1454), August (10,325), and October (1880) which led Cimberg et al.[2] to speculate that there was a large-scale seasonal migration of sea otters between the Bering Sea and North Pacific Ocean. Sea otter distribution and abundance

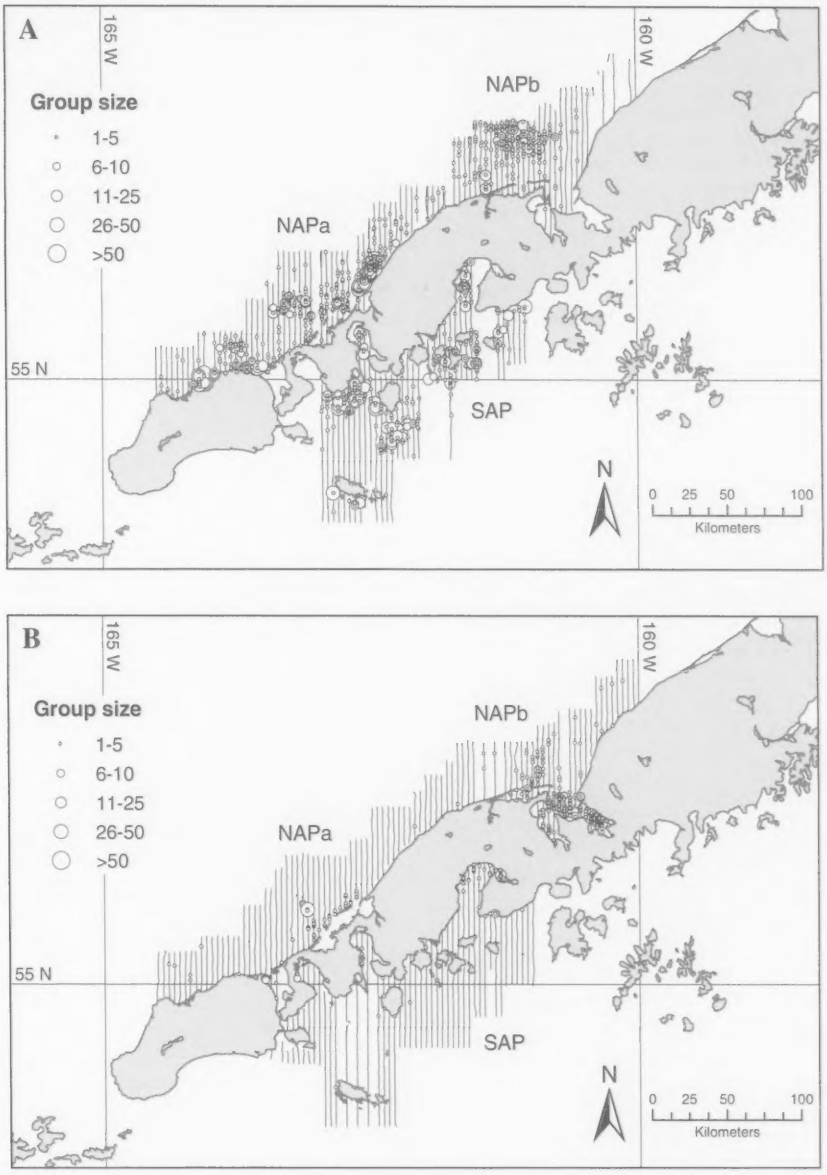

Figure 3

All survey transects and sea otter (*Enhydra lutris*) sightings in offshore areas. (**A**) Late June–early July 1986. (**B**) May 2000 (north Alaska Peninsula [NAP], a and b), April 2001 (south Alaska Peninsula [SAP]).

remained relatively constant over the spring, summer, and fall seasons for both the NAP and SAP study areas in 1986 which led Brueggeman et al.[1] to conclude that there was no indication that sea otters were redistributed from the northern to the southern Peninsula during the winter months. Instead, Brueggeman et al.[1] attributed the differences in the survey results between 1982–83 and 1986 to the viewing conditions and wind speed in which Cimberg et al.[2] conducted their March and October surveys. Although both the 1976 and 1983 estimates were adjusted for sea otters missed by observers, the 1986 estimates were not. Evans et al.[4]

Table 2

Alaska Peninsula island coastline lengths, sea otter (*Enhydra lutris*) counts, sea otter densities, and estimated population change. Survey strip width for the 1986 survey was 0.92 km, for 1989 it was 0.4 km, and for 2001 it was 0.46 km.

Island name	Coastline length (km)	Sea otters counted			Sea otter density (otters/km^2)			% change in density 1989–2001
		1986	1989	2001	1986	1989	2001	
Sanak and Caton	178	13	168	12	0.08	2.36	0.15	+84.6
Deer Island	61	245	71	19	4.35	2.90	0.67	–84.5
Dolgoi	94	185	93	15	2.14	2.47	0.35	–83.8
Goloi	14	113	62	1	8.77	11.07	0.16	–98.2
Inner Illiask	13	77	68	9	6.44	13.07	1.51	–76.6
Outer Illiask	17	82	305	4	5.24	44.85	0.51	–90.2
Wosnesenski	32	29	28	3	0.99	2.19	0.20	–79.3
Ukolnoi	38	54	133	21	1.54	8.75	1.20	–22.2
Poperechnoi	22	80	26	1	3.96	2.95	0.10	–97.5
Unga	231	568	275	182	2.67	2.98	1.71	–35.9
Popof	72	72	73	4	1.09	2.53	0.12	–88.9
Korovin	65	101	47	9	1.69	1.81	0.30	–82.2
Andronica	22	31	15	0	1.53	1.70	0.00	–100.0
Nagai	342	184	141	52	0.58	1.03	0.33	–43.5
Big Koniuji	160	52	18	33	0.35	0.28	0.45	+26.9
Turner and the Twins	16	6	9	0	0.41	1.41	0.00	–100.0
Bendel	17	35	7	2	2.24	1.03	0.26	–88.6
Spectacle	15	17	12	7	1.23	2.00	1.01	–17.6
Little Koniuji	95	65	20	0	0.74	0.53	0.00	–100.0
Simeonof	49	65	5	24	1.44	0.26	1.06	–26.2
Chernabura	30	20	2	0	0.72	0.17	0.00	–100.0
Bird	31	80	11	4	2.81	0.89	0.28	–90.0
Total	1614	2174	1589	402	1.46	2.46	0.54	–63.0

Table 3

Alaska Peninsula coastline segment lengths, sea otter (*Enhydra lutris*) counts, sea otter densities, and estimated population change. Survey strip width for the 1989 survey was 0.4 km; for 2001 it was 0.46 km.

Coastline segment 1989–2001	Coastline length (km)	Sea otters counted		Sea otter density (otters/km^2)		% change in density
		1989	2001	1989	2001	
False Pass to Seal Cape	715	622	461	2.17	1.40	–35.6
Seal Cape to Kupreanof Point	370	196	50	1.32	0.29	–77.8
Kupreanof Point to Castle Cape	697	48	25	0.17	0.08	–54.7
Castle Cape to Cape Kuyuyukak	639	1007	1193	3.94	4.06	+3.0
Cape Kuyuyukak to Cape Aklek	495	177	352	0.89	1.55	+72.9
Cape Aklek to Cape Douglas	814	570	497	1.75	1.33	–24.2
Sutwick Island	70	12	73	0.43	2.27	+429.0
Total	3800	2632	2651	1.73	1.52	–12.4

estimated that observers flying in a Twin Otter aircraft recorded 42% of the sea otters present within the area surveyed. Adjusting the 1986 results by this amount yields a range of 10,086–17,238; therefore the population may not have changed substantially between 1976 and 1986. By 2000 however, it is clear that sea otters had declined within the NAP study area, and although the data history for the SAP study area is even more sparse, there is little doubt that the population in this area has also declined severely since 1986.

The distribution of sea otters along the north side of the Alaska Peninsula is rather unique. Because of the broad shelf, large rafts of otters have been observed at distances of 50 km or more from shore. The area is also subject to seasonal sea ice that can have a profound impact on sea otter distribution, and in extreme ice years, result in significant mortality (Schneider and Faro, 1975). It is unclear if behavior and movement patterns in the NAP area are different from other areas in the north Pacific. In the 1960s and 1970s it was thought that sea otters along the northern Alaska Peninsula spent much, if not all, of their life in offshore waters (Kenyon, 1969; Lensink, 1962; Schneider, 1976). Cimberg et al.[2] suggested that sea otters may migrate through False Pass from the Bering Sea to the north Pacific Ocean during the winter months to avoid being trapped by shore-fast sea ice. Of the two study areas along the north side of the Alaska Peninsula, the NAPa study area located farther south and west is more likely to remain ice-free, and therefore may be important for the overall survival of sea otters in this area (Schneider and Faro, 1975). If sea otters remain concentrated throughout the year in Port Moller, which is in the NAPb study area, they may be vulnerable to mortality by extensive sea ice events in the future.

Information derived from sea ice data with spatial and temporal resolution suitable for evaluating the impacts of extensive sea ice on sea otters is not readily available. Detailed sea ice data for the NAP study area from the National Ice Center is only available for the period from 1997 to the present. In March 1999 shore-fast ice was present in both Port Moller and Izembek Lagoon, and nearshore areas were almost totally covered by sea ice. Similar conditions also occurred in January 2000. In both instances, sea otter mortality was reported by residents of Port Heiden, Alaska, located to the northeast of the NAP study area (Esslinger[5]; Snyder[6]). Human habitation in the NAP study area is extremely sparse in winter, which may explain why there were no reports of sea otter mortality in this area. Given the degree of sea ice present, it is possible that the extreme ice conditions in 1999 and 2000 may have resulted in the death of some sea otters within our study area. The geographic pattern of the decline does not exactly fit what would be expected from sea ice however, because the decline occurred in the NAPa study area, which is presumed to be less vulnerable to these events. Although it is possible that extreme sea ice conditions may have been a contributing factor, it was likely not the sole cause of the decline in the NAP study area.

In our surveys of the NAP study area, sea otter abundance declined severely in NAPa but had increased in NAPb. It is unclear to what degree otters may move between these respective study areas. Quarterly surveys in 1986 did not indicate seasonal changes in distribution between the NAPa and NAPb portions of the study area. Monnett et al.[7] used radio telemetry to study sea otter movements in the NAPa study area from 1986 through 1988 and found that study animals did not move between NAPa and NAPb or to the SAP study area as previously hypothesized by Cimberg et al.[2] The average distance between extreme locations was only 18.4 km; however, the sample size of sea otters in the Monnett et al.[7] study was small (n=14). The large concentration of sea otters observed in Port Moller and Nelson Lagoon in May 2000 may be a seasonal event; large numbers of sea otters are typically observed in that area in May, but disperse by June (Murphy[8]). Compared to the ecology of other areas, the ecology of sea otters along the north side of the Alaska Peninsula is poorly understood and additional study is warranted.

In addition to changes in abundance there were also changes in sea otter distribution in the 2000–01 surveys. In 1986, sea otters were observed up to 50 km from shore during all surveys. In the 1970s and 1980s, large rafts of up to 1000 sea otters were distributed well offshore (Kenyon, 1969; Schneider, 1976; Brueggeman et al.[1]). By 2001 sea otters were, with rare exception, located in bays and lagoons along the Peninsula rather than in the offshore habitat in both the NAP and SAP study areas. Estes et al. (1998) hypothesized that declines in sea otters in the Aleutian islands during the 1990s may have been caused by increased predation by killer whales (*Orcinus orca*). One line of evidence that led to this conclusion was a lower sea otter mortality in the sheltered area of Clam Lagoon than in the exposed area of Kuluk Bay on Adak Island. The observed distribution of sea otters within bays and lagoons along the Alaska Peninsula in 2000–01 is not inconsistent with the predation hypothesis of Estes et al. (1998). Alternatively, nearshore waters may constitute preferred

[4] Evans, T. J., D. M. Burn, and A. R. DeGange. 1997. Distribution and relative abundance of sea otters in the Aleutian archipelago. Tech. Rep. MMM 97-5, 29 p. U. S. Fish and Wildl. Serv. Mar. Mamm. Manage. Office 1011 E Tudor Road, Anchorage, AK 99503.

[5] George Esslinger. 1999. Personal commun. U.S. Geological Survey, Alaska Science Center. 1011 East Tudor Road, Anchorage, AK 99503-6103.

[6] Jonathan Snyder. 2000. Personal commun. U.S. Fish and Wildl. Serv., Mar. Mamm. Manage. Office, 1011 East Tudor Road, Anchorage, AK 99503-6103.

[7] Monnett, C., L. M. Rotterman, D. B. Sniff, and J. Sarvis. 1988. Movement patterns of western Alaska Peninsula sea otters. Minerals Management Service, OCSEAP (Offshore Continental Shelf Engineering Assessment Program) Research Unit 688, 51 p.

[8] Murphy, B. 2002. Personal commun. Alaska Department of Fish and Game, Division of Commercial Fisheries, 211 Mission Road, Kodiak, AK 99615-6399.

habitat for sea otters, and at low densities it is possible that these may be the only areas where they occur.

We are reasonably confident that the 2000–01 surveys yielded results that were comparable to baseline surveys because the methods were closely repeated. The difference in distribution of sea otter sighting zones may have been a result of different aircraft configurations. Although both aircraft were equipped with bubble windows, the size and shape of these windows were probably not identical. We accounted for any differences by selecting the zones best suited to estimate sea otter abundance for each survey period. In our data analysis, we also accounted for the effects of survey conditions (Beaufort sea state and viewing condition) in both data sets. Our results indicate that in addition to changes in sea otter abundance, distribution had changed markedly between study periods as well. Because sea otter distribution is currently concentrated closer to the coast, we recommend revising the survey design for future population surveys in this area. Rather than considering the offshore area as a single survey stratum, it would be more efficient to define nearshore and offshore survey strata and allocate survey effort accordingly.

To the west of the Alaska Peninsula study areas, the sea otter population in the Aleutian archipelago has declined to less than 10% of the estimated carrying capacity (Burn et al., 2003). Further westward in the Commander Islands, Russia, the sea otter population appears to have remained stable over the same time period (Burkanov and Burdin[9]). To the east of the Alaska Peninsula, sea otters have declined by an estimated 56% in the nearby Kodiak archipelago since 1989 (Doroff et al.[10]), but they appear to have remained relatively stable in the areas of Cook Inlet and Kenai Fiords (Bodkin et al.[11]) According to the most recent population surveys, the geographic extent of the sea otter decline does not appear to have exceeded the range of the southwest Alaska population stock as described by Gorbics and Bodkin (2001), where the overall decline has been estimated at 56–68%. Because the cause of the decline remains unknown, areas at the periphery of the current decline should be regularly monitored in the future. Given the close proximity between the Aleutian Islands and the Commander Islands, Russia, future research there may improve our understanding of the cause of the decline in southwest Alaska.

[9] Burkanov, V. N., and A. M. Burdin. 2002. Distribution and abundance of sea otter, steller sea lion, and killer whale in the Commander Islands (Russia) during 2002. North Pacific Wildlife Consulting, LLC Interim Report, 37 p. North Pacific Wildlife Consulting , 12600 Elmore Rd., Anchorage, AK 99516.

[10] Doroff, A. M., D. M. Burn, R. A. Stovall, and V. A. Gill. In prep. Unexpected population declines of sea otters in the Kodiak archipelago, Alaska.

[11] Bodkin, J. L. D. H. Monson, and G. E. Esslinger. 2003. A report on the results of the 2002 Kenai Peninsula and Lower Cook Inlet aerial sea otter survey, 10 p. U.S. Geological Survey, Alaska Science Center Report. 1011 East Tudor Road, Anchorage, Alaska 99503.

The sea otter decline, which has occurred over a broad geographic area, encompasses different habitat types in southwest Alaska. The Aleutian Island chain is primarily volcanic in origin and the majority of habitat for foraging (waters <40 m) is concentrated relatively near shore and is primarily a rocky substrate. The Alaska Peninsula includes extensive soft-sediment offshore habitat available to sea otters. Despite these differences, the declines in sea otter populations are similar between the Alaska Peninsula and the Aleutian archipelago in both severity and time period, which may imply a common cause. In addition to sea otters, severe declines of harbor seals (*Phoca vitulina*), Steller sea lions (*Eumetopias jubatus*), and fur seals (*Callorhinus ursinus*) have also been documented within the same general region, which suggests broader ecosystem-level changes may be involved. Our survey results, along with evidence of a declining sea otter population in the Kodiak archipelago, prompted the U.S. Fish and Wildlife Service to propose listing sea otters in southwest Alaska as threatened under the U.S. Endangered Species Act. The population decline in southwest Alaska is one of the most significant conservation issues for the sea otters in our time.

Acknowledgments

We thank the following individuals and organizations for their contributions to 2000-01 surveys: Linda Comerci, Thomas Evans, Susanne Kalxdorff, and Rosa Meehan for their work as observers and data recorders during survey operations; Ralph Aiken, Tom Blaesing, and Dave Weintraub for their incomparable piloting skills; Izembek National Wildlife Refuge manager Rick Poetter and his staff for logistical support. Jay Brueggeman and Greg Green provided the original 1986 aerial survey information and assisted with data interpretation. We thank John Haddix for assistance with GIS analysis of the 1986 survey data. We also thank James Bodkin, Verena Gill, Mark Udevitz, and two anonymous reviewers for comments on an earlier draft of this manuscript.

Literature cited

Burn, D. M., A. M. Doroff, and M. T. Tinker.
2003. Carrying capacity and pre-decline abundance of sea otters (*Enhydra lutris kenyoni*) in the Aleutian Islands. Northwest. Nat. 84:145–148.

Doroff, A. M., J. A. Estes, M. T. Tinker, D. M. Burn, T. J. Evans.
2003. Sea otter population declines in the Aleutian archipelago. J. Mammal. 84:55–64.

Estes, J. A.
1977. Population estimates and feeding behavior of sea otters. *In* The environment of Amchitka Island, Alaska (M. L. Merritt and R. G. Fuller, eds.), p. 511–526. U. S. Energy Resource and Development Administration, Springfield, VA.
1990. Growth and equilibrium in sea otter populations. J. Anim. Ecol. 59:385–401.

Estes, J. A., and J. R. Gilbert.
1978. Evaluation of an aerial survey of Pacific walruses (*Odobenus rosmarus divergens*). J. Fish. Res. Board Can. 53:1130–1140.

Estes, J. A., M. T. Tinker, T. M. Williams, and D. F. Doak.
1998. Killer whale predation on sea otters linking oceanic and near shore ecosystems. Science 282:473–476.

Garshelis, D. L., and J. A. Garshelis.
1984. Movements and management of sea otters in Alaska. J. Wild. Manag. 48(3):665–678.

Gelatt, T. S., D. B. Siniff, and J. A. Estes.
2002. Activity patterns and time budgets of the declining sea otter population at Amchitka Island, Alaska. J. Wild. Manag. 66:29–39.

Gorbics, C. S., and J. L. Bodkin.
2001. Stock structure of sea otters (*Enhydra lutris kenyoni*) in Alaska. Mar. Mamm. Sci. 17(3):632–647.

Kenyon, K. W.
1969. The sea otter in the eastern Pacific Ocean. N. Am. Fauna 68:1–352.

Lensink C. J.
1962. The history and status of sea otters in Alaska. Ph. D. diss., 188 p. Purdue Univ., West La Fayette, IN.

Schneider, K. B.
1976. Assessment of the distribution and abundance of sea otters along the Kenai Peninsula, Kamishak Bay, and the Kodiak archipelago. OCSEAP (Offshore Continental Shelf Engineering Assessment Program) final rep. no. 37, p. 527–626. Dept. of Commerce, National Oceanographic and Atmospheric Administration, Anchorage, AK.

Schneider, K. B., and J. B. Faro.
1975. Effects of sea ice on sea otters (*Enhydra lutris*). J. Mammal. 56:91–101.

Growth dynamics of the spinner shark (*Carcharhinus brevipinna*) off the United States southeast and Gulf of Mexico coasts: a comparison of methods

John K. Carlson

Ivy E. Baremore

Southeast Fisheries Science Center
National Marine Fisheries Service, NOAA
3500 Delwood Beach Road
Panama City, Florida 32408

E-mail address (for J. K. Carlson): john.carlson@noaa.gov

Abstract—The age and growth dynamics of the spinner shark (*Carcharhinus brevipinna*) in the northwest Atlantic Ocean off the southeast United States and in the Gulf of Mexico were examined and four growth models were used to examine variation in the ability to fit size-at-age data. The von Bertalanffy growth model, an alternative equation of the von Bertalanffy growth model with a size-at-birth intercept, the Gompertz growth model, and a logistic model were fitted to sex-specific observed size-at-age data. Considering the statistical criteria (e.g., lowest mean square error [MSE], high coefficient-of-determination, and greatest level of significance) we desired for this study, the logistic model provided the best overall fit to the size-at-age data, whereas the von Bertalanffy growth model gave the worst. For "biological validity," the von Bertalanffy model for female sharks provided estimates similar to those reported in other studies. However, the von Bertalanffy model was deemed inappropriate for describing the growth of male spinner sharks because estimates of theoretical maximum size (L_∞) indicated a size much larger than that observed in the field. However, the growth coefficient (k=0.14/yr) from the Gompertz model provided an estimate most similar to that reported for other large coastal species. The analysis of growth for spinner shark in the present study demonstrates the importance of fitting alternative models when standard models fit the data poorly or when growth estimates do not appear to be realistic.

Manuscript submitted 3 May 2004
to the Scientific Editor's Office.

Manuscript approved for publication
29 December 2004 by the Scientific Editor.

Fish. Bull. 103:280–291 (2005).

Virtually every study concerned with describing the growth of elasmobranchs uses the von Bertalanffy growth equation (von Bertalanffy, 1938), despite criticism of the model (Knight, 1968; Roff, 1980). A review of the existing literature from 1962 to 2002 indicates that only about 12% of the published papers concerned with elasmobranch age and growth provide or have examined an alternative model (I.E.B., unpubl. data). Most studies on elasmobranch age and growth have simply fitted the von Bertalanffy model to observed or back-calculated size-at-age data without much concern about goodness-of-fit. In addition, appropriate age-structured assessments require accurate measures of the growth coefficient (k) of the population when calculating, for example, indirect estimates of natural mortality. A complete study on the age and growth of a species may require the application of multiple growth models, especially when data do not appear to fit a given model (e.g., when there is no statistical significance or when there is poor goodness-of-fit) or when results do not appear to be biologically realistic.

The spinner shark (*Carcharhinus brevipinna*) is a cosmopolitan species occurring in warm-temperate areas of the Atlantic Ocean, the Indian Ocean, and the western Pacific Ocean (Compagno, 1984). Off the United States east and Gulf of Mexico coasts, the spinner shark is managed under a large coastal shark complex (NMFS, 1993). Sharks within this complex are considered to be relatively large, slow growing, long lived, and are currently overfished (Cortés et al.[1]).

Although Allen and Wintner (2002) recently examined the age and growth of the spinner shark off South Africa, the only existing information on spinner sharks from U.S. waters is from Branstetter (1987), who examined just 15 animals from the Gulf of Mexico. The purpose of the present study is to re-examine the age and growth dynamics of the spinner shark off the U.S. southeast and Gulf of Mexico coasts. We compare and contrast four growth models to determine the model that best describes the growth data of the spinner shark.

Materials and methods

Sharks (n=273) were collected from 1995 to 2003 in the U.S. Exclusive Economic Zone from Galveston, Texas to Key West, Florida, in the Gulf of Mexico and in the U.S. south Atlantic Ocean from Charleston, South Carolina, to West Palm Beach, Florida (Fig. 1). Precaudal (PC), fork (FL) or total (TL) length (cm) were measured, and sex and maturity state were determined for each shark. Total

[1] Cortés, E., L. Brooks, and G. Scott. 2002. Stock assessment of large coastal sharks in the U.S. Atlantic and Gulf of Mexico. Sustainable Fisheries Division contribution SFD-02/03-177, 64 p. Southeast Fisheries Science Center, 3500 Delwood Beach Rd., Panama City, FL, 32408.

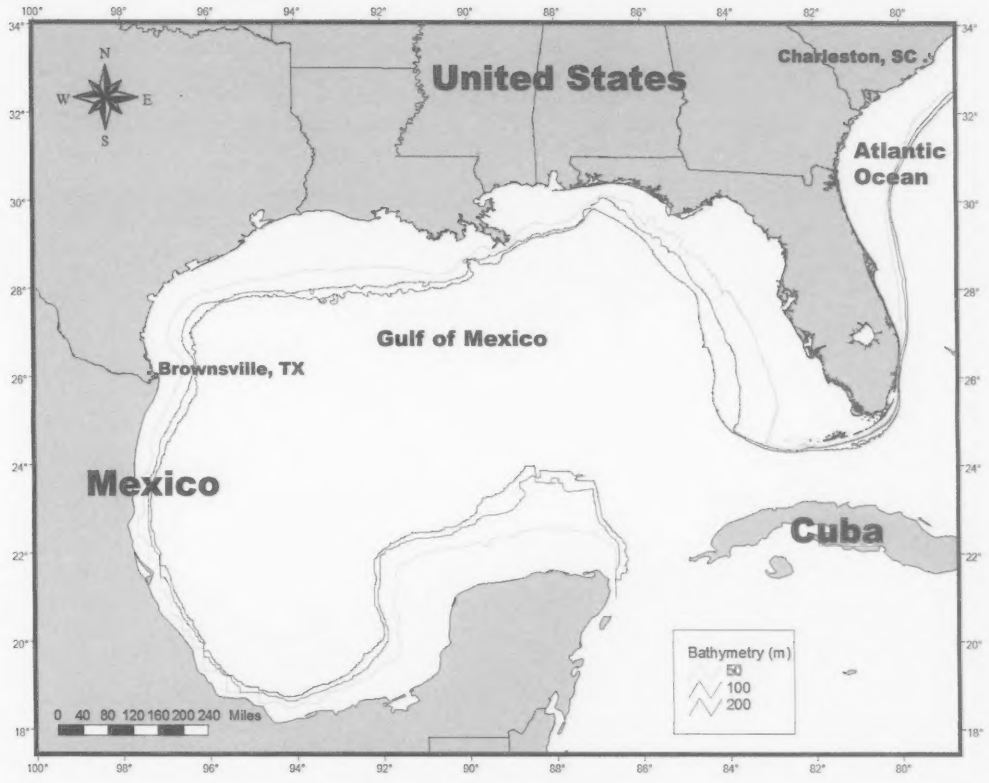

Figure 1

Map of the sampling area for spinner sharks (*Carcharhinus brevipinna*) showing areas and locations stated in the text.

length was measured as a straight line from the tip of the snout to the tip of the tail in a natural position. The weight (kg) of each shark was obtained when sampling conditions permitted. Vertebrae were removed from an area anterior to the first dorsal fin.

Vertebral sections were placed on ice after collection and frozen upon return to the laboratory. Thawed vertebrae were cleaned of excess tissue and soaked in a 5% sodium hypochlorite solution for 5–30 min to remove remaining tissue. After cleaning, vertebrae were soaked in distilled water for 30 minutes and stored in 95% isopropyl alcohol. Prior to examination, one vertebra from each shark was chosen at random, removed from alcohol, and dried. The vertebra was fixed to a clear glass slide with resin and sectioned with a Buehler 82 Isomet low-speed saw.

Sagittal sections of different thicknesses were cut from the vertebral centrum and stained with crystal violet, or alizarin red, or left unstained according to the methods of Carlson et al. (2003). Each vertebral section was mounted on a glass microscope slide with ProTex cytoseal (Lerner Laboratories, Pittsburg, PA) and examined by using a dissecting microscope under transmitted light. The banding pattern was found to be most apparent on unstained sagittal sections with a thickness of 0.3 mm.

Opaque bands representing summer growth and translucent bands representing winter growth were identified following the description and terms in Cailliet and Goldman (2004) (Fig. 2). Because no validation is available for this species, verification of the annual period of band formation was performed by using the relative marginal increment analysis (Branstetter and Musick, 1994; Natanson et al., 1995):

$$MIR = (VR - R_n)/(R_n - R_{n-1}),$$

where MIR = the marginal increment ratio;
VR = the vertebral radius;
R_n = distance to the outer edge of the last complete band; and
R_{n-1} = distance to the outer edge of the next-to-last complete band.

Mean MIR was plotted against month to determine trends in band formation. A single factor analysis of variance was used to test for differences in arcsine-transformed (Zar, 1984) MIR data among months.

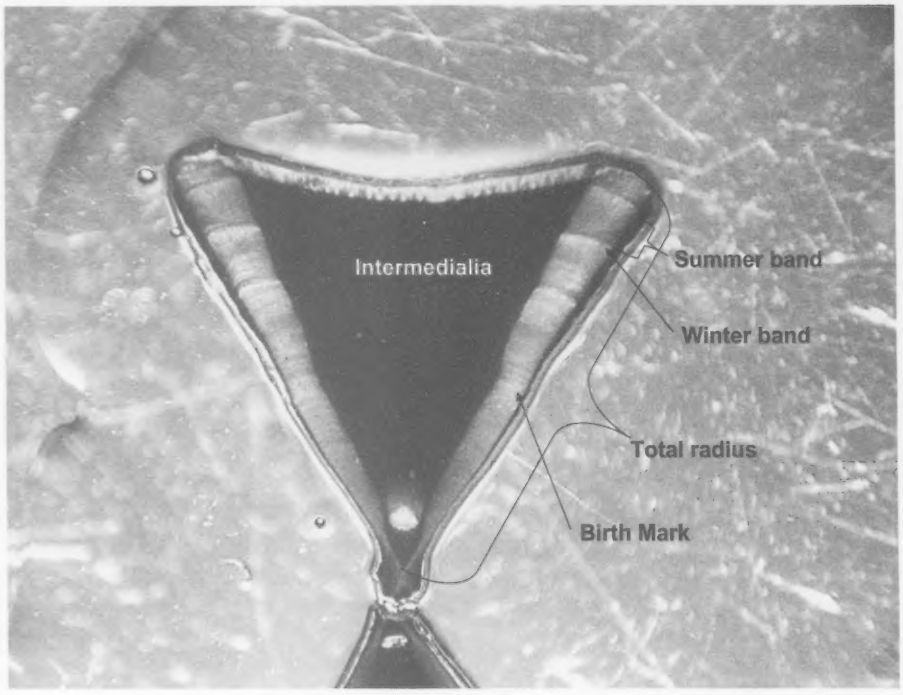

Figure 2

Sagittal section from a 3.5+ year-old spinner shark (*Carcharhinus brevipinna*) illustrating the banding pattern and winter marks (annuli) used to assign age.

Both authors randomly read vertebrae independently without knowledge of sex or length of specimens. Vertebral age estimates for which the readers disagreed were reread simultaneously by using a digital camera and software (Pixera Studio version 2, Pixera Corporation, Los Gatos, CA). If no agreement between readings was reached, samples were discarded.

Several methods were used to evaluate precision and bias among age determinations following the recommendations in Cailliet and Goldman (2004). Percent agreement (PA=number agreed/number read)×100 and percent agreement plus or minus one year were calculated for 10 cm (e.g. 76–85 cm FL) length intervals to evaluate precision (Goldman, 2002). The index of average percent error (APE: Beamish and Fournier, 1981) was calculated to compare the average deviation of readings from the means of all readings for each vertebral section:

$$IAPE = \frac{1}{n}\sum_{j=1}^{N}\left[\frac{1}{r}\sum_{i=1}^{R}\frac{\left|x_{ij}-x_j\right|}{x_j}\right],$$

where n = number of sharks aged;
r = number of readings;
x_{ij} = i^{th} age estimation of j^{th} shark at i^{th} reading; and
x_j = mean age calculated for the j^{th} shark.

Chi-square tests of symmetry following Hoenig et al. (1995) were used to determine if differences between readers were systematic or due to random error.

Several models were fitted to sex-specific observed size-at-age data to estimate the growth dynamics in spinner shark. Although back-calculated size-at-age length data would increase sample sizes for some ages (Cailliet, 1990), multiple back-calculated lengths-at-age are not independent samples and violate statistical assumptions in estimating parameters for a growth model (Vaughan and Burton, 1994). Vaughan and Burton (1994) pointed out that estimates of the model parameters may be biased because multiple back-calculated lengths cause an inaccurate number of degrees of freedom. Thus, we used data only from observed size-at-age.

In developing theoretical growth models, we assumed that 1) the birth mark is the band associated with a pronounced change in angle in the intermedialia, and we assigned an arbitrary birth date of 1 June, the approximate mid-point date when neonates were present in field collections, 2) translucent bands representing

winter growth form approximately six months later (i.e., 0.5 years) and 3) subsequent translucent bands representing winter growth form at yearly intervals, thereafter. Thus, ages (yr) were calculated by following the algorithm of Carlson et al. (1999): *age = birth mark + number of translucent winter bands* − 1.5. If only the birth mark was present, the age was 0+ years. All age estimates from growth band counts were based on the hypothesis of annual growth band deposition (Branstetter, 1987).

The von Bertalanffy growth model (von Bertalanffy, 1938) is described by using the equation

$$L_t = L_\infty(1-e^{-k(t-t_0)},$$

where L_t = mean fork length at time t;
L_∞ = theoretical asymptotic length;
k = growth coefficient; and
t_0 = theoretical age at zero length.

An alternative equation of the von Bertalanffy growth model, with a size-at-birth intercept rather than the t_0 parameter (Van Dykhuizen and Mollet, 1992, Goosen and Smale, 1997; Carlson et al., 2003) is described as

$$L_t = L_\infty(1-be^{-kt}),$$

where b = $(L_\infty - L_0)/L_\infty$; and
L_0 = length at birth.

Estimated median length at birth for spinner shark is 52 cm FL (Carlson, unpubl. data).

We also used the modified form of the Gompertz growth model (Ricker, 1975). The model is expressed following Mollet et al. (2002) as

$$L_t = L_0\left(e^{G(1-e(-kt))}\right),$$

where $G = \ln(L_0/L_\infty)$.

For the Gompertz model, the estimated median asymptotic length for spinner shark is 220 and 200 cm FL for females and males, respectively (Carlson, unpubl. data).

A logistic model (Ricker, 1979) was also considered in the form

$$W_t = W_\infty/(1+e^{-k(t-a)}),$$

where W_t = mean weight (kg) at time t;
W_∞ = theoretical asymptotic weight;
k = (equivalent to g in Ricker, 1979) instantaneous rate of growth when $w \rightarrow 0$; and
a = (equivalent to t_0 in Ricker, 1979) time at which the absolute rate of increase in weight begins to decrease or the inflection point of the curve.

If weight was not available, length was converted to weight by using the regression: $weight = 0.0000209 \times FL^{2.9524}$ (n=226, r^2=0.98, range: 1.1–66.1 kg).

Table 1

A summary of the number of spinner sharks (*Carcharhinus brevispinna*), by month and sex, used for our estimates of age.

Month	Male	Female
January	8	3
February	0	0
March	0	13
April	0	3
May	25	6
June	15	47
July	35	22
August	30	35
September	4	13
October	0	0
November	0	0
December	0	0

All growth model parameters were estimated with Marquardt least-squares nonlinear regression. All models were implemented by using SAS statistical software (SAS version 6.03, SAS Institute Inc., Cary, NC). The goodness-of-fit of each model was assessed by examining residual mean square error (MSE), coefficient-of-determination (r^2), F from analysis of variance, level of significance (P<0.05), and standard residual analysis (Neter et al., 1990).

Results

Morphometric relationships were developed to convert length measurements. Linear regression formulae were determined as PC=0.880(FL)+1.503, n=163, r^2=0.88, P<0.0001; and FL=0.847(TL)−3.497, n=260, r^2=0.99, P<0.0001.

Of the original 273 samples, 14 were deemed unreadable and were discarded (Table 1). The index of average percent error for the initial reading between authors was 10.6%. When grouped by 10-cm length intervals, agreement for combined sexes was reached for an average of 30.2% and 58.2% (±1 band) of band counts for sharks less than 115 cm FL (Table 2). Above 115 cm FL, agreement was reached for 33.5% and 74.0% (±1) of band counts for samples initially read. Hoenig's et al. (1995) test of symmetry indicated that there was bias between readers (χ^2=98.33, df=40, P<0.001).

Relative marginal increment analysis indicated that bands form annually during winter months (Fig. 3). The smallest relative increment was found in January and the greatest in July. The relative marginal increment ratio increased through spring months (March–May), peaked in summer (June–August), and then declined to fall. However, no statistical difference was found in MIR

values among months (F=1.63, df=7, P=0.129), likely because of the large variation in increment by months.

Under the statistical criteria established in our study, all growth models fitted the data well (Table 3). For males and females, models were highly significant (P<0.001) and exhibited high coefficients of determination (r^2≥0.88). Residual mean square error (MSE) was lowest for the logistic models. Notably, MSE was much higher for the von Bertalanffy model males than for any other model. Plots of the residuals against predicted sizes indicated no pattern in the residuals for any model. The standard deviation of the residuals was lowest for the logistic models (Table 3).

Estimates of the asymptotic size varied depending on sex and model (Table 3; Figs. 4 and 5). For males, the highest asymptotic length was produced by the von Bertalanffy model (L_∞=421 cm FL), intermediate lengths came from the von Bertalanffy model with a size-at-birth intercept (L_∞=279 cm FL) and the Gompertz model (L_∞=200, G=1.38), and lowest length was produced by the logistic model (W_∞=60.2 kg, ~161 cm FL). For females, asymptotic sizes were highest and similar with the von Bertalanffy, von Bertalanffy model with a size-at-birth, and the Gompertz models (226, 202, and 220 cm FL, respectively) and lowest with the logistic model (62.6 kg or ~162 cm FL).

Among models with comparable growth coefficients, the von Bertalanffy model produced the lowest growth coefficient for both males and females (k=0.03 and 0.08/yr, respectively). Growth coefficients were higher and fairly similar for the other two length models. The growth coefficient from the logistic weight model was 0.44 and 0.37 for males and females, respectively.

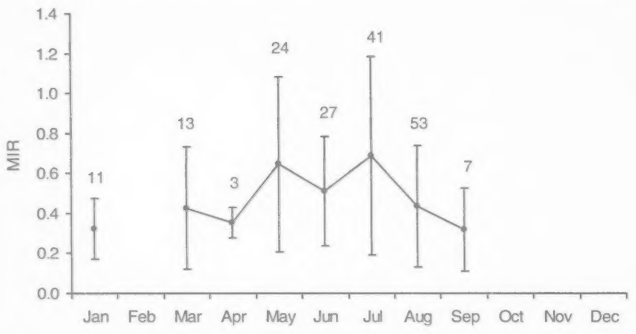

Figure 3

Mean marginal increment analysis (MIR) by month for combined sexes of spinner sharks (*Carcharhinus brevipinna*). Vertical bars are ± the standard deviation of the mean and numbers above each month represent the sample size.

Table 2

Percent agreement and percent agreement (±1 band) from the initial set of readings for spinner shark (*Carcharhinus brevispinna*).

	Sexes combined			Males			Females		
FL interval	Total read	Percent agreement	Percent agreement ±1 band	Total read	Percent agreement	Percent agreement ±1 band	Total read	Percent agreement	Percent agreement ±1 band
46–55	8	75.0	100.0	2	100.0	100.0	6	66.7	100.0
56–65	62	32.3	83.9	25	20.0	64.0	37	40.5	81.1
66–75	10	20.0	60.0	4	0.0	50.0	6	33.3	66.7
76–85	36	30.6	66.7	17	29.4	47.1	19	31.6	84.2
86–95	28	14.3	28.6	13	23.1	30.8	15	6.7	26.7
96–105	15	20.0	40.0	5	0.0	40.0	10	30.0	40.0
106–115	21	19.0	28.6	10	10.0	20.0	11	27.3	36.4
116–125	16	37.5	68.8	10	40.0	90.0	6	33.3	33.3
126–135	12	41.7	75.0	2	50.0	50.0	10	40.0	80.0
136–145	5	60.0	100.0	5	60.0	100.0	0	—	—
146–155	10	40.0	60.0	6	50.0	83.3	4	25.0	25.0
156–165	12	41.7	58.3	8	62.5	87.5	4	0.0	25.0
166–175	11	36.4	63.6	4	50.0	75.0	7	28.6	57.1
176–185	12	16.7	66.7	6	33.3	83.3	6	0.0	50.0
186–195	1	0.0	100.0	0	—	—	1	0.0	100.0

The Gompertz model estimated size-at-birth (61 cm FL) within the range reported for spinner sharks. Size-at-birth off the United States southeast and Gulf of Mexico coasts has been reported to range from 50 to 65 cm FL depending on the study (Branstetter, 1987; Castro, 1993; Carlson, unpubl. data).

Observed size-at-age and longevity were different between males and females (Table 4). For most ages, females were larger. The oldest animals aged were 17.5+ years (female) and 13.5+ years (male).

Discussion

Considering our statistical criteria (e.g., lowest MSE, high r^2, and level of significance), logistic models provided the best fits to the size-at-age data. The von Bertalanffy growth models, on the other hand, gave the worst fits. However, the criteria used to evaluate the models in this study may not be adequate. Because statistical fits have not been reported by other elasmobranch age and growth studies, we were not able to compare our criteria with other studies. Although not directly comparable, goodness-of-fit criteria used to select the best nonlinear gastric evacuation models have employed a combination of r^2, residual sum of squares, standard deviation, or coefficient of variation of residuals (review in Cortés, 1997). Until a more rigorous criterion is developed for growth models, efforts should continue to identify a best-fitting growth model.

We feel the von Bertalanffy model is inappropriate for describing the growth of male spinner shark. Asymptotic values indicated an unreasonable theoretical maximum size of 421 cm FL—much larger than sizes from recent fishery-dependent and fishery-independent sources (176–220 cm FL; Grace and Henwood, 1997; Morgan[3]; Carlson, unpubl. data). Asymptotic values from other models approach those actual values. Because of the relationship between k and L_∞, the von Bertalanffy growth coefficient was also much lower than expected. The growth coefficient from the Gompertz model was 0.14/yr, similar to those reported for other large coastal species in general (Cortés, 2000) and to those reported by Allen and Wintner (2002) for spinner sharks from South Africa.

The poor statistical fit and unrealistic biological estimates of the von Bertalanffy growth model for male spinner shark illustrates the importance of fitting alternative models to the data when estimates do not appear to be biologically real. Although sample size was well represented for most ages, the von Bertalanffy growth model did not reach an asymptote until well beyond the

[3] Morgan, A. Personal commun. Program for Shark Research, Florida Museum of Natural History, Univ. Florida, P.O. Box 117800, Gainesville, FL, 32611.

Table 3

Estimates of growth and goodness-of-fit from four growth models fitted to observed size-at-age data for male and female spinner sharks (*Carcharhinus brevispinna*). Values in parentheses are standard errors. L_0 = size at birth. The standard deviation (SD) of the residuals is from standard residual analysis. MSE=mean square error. n/a=not available.

Model	Asymptotic size[1] (cm FL)	Growth coefficient (/yr)	t_0[2] (yr)	L_0 (cm FL)	F	P	r^2	MSE	SD of residuals
Male									
von Bertalanffy	421.0 (±157.6)	0.03 (±0.02)	−4.58 (±0.65)	—	543.91	<0.001	0.91	543.91	11.91
von Bertalanffy with size-at-birth	279.1 (±39.4)	0.07 (±0.02)	n/a	52	946.24	<0.001	0.89	163.65	12.49
Gompertz	200 (G=1.38±0.09)	0.14 (±0.02)	n/a	60.5 (±1.9)	557.83	<0.001	0.91	141.23	11.78
Logistic	60.2 (±39.4)	0.44 (±0.05)	6.75 (±0.47)		483.00	<0.001	0.93	47.44	6.83
Female									
von Bertalanffy	226.2 (±18.6)	0.08 (±0.02)	−3.84 (±0.40)	—	612.20	<0.001	0.90	150.70	12.19
von Bertalanffy with size-at-birth	202.7 (±10.9)	0.11 (±0.01)	n/a	52	1047.19	<0.001	0.88	173.07	12.78
Gompertz	220 (G=1.17±0.4)	0.16 (±0.02)	n/a	60.7 (±1.6)	609.09	<0.001	0.90	151.39	12.21
Logistic	62.6 (±3.2)	0.37 (±0.03)	7.62 (±0.43)		572.84	<0.001	0.93	43.82	6.57

[1] Asymptotic size for the von Bertalanffy, von Bertalanffy with size-at-birth, and Gompertz models are in cm, whereas asymptotic size for the logistic model is in kg.

[2] t_0 is the theoretical age at zero length for the von Bertalanffy whereas t_0 for the logistic model represents time at which the absolute rate of increase in weight begins to decrease.

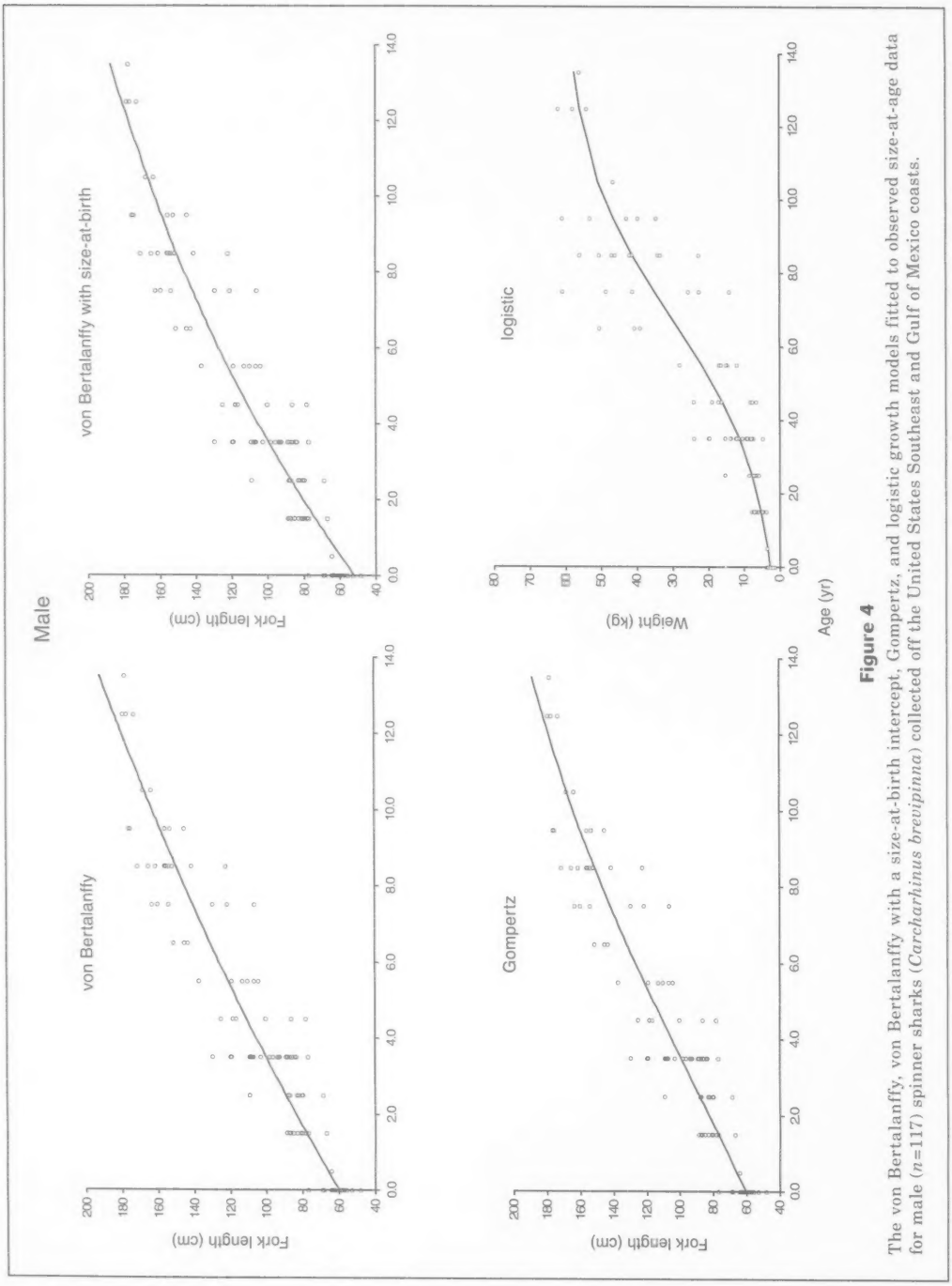

Figure 4

The von Bertalanffy, von Bertalanffy with a size-at-birth intercept, Gompertz, and logistic growth models fitted to observed size-at-age data for male (n=117) spinner sharks (*Carcharhinus brevipinna*) collected off the United States Southeast and Gulf of Mexico coasts.

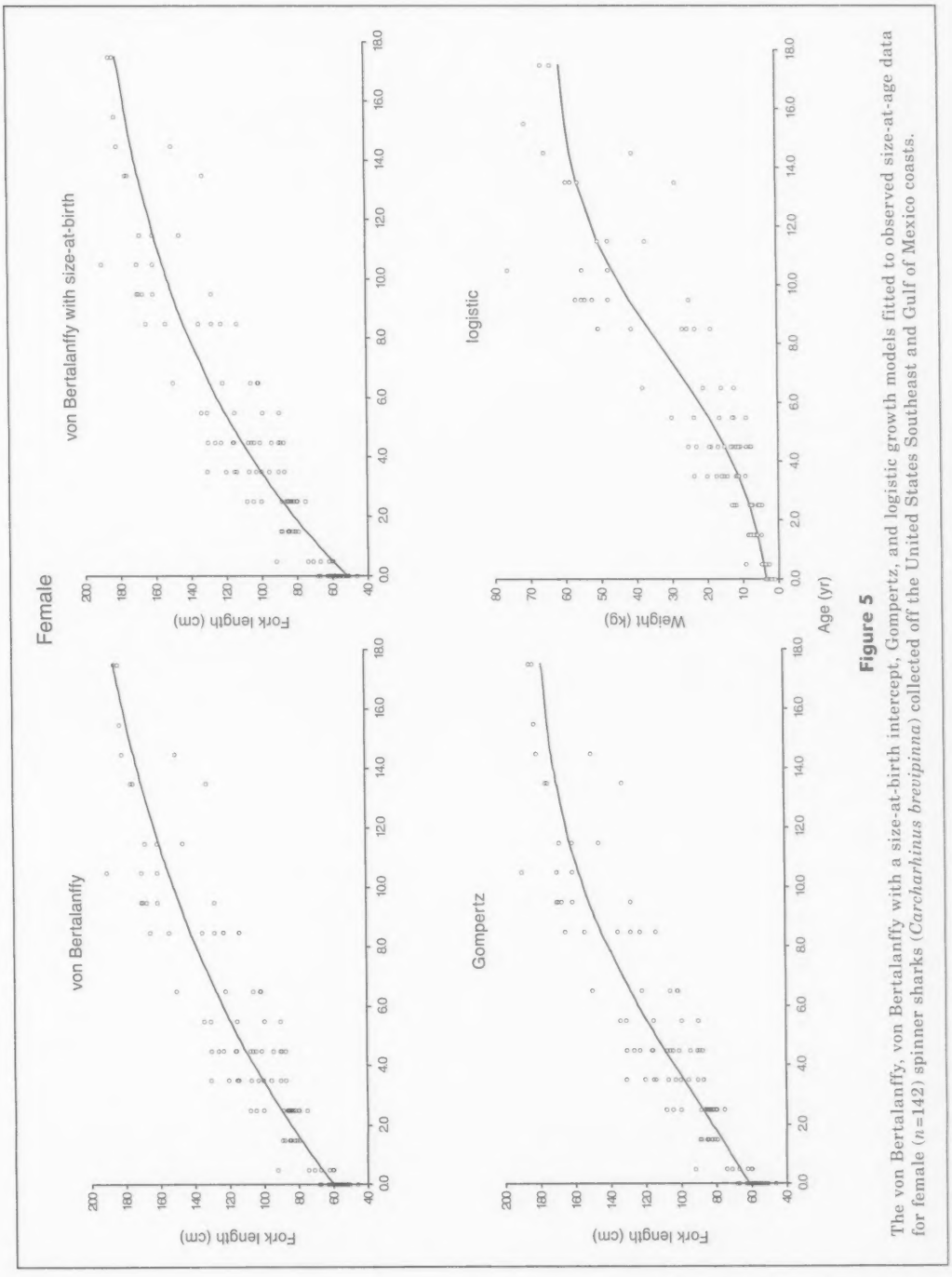

Figure 5

The von Bertalanffy, von Bertalanffy with a size-at-birth intercept, Gompertz, and logistic growth models fitted to observed size-at-age data for female (n=142) spinner sharks (*Carcharhinus brevipinna*) collected off the United States Southeast and Gulf of Mexico coasts.

Table 4

Mean size-at-age (cm FL) for male and female spinner sharks (*Carcharhinus brevispinna*). SD=standard deviation.

	Age (yr)																	
	0.0	0.5	1.5	2.5	3.5	4.5	5.5	6.5	7.5	8.5	9.5	10.5	11.5	12.5	13.5	14.5	15.5	16.5	17.5
Male																			
Size	60.7	64.1	81.2	84.6	99.9	105.8	115.5	146.3	138.9	154.2	165.3	165.9	—	176.3	178.0	—	—	—	—
SD	5.3		5.9	11.4	13.8	17.9	11.0	4.2	23.4	13.9	13.4	3.0	—	3.1		—	—	—	—
n	29	1	12	8	21	7	7	3	6	10	7	2	—	3	1	—	—	—	—
Female																			
Size	59.0	69.3	84.4	86.9	106.9	106.9	117.1	116.2	—	136.3	160.8	173.7	158.3	—	164.7	165.5	182.0	—	184.0
SD	4.1	11.5	2.9	8.7	13.3	13.9	19.1	20.7	—	19.6	16.4	14.8	11.2	—	21.7	21.9	—	—	1.4
n	42	7	12	18	11	14	6	5	—	6	6	3	3	—	4	2	1	—	2

expected maximum size, resulting in an inflated asymptote and low growth coefficient. Branstetter and Stiles (1987) also encountered this problem with bull sharks (*Carcharhinus leucas*) but rather than fit an alternative growth model, those authors hand-fitted a curve through the upper data points. Results such as these may seriously bias estimates of k and any resulting population models because several indirect estimates of natural mortality (M) and longevity rely heavily on accurate estimates of k from a growth model (Fabens, 1965; Pauly, 1980; Chen and Watanabe, 1989; Jensen, 1996). For example, the method of Jensen (1996) for estimating M yields values ranging from 0.05/yr (with results from the von Bertalanffy model) to 0.23/yr (with results from the Gompertz model). Similarly, theoretical longevity estimates determined by the method of Fabens (1965) are 115.5 years and 21.6 years from the von Bertalanffy model and the Gompertz model, respectively.

In general, our estimates of age and growth for female spinner sharks from the von Bertalanffy model were similar to those reported by Allen and Wintner (2002) for spinner sharks collected off South Africa. Growth coefficients in their study were about 0.13/yr, L_∞ was 250 cm FL, and observed longevity for females was up to 19+ years. Branstetter (1987), in his study on sharks collected in the Gulf of Mexico, reported an observed longevity up to 11+ years (combined sexes) and growth coefficients of about 0.21/yr. Because differences in life history traits (e.g., growth rates, size and age at maturity) between populations of blacktip and bull sharks from South Africa and United States waters have been proposed (Wintner and Cliff, 1995; Wintner et al., 2002, respectively), results from our study for spinner shark may be expected to be more similar to those of Branstetter (1987) rather than those of Allen and Wintner (2002). Although techniques (e.g., counting winter bands on sagittal vertebral sections) in Branstetter (1987) were similar to ours, the differences are likely a result of low sample size in the earlier study.

The index of average percent error (IAPE) in aging was at the higher end of the range of estimates provided in other studies that also used sagittal sections for aging. Values have been reported as low as 3.0% for the oceanic whitetip shark (*Carcharhinus longimanus*) (Lessa et al., 1999), and up to 13.0% for the blacktip shark (*Carcharhinus limbatus*) (Wintner and Cliff, 1995). Although IAPE indices are most commonly used to evaluate precision among age determinations, IAPE does not test for systematic differences and does not distinguish all sources of variation (Hoenig et al., 1995). In addition, comparing IAPE values among studies may not be valid unless the study species is the same and from the same geographic area (Cailliet and Goldman 2004).

Although bands were readily discernible in most samples, the inexperience of one of the authors (reader 2) in reading and counting vertebral bands likely led to the higher IAPE and systematic bias. Generally, most systematic bias is a shift to increasing or decreasing counts with age (Morison et al. 1998), yet the bias in this study was the result of reader 2 consistently over aging sharks from the final agreed age regardless of the band count of the sample. Percent agreement was similar for samples above 115 cm FL as it was for samples below this size. Although a reference collection was aged by reader 2 prior to beginning this study, finely honed skills through experience are key elements in the technique of aging.

The trend in marginal increment analysis indicated that band formation occurs once a year during winter months—a result common to most studies where relative marginal increment analysis is used for carcharhinid sharks (e.g., Natanson et al., 1995; Carlson et al., 1999; Carlson et al., 2003). However, high variance in marginal increment analysis (MIR) within each month resulted in months not being statistically different, which is a widespread occurrence when using this method. Marginal increment analysis has been criticized as one of the most abused methods for validation of band formation (Campana, 2001). Problems with differentiating bands on the vertebral edge and application to older age classes may provide misleading results (Campana,

2001). Other methods have been used recently to report yearly band formation in sharks, including oxytetracycline marking (Simpfendorfer et al., 2002; Skomal and Natanson, 2003; Driggers et al., 2004) and bomb radiocarbon methods (Campana et al., 2002). However, validation exists for relatively few elasmobranch species (Cortés, 2000).

Two-phase growth models may be more appropriate for describing the growth of sharks, especially those that are longer lived. Soriano et al. (1992) developed a biphasic growth model which they applied to the long-lived Nile perch (*Lates niloticus*) to better describe their change in growth from zooplanktivores as juveniles to piscivores as adults. Growth by sharks could be regarded as being found in two phases: a rapid juvenile growth followed by a slower adult growth. From a bioenergetic perspective, this would follow a change from energy devoted to growth to energy devoted to reproduction. The logistic model could be regarded as a two-phase model and may help to describe this change. The shift from juvenile to adult would correspond to the inflection point (t_0) of the curve, which approximates biological age-at-maturity. In spinner sharks, age at maturity was reported to be about 6–7 years for males and 7–8 years for females (Branstetter, 1987). This estimate of age-at-maturity is similar to the inflection points from our logistic model of 6.75 and 7.62 years for males and females, respectively. Although each species should be evaluated separately, future studies should investigate the use of two-phase models to provide a more accurate description of the growth of elasmobranchs.

There have been few other examples of fitting alternative growth models to size-at-age data when results from the von Bertalanffy model were biologically incorrect or when models did not fit the data well. The present study represents the first attempt to do so for a species of shark. Comparison of age and growth models by Mollet et al. (2002) and Neer and Cailliet (2001) for two species of rays revealed that the Gompertz model best described their respective data although all models they tested fitted the data fairly well. For pelagic stingray (*Dasyatis violacea*) the Gompertz model predicted a more reasonable size-at-birth and growth rate than the von Bertalanffy growth model (Mollet et al., 2002). Neer and Cailliet (2001) reported a slightly better statistical fit for the Pacific electric ray (*Torpedo californica*) when using the Gompertz model. However, because the difference in model parameters was negligible, results were reported only for the von Bertalanffy model.

The von Bertalanffy growth model is still the most common model used to describe growth in fisheries literature, despite criticism by Roff (1980) who recommended its retirement. As pointed out by Roff (1980), the choice of using another equation should be determined by the variables that are being investigated and the results that are produced by the equation; for example, if the results appear to be biologically unrealistic. Our analysis of the growth of the spinner shark clearly demonstrates the value of this approach. Use of the von Bertalanffy growth model should continue because it permits comparison of growth curves to information already published and in some cases adequately describes the growth of a given organism. However, the variety of statistical techniques and quality of each study make comparisons of von Bertalanffy growth curves between different populations difficult and results should be interpreted with caution regardless of what growth model is used (Roff, 1980).

Acknowledgments

We thank Enric Cortés, Pete Sheridan (NOAA Fisheries, Panama City Laboratory), and Miguel Arraya (Universidad Arturo Prat, Chile) for providing comments on earlier versions of this manuscript. Ken Goldman (Jackson State University) was especially helpful in discussion on precision and bias in age estimation, Miguel Arraya on the validity of the comparison of growth models, and Henry Mollet (Monterey Bay Aquarium) with the Gompertz model. Many different laboratories and institutions aided with the collection of vertebrae. George Burgess and Matt Callahan (University of Florida) provided samples from the directed shark longline fishery. Lisa Natanson (NOAA Fisheries, Narragansett Laboratory) obtained samples during their longline surveys from the U.S. south Atlantic Ocean. Observers Armando de ron Santiago, Carl Greene, Matt Rayl, Bill Habich, Mike Farni, Jacques Hill, and Jeff Pulver collected samples from the directed shark gillnet fishery. Mark Grace and Lisa Jones (NOAA Fisheries, Pascagoula Laboratory) provided samples from fishery-independent longline surveys. We also thank Linda Lombardi, Lori Hale, and numerous interns who assisted with the cleaning and processing of vertebrae samples.

Literature cited

Allen, B. R. and S. P. Wintner.
2002. Age and growth of the spinner shark *Carcharhinus brevipinna* (Müller and Henle, 1839) off the Kwazulu-Natal coast, South Africa. S. Afr. J. Mar. Sci. 24: 1–8.

Beamish, R. J., and D. A. Fournier.
1981. A method for comparing the precision of a set of age determinations. Can. J. Fish. Aquat. Sci. 38: 982–983.

Branstetter, S.
1987. Age and growth estimates for blacktip, *Carcharhinus limbatus*, and spinner, *C. brevipinna*, sharks from the northwestern Gulf of Mexico. Copeia 1987:964–974.

Branstetter, S., and J. A. Musick.
1994. Age and growth estimates for the sand tiger in the northwestern Atlantic Ocean. Trans. Am. Fish. Soc. 123:242–254.

Branstetter, S., and R. Stiles.
1987. Age and growth estimates of the bull shark, *Carcharhinus leucas*, from the northern Gulf of Mexico. Environ. Biol. Fish. 20:169–181.

Cailliet, G. M.
1990. Elasmobranch age determination and verifica-

tion: an updated review. *In* Elasmobranchs as living resources: advances in biology, ecology, systematic and the status of the fisheries (H. L. Pratt Jr., S. H. Gruber and T. Taniuchi, eds.), p. 157–165. NOAA Tech. Rep. NMFS 90.

Cailliet, G. M., and K. J. Goldman.
2004. Age determination and validation in chondrichthyan fishes. *In* The biology of sharks and their relatives (J. Carrier, J.A. Musick and M. Heithaus, eds.). p. 399–447. CRC Press, Boca Raton, FL.

Campana, S. E.
2001. Accuracy, precision, and quality control in age determination, including a review of the use and abuse of age validation methods. J. Fish. Biol. 59:197–242.

Campana, S. E., L. J. Natanson, and S. Myklevoll.
2002. Bomb dating and age determination of large pelagic sharks. Can. J. Fish. Aquat. Sci. 59(3):450–455.

Carlson, J. K., E. Cortés, and D. M. Bethea.
2003. Life history and population dynamics of the finetooth shark, *Carcharhinus isodon*, in the northeastern Gulf of Mexico. Fish. Bull. 101:281–292.

Carlson, J. K., E. Cortés, and A. G. Johnson.
1999. Age and growth of the blacknose shark, *Carcharhinus acronotus*, in the eastern Gulf of Mexico. Copeia 1999:684–691.

Castro, J. I.
1993. The shark nurseries of Bulls bay, South Carolina, with a review of the shark nurseries of the southeastern coast of the United States. Environ. Biol. Fish. 38:37–48.

Chen, S. B., and S. Watanabe.
1989. Age dependence of natural mortality coefficient in fish population dynamics. Nippon Suisan Gakkaishi 55:205–208.

Compagno, L. J. V.
1984. FAO species catalogue: sharks of the world. An annotated and illustrated catalogue of shark species known to date. FAO Fisheries Synopsis (125), vol. 4, part 1: Hexanchiformes to Lamniformes, 249 p. FAO, Rome.

Cortés, E.
1997. A critical review of methods of studying fish feeding based on analysis of stomach contents: application to elasmobranch fishes. Can. J. Fish. Aquat. Sci. 54:726–738.
2000. Life history patterns and correlations in sharks. Rev. Fish. Sci. 8:299–344.

Driggers, W. B., J. K. Carlson, D. Oakley, G. Ulrich, B. Cullum, and J. M. Dean.
2004. Age and growth of the blacknose shark, *Carcharhinus acronotus*, in the western North Atlantic Ocean with comments on regional variation in growth rates. Environ. Biol. Fish. 71:171–178.

Fabens, A. J.
1965. Properties and fitting of the von Bertalanffy growth curve. Growth 29:265–289.

Goldman, K. J.
2002. Aspects of age, growth, demographics, and thermal biology of two Lamniform shark species. Ph.D. diss., 219 p. Virginia Institute of Marine Science, Glocester Point, VA

Goosen, A. J. J., and M. J. Smale.
1997. A preliminary study of the age and growth of the smoothhound shark *Mustelus mustelus* (Triakidae). S. Afr. J. Mar. Sci. 18:85–91.

Grace, M., and T. Henwood.
1997. Assessment of the distribution and abundance of coastal sharks in the U.S. Gulf of Mexico and eastern seaboard, 1995 and 1996. Mar. Fish. Rev. 59(4):23–32.

Hoenig, J. M., M. J. Morgan, and C. A. Brown.
1995. Analysing differences between two age determination methods by tests of symmetry. Can. J. Fish. Aquat. Sci. 52:364–368.

Jensen, A. L.
1996. Beverton and Holt life history invariants result from optimal trade-off of reproduction and survival. Can. J. Fish. Aquat. Sci. 53:820–822.

Knight, W.
1968. Asymptotic growth: an example of non-sense disguised as mathematics. J. Fish. Res. Board Can. 25: 1303–1307.

Lessa, R., F. M. Santana, and R. Paglerani.
1999. Age, growth, and stock structure of the oceanic whitetip, *Carcharhinus longimanus*, from the southwestern equatorial Atlantic. Fish. Res. 42:21–30.

Mollet, H. F., J. M. Ezcurra, and J. B. O'Sullivan.
2002. Captive biology of the pelagic stingray, *Dasyatis violacea* (Bonaparte, 1832). Mar. Freshw. Res. 53: 531–541.

Morison, A. L., S. G. Robertson, and D. G. Smith.
1998. An integrated system for production fish aging: image analysis and quality assurance. N. Am. J. Fish. Manag. 18:587–598.

Natanson, L. J., J. G. Casey, and N. E. Kohler.
1995. Age and growth estimates for the dusky shark, *Carcharhinus obscurus*, in the western North Atlantic Ocean. Fish. Bull. 193:116–126.

Neer, J. A., and G. M. Cailliet.
2001. Aspects of the life history of the Pacific electric ray, *Torpedo californica* (Ayres). Copeia 2001:842–847.

Neter, J., W. Wasserman, and M. H. Kutner.
1990. Applied linear statistical models, 1408 p. Richard D. Irwin, Inc. Boston, MA.

NMFS (National Marine Fisheries Service).
1993. Fishery management plan for sharks of the Atlantic Ocean, 167 p. Office of Fisheries Conservation and Management, National Marine Fisheries Service, NOAA, 1334 East-West Highway, Silver Springs, MD.

Pauly, D.
1980. On the interrelationships between natural mortality, growth parameters, and mean environmental temperature in 175 fish stocks. J. Cons. Int. Explor. Mer 39:175–192.

Ricker, W. E.
1975. Computation and interpretation of biological statistics of fish populations. Bull. Fish. Res. Board Canada 191:1–382.
1979. Growth rates and models. *In* Fish physiology, vol. VIII: Bioenergetics and growth (W. S. Hoar, D. J. Randall, and J. R. Brett, eds). p. 677–743. Academic Press. New York, NY.

Roff, D. A.
1980. A motion for the retirement of the von Bertalanffy function. Can. J. Fish. Aquat. Sci. 37:127–129.

Simpfendorfer, C. A., R. B. McAuley, J. Chidlow, and P. Unsworth.
2002. Validated age and growth of the dusky shark, *Carcharhinus obscurus*, from western Australian waters. Mar. Freshw. Res. 53:567–573.

Skomal, G. B., and L. J. Natanson.
2003. Age and growth of the blue shark (*Prionance*

glauca) in the North Atlantic Ocean. Fish. Bull. 101:627–639.

Soriano, M., J. Moreau, J. M. Hoenig, and D. Pauly.
1992. New functions for the analysis of two-phase growth of juvenile and adult fishes, with application to Nile perch. Trans. Am. Fish. Soc. 121:486–493.

Van Dykhuizen, G., and H. F. Mollet.
1992. Growth, age estimation, and feeding of captive sevengill sharks, *Notorynchus cepedianus*, at the Monterey Bay Aquarium. Aust. J. Mar. Freshw. Res. 43:297–318.

Vaughan, D. S., and M. L. Burton.
1994. Estimation of von Bertalanffy growth parameters in the presence of size-selective mortality: a simulated example with red grouper. Trans. Am. Fish. Soc. 123:1–8.

von Bertalanffy, L.
1938. A quantitative theory of organic growth (inquiries on growth laws. II). Human Biology 10:181–213.

Wintner, S. P., and G. Cliff.
1995. Age and growth determination of the blacktip shark, *Carcharhinus limbatus*, from the east coast of South Africa. Fish. Bull. 94:135–144.

Wintner, S. P., S. F. J Dudley, N. Kistnasamy, and B. Everett.
2002. Age and growth estimates for the Zambezi shark, *Carcharhinus leucas*, from the east coast of South Africa. Mar. Freshw. Res. 53:557–566.

Zar, J. H.
1984. Biostatistical analysis, 718 p. Prentice Hall, Inc. Englewood Cliffs, NJ.

Tracking Pacific bluefin tuna (*Thunnus thynnus orientalis*) in the northeastern Pacific with an automated algorithm that estimates latitude by matching sea-surface-temperature data from satellites with temperature data from tags on fish

Michael L Domeier
Pfleger Institute of Environmental Research
901B Pier View Way
Oceanside, California 92054
E-mail address: Domeier@cs.com

Dale Kiefer
System Science Applications Inc.
PO Box 1589
Pacific Palisades, California 90272

Nicole Nasby-Lucas
Adam Wagschal
Pfleger Institute of Environmental Research
901B Pier View Way
Oceanside, California 92054

Frank O'Brien
System Science Applications Inc.
PO Box 1589
Pacific Palisades, California 90272

Abstract—Data recovered from 11 popup satellite archival tags and 3 surgically implanted archival tags were used to analyze the movement patterns of juvenile northern bluefin tuna (*Thunnus thynnus orientalis*) in the eastern Pacific. The light sensors on archival and pop-up satellite-transmitting archival tags (PSATs) provide data on the time of sunrise and sunset, allowing the calculation of an approximate geographic position of the animal. Light-based estimates of longitude are relatively robust but latitude estimates are prone to large degrees of error, particularly near the times of the equinoxes and when the tag is at low latitudes. Estimating latitude remains a problem for researchers using light-based geolocation algorithms and it has been suggested that sea surface temperature data from satellites may be a useful tool for refining latitude estimates. Tag data from bluefin tuna were subjected to a newly developed algorithm, called "PSAT Tracker," which automatically matches sea surface temperature data from the tags with sea surface temperatures recorded by satellites. The results of this algorithm compared favorably to the estimates of latitude calculated with the light-based algorithms and allowed for estimation of fish positions during times of the year when the light-based algorithms failed. Three near one-year tracks produced by PSAT tracker showed that the fish range from the California–Oregon border to southern Baja California, Mexico, and that the majority of time is spent off the coast of central Baja Mexico. A seasonal movement pattern was evident; the fish spend winter and spring off central Baja California, and summer through fall is spent moving northward to Oregon and returning to Baja California.

Manuscript submitted 11 June 2004
to the Scientific Editor's Office.
Manuscript approved for publication
21 December 2004 by the Scientific Editor.
Fish. Bull. 103:292–306 (2005).

Current theories indicate the presence of a single stock of northern Pacific bluefin tuna (*Thunnus thynnus orientalis*) in the Pacific Ocean. Spawning adults have been recorded only from the western Pacific (Yamanaka et al., 1963; Yabe et al., 1966; Okiyama, 1974; Okiyama and Yamamoto, 1979; Nishikawa et al., 1985) but resulting offspring are known to either inhabit the western Pacific or to travel to the eastern Pacific (Sund et al., 1981; Bayliff, 1994; Itoh et al., 2003a) where they remain for an undetermined amount of time. Although it is believed that only a small fraction of the population migrates to the eastern Pacific, these fish are the basis for a fishery that occurs from May through October. A recent study has documented the migration of an archival-tagged juvenile northern Pacific bluefin tuna from the western Pacific to the eastern Pacific in about two months, where it remained for eight months before being recaptured (Itoh, et al., 2003a). Conventional tagging studies have shown that Pacific bluefin tuna in the eastern Pacific eventually return to the western Pacific where they are believed to remain as adults (Sund et al., 1981; Bayliff, 1994). We provide this cursory summary merely as an introduction to our work, deferring the known details of Pacific bluefin biology to the excellent reviews that have been previously published (Bayliff, 1980, 1994; Sund et al., 1981). Work presented in the present study describes the use of electronic tags (pop-up satellite-transmitting archival tags and archival tags obtained from fish) and a newly developed sea surface temperature (SST) based geo-

location algorithm to further our understanding of bluefin tuna movements in the eastern Pacific.

The light sensors on archival and pop-up satellite tags provide data on the time of sunrise and sunset, allowing one to calculate the approximate geographic position of an animal (Delong et al., 1992; Wilson et al., 1992; Hill, 1994; Bowditch, 1995; Sobel, 1995; Welch and Eveson, 1999; Hill and Braun, 2001; Metcalfe, 2001;Smith and Goodman;[1] Gunn et al.[2]). The accuracy of the light-based geolocation estimates have been studied under controlled conditions (tags tethered to a moored buoy) and field conditions (tags attached to fish at a known location). Locations from tethered tags have been reported to be accurate to within ±0.2–0.9° in longitude and ±0.6–4.4° in latitude (Welch and Eveson, 1999, 2001; Musyl et al., 2001). Tagged tuna have provided light-based geolocation estimates within ±0.5° of longitude and ±1.5–2.0° latitude (means) of known locations (Schaefer and Fuller, 2002; Gunn et al.[1]).

Light-based estimates are not precise and comparing studies that have examined the accuracy of this method is complicated by differences in tag hardware and geolocation algorithms used by different researchers. Other physical and biological factors complicate the issue further. Day length is not a good predictor of latitude during the spring and fall equinox, therefore estimates of latitude at times surrounding the equinox contain more error than at other times of the year (Hill and Braun, 2001). Latitude estimates are also more prone to error the closer the animal is to the equator (Hill and Braun, 2001). Additional errors can be introduced into estimates of both latitude and longitude by the behavior of the tagged animal (e.g., diving), bio-fouling of the tag, cloud cover, and wave action (Metcalfe, 2001).

Poor resolution of latitude estimates continues to be a problem for researchers using light-based geolocation algorithms. Under ideal theoretical conditions the variability in latitude error cannot be less than 0.7° and the expected variability in longitude will be a constant 0.32° (Hill and Braun, 2001). Sibert et al. (2003) developed an algorithm that applies a Kalman filter to light-based geolocation estimates in an attempt to reduce the error of these estimates. Although this approach smoothes data, it does not incorporate external data (data not collected by the tag) and therefore is still affected by errors inherent in the use of light-based geolocation estimates of latitude. It has been suggested that sea-surface-temperature (SST) and bathymetry data be used to refine light-based geolocation estimates (Block et al., 2001). These techniques are particularly useful when there is a north-to-south gradient of bathymetry or SST. The use of bathymetry to refine latitude requires an assumption that maximum diving depth is limited by the bottom depth; certainly this assumption introduces a new source of error. In addition, for animals that move off the continental shelf, bathymetry would be useless. The use of SST or bathymetry data to refine latitude necessitates the arduous task of matching tag data with another source of data.

It was our opinion that the accuracy of tracking marine animals could be improved through the development of an algorithm that automatically resolved latitude estimates by matching SST measurements from the tag to those taken from satellites. Here we present such an algorithm; one that was designed to operate in a geographic information system (GIS) environment, allowing for rapid analysis and display of archival and PSAT tag data. We demonstrate the algorithm and its product through the analyses of data we collected from Pacific bluefin tuna tagged in the eastern Pacific.

Materials and methods

Tagging in the field

Pacific bluefin tuna were captured on rod and reel from a recreational fishing vessel by using live bait and circle hooks. Fishing took place 123 nmi southwest, 86 nmi southwest, and 178 nmi south of San Diego in years 2000, 2001, and 2002, respectively. Fish were lifted into the boat with a vinyl sling and then placed on a soft mat, eyes were covered with a cloth, and the gills irrigated with seawater. The fish were then measured (fork length and girth), tagged, and immediately released. Sixteen fish were tagged with Wildlife Computers Inc. (Redmond, WA) pop-up satellite archival tags (PSATs), one fish was tagged with a Microwave Telemetry Inc.(Columbia, MD) PTT-100 PSAT, and seventeen fish were tagged with Lotek Wireless Inc. (Newmarket, Ontario) LTD2310 nontransmitting archival tags. The two types of PSATs either provided data once an hour (depth, water temperature, light level [Microwave Telemetry, Inc.]) or summarized data that had been collected every two minutes (Wildlife Computers, Inc.)—the difference being an artifact of the two tag manufacturers. The Lotek archival tags provided us with data every two minutes detailing the swimming depth, water temperature, internal fish temperature, and light level. Pressure sensor drift was adjusted by the tag manufacturers' software for PSAT tags and in the laboratory for the Lotek tags.

The PSAT tags were rigged with 300-lb monofilament leaders and a nylon dart. In 2000 and 2001 the dart was a "bluefin-type" provided by Eric Prince (NMFS-SEFSC); in 2002 a Pfleger Institute of Environmental Research (PIER) "umbrella" dart was used (Fig. 1).

[1] Smith, P., and D. Goodman. 1986. Determining fish movements from an "archival" tag: precision of geographical positions made from a time series of swimming, temperature and depth. NOAA. Tech. Memo. NMFS-SWFC-60, 13 p. Southwest Fisheries Science Center, La Jolla, CA 92038.

[2] Gunn, J. S., T. W. Polacheck, T. L. O. Davis, M. Sherlock, and A. Betlehem. 1994. The development and use of archival tags for studying the migration, behavior and physiology of southern bluefin tuna, with an assessment of the potential for transfer of the technology to groundfish research. *In* Proceedings of ICES mini-symposium on fish migration, 23 p. International Council for the Exploration of the Sea, Palaegade 2-4, DK-1261 Copenhagen K, Denmark.

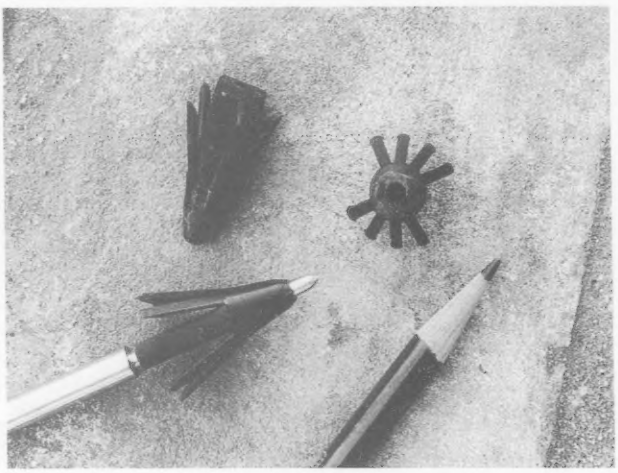

Figure 1
PIER umbrella dart used for external attachment of tags.

Each style of dart was inserted through the midline of the fish at the base of the second dorsal fin according to the method of Block et al. (1998).

Archival tags were surgically implanted either in the dorsal musculature below the first dorsal fin (when fork length was >110 cm) or into the peritoneal cavity (when fork length was <110 cm). The dorsal musculature implant was performed by making a 1-cm incision 3–5 cm below the first dorsal fin. A cold-sterilized trocar (14 mm diameter) was then inserted into the muscle, to a depth of 13–14 cm, within a plane parallel to the pterygiophores but angled 45 degrees to the anterior. The trocar was then removed and the tag was inserted so that the light stalk was angled toward the tail. The incision was then closed with a monocryl suture material. This method was similar to that used by Musyl et al. (2003). Interperitoneal implants were done according to the method of Block et al. (1998).

PSAT Tracker algorithm and analysis system

We have developed an automated system, called the PSAT Tracker Information System (PTIS), to improve the accuracy and minimize the subjectivity and tedium of matching data from different sources (tag and satellite). It is an application of the Environmental Analysis System (EASy) (System Science Applications, Redondo Beach, CA) software that is specifically designed for handling four-dimensional information (latitude, longitude, depth, and time). We describe the system in terms of three processes; importing tag data and satellite imagery, calculation of the optimal path of the tag, and dynamic display of the path and associated tag information.

Importing tag data and setting parameters

The PSAT tracker information system was designed to support data formats of three tag manufacturers: Wildlife Computers, Microwave Telemetry, and Lotek. All three tag formats are imported into FIS and stored in a universal relational database format for processing. Key parameters used in the calculation of tracks include time and position of tag deployment, time and position of tag recovery, light-based estimates of longitude (provided by tag manufacturers), maximum swimming speed of the tagged fish (estimated and determined by the user), and a bracketed range of latitude within which the program will search for SST matches. Processing involves the temporal matching of SST as recorded by the tag with that measured from satellite imagery. It is important to note that the PTIS user-defined latitude bracket is unrelated to the light-based latitude estimates provided by the tag manufacturers; instead, it is simply a range set by the user to include all possible movement of the animal during the tag deployment. However, longitude estimates are tied to the tag manufacturers' light-based estimates; the user has the option of tying PTIS position estimates directly to the light-based estimates or allowing the algorithm to search a specified distance on either side of the light-based estimate.

For this study the maximum fish velocity was set at 4 knots. This was meant to be an inclusive rather than an exclusive value, broadening the range PSAT Tracker could search for SST matches. SST matches were also constrained to remain within ±20 nautical miles (±0.33°) of the manufacturers' light-based estimates of longitude, based upon the observance by Hill and Braun

Table 1

Resolution of sea-surface-temperature data from satellites and tags (advanced very high resolution radiometer [AVHRR], moderate resolution spectroradiometer [MODIS], multichannel sea surface temperature algorithm [MCSST].

Source	Accuracy (+C)	Spatial scale (km)	Temporal scale	Availability
AVHRR pathfinder	0.3–0.5	9	Daily	1985–present
AVHRR pathfinder	0.3–0.5	9	8-day composite	1985–present
MODIS	0.3	4.6	Daily	Oct 2000–present
MODIS	0.3	4.6	8-day composite	Oct 2000–present
MCSST (Miami)	0.5–0.7	18	Weekly composite	1981–Feb 2001
MCSST (NAVOCEANO)	0.5–0.7	18	Weekly composite	Sep 2001–present
Wildlife computer tag	0.05	—	1–12/day	—
Microwave telemetry tag	0.17	—	60 minutes	—
Lotek 2300 tag	0.1	—	2 minutes	—

(2001) that light-based longitude estimates have a year round constant error of ±0.32 degrees.

Satellite imagery, temperature sensors, and land mask

The PSAT Tracker code provides an interface to automatically download, georeference, and display SST imagery. As many as three different types of imagery can be layered and prioritized to produce a collage of imagery for processing and display. Higher priority layers are searched first for SST matches before "drilling down" to lower layers. The sources and types of available SST data are numerous and have varied over the time frame of this study; different sensors and algorithms produced data of differing spatial and temporal resolution or accuracy (Table 1). To maximize the quality of the latitude estimates produced by the PSAT Tracker algorithm, we substituted better SST data as it became available. For this study SST imagery was prioritized as follows: 1) advanced very high resolution radiometer (AVHRR) or moderate resolution spectroradiometer (MODIS) daily data, 2) AVHRR or MODIS weekly data, and 3) multichannel sea surface temperature algorithm (MCSST) weekly data. The MCSST algorithm is a weekly (or 8-day) composite that is most helpful in analyzing regions of frequent cloud cover; this algorithm was applied by the University of Miami (Miami) from 1981 through February 2000 and has been applied by the Naval Oceanographic Office (NAVOCEANO) since September 2001. The MCSST algorithm provides a near complete picture of SST data for the study area; although AVHRR and MODIS data are higher resolution and more accurate.

The difference in the resolution and accuracy of temperature sensors on the tags verses those on the satellites (Table 1) are worth mentioning. The accuracy of the satellite SST data, particularly for MCSST/NAVOCEANO, is the limiting factor when attempting to match tag data to satellite data. The degree to which the satellite data and tag data must match can be set by the user in PSAT Tracker; for this study it was set between the limit of MODIS and NAVOCEANO resolution (0.4°C).

There is a fourth layer that is superimposed upon the imagery. This is a land mask that is used to eliminate placing a tag on land and to insure that tags move around land barriers rather than across them.

Computation of the track

A detailed mathematical description of the computation for the best track would take more space than is available. Instead, we present a more general description of the algorithm and its logic, consisting of the following five steps that are summarized below and then subsequently described in detail.

1 Define the daily search area found within satellite SST imagery.
2 Define appropriate tag data (termed selection set) to match to satellite SST values found within the daily search area.
3 Select candidate points within each daily search area that provide the best match to the temperatures found in the selection set. The cost of each candidate point is largely determined by the difference between the tag and satellite SST values.
4 Calculate the cost for all possible steps, called arcs, between pairs of candidate points of adjacent daily search areas. The cost of each step is a function of the length of the arc that connects adjacent candidate points (the greater the distance, the greater the cost) and the cost of each individual candidate point (see step 3).
5 Sum the costs of all tracks and identifying the track with the lowest cost.

Step 1: Defining the daily search area A daily search area is defined by the tag manufacturers' light-based solution for longitude, a user defined bracket for latitude and the value entered for maximum swimming

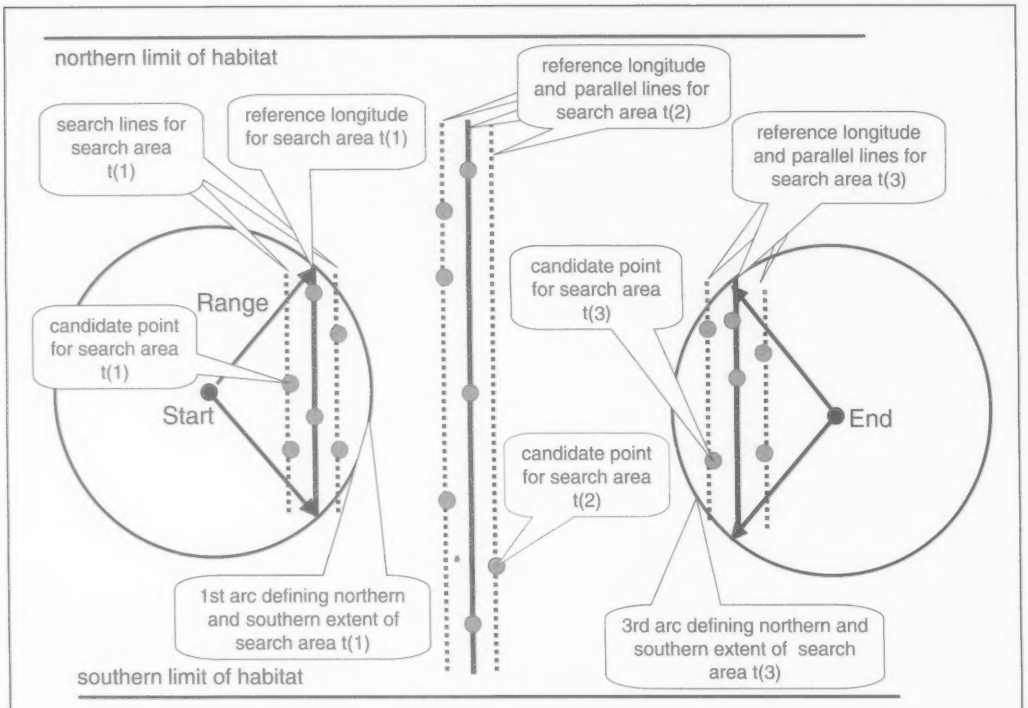
northern limit of habitat
search lines for search area t(1)
reference longitude for search area t(1)
reference longitude and parallel lines for search area t(2)
reference longitude and parallel lines for search area t(3)
candidate point for search area t(3)
Range
candidate point for search area t(1)
Start
End
candidate point for search area t(2)
1st arc defining northern and southern extent of search area t(1)
3rd arc defining northern and southern extent of search area t(3)
southern limit of habitat

Figure 2

Definition of terms used to describe the PSAT Tracker algorithm. A search area is a region in a satellite thermal image where a search is conducted for pixels whose temperature values match those recorded by the tag at that time and when it is at the surface. The search area consists of a reference longitude line, defined by the daily calculation of latitude provided by the manufacturer's processed data record and parallel search lines that provide a hedge on this determination. The search area is uniquely defined by the time at which this calculation was determined. The northern and southern bounds of the search area are determined by either the habitat range or the maximum distance that the tagged fish can swim during each time step. Those pixels underlying the reference and search line, whose temperature best match the temperatures of the selection set of points from the tag, are chosen as candidate points. One candidate point from each search area will eventually define the best track.

speed of the fish. The latitudinal bounds of the daily search area are constrained in two ways, by the known (or unknown) bounds of the fish's habitat and by its maximum swimming speed. The northern and southern bounds of the habitat are entered by the user, and no areas are searched that are beyond these latitudes. These values are meant to be inclusive and can be determined from the literature or estimated by using latitude values provided by light-based geolocation algorithms. These bounds are set prior to processing and do not change throughout the processing; in this study the latitude search area was restricted to waters between 15 and 50 degrees north.

Each search area is centered on the light-based longitude estimate (termed the reference longitude). PSAT Tracker does not search every pixel of SST data for matches, but instead searches along parallel lines of longitude on either side of, and including, the reference longitude. These lines, termed search lines, are spaced at equal distances from the reference longitude (Fig. 2). The user establishes the extent to which PSAT Tracker searches to the east and west of the reference longitude by choosing the number of search lines as well as their distance of separation. In this study four search lines were drawn on either side of the reference longitude; these parallels were drawn 5 nmi apart resulting in a 40 nmi wide daily search area. We refer to each search according to the time at which the reference longitude was determined, $t(i)$ (where t is the time for which the reference longitude was determined and i is the index for the sequence of daily search areas in the time series).

The maximum swimming speed of the fish can also constrain the latitudinal bounds of a daily search area. The farthest a fish can swim in a given time interval is simply the product of its maximum swimming speed and the length of the time interval. Thus, all possible posi-

tions that a fish can occupy when swimming in a fixed direction from the starting point of a track is the locus of points forming a circle whose center is at the starting point and whose radius is the product of its maximum swimming speed and the length of the time interval. Likewise, the farthest positions from which a fish can swim in given direction and reach the end point of the track is the locus of points forming a circle whose center is at the end point and whose radius is the product of its maximum swimming speed and the length of the time interval. The intersection of loci originating from either the start point or end point with a reference to longitude defines the most northern and southern extent of the search area for that reference longitude.

Because the distance of arcs whose center lies at the start point increases with time, whereas the distance of arcs whose center lies at the end point decreases with time, the latitudinal range of the search area is usually smallest at the start of the time series and at the end of the time series and is usually largest midway through the time series. The long time series obtained from the recovered archival tags creates a situation where the latitudinal extent of the search areas is largely determined by the northern and southern bounds of the habitat rather than by swimming speed. Swimming speed does, however, constrain east-west movement on a daily basis because the reference longitudes anchor the search areas.

Step 2: Selection sets for tag data The second step of processing involves selecting SST records (from the tag data set) that are coincident in time with the daily search area. The user can define the sea surface layer by entering a maximum depth of this layer; for this study the surface layer was defined as 0–1 m. The user can also determine how many values from the selection set should be used to search for SST matches. We chose a selection set consisting of three individual values for PSAT tags; however, because of the much higher frequency of measurements from the archival tags, we chose a selection set that consisted of a single average SST value for each day. The temperatures found in the selected set of points for a given daily search area would be used to calculate the location of pixels within the search area that the tag most likely visited.

Step 3: Choosing candidate points Selecting candidate points from which a best track will be chosen begins by assigning a temperature cost to pixels within the search area. The temperature cost for a given pixel, j, with a search area referenced by time, $t(i)$, $\Delta T[j, t(i)]$, is simply the absolute value of the difference in its temperature, $Tsat(j, t(i))$, and that of its closest match, k, from the selected set of tag points, $Ttag[k, t(i)]$:

$$\Delta T\left[j,t(i)\right]=\left|Tsat\left[j,t(i)-Ttag\left[k,t(i)\right]\right]\right|.$$

The temperature cost, $\Delta T\ [j, t(i)]$, is an inherited trait of a pixel and will be applied to all further calculations of the best track(s). If the temperature cost of any pixel examined in a search area exceeds the cutoff value entered by the user, that pixel will be removed from further consideration. Pixels will also be removed if they lie over land.

Those pixels that remain are next subjected to an evaluation to determine if they qualify as candidate points. This evaluation is based upon the value of a cost function that weighs both the pixel's temperature cost described above, $\Delta T[j, t(i)]$, and the pixel's contribution to spreading coverage over the search area:

$$\mathrm{Cost}\left[j,t(i)\right]=\Delta T\left[j,t(i)\right]+Spread\ Factor\times\Delta L\left[j,t(i)\right].$$

$\Delta L\ [j, t(i)]$ is the relative contribution a pixel makes to providing even latitudinal distribution along the reference longitude and search lines of the daily search area; the *Spread Factor* weights the relative importance of temperature costs with the benefit of obtaining an even distribution. Although the primary criterion for selecting candidate points is how well tag SST matches satellite imagery SST, we have found that this criterion alone can cause all the selected candidate points to be bunched together. Such aggregation will force the computed track into small regions of the search area without regard to the distribution of matching pixels in proceeding or succeeding search areas. To avoid this problem the *Spread Factor* function spreads candidate points in a north–south direction thereby providing smoother and more economical tracks. The degree to which the *Spread Factor* function spreads candidate points is controlled by the user by entering a weighted value. For this study we chose an intermediate value (5000 out of a possible 9999) and this value was constant for all evaluations.

The number of candidate points finally determined is determined by the user. For this study, five candidate points were identified for each search area. When the user defines the number of points to be evaluated in the search areas, pixels having the lowest cost are ranked and selected accordingly.

Step 4: Enumerate and calculate the cost of arcs After the candidate points have been chosen, the best track(s) is computed by choosing a single candidate point from each of the daily search areas in the time series. The best track is selected from all possible tracks by choosing the one of least cost. Thus, the solution is global rather than serial. The computation begins by calculating the cost of arcs between candidate points from adjacent search areas, and ends by summing the cost of all the arcs of a given track (Figs. 3 and 4).

The cost of an arc is a function of the temperature match for the pair of candidate points that define the arc, $\Delta T[j, t(i)]$ and $\Delta T[k, t(i+1)]$, as defined above. It also depends upon the minimum swimming speed required of the fish traveling between the two candidate points, *arc velocity min*, where

$$arc\ velocity\ min=\frac{distance\ between\ candidate\ pixels}{\left(t(i+1)-t(i)\right)}.$$

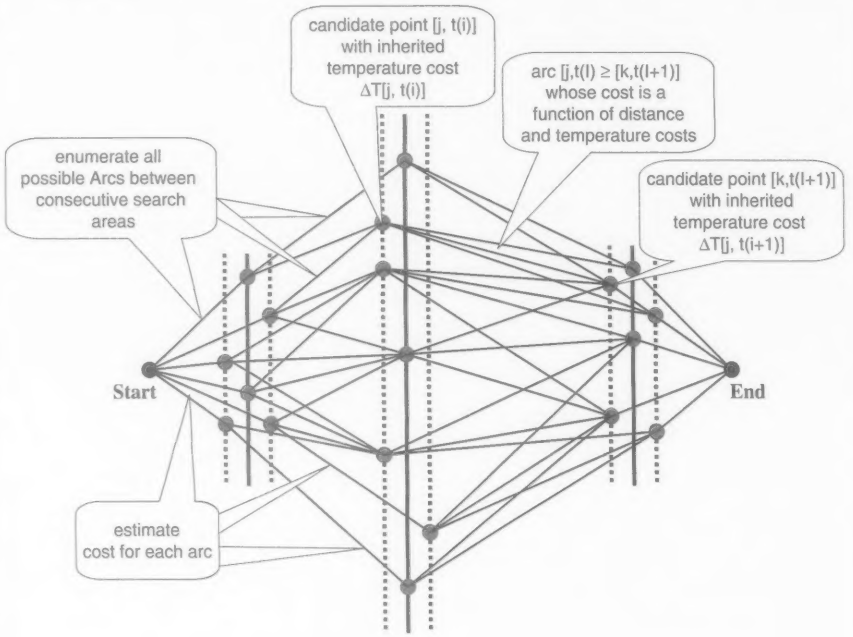
candidate point [j, t(i)] with inherited temperature cost ΔT[j, t(i)]
arc [j,t(I) ≥ [k,t(I+1)] whose cost is a function of distance and temperature costs
enumerate all possible Arcs between consecutive search areas
candidate point [k,t(I+1)] with inherited temperature cost ΔT[j, t(i+1)]
Start
End
estimate cost for each arc

Figure 3

Enumerating and costing arcs. An arc is defined as the arc between any two candidate points of adjacent search areas. The cost of an arc depends upon the temperature cost, ΔT, of the two candidate points of the arc. It is also depends upon the swimming speed required to travel the distance of the arc.

The cost of the arc between candidate point j and candidate point k is

$$\arccos t\left(\{j,t(i)\}->\{k,t(i+1)\}\right)=\left(\Delta T\left(j,t(i)\right)+\Delta T\left(k(t,i+1)\right)\right)+$$

$$DistFactor\left(\frac{arcv\min}{velocity}\right)$$

where velocity = the maximum sustained swimming speed of the fish; and

DistFactor = a factor that scales the cost of swimming at a given speed in relation to the sum of the temperature costs of the two candidate points.

Values for the *DistFactor* and *Velocity* are determined by the user. The rationale for such cost is that the best track should include an assessment of variations in swimming velocity as well as the costs of temperature. If swimming speed is judged to be an insignificant cost or too difficult to quantify, the *DistFactor* can be set to 0. If a land barrier lies between the pair of candidate points, the distance to swim around the barrier is calculated and included in the cost of the arc. In this study an intermediate value (5000 out of 9999) was assigned for the *DistFactor*, and this value was constant for all evaluations.

Step 5: Calculating the best track Finally, the algorithm calculates the sum of the arc costs for each track:

$$Cost\ of\ tract=\sum_{tstart}^{tend}\arccos t\left(\{j,t(i)\}->\{k,t(i+1)\}\right).$$

The costs for all possible tracks are then ranked, and the track(s) with the lowest cost(s) is then saved and available for display (Fig. 4). The track is saved in a table of the PSAT Tracker database; the table contains records of the latitude, longitude, time, and surface temperature of the candidate points that comprise the track, as well as records of surface temperature from the satellite imagery at regular intervals along the arcs between candidate points. Depending on the length of the time series, this process analyzes tens of thousands to hundreds of thousands of tracks and thus is the most time-consuming step of the algorithm.

Analyzing position data from PSAT Tracker

Location estimates provided by PSAT Tracker were subjected to spatial analysis to describe the move-

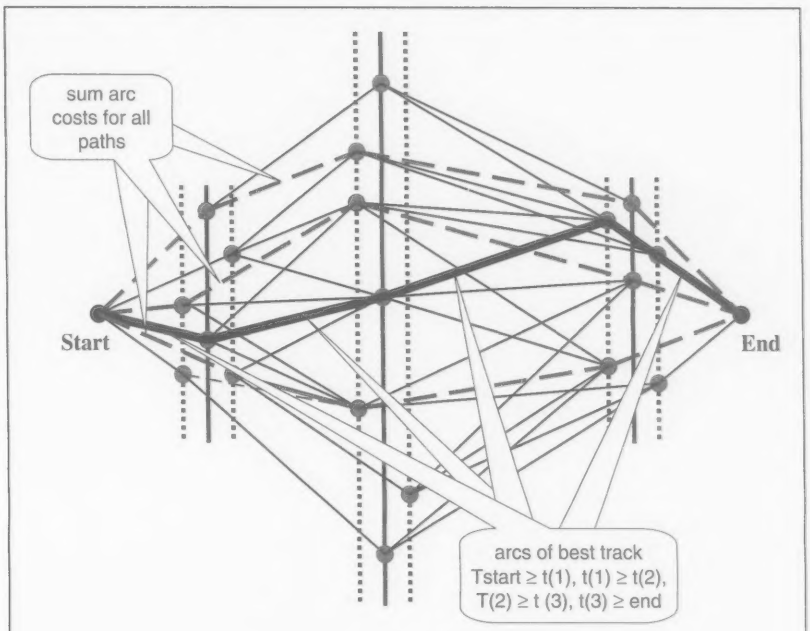

Figure 4

Diagram to show how the best track is calculated by summing the cost of arcs for all possible paths and then choosing the track of least cost.

ment patterns and habitat use of Pacific bluefin tuna in the eastern Pacific. Monthly data were combined within each tag data set prior to performing utilization distribution analyses with the Home Range Extension for ArcView (version. 1.1c, BlueSky Telemetry, Aberfeldy, Scotland) that employs the fixed kernel method (Rodgers and Carr, 1998). Results were displayed as volume contours displaying the main centers of activity for each fish during a given time period. Initial analyses allowed us to combine data so that figures could be minimized. For the archival tag data, consecutive months with similar spatial distribution were combined and individual fish with very similar tracks were combined. All data from fish that were PSAT tagged were combined by month because of the relatively sparse data compared with the data from the archival tags. PSAT tag data provided a glimpse at year-to-year variations in bluefin distribution (August 2000 through October 2002), whereas the archival tag data were for a single year and allowed for a monthly comparison within one year (August 2002 to September 2003).

The near daily position data provided through the PSAT Tracker analyses allowed us to calculate the swimming speed of each fish. This was done by simply dividing the horizontal distance between consecutive data records by the time between consecutive data records (1–4 days).

Results

Tag recoveries

Fifteen of the PSAT tags transmitted data after remaining on the fish from 2 to 191 days (Table 2). Unfortunately some of these tags did not transmit usable data. Fourteen of them provided a pop-up location and eleven of them transmitted enough data for some level of analyses of behavioral and movement patterns. The Microwave Telemetry PSAT tag provided an archival data set with a one-hour sampling schedule. The Wildlife Computer PSATs transmitted data summaries that included a daily water column profile of temperature (obtained from the deepest dive) and the percent time each fish spent within predetermined temperature and depth bins.

Four archival tags were recovered after a period at liberty of 16 hours to 385 days (Table 2). The 16-hour archival tag recovery was made from a recreational angler very near the point of release; this tag was not used for any analyses. The three tag recoveries made after 300 days came from a purse-seine vessel. Two of these three recaptured fish spent several weeks in a grow-out pen before the tags were discovered; the dates the fish were in the pen were not used for any analyses. The light stalks of tags 441 and 159 were damaged during recovery. For these tags, the internal temperature and pressure sensors were verified by Lotek data, but external

temperature and light level sensors could not be checked. For tag 233, none of the sensors could be verifed because the tag had to be disassembled and destroyed by Lotek personnel in order to recover the data.

Table 2

Details of tagged Pacific bluefin tuna (*Thunnus thynnus orientalis*). WC=Wildlife Computer Tag, MT=Microwave Telemetry Tag, Lot=Lotek Tag).

Fish	Tag date	Weight (kg)	Time at liberty (days)
4 WC	13 August 2002	36	23
184 WC	13 August 2002	60	62
200 WC	13 August 2002	41	51
245 WC	2 August 2000	51	19
247 WC	2 August 2000	57	38
249 WC	2 August 2000	50	102
265 WC	2 August 2000	52	33
301 WC	2 August 2000	60	191
961 WC	3 August 2001	32	9
962 WC	3 August 2001	35	4
964 WC	3 August 2001	35	23
1041 WC	3 August 2001	26	2
1042 WC	2 August 2000	42	72
283 MT	13 August 2002	41	61
114 Lot	13 August 2002	52	16 (hours)
159 Lot	13 August 2002	52	375
233 Lot	14 August 2002	43	385
441 Lot	30 August 2002	12	323

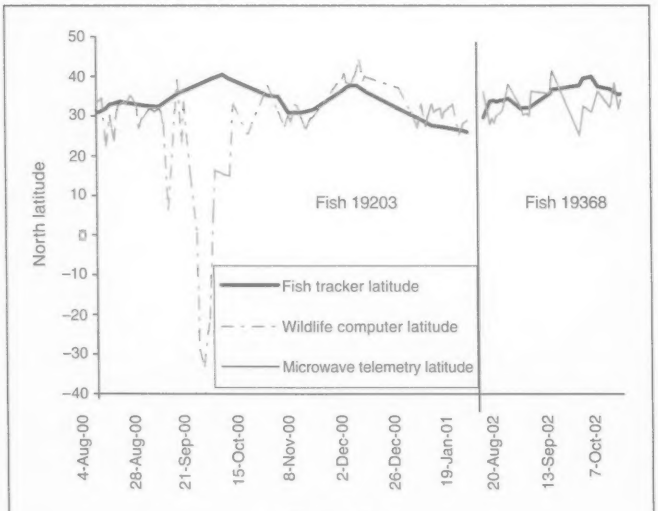

Figure 5

PSAT Tracker SST-based latitude solutions vs. Wildlife Computers and Microwave Telemetry light-based latitude estimates.

PSAT Tracker algorithm

The archival tags provided large data sets that allowed for the comparison of the PSAT Tracker algorithm to the manufacturer's light-based geolocation solution. Because longitude estimates generated by PSAT Tracker are constrained by the light-based estimates, these values differed very little from the position estimates from the various tag manufacturers. Although similar, the PSAT Tracker latitude solutions were generally less erratic than those produced from the three light-based algorithms, particularly surrounding the times of the equinoxes (Figs. 5 and 6). The spring and fall equinoxes each produced approximately two months of unreliable latitude estimates for light-based algorithms.

Pacific bluefin tuna habitat use

Horizontal movement Tagged bluefin tuna ranged as far north as the California–Oregon border and nearly to the tip of Baja California, Mexico, to the south. Although this distance encompasses 2400 km of coastline, these fish spent the majority of their time in the southern part of the range, best illustrated by a home range analysis of the combined approximately year-long tracks of the three archival tagged bluefin (Fig. 7). Tagged off the northern coast of Baja California, Mexico, these three bluefin moved northward until November, followed by a southward migration to south-central Baja California where they spent the months of January through June (Fig. 8). The two larger archival-tagged fish reached the offshore waters of Oregon before turning south and the smaller fish did not venture north of San Francisco, California. The two larger fish spent much of the winter and spring (January–June) in the coastal bight between Punta Eugenia, Mexico, to the north and Cabo San Lazaro, Mexico, to the south, and the smaller fish had a more dispersed spring range north of Punta Eugenia. In July all three fish began to move to northern Baja, back into the general area where they were originally tagged and where they were subsequently recaptured (Fig. 8). This general pattern of summer–fall movement northward followed by a winter migration southward and a winter–spring holding pattern off south-central Baja California was supported by data from fish with PSATs in years 2000 through 2002 (Fig. 9).

Although position data for the months of January through June generally placed the tagged bluefin off southern Baja, two of the three fish tagged with archival tags underwent rapid April excursions to the north before returning to the south (Fig. 10). Fish 159 traveled 2130 km, one way, before returning by 1 May; fish 441 made a similar move but did not go as far north (1285 km) and stopped its southward return 480 km north of its original starting point. The extreme

northern latitude estimates calculated by PSAT Tracker placed fish 441 slightly north of Point Conception, California, and fish 159 near the California–Oregon border before it returned to wintering grounds off Baja California (Fig. 10). This movement is corroborated by a westerly trend in longitudes and a dramatic drop in SSTs. For fish 159, SST dropped from 19.1°C on 4 April 2003 to 12.4°C on 18 April 2003. Similarly, fish 441 experienced an SST drop from 19.5° to 13.5°C between 1 and 18 April.

Data from the archival tags provided near daily positions for each fish. The longest time between successive fixes was four days. The calculated swimming speeds between successive position fixes ranged from 0 to 14.7 knots for all three fish combined. The mean swimming speed for all three fish was 1.3 knots (±1.3 kn).

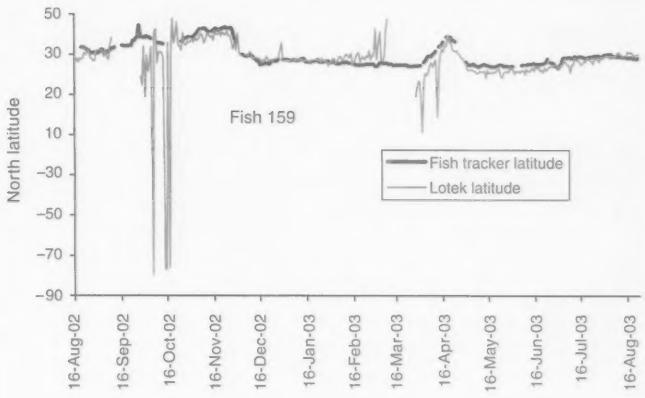

Figure 6

PSAT Tracker SST-based latitude solutions and Lotek light-based latitude estimates.

Depth and temperature ranges Vertical movement was similar to that reported for other bluefin tuna (Block et al., 1997; Block, 2001; Kitagawa et al., 2004). Detailed analyses of vertical movement and temperature preferences and tolerances are beyond the scope of this article and will be presented in a future publication. In general, dives were most common during the day; maximum dive depths ranged from 341 to 382 m. Fish with archival tags spent nearly 70.1% of the time near the surface (<20 m deep). Ambient water temperatures ranged from 5.7° to 25.0°C (mean=17.4°C). The internal temperature of fish tagged with archival tags ranged from 14.1° to 29.5°C (mean=21.8°C); average internal temperatures of the fish were 4.4°C warmer than ambient waters and at times were up to 19.2°C warmer.

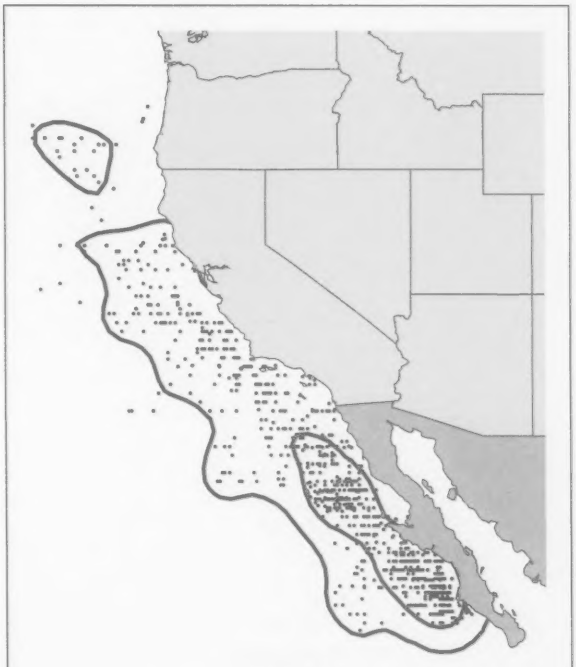

Figure 7

Fixed kernel home range analysis illustrating relative importance of the range of juvenile Pacific bluefin tuna (*Thunnus thynnus orientalis)* in the eastern Pacific; displayed are all points for fish 159, 233, and 441 and volume contours of 95% (outer line) and 50% (inner line) for all three fish combined. Isolated circle to the north is a 95% contour.

Discussion

Although we used SST matching as the sole means of estimating latitude for the fish tracks and spatial analyses presented in our study, the extent of the northward fall migration of juvenile Pacific bluefin tuna in the eastern Pacific has been corroborated by occasional commercial landings of Pacific bluefin tuna in Oregon (McCrae[3]). Because Pacific bluefin tuna are apparently capable of existing in the northern part of the eastern Pacific range, even during the colder months of the year, it is not clear what dictates the movement pattern of these fish. It is reasonable to speculate that the tuna are taking advantage of seasonal ocean warming to exploit distant prey when the physiological expense to maintain optimum body

[3] McCrae, J. 2004. Personal commun. Oregon Dept. Fish & Wildlife, Newport, OR 97365.

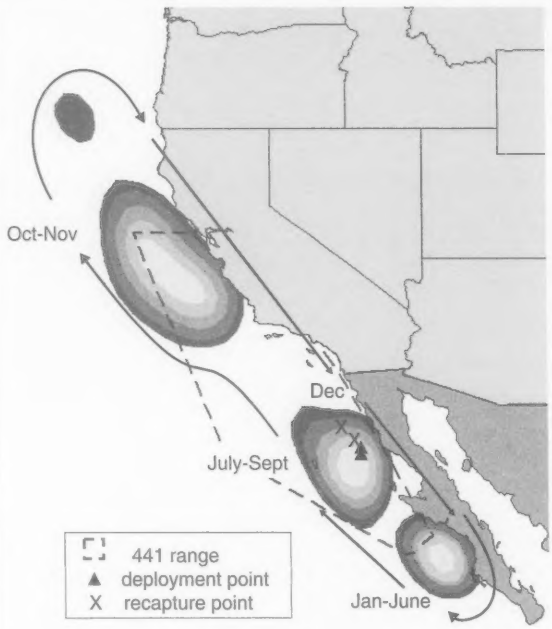

Figure 8

Grayscale contours of seasonal spatial use and movement pattern for fish 159 and 233 combined, displaying "core areas" of use represented by volumes of 10–50%. The smaller total range of fish 441 is illustrated by the polygon.

temperature is less. Temperature and depth tolerances and preferences indicated in our study are similar to those of bluefin tuna studied in other parts of the world (Carey and Teal, 1969; Carey and Lawson, 1973; Block et al., 1997; Kitagawa et al., 2000, 2004; Block et al., 2001; Brill et al., 2002; Itoh et al., 2003b).

The migration of a fish with an archival tag from the western Pacific to the eastern Pacific (Itoh et al., 2003a) provides an interesting comparison to our data. This individual, tagged off Japan, made the trans-Pacific migration in about two months and then resided in the eastern Pacific for about eight months before being recaptured by a recreational angler. The fish arrived off the coast of northern California in the month of January—a time when fish from our study were found to be at the southern extreme of their eastern Pacific range. By the month of March, the western Pacific migrant had traveled to the winter–spring grounds where it then seemed to behave in a pattern similar to that of fish tagged for our study. Whether or not the Itoh et al. (2003a) tagged fish illustrated a typical transition from trans-Pacific migrant to eastern Pacific resident will require more tag recoveries. It will be equally interesting to see future descriptions, from archival-tag data, of maturing Pacific bluefin tuna making the trip back to the western Pacific.

Two of the Pacific bluefin tuna with archival tags were captured and recaptured in very close proximity in both space and time of year. The computed tracks for these two fish, both relatively large for the eastern Pacific, also showed that they kept close to each other for most of the year. A smaller fish, tagged a month later, underwent a similar north to south movement, but did not range as far north, particularly, or south. Given our extremely low sample sizes, very little can be concluded, but the question is raised as to whether or not Pacific bluefin tuna of different year classes have distinct schools and migratory behaviors. It is also important to point out that the two larger fish were tagged in the dorsal musculature, whereas the smaller fish was tagged in the peritoneal cavity. The orientation of the light stalk is different for these two methods, one pointing towards the surface and the other in the shadow of the fish and pointing down. How this tag orientation may influence the detection of light and subsequent position estimates is unknown.

Two of our fish with archival made rapid northward migrations into much colder water in the early spring. This northward migration is similar to that made by Itoh's fish in the early spring of 1998. Because these movements occurred at a time when the light-based latitude estimates prove unreliable, it would not have

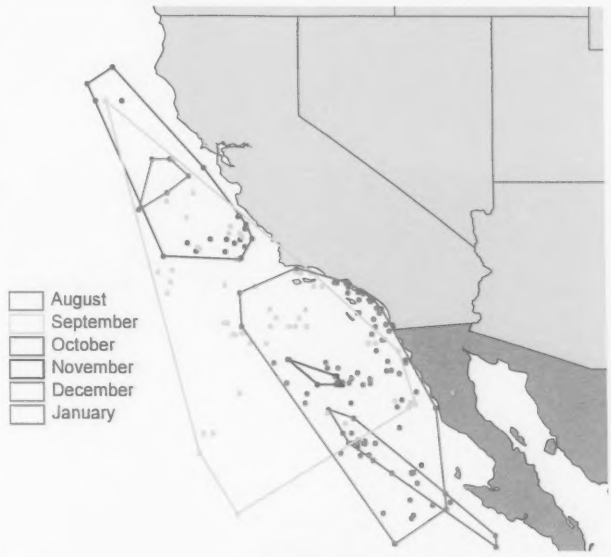

Figure 9

Positions for eleven Pacific bluefin tuna (*Thunnus thynnus orientalis)* tagged with satellite pop-up tags from 2000, 2001, and 2002 showing the 100% minimum convex polygon for fish positions within a given month.

been possible to be certain that this rapid excursion was authentic without the aid of SST matching (as was also done by Itoh et al. [2003a]).

The PSAT Tracker algorithm provided relatively quick and automated geolocation estimates for data recovered from three separate types of tags deployed on Pacific bluefin tuna. Furthermore, the PSAT Tracker latitude solutions compared favorably to the light-based latitude estimates during non-equinox times of the year. The use of SSTs to resolve latitude allowed for spatial analyses of individual bluefin positions for every month of the year, whereas a strictly light-based approach would not provide reliable latitude position estimates for approximately 30% of a year-long track. PSAT Tracker also results in a global, rather than serial track solution. In essence this means that no single position estimate is selected without regard to the influence this position has on the overall track. A serial track is one that is produced by selecting each position without regard to the effect each selection has on the overall track. A serial track is also heavily biased by the start point and may weight the location estimates based upon the previous location estimate, allowing a single poor location estimate to ruin the remainder of the location estimates for the track.

It is instructive to compare our SST matching algorithm to the Kalman filter-based algorithm developed by Sibert et al. (2003). The Sibert et al. algorithm depends solely upon light data collected by the tag to estimate latitude and longitude, whereas the PSAT Tracker algorithm depends upon the light field to provide an estimate of longitude and solely upon the sea surface temperature to provide an estimate of latitude. The initial estimates of both approaches are then refined according to a goodness-of-fit criterion that depends upon assumptions regarding the swimming behavior of the tagged fish. In the case of the Sibert et al.'s algorithm, the behavior of the fish is modeled in terms of a biased random walk model that describes the movement of the fish in terms of an advection-diffusion equation; the advective term describes the most probable displacement of the fish during a time step and the diffusive term describes the distribution of less likely displacements. The usefulness of the random walk model is largely determined by the adequacy of describing the distribution of swimming speed and direction of the fish. The algorithm also includes formulations of the dependence of the accuracy and precision of the estimates of latitude and longitude from the tag upon other factors. For example, around the equinox the weighting of the estimate of latitude from the tag measurements is greatly reduced (specifically an inverse cosine squared function of date.) The Sibert et al. algorithm simply searches for a track that minimizes discrepancies between the positions predicted from random walk model (the transition equation) and those predicted from the tag measurements (the measurement equation).

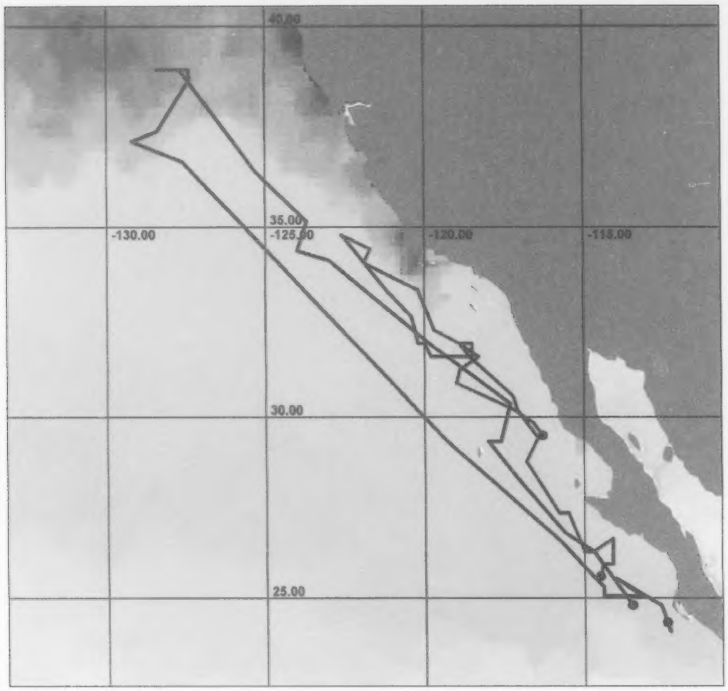

Figure 10

Track showing northward excursions of fish 159 (track extending to 38°) and 441 (track extending to 34.5°) between 1 April and 10 May 2003. Displayed SST imagery is a composite for the month of April showing a 7°C temperature gradient.

PSAT Tracker is similar to the Sibert et al. algorithm in that it invokes a model of fish behavior; there is a simple constraint on the maximum distance that a fish can swim during a time step, and shorter tracks that require lesser expenditures of energy by the fish are favored. Like the Sibert et al. algorithm, the PSAT Tracker also incorporates candidate points that are not limited to the initial light-based estimate of longitude but includes adjacent longitudes based upon the user's assessment of the accuracy of the initial estimate. Finally, both the Sibert et al. and the PSAT Tracker algorithms yield a solution that provides a best fit to the time series of satellite (in the case of PSAT Tracker) and tag measurements to the model of fish behavior.

Unfortunately, it is difficult to make a general assessment of the accuracy of either approach. In the case of the PSAT Tracker algorithm, the accuracy of the track will decrease in the absence of a north–south temperature gradient. We have not found a means of quantitatively determining the accuracy of PSAT Tracker calculations. However, the quality of the fit between pixel values of temperature from imagery and tag values for positions along the track is calculated as a χ^2 value. In the case of the Sibert et al. algorithm, the accuracy of the track will decrease during the period of the equinox when the latitudinal errors of the light-based estimates are extremely large. Our data indicate that this period can be as long as two months surrounding each equinox (skewed towards winter). At such times the estimates of position derived by the Sibert et al. algorithm depend largely on the random walk model of fish movement, which provides only a generic description of movement. Although the algorithm provides values for the mean square errors of bias and randomness for the tag estimates of latitude and longitude, these values are not true values for error of predicting location; rather they represent of the discrepancy between the estimates of position by the random walk model, the formulation of the latitude estimation error, and the tag measurements. Additionally, the Sibert et al. algorithm does not exclude the possibility of placing a fish on land.

The PSAT Tracker worked well for this study because of the strong north-to-south temperature gradient that is presented in the northeastern Pacific. Studies conducted in regions with poor temperature gradients will continue to rely on light-based latitude estimates and approaches like the Sibert et al. algorithm. Further development of PSAT Tracker, or other SST-based geolocation algorithms, should explore a means of using light-based latitude positions in combination with SST matching when light data are reliable, but excluding light-derived latitude positions when they are unreliable.

Acknowledgments

This study was made possible through the support of the George T. Pfleger Foundation and the Offield Family Foundation. We thank those who helped us capture the fish in our study: Tom Pfleger, Tom Fullam, Tom Rotherie, Greg Stutzer and Chugey Sepulveda. Archival tags were recovered with the assistance of the Inter-American Tropical Tuna Commission.

Literature cited

Bayliff, W. H.
1980. Synopsis of biological data on the northern bluefin tuna, *Thunnus thynnus* (Linnaeus, 1758), in the Pacific Ocean. Inter-Am. Trop. Tuna Comm. Spec. Rep. 2: 261–293.
1994. A review of the biology and fisheries for northern bluefin tuna, *Thunnus thynnus*, in the Pacific Ocean. FAO Fish. Tech. Paper 336, part 2:244–295.

Block, B. A., H. Dewar, S. B. Blackwell, T. D. Williams, E. D. Prince, A. Boustany, C. F. Farwell, D. J. Dau, and A. Seitz.
2001. Archival and pop-up satellite tagging of Atlantic bluefin tuna. *In* Electronic tagging and tracking in marine fishes (J. R. Sibert and J. L. Nielsen, eds.), p. 65–68. Kluwer Academic Publs, The Netherlands.

Block, B.A., H. Dewar, T. Williams, E. Prince, C. Farwell, and D. Fudge.
1997. Archival and pop up satellite tagging of Atlantic bluefin tuna, *Thunnus thynnus*. *In* Proceedings of the 48th annual tuna conference, p. 10. Inter-Am. Trop. Tuna Comm., Lake Arrowhead, CA.
1998. Archival tagging of Atlantic bluefin tuna (*Thunnus thynnus thynnus*). MTS Journal 32:37–46.

Bowditch, N.
1995. The American practical navigator: an epitome of navigation. Originally by Nathaniel Bowdich (1802), Publ. 9., 873 p. Defense Mapping Agency Hydrographic/ Topographic Center, Bethesda, MD.

Brill, R., M. Lutcavage, G. Metzger, P. Bushnell, M. Arendt, J. Lucy, C. Watson, and D. Foley.
2002. Horizontal and vertical movements of juvenile bluefin tuna (*Thunnus thynnus*), in relation to oceanographic conditions of the western North Atlantic, determined with ultrasonic telemetry. Fish. Bull. 100:155–167.

Carey, F. G., and K. D. Lawson.
1973. Temperature regulation in free-swimming bluefin tuna. Comp. Biochem. Physiol. 44a:375–395.

Carey, F. G., and J. M. Teal.
1969. Regulation of body temperature by the bluefin tuna. Comp. Biochem. Physiol. 28:205–213.

Delong, R. I., B. S. Stewart, and R. D. Hill.
1992. Documenting migrations of northern elephant seals using day length. Mar. Mamm. Sci. 8:155–159.

Hill, R.
1994. Theory of geolocation by light levels. *In* Elephant seals: population ecology, behavior, and physiology (B. J. LeBoeuf and R. M. Laws, eds.), p. 227–236. Univ. California Press, Berkeley, CA.

Hill, R. D., and M. J. Braun.
2001. Geolocation by light-level. The next step: latitude. *In* Electronic tagging and tracking in marine fisherie (J. Sibert and J. Nielsen, eds.), p. 315–330. Kluwer Academic Press, Dordrecht, The Netherlands.

Itoh, T., S. Tsuji and A. Nitta.
2003a. Migration patterns of young Pacific bluefin tuna (*Thunnus orientalis*) determined with archival tags. Fish. Bull. 101:514–534.
2003b. Swimming depth, ambient water temperature preference, and feeding frequency of young Pacific bluefin tuna (*Thunnus thynnus orientalis*) determined with archival tags. Fish. Bull. 101:535–544.

Kitagawa, T., S. Kimura, H. Nakata, and H. Yamada.
2004. Diving behavior of immature, feeding Pacific bluefin tuna (*Thunnus thynnus orientalis*) in relation to season and area: the East China Sea and the Kuroshio-Oyashio transition region. Fish. Oceanogr. 13(3):161–180.

Kitagawa, T., H. Nakata, S. Kimura, T. Itoh, S. Tsuji, and A. Nitta.
2000. Effect of ambient temperature on the vertical distribution and movement of Pacific bluefin tuna *Thunnus thynnus orientalis*. Mar. Ecol. Prog. Ser. 206:251–260.

Metcalfe, J. D.
2001. Summary report of a workshop on daylight measurements for geolocation in animal telemetry. *In* Electronic tagging and tracking in marine fisheries (J. Sibert and J. Nielsen, eds.), p. 331–342. Kluwer Academic Press, Dordrecht, The Netherlands.

Musyl, M. K., R. W. Brill, D. S. Curran, J. S. Gunn, J. R. Hartog, R. D. Hill, D. W. Welch, J. P. Eveson, C. H. Boggs, and R. E. Brainard.
2001. Ability of archival tags to provide estimates of geographical position based on light intensity. *In* Electronic tagging and tracking in marine fisheries (J. Sibert and J. Nielsen, eds), p. 343–368. Kluwer Academic Press, Dordrecht, The Netherlands.

Musyl, M. K., R. W. Brill, C. H. Boggs, D. S. Curran, T. K. Kazama, and M. P. Seki.
2003. Vertical movements of bigeye tuna (*Thunnus obesus*) associated with islands, buoys, and seamounts near the main Hawaiian islands from archival tagging data. Fish. Oceanogr. 12:152–169.

Nishikawa, Y., M. Honma, S. Ueyanagi, and S. Kikawa.
1985. Average distribution of larvae of oceanic species of scombrid fishes, 1956–1981. Nat. Res. Institute of Far Seas Fisheries, Shimizu. 12:99.

Okiyama, M.
1974. Occurrence of the postlarvae of bluefin tuna, *Thunnus thynnus*, in the Japan Sea. Japan Sea Reg. Fish. Res. Lab. Bull. 25:89–97.

Okiyama, M., and G. Yamamoto.
1979. Successful spawning of some holepipelagic fishes in the Sea of Japan and zoogeographical implications. *In* Proceedings of the seventh Japan-Soviet joint symposium on aquaculture, p. 223–233. Tokai Univ. Press, Tokyo, Japan.

Rodgers, A. R., and A. P. Carr.
1998. HRE: the home range extension for ArcView. User's manual, 27 p. Centre for Northern Forest Ecosystem Research, Ontario Ministry of Natural Resources, Thunder Bay, Ontario, Canada.

Schaefer, K. M., and D. W. Fuller.
2002. Movements, behavior, and habitat selection of bigeye tuna (*Thunnus obesus*) in the eastern equatorial Pacific, ascertained through archival tags. Fish. Bull. 100:765–788.

Sibert, J. R., M. K. Musyl, and R. W. Brill.
2003. Horizontal movements of bigeye tuna (*Thunnus obesus*) near Hawaii determined by Kalman filter analyis of archival tag data. Fish. Oceanogr. 12(3):141–151.

Sobel, D.
1995. Longitude: the true story of a lone genius who solved the greatest scientific problem of his time, 184 p. Penguin Books, New York, NY.

Sund, P. N., M. Blackburn, and F. Williams.
1981. Tunas and their environment in the Pacific Ocean: a review. Oceanogr. Mar. Biol. Ann. Rev. 19:443–512.

Welch, D. W., and J. P. Eveson.
1999. An assessment of light-based geoposition estimates from archival tags. Can. J. Aquat. Sci. 56:13171–1327.
2001. Recent progress in estimating geoposition using daylight. *In* Electronic tagging and tracking in marine fisheries (Sibert and J. Nielsen, eds.), p. 3693–83. Kluwer Academic Press, Dordrecht, The Netherlands.

Wilson, R. P., J. J. Ducamp, W. G. Rees, B. M. Culik, and K. Neikamp.
1992. Estimation of location: global coverage using light intensity. *In* Wildlife telemetry: remote monitoring and tracking of animals (I. G. Priede and S.M. Swift, eds.) p. 131–134. Ellis Horwood, New York, NY.

Yabe, H., S. Ueyanagi, and H. Watanabe.
1966. Studies on the early life history of bluefin tuna *Thunnus thynnus* and on the larvae of the southern bluefin tuna *T. maccoyii*. Rep. Nankai Reg. Fish. Res. Lab. 23:95–129.

Yamanaka, H., and staff (*sic*).
1963. Synopsis of biological data on kuromaguro *Thunnus orientalis* (Temminck and Schlegel) 1942 (Pacific Ocean). FAO Fish Rep, 6(2):180–217.

Age, growth, mortality, and radiometric age validation of gray snapper (*Lutjanus griseus*) from Louisiana

Andrew J. Fischer
Coastal Fisheries Institute
School of the Coast and Environment
Louisiana State University
Baton Rouge, Louisiana 70803-7503
E-mail address: afische@lsu.edu

M. Scott Baker Jr.
North Carolina Sea Grant
UNC-W Center for Marine Science
5001 Masonboro Loop Rd.
Wilmington, North Carolina 28409

Charles A. Wilson
Louisiana Sea Grant College Program
Louisiana State University
Baton Rouge, Louisiana 70803-7507

David L. Nieland
Coastal Fisheries Institute
School of the Coast and Environment
Louisiana State University
Baton Rouge, Louisiana 70803-7503

Abstract—The gray snapper (*Lutjanus griseus*) is a temperate and tropical reef fish that is found along the Gulf of Mexico and Atlantic coasts of the southeastern United States. The recreational fishery for gray snapper has developed rapidly in south Louisiana with the advent of harvest and seasonal restrictions on the established red snapper (*L. campechanus*) fishery. We examined the age and growth of gray snapper in Louisiana with the use of cross-sectioned sagittae. A total of 833 specimens, (441 males, 387 females, and 5 of unknown sex) were opportunistically sampled from the recreational fishery from August 1998 to August 2002. Males ranged in size from 222 to 732 mm total length (TL) and from 280 g to 5700 g total weight (TW) and females ranged from 254 to 756 mm TL and from 340 g to 5800 g TW. Both edge analysis and bomb radiocarbon analyses were used to validate otolith-based age estimates. Ages were estimated for 718 individuals; both males and females ranged from 1 to 28 years. The von Bertalanffy growth models derived from TL at age were $L_t = 655.4\{1-e^{[-0.23(t)]}\}$ for males, $L_t = 657.3\{1-e^{[-0.21(t)]}\}$ for females, and $L_t = 656.4\{1-e^{[-0.22(t)]}\}$ for all specimens of known sex . Catch curves were used to produce a total mortality (Z) estimate of 0.17. Estimates of M calculated with various methods ranged from 0.15 to 0.50; however we felt that M=0.15 was the most appropriate estimate based on our estimate of Z. Full recruitment to the gray snapper recreational fishery began at age 4, was completed by age 8, and there was no discernible peak in the catch curve dome.

Manuscript submitted 19 September 2003 to the Scientific Editor's Office.

Manuscript approved for publication 20 November 2004 by the Scientific Editor.

Fish. Bull. 103:307–319 (2005).

The gray snapper (*Lutjanus griseus*), commonly referred to as the mangrove snapper, is a temperate and tropical reef species that is found along the southeastern Atlantic coast of the United States from North Carolina to Bermuda, throughout the Gulf of Mexico (GOM), and south to Brazil (Johnson et al., 1994; Allman and Grimes, 2002). Gray snapper are fairly common along the Louisiana coast and are usually associated with complex structures such as oil and gas platforms, artificial reefs and other hard bottom substrates. In 1991 restrictions were put on the recreational red snapper (*Lutjanus campechanus*) fishery; these restrictions coincided with a rapid expansion of the gray snapper fishery in south Louisiana. Recreational anglers now typically target gray snapper once they have reached their bag limit of red snapper; thus peak gray snapper landings generally coincide with the red snapper recreational season (April–October). As a result, recreational landings of gray snapper in Louisiana have increased exponentially from 3.25 metric tons (t) in 1983 to 175 t in 2002 (NMFS[1]). Currently there is a 305 mm (12 inches) minimum size and a recreational bag limit of 10 fish/person/day for gray snapper in the GOM.

Some background information is available for gray snapper in the southeastern United States, mainly from south Florida. Scientists have reported on early life history (Ruth-

[1] NMFS (National Marine Fisheries Service). 2003. Fisheries Statistics and Economics Division. Unpubl. data. Website: http://www.st.nmfs.gov/pls/webpls/MF_ANNUAL_LANDINGS.RESULTS. [Accessed 25 August 2003.]

erford et al., 1989; Domier et al., 1997), population dynamics (Rutherford et al., 1989), juvenile food habits (Hettler, 1989), juvenile distribution (Chester and Thayer, 1990), and reproduction (Domeier et al., 1997; Allman and Grimes, 2002).

Few reports have been conducted on the age and growth of gray snapper. Manooch and Matheson (1981) used sectioned otoliths to age gray snappers from eastern Florida but did not validate their methods. Johnson et al. (1994) also used sectioned otoliths to age fish sampled from Fort Pierce, FL, to Grand Isle, LA, again without validation of methods. Burton (2001) validated the periodicity of opaque zone formation in gray snapper from east coast Florida waters with the use of marginal increment analysis of distal edge measurements. But gray snapper have never been fully examined in the northern GOM and comprehensive age, growth, and mortality data from the thriving Louisiana recreational fishery are virtually nonexistent.

The objectives of our study were to describe the age, growth, and mortality of gray snapper from the Louisiana recreational fishery. We obtained age information through examination of cross-sectioned sagittal otoliths, validated our aging techniques with the use of bomb-radiocarbon ^{14}C and edge analyses, produced mortality estimates with standard procedures, and modeled growth with the von Bertalanffy growth equation.

Methods and materials

Gray snapper were sampled from the Louisiana recreational harvest from August 1998 to August 2002 by personnel from the Louisiana State University Coastal Fisheries Institute and the Louisiana Department of Wildlife and Fisheries. Fish were opportunistically sampled at charter boat facilities in Port Fourchon, LA, and at spearfishing and hook and line fishing tournaments in Grand Isle and New Orleans, LA. Morphometric measurements (fork length [FL] and total length [TL] in mm, total weight [TW] in g) were taken, sex was determined by macroscopic examination of the gonads, and both sagittae were removed, rinsed, and air dried, weighed to the nearest 0.1 mg, and stored in coin envelopes until processed. For specimens in which TL was unavailable, TL was estimated from FL with the equation $TL = 1.048(FL) + 8.35$ (linear regression, df=275; $P<0.001$; $r^2=0.98$) calculated from specimens in which both TL and FL were available.

In order to estimate age of gray snapper, a transverse section (~1 mm thick) was taken containing the core of the left sagittal otolith of each specimen. Sections were made with a Hillquest model 800, thin-sectioning machine equipped with a diamond embedded wafering blade and precision grinder (Cowan et al., 1995). In instances where the left otolith was unavailable, the right was substituted. Examinations of otolith cross-sections were made under a dissecting microscope with transmitted light and polarized light filter from 20× to 64×. Opaque zones were enumerated along the ventral side of the sulcus acousticus from the core to the proximal edge (Wilson and Nieland, 2001). Two readers (AJF and MSB) performed opaque zone counts independently without knowledge of capture date or morphometric data. Otolith marginal edge condition was coded as opaque or translucent by using the criteria described by Beckman et al. (1989). Opaque zones were counted a second time when initial counts differed. In instances where a consensus between readers could not be reached, counts of the more experienced reader (AJF) were used. Between-reader variation in opaque zone counts was examined after the second readings of otolith sections were completed. Differences in counts were evaluated with the coefficient of variation (CV), index of precision (D) (Chang, 1982), and average percent error (APE) (Beamish and Fournier, 1981).

Ages of gray snapper were estimated from opaque annulus counts and capture date with the equation described by Wilson and Nieland (2001):

$$Day\ age = -182 + (opaque\ increment\ count \times 365) + \left((m-1)\times 30\right) + d,$$

where m = the ordinal number (1–12) of month of capture; and
d = the ordinal number (1–31) of the day of the month of capture.

The 182 days subtracted from each age estimate are to account for the uniform hatching date of 1 July assigned for all gray snapper to coincide with peak spawning activity occurring in July (Domeier et al., 1997; Allman and Grimes, 2002). Age in years was assigned by dividing age (in days) by 365. Year of birth (YOB) was back calculated by subtracting our otolith-based age estimates from year of capture.

Validation of the periodicity of opaque zone formation in gray snapper otoliths was examined with two approaches. An advanced and accurate method of age validation uses a quantitative measurement of nuclear bomb-produced radiocarbon (^{14}C) that was accumulated in carbon-containing hard parts of marine organisms before, during, and after the atmospheric testing period of nuclear weapons (1958–65) (Baker and Wilson, 2001). Elevated levels of ^{14}C have been observed in hermatypic corals (Druffel, 1980, 1989) and this time-specific marker can be used to validate age estimates derived from hard parts in marine fishes (Kalish, 1993; Campana and Jones, 1998). Baker and Wilson (2001) recently validated red snapper otolith section age estimates using this technique with excellent results. This same method was applied in our study to the otolith cores of gray snapper hatched after the nuclear testing periods.

Gray snapper hatched prior to 1973 were not available for our study, and thus the steepest portion of the radiocarbon uptake curve could not be used to confirm age estimates. Consequently, no coral reference data for the general area were available after 1983. Because red snapper otoliths have been previously validated

with this same method (Baker and Wilson, 2001), we anticipated that gray snapper radiocarbon values would be roughly similar to red snapper values for a given YOB.

To obtain the oldest portion of the otolith for radiocarbon analysis, right otoliths of older gray snapper with an estimated YOB after the period of atmospheric testing (1973–95) were embedded in araldite epoxy resin and thin sectioned (~1 mm in thickness) through the core with an Isomet low-speed saw. The otolith core region was isolated from the otolith section by using the technique described in Baker and Wilson (2001). Cores were rinsed in double-distilled de-ionized water, allowed to air dry, weighed to the nearest 0.1 mg, and submitted to the accelerator mass spectrometry (AMS) facility in acid-washed 20-mL glass scintillation vials. The mean sample weight submitted for analyses was 12.8 mg.

At the AMS facility, otolith cores underwent acid hydrolysis with 85% phosphoric acid to yield CO_2 which was then made into graphite (pure C) by reduction at high temperature under vacuum. The graphite was pressed onto a target, loaded on the AMS unit and analyzed for radiocarbon. Samples were also analyzed for ^{13}C to correct for natural and machine fractionation effects. Radiocarbon values from individual otolith cores were reported as $\Delta^{14}C$ (mean ±SD), the adjusted deviation from the radiocarbon activity of 19th century wood (Stuiver and Polach, 1977).

The periodicity of opaque zone formation was also examined with edge analysis. The marginal edge of each otolith was examined and coded as

1 opaque zone forming on otolith margin;
4 translucent zone forming on margin up to 1/3 complete;
5 translucent zone forming on margin 1/3 to 2/3 complete;
6 translucent zone forming on margin 2/3 to fully complete.

Percentages of otoliths with opaque margins were plotted by month of capture (Beckman et al., 1989; Campana, 2001; Wilson and Nieland, 2001) for all months in which specimens were available.

In order to examine the predictive capacity of otolith weight (W_o) to determine age in gray snapper, sex specific W_o-age relationships were fitted by using a power function with least squares with the model: $Age = aW_o^b$. A likelihood ratio test (Cerrato, 1990) was used to test for differences between male and female models.

Male and female TW-TL relationships were independently fitted with linear regression to the model $W = aTL^b$ from $\log^{10}$-transformed data. Male and female regression coefficients were compared with an ANCOVA. Variability in age, TL, and TW-frequency distributions of males and females were compared with Komolgorov-Smirnov two-sample tests (Tate and Clelland, 1957; Sokal and Rohlf, 1995). Growth of gray snapper was modeled by using all specimens of known sex. Von Bertalanffy growth models of TL at age were fitted with nonlinear regression by least squares (SAS 6.11, SAS Institute, 1996, Cary, NC) in the form:

$$TL_t = L_\infty(1 - e^{[-k(t)]}),$$

where t = age in years;
TL = TL at age t;
L_∞ = the theoretical maximum TL; and
k = the growth coefficient.

Because of a lack of smaller individuals in our sample population, no y-intercepts for t_0 were specified and models were forced through 0 (Szedlmayer and Shipp, 1994; Fischer et al., 2004) to better estimate juvenile growth. One growth model was generated for all specimens of known sex. Additional models were fitted independently for males and females. Likelihood ratio tests (Cerrato, 1990) were used to test for differences between male and female models.

The instantaneous total mortality rate (Z) was estimated from a catch curve (Nelson and Manooch, 1982; Burton, 2001) assuming our collections represented the actual age distribution of the population. These estimates were made with the regression method of plotting the $\log_e$ age frequency on age. We used the absolute value of the slope of the linear descending right limb of the curve after full recruitment to estimate Z.

Estimates of instantaneous natural mortality (M) were computed with several methods. The first estimate of M was based on Hoenig's (1983) longevity-mortality relationship, where the mortality rate is based solely on the oldest specimen encountered in the data set. We also used Hoenig's (1983) relationship for natural mortality with modifications for sample size. Natural mortality was also computed with the method of Pauly (1980) assuming a mean annual water temperature of 25°C. Our mean annual water temperature estimate was derived from the data buoys operated by the National Oceanic and Atmospheric Administration's National Oceanographic Data Buoy Center from 1995 to 2001. Finally, M was calculated with the Ralston (1987) method, where the estimate of M is based solely on a simple regression involving the Brody growth coefficient (k). A significance level of 0.05 was used for all statistical analyses.

Results

We sampled 833 gray snapper (441 males, 387 females, and 5 individuals of unknown sex) from the recreational fishery of Louisiana for morphometric data and otoliths. The male:female ratio was 1:0.88; a χ^2 test indicated no significant difference between the proportions of males and females (χ^2=3.52, P=0.06). Male and female specimens ranged from 222 to 732 mm TL and from 254 to 756 mm TL, respectively (Fig. 1A). Both sexes exhibited multimodal distributions; males were represented in the greatest numbers at 450 mm TL, compared to 400 mm

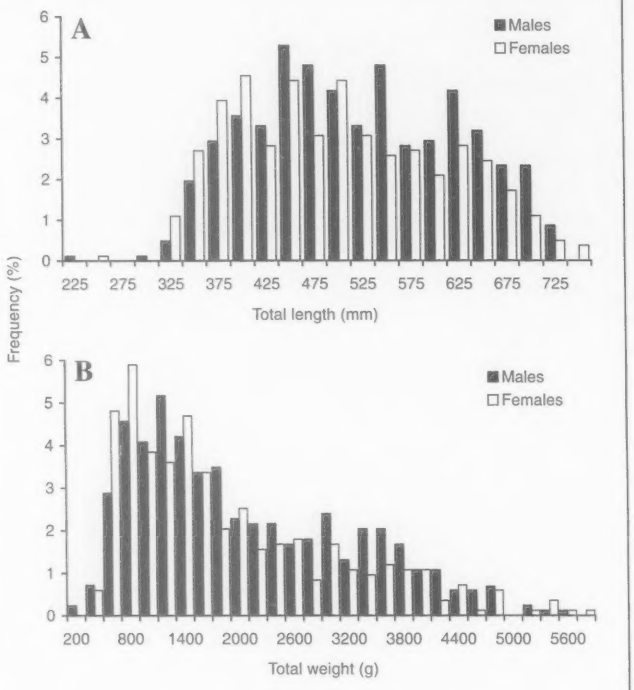

Figure 1

Distributions of (**A**) total length in mm (n=837) and (**B**) total weight in g (n=832) for gray snapper (*Lutjanus griseus*) sampled from the Louisiana 1998–2002 recreational harvest.

TL for females. A Komolgorov-Smirnov two-sample test indicated no significant difference between male and female TL frequencies (maximum difference=9.45). Male and female TW ranged from 200 to 5700 g and 300 to 5800 g TW, respectively (Fig. 1B). Both sexes also displayed multimodal distributions in TW. A Komolgorov-Smirnov two-sample test indicated a significant difference between sexes at 1600 g TW (maximum difference=9.67). A single predictive TL-TW regression was generated for both males and females:

$$TW = 3.31 \times 10^{-5} (TL^{2.85})$$
$$(F_{1, 822}=9{,}326.54;\ P<0.001;\ r^2=0.92).$$

Significant differences were found between sexes in TL-TW relationships (ANCOVA test of homogeneity of slopes, $F_{3,822}=7.25$; $P=0.007$; $r^2=0.92$). Therefore, separate models were fitted for each sex:

$$\text{Males} = TW = 2.04 \times 10^{-5}(x^{2.93})$$
$$(F_{1, 436}=7588.29;\ P<0.001;\ r^2=0.95)$$

$$\text{Females} = TW = 5.5 \times 10^{-5}(TL^{2.77})$$
$$(F_{1,385}=3{,}089.16;\ P<0.001;\ r^2=0.89)$$

Gray snapper otoliths are very similar in physical structure, although much smaller in actual size, to those of the red snapper. Opaque zones are easily distinguishable on the ventral side of the sulcus groove (Manooch and Matheson, 1981; Johnson et al., 1994; Shipp[2]) (Fig. 2, A and B).

Sagittae were collected from 721 gray snapper of which 718 were aged. Readers were unable to resolve opaque zones in three otolith sections because of poor sectioning. Readers agreed on the ages of 568 individuals (78.8%) after initial counts and differed by one opaque annulus for 154 specimens, two annuli for 18 specimens, and three annuli for 2 specimens. Readers agreed on 709 ages (98.7%) after the second reading. The average percent error (APE) was 0.5, coefficient of variation (CV) was 0.00078, and index of percent (D) was 0.0006.

[2] Shipp, R. L. 1991. Investigations of life history parameters of species of secondarily targeted reef fish and dolphin in the northern Gulf of Mexico. Proc. Fourth Annu. MARFIN Conf., San Antonio, TX, p 80–85. [Available from National Marine Fisheries Service, State/Federal Liaison Office, 9721 Executive Center DR. N., St. Petersburg, FL 33702.]

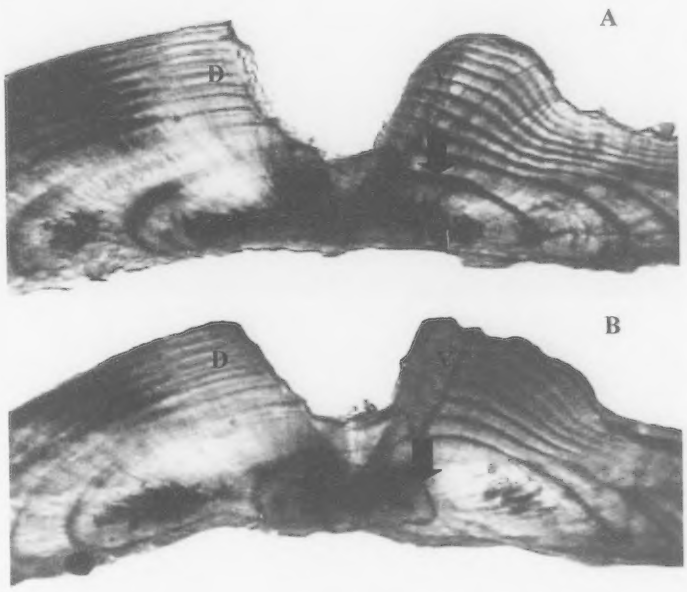

Figure 2

(**A**) Transverse section of a gray snapper (*Lutjanus griseus*) otolith with first opaque zone distant from the core, with 10 opaque zones and an edge condition of 4 and (**B**) transverse section of a gray snapper otolith with first opaque zone close to the core, with 8 opaque zones, and an edge condition of 4. D indicates dorsal side and V indicates ventral side of otolith section.

Table 1

List of gray snapper (*Lutjanus griseus*) otoliths analyzed for stable carbon and bomb radiocarbon. "AMS wt." is the amount of otolith separated from the otolith section and submitted for accelerator mass spectrometry (AMS) radiocarbon analysis; FL=fork length. I.D.= our identification number.

NOS-AMS number	I.D.	Date caught	Otolith section age (yr)	Birth date	Otolith wt. (mg)	AMS wt. (mg)	$\delta^{13}C$ (‰)	$\Delta^{14}C$ (‰)	
								Mean	±SD
OS–36337	320	2001	28	1973	639.1	9.9	–2.67	142.8	9.7
OS–36338	33	2000	25	1975	635.2	14.7	–2.55	126.2	6.7
OS–36339	5	2000	20	1980	536.7	15.0	–3.34	115.3	6.5
OS–36340	322	2001	16	1985	414.6	15.1	–5.27	113.5	11.9
OS–36341	316	2001	11	1990	306.5	9.8	–4.49	91.4	6.1
OS–36342	304	2001	6	1995	154.0	12.2	–5.73	74.5	5.9

The gray snapper (n=6) used for the radiocarbon age validation procedure ranged from 6 to 28 years of estimated age and were collected during 2000 and 2001 (Table 1). Furthermore, YOB ranged from 1973 to 1995. Gray snapper radiocarbon values were plotted along with red snapper radiocarbon values from the northern Gulf of Mexico (Baker and Wilson, 2001) and coral radiocarbon values from Bermuda (Druffel, 1989), South Florida (Druffel, 1989), and Belize (Druffel, 1980) (Fig. 3). Radiocarbon values of gray snapper cores were

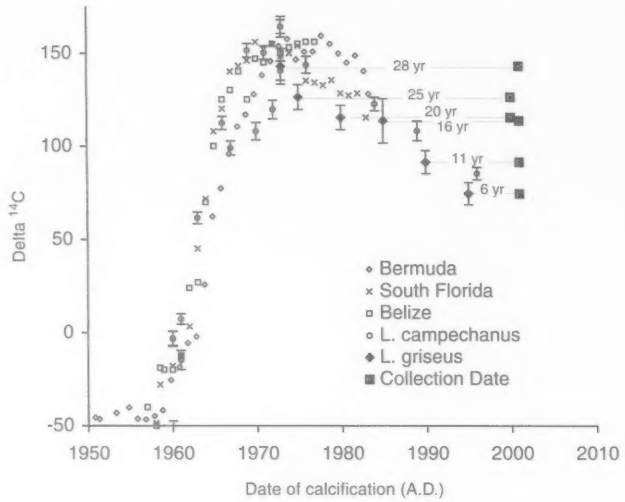

Figure 3

Plot of radiocarbon (^{14}C) values versus date of calcification for gray snapper (*Lutjanus griseus*) (present study) and red snapper (*Lutjanus campechanus*) (Baker and Wilson, 2001) from the northern Gulf of Mexico and from corals off Bermuda (Druffel, 1989), South Florida (1989), and Belize (Druffel, 1980). Solid squares (■) indicate collection dates for the gray snapper samples (n=6) and the age listed are the estimated ages as read from the otolith sections.

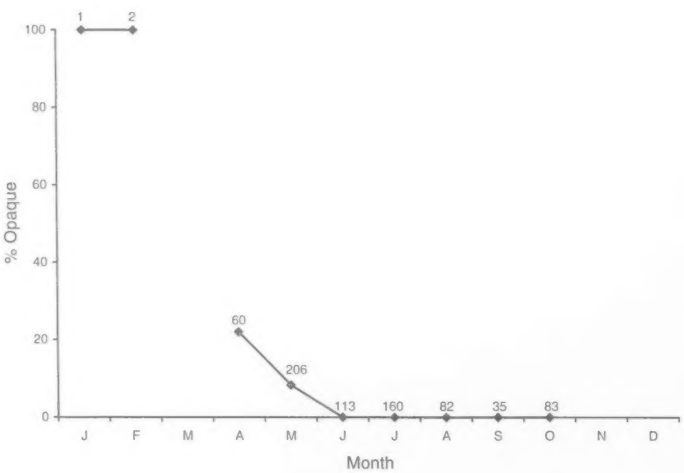

Figure 4

Marginal edge analysis of gray snapper (*Lutjanus griseus*) otoliths sampled from the 1998–2002 Louisiana recreational harvest (n=718). Numbers above data points indicate the number of otoliths analyzed for each month.

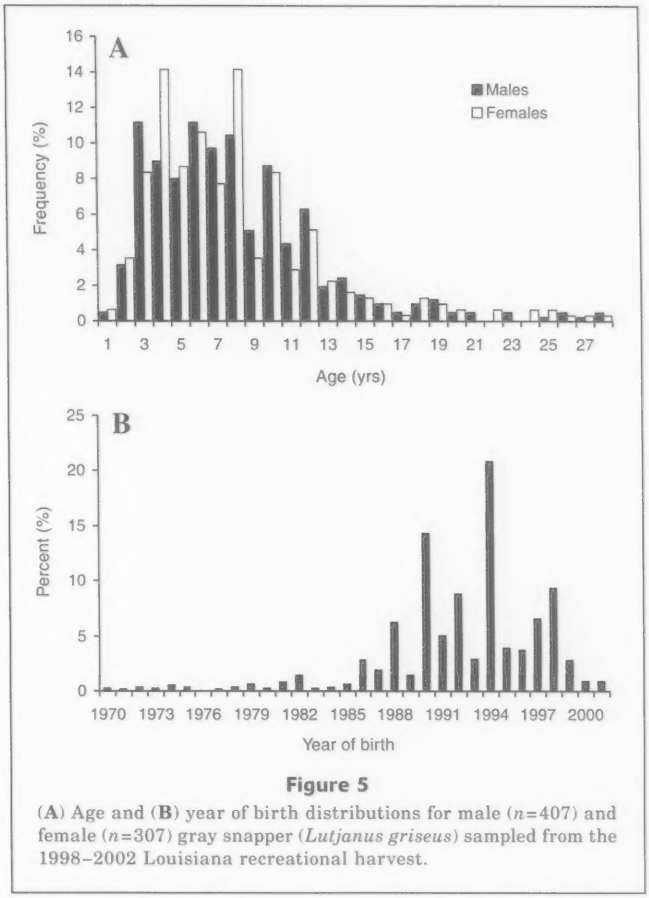

Figure 5

(**A**) Age and (**B**) year of birth distributions for male (n=407) and female (n=307) gray snapper (*Lutjanus griseus*) sampled from the 1998–2002 Louisiana recreational harvest.

highest in 1973 and exhibited a steady decline to a low in 1995.

The periodicity of opaque annulus formation in gray snapper otoliths was further examined by plotting the monthly percentages of otoliths with opaque margins (Fig. 4). Although little data were available for the winter months, one specimen sampled in January and two specimens sampled in February 2001 each exhibited opaque marginal otolith edges indicating that opaque annulus formation occurs during the winter. Minimum percentages of otoliths with opaque margins during the months of April (22%) and May (8%) followed by an absence of opaque margins during the months of June through October indicate the cessation of opaque annulus formation by early spring and the onset of translucent annulus formation beginning in April and continuing through November.

Male and female gray snapper ranged in age from 1 to 28 years (Fig. 5A). There was no significant difference in age distributions between males and females (maximum difference=6.92 yr), but both sexes exhibited variable multimodal distributions in age frequency. Year of birth (YOB) frequency was also multimodal, and the population was dominated by younger fish; 77% of males and 80% of females were aged at 10 years or younger (Fig. 5B).

Significant differences in slopes were detected when plotting age-W_0 relationships between sexes (ANCOVA test of homogeneity of slopes, $F_{3,353}$= 8.06; P=0.0005). Therefore, predictive models of age-W_0 were fitted separately for males and females using a power function with least squares as (Fig. 6)

$$\textit{Male age} = 0.0278\ (W_0)^{1.06}$$
$$(F_{2,\ 204}=3{,}956.29,\ P<0.001,\ r^2=0.89).$$

$$\textit{Female age} = 0.0460\ (W_0)^{0.97}$$
$$(F_{2,148}=4{,}504.05,\ P<0.001,\ r^2=0.90).$$

The single von Bertalanffy growth model to describe gray snapper TL at age (Fig. 7) was

$$L_t = 656.4\{1 - e^{[-0.22(t)]}\}$$
$$(F_{2,714}=32{,}217.6;\ P<0.0001;\ r^2=0.72).$$

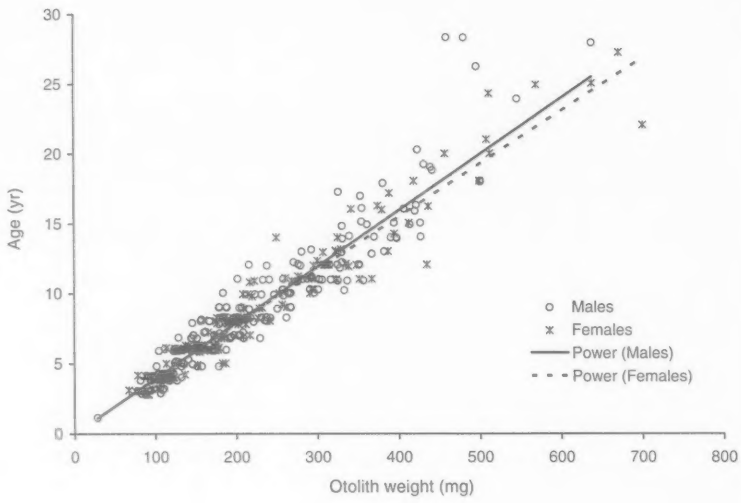

Figure 6

Observed otolith weight (mg) at age for male (n=204) and female (n=148) gray snapper (*Lutjanus griseus*) sampled from the 1998–2002 Louisiana recreational harvests. Plotted lines are power functions fitted to the data.

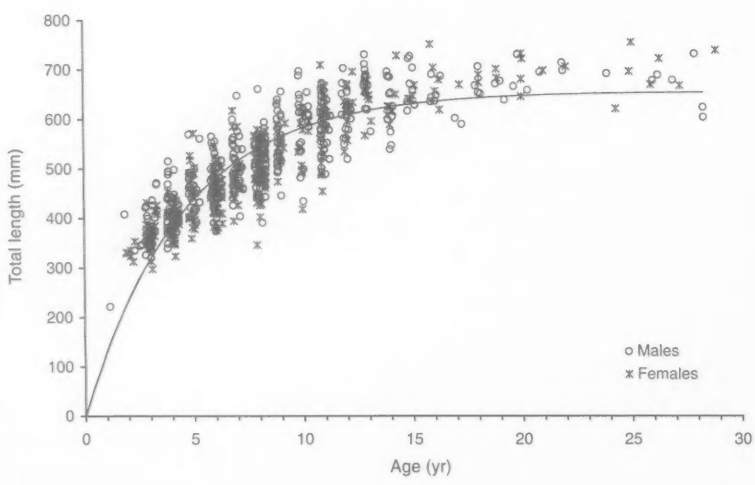

Figure 7

Observed total length (mm) at age for male (n=407) and female (n=307) gray snapper (*Lutjanus griseus*) sampled from the 1998–2002 Louisiana recreational harvests. Plotted lines are von Bertalanffy growth functions fitted to the data.

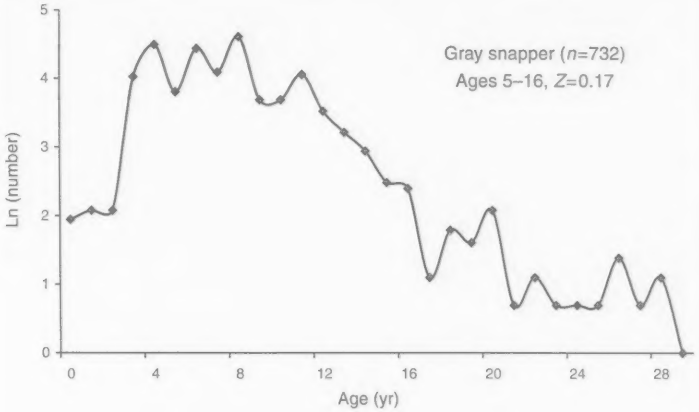

Figure 8

Catch curve for Louisiana gray snapper (*Lutjanus griseus*) (n=742) sampled from 1998 to 2002 Louisiana recreational harvests.

Table 2

Degrees of freedom (df), sum of squares (SS), mean square (MS), F value, and P values for the likelihood ratio test by which the full von Bertalanffy growth model (in which sexes were fitted independently) is compared with the reduced von Bertalanffy model (by fitting all specimens of known sex).

Model	df	SS	MS	F	P
Full	4714	1.9493×10^8	48,732,614	16,341	<0.0001
Reduced	2714	1.9489×10^8	97,447,139	32,217.6	<0.0001

However, a likelihood ratio test indicated growth models for males and females were significantly different from one another (χ^2=494.77; df=2,714; P<0.001) (Table 2). The resultant sex-specific von Bertalanffy growth models were

$$\text{Male} \quad L_t = 655.4\{1 - e^{[-0.23(t)]}\} \quad (F_{2,407}=19{,}732.9;\ P<0.001;\ r^2=0.73)$$

$$\text{Female} \quad L_t = 657.3\{1 - e^{[-0.21(t)]}\} \quad (F_{2,307}=13{,}015.2;\ P<0.0001;\ r^2=0.72).$$

Instantaneous total mortality (Z) was calculated with catch curve analysis. Full recruitment to the gray snapper fishery began at age 4 and was completed by age 8 and there was no discernible peak in the catch curve dome (Fig. 8). For the purposes of Z estimation, age 4 was used as the age of full recruitment to the fishery. Z was estimated at 0.18 for all fish (age range: 5–28 years) and 0.17 for all fish when the age range was truncated at 16 years. The age range was truncated at 16 years because older age classes contained fewer than 10 individuals.

Estimates for natural mortality (M) for gray snapper varied substantially and were dependent upon the method used. Hoenig's (1983) longevity-mortality relationship produced the lowest estimate of 0.15. Hoenig's (1983) relationship modified for sample size yielded an estimate of 0.30. The regression method of Ralston (1987) produced an estimate of 0.40. Finally, Pauly's (1980) method using a mean annual water temperature of 25°C and parameter estimates L_∞ and k derived from the von Bertalanffy growth equations produced the highest estimate of 0.51.

Discussion

Validation of the periodicity of opaque zone formation is critical when using otoliths to determine the ages of fish (Beamish and McFarlane, 1983). The lack of data during the winter months prevented us from making a definitive statement on the timing of opaque zone formation based on edge analysis alone. However, we present evidence that suggests that opaque zone formation may

begin as early as December and proceed through May. Opaque zone formation beginning in December through spring has been shown to occur in the congeneric red snapper (Render, 1995; Patterson et al., 2001; Wilson and Nieland, 2001) as well as in a number of other teleosts in the northern GOM (Beckman et al., 1989, 1990, 1991; Thompson et al., 1999). Burton (2001) validated the periodicity of opaque zone formation for gray snapper along the Atlantic coast but reported the period of formation to occur during the summer months of June and July.

The natural decay of radiocarbon in the world ocean after the nuclear testing period is well documented (Broecker et al., 1985) and close agreement between gray snapper data and existing radiocarbon chronologies from the Gulf of Mexico, U.S. South Atlantic, and Caribbean provided additional evidence that our otolith-section-based age estimates of gray snapper were valid (Fig. 3). The ^{14}C values obtained from gray snapper otolith cores formed after the period of atmospheric testing of nuclear weapons were comparable to, if not slightly less than, those values found in red snapper from the northern Gulf of Mexico (GOM) (Baker and Wilson, 2001).

Although published coral radiocarbon chronologies are available for review and are made available in the present study, we are most confident in comparing gray snapper to the red snapper data for several reasons. First and foremost, these two species were collected from the same general area of the northern Gulf of Mexico and thus in theory should have similar radiocarbon chronologies (Broecker et al., 1985). Second, although the coral samples would seem to be the best possible items for comparison because of their known age, stationary location, and most importantly because multiple "birth dates" can be analyzed from one coral head, the gray snapper and red snapper samples were taken from different geographic areas and thus different water bodies. No known coral radiocarbon chronologies exist for the northern Gulf of Mexico. Radiocarbon chronologies have been shown to vary significantly in the world ocean by latitude (Broecker et al., 1985) and this trend in the reference corals can be seen in Figure 3, especially during the period of rapid radiocarbon uptake (1958–75). Finally, all otolith samples (gray snapper and red snapper) were analyzed for radiocarbon by the same AMS facility by using identical laboratory methods (Baker and Wilson, 2001). Delta ^{14}C data from the otoliths of gray snapper with presumed YOB back to 1973 (the oldest fish in our data set) clearly reflected the same pattern found in red snapper; high levels of oceanic radiocarbon attributable to previous nuclear testing followed by a slow but steady decline to a low in 1995 (Fig. 3). The gray snapper curve is slightly lower but parallel to the red snapper curve. Because of the inherent variability associated with individual fishes, it is inconceivable to think that the two species of snapper would have curves that completely lie on top of each other or on top of the coral chronologies for that matter. Although the two species are very similar in many regards, we can only speculate that differences in juvenile life history patterns, habitat preferences, water column chemistry, and possibly otolith formation may account for the variation in radiocarbon chronologies. However, both the gray snapper and previously validated red snapper chronologies exhibit the same trend and indicate that our otolith-based age estimates are accurate.

The majority of radiocarbon fisheries age validation has produced otolith-based chronologies that resemble those from nearby reference corals or other fish species in the same general location (Campana, 2001). Campana and Jones (1998) observed extremely high and erratic radiocarbon values for black drum (*Pogonias cromis*) in the Chesapeake Bay. In that study, the radiocarbon values resembled the intermediate of surface oceanic (corals) and the much higher atmospheric values (Campana and Jones, 1998). The reasons for the erratic $\Delta^{14}C$ values remain unknown, but Campana and Jones speculated that the estuarine dependency of the species produced the variable activities of radiocarbon in individual fish for a given YOB. This was not the case with gray snapper, also a species that uses the shallow estuarine environment during the first years of its life. Because gray snapper is estuarine dependent, we fully expected the gray snapper radiocarbon values to be erratic and much higher than the reference corals. In contrast, gray snapper radiocarbon values were strikingly similar to, if not less than, red snapper and the reference coral radiocarbon values at all comparable YOBs (Fig. 3). Contrary to the opinions expressed by Campana and Jones (1998), our limited data suggested that estuarine dependency may have no effect on observed radiocarbon values, at least for gray snapper.

Although opaque zones are distinct in gray snapper otolith cross sections, the small size and apparent longevity of the species pose some challenges for age interpretation. In older fish, opaque zones are formed more closely together in the otolith, making accurate counts and accurate interpretation of the otolith margin more difficult. We observed considerable variability in the location of the first opaque zone in gray snapper; the first annulus was variously located somewhat distant from the core to close to and continuous with the otolith core (Fig. 2, A and B). Wilson and Nieland (2001) noted the same pattern in red snapper otoliths suggesting that this variability may be a function of the protracted red snapper spawning season, which is similar to that of gray snapper, and of the rapid growth rate during the juvenile stage. This variability in first opaque zone position accounted for the majority of disagreement between readers in initial age estimates; there was only 76.5% agreement. However, experience by both readers (AJF and MSB) with red snapper otoliths produced consensus of 98.8% after second readings.

Male and female gray snapper ranged in age from 1 to 28 years. Younger individuals composed the major portion of the fishery; 90% of the catch was aged less than 15 years. Maximum ages were greater than those reported in previous studies. Johnson et al. (1994) re-

ported maximum ages of 23 and 25 years for males and females, respectively; the oldest fish in the study was actually sampled from Grand Isle, LA. Burton (2001) reported a non-sex-specific maximum age of 24 years. Sampling for both of these studies was focused in Florida where there is higher fishing pressure on gray snapper (Burton, 2001) and this fishing pressure may explain the lesser maximum ages and paucity of older individuals in their sample populations.

Gray snapper exhibit multimodal distributions in age and YOB frequencies. Due to minimum size limits, very few individuals were represented below age 3. Age distributions exhibited an initial peak at 3 years, when gray snapper are beginning to recruit to the recreational fishery. Successive peaks in age-class abundance in our data set occurred every two years. In an examination of abundance by YOB a similar pattern was observed; strong year classes were followed by diminished year classes. Similar patterns of variability in year-class strength have been observed in black drum (*Pogonias chromis*) and red drum (*Scienops ocellatus*) in the northern GOM. Beckman et al. (1989) suggested that year-class variability in these species might be due to environmental factors during early life stages or biological controls on the population. If this observed consistent pattern is reflective of the gray snapper population off Louisiana, we suggest that the variation in year-class strength may be reflective of intra-species-specific year-class competition of juveniles competing for resources within the estuaries before recruiting to the offshore fishery.

Researchers continually search for effective, cost-efficient ways to acquire fish age data. Body size has been shown to be a poor value to use for estimating age in a number of fish species because of the considerable variability in size at age. Otolith growth has been shown to continue with age, independent of somatic growth. Otolith weight (W_o) has been used as a predictive tool to determine age in a number of fish species (Templeman and Squires, 1956; Beamish, 1979; Wilson and Dean, 1983; Secor et al., 1989; Beckman et al., 1991). Although a strong relationship has been demonstrated between W_o and age, especially for the younger age classes, considerable variability exists in W_o at age in older age classes. For example, the W_o of a 10-yr-old male gray snapper can range from 180 mg to 357 mg thus preventing a precise age estimate based on W_o alone. Although W_o data may provide general information on overall age distribution patterns of a population, we feel that annulus counts from otolith cross sections provide the most accurate age estimates for gray snapper.

Our overall (sexes combined) von Bertalanffy growth model estimated a maximum theoretical length (L_∞) of 656.4 mm TL. Although a likelihood ratio test indicated a significant difference between male and female models, this difference may be of limited biological significance because male and female models appear to be very similar. The presence of larger, older fish in our sample population resulted in our overall model coming to an asymptote at a smaller L_∞ and having a larger respective k than previously reported (Manooch and Matheson, 1981; Johnson et al., 1994). Johnson et al. (1994) predicted an L_∞ of 792.25 mm using the regression method of Manooch and Matheson (1981) to back calculate lengths at age. Johnson et al. (1994) also obtained a much smaller estimate of k at 0.08 compared with a k value of 0.22 predicted in our model. A smaller estimate was not unexpected given the inverse correlation between L_∞ and k noted by Knight (1968). Because of the minimum size limitations on the recreational fishery, smaller (presumably younger) individuals below 304 mm TL were almost absent in our sample population. We chose to not specify a y-intercept for t_0 and to force our growth models through zero in order to obtain more accurate estimates of k. Forcing our models through zero also contributed to the differences in growth parameters between our study and those of Johnson et al. (1994). Like Johnson et al. (1994), Burton (2001) also estimated growth parameters by fitting back-calculated lengths at age. Burton's (2001) L_∞ estimates of 717 mm and 625 mm for north and south Florida, respectively, are similar to those found in our study. Burton's (2001) sample populations consisted of a number of fish below 200 mm TL. These smaller individuals had similar effects on his models as that of forcing our models through zero. Burton's estimates of k were 0.17 and 0.13 for north and south Florida, respectively, compared with a k of 0.22 for our overall model.

We estimated total instantaneous mortality (Z) to be 0.17 and full recruitment to the fishery at age 4. We chose to use the truncated age range of 5–16 years (versus 5–28 years) for Z estimation in order to have at least 10 samples in each age category. Our estimation of Z based on all age categories (5–28) was 0.18. Our estimate of Z is at the low end of the range of values reported by Johnson et al. (1994) (Z=0.17–0.26) for the Gulf of Mexico. It should be noted, however, that Johnson et al. (1994) pooled fish from five distinct geographical locations. Of the 432 fish analyzed in their study, 69% came from Grand Isle, LA (n=104) and Panama City, FL (n=193). The remaining 31% came from the central and southern coasts of Florida. Perhaps Johnson et al.'s (1994) estimates of Z would be lower if only the Louisiana samples were used. Our Z values, however, are much lower than those reported by Manooch and Matheson (1981) (Z=0.39–0.60) and Burton (2001) (Z=0.34–0.95) for the east coast of Florida.

Our low estimate of Z for gray snapper in Louisiana waters is clearly associated with the abundance of older, larger individuals in the population. Unlike the catch curves in previous studies that dealt with gray snapper populations on the east coast of Florida (Manooch and Matheson 1981; Burton 2001) and in the southeast in general (Johnson et al. 1994), the mode of our catch curve is not well defined. It is evident that gray snapper in the South Atlantic are heavily exploited (Burton, 2001), as evidenced from their age-frequency distribution and high estimates of Z.

Estimates of M ranged from 0.15 to 0.51 and were comparable to previous studies on gray snapper from the southeastern United States. Johnson et al. (1994) used the Pauly (1980) and Ralston (1987) methods to estimate M to range from 0.12 to 0.32 for the west coast of Florida, including Louisiana. Manooch and Matheson (1981) used the Pauly (1980) relationship to calculate M = 0.22. Burton (2001) used the same four methods as in our study and found M to range from 0.18 to 0.43. It is well known that estimates of mortality are highly variable and depend upon the parameters used to calculate them. The purpose of providing various estimates of M was to demonstrate to the reader the variability in this important life history parameter and to demonstrate how little we actually know about it. Adopting our estimate of Z, we feel that the Hoenig (1983) method (M=0.15) produced the most suitable estimate of M for gray snapper in Louisiana waters of the northern Gulf of Mexico. Based on the apparent age-size structure of the stock, historical landings data, and personal observation, all indications are that this species is lightly fished in this study area. Hoenig (1983) indicated that M should be roughly equivalent to Z if the population is lightly exploited. Our estimate of Z (0.17) was indeed roughly equivalent to M (0.15), supporting our belief that fisheries mortality (F) is not yet a significant threat to this fishery.

Gray snapper could become over-exploited if a large, intensive fishery developed in the northern Gulf of Mexico. Landings of gray snapper in Louisiana have increased dramatically over the last few years, partly because of the recent restrictions imposed on red snapper in the Gulf of Mexico. Compared to the gray snapper population structure in the South Atlantic, especially off the coast of south Florida (Manooch and Matheson, 1981; Burton, 2001), the Louisiana population appears to be healthy. Long-term heavy fishing pressure has probably affected the south Florida gray snapper population (Burton, 2001). As a result, the population structure of south Florida is dramatically different from that of Louisiana. Our estimates of Z are extremely low and indicate that fishing mortality (F) is currently not a significant factor for the gray snapper population in Louisiana waters. A low-intensity gray snapper fishery could take most of the resource without endangering future production.

Acknowledgments

Funding and assistance with sampling was provided by the Louisiana Department of Wildlife and Fisheries. We would also like to thank Josh Maier, Brett Blackmon, and Candace Aiken for sampling efforts and otolith processing as well as Brain Milan for providing juvenile gray snapper samples. We thank Steve Tomeny, the boat captains, and deck hands of Captain Steve Tomeny's charters in Port Fourchon, LA, as well as all the recreational fishermen that allowed us to sample their catch. We wish to thank Ann P. McNichol of National Ocean Sciences (Accelerator Mass Spectrometry facility at the Woods Hole Oceanographic Institution) for otolith radiocarbon analyses.

Literature cited

Allman, J. A., and C. B. Grimes.
2002. Temporal and spatial dynamics of spawning, settlement, and growth of gray snapper (*Lutjanus griseus*) from the West Florida shelf as determined from otolith microstructures. Fish. Bull. 100:391–403.

Baker, M. S. Jr., and C. A. Wilson.
2001. Use of bomb radiocarbon to validate otolith section ages of red snapper *Lutjanus campechanus* from the northern Gulf of Mexico. Limnol. Oceanogr. 46:1819–1824.

Beamish, R. J.
1979. New information on the longevity of the Pacific ocean perch (*Sebastes alutus*). J. Fish. Res. Board Can. 36: 1395–1400.

Beamish, R. J., and D. A. Fournier.
1981. A method for comparing the precision of a set of age determinations. Can. J. Fish. Aquat. Sci. 38:982–983.

Beamish, R. J., and G. A. McFarlane.
1983. The forgotten requirement for age for age validation in fisheries biology. Trans. Am. Fish. Soc. 112:735–743.

Beckman, D. W., A. L. Stanley, J. H. Render, and C. A. Wilson.
1990. Age and growth of black drum in Louisiana waters of the Gulf of Mexico. Trans. Am. Fish. Soc. 119:537–544.
1991. Age and growth-rate estimation of sheepshead, *Archosargus probatocephalus*, in Louisiana waters using otoliths. Fish. Bull. 89:1–8.

Beckman, D. W., C. A. Wilson, and A. L. Stanley.
1989. Age and growth of red drum, *Sciaenops ocellatus*, from offshore waters of the northern Gulf of Mexico. Fish. Bull. 87:17–28.

Broecker, W. S., T. Peng, G. Ostlund, and M. Stuiver.
1985. The distribution of bomb radiocarbon in the world ocean. J. Geophys. Res. 90:6953–6970.

Burton, M. L.
2001. Age, growth, and mortality of gray snapper, *Lutjanus griseus*, from the east coast of Florida. Fish. Bull. 99:254–265.

Campana, S. E., and C. M. Jones.
1998. Radiocarbon from nuclear testing applied to age validation of black drum, *Pogonias cromis*. Fish. Bull. 96: 185–192

Campana, S. E.
2001. Accuracy, precision and quality control in age determination, including a review of the use and abuse of age validation methods. J. Fish Biol. 59:197–242.

Cerrato, R. M.
1990. Interpretable statistical tests for growth comparisons using parameters in the von Bertalanffy equation. Can. J. Fish. Aquat. Sci. 47:1416–1426.

Chang, W. B.
1982. A statistical method for evaluating the reproducibility of age determination. Can. J. Aquat. Sci. 39:1208–1210.

Chester, A. J., and G. W. Thayer.
1990. Distribution of spotted seatrout (*Cynoscion nebul-*

sus) and gray snapper (*Lutjanus campechanus*) juveniles in seagrass habitats of western Florida Bay. Bull. Mar. Sci. 46(2):345–357.

Cowan, J. H. Jr., R. L. Shipp, H. K. Bailey IV, and D. W. Haywick.
1995. Procedure for rapid processing of large otoliths. Trans. Am. Fish. Soc. 124:280–282.

Domeier, M. L., C. C. Loenig, and F. C. Coleman.
1997. Reproductive biology of the gray snapper (*Lutjanus griseus*), with notes on spawning for other Western Atlantic snappers (*Lutjanidae*). *In* Biology and culture of tropical groupers and snappers (F. Arreguin-Sanchez, J. L. Munro, M. C. Balgos, and D. Pauly, eds.), p. 189–201. ICLARM Conf. Proc. 48.

Druffel, E. M.
1980. Radiocarbon in annual coral rings of Belize and Florida. Radiocarbon 22:363–371.
1989. Decadal time scale variability of ventilation in the North Atlantic: high-precision measurements of bomb radio-carbon in banded corals. J. Geophys. Res. 94:3271–3285.

Fischer, A. J., M. S. Baker Jr., and C. A. Wilson.
2004. Red snapper, Lutjanus campechanus, demographic structure in the northern Gulf of Mexico based on spatial patterns in growth rates and morphometrics. Fish. Bull. 102:593–603.

Hettler, W. F., Jr.
1989. Food habits of juveniles of spotted seatrout and gray snapper in western Florida Bay. Bull. Mar. Sci. 44(1): 155–162.

Hoenig, J. M.
1983. Empirical use of longevity data to estimate mortality rates. Fish. Bull. 82:898–903.

Johnson, A. G., L. A. Collins, C. P. Keim.
1994. Age-size structure of gray snapper from the Southeastern United States: a comparison of two methods of back-calculating size at age from otolith data. Proc. Annu. Conf. Southeast Assoc. Fish and Wildl. Agencies 48:592–600.

Kalish, J. M.
1993. Pre- and post-bomb radiocarbon in fish otoliths. Earth Planet. Sci. Lett. 114:549–554.

Knight, W.
1968. Asymptotic growth: an example of nonsense disguised as mathematics. J. Fish. Res. Board Can. 25(6):1303–1307.

Manooch, C. S., III, and R. H. Matheson III.
1981. Age, growth and mortality of gray snapper collected from Florida waters. Proc. Annu. Conf. Southeast Assoc. Fish Wildl. Agencies 35:331–344.

Nelson, R. S., III, and C. S. Manooch III.
1982. Growth and mortality of red snappers in the west-central Atlantic Ocean and northern Gulf of Mexico. Trans. Am. Fish Soc. 111:465–475.

Patterson, W. F. III, James H. Cowan Jr., Charles A. Wilson, and Robert L. Shipp.
2001. Age and growth of red snapper, *Lutjanus campechanus*, from an artificial reef area off Alabama in the northern Gulf of Mexico. Fish. Bull. 99: 617–627.

Pauly, D.
1980. On the interrelationshops between natural mortality, growth parameters, and mean environmental temperature in 175 fish stocks. J. Cons. Int. Explor. Mer 39:175–192.

Ralston, S.
1987. Mortality rates of snappers and groupers. *In* tropical snappers and groupers: biology and fisheries management (J. J. Polovina and S. Ralston, eds.), p. 375–404. Westview Press, Boulder, CO.

Render, J. H.
1995. The life history (age, growth, and reproduction) of red snapper (*Lutjanus campechanus*) and its affinity for oil and gas platforms. PhD. diss., 76 p. Louisiana State University, Baton Rouge, LA.

Rutherford, E. S., T. W. Schmidt, and J. T. Tilmant
1989. Early life history of spotted sea trout (*Cynoscion nebulosus*) and gray snapper (*Lutjanus griseus*) in Florida Bay, Everglades National Park, Florida. Bull. Mar. Sci. 44(1):49–64.

Rutherford, E. S., J. T. Tilmant, E. B. Thue, and T. W. Schmidt.
1989. Fishery harvest and population dynamics of gray snapper, *Lutjanus griseus*, in Florida Bay and adjacent waters. Bull. Mar. Sci. 44:139–154.

Secor, D. H., J. M. Dean, and R. B. Baldevarona.
1989. Comparison of otolith growth and somatic growth in larval and juvenile fishes based on otolith length/fish length relationships. Rapports et Proces-Verbaux des Reunions, Counseil International pour l'Exploration de la Mer 191:431–438.

Sokal, R. R., and F. J. Rohlf.
1995. Biometry: the principles and practice of statistics in biological research. 3rd ed., 887 p. W.H. Freeman and Co., NewYork, NY. [ISBN:0-7167-2411-1.]

Stuiver, M., and H. Polach.
1977. Reporting of ^{14}C data. Radiocarbon 19:355–363.

Szedlmayer, S. T., and R. L. Shipp.
1994. Movement and growth of red snapper, *Lutjanus campechanus*, from an artificial reef area in the northeastern Gulf of Mexico. Bull. Mar. Sci. 55(2-3):887–896.

Tate, M. W., and R. C. Clelland.
1957. Non-parametric and shortcut statistics in the social, biological, and medical sciences, p 93–94. Interstate Printers and Publishers, Inc., Danville, IL.

Templeman , W., and H. J. Squires
1956. Relationship of otolith lengths and weights in the haddock *Melanogrammus aeglefinus* (*L.*) to the rate of growth of the fish. J. Fish. Res. Board Can. 13:467–487.

Thompson, B. A., M. Beasley, and C. A. Wilson .
1999. Age distribution and growth of greater amberjack, *Serioloa dumerilli*, from the north-central Gulf of Mexico. Fish. Bull. 97:362–372.

Wilson, C. A., and J. M. Dean.
1983. The potential use of sagittae for estimating the age of Atlantic swordfish, *Xiphias gladius*. NOAA Tech. Rep. NMFS 8:151–156.

Wilson, C. A., and D. L. Nieland.
2001. Age and growth of red snapper, *Lutjanus campechanus*, from the Northern Gulf of Mexico off Louisiana. Fish. Bull. 99:653–664.

Abstract—The objective of this study was to investigate the spatial patterns in green sea urchin (*Strongylocentrotus droebachiensis*) density off the coast of Maine, using data from a fishery-independent survey program, to estimate the exploitable biomass of this species. The dependence of sea urchin variables on the environment, the lack of stationarity, and the presence of discontinuities in the study area made intrinsic geostatistics inappropriate for the study; therefore, we used triangulated irregular networks (TINs) to characterize the large-scale patterns in sea urchin density. The resulting density surfaces were modified to include only areas of the appropriate substrate type and depth zone, and were used to calculate total biomass. Exploitable biomass was estimated by using two different sea urchin density threshold values, which made different assumptions about the fishing industry. We observed considerable spatial variability on both small and large scales, including large-scale patterns in sea urchin density related to depth and fishing pressure. We conclude that the TIN method provides a reasonable spatial approach for generating biomass estimates for a fishery unsuited to geostatistics, but we suggest further studies into uncertainty estimation and the selection of threshold density values.

Estimating exploitable stock biomass for the Maine green sea urchin (*Strongylocentrotus droebachiensis*) fishery using a spatial statistics approach

Robert C. Grabowski

School of Marine Sciences
5741 Libby Hall
University of Maine
Orono, Maine 04469
Present address: Flat 6, Falmer House
16-17 Marylebone High St.
London, W1U 4NY, England
E-mail address: grabowskirc6@yahoo.com

Thomas Windholz

The GIS Training and Research Center
Idaho State University
Pocatello, Idaho 83209-8130

Yong Chen

School of Marine Sciences
5741 Libby Hall
University of Maine
Orono, Maine 04469

Manuscript submitted 27 January 2003 to the Scientific Editor's Office.

Manuscript approved for publication 21 December 2004 by the Scientific Editor.

Fish. Bull. 103:320–330 (2005).

The green sea urchin (*Strongylocentrotus droebachiensis*) is an important resource of the fishing industry in the State of Maine, where it currently ranks fourth by value. The commercial fishing industry began in the late 1980s as a result of expanding foreign markets. Landings reached a peak of more than 22,000 metric tons (t) in 1993. However, declining stock abundances have caused landings to diminish over the last decade, and in 2001, less than 5,000 t were landed (Chen and Hunter, 2003). Considering the economic importance of the fishery and its persistent decline in yield, it is essential that we establish an accurate quantitative assessment of the stock in order to develop an effective management plan.

The Maine Department of Marine Resources (DMR) has collected fishery-dependent information since the beginning of the state's commercial fishery. This information, including catch and size-composition data, has formed the basis of most management decisions in the fishery. The fishery is currently managed through limited entry, a restricted number of opportunity days, and sea urchin size limits, in which legal-size sea urchins have a test diameter between 52 mm and 76 mm. The fishing grounds are divided into two management areas based on spatial and temporal variations in spawning (Fig. 1), in which management differs only by fishing seasons (Vadas et al., 2002).

Chen and Hunter (2003) conducted the first formal stock assessment for the Maine green sea urchin in 2001. Fishery-dependent data and sea urchin life history parameters were used to assess the population dynamics of the Maine urchin stock. A length-based stock assessment model was used with a Bayesian approach to determine probabilistic estimates of current stock biomass and exploitation rate. The study estimated that the current stock biomass was extremely low, about 10% of the virgin biomass. Only fishery-dependent data were available at the time the stock assessment was conducted, but in

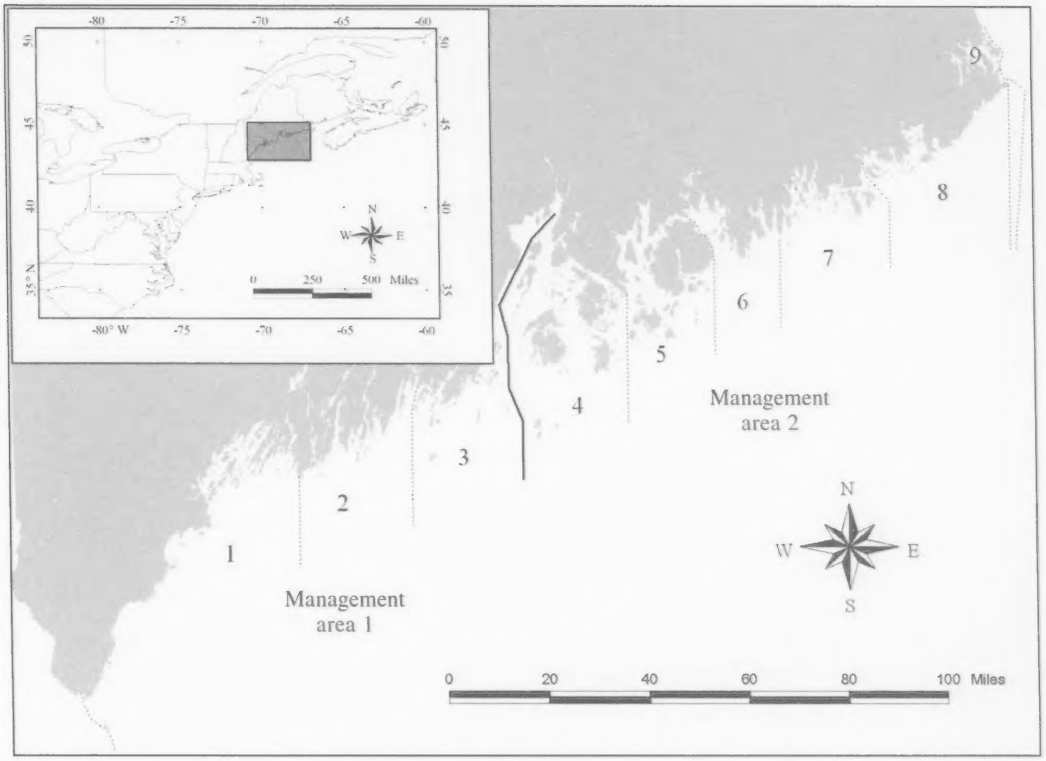

Figure 1

Map of the Maine coastline, showing the two management areas and the nine study strata from the fishery-independent survey program for green sea urchins (*Strongylocentrotus droebachiensis*).

2001 the DMR began an extensive fishery-independent survey program. This program generates large, spatially referenced, scientific data sets each year, which can be incorporated into stock assessments by using either fisheries population dynamics models or spatial analysis techniques.

Spatial statistics, also known as spatial statistics or geostatistics, encompasses a diverse group of techniques that can be used to model the spatial variability of a process, such as sea urchin density, to estimate the value at unobserved locations (Bailey and Gatrell, 1995; Petitgas, 2001). Spatial variability is routinely divided into two categories: first- and second-order effects, or similarly, large- and small-scale variability. Large-scale variability is the variation in the mean value of the process over the study area, whereas small-scale variability is the spatial dependence of the process, in other words the similarity between neighboring sites (Bailey and Gatrell, 1995).

Intrinsic second-order methods, along with kriging, have become the most popular geostatistical tools and are now commonly used to estimate exploited fish stock biomass (e.g., Simard et al., 1992; Petitgas, 1993; Pelletier and Parma, 1994; Maravelias et al., 1996; Lembo et al., 1998; Maynou et al., 1998; Rivoirard et al., 2000; Petitgas, 2001). Two assumptions must be met to use intrinsic geostatistical methods: 1) independence between the variable and the region's geometry and 2) stationarity (Petitgas, 1993; Warren, 1998; Rivoirard et al., 2000). If these assumptions are violated, we can attempt to modify the data to make them more applicable or we must use other spatial analysis techniques to estimate the spatial patterns.

Tessellation is a spatial analysis technique that investigates first-order, or large-scale, spatial variability of a process (Ripley, 1981; Bailey and Gatrell, 1995). Triangulated irregular networks (TINs), or Delaunay triangulation, are the simplest and most common tessellation technique, in which a three-dimensional surface of contiguous, non-overlapping triangles is created by linear interpolation of the variable. TINs are most commonly used for visualization purposes but can be used to estimate the biomass of a process (Simard et al., 1992; Guan et al., 1999). They have received limited use in fisheries stock assessment, however, because if a stock exhibits stationarity, second-order methods tend

to provide more precise biomass estimates, as well as a quantification of their variances (Simard et al., 1992; Bailey and Gatrell, 1995; Guan et al., 1999).

The objective of our study is to investigate the spatial trends in green sea urchin density using spatial analysis techniques to estimate stock biomass. In doing so, we address the suitability of second-order methods to analyze a fishery with a target species that is highly spatially variable over a large, complex study area. We compare biomass estimates from several techniques to address the suitability of TINs for biomass estimation in the green sea urchin fishery.

Materials and methods

Data collection and processing

Sea urchin density and size-frequency information were obtained from the 2001 pilot study for the State's annual fishery-independent survey. The Department of Marine Resources conducted the survey in June and early July, after the fishing season had ended. The survey was restricted to rock and gravel habitats along the Maine coast and we used two modes of data collection, divers and video. In the first part of the study, divers sampled 144 sites according to a stratified random sampling design. The design consisted of 16 sites in each of 9 survey strata, where the width of a survey stratum was inversely proportional to the commercial landings in the region. At each site, SCUBA divers randomly sampled 30 quadrats (1 m^2 each) along three parallel linear transects set perpendicular to shore, for a total of 90 quadrats per site. The sampling intensity was divided equally among three depth zones: 0–5 m, 5–10 m, and 10–15 m. At each site, size-frequency data were obtained by randomly subsampling one quadrat in each depth zone, in which test diameters were measured for all individuals in the quadrat. An additional 148 sites were sampled, in a 15–40 m depth zone, with a video camera that recorded 10 quadrats (0.5 m^2 each) at each site. Because of the low sea urchin densities at these sites, test diameters were measured for all recorded specimens. Mean sea urchin density values were calculated for each site (n=292) and for each depth zone within a site (n=580). An analysis of variance (ANOVA) was used to test if there were significant differences in mean sea urchin density and test diameter among survey strata.

Five test diameter categories were created to more accurately represent the wide range of individual sea urchin weights. The categories were based on the state's minimum and maximum size restrictions, allowing us to separately estimate the biomass of sea urchins that have not yet recruited to the fishery, sea urchins within the fishery, and sea urchins that have escaped the fishery. The minimum (50 mm) and maximum (80 mm) size limits for our study were set slightly wider than the those of the state, because, according to the fishery regulations, up to 10% of the catch can be illegal-size sea urchins. Size-frequency data from subsampled quadrats were applied to the mean sea urchin density for the specific depth zone and site, to generate density values for each size category. Weight per sea urchin was calculated from the mean length of the category by using a length-weight relationship (Scheibling et al., 1999).

Spatial interpolation

A sample semivariogram, often abridged to variogram, was generated from mean sea urchin densities by site, to examine the second-order spatial variation in the data set. The sample variogram was calculated with the following equation (Bailey and Gatrell, 1995):

$$\gamma(h)=\frac{1}{2n(h)}\sum_{S_i-S_j=h}(z_i-z_j)^2, \quad (1)$$

where S_i and S_j = sampling point pairs with (x,y) coordinates;
n = the number of sample point pairs;
h = the distance between pairs; and
z = mean urchin density for the sample.

Trends in the variogram provide insights into the viability of second-order methods for the sea urchin data.

Representations of the large-scale trends in sea urchin density were created by using Delaunay triangulated irregular networks (TINs) (ArcView 3.2a, 3D and Spatial Analyst Extensions, Redlands, CA). First, the sample points were plotted by using sea urchin density (/m^2) as the z value. Second, each point was connected to the three nearest sites by linear interpolation, forming a continuous surface of nonoverlapping triangles (Fig. 2) (Bailey and Gatrell, 1995; Guan et. al., 1999). Thus, the z value of any location within a triangular surface is based solely on the three nearest sites. TIN surfaces were generated for 40 different scenarios, according to the size category, depth zone, and management area, which minimizes variability and allows us to produce more realistic biomass estimates. Finally, using a customized C++ program,[1] we modified each surface to include only areas of appropriate sea urchin habitat. The green sea urchin is most commonly found on rocky substrate in the shallow subtidal (Scheibling and Hatcher, 2001), and, accordingly, the original survey program was limited to areas with predominately rock or gravel substrata in areas less than 40 meters deep. Therefore, we used a map of surficial geology to identify areas of the correct substrate type (1:100,000 scale) (Kelley et al., 1997) and digital gridded bathymetry data to create a plot of 5-m isoline contours. The bathymetry data source consisted of digital bathymetry data sets from sources such as NOAA and the Naval Oceanographic Office (15 arc second resolution) (Roworth and Signell, 2002).

[1] The C++ code used in this study is available upon request from the principal author (RCG).

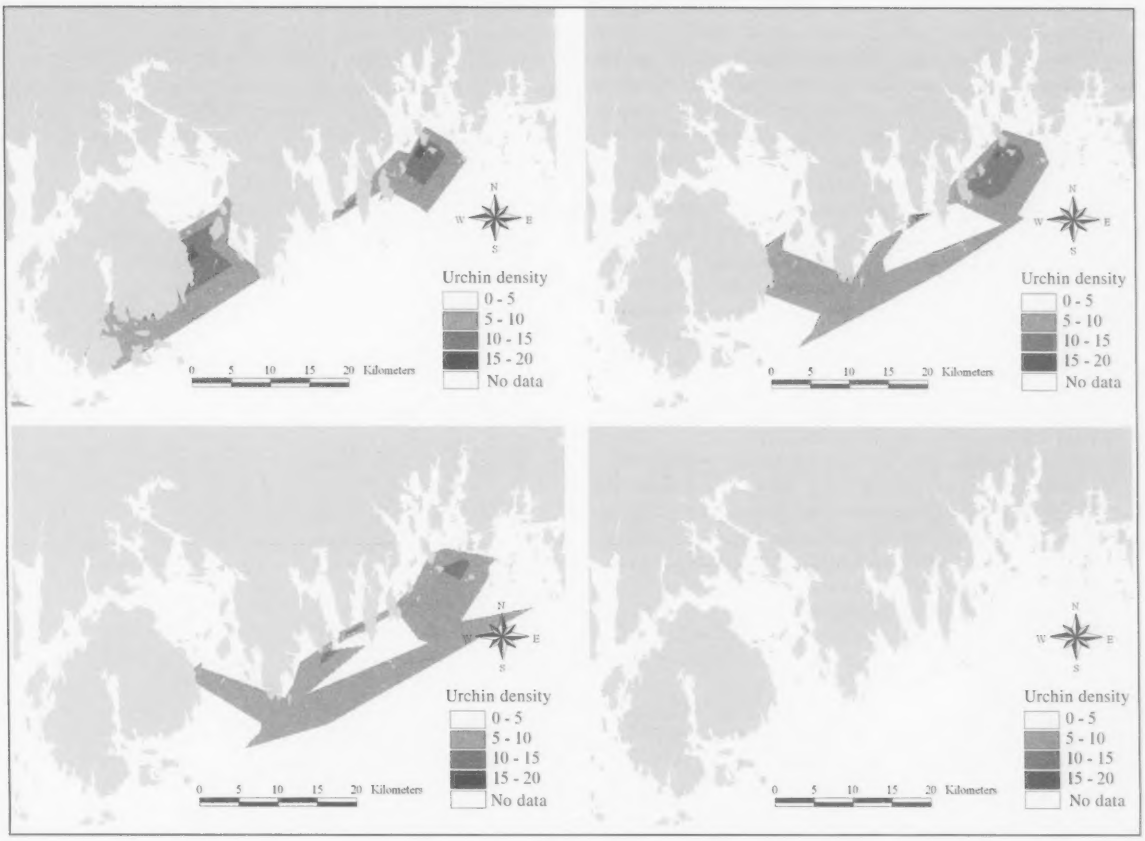

Figure 2

Representations of the triangulated irregular networks (TINs), used to characterize the large-scale patterns in green sea urchin (*Strongylocentrotus droebachiensis*) density (number of sea urchins/m^2), for the 50–64 mm sea urchin size category in the central portion of management area 2. Top left, 0–5 m depth zone; top right, 5–10 m depth zone; bottom left, 10–15 m depth zone; bottom right, 15–40 m depth zone.

To determine total sea urchin biomass (b) for each scenario, the volume beneath the modified TIN surface was calculated, from Riemann sums, and multiplied by the mean weight (w) according to the following equation:

$$b = w\sum_{i=1}^{n} f(s_i)g, \qquad (2)$$

where s_i = the spatial location (x,y) on an ASCII grid;
n = the number of grids squares;
$f(s_i)$ = the TIN surface and corresponds to a z value for each grid cell; and
g = the grid cell size, which was 1.72 hectares for area 1 and 1.82 hectares for area 2.

Fishable biomass is defined as the biomass of all legal-size sea urchins and is simply the subset of the total biomass corresponding to legal-size sea urchins. Exploitable biomass corresponds to the legal-size sea urchins that are available to the fishery. Some areas included in this study may not be subject to fishing pressure because of geographic isolation or low sea urchin densities. Because information on historical fishing grounds is insufficient, exploitable biomass was estimated by using a threshold density value. Only areas with densities greater than the threshold were included in the exploitable biomass estimates.

Two different types of threshold values were tested: 1) a threshold based on total sea urchin density and 2) a threshold based on the density of legal-size sea urchins. The threshold values make different assumptions about the fishery: method 1 assumes that fishermen target areas based on total sea urchin density, whereas method 2 assumes that fishermen target areas based on the density of legal-size sea urchins. Interviews were conducted with state sea urchin biologists and fishermen to determine an appropriate threshold value. The reported threshold values, the minimum total sea

urchin density that could attract fishermen, ranged from 20–50 sea urchin/m^2. For the first scenario, the mean density from the range of recommended values, 35 sea urchin/m^2, was selected. Therefore, the biomass of legal-size sea urchins was calculated only in areas where total sea urchin density was equal to or greater than 35/m^2. For the second scenario, we estimated that commercial divers target areas that have greater than 10 legal-size sea urchins/m^2.

Estimation of uncertainty and stock assessment

Because information on uncertainty cannot be directly obtained from the TIN method, cross validation was employed to approximate uncertainty in the estimation process. Cross validation involves randomly removing a site from a data set and predicting its value based on the other data points using the TIN process (Bailey and Gatrell, 1995). Residuals, or prediction errors, are calculated between the predicted and true values at the site. The process is repeated n times, resulting in an observed set of n prediction errors, or residuals. The frequency distribution and spatial distribution of residuals provide insights into the accuracy of the model; an ideal model would have a mean residual value of 0 and positive and negative residuals would be distributed randomly over the study area.

Sea urchin biomass values were also calculated with the arithmetic mean to provide comparisons with the spatially derived estimates. For total biomass, mean sea urchin densities by survey strata were multiplied by a spatially derived area estimate of suitable sea urchin habitat (<40 meters in depth) in the strata and the mean sea urchin mass per strata. Fishable biomass was calculated the same way but sea urchin density values were scaled by the proportion of legal-size sea urchins in the stratum. Finally, exploitation rates, or the ratio of commercial landings to the exploitable biomass estimates, were calculated to facilitate comparison with the results generated from the population dynamics stock assessment and a recent study on biological reference points (Chen and Hunter, 2003; Grabowski and Chen, 2004).

Table 1

Quadrat density counts (/m^2) for the green sea urchin (*Strongylocentrotus droebachiensis*) by management area and survey strata. Sample size, n, is the number of quadrats observed.

		Density				
Area	Stratum	Min.	Max.	Mean	SD	n
1	1	0	36	0.17	1.62	1706
	2	0	130	2.57	10.63	1600
	3	0	141	3.20	11.29	1580
2	4	0	180	4.20	14.13	1490
	5	0	127	4.24	12.52	1580
	6	0	147	10.06	17.59	1530
	7	0	113	7.90	13.85	1498
	8	0	113	13.50	20.38	1570
	9	0	280	34.45	44.03	1540

Table 2

Sea urchin test diameter (mm) for green sea urchins (*Strongylocentrotus droebachiensis*) subsampled in the fishery-independent survey program.

		Density				
Area	Stratum	Min.	Max.	Mean	SD	n
1	1	7	80	38,69	21,07	29
	2	3	81	39,01	22,19	627
	3	4	89	45,25	18,90	855
2	4	3	89	32,99	19,82	1148
	5	3	77	29,25	17,56	1034
	6	4	110	39,87	16,23	1734
	7	5	92	47,23	16,07	1283
	8	3	114	42,11	16,86	2567
	9	3	114	28,84	12,90	5263

Results

Sea urchin density and size frequency, which were used to calculate biomass, varied considerably along the coast of Maine. Density (number of sea urchins/m^2) differed significantly among survey strata ($P<0.05$; ANOVA), showing a general large-scale trend of increasing density from stratum 1 to 9 (Table 1). Density also varied by depth; the sea urchin density in the 15–40 m depth zone was 0.32 sea urchins/m^2, significantly lower than those of the three shallow (<15 m) depth zones ($P<0.05$, t-test), which each had approximately 9.50 sea urchins/m^2. Sea urchin test diameter varied from 3 mm to 114 mm (mean at 35.90 mm). Test diameter differed significantly among survey strata ($P<0.05$; ANOVA), in which strata 4, 5, and 9 had the smallest size sea urchins, and strata 3 and 5 had the largest (Table 2). No meaningful trend was evident in the sample variogram, which showed a pure nugget effect (Fig. 3). This result indicates that the sea urchin density data were too spatially variable to be analyzed by intrinsic small-scale methods.

Total sea urchin biomass was estimated at approximately 250,000 metric tons (t), and legal-size sea urchins accounted for 165,000 t (Fig. 4). Most of the biomass was found in management area 2, which accounted for over 75% and 80% of the total and fishable biomass, respectively (Table 3). For both estimates, biomass varied by depth, being highest in the 0–5 m depth zone and lowest in the 15–40 m depth zone (Fig. 5).

The two methods used to estimate exploitable biomass produced different biomass estimates with unique

Table 3

A summary of 2001 biomass estimates and 2000-2001 landings, in metric tons, for the Maine green sea urchin fishery. Biomass estimates for the TIN method and arithmetic mean were generated in this study, whereas the population dynamics estimates are from Chen and Hunter (2003). Area 1 consists of strata 1–3 and area 2 consists of strata 4–9. When possible, 95% confidence intervals are included, in italics.

	Area 1	Area 2	Total
TIN method			
Total biomass	45,868	204,304	250,172
Fishable biomass	39,060	126,725	165,786
Exploitable biomass			
Method 1	3645	5793	9438
Method 2	10,886	12,069	22,955
Arithmetic mean			
Total biomass	47,933	290,954	338,887
	(42,399–54,331)	*(274,632–307,977)*	*(317,031–362,308)*
Fishable biomass	24,241	90,185	114,426
	(21,575–27,287)	*(85,144–95,144)*	*(106,719–122,723)*
Population dynamics	6550	8452[1]	15,002
	(4041–9450)	*(5866–11,701)*	*(10,307–21,151)*
2000–2001 landings	2148	3213	5361

[1] 2000 value.

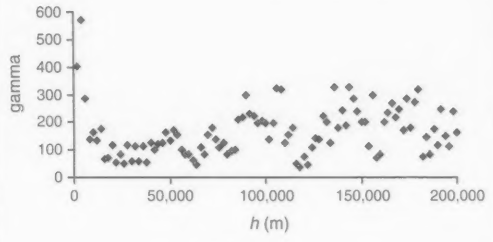

Figure 3

Sample variogram of mean green sea urchin (*Strongylocentrotus droebachiensis*) density by site, showing small-scale variability, gamma (γ), with respect to the distance between sample point pairs, h.

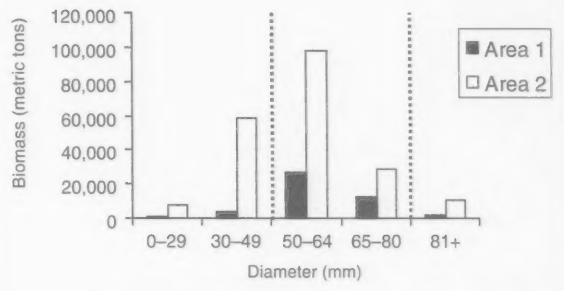

Figure 4

Total biomass by green sea urchin (*Strongylocentrotus droebachiensis*) test diameter according to management area. Sea urchins between 50 and 80 mm were considered legal size for this study, and the biomass within these limits, indicated by the dashed lines, constitutes the fishable biomass.

spatial distributions. Exploitable biomass estimates for method 2 were more than 2 times greater than those for method 1 (Table 3). With method 1, legal-size sea urchins were concentrated in the northeastern corner of management area 2, but with method 2, they were concentrated in the northeastern portion of area 1 and the central portion of area 2 (Fig. 6). Exploitable sea urchin biomass showed different patterns by management area and depth than did total biomass and fishable biomass (Fig. 5). For example, management area 1 had a larger share of the total exploitable biomass, 39% or 47%, for methods 1 and 2, respectively, and this biomass was almost exclusively found in the 0–5 m depth zone, accounting for 98% or 93%, respectively, of the area's biomass.

TIN biomass estimates were similar to ones produced with the arithmetic mean but were higher for total biomass and lower for fishable biomass. Exploitation rates for method 1 were estimated at 0.59 and 0.55 for management areas 1 and 2, respectively, and 0.20 and 0.27 for method 2, respectively. Exploitation rates

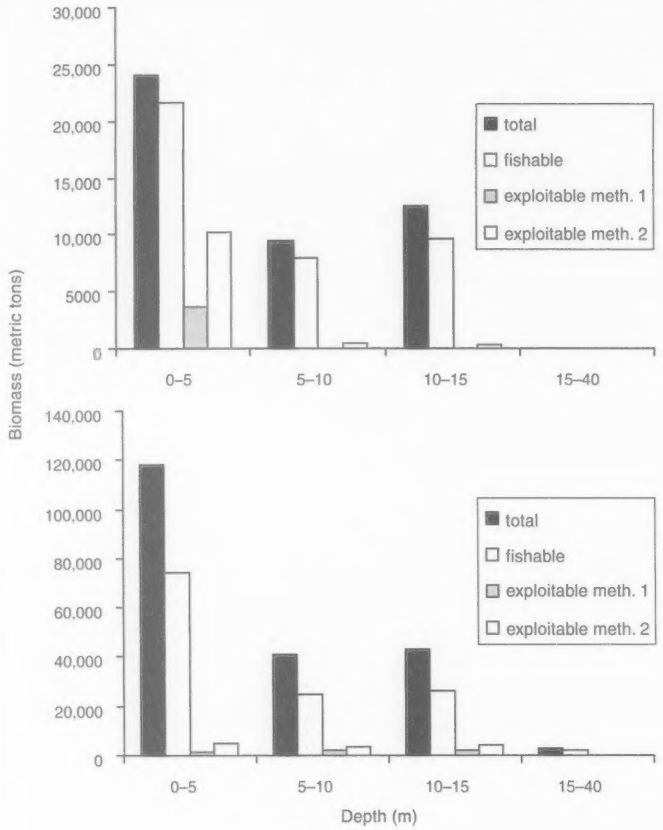

Figure 5

Total, fishable, and exploitable green sea urchin (*Strongylocentrotus droebachiensis*) biomass estimates by depth zone. Top, area 1; bottom, area 2.

from the population dynamics modeling approach were 0.38 and 0.57 (2000) for management areas 1 and 2, respectively.

Cross validation of sea urchin density surfaces yielded a mean residual of 0.50 (median=0, standard deviation=1.86, skewness=2.80, n=60) (Fig. 7). Residuals were greatest in regions with the highest spatial variability, such as sites within depth zones 1 and 2 and in the eastern survey strata.

Discussion

Spatial variability and distribution

The objective of this study was to investigate the spatial variability in green sea urchin density to estimate the biomass of the Maine stock. However, several factors limited the choice of spatial statistical approaches that could be used to assess the fishery. In particular, the physical structure of the study area, the dependence of sea urchin variables upon the environment and a high degree of small-scale spatial uncertainty make small-scale approaches inappropriate.

First, the study area was neither uniform nor continuous. Because the aim of the fishery-independent survey program was to assess the whole population of sea urchins in Maine, the study area had to span the entire coastline. Consequently, the study area encompassed many features that create discontinuities in a spatial model at varying, yet relatively small, spatial scales. These features included the highly indented coastline, the presence of several hundred islands and the exclusion of regions because of environmental constraints. Second, green sea urchin variables were not independent of the study area; rather, they were dependent on several environmental, ecological, and anthropogenic factors. In particular, depth, substrate type,

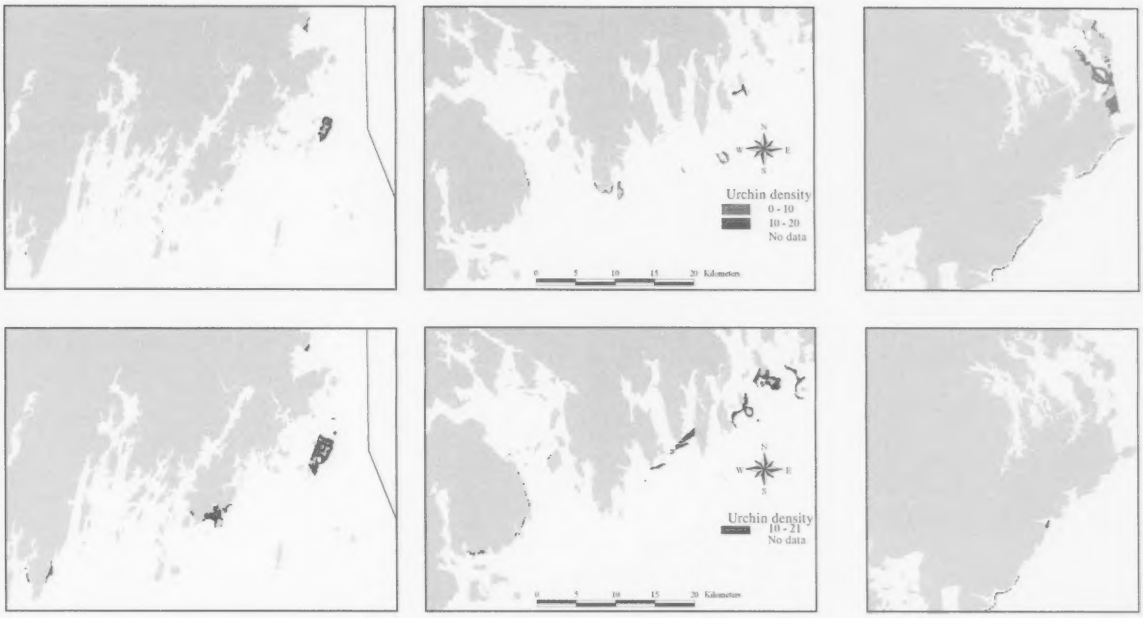

Figure 6

Final spatial representations of the density of exploitable green sea urchins (*Strongylocentrotus droebachiensis*). Top row, method 1: threshold was based on total sea urchin density. Bottom row, method 2: threshold was based on legal-size sea urchin density. Left column, eastern portion of management area 1; middle column, central portion of management area 2; right column, northeastern corner of management area 2.

benthic algal presence, and the presence and level of fishing or predatory activity all greatly affect urchin density, growth rates, and size frequency (Vadas et al., 1986; Scheibling and Hatcher, 2001). Mean sea urchin density and size frequency were not constant over the study area (Tables 1 and 2). Density exhibited large-scale spatial trends along the coast, which are related, at least, to depth and fishing activity. The eastward increase in total sea urchin density along the coast corresponded well with the historical patterns of commercial sea urchin fishing in the State of Maine (Table 1). The fishery began in the southwest, but as sea urchin densities dropped in those regions, the fishery steadily progressed northeastward along the coast. Spatial patterns in density by depth (0–15 m vs. 15–40 m) may have been caused, in part, by the difference in sampling techniques, yet the magnitude of the differences and support from ecological studies indicate that there is a pattern. Finally, sea urchin densities varied dramatically on small spatial scales—variations on the order of one magnitude within the same habitat, and sometimes only meters apart, are not uncommon (Scheibling and Hatcher, 2001). This variability was evident in the variogram analysis, which showed no meaningful small-scale spatial structure and thus no stationarity (Fig. 3).

We were interested in identifying a spatial statistical approach that would generate reasonable estimates of stock biomass. The numerous discontinuities in the study area, the dependence of variables on ecological factors, and the high spatial variability indicated that an intrinsic spatial statistical approach was not appropriate for the investigation. Therefore, we needed an approach that was geared towards the detection and modeling of large-scale variability and that also exhibited some robustness to discontinuities caused by the indented coastline, islands, and habitat constraints. We believe the TIN approach used in this study satisfies these requirements, and, additionally, allows for varying levels of resolutions, with finer resolution in high density sampling areas.

Biomass estimates

We calculated exploitable biomass in two different ways because of the different assumptions they make about the fishery. Method 1 assumes that fishermen target areas based on total sea urchin density, whereas method 2 assumes that fishermen target areas based on the density of legal-size sea urchins. The spatial distributions of legal-size sea urchin density, which were used to calculate exploitable biomass, were distinctive and showed little overlap between methods (Fig. 6). The spatial distributions appear to reflect different aspects of the sea urchin fishery. When the threshold was based on total density (method 1), exploitable biomass was

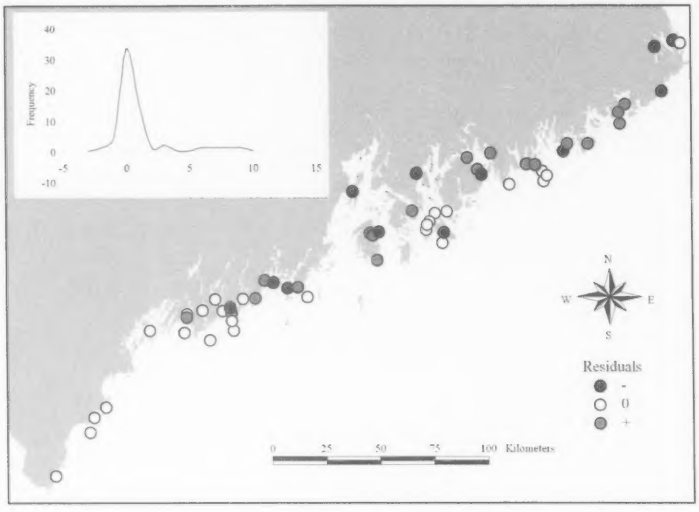

Figure 7

Spatial distribution of residuals and frequency distribution, insert (median=0, standard deviation=1.86, skewness=2.80, n=60), from the cross-validation study that addressed uncertainty in the TIN estimation process for estimating biomass for the green sea urchin (*Strongylocentrotus droebachiensis*) fishery.

concentrated in the eastern corner of management area 2, which is the most northeastern location on the coast of Maine. This area has high total sea urchin densities, but relatively low densities of legal-size adults, and is an important location for the trawling industry. When the threshold was based on the density of legal-size sea urchins (method 2), however, exploitable biomass was concentrated in the eastern portion of management area 1 and the central portion of area 2. These regions have lower average sea urchin densities, but higher percentages of legal-size adults, and are key fishing grounds for the state's dive-based fishery.

Because the two methods reflected different aspects of the fishery, it is not surprising that they produced different estimates of exploitable biomass (Table 3). Nevertheless, these estimates did not differ considerably from those of the population dynamics model. The spatial analysis estimates bordered the ones derived from the population dynamics model; method-1 estimates were smaller than those derived from the population dynamics model whereas method-2 estimates were larger. The biomass estimates were similar despite the fact that they were derived from different models (spatial analysis and population dynamics model) using entirely different data sources (fishery-independent and fishery-dependent).

The status of a fishery is often determined by comparing the current fishing mortality or stock biomass with biological reference points (BRPs) (Hilborn and Walters, 1992). The previous stock assessment study estimated that the sea urchin stock biomass in Maine is only about 10% of the virgin biomass, implying that the fishery has been severely overfished. A preliminary investigation into BRPs recently estimated a BRP $F_{0.1}$ for the urchin fishery, based on a yield per recruit analysis, and concluded that estimates of the current exploitation rate are much higher than the BRP, which means that the fishery is being overfished (Grabowski and Chen, 2004). However, when we compare the TIN exploitation rates with the preliminary mean BRP $F_{0.1}$, which ranged from 0.37 to 0.43 depending upon uncertainty levels, we get an unclear assessment of the stock status. The fishery is being drastically overfished according to method 1, but is healthy according to method 2. We believe that the assessment generated by method 2 was unrealistically optimistic, considering the results from the stock assessment and the decade-long declining trend in landings.

Uncertainty and further studies

The TIN method was an appropriate spatial statistical approach for estimating biomass for the sea urchin fishery; however, a disadvantage of this technique is that there is no straightforward method to estimate the uncertainty in the biomass estimates. Because the technique does not incorporate a variance structure into the estimation process, we could not directly estimate uncertainty. Therefore, we used cross-validation to approximate the uncertainty associated with the TIN method (Fig. 7). We found that the mean residual did not equal zero, indicating that there is a global bias in the TIN surfaces and that biomass estimates were likely overestimated (Simard et al., 1992). This bias was most likely caused

by a combination of the underlying patterns in spatial variability, the linear interpolation method employed in TIN formation, and the effects of sample selection in the cross-validation study. There are several possible ways to reduce the bias in the estimation process, such as incorporating a smoothing function or weighting based on neighbors into the TIN model. This procedure would not completely address uncertainty, however, because it would only acknowledge uncertainty in the TIN estimation process. To obtain confidence intervals for biomass estimates, we needed to incorporate uncertainty in mean density and in TIN estimation. We are currently investigating methods to estimate confidence intervals, such as using a Monte Carlo simulation approach. A thorough examination and quantification of uncertainty is beyond the scope of this article.

In this study, we identified a basic approach for investigating spatial patterns, and estimating stock biomass in situations where second-order methods are inappropriate. The TIN technique generated realistic biomass estimates that are similar to those derived with other approaches, but before we can recommend this technique for the green sea urchin fishery, several points must be addressed. First, the two methods used to estimate exploitable biomass must be integrated because they reflect different aspects of the fishery and result in different stock assessments. Second, a process must be established to estimate threshold levels because they have a large control over exploitable biomass estimates. Finally, a technique must be developed to estimate uncertainty in biomass. We would also recommend further investigations into tracking fishing pressure and identifying its effects on the benthic ecosystem and the spatial distribution of sea urchins.

Acknowledgments

We would like to thank the staff at the Maine Department of Marine Resources for collecting and compiling the sea urchin fishery data. We would especially like to thank Margaret Hunter and Robert Russell from the DMR, Kathryn Wisz, our laboratory assistant, Ryan Weatherbee, for his help with the manuscript, and Olivier Mette, for his technical assistance. This project was partially supported by grants from the Northeast Consortium (UNH SUB 302-628), the Maine Department of Marine Resources (G1102012), and the Sea Urchin Zone Council to Y. Chen and a Maine Marine Science Fellowship from the Marine Department of Marine Resources and the University of Maine School of Marine Sciences to R. Grabowski.

Literature cited

Bailey, T., and A. Gatrell.
1995. Interactive spatial data analysis, 413 p. Pearson Education, Essex, England.

Chen, Y., and M. Hunter.
2003. Assessing the green sea urchin (*Strongylocentrotus droebachiensis*) stock in Maine, USA. Fish. Res. 60:527–537

Guan, W., R. H. Chamberlain, B. M. Sabol, and P. H. Doering.
1999. Mapping submerged aquatic vegetation with GIS in the Caloosahatchee Estuary: evaluation of different interpolation methods. Mar. Geod. 22:69–92.

Grabowski, R., and Y. Chen.
2004. Incorporating uncertainty into the estimation of the biological reference points $F_{0.1}$ and F_{max} for the Maine green sea urchin (*Strongylocentrotus droebachiensis*) fishery. Fish. Res. 68:367–371

Hilborn, R., and C. J. Walters.
1992. Quantitative fisheries stock assessment: choice, dynamics and uncertainty, 570 p. Chapman and Hall, New York, NY.

Kelley, J. T., W. A. Barnhardt, D. F. Belknap, S. M. Dickson, and A. R. Kelley.
1997. The seafloor revealed: the geology of the northwestern Gulf of Maine inner continental shelf, 55 p. Open file source 96-6. Maine Geological Survey, Natural Resources Information and Mapping Center, Augusta, ME.

Lembo, G., T. Silecchia, P. Carbonara, A. Acrivulis, and M. T. Spedicato.
1998. A geostatistical approach to the assessment of the spatial distribution of *Parapenaeus longirostris* (Lucas, 1846) in the central-southern Tyrrhenian Sea. Crustaceana 72:1093–1095.

Maravelias, C. D., D. G. Reid, E. J. Simmonds, and J. Haralabous.
1996. Spatial analysis and mapping of acoustic survey data in the presence of high local variability: geostatistical application to North Sea herring (*Clupea harengus*). Can. J. Fish. Aquat. Sci. 53:1497–1505.

Maynou, F. X., F. Sarda, and G. Y. Conan.
1998. Assessment of the spatial structure and biomass evaluation of *Nephrops norvegicus* (L.) populations in the northwestern Mediterranean by geostatistics. ICES J. Mar. Sci. 55:102–120.

Pelletier, D., and A. M. Parma.
1994. Spatial distribution of Pacific halibut (*Hippoglossus stenolepis*): an application of geostatistics to longline survey data. Can. J. Fish. Aquat. Sci. 51:1506–1518.

Petitgas, P.
1993. Geostatistics for fish stock assessments: a review and an acoustic application. ICES J. Mar. Sci. 50: 285–298.
2001. Geostatistics in fisheries survey design and stock assessment: models, variances and applications. Fish and Fisheries 2:231–249.

Ripley, B. R.
1981. Spatial statistics, 252 p. John Wiley & Sons, New York, NY.

Rivoirard, J., J. Simmonds, K. G. Foote, P. Fernandes, and N. Bez.
2000. Geostatistics for estimating fish abundance, 206 p. Blackwell Science, Oxford, UK.

Roworth, E., and R. Signell.
2002. Construction of a digital bathymetry for the Gulf of Maine. http://woodshole.er.usgs.gov/project-pages/oracles/gomaine/bathy/data.htm. [Accessed 22 October 2002.]

Scheibling, R. E., A. W. Hennigar, and T. Balch.
1999. Destructive grazing, epiphytism, and disease: the dynamics of sea urchin-kelp interactions in Nova Scotia. Can. J. Fish. Aquat. Sci. 56:2300–2314.

Scheibling, R. E., and B. G. Hatcher.
2001. The ecology of *Strongylocentrotus droebachiensis*. *In* Edible sea urchin biology and ecology (J. M. Lawrence, ed.), p. 271–304. Elsevier, New York, NY.

Simard, Y., P. Legendre, G. Lavoie, and D. Marcotte.
1992. Mapping, estimating biomass, and optimizing sampling programs for spatially autocorrelated data: case study of the northern shrimp (*Pandalus borealis*). Can. J. Fish. Aquat. Sci. 49:32–45.

Vadas, R. L., R. W. Elner, P. E. Garwood, and I. G. Babb.
1986. Experimental aggregation behavior in the sea urchin *Strongylocentrotus droebachiensis*. Mar. Biol. 90: 433–448.

Vadas, R. L., Sr., B. D. Smith, B. Beal, and T. Dowling.
2002. Sympatric growth morphs and size bimodality in the green sea urchin (*Strongylocentrotus droebachiensis*). Ecol. Monogr. 72:113–132.

Warren, W. G.
1998. Spatial analysis for marine populations: factors to be considered. *In* Proceedings of the North Pacific symposium on invertebrate stock assessment and management (G. S. Jamieson and A. Campbell, eds.), p. 21–28. Can. Spec. Publ. Fish. Aquat. Sci. 125.

Abundance and distribution of California sea lions (*Zalophus californianus*) in central and northern California during 1998 and summer 1999

Mark S. Lowry
National Marine Fisheries Service
Southwest Fisheries Science Center
8604 La Jolla Shores Dr.
La Jolla, California 92037
E-mail address: mark.lowry@noaa.gov

Karin A. Forney
National Marine Fisheries Service
Southwest Fisheries Science Center
110 Shaffer Road
Santa Cruz, California 95060

Abstract—The abundance and distribution of California sea lions (*Zalophus californianus*) in central and northern California was studied to allow future evaluation of their impact on salmonids, the ecosystem, and fisheries. Abundance at-sea was estimated by using the strip transect method from a fixed-wing aircraft with a belly viewing port. Abundance on land was estimated from 126-mm-format aerial photographs of animals at haulouts between Point Conception and the California–Oregon border. The sum of these two estimates represented total abundance for central and northern California. Both types of survey were conducted in May–June 1998, September 1998, December 1998, and July 1999. A haulout survey was conducted in July 1998. The greatest number of sea lions occurred near Monterey Bay and San Francisco Bay for all surveys. Abundance was high in central and northern California in 1998 when warm water from the 1997–98 El Niño affected the region and was low in July 1999 when cold water La Niña conditions were prevalent. At-sea abundance estimates in central and northern California ranged from 12,232 to 40,161 animals, and haulout abundance was 13,559 to 36,576 animals. Total abundance of California sea lions in central and northern California was estimated as 64,916 in May–June 1998, 75,673 in September 1998, 56,775 in December 1998, and 25,791 in July 1999. The proportion of total abundance to animals hauled-out for the four complete surveys ranged from 1.77 to 2.13, and the mean of 1.89 was used to estimate a total abundance of 49,697 for July 1998. This multiplier may be applicable in the future to estimate total abundance of California sea lions off central and northern California if only the abundance of animals at haulout sites is known.

Manuscript submitted 1 October 2002 to the Scientific Editor's Office.

Manuscript approved for publication 14 December 2004 by the Scientific Editor.

Fish. Bull. 103:331–343 (2005).

The California sea lion (*Zalophus californianus*) is distributed from central Mexico to British Columbia, Canada. Four islands off southern California (Santa Barbara, San Clemente, San Nicolas, and San Miguel Islands) form the reproductive center for the U.S. population, although some pupping occurs at various other haulout sites in central California (Pierotti et al., 1977; Keith et al., 1984). The number of individuals off California varies throughout the year because sea lions from Mexico enter and leave California waters and individuals from California migrate southward into Mexico or northward as far as British Columbia, Canada (Bartholomew, 1967; Bigg, 1988; and Huber, 1991). In southern California, the abundance of California sea lions peaks during the summer breeding season (Bartholomew, 1967; Odell, 1975). In central and northern California, the number of sea lions typically increases in the autumn during the northward migration, declines in winter, increases in spring as sea lions move to rookeries in southern California and Mexico, and declines in summer (Orr and Poulter, 1965; Mate, 1975; Sullivan, 1980; and Griswold, 1985; Bonnell et al.[1]).

Since the mid-1970s, the California sea lion population in the United States has expanded at an average of 5.0% per year and was most recently estimated to be between 204,000 and 214,000 individuals in 1999 (Forney et al.[2]). This estimate is roughly 2.7 times greater than in 1981–83 (Bonnell et al.[1]). As the U.S. sea lion population has grown, concerns have arisen about potential impacts on commercially harvested fish stocks. California sea lions feed on a variety of fish and cephalopods, some of which are commercially important species, such as salmonids (*Oncorhynchus* spp.), Pacific sardines (*Sardinops sagax*), northern anchovy (*Engraulis mordax*), Pacific mackerel (*Scomber japonicus*), Pacific whiting (*Merluccius productus*), rockfish (*Se-*

[1] Bonnell, M. L., M. O. Pierson, and G. D. Farrens. 1983. Pinnipeds and sea otters of central and northern California, 1980–1983: status, abundance, and distribution. Center for Marine Studies, Univ. California, Santa Cruz. OCS Study MMS 84-0044, 220 p. Prepared for Pacific OCS Region, Minerals Management Service, U.S. Department of Interior, Camarillo, Calif. 93010, contract no. 14-12-0001-29090.

[2] Forney, K. A., J. Barlow, M. M. Muto, M. Lowry, J. Baker, G. Cameron, J. Mobley, C. Stinchcomb, and J. V. Carretta. 2000. U.S. Pacific marine mammal stock assessments: 2000. NOAA Tech. Memo.: NOAA-TM-NMFS-SWFSC-300, 276 p. National Marine Fisheries Service, Southwest Fisheries Science Center, 8604 La Jolla Shores Drive, La Jolla, CA 92037.

bastes spp.), and market squid (*Loligo opalescens*) (Lowry et al., 1990, 1991; Lowry and Carretta, 1999; Weise, 2000). Effects on these resources have been estimated for Monterey Bay only, where during the 1997–98 El Niño sea lions consumed an estimated 269.1 to 804.7 metric tons (t) of salmon, 988.4 to 2206.8 t of sardine, and 533.4 to 1827.4 t of rockfishes annually (Weise, 2000). Recently, salmon in central and northern California have experienced population declines and some stocks have been listed as threatened or endangered under the U.S. Endangered Species Act. Although a variety of factors are responsible for the decline (e.g., logging, dams, agriculture, fishing), some salmonid populations are at such reduced levels that predation by sea lions may negatively affect their recovery (NMFS[3]). Sea lions also have been documented as interfering with recreational fisheries by consuming bait and chum and depredating hooked fish (Fluharty[4]).

Existing methods of population assessment have been based on pup counts obtained at California sea lion rookeries near the end of the breeding season and total population has been estimated by extrapolating data from a life history model (Barlow and Boveng, 1991; Boveng[5]; Barlow et al.[6, 7]; Forney et al.[2]). However, this approach cannot be used outside of the breeding season or in nonbreeding areas. Previous studies of California sea lion abundance and distribution in central and northern California during 1980–82 (Bonnell et al.[1]) and 1995–96 (Beeson and Hanan[8]) included only animals on land; animals at sea were either not considered or were included as a rough estimate. An assessment approach was, therefore, needed to provide quantitative estimates of California sea lion abundance in central and northern California that included both animals at sea and on land.

This study uses a combination of the strip-transect method (to estimate at-sea abundance) and aerial photographic counts (to estimate abundance of sea lions on land) in order to estimate the total abundance of California sea lions in central and northern California. Abundances were estimated separately for seven latitudinal zones within central and northern California. This study also describes distribution of sea lions by age and sex class in central and northern California, describes offshore distribution of sea lions, and introduces a new multiplier that can be used to estimate the total abundance of California sea lions at sea and on land, when only an estimate of the number of animals on land is available.

Methods

Survey dates and areas

Surveys were conducted during May–June, July, September, and December 1998, and July 1999. The May–June survey occurred when salmonid smolts were migrating out of rivers (NMFS[3]), the July survey when the United States stock of California sea lions was expected to be distributed mostly in California coastal waters, and the September and December surveys when adult salmon were migrating into rivers (NMFS[3]). The study area encompassed the waters and shoreline of central and northern California from Point Conception (34°26.8′N, 120°28.0′W) to the California–Oregon border (42°00.0′N, 124°12′W) within approximately sixty nautical miles of the coast (Fig. 1).

Strip-transect surveys

A twin-engine, high-wing Partenavia PN68C- or PN68-observer model aircraft was flown at an airspeed of 185 km/h during strip-transect and coastal haulout surveys. Abundance of sea lions at sea was determined by using the strip-transect method because previous aerial surveys in central California indicated that densities of sea lions would be too great in some areas to obtain reliable measures of perpendicular distances for line-transect density estimation. Previous aerial surveys using line transect methods, conducted at 213 m altitude, indicated a relatively flat detection function for sea lions between

[3] NMFS (National Marine Fisheries Service). 1997. Investigation of scientific information on the impacts of California sea lions and Pacific harbor seals on salmonids and on the coastal ecosystems of Washington, Oregon, and California. NOAA Tech. Memo. NMFS-NWFSC-28, 172 p. Northwest Fisheries Science Center, 2527 Montlake Blvd. E., Seattle, WA 98112-2097 and National Marine Fisheries Service, Northwest Region, 7600 Sand Point Way N.E., Seattle, WA 98115-0070.

[4] Fluharty, M. J. 1999. California sea lion interactions with commercial passenger fishing vessel fisheries: a review of log book data from 1994, 1995, and 1996. California Department of Fish and Game Admin. report 99-2, 21 p. [Available from California Department of Fish and Game, Marine Region, San Diego Field Office, 4949 Viewridge Avenue, San Diego, CA 92123.]

[5] Boveng, P. 1988. Status of the California sea lion population on the U. S. west coast. National Oceanographic and Atmospheric Administration admin. report LJ-88-07, 26 p. Southwest Fisheries Science Center, 8604 La Jolla Shores Drive, La Jolla, CA 92037.

[6] Barlow, J., R. L. Brownell Jr., D. P. DeMaster, K. A. Forney, M. S. Lowry, S. Osmek, T. J. Ragen, R. R. Reeves, and R. J. Small. 1995. U.S. Pacific marine mammal stock assessments. NOAA Tech. Memo. NMFS, NOAA-TM-NMFS-SWFSC-219, 162 p. National Marine Fisheries Service, Southwest Fisheries Science Center, 8604 La Jolla Shores Drive, La Jolla, CA 92037.

[7] Barlow, J., K. A. Forney, P. Scott Hill, R. L. Brownell Jr., J. V. Carretta, D. P. DeMaster, F. Julian, M. S. Lowry, T. Ragen, R. and R. Reeves. 1997. U.S. Pacific marine mammal stock assessments: 1996. NOAA Tech. Memo. NMFS, NOAA-TM-NMFS-SWFSC-248, 223 p. National Marine Fisheries Service, Southwest Fisheries Science Center, 8604 La Jolla Shores Drive, La Jolla, CA 92037.

[8] Beeson, M. J., and D. A. Hanan. 1996. An evaluation of pinniped-fishery interactions in California. Report to the Pacific States Marine Fisheries Commission, 47 p. [Available from Pacific States Marine Fisheries Commission, 205 SE Spokane St., Suite 100, Portland, OR, 97202-6413.]

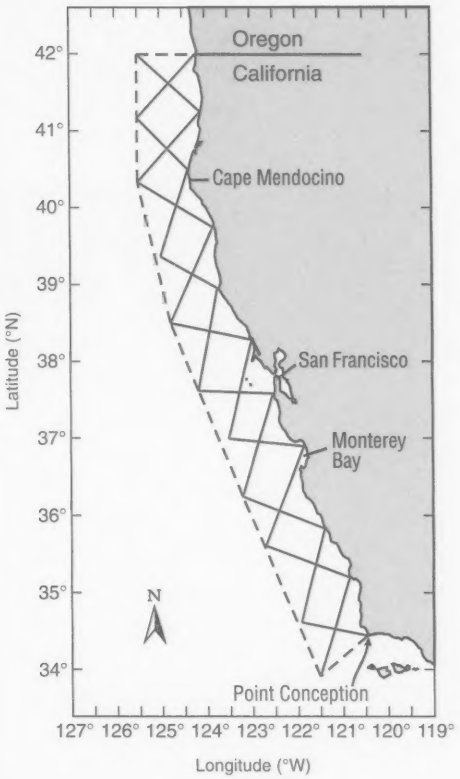

Figure 1

Strip-transect lines (solid lines) within the study area (dashed line) used for estimating at-sea abundance of California sea lions (*Zalophus californianus*) in central and northern California.

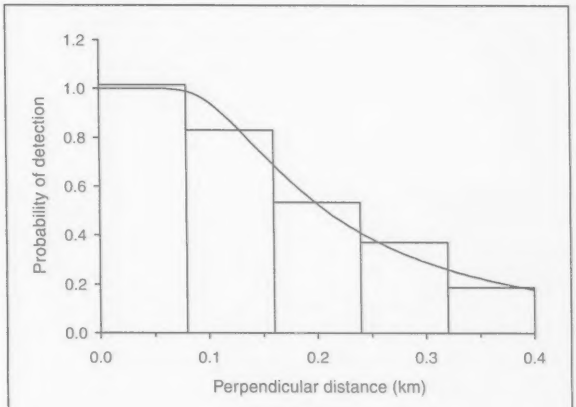

Figure 2

Probability density function for California sea lion (*Zalophus californianus*) sightings from an aircraft flying at an altitude of 213 meters in Beaufort sea states 0–4. Figure was provided by J. Carretta, National Marine Fisheries Service, Southwest Fisheries Science Center, La Jolla, CA, 92037.

approximately 85 meters left and right of the transect line (Fig. 2; Carretta, personal commun.[9]). Therefore, strip transect assumptions, that all individuals within the observed strip are detected, were expected to be valid within 85 meters left and right of the transect line. In our study we lowered the altitude of the aircraft to 183 m to increase the detection probability for sea lions in the water, especially in Beaufort 3–4 sea states. At that altitude, the viewing area of a single observer viewing from the belly window extended from directly below (90°) to a declination angle of 65° on each side, resulting in a total strip width of 170 m, or 85 m on each side of the viewing window.

Transects followed predetermined lines that systematically zig-zagged the study area (Fig. 1). Surveys were conducted in Beaufort sea states of 0–4. The lines were flown from south to north to take advantage of sun angle and to minimize sun glare, except on a few overcast days when southbound flights provided ample visibility. Geographical positions were recorded at one-minute intervals directly to a laptop computer by a serial cable connected to the aircraft's global positioning system (GPS). The following data were collected: number of California sea lions, GPS position, percentage of cloud cover over the survey area, name of the observer and data recorder, Beaufort sea state, transect number, and percentage of glare. Percentage of glare was defined as the proportion of the viewing area in which the observer could not see into the water because of surface reflection caused by sun or cloud glare. During the May–June survey we used a recorder, observer, and a resting person—the resting person rotating with the observer approximately every 30 minutes. During the July, September, and December surveys, the resting person was eliminated and the observer and recorder rotated at approximately 30-minute intervals.

Abundance at sea

We used the nonparametric Kruskal-Wallis test for two-way comparisons of the effects of glare and sea state on California sea lion sighting rates. For these tests, each transect segment with constant viewing conditions was randomly assigned to one of five substrata, which served as replicate samples for the tests. Viewing conditions with significantly lower sighting rates were excluded from the abundance analyses to reduce bias caused by missed animals.

Two *a posteriori* geographic strata were created, inshore (50,546 km^2 total surface area) and offshore

[9] Carretta, J. 1998. Personal commun. Southwest Fisheries Science Center, NMFS, La Jolla, California, 92037.

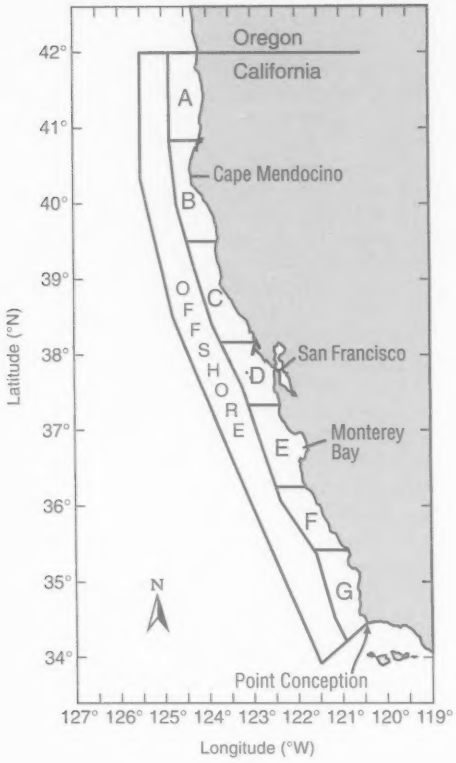

Figure 3

A posteriori stratification of study area into "offshore" stratum and into seven zones (**A** through **G**) within the "inshore" stratum for estimating abundance of California sea lions (*Zalophus californianus*) from strip-transect data and haulout count data.

(56,526 km^2 total surface area), using transect intersect points as the dividing line (Fig. 3). Differences between the definition of haulout sites for the surveys in this study and during previous surveys in 1980–82 and 1995 (Bonnell et al.[1], and Beeson and Hanan[8]) made it necessary to create additional zones within the inshore stratum to allow comparisons of the three data sets. The inshore stratum was thus divided into seven zones ("A" through "G"), separated at the following latitudes: 1) 35°25′N; 2) 36°15′N; 3) 37°20′N; 4) 38°10′N; 5) 39°30′N; and 6) 40°50′N (Fig. 3). The zones were separated where gaps occurred in the distribution of haulout areas along the coastline. Total area sizes for the seven zones were the following: A: 7647 km^2; B: 7206 km^2; C: 8025 km^2; D: 6153 km^2; E: 7790 km^2, F: 6030 km^2, and G: 7695 km^2. At-sea abundance was obtained separately for offshore and inshore strata, and for each zone within the inshore stratum, by using a modified strip-transect formula that included a correction, $g(0)$, for diving animals that were not available to be seen:

$$N_c = \frac{nA}{WLg(0)}, \quad (1)$$

where N_c = corrected total abundance (corrected for animals below the surface);
n = number of individuals sighted within the strip-transect;
A = total size of study area (in km^2);
W = the strip width (in km);
L = distance surveyed (in km) calculated as the sum of the great circle distances between position fixes; and
$g(0)$ = probability that a sea lion will be visible at the surface within the strip viewed by the observer as the aircraft passes over the water.

Coefficients of variation (CV) and lognormal 95% confidence limits of these abundance estimates were calculated by using standard formulae (Buckland et al., 1993).

Probability of missing submerged sea lions

We estimated the probability of seeing sea lions at the surface, $g(0)$, from dive data in Feldkamp et al. (1989) derived from 14 foraging trips made by seven lactating adult female California sea lions during late breeding-season:

$$g(0) = \frac{t+s+r}{t+s+r+d}, \quad (2)$$

where t = average time (hours) spent at the surface between dives within diving bouts by an adult female sea lion;
s = average time (h) spent swimming near the surface between diving bouts by an adult female sea lion;
r = average time (h) spent resting at the surface between diving bouts by an adult female sea lion; and
d = average time (h) spent diving during diving bouts by an adult female sea lion.

From seven female sea lions, Feldkamp et al. (1989) calculated averages of 12.0 hours (no SD given) spent at the surface between dives within diving bouts (t), 21.9 hours (SD=9.5 hours) spent swimming near the surface between diving bouts (s), 1.6 hours (SD=1.6) spent resting at the surface between diving bouts (r), and 17.3 hours (SD=6.7) spent diving during diving bouts (d). We calculated the CV for $g(0)$ from the standard deviations of diving data. In using these data we assumed that between dives, sea lions swam near the surface and at a depth where they would be seen by an observer in the aircraft and that sea lions were not visible to an observer in the aircraft during dives. Dive data were not available for other age and sex classes; therefore,

it was assumed that the proportion of time spent at or near the surface was similar for adult females and other age and sex classes and did not vary significantly within region, season, and year.

Photographic surveys

The aircraft was flown from north to south directly over the coastline or slightly offshore at an altitude of 183 to 213 m (typically 213 m) to locate sea lions onshore. The low altitude ensured that California sea lions could be detected on rocky substrates, aided in identification of different pinniped species, and enabled accurate counts from aerial photographs. All hauled-out California sea lions onshore were photographed. At the Farallon Islands, the aircraft was flown at an altitude of 366 to 457 m (typically 396 m) to prevent disturbance of nesting seabirds. Multiple passes were made over large rocks or islands to ensure that the entire rock or island was photographed. Surveys were made without regard to tidal conditions at any time of day between approximately two hours after sunrise and two hours before sunset.

Sea lions were photographed with a 126-mm-format KA-76 camera (Chicago Aerial Industries, Inc., Chicago, IL) equipped with image motion compensation (IMC) and operated at a cycle rate that achieved 67% overlap between adjacent frames. The geographical position of each photograph was recorded by linking the camera (mounted vertically inside the belly of the aircraft) to a computer and GPS unit. A 152-mm focal-length lens was used for low altitude photography (i.e., 183–213 m) and a 305-mm focal-length lens was used for higher altitude photography (i.e., 366–457 m). Kodak Aerochrome MS Film 2448, a very fine-grained, medium-speed, color transparency film, or Aerochrome HS Film SO-359, a very fine-grained, high-speed, color transparency film, was used. The camera was set at an aperture of f/5.6 and a shutter speed between 1/400 and 1/2000 second.

Photographic counts

Sea lions were counted from photographs illuminated with a light table by using a 7-30X zoom binocular microscope. Counts were obtained for five age and sex class categories: pups, juveniles, adult females or young males of similar size, subadult males, and adult males. Age and sex class distinctions were determined from size and other external characteristics (e.g., hair color on head, presence of sagittal crest, chest size, fore flipper width, snout shape, and body coloration). Animals of each age and sex class were marked on a clear acetate plastic overlay with different colored pens as each was counted. Marks on the acetate were then compared and verified with overlapping photographs. The acetate was placed on another photograph at the exact position of the coastline where the count ended previously and the count was continued on the uncounted portion. One count was made for each rock, island, or mainland haulout site. All counts were conducted by the first author, who is an experienced counter with high intercount reliability (Lowry, 1999). Geographical positions (latitude and longitude) were assigned to each haulout site.

Analysis of haulout data

Counts of sea lions made in this study were compared to those obtained by earlier investigators in 1980–82 (Bonnell et al.[1]) and 1995–96 (Beeson and Hanan[8]) by using nested ANOVAs and paired t-tests. The null hypothesis of no difference in zonal counts was used to examine differences in counts by zone, season, year, and survey. The counts were 0.45 power transformed (with Systat 6.0 for Windows, SPSS Inc., Chicago, IL) because their distribution was skewed toward zero.

Results

Sighting rates and $g(0)$

No difference was found ($P>0.05$) for number of sightings, total animals seen, and mean group size during Beaufort sea state conditions 1 through 4. A sharp decline in sighting rates was observed when sightings were grouped into glare categories of 0–24% (n=27.3 sightings/1000 km), 25–49% (n=17.5 sightings/1000 km), 50–74% (n=10.7 sightings/1000 km), and 75–100% (n=0 sightings/1000 km). Sighting rates were significantly greater at 0–49% glare than at 50–100% glare ($P<0.001$ for all surveys combined); therefore, only data collected in 0–49% glare were used for at-sea abundance estimation. With only data collected in 0–49% glare, we used 48–76% of kilometers surveyed and 79–89% of sightings.

The probability of sighting a sea lion at the surface, $g(0)$, was estimated as 0.67 (with a CV of $g(0)$=0.12).

At-sea abundance

Strip-transect survey effort totaled 1272 km during 26–30 May 1998, 2856 km during 12–28 September 1998, 2993 km during 1–11 December 1998, and 1175 km during 13–21 July 1999 (Fig. 4). No transect survey was conducted in July 1998 because of persistent low clouds and high winds. Transect distances in 0–49% glare conditions are given in Table 1. Nearly all sightings were within the inshore stratum, and most were within 20 nautical miles from the mainland coast (Fig. 5). Corrected at-sea abundance estimates for sea lions in the study area (Table 1) were 28,340 (May 1998), 40,161 (September 1998), and 24,720 animals (December 1998). For July 1999, a corrected abundance estimate for the inshore stratum in July 1999 was 11,492 animals (Table 1). From the total abundance estimated in the three 1998 surveys, the average proportion represented by the offshore stratum was 0.073 (range: 0.000–0.204). From this proportion, we estimated that there were about 829 sea lions in the unsurveyed offshore stratum

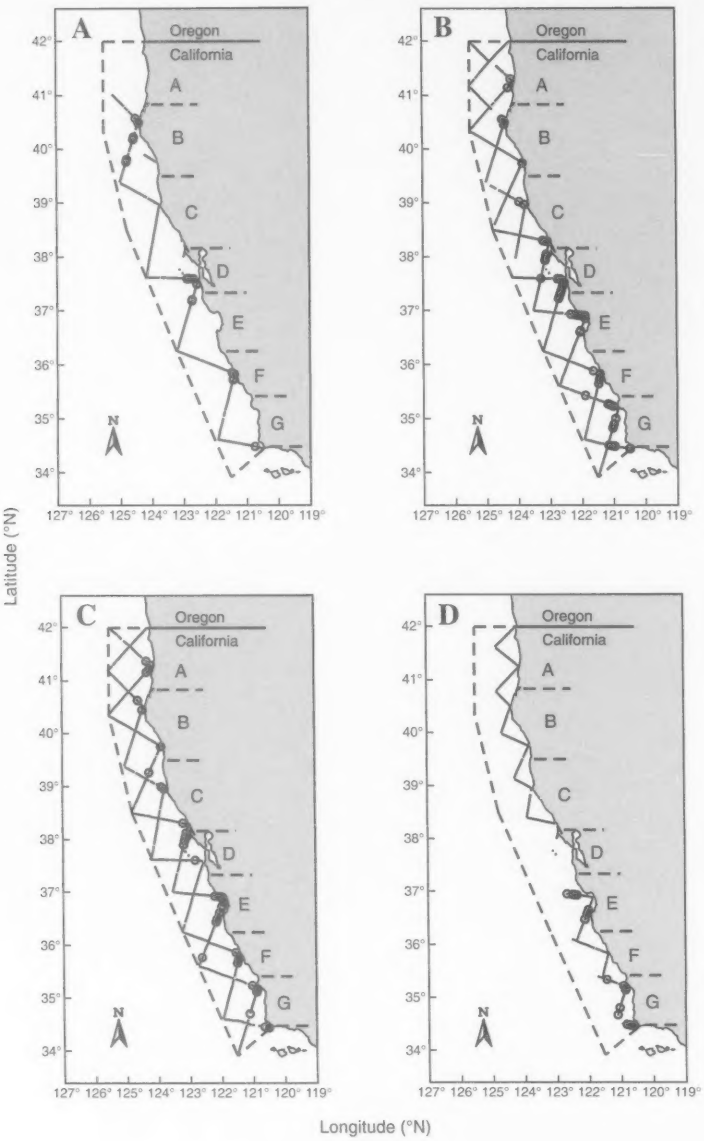

Figure 4

California sea lions (*Zalophus californianus*) sightings (o) during strip-transect surveys flown in Beaufort sea states 0–4 and 0–49% glare conditions (solid zig-zag line). (**A**) 26–30 May 1998, (**B**) 12–28 September 1998, (**C**) 1–11 December 1998, and (**D**) 13–21 July 1999.

in July 1999, and this number was used to extrapolate a total at-sea abundance estimate within the study area of 12,232 sea lions. CVs of corrected estimates were 0.32 (May 1998), 0.26 (September 1998), 0.50 (December 1998), and 0.43 (July 1999; Table 1).

During the May–June 1998 survey, sea lions were most abundant in the northern part of the study area (Table 1). In September 1998, sea lions were most abundant in the central part of the study area (zones D and E). In December 1998 they were most abundant in the southern portion of the study area (zones E and F). During July 1999, sea lions were most abundant in the south-central portion of the study area (zone E).

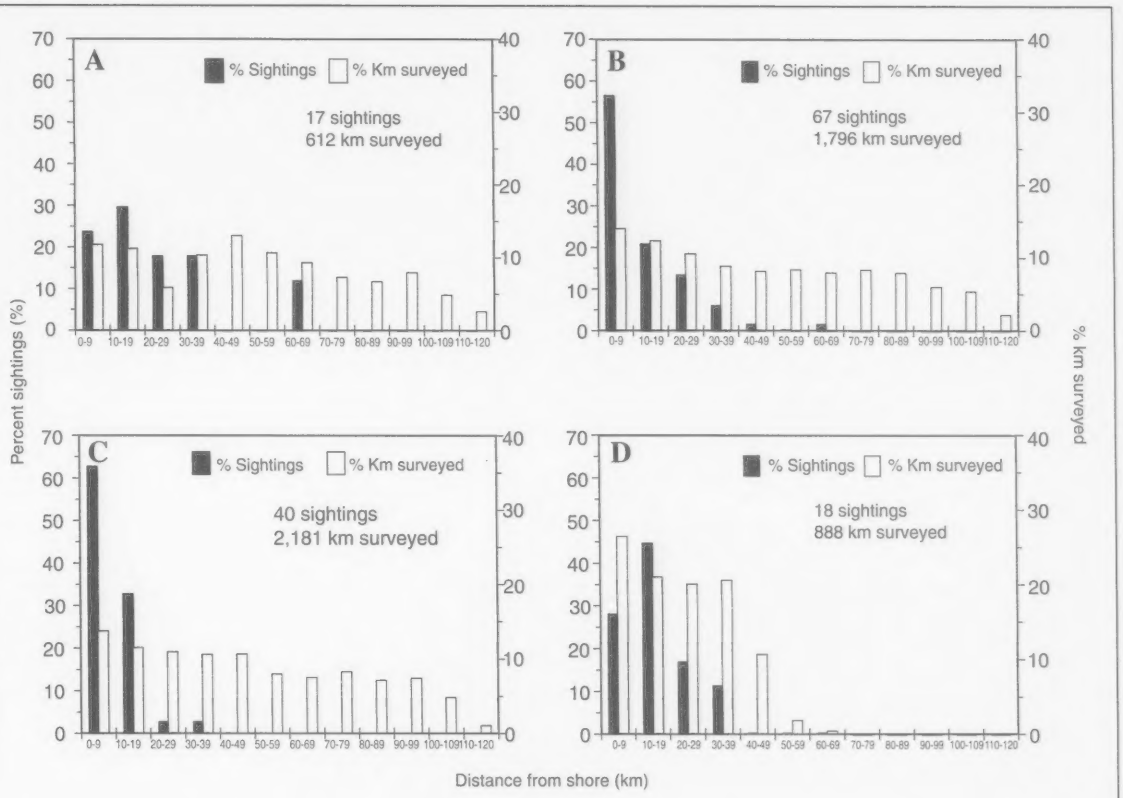

Figure 5

Distances from shore for California sea lions (*Zalophus californianus*) sighted and kilometers from shore for California sea lions that were surveyed during strip transect surveys in Beaufort sea state 0–4 and 0–49% glare conditions. (**A**) 26–30 May 1998, (**B**) 12–28 September 1998, (**C**) 1–11 December 1998, and (**D**) 13–21 July 1999.

Haulout abundance

In 1998 and 1999, aerial photographic surveys of sea lion haulouts in central and northern California were conducted during 31 May–8 June 1998, 7–18 July 1998, 11–20 September 1998, 14–16 December 1998, and 6–11 July 1999. For the July 1998 survey, low clouds prevented aerial surveys of the coastline from Point Sal (34°54.1′N, 120°40.0′W) to Point Conception (counts from 1999 were used for these areas) and from the Klamath River (41°32.5′N, 124°04.7′W) to Humboldt Bay (40°45.4′N, 124°14.4′W). To estimate abundance in the latter missed area, we obtained ground counts from the mainland at all haulouts except Turtle Rocks (41°08.0′N, 124°10.9′W) and Redding Rock (41°20.6′N, 124°10.5′W). In July 1999 a low cloud layer prevented surveys of the coastline between Golden Gate Bridge (37°51.1′N, 122°34.0′W) and just north of Año Nuevo Island (37°06′N, 122°20′W). This gap should have had virtually no effect on the total counts, however, because there is only one minor haulout in this region.

The number of sea lions hauled-out in the study area (Table 2) were 36,576 (May 1998), 26,260 (includes estimate, July 1998), 35,512 (September 1998), 32,055 (December 1998), and 13,559 (July 1999). There was no significant difference in total number of sea lions between the seven zones (P=0.229) and between seasons (P=0.179; Table 3). More sea lions were counted in 1998–99 than during previous surveys in 1980–82 and 1995–96 (P<0.003 for both tests), but no difference in counts was found between 1980–82 and 1995–96 surveys (P=0.232; Table 3).

In 1998, the greatest numbers of sea lions were found in zone D and E (Table 2), corresponding to the San Francisco and Monterey Bay regions; most animals hauled out at Año Nuevo Island and South Farallon Islands. Juveniles and adult-females or young-males were the most prevalent age and sex classes found in the study area in 1998 (Table 2). More adult males were counted during the May–June 1998 survey than during other surveys. In 1998 the number of pups in the study area ranged from 22 (December 1998) to 149 (May–June 1998).

Table 1

Abundance estimates for California sea lions (*Zalophus californianus*) at sea from sightings during strip-transect surveys in the central and northern California study area during three surveys in 1998 and one survey in 1999, under 0–49% glare and Beaufort 0–4 sea state conditions. No survey was conducted within the offshore stratum in July 1999. Insufficient kilometers were surveyed for estimating at-sea abundance, CV(N_c), and 95% confidence limits for strata noted with a dash (—). Corrected estimates are based on $g(0)$ calculated from dive studies on lactating adult females during late breeding-season (Feldkamp et al., 1989).

				Corrected			
Stratum	No. of sightings	No. of animals	Kilometers surveyed (km)	CV (N_c)	Abundance (N_c)	Lower 95% CL	Upper 95% CL
26–30 May 1998							
Inshore: zone A	—	—	0	—	—	—	—
Inshore: zone B	5	6	96	—	3977	—	—
Inshore: zone C	—	—	19	—	—	—	—
Inshore: zone D	6	6	63	—	5156	—	—
Inshore: zone E	—	—	0	—	—	—	—
Inshore: zone F	4	4	118	—	1793	—	—
Inshore: zone G	—	—	6	—	—	—	—
Inshore: total	15	16	302	0.29	23,541	11,224	49,376
Offshore	2	3	310	1.01	4799	561	41,040
Inshore + offshore	17	19	612	0.32	28,340	15,237	52,713
12–28 September 1998							
Inshore: zone A	1	1	121	—	556	—	—
Inshore: zone B	5	5	140	—	2256	—	—
Inshore: zone C	6	7	117	—	4235	—	—
Inshore: zone D	18	23	108	—	11,552	—	—
Inshore: zone E	16	25	146	—	11,752	—	—
Inshore: zone F	5	5	69	—	3852	—	—
Inshore: zone G	15	16	220	—	4919	—	—
Inshore: total	66	82	919	0.27	39,595	24,210	64,757
Offshore	1	1	877	1.1	566	82	3923
Inshore + offshore	67	83	1796	0.26	40,161	24,205	66,635
1–11 December 1998							
Inshore: zone A	4	4	213	—	1262	—	—
Inshore: zone B	6	7	219	—	2026	—	—
Inshore: zone C	4	4	238	—	1185	—	—
Inshore: zone D	2	3	124	—	1303	—	—
Inshore: zone E	15	25	175	—	9773	—	—
Inshore: zone F	3	18	59	—	16,129	—	—
Inshore: zone G	6	6	175	—	2316	—	—
Inshore: total	40	67	1203	0.5	24,720	9333	65,479
Offshore	0	0	977	0	0	0	0
Inshore + offshore	40	67	2181	0.5	24,720	9726	62,831
13–21 July 1999							
Inshore: zone A	0	0	124	—	0	—	—
Inshore: zone B	0	0	174	—	0	—	—
Inshore: zone C	0	0	185	—	0	—	—
Inshore: zone D	—	—	0	—	—	—	—
Inshore: zone E	11	14	146	—	6573	—	—
Inshore: zone F	0	0	135	—	0	—	—
Inshore: zone G	7	9	128	—	4762	—	—
Inshore: total	18	23	888	0.5	11,492	4,358	30,304
Offshore (estimated)	0	0	23	0.9	829	183	3752
Inshore + offshore	18	23	911	0.43	12,232	5427	27,572

Table 2

Counts of California sea lions (*Zalophus californianus*) made from 126-mm-format aerial color photographs for five age- and sex-class categories found in seven zones along the central and northern California coast during four surveys in 1998 and one survey in 1999.

Zone	Pups	Juveniles	Adult females or young males	Subadult males	Adult males	Total
31 May–8 June 1998						
A	0	299	1948	1554	528	4329
B	0	3195	1534	2371	911	8011
C	0	698	751	513	530	2492
D	11	3639	5821	1636	555	11,662
E	99	3481	2993	678	464	7715
F	5	186	380	93	52	716
G	34	684	886	32	15	1651
All	149	12,182	14,313	6877	3055	36,576
7–18 July 1998						
A	0	358	206	148	22	734
B	0	2382	116	162	62	2722
C	0	320	287	190	101	898
D	55	1918	7318	1283	290	10,864
E	54	2920	3226	564	178	6942
F	12	63	510	125	50	760
G	0	779	1362	92	30	3340[1]
All	121	8740	13,025	2564	733	26,260[1]
11–20 September 1998						
A	0	73	1325	1548	559	4165
B	0	1136	351	938	173	2598
C	0	524	594	584	56	2028
D	18	1506	8453	1136	100	11,213
E	22	2122	8056	671	188	11,059
F	6	470	1440	78	24	2018
G	0	1224	1175	29	3	2431
All	46	7985	21,394	4984	1103	35,512
14–16 December 1998						
A	0	27	105	162	123	663
B	0	193	1790	2950	429	5362
C	0	54	201	995	516	1766
D	1	765	10,310	632	97	11,805
E	12	1566	8035	311	103	10,027
F	9	307	903	84	15	1318
G	0	201	831	63	19	1114
All	22	3359	22,175	5197	1302	32,055
6–11 July 1999						
A	0	111	167	5	4	287
B	0	6	6	1	1	14
C	0	0	0	1	0	1
D	3	193	970	109	91	1366
E	4	1226	5652	398	65	7345
F	0	270	578	90	14	952
G	0	919	2426	186	63	3594
All	7	2725	9799	790	238	13,559

[1] Includes 1077 unknown age- and sex-class sea lions that were estimated to have been missed in zone G.

Table 3

Results of four nested ANOVAs on haulout counts of California sea lions (*Zalophus californianus*) found in 7 zones within central and northern California (refer to text and Fig. 3 for zone descriptions). The tests of ANOVA revealed differences between zones, season, years, and surveys. 1980–82 surveys were conducted by Bureau of Land Management (Bonnell et al.[1]) and 1995–96 surveys were conducted by the California Department of Fish and Game (Beeson and Hanan[8]). Year was nested within survey, season was nested within year, and zone was nested within season.

Source	Sum-of-squares	df	Mean-square	*F*-ratio	*P*
1998–99 surveys					
Season	1427.2	3	475.7	2.177	0.179
Zone (season)	9157.0	24	381.5	1.746	0.229
1998–99 surveys *vs.* summer and autumn 1995 and winter 1996 surveys					
Survey	1610.7	1	1610.7	11.449	0.003
Season (survey)	2019.4	5	403.9	2.871	0.037
Zone (season)	11,008.8	24	458.7	3.260	0.003
1998–99 surveys *vs.* 1980–82 surveys					
Survey	1731.6	1	1731.6	21.224	<0.001
Year (survey)	2235.9	3	745.3	9.135	<0.001
Season (year)	3576.5	12	298.0	3.653	<0.001
Zone (season)	14,761.2	24	615.0	7.538	<0.001
1980–82 surveys *vs.* summer and autumn 1995 and winter 1996 surveys					
Survey	81.9	1	81.9	1.457	0.232
Year (survey)	649.0	3	216.3	3.849	0.013
Season (year)	3491.5	10	349.1	6.211	<0.001
Zone (season)	11,027.6	24	459.5	8.174	<0.001

In 1999, the majority of sea lions were found between the San Francisco Bay area and Point Conception (zones D through G). Zone E had the greatest number of sea lions (Table 2); the majority of these animals hauled out at Año Nuevo Island. As in 1998, juveniles and adult-females or young-males were the most prevalent age and sex classes (Table 2). Only seven pups were counted in the study area during July 1999. The number of sea lions counted in 1999 was 52% of that counted in July 1998.

Total abundance

There was a significant correlation (r=0.468, P=0.024) between at-sea abundance and haulout abundance within zones. Total abundance of California sea lions in central and northern California during 1998 was estimated to be 64,916 in May–June, 75,673 in September, and 56,775 in December. Total abundance in July 1999 was estimated at 25,791 individuals. The proportion of total abundance to animals hauled-out was 1.77, 2.13, 1.77, and 1.90, respectively, with a mean of 1.89 and a CV for small samples (Sokal and Rohlf, 1995) of 0.09. Using the mean multiplier of 1.89 on haulout counts obtained in July 1998 (Table 2), when at-sea abundance could not be estimated, we estimated total abundance as 49,697 (CV=0.09) animals for that period.

Discussion

This abundance study of California sea lions in central and northern California successfully integrated two methods: 1) strip transect surveys to estimate abundance at sea; and 2) aerial photographic surveys to estimate haulout abundance. The $g(0)$ detection probability derived from previously published dive data allowed estimation of total abundance, including animals expected to be underwater during at-sea strip transect surveys. Previous surveys where transect methods similar to ours were used in the Southern California Bight in 1975–78 and in central and northern California in 1980–83 (Bonnell and Ford, 1987; Bonnell et al.[1, 10]) did not have information for deriving $g(0)$, and, therefore, densities of sea lions at sea were underestimated in these studies.

California sea lions were abundant in central and northern California during May through September

[10] Bonnell, M. L., B. J. Le Boeuf, M. O. Pierson, D. H. Dettman, G. D. Farrens, C. B. Heath, R. F. Gantt, and D. J. Larsen. 1980. Summary of marine mammal and seabird surveys of the Southern California Bight area 1975–1978. Vol. 3: Investigators reports, part 1—pinnipeds of the Southern California Bight, 535 p. Univ. Calif., Santa Cruz, Calif. 95064. Final Report to the Bureau of Land Management, under Contract AA550-CT7-367. [NTIS PB81-248-71.]

1998 when waters were warm because of the strong 1997–98 El Niño. Increased abundance of juveniles and adult females were observed in this region during previous El Niños (Huber, 1991; Sydeman and Allen, 1999) and during our May–June, July, and September 1998 surveys. The increase in adult females in central California in 1998 resulted in an increase in the number of pups counted at Año Nuevo and South Farallon Islands (106 pups in 1998 *vs.* 23 in 1997), and below normal births at rookeries in southern California (Lowry, unpubl. data, Forney et al.[2]). In contrast to 1998, during the summer of 1999 fewer sea lions were found in central and northern California, especially north of San Francisco (zones A, B, and C), and greater numbers were found at rookeries in southern California (M. Lowry, unpubl. data) when waters were cold as a result of the La Niña oceanographic condition that began in October 1998 (Hayward et al., 1999).

The abundance and distribution of California sea lions were distinctly different between El Niño and La Niña periods. During El Niño, sea lions were very abundant in central and northern California, and were distributed throughout the region. In contrast, during summer 1999 (our only survey that year [La Niña]), sea lions were less abundant than during summer 1998, and they were distributed only south of the San Francisco Bay area. The abundance and distribution pattern of summer 1999 is similar to the observed abundance and distribution pattern described by earlier studies (Chambers, 1979; Griswold, 1985; Weise, 2000; Bonnell et al.[1]). During periods of elevated sea lion abundance in central and northern California, such as those observed during the 1998 El Niño, we would expect 1) increased consumption of prey species because of more sea lions feeding in the area, 2) increased pressure on coastal fisheries resources because sea lions feed on commercially valuable species (see Lowry et al., 1990, 1991; Lowry and Carretta, 1999; Weise, 2000), and 3) increased interactions with commercial and sport fisheries. The opposite would occur during periods of low sea lion abundance during non-El Niño years. Greater abundance of California sea lions in central and northern California during the 1997–98 El Niño event, therefore, would be expected to have a greater effect on salmonids and other sea lion prey species, and on fisheries than would occur during non-El Niño years.

Abundance of sea lions in central and northern California during 1998 was greater in May–June (spring) and September (fall) and less in July (summer) and December (winter). This bimodal phenomenon, also observed in the past (Sullivan, 1980; Bonnell et al.[1]), is due to migrating subadult and adult male sea lions on their way to (in fall) and from (in spring) Oregon (Mate, 1975), Washington, and British Columbia (Bigg, 1988). However, these seasonal differences were not significantly different, likely because of low power (only one year of data), or because the animals behaved differently from other years. In fact, fewer subadult and adult males were present at southern California rookeries during the 1998 July census (near the end of breeding season) than were present during 1997 and 1999 (M. Lowry, unpubl. data). The large number of sea lions in central and northern California during 1998 was the result of a more numerous population (U.S. population estimated at 204,000 to 214,000 in 1999) than existed when previous surveys were conducted in 1980–82 and 1995–96 (U.S. population estimated at 76,000 in 1982 and at 167,000 to 188,000 in 1995) (Barlow et al.[7]; Forney[2]; Bonnell et al.[1], and Beeson and Hanan[8]).

In central and northern California, California sea lions have been sighted during aerial surveys (Carretta and Forney[11]; present study) and tracked with satellite tags (Melin and DeLong, 2000; Melin, 2002) up to 100 nautical miles from shore. However, our surveys indicated that they forage predominantly within 20 nautical miles from shore.

The strip transect method assumes that all animals within a strip are sighted by the observer. Although we found no difference in sighting rate between Beaufort sea state scales 0–1, 2, 3, and 4, Carretta et al.[12] found during their 1998–99 line transect survey in waters off San Clemente Island, California, that the effective strip width of pinniped sightings at 213 m altitude was slightly less in Beaufort sea states 3–4 (184 m on each side) than in Beaufort sea states 0–2 (256 m on each side). Their results suggest that if our analysis suffered from reduced detection probability at high sea states, then we may have underestimated at-sea abundance of sea lions or increased the variance of at-sea sea lion abundance. This potential negative effect was minimized in our surveys by surveying at a lower altitude (183 m) than the 213 m altitude surveyed by Carretta et al.[12]

The $g(0)$ correction derived from dive and foraging studies of lactating adult-female California sea lions during late breeding season (July–August) may be an additional source of error in our at-sea abundance estimates. It may not be representative of nonlactating adult females and other age- and sex-class sea lions, and it may not be representative for all seasons or different oceanographic cycles (e.g., El Niño and non-El Niño). Dive data from various ages and sexes are needed to test these assumptions, but existing dive data from a single age+sex group provided a rough correction to account for animals underwater during at-sea

[11] Carretta, J. V. and K. A. Forney. 1993. Report of two aerial surveys for marine mammals in California coastal waters utilizing a NOAA DeHavilland twin otter aircraft March 9–April 7, 1991 and February 8–April 6, 1992. NOAA Tech. Memo. NMFS, NOAA-TM-NMFS-SWFSC-185, 77 p. National Marine Fisheries Service, Southwest Fisheries Science Center, 8604 La Jolla Shores Drive, La Jolla, CA 92037.

[12] Carretta, J. V., M. S. Lowry, C. E. Stinchcomb, M. S. Lynn, and R. E. Cosgrove. 2000. Distribution and abundance of marine mammals at San Clemente Island and surrounding offshore waters: results from aerial and ground surveys in 1998 and 1999. National Oceanographic and Atmospheric Administration admin. report LJ-00-02, 51 p. Southwest Fisheries Science Center, 8604 La Jolla Shores Drive, La Jolla, CA 92037.

surveys. Seasonal differences may exist, but data in Feldkamp et al., (1989, 1991) and Melin (2002) indicate that these differences are negligible. Feldkamp et al. (1991) showed differences in diving behavior during El Niño and non-El Niño, but Melin (2002) did not find as much difference in diving behavior during El Niño and non-El Niño (with the exception of longer transit time to foraging grounds during El Niño).

Error in age- and sex-class abundance estimates at haulouts is also affected by subjectivity and inter-observer differences in age and sex classification of sea lions. Therefore, age- and sex-class counts provided in these surveys, although conducted by a single experienced observer (M. Lowry), serve as approximate indices of sea lion age- and sex-class distributions in central and northern California. These indices will be useful for future attempts to estimate consumption of prey by sea lions along central and northern California, given that nutritional requirements differ among age and sex classes.

By estimating abundance of sea lions on land as well as at-sea, we were able to derive a multiplier for estimating total abundance from counts of animals hauled out on land. This multiplier can be applied to future land counts of California sea lions in central and northern California to estimate total abundance, as has been done for harbor seals in California, Oregon, and Washington (Huber et al., 2001; Barlow et al.[6]; Forney et al.[2]). It may also be useful for estimating total abundance from counts of sea lions hauled out in Oregon, Washington, and British Columbia because the age- and sex-class structure of sea lions is similar to that found in central and northern California. However, the multiplier should not be used for smaller areas (such as the zones in the inshore stratum) or for other species, because regional and interspecies differences may exist. In particular, it would not be appropriate for regions where sea lions reproduce, such as in the Southern California Bight (SCB) and in Mexico, because adult females that are rearing pups may spend a different proportion of their time at sea. For that reason, it would be judicious to conduct concurrent offshore and haulout surveys in the SCB and Mexico to derive a correction factor for each geographical region of the sea lion's range. Multipliers could also be derived for smaller areas (such as our zones) by conducting suitably designed smaller-scale at-sea surveys in conjunction with counts of animals hauled out, or by using satellite or radio telemetry tags to directly measure the relative times at sea and on land.

The multiplier for deriving total abundance from haulout counts provides researchers and resource managers with an alternative method for estimating total population abundance or abundance of a stock. Abundance estimates derived with this new approach can be compared to abundance estimates obtained with more conventional methods (such as the life history model), and may provide a means for estimating total abundance when life history data are unavailable. The approach used in the present study may be particularly useful for estimating abundance at times and places unrelated to breeding activities, or for periods when breeding is disrupted, as with El Niño conditions. Abundance estimates and distributional data provided by these methods can be used to determine where and when the greatest effects on salmon and other prey species may occur. Diet studies at major hauling areas in conjunction with abundance surveys to derive consumption estimates are required to determine the effect of California sea lions on salmon and other sea lion prey species of the region.

Acknowledgments

This research was supported financially by the Office of Protected Resources, National Marine Fisheries Service. We greatly appreciate the assistance given by Jim Gilpatrick, Charlie Stinchcomb, and, especially, Scott Benson of Moss Landing Marine Laboratories during the surveys. Jay Barlow provided guidance. Special thanks to Morgan Lynn of the Southwest Fisheries Science Center who kept the photographic equipment functioning properly. Henry Orr of the Southwest Fisheries Science Center helped with illustrations. Research within Gulf of the Farallones National Marine Sanctuary and Monterey Bay National Sanctuary was conducted under National Marine Sanctuary Permit GFNMS/MBNMS-20-98. This research was conducted under MMPA Research Permit No. 774-1437. We greatly appreciated the reviews and comments by Jay Barlow, Jeff Laake, Jim Harvey, and three anonymous reviewers.

Literature cited

Barlow, J., and P. Boveng.
1991. Modeling age-specific mortality for marine mammal populations. Mar. Mamm. Sci. 7:50–65.

Bartholomew, G. A.
1967. Seal and sea lion populations of the Channel Islands. *In* Proc. of the symp. on the biology of the Calif. Islands (R. N. Philbrick, ed.), p. 229–243. Santa Barbara Botanic Garden, p. 229–243. Santa Barbara, CA.

Bigg, M. A.
1988. Status of the California sea lion, *Zalophus californianus*, in Canada. Can. Field Nat. 102:307–314.

Bonnell, M. L., and R. G. Ford.
1987. California sea lion distribution: a statistical analysis of aerial transect data. J. Wildl. Manage. 51: 13–20.

Buckland, S. T., D. R. Anderson, K. P. Burnham, and J. L. Laake.
1993. Distance sampling: estimating abundance of biological populations, 446 p. Chapman and Hall, London.

Chambers, J. R.
1979. Population studies of California sea lions near Diablo Canyon, California. M.A. thesis, 154 p. California Polytechnic State Univ., San Luis Obispo, CA.

Feldkamp, S. D., R. L. DeLong, and G. A. Antonelis.
1989. Diving patterns of California sea lions, *Zalophus californianus*. Can. J. Zool. 67:872–883.

Feldkamp, S. D., R. L. DeLong, and G. A. Antonelis.
1991. Effects of El Niño 1983 on the foraging patterns of California sea lions (*Zalophus californianus*) near San Miguel Island, California. *In* Pinnipeds and El Niño: responses to environmental stress (F. Trillmich and K. A. Ono, eds.) p. 146–155. Springer-Verlag, Berlin and Heidelberg, Germany.

Griswold, M. D., Jr.
1985. Distribution and movements of pinnipeds in Humboldt and Del Norte counties, California. M.A. thesis, 101 p. Humboldt State University, Arcata, CA.

Hayward, T. L., T. R. Baumgartner. D. M. Checkley, R. Durazo, G. Gaxiola-Castro, K. D. Hyrenbach, A. W., Mantyla, M. M. Mullin, T. Murphree, F. B., Schwing, P. E., Smith, and M. J. Tegner.
1999. The state of the California Current in 1998–1999: transition to cool-water conditions. CalCOFI Rep. 40:29–62.

Huber, H. R.
1991. Changes in the distribution of California sea lions north of the breeding rookeries during the 1982–83 El Niño. *In* Pinnipeds and El Niño: responses to environmental stress (F. Trillmich and K. A. Ono, eds.) p. 129–137. Springer-Verlag, Berlin and Heidelberg, Germany.

Huber, H. R., S. J. Jeffries, R. F. Brown, R. L. DeLong, and G. VanBlaricom.
2001. Correcting aerial survey counts of harbor seals (*Phoca vitulina richardsi*) in Washington and Oregon. Mar. Mamm. Sci. 17:276–293.

Keith, E. O., R. S. Condit, and B. J. Le Boeuf.
1984. California sea lions breeding at Año Nuevo Island, California. J. Mamm. 65:695.

Lowry, M. S.
1999. Counts of California sea lion (*Zalophus californianus*) pups from aerial color photographs and from the ground: a comparison of two methods. Mar. Mamm. Sci. 15:143–158.

Lowry, M. S, and J. V. Carretta.
1999. Market squid (*Loligo opalescens*) in the diet of California sea lions (*Zalophus californianus*) in southern California (1981–1995). CalCOFI Rep. 40:196–207.

Lowry, M. S., C. W. Oliver, C. Macky, and J. B. Wexler.
1990. Food habits of California sea lions, *Zalophus californianus*, at San Clemente Island, California, 1981–1986. Fish. Bull. 88:509–521.

Lowry, M. S., B. S. Stewart, C. B. Heath, P. K. Yochem, and J. M. Francis.
1991. Seasonal and annual variability in the diet of California sea lions, *Zalophus californianus*, at San Nicolas Island, California, 1981–86. Fish. Bull. 89:331–336.

Mate, B. R.
1975. Annual migrations of the sea lions *Eumetopias jubatus* and *Zalophus californianus* along the Oregon USA coast. Rapp. P.-V. Reun. Cons. Int. Explor. Mer 169:455–461.

Melin, S. R.
2002. The foraging ecology and reproduction of California sea lion (*Zalophus californianus californianus*). Ph.D. diss., 150 p. Univ. Minnesota, Minneapolis, MI.

Melin, S. R., and R. L. DeLong.
2000. At-sea distribution and diving behavior of California sea lion females from San Miguel Island, California. *In* Proceedings of the fifth California Islands symposium (D. R. Browne, K. L. Mitchell, and H. W. Chaney), p. 407–412. Prepared by MBC Applied Environmental Sciences, 3000 Redhill Ave., Costa Mesa, CA 92626 under MMS (Minerals Management Service) contract no. 14-35-01-96-RC-30801 from the U.S. Dep. Interior, MMS, Pacific OCS Region.

Odell, D. K.
1975. Breeding biology of the California sea lion, *Zalophus californianus*. Rapports et Proces-verbaux de Reunions 169:374–378.

Orr, R. T., and T. C. Poulter.
1965. The pinniped population of Año Nuevo Island, California. Proc. Calif. Acad. Sci. 32:377–404.

Pierotti, R. J., D. G. Ainley, and T. J. Lewis.
1977. Birth of a California sea lion on Southeast Farallon Island. Calif. Fish Game 63:64–66.

Sokal, R. R., and F. J. Rohlf.
1995. Biometry: the principles and practice of statistics in biological research, 887 p. W.H. Freeman and Co., New York, NY.

Sullivan, R. M.
1980. Seasonal occurrence and haul-out use in pinnipeds along Humboldt County, California. J. Mamm. 61:754–760.

Sydeman, W. J., and S. G. Allen.
1999. Pinniped population dynamics in central California: correlations with sea surface temperature and upwelling indices. Mar. Mamm. Sci. 15:446–461.

Weise, M. J.
2000. Abundance, food habits and annual fish consumption of California sea lions (*Zalophus californianus*) and its impact on salmonid fisheries in Monterey Bay, California. M.S. thesis, 103 p. Moss Landing Marine Laboratories, Moss Landing, CA, and San Jose State Univ., San Jose, CA.

Variability in spawning frequency and reproductive development of the narrow-barred Spanish mackerel (*Scomberomorus commerson*) along the west coast of Australia

Michael C. Mackie
Paul D. Lewis
Daniel J. Gaughan
Stephen J. Newman

Western Australian Marine Research Laboratories
Department of Fisheries
Government of Western Australia
West Coast Drive
Waterman, Western Australia 6020, Australia
E-mail address (for M.C. Mackie): mmackie@fish.wa.gov.au

Abstract—The narrow-barred Spanish mackerel (*Scomberomorus commerson*) is widespread throughout the Indo-West Pacific region. This study describes the reproductive biology of *S. commerson* along the west coast of Australia, where it is targeted for food consumption and sports fishing. Development of testes occurred at a smaller body size than for ovaries, and more than 90% of males were sexually mature by the minimum legal length of 900 mm TL compared to 50% of females. Females dominated overall catches although sex ratios within daily catches vary considerably and females were rarely caught when spawning. *Scomberomorus commerson* are seasonally abundant in coastal waters and most of the commercial catch is taken prior to the reproductive season. Spawning occurs between about August and November in the Kimberley region and between October and January in the Pilbara region. No spawning activity was recorded in the more southerly West Coast region, and only in the north Kimberley region were large numbers of fish with spawning gonads collected. Catches dropped to a minimum when spawning began in the Pilbara region, when fish became less abundant in inshore waters and inclement weather conditions limited fishing on still productive offshore reefs. Final maturation and ovulation of oocytes took place within a 24-hour period, and females spawned in the afternoon-evening every three days. A third of these spawning females released batches of eggs on consecutive days. Relationships between length, weight, and batch fecundity are presented.

Manuscript submitted 1 October 2002 to the Scientific Editor's Office.

Manuscript approved for publication 14 December 2004 by the Scientific Editor.

Fish. Bull. 103:344–354 (2005).

The narrow-barred Spanish mackerel (*Scomberomorus commerson*) is a prized food fish targeted by fishermen throughout its range in the Indo-West Pacific region (Collette and Nauen, 1983). Reaching over 2.4 m in length and 45 kg in weight, this pelagic species is seasonally abundant in coastal waters where it often schools in large numbers. In Australian waters, the commercial mackerel fishery targets these schools using trolling methods, and 2362 metric tons were caught in 2001–02 for domestic and overseas markets (ABARE, 2003).

Scomberomorus commerson is also a premier sport fishing species, targeted by an increasing number of recreational anglers throughout its broad Australian distribution. The combined commercial and recreation take of *S. commerson* has put significant pressure on stocks in Queensland (QLD) waters, leading to a possible decline in the spawning stock abundance (McPherson and Williams, 2002). The biology of *S. commerson* in these waters has been well studied (e.g., Munro, 1942; McPherson, 1981, 1992, 1993). Biological information is also available for *S. commerson* in waters of the Northern Territory (NT; Buckworth[1]), where stocks are still recovering from a prolonged period of exploitation by foreign gill-net operators that ended in 1986. In contrast, little is known about the stock status and biology of *S. commerson* in Western Australian (WA) waters, despite the fact that catches are similar to those taken in QLD and the NT, and commercial fishermen have expressed concern about increasing fishing pressure on this species in WA. Recent moves to overhaul management of the mackerel fishery in WA (in which *S. commerson* is the dominant species) have further highlighted the need for more information on the biology and stock status of *S. commerson* along the WA coast.

Research to enable a stock assessment of *S. commerson* in WA waters was therefore commenced in 1999. Description of reproductive biology was a key focus of this study, since this information is required for stock assessment models and for management controls such as minimum legal lengths, which were previously set with little knowledge of the biology of *S. commerson* in WA. Information on other reproductive parameters, such as batch fecundity and spawning behavior, which are also required for

[1] Buckworth, R. C. 1999. Age structure of the commercial catch of Northern Territory narrow-barred Spanish mackerel. Final Report to the Fisheries Research and Development Corporation (FRDC) on project no. 1998/159. Fishery report 42, 27 p. Department of Business Industry and Resource Development, Darwin, Northern Territory, 0800, Australia.

stock assessments, is unavailable or insufficiently described in the literature for this species. The objective of our study was, therefore, to provide a comprehensive description of the reproductive biology of *S. commerson* in Western Australian waters.

Material and methods

Collection and processing of samples

Scomberomorus commerson were collected onboard vessels operating from a number of locations along the WA coast between 1998 and 2002 (Fig. 1). These locations were pooled into three regions to reflect differences in fishing methods within the mackerel fishery (Kimberley—east of 120°E, Pilbara—north of 23°S to the Kimberley border, and West Coast—south of 23°S; Fig. 1). *Scomberomorus commerson* are seasonally abundant in coastal waters although low numbers are caught in the Pilbara region during the "off-season." Samples were therefore collected throughout the year from this region only.

Fresh *S. commerson* collected from commercial and recreational fishermen were measured (total length [TL] and fork length [FL] in mm) and, where possible, weighed to 0.1 kg (whole weight [WW] and clean weight [viscera and gonads removed]). Heads were removed and measured from tip of the mouth to firm edge of the operculum (mm), and weighed with gills intact (±0.1 gm). Gonads were removed from the fish within hours of capture, macroscopically staged (see below), weighed where possible (±0.01 g), and preserved in 10% formalin and seawater solution. Frozen head and viscera obtained from commercial and recreational fishermen were also measured and weighed as above. The thawed gonads were macroscopically staged by using a simplified staging system (see below) that is used in less detailed reproductive analyses.

Preserved gonads were blotted dry with a paper towel and weighed. A 4-mm slice from the mid-region was processed by using standard histological techniques and stained with Harris's haematoxylin and eosin for microscopic examination. Full details of methods used in the collection and analysis of *S. commerson* gonads are provided in Mackie and Lewis.[2]

Biological analyses

Gonads were staged macroscopically and microscopically. Macroscopic staging employed five developmental steps that were compatible with the microscopic staging system (Mackie and Lewis[2]):

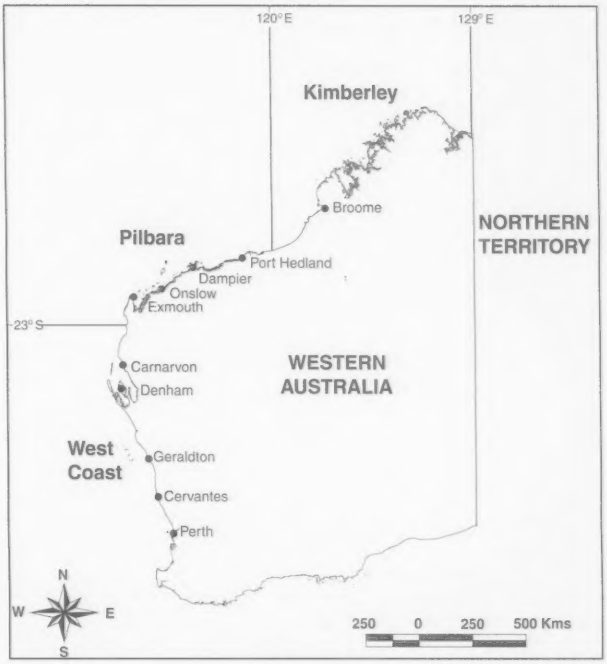

Figure 1

Sampling locations used in the study of the narrow-barred Spanish mackerel (*Scomberomorus commerson*) reproductive biology.

Juvenile (J)	undifferentiated.
Females	
stage 1	immature ("virgin" in other studies);
stages 2–3	mature, resting;
stage 4	reproductively developed;
stage 5	spawning ("running, ripe" in other studies).
Males	
stage 1	immature ("virgin" in other studies);
stage 2	mature resting;
stage 3	reproductively developed, ripe;
stage 4	spawning ("running, ripe" in other studies).

The microscopic staging system had more stages and allowed a more detailed description of spawning:

Juvenile (J)	undifferentiated.
Females	
stage 1	immature ("virgin" in other studies);
stage 1a	immature, developing;
stage 2	mature, resting;
stage 3	mature, developing;
stage 4	reproductively developed;
stage 5a	prespawning;
stage 5b	spawning ("running, ripe" in other studies);
stage 5c	postspawning;
stage 6	spent.

[2] Mackie, M. C., and P. D. Lewis. 2001. Assessment of gonad staging systems and other methods used in the study of the reproductive biology of narrow-barred Spanish mackerel, *Scomberomorus commerson*, in Western Australia. Fisheries Research Report 136, 25 p. Department of Fisheries, Perth, Western Australia 6020, Australia. http://www.fish.wa.gov.au/res/broc/frr/frr136/index.html. [Accessed January 15 2002.]

Males

stage 1	immature ("virgin" in other studies);
stage 1a	immature, developing;
stage 2	mature, resting;
stage 3	reproductively developed, ripe;
stage 4	spawning.

The immature, developing stage identified females that were immature and unlikely to spawn but had ovaries containing cortical alveoli stage oocytes (which otherwise identified mature, developing females).

Division of the microscopic staging system for ovaries into three spawning stages was based on the presence of migratory nucleus stage or hydrated oocytes within the ovarian lamellae (stage 5a), the presence of hydrated oocytes within the ovarian lumen (stage 5b), and the presence of postovulatory follicles (POFs) in the lamellae (stage 5c). In tropical fish species POFs may remain up to 24 hours in the ovaries before being resorbed (West, 1990), and there is evidence suggesting this is the case for *S. commerson* in Queensland waters (McPherson, 1993). In the present study POFs observed in the ovaries of females were categorized as either "new" or "old" based on their degree of degeneration (Mackie and Lewis[2]).

Gonadosomatic indices (GSIs) were calculated by using ratios of gonad weight to whole body weight, head weight, and head length. The latter two ratios were used to assess the usefulness of head and viscera samples in future monitoring of *S. commerson*.

Scomberomorus commerson is a serial-spawning species (Munro, 1942). Estimates of batch fecundity were made for preserved prespawning (stage 5a) ovaries from counts of hydrated oocytes within three samples taken from the anterior, middle, and posterior region of one lobe (each 130–200 mg). A section of each ovary was also processed by using histological methods to confirm suitability for estimation of fecundity. Some ovaries were subsequently rejected for fecundity estimates because the most mature batch of oocytes had not fully hydrated and were less easy to distinguish from earlier stage oocytes. These ovaries tended to provide an overestimate of batch fecundity (Mackie et al.[3]).

The daily timing and frequency of spawning were determined for females captured in the Kimberley region during September 1999 when 94% of ovaries were retained for histological analysis (n=344). Spawning frequency was determined as the inverse of the spawning fraction (the number of ovaries with hydrated or migratory nucleus stage (MNS) oocytes divided by the total number of mature ovaries in the catch). These data were compared with estimates made by using the number of ovaries macroscopically identified as having hydrated oocytes. Analyses of sex ratios were based on data where the whole catch or a known random sample of the catch was processed.

Results

The gonads of 5128 male, female, and juvenile *S. commerson* were macroscopically staged during this study. Of these, 1624 were also processed with histological techniques for more detailed analyses.

Biological analyses

Body lengths ranged from 58 to 1720 mm FL (62 to 1840 mm TL), and whole weights ranged from 0.0015 to 40.6 kg. Regression analyses incorporating step-wise reduction (using analysis of variance) of a fully parameterized model indicated that differences in length and weight relationships between regions and sex were minor compared to measurement error. Thus, the simplest models which adequately explain the pooled data were

$$\textit{Whole weight}\ (\text{kg}) = 3.40e-9 \times FL\ (\text{mm})^{3.12} \quad (n=2842)$$
(SE of constants: a=2.78e–10, b=0.01)

$$TL\ (\text{mm}) = 42.74 + (1.06 \times FL\ (\text{mm})) \quad (n=1679,\ r^2=0.996).$$

Overall sex ratios were biased towards females, with the M:F ratio varying between 1:1.2 and 1:1.6 in the three regions. However, there was considerable variation between samples, from a peak M:F ratio of 1:2.6 for samples obtained in the nonreproductive period, to a male bias of 1.1:1 in pooled samples obtained during the peak spawning period. This slight male bias during the spawning period occurred in successive years; the sex bias, however, was variable between daily samples. Sex ratios also changed over from a male to female bias with increasing size class, with a 1:1 ratio occurring at about 1000–1050 mm FL.

Ovarian weight ranged from 2.00 to 1908.30 g and testes from 0.84 to 840.10 g. Gonads of juvenile *S. commerson* were small and contained no recognizable germ tissue. The smallest fish with differentiated gonads was a 301-mm-FL male. The smallest female was 396 mm FL. Two abnormally large juveniles (1170 and 1251 mm FL) were captured whose gonads had remained unusually small and undifferentiated. Body lengths of immature females (largest=1195 mm FL [13.8 kg WW]) overlapped substantially with those of mature females (smallest=641 mm FL [2.3 kg WW]).

Estimates of the size at which 50% of females were mature were calculated by using all available data as well as data taken only during the reproductive season (October to April). Data for each area were pooled to provide sufficient samples (virtually all samples of immature fish were obtained from the Pilbara region). Both data sets provided similar estimates; 809 mm FL, ±9.8 SE (898 mm TL) for all data, and 788 mm

[3] Mackie, M. C., D. J., Gaughan, and R. C. Buckworth. 2003. Stock assessment of narrow-barred Spanish mackerel (*Scomberomorus commerson*) in Western Australia. Final report to the Fisheries Research and Development Corporation (FRDC) on project no. 1999/151, 242 p. Department of Fisheries, Perth, Western Australia, 6020.

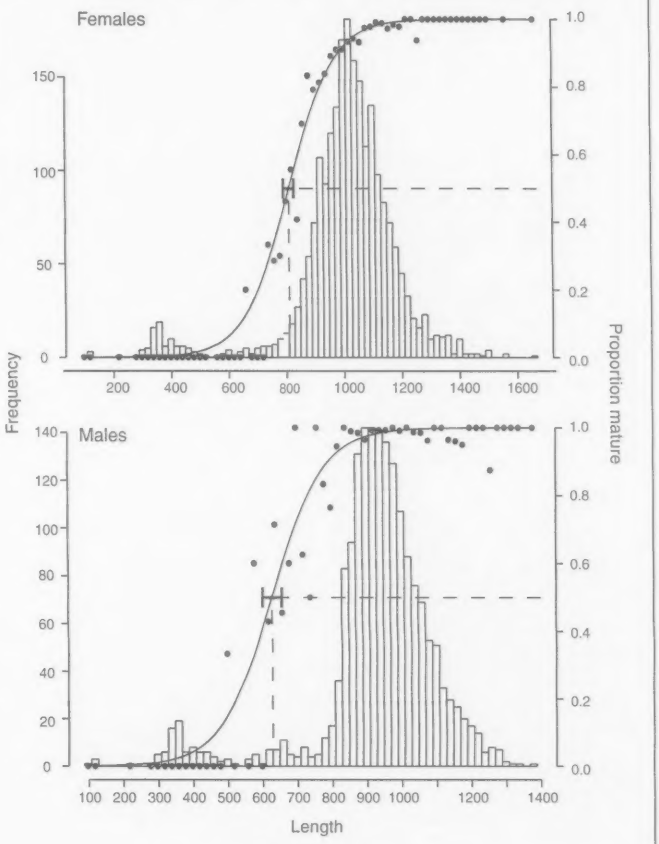

Figure 2

Proportion of mature female and male *S. commerson* within samples. The number of fish within each length class is indicated by the vertical bars and the left *y*-axis and the proportion of mature fish by the black circles and the right *y*-axis. The length at which 50% of fish within the samples were mature is indicated on the fitted maturity curve (±95% CI). Lengths are fork length in mm. Note that data for juvenile fish of undifferentiated sex are included in both graphs. The dashed lines indicate the length at 50% mature (P=0.5).

FL (±14.5 SE) for data taken during the reproductive period. The size at which 10% of females were mature was 638 mm FL (±19.6 SE), with 90% mature by 981 mm FL (±7.2 SE) (Fig. 2A).

There was also considerable overlap between the lengths of immature and mature males. The largest immature male was 1140 mm FL (11.3 kg WW), whereas the smallest mature male (stage 3) was 491 mm FL (1.0 kg WW). The size at which 10% of males were mature was 465 mm FL (±24.9 SE), the size at which 50% of males were mature was 628 mm FL (±13.8 SE) or 706 mm TL, and the size at which 90% were mature was 791 mm FL (±10.5 SE) (Fig. 2B).

Development of oocytes is asynchronous and all stages of oocytes are present at the same time within reproductively active ovaries. This reproductive feature, along with the maturation of multiple batches of oocytes (as evidenced by presence of both POFs and hydrated or MNS oocytes in spawning ovaries), confirms that female *S. commerson* are serial or partial spawners (Hunter et al., 1985).

Relationships between batch fecundity and body parameters were obtained from counts of hydrated oocytes within prespawning (stage 5a) ovaries. Size of females for which batch fecundity was determined ranged from 857 to 1143 mm FL and from 5.3 to

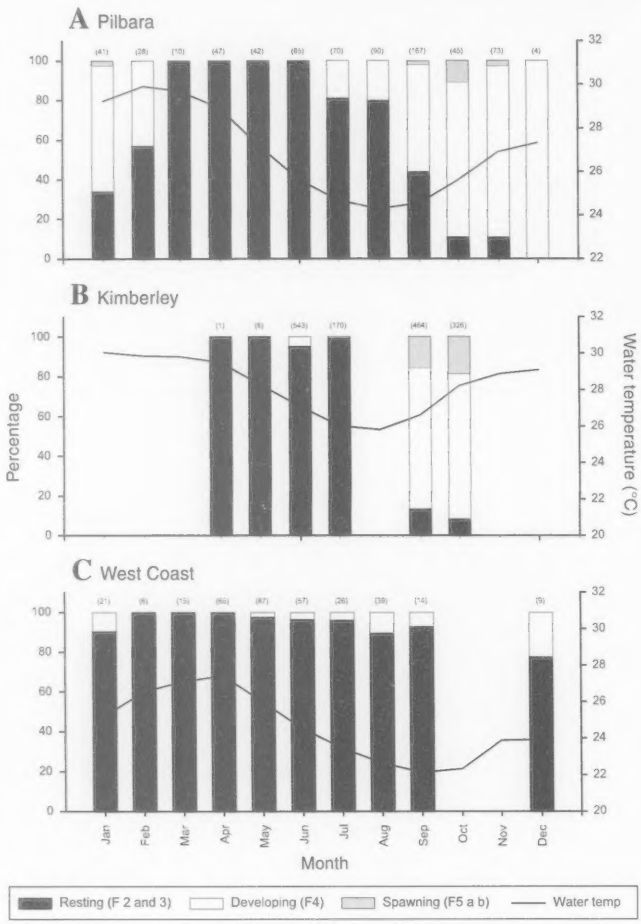

Figure 3

Annual cycle of *Scomberomorus commerson* reproduction within each region, as indicated by macroscopically staged ovaries. Mid-month sea surface temperatures are overlaid (solid line) and sample sizes are shown above each column.

12.7 kg WW. Both relationships were explained with power curves:

$$Batch\ fecundity = 0.0011 \times FL^{2.896} \quad (r^2=0.441,\ n=21)$$
$$Batch\ fecundity = 31087 \times WW^{1.384} \quad (r^2=0.714,\ n=19).$$

Annual reproductive cycle

Female *S. commerson* within the Pilbara region were non-reproductive between March and June, during the downward cycle of water temperatures (Figs. 3 and 4). As water temperatures reached a minimum in July and August (around 24°C), a small proportion of mature ovaries had become reproductively developed (stage 4). The proportion of developed ovaries during September (the start of the upward cycle of water temperatures) varied noticeably between years in the Pilbara region, from 18.5% to 79% in 2001 and 2000, respectively. A small number of females were also actively spawning when sampled during September 2000. Peak reproductive activity extended from October to January, and spawning females were captured during this period in 1999 and 2000 when the sea surface temperature (SST) was rising from about 25.5° to 28.5°C. By February, when SST peaked at approximately 30°C, reproductive development was declining and the ovaries of most females were spent or resting.

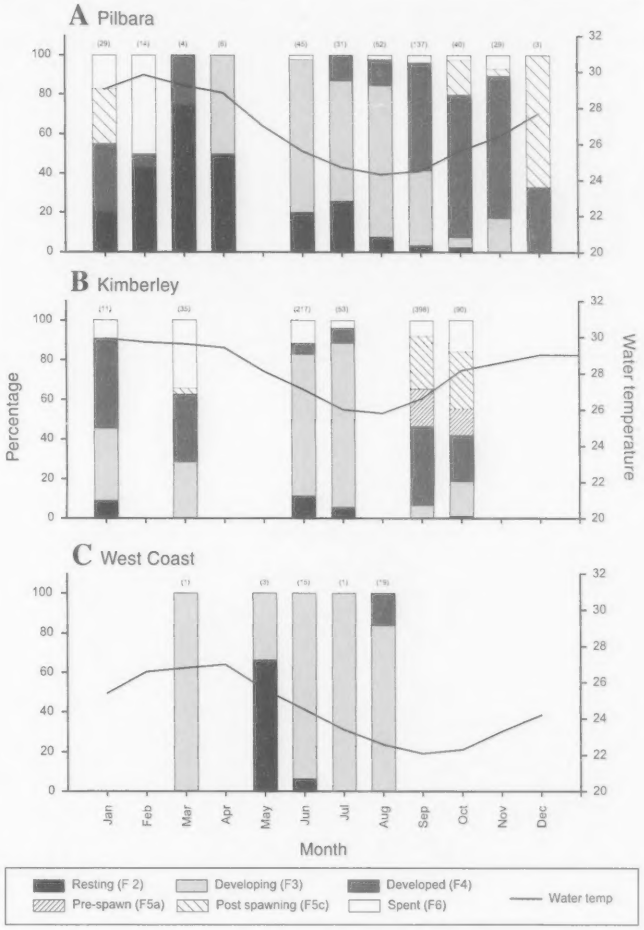

Figure 4

Annual cycle of *Scomberomorus commerson* reproduction in Western Australia for (**A**) Pilbara, (**B**) Kimberley, and (**C**) West Coast regions, as indicated by histologically staged ovaries. Mid-month sea surface temperatures are overlaid (solid line) and sample sizes are shown above each column.

The annual reproductive cycle of ovaries in the Kimberley region follows a similar pattern to that in the Pilbara region (Figs. 3 and 4). However, because 30–50% of females captured in Kimberley waters during September 1999 and 2000 were actively spawning, it appears that *S. commerson* commence spawning at least one month earlier in this region. About 60% of females were also spawning when sampled during October 1999 and 2000, although only 35% were spawning during this month in 2001. If spawning in the Kimberley region commenced in August and concluded in November (same duration as in the Pilbara region), the associated SST ranged from approximately 26.5–27°C to 29–30°C (annual maximum approx 30–31°C; Figs. 3 and 4). Sampling of developed ovaries in March also indicated that the reproductive period for *S. commerson* in the Kimberley region may be more protracted than in the Pilbara region.

In the West Coast region few reproductively developed ovaries and no spawning ovaries were obtained; *S. commerson* are rarely captured in this region during the peak spawning period observed in the northern regions. The maximum sea surface temperature (SST) in this region of around 28°C is above the lower temperature range of spawning in the two northern regions. Reproductively developed ovaries obtained from the

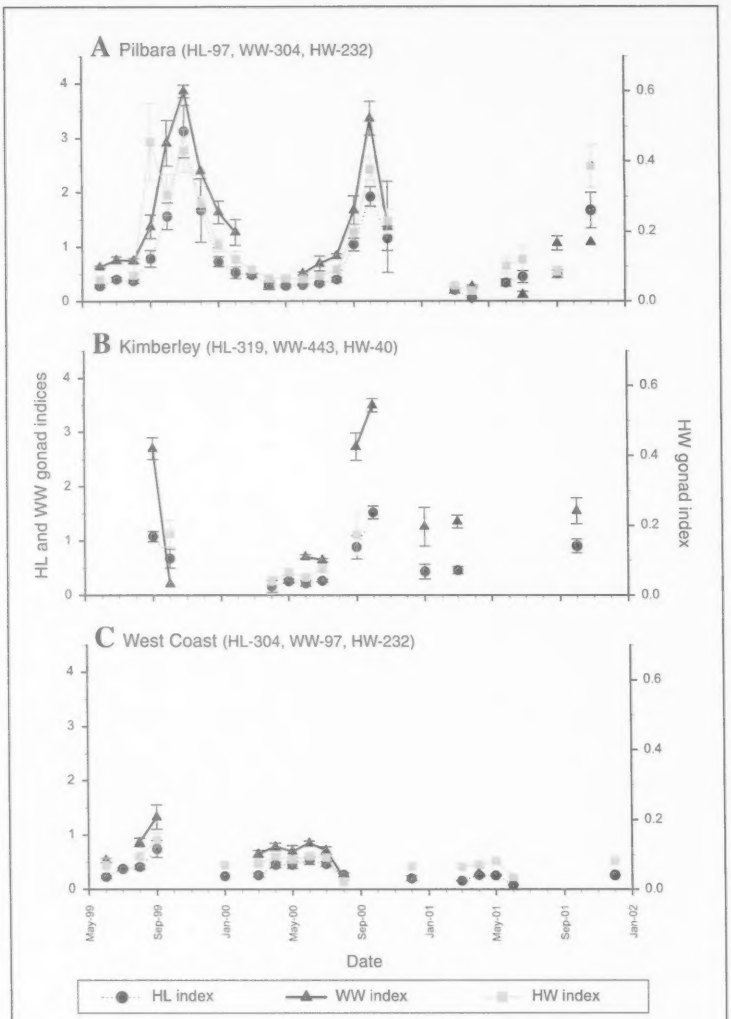

Figure 5

Annual cycle of gonad indices for *Scomberomorus commerson* in Western Australia for (**A**) Pilbara, (**B**) Kimberley, and (**C**) West Coast regions. Sample sizes are given for each index, where HL=head length index, WW=whole weight index, and HW=head weight index.

West Coast region were collected over a range of SSTs, including when it was at a minimum (Figs. 3 and 4).

Gonadosomatic indices calculated from whole weight, head weight, and head length exhibited similar patterns and confirmed the spawning cycle determined from examination of ovaries (Fig. 5). The most complete data set was for females from the Pilbara region. In this region indices were minimal between March and August and increased considerably during September as ovaries became reproductively developed. Peak indices occurred in November 1999 and October 2000, coinciding with peaks in the proportion of spawning (stage 5) ovaries in the samples. The drop in gonad indices during December 1999 showed that the supplies of vitellogenic oocytes within the ovaries were reduced by this time, even though many females were still spawning (Fig. 4). This drop continued until March when all the ovaries in the samples were in the resting stage. Data for 2001 indicate that decreased GSIs during the reproductive season were comparable to data from the previous two

Table 1

Ovarian development of *Scomberomorus commerson* sampled in the Kimberley region during the spawning season. POFs= postovulatory follicles. Ovaries in prespawning, spawning, postspawning, and spent stages of development are indicated by 5a, 5b, 5c, and 6, respectively. Note that data for stage 5c includes only females that had spawned on the day of capture (i.e., excluding ovaries containing old POFs only). Data for "Old POFs" includes all ovaries containing old POFs as well as other evidence of recent or imminent spawning.

		Histological analysis		Morning					Afternoon				
Year	Total caught	Total	Number mature	Total	5a	5b	5c	Old POFs	Total	5a	5b	5c	Old POFs
1999	344	325	306	171	59	0	0	70	135	1	1	23	51
2000	406	115	103	59	22	0	0	21	44	0	0	15	13

years. Data for the Kimberley and West Coast regions were limited but concurred with gonad staging data and also confirmed the low reproductive status of *S. commerson* within the West Coast region.

Spawning

Evidence of spawning was found in 237 of the histologically processed ovaries. Thirty-eight percent (n=90) of these were about to spawn when captured (stage 5a), 62% (n=147) had recently spawned (stage 5c), and one was running, ripe (stage 5b). The ovaries of only two macroscopically staged females were also running, ripe. Most of these spawning fish (n=219) were captured in the north Kimberley region (eighteen from the Pilbara region). The most southern location from which a spawning female was obtained was Exmouth (one recently spawned fish), and no females captured in the West Coast or more southern regions showed histological (or macroscopic) evidence of spawning.

Spawning females collected during 1999 and 2000 were either prespawning (stage 5a) and caught in the morning, or had recently spawned (stage 5c) and were caught in the afternoon (Table 1). The absence of hydrated oocytes in the afternoon and new POFs in the morning showed that the entire cycle of oocyte maturation, ovulation, and spawning is completed within a 24-hour period. Because no new POFs were present in ovaries sampled during the morning the transition from new to old POFs occurs during the night, within about 12 hours of spawning. The lack of evidence to show that females spawned on more than two consecutive days indicates that old POFs are unrecognizable after 24 hours.

Spawning fraction was estimated by using data obtained in the Kimberley region during September 1999 when 95% (n=344) of ovaries were examined by using histological methods. Analyses were based on the number of prespawning (stage 5a) ovaries sampled during the morning (usually between 0600–0900 h). Afternoon samples (usually 1500–1800 h) were not used because the number of spawning fish was likely to be underestimated because of the low catchability of running, ripe (stage 5b) females. Thirty-five percent (n=59) of mature females in the morning samples were about to spawn (stage 5a). Spawning frequency was therefore 2.9 days. Comparison of spawning fractions in samples of at least ten females showed higher spawning fractions (33–56%) for the Kimberley region compared with the Pilbara region (4–28%).

Spawning fraction was also estimated for the morning samples as the proportion of macroscopically staged mature ovaries that contained hydrated oocytes. Thirty-one of the 180 mature females were identified as such, providing an estimated spawning fraction of 17.2%, and a spawning frequency of 5.8 days.

Thirty-six percent (n=54) of spawning females (stages 5, a–c) had spawned on two consecutive days. For example, 39 ovaries contained oocytes in the MNS or hydrated stage of development (i.e., spawning was imminent when fish were captured) and also contained old POFs. Another 15 ovaries had both old and new POFs.

Discussion

Scomberomorus commerson has a gonochoristic life history in which the gonad differentiates into an ovary or testis at around 300–400 mm FL. Males differentiate and reach sexual maturity at a smaller body size than females, as is the case with the congeneric species *S. maculatus* and *S. cavalla* (Beamariage, 1973; Schmidt et al., 1993). Consequently, more than 90% are sexually mature by the time the minimum legal length of 900 mm TL is reached in the fishery. In contrast only 50% of females are mature at 898 mm TL. Although mortality of released undersize fish may be high because of difficulties in removing fishing hooks, this size limit deters fishermen from targeting small fish and relatively few are captured (Mackie et al.[3]).

Biases in sex ratios have been observed in several species of *Scomberomorus* (e.g. Trent et al., 1981; Sturm

and Salter, 1990; Begg, 1998). In the case of *S. commerson*, females usually dominate size classes above the MLL because they grow faster and reach a larger maximum size (McPherson, 1992; Mackie et al.[3]). However, they are rarely caught when actively spawning, despite observations by fishermen of leaping fish that might indicate that they are still present on the fishing grounds. Regional differences in fishing gear can also affect catchability. The lighter monofilament and reel outfits used in the Pilbara and West Coast regions likely catch larger fish than the heavier rope and thick monofilament hand-hauled rigs used by Kimberley fishermen that do not allow the fish to be "played" (i.e. do not allow the fish to swim) and may result in more gear failure.

The spring-summer spawning pattern observed in our study is similar to that of *S. commerson* along the east coast of Australia (McPherson, 1981). Water temperature may influence spawning in fish by affecting gametogenesis, gonad atresia, and spawning behavior (Lam, 1983). In WA waters *S. commerson* spawn as water temperatures are rising and, as found in Queensland, may compensate for latitudinal differences in temperatures by spawning earlier in northern waters (McPherson, 1981). No evidence of spawning activity was found within the West Coast region although the annual range of water temperatures overlap with those in which spawning occurs farther north. Restricted spawning by *S. commerson* on the east coast occurs at similar latitudes to northern parts of the West Coast region, and anecdotal evidence suggests that spawning may be restricted in some years in this region.

During the spawning period the average female *S. commerson* may spawn every three days and about one third of fish spawn on consecutive days. Female fish similarly spawn every 2–6 days and possibly on consecutive days in Queensland waters (McPherson, 1993). Our study showed that estimates based on the fraction of histologically staged prespawning (stage 5a) ovaries provided the best estimate of spawning frequency. However, only samples taken during the morning can be used for this analysis because of decreased catchability of running, ripe females in the afternoon. In comparison, macroscopic staging of ovaries with hydrated oocytes underestimated spawning frequency because migratory nucleus oocytes (which comprised 54% of histologically staged, prespawning [stage 5a] ovaries) cannot be identified. It is also impossible to identify fish that have spawned on more than one occasion with macroscopic criteria, resulting in a further underestimate of spawning activity (by 25% for *S. commerson*).

Maturation, ovulation, and spawning of oocytes by female *S. commerson* was completed within a 24-h cycle in the Kimberley region compared to 24–36 hours in Queensland waters (McPherson, 1993). Maturation of the oocytes is underway by sunrise and probably completed in all spawning ovaries by mid to late morning to allow for ovulation prior to spawning in the afternoon. Few samples were obtained at or after dusk because fish are generally not catchable, indicating that a high incidence of spawning at this time because only one spawning fish was obtained during the study. Dusk spawning is prominent among pelagic spawning species that inhabit tropical reefs (Thresher, 1984). However, spawning in the afternoon is less common and may be linked to large tidal cycles and strong currents in the north of WA, as indicated for the brown stripe snapper (*Lutjanus vitta*) that also spawns in the afternoon in the Pilbara region (Davis and West, 1993).

Batch fecundity of *S. commerson* has not previously been recorded and such data are rare for other *Scomberomorus* species. Fecundity estimates for *S. commerson* from the Indian Peninsula (Devaraj, 1983) were not comparable because those data appeared to be obtained from counts of both vitellogenic and previtellogenic oocytes. Although the current study provided fecundity estimates only for females up to 13 kg whole weight, it shows that *S. commerson* is highly fecund (the highest estimated batch fecundity of 1.2 million eggs was obtained from an ovary that was less than half the weight of the heaviest ovary sampled). This study highlighted the need to histologically check that oocytes in the spawning batch are fully hydrated because fecundity may otherwise be over-estimated. Similarly, fecundity will be under-estimated if ovulation has commenced. The best time to collect gonad samples so that these biases are minimized is during the mid to late afternoon for this species.

Fishing activity is also regulated by the reproductive cycle. About 3–6 months prior to the spawning season catches of *S. commerson* by commercial fishermen increase as large numbers of smaller *S. commerson* appear on offshore reefs sometime between March and May, and soon after throughout the coastal waters of WA (Mackie[4]). By the time reproductive development in ovaries begins (approximately August and September in the Kimberley and Pilbara regions, respectively) catches have peaked or are declining. In the Pilbara region commercial catches have dropped to a minimum when spawning begins, as fish become less abundant in inshore waters and inclement weather conditions limit fishing on still productive offshore reefs. Because *S. commerson* generally do not make substantial longshore movements (Buckworth et al.[5]), it is likely that most spawning activity occurs at offshore locations in this region (e.g., in mid to outer areas of the continental shelf), although anecdotal evidence indicates that

[4] Mackie, M. C. 2001. Spanish mackerel stock status report. *In* State of the fisheries report 1999/2000 (J. W. Penn, W. J. Fletcher, and F. Head, eds.), p. 71–75. Department of Fisheries, Perth, Western Australia, 6020. http://www.fish.wa.gov.au/sof/1999/comm/nc/commnc26.html, Accessed 10/2/2001.

[5] Buckworth, R. C., S. J. Newman, J. R. Ovenden, R. J. G. Lester, and G. R. McPherson. 2004. In prep. The stock structure of northern and western Australian spanish mackerel. Final report to the Fisheries Research and Development Corporation (FRDC) on project no. 1998/159. Department of Business Industry and Resource Development, Darwin, Northern Territory, 0800, Australia.

large, more solitary individuals may spawn in inshore waters.

Catches of *S. commerson* peak and decline rapidly along the Kimberley coast during the main spawning period because of declining fish abundance and weather conditions. As in the Pilbara region, few *S. commerson* are caught at this time in southern or midsections of the Kimberley coast. Fishermen must therefore undertake extensive trips north to the remaining productive grounds located between 12.5° and 15°S latitude where the majority of *S. commerson* spawning activity was encountered in the present study. Although it is possible that *S. commerson* in other areas of the Kimberley region may move offshore to spawn, it is also possible that some move northward, mixing and spawning with otherwise temporally and spatially discrete northern populations, in a similar manner to *S. cavalla* in U.S. waters (Broughton et al., 2002).

Monitoring of the WA fishery for *S. commerson* is likely to be based on the collection of head and gonad samples because limited funding and large distances will restrict future research trips. Onboard storage of filleted frames for research purposes is also prohibited by the large body size of *S. commerson*. In contrast, the head of this species is relatively small and easy to store, and as shown in the present study, provides a general measure of reproductive activity through calculation of head-to-gonad ratios. These ratios can also be supplemented by staging the gonads by using the macroscopic staging system developed for this species (Mackie and Lewis[2]). Head length can also be used to estimate body length of *S. commerson* (Mackie et al.[3]) and the otoliths contained in the head can be used to determine age. Although data gathered by such means is less accurate than that obtained from whole, fresh samples, it presents the best option for gathering ongoing data in sufficient quantities for meaningful analyses.

Acknowledgments

The authors thank the numerous commercial and recreational fishermen who assisted in the collection of samples and provided invaluable advice. The assistance of Department of Fisheries staff and volunteers on field trips is also appreciated. We also thank Rod Lenanton, Rick Fletcher, and Peter Stephenson for reviewing the manuscript, and to the Fisheries Research and Development Corporation for funding Project 1999/151, of which this study formed a part.

Literature cited

ABARE (Australian Bureau of Agricultural and Resource Economics).
2003. Australian fisheries statistics 2002, 69 p. ABARE, Canberra, New South Wales,Australia.

Beaumariage, D. S.
1973. Age, growth and reproduction of king mackerel *Scomberomorus cavalla*, in Florida. Florida Mar. Res. Pub. 1:1–45.

Begg, G. A.
1998. Reproductive biology of school mackerel (*Scomberomorus queenslandicus*) and spotted mackerel (*S. munroi*) in Queensland east-coast waters. Mar. Freshw. Res. 49:261–270.

Broughton, R. E., L. B. Stewart, and J. R. Gold.
2002. Microsatellite variation suggests substantial gene flow between king mackerel (*Scomberomorus cavalla*) in the western Atlantic Ocean and Gulf of Mexico. Fish. Res. 54:305–316.

Collette, B. B., and C. E. Nauen.
1983. FAO Species catalogue. Vol 2: scombrids of the world. FAO Fish. Synop. 125:1–137.

Davis, T. L. O., and G. J. West.
1993. Maturation, reproductive seasonality, fecundity, and spawning frequency in *Lutjanus vittus* (Quoy and Gaimard) from the North West Shelf of Australia. Fish. Bull. 91:224–236.

Devaraj, M.
1983. Maturity, spawning and fecundity of the king seer, *Scomberomorus commerson* (Lacepede), in the seas around the Indian Peninsula. Ind. J. Fish. 30(2):203–230.

Hunter, J. R., N. C. H. Lo, and R. J. H. Leong.
1985. Batch fecundity in multiple spawning fishes. *In* An egg production method for estimating spawning biomass of pelagic fish: application to the northen anchovy (*Engraulis mordax)* (R. Lasker, ed.), p. 67–77. NOAA Tech. Rep. NMFS 36.

Lam, T. J.
1983. Environmental influences on gonadal activity in fish. *In* Reproduction, part B, Behaviour and fertility control (W. S. Hoar, D. J. Randall, and E. M. Donaldson, eds.), p. 65–115. Academic Press, New York and London.

McPherson, G. R.
1981. Preliminary report: Investigations of Spanish mackerel (*Scomberomorus commerson)* in Queensland waters. *In* Northern pelagic fish seminar (D. J. Grant and D. G. Walter, eds.), p. 51–58. Australian Government Publishing Service, Canberra, New South Wales, Australia.
1992. Age and growth of the narrow-barred Spanish mackerel (*Scomberomorus commerson* Lacepede, 1800) in north-eastern Queensland waters. Aust. J. Mar. Fresh. Res. 43:1269–1282.
1993. Reproductive biology of the narrow-barred Spanish mackerel (*Scomberomorus commerson* Lacepede, 1800) in Queensland waters. Asian Fish. Sci. 6:169–182.

McPherson, G. R., and L. E. Williams.
2002. Narrow-barred Spanish mackerel. *In* Queensland's fisheries resources: current condition and recent trends 1988–2000 (L. E. Williams, ed.), p. 88–93. Information Series QI02012, Department of Primary Industries Queensland, Brisbane, Australia.

Munro, I. S. R.
1942. The eggs and early larvae of the Australian barred Spanish mackerel, *Scomberomorus commersoni* (Lacepede) with preliminary notes on the spawning of that species. Proc. Royal Soc. Qld. 54:33–48.

Schmidt, D. J., M. R. Collins, and D. M. Wyanski.
1993. Age, growth, maturity and spawning of Spanish mackerel, *Scomberomorus maculatus* (Mitchell), from the Atlantic coast of the southeastern United States. Fish. Bull. 91:526–533.

Sturm, M. G. deL., and P. Salter.
1990. Age, growth and reproduction of the king mackerel, *Scomberomorus cavalla* (Cuvier), in Trinidad waters. Fish. Bull. 88:361–370.
Thresher, R. G.
1984. Reproduction in reef fishes, 391 p. T.F.H. Publications Pty Ltd., Neptune City, NJ.
Trent, L., R. O. Williams, R. G. Taylor, C. H. Saloman, and C. S. Manooch.
1981. Size and sex ratio of king mackerel, *Scomberomorus cavalla*, in the southeastern United States. NOAA Tech. Memo. NMFS-SEFC 62:1–59.
West, G.
1990. Methods of assessing ovarian development in fishes: areview. Aust. J. Mar. Freshw. Res. 41:192–222.

Seasonal marine growth of Bristol Bay sockeye salmon (*Oncorhynchus nerka*) in relation to competition with Asian pink salmon (*O. gorbuscha*) and the 1977 ocean regime shift

Gregory T. Ruggerone
Natural Resources Consultants, Inc.
1900 West Nickerson Street, Suite 207
Seattle, Washington 98119
E-mail address: GRuggerone@nrccorp.com

Ed Farley
National Marine Fisheries Service
11305 Glacier Highway
Juneau, Alaska 99801

Jennifer Nielsen
Biological Resources Division
U.S. Geological Survey
Anchorage, Alaska 99503

Peter Hagen
Alaska Dept. of Fish and Game
P.O. Box 25526
Juneau, Alaska 99802-5526

Abstract—Recent research demonstrated significantly lower growth and survival of Bristol Bay sockeye salmon (*Oncorhynchus nerka*) during odd-numbered years of their second or third years at sea (1975, 1977, etc.), a trend that was opposite that of Asian pink salmon (*O. gorbuscha*) abundance. Here we evaluated seasonal growth trends of Kvichak and Egegik river sockeye salmon (Bristol Bay stocks) during even- and odd-numbered years at sea by measuring scale circuli increments within each growth zone of each major salmon age group between 1955 and 2000. First year scale growth was not significantly different between odd- and even-numbered years, but peak growth of age-2. smolts was significantly higher than age-1. smolts. Total second and third year scale growth of salmon was significantly lower during odd- than during even-numbered years. However, reduced scale growth in odd-numbered years began after peak growth in spring and continued through summer and fall even though most pink salmon had left the high seas by late July (10–18% growth reduction in odd *vs.* even years). The alternating odd and even year growth pattern was consistent before and after the 1977 ocean regime shift. During 1977–2000, when salmon abundance was relatively great, sockeye salmon growth was high during specific seasons compared with that during 1955–1976, that is to say, immediately after entry to Bristol Bay, after peak growth in the first year, during the middle of the second growing season, and during spring of the third season. Growth after the spring peak in the third year at sea was relatively low during 1977–2000. We hypothesize that high consumption rates of prey by pink salmon during spring through mid-July of odd-numbered years, coupled with declining zooplankton biomass during summer and potentially cyclic abundances of squid and other prey, contributed to reduced prey availability and therefore reduced growth of Bristol Bay sockeye salmon during late spring through fall of odd-numbered years.

Manuscript submitted 7 April 2004
to the Scientific Editor's Office.

Manuscript approved for publication
14 December 2004 by the Scientific Editor.

Fish. Bull. 103:355–370 (2005).

Competition among Pacific salmon (*Oncorhynchus* spp.) for food resources in the North Pacific Ocean and Bering Sea is a potentially important mechanism affecting salmon growth and population dynamics. Reduced growth at sea may lead to delayed maturation (Rogers, 1987), lower reproductive potential (Groot and Margolis, 1991), or greater risk of predation (Juanes, 1994).

Density-dependent growth in the ocean has been observed among sockeye (*O. nerka*), pink (*O. gorbuscha*), and chum salmon (*O. keta*), which are the most abundant species among Pacific salmon (Rogers[1]; Eggers et al.[2]). Density-dependent growth may occur during early marine life (Peterman, 1984) or during the homeward migration period when the potential for high growth rate (Ishida et al., 1998) may be influenced by high concentrations of salmon (Rogers and Ruggerone, 1993).

Since the early 1970s, salmon abundance in the North Pacific Ocean has increased, whereas body size for many populations of all salmon species has declined (Bigler et al., 1996). However, greater abundance of adult sockeye salmon returning to Bristol Bay, Alaska, was associated with increased growth during the first and second years at sea, followed by relatively low growth during the third year at sea, and greater adult size at a given abundance (Ruggerone et al.,

[1] Rogers, D. E. 2001. Estimates of annual salmon runs from the North Pacific, 1951–2001. Report SAFS-UW-0115, 11 p. School of Aquatic Sciences, Univ. Washington, Seattle, WA.

[2] Eggers, D. M, J. Irvine, M. Fukawaki, and V. Karpenko. 2003. Catch trends and status of North Pacific salmon. Doc. no. 723, 34 p. North Pacific Anadromous Fisheries Commission (NPAFC), 889 Pender Street, Vancouver, Canada.

2002). Increased growth of Bristol Bay sockeye salmon during the first two years at sea was associated with greater adult returns, but high abundance apparently led to increased competition and reduced growth during the third year.

The potential for competition for food between Asian pink salmon and Bristol Bay sockeye salmon stocks is great in the North Pacific Ocean and Bering Sea. Trophic level, diet, and feeding behavior of pink salmon overlap significantly with sockeye salmon (Welch and Parsons, 1993; Davis et al., 2000; Kaeriyama et al., 2004). Asian pink salmon are highly abundant, averaging approximately 162 million adults in odd-numbered years and 104 million adults in even-numbered years, 1955 to 2000 (Rogers[1]). Bristol Bay sockeye salmon and Asian pink salmon overlap in the central North Pacific Ocean and the Bering Sea. Greatest overlap is with pink salmon from the eastern Kamchatka Peninsula and Sakhalin Island (French et al., 1976; Takagi et al., 1981; Myers et al.[3]), which are especially abundant, as shown by average harvests of 79,000 metric tons (t) in odd-numbered years and 33,000 t in even-numbered years, 1955–99 (Sinyakov, 1998; Anonymous[4]).

Evidence for competition between Asian pink and Bristol Bay sockeye salmon was provided in a recent investigation by Ruggerone et al. (2003). During 1955–97, annual sockeye salmon scale growth during the second and third years at sea was significantly reduced during odd- compared to even-numbered years. Adult sockeye salmon length was relatively low when sockeye salmon overlapped with abundant odd-year pink salmon during the year prior to homeward migration. Furthermore, smolt-to-adult survival of Bristol Bay sockeye salmon was significantly lower when they encountered odd-year pink salmon during the second year at sea. However, Bristol Bay sockeye salmon encountered relatively few pink salmon during their first year at sea and no competition effect was observed during this early marine period.

In our study we examined the seasonal growth of Bristol Bay sockeye salmon scales in an effort to determine the approximate timing and duration of reduced growth during odd-numbered years at sea that was observed by Ruggerone et al. (2003). Scale circuli increments and annuli are correlated with salmon body size (Clutter and Whitesel, 1956; Fukuwaka and Kaeriyama, 1997; Fukuwaka, 1998). We compared seasonal scale growth before and after 1977 to examine seasonal growth trends associated with the twofold increase in Bristol Bay sockeye salmon abundance and the 1977 ocean regime shift (Rogers, 1984; Beamish and Bouillon, 1993; Rogers[1]). We also examined the hypothesis that seasonal growth during the second growing season was dependent on previous marine growth (Aydin, 2000). These hypotheses were tested by using scales from Kvichak River and Egegik River sockeye salmon, which averaged approximately 16 million fish per year or approximately 57% of the annual sockeye salmon run to Bristol Bay, 1955–2000.

Methods

For our study, we used scales from four age groups of Kvichak River sockeye salmon and three age groups of Egegik River sockeye salmon collected from the late 1950s through 2000 (Fig. 1). Adult salmon scales were obtained from the Alaska Department of Fish and Game (ADFG) archive in Anchorage, Alaska, and from the School of Aquatic and Fishery Sciences, University of Washington. Scales have been collected annually for measuring and quantifying age composition for management of the fisheries in Alaska. We selected scales from salmon sampled in the Kvichak and Egegik rivers rather than in the ocean fisheries to reduce the possibility of mixed stocks in the scale collection. Scale collections from the Kvichak River began in 1955, whereas collections from Egegik River began in 1960. Major freshwater and ocean age groups from Kvichak (ages 1.2, 1.3, 2.2, 2.3) and Egegik (ages 1.3, 2.2, 2.3) sockeye salmon were measured. Age was designated by European notation, i.e. the number of winters spent in freshwater before going to sea (1 winter=age-1. or two winters=age-2.) followed by the number of winters spent at sea (two winters=age-.2 or 3 winters=age-.3.). Nearly all Bristol Bay sockeye salmon mature after spending two or three winters at sea.

Scales were selected for measurement in this study only when 1) we agreed with the age determination previously made by ADFG, 2) the scale shape indicated that the scale was removed from the "preferred area" (Koo, 1962), and 3) circuli and annuli were clearly defined and not affected by scale regeneration or significant resorption along the measurement axis. We measured up to 50 scales per year, representing equal numbers of male and female salmon from each age group within each stock.

Scale measurements followed procedures described by Davis et al. (1990) and Hagen et al.[5] After selecting a scale for measurement, the scale was scanned from a microfiche reader and its image was stored as a high resolution digital file. High resolution (3352×4425 pixels) allowed the entire scale to be viewed and provided enough pixels to be seen between narrow circuli

[3] Myers, K. W., K. Y. Aydin, R. V. Walker, S. Fowler, and M. L. Dahlberg. 1996. Known ocean ranges of stocks of Pacific salmon and steelhead as shown by tagging experiments, 1956–1995. Report FRI-UW-9614, 159 p. School of Aquatic and Fishery Sciences, Univ. Washington, Seattle, WA

[4] Anonymous. 2002. Biostatistical information on salmon catches, escapement, outmigrants number, and enhancement production in Russia in 2001. Doc. no. 646, 14 p. NPAFC, 889 Pender Street, Vancouver, Canada.

[5] Hagen, P. T., D. S. Oxman, and B. A. Agler. 2001. Developing and deploying a high resolution imaging approach for scale analysis. Doc. 567, 11 p. North Pacific Anadromous Fish Commision, 889 Pender Street, Vancouver, Canada.

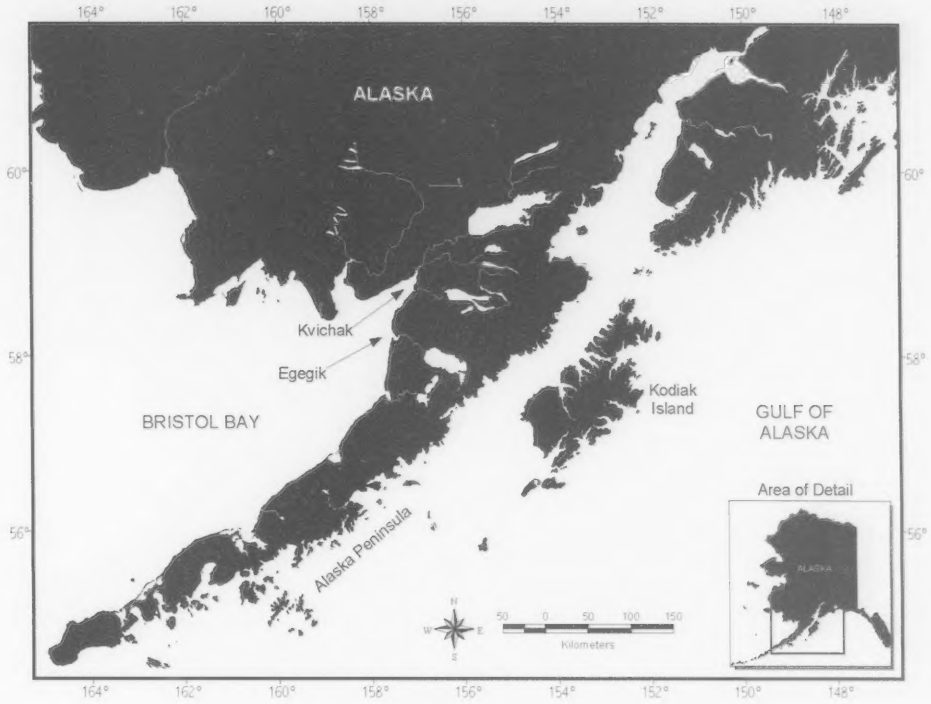

Figure 1

Map of Bristol Bay, Alaska, and the location of the Kvichak and Egegik river systems.

to ensure accurate measurements of circuli spacing. The digital image was loaded in Optimas 6.5 (Media Cybernetics, Inc., Silver Spring, MD) image processing software to collect measurement data with a customized program. The scale image was displayed on a digital LCD flat panel tablet. The scale measurement axis was determined by a perpendicular line drawn from a line intersecting each end of the first saltwater annulus. Distance (mm) between circuli was measured within each growth zone (i.e., from the scale focus to the outer edge of the first freshwater (FW1) annulus, between the first and second freshwater (FW2) annuli, within the spring plus (FWPL) growth zone, within each annual saltwater (SW1, SW2, SW3) growth zone, and from the last ocean annulus to the edge of the scale (i.e., the saltwater plus [SWPL] growth zone).

Data analysis

Mean scale circuli increments (distance between adjacent circuli pairs) of each age group and stock were calculated for each year when 10 or more scales were available. Typically, 40 to 50 scales of each age group and stock were measured in a given year. To facilitate evaluation of trends between odd- and even-numbered years at sea, scale circuli measurements were described in terms of the odd- or even-numbered year when the salmon entered the ocean. Thus, a salmon smolt entering the Bering Sea during an even-numbered year interacted with abundant odd-year Asian pink salmon during its second growing season (SW2) and less abundant even-year pink salmon during its third year, if it remained at sea. The number of circuli pairs considered in our analysis differed by growth zone, ranging from 22 circuli (SW1) to 20 circuli (SW2) to 15 circuli (SW3) in order to represent the majority of salmon. Analyses of seasonal scale growth trends were based on the mean of annual mean scale circuli increments, percentage change in scale circuli increments during odd- versus even-numbered years, and percentage change in odd- and even-year growth during periods before and after the 1977 ocean regime shift. A two-sample t-test was used to test for differences between odd- and even-numbered year scale growth at each circuli pair. Correlation was used to determine whether an individual's growth during the second growing season was related to previous growth at sea.

Results

First year (SW1) growth of ocean age-3 sockeye salmon

Kvichak and Egegik river sockeye salmon scale growth (distance between adjacent circuli) increased rapidly

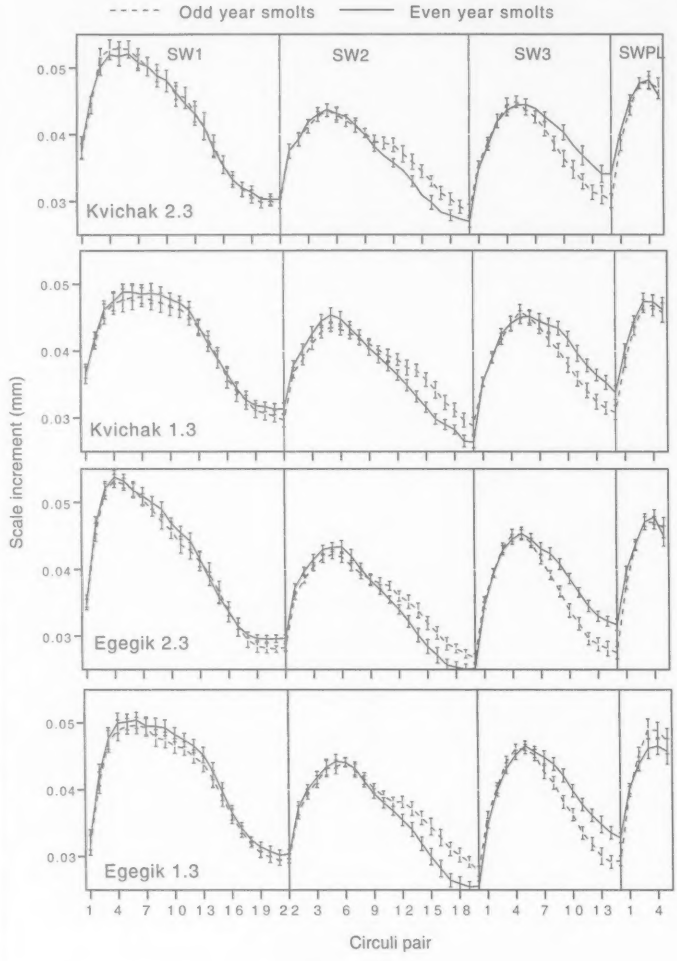

Figure 2

Average seasonal scale growth for Kvichak and Egegik ocean age-3 sockeye salmon (*Oncorhynchus nerka*) that entered the ocean as smolts during odd (- - - - -) and even (———) numbered years, 1952–2000. Growth of salmon spending one (age 1.3) and two years (age 2.3) in freshwater are shown separately. Circuli pair ordering restarts at the beginning of each new growing season (SW1, SW2, SW3, SWPL). 95% confidence intervals (CIs) are shown at each measurement.

after the fish entered Bristol Bay during May and early June, reaching peak growth near the fifth circuli (Fig. 2). Thereafter, growth declined steadily to a minimum at the first ocean annulus (circuli 18–22).

Peak scale growth of age-2. smolts was significantly greater compared with that of age-1. smolts for both Kvichak (df=79, t=5.757, P<0.001) and Egegik salmon (df=73, t=4.667, P<0.001). During the first eight circuli, age-2. smolts averaged 6.5% greater growth than age-1. smolts. Thereafter (circuli 11–20), growth of age-2. smolts declined more rapidly and averaged 2.3% (Kvichak) to 6.1% (Egegik) less than growth of age-1. smolts.

Within the SW1 growth period, no statistically significant difference in circuli growth was detected between smolts entering the ocean during odd- and even-numbered years (P>0.05). However, there was a trend for greater growth among even-year smolts in some

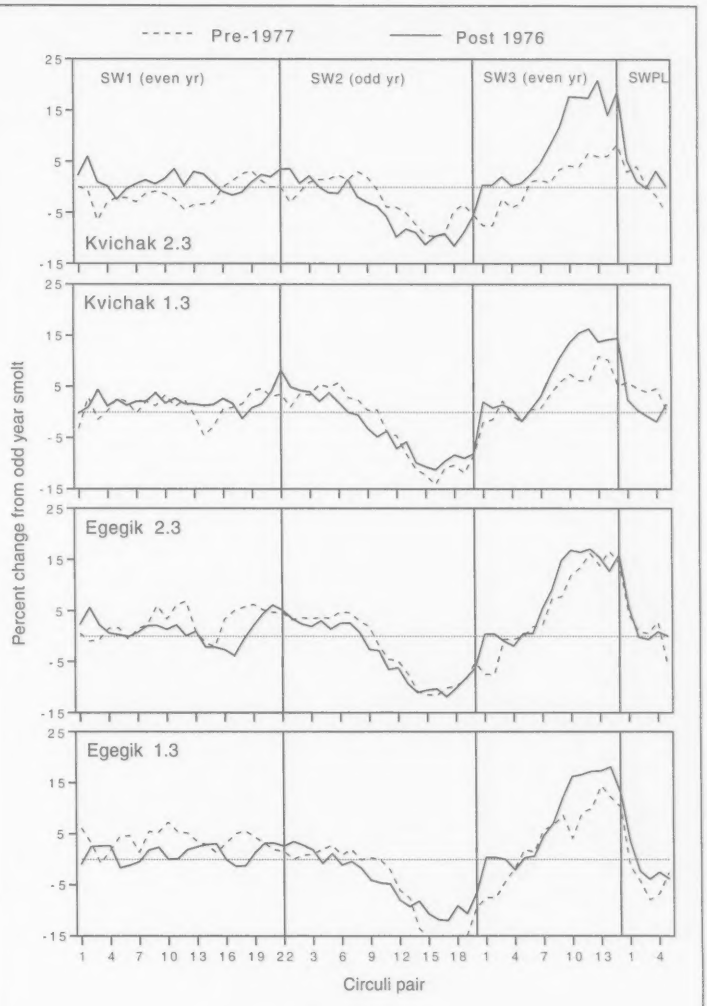

Figure 3

Percent change in scale growth of ocean age-3 sockeye salmon (*O. nerka*) entering the ocean during even-numbered years compared to odd-numbered years. Growth patterns represent ocean developmental periods prior to 1977 (- - - - -) and after 1976 (———). Even-year smolts encountered odd-year pink salmon (*O. gorbuscha*) during their second year at sea (SW2), but they encountered even-year pink salmon during their third year at sea (SW3). Age 1.3=1 year in freshwater and 3 years in saltwater; age 2.3= 2 years in freshwater and 3 years in saltwater.

portions of SW1, including the annulus (circuli 18–22) and immediately after peak growth (circuli 7 to 13) (Figs. 2 and 3).

SW1 growth of both even- and odd-year smolts tended to be greater after the 1977 climate shift than prior to this period, except for the last few circuli (Fig. 4). The greatest difference in growth between these two periods occurred immediately after entry into Bristol Bay (circuli 1–3) and during the last part of the SW1 growth period (circuli 13–19). This bimodal pattern of growth between the two periods was somewhat consistent among both stocks and freshwater age groups. However, Kvichak age 2.3 salmon experienced especially high early marine growth that was 17% greater, on average, after 1976. Following peak scale growth in spring, Egegik age 1.3 sockeye salmon experienced a

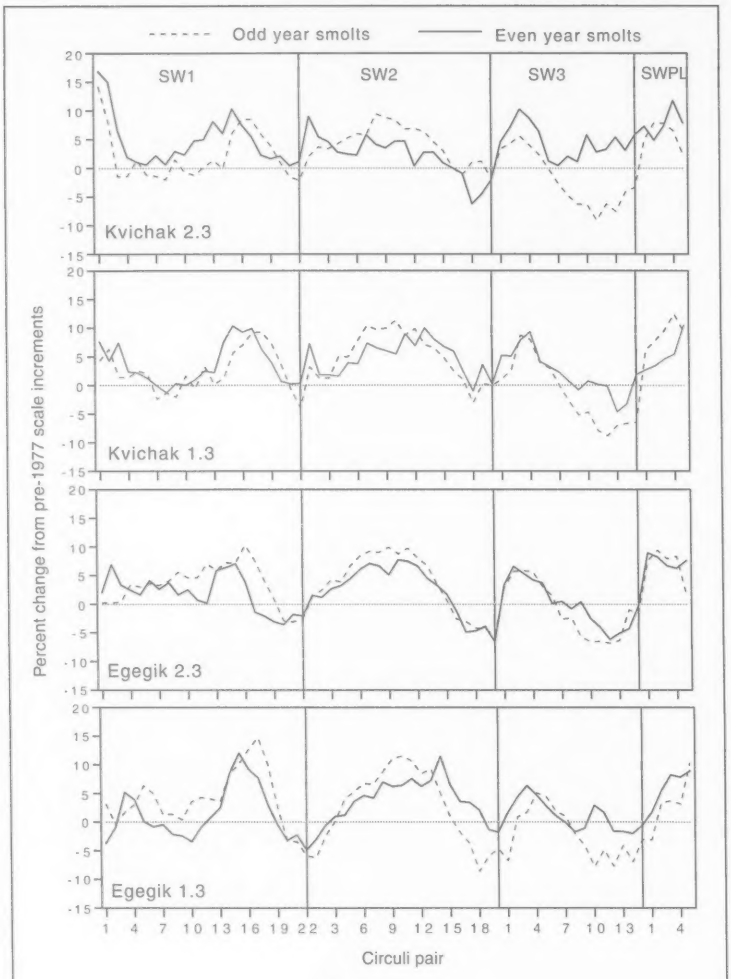

Figure 4

Percent change in scale growth of ocean age-3 sockeye salmon (*O. nerka*) entering the ocean during 1977–97 from those entering the ocean during 1952–76. Growth patterns represent smolts entering the ocean during odd- (- - - - -) and even-numbered years (———). Even-year smolts encounter odd-year pink salmon (*O. gorbuscha*) during their second year at sea (SW2), but they encountered even-year pink salmon during the their third year at sea (SW3).

15% increase in growth after 1976. In contrast, growth near the winter annulus (circuli 20–22) was up to 5% lower after the 1977 climate shift.

Second year (SW2) growth of ocean age-3 sockeye salmon

At the beginning of the second growing season (SW2), when Bristol Bay sockeye salmon are farthest south in the North Pacific Ocean (French et al., 1976), scale growth of both stocks and age groups increased rapidly, but the rate of increase was 59% less than that of SW1 and 37% less than SW3 growth (Fig. 2). Peak growth occurred near circuli 5 or 6 and it averaged 15% lower than that of SW1 growth.

During their second year at sea, even-year sockeye smolts inhabited the North Pacific and Bering Sea when Asian pink salmon were abundant in offshore waters

Table 1

Summary of two sample *t*-tests for evaluating the circuli number at which sockeye scale growth began to differ between odd- versus even-numbered years of the second and third seasons at sea. Between-year differences in circuli growth were greater after the circuli number shown in this table. No consistent pattern of differences between odd- and even-numbered years was observed during the first season at sea. Age "1.2" is a fish that has spent one year in fresh water and two years in salt water. SW2=2 years in saltwater.

Age	Ocean period	Stock	Circuli no.	df	*t*-value	*P* (two tailed)
1.2	SW2	Kvichak	C11	43	2.412	0.020
2.2	SW2	Kvichak	C11	44	3.283	0.002
2.2	SW2	Egegik	C11	39	3.434	0.001
1.3	SW2	Kvichak	C12	42	3.068	0.004
	SW3	Kvichak	C8	42	3.126	0.003
1.3	SW2	Egegik	C11	38	2.140	0.038
	SW3	Egegik	C7	38	2.527	0.016
2.3	SW2	Kvichak	C11	43	2.711	0.010
	SW3	Kvichak	C8	43	2.384	0.022
2.3	SW2	Egegik	C11	39	3.061	0.004
	SW3	Egegik	C7	39	2.728	0.010

(i.e., during odd-numbered years). Initial scale growth prior to the SW2 peak in spring was the same between odd- and even-numbered years, although there was a tendency for greater growth following the SW1 annulus of even-year smolts (Fig. 3). Immediately after peak growth near circuli 11, scale growth of even-year smolts became significantly less than that of odd-year smolts (Table 1). The growth differential continued through the end of the SW2 growing season and it reached a maximum reduction of –10% to –18% near circuli 14 to 18 (Fig. 3). This pattern was consistent before and after the 1977 climate shift and among each stock and age group. The reduced growth of even-year smolts during SW2 corresponded with high abundance of pink salmon in the central North Pacific Ocean during odd-numbered years.

Scale growth during SW2 of both odd- and even-year smolts tended to be greater after the 1977 climate shift (Fig. 4), a period when abundance of Bristol Bay sockeye salmon and Asian pink salmon was great. This pattern was consistent among both age groups of Kvichak and Egegik River sockeye salmon. Greatest growth differential between the two periods (up to 10%) occurred just after peak growth (circuli 5 to 15), a pattern that differed markedly from both SW1 and SW3. In contrast to the relatively large increase in growth shown in the central portion of SW2 after 1977, growth at the beginning of SW2 was similar during both periods and growth at the end of SW2 was relatively low after the climate shift.

Third year (SW3) growth of ocean age-3 sockeye salmon

Scale growth at the beginning of the third year at sea increased rapidly, peaked near circuli 5–6, then declined steadily through the year (Fig. 2). Peak growth during SW3 was intermediate to the relatively high peak growth during SW1 and relatively low peak growth during SW2.

During their third year at sea, even-year sockeye smolts inhabited the North Pacific and Bering Sea when relatively few Asian pink salmon were in offshore waters (i.e., even-numbered years). Prior to peak growth, SW3 growth of even-year smolts was similar or below that of odd-year smolts (Fig. 3), a pattern that continued from the previous season. Immediately following the peak, growth of even-year smolts significantly increased in relation to odd-year smolts (Table 1), and growth remained relatively high throughout the remaining season (Fig. 2). Growth of even-year smolts was approximately 5% to 15% greater than that of odd-year smolts from circuli 8 to the annulus (Fig. 3). Differences in growth during even- versus odd-numbered years tended to be greater after 1976 when both pink and sockeye salmon were relatively abundant.

Peak SW3 scale growth was up to 10% greater after the mid-1970 regime shift during both odd- and even-numbered years (Fig. 4). However, after the peak growing season, scale growth was typically lower after 1976. The relatively low growth after 1976 was especially pronounced among odd-year smolts that inhabited the ocean during odd-numbered years when Asian pink salmon were abundant in offshore waters. Scale growth of odd-year smolts during SW3 was as much as 10% lower than that prior to 1977.

Scale growth during both SW3 and SW2 were significantly reduced during odd-numbered years at sea (Table 1). However, SW3 scale growth during odd- versus even-years diverged immediately after the peak, whereas

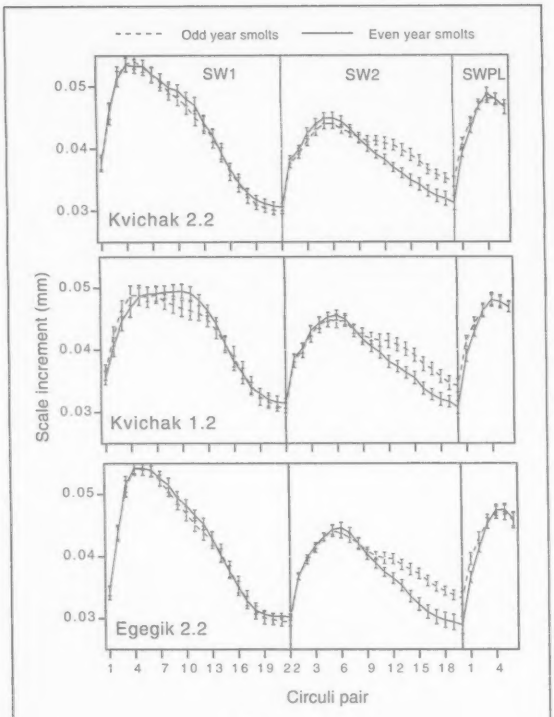

Figure 5

Seasonal scale growth of Kvichak and Egegik ocean age-2 sockeye salmon (*O. nerka*) that entered the ocean as smolts during odd- (- - - - -) and even- (———) numbered years, 1952–2000. Growth of salmon spending one (age 1.2) and two years (age 2.2) in freshwater are shown separately. Circuli pair ordering restarts at the beginning of each new growing season (SW1, SW2, SWPL). 95% CIs are shown at each measurement. Age 1.2=1 year in freshwater and 2 years in saltwater.

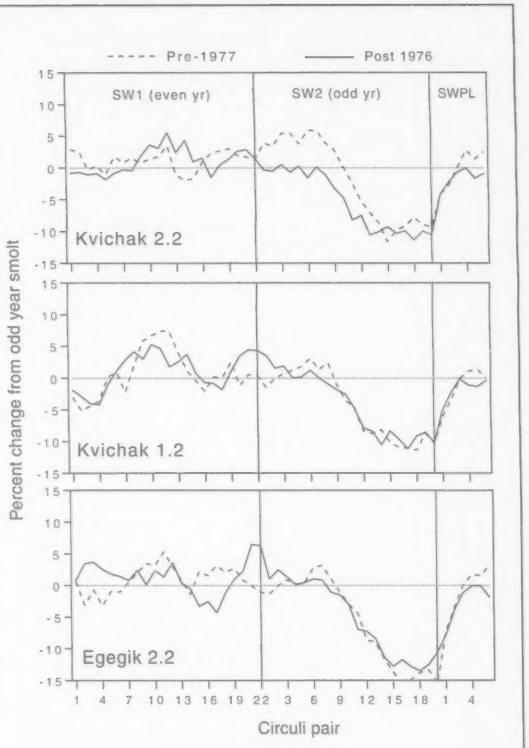

Figure 6

Percent change in scale growth between ocean age-2 sockeye salmon (*O. nerka*) entering the ocean during even years and those entering during odd-numbered years. Growth patterns represent ocean rearing periods prior to 1977 (- - - - -) and after 1976 (———). Even-year smolts encountered odd-year pink salmon (*O. gorbuscha*) during the second year at sea (SW2).

growth during SW2 diverged two or three circuli after the peak (Fig. 2). Late season growth of even-year smolts during SW3 was greater than late season growth during SW1 and SW2, whereas growth of odd-year smolts during SW3 was intermediate to SW1 and SW2 growth. These relatively large, older fish experienced a longer growing season, especially during even-numbered years, when few pink salmon were present.

Growth during homeward migration (SWPL) of ocean age-3 sockeye salmon

The peak return of sockeye salmon to Bristol Bay occurs near 3 July. Scale growth during the homeward migration peaked at circuli 3 and 4, then declined (Fig. 2). Peak growth was less than that of SW1, but greater than SW2 and SW3 growth. No growth difference was detected between odd- and even-year migrants during the period of homeward migration. Spring growth after 1976 was 5–10% greater than that during the earlier time period (Fig. 4).

First year ocean (SW1) growth of ocean age-2 sockeye salmon

Scale growth patterns of ocean age-2 Kvichak and Egegik sockeye salmon were remarkably similar to that of ocean age-3 sockeye, especially among those having the same freshwater age (Fig. 5). Sockeye salmon that had spent two winters in freshwater had significantly greater SW1 peak growth compared with those spending one winter in freshwater (Kvichak stock: df=85, t=6.772, P<0.001). Growth of age-2. smolts during the first eight circuli averaged 9% higher compared to age-1. smolts. However, as with ocean age-3 salmon, postpeak growth of age-2 smolts averaged 3.5% less than that of age-1.

smolts. Growth of even- and odd-year smolts during the first growing season was not significantly different but even-year smolts tended to have somewhat greater growth immediately following peak growth (circuli 7–13) and at the end of the growing season (circuli 19–22) (Fig. 6).

SW1 growth was markedly greater after 1976 when salmon abundance was relatively high compared with the growth during 1952–1976 (Fig. 7). Greater growth during the recent time period was most pronounced immediately after entry to Bristol Bay and after peak growth (circuli 13–18), but it was relatively low at the end of the growing season (circuli 20–22). These patterns were generally consistent between odd- and even-year smolt years.

Second year (SW2) growth of ocean age-2 sockeye salmon

SW2 scale growth patterns of ocean age-2 sockeye salmon were similar to SW2 patterns of ocean age-3 sockeye salmon. Scale growth of odd- and even-year smolts was similar until scale growth of even-year smolts significantly declined approximately three circuli after peak growth (Fig. 5, Table 1). Lower growth of even-year smolts continued to the end of the growing season. Scale growth of even-year migrants during their second year at sea was approximately 10% to 15% less than that of odd-year migrants (Fig. 6). Low growth of even-year migrants was associated with odd-numbered years at sea—a trend that was observed among SW2 and SW3 growth periods of ocean age-3 sockeye salmon.

Scale growth during SW2 was greater after 1976 when salmon abundance was relatively high compared with the growth before 1977, especially during the middle of the growing season (Fig. 7). However, after 1976, growth near the end of the growing season (circuli 17–20) tended to be below average. These patterns were consistent among the two stocks and three age groups.

Late season growth of ocean age-2 sockeye salmon during the second year at sea differed from that of ocean age-3 sockeye salmon (Figs. 2 and 5). Growth after circuli 8 of SW2 was significantly greater among ocean age-2 compared with ocean age-3 sockeye salmon (df=283, t=12.81, P<0.001), averaging 11% greater growth.

Growth during homeward migration (SWPL) of ocean age-2 sockeye salmon

Scale growth of ocean age-2 sockeye salmon during the homeward migration peaked at circuli 4, then declined. Prior to peak growth, even-year migrants experienced approximately 5% less growth than odd-year migrants, a pattern that was similar prior to and after the climate shift (Fig. 6). Low initial growth during SWPL appeared to be a continuation of relatively low growth during SW2. No difference in peak growth between odd- and even-years was apparent. Growth tended to be higher after the mid-1970s (Fig. 7).

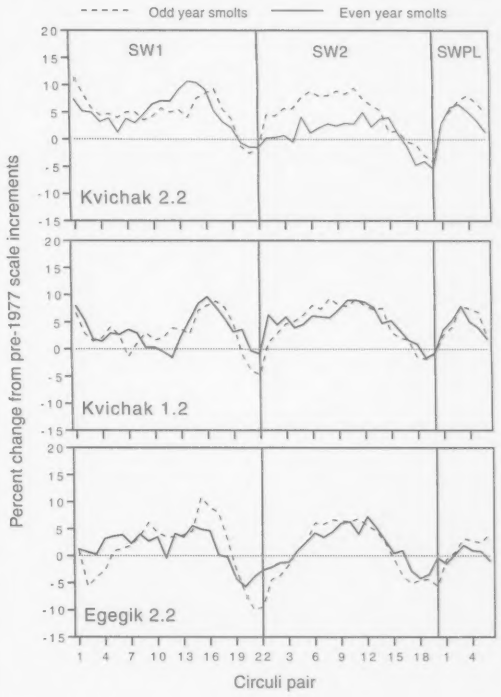

Figure 7

Percent change in ocean age-2 sockeye salmon (*O. nerka*) scale growth entering ocean during 1977 to 1998 compared with 1952–1976. Growth patterns represent smolts entering ocean during odd- (- - - - -) and even-numbered years (———). Even-year smolts encountered odd-year pink salmon (*O. gorbuscha*) during the second year at sea (SW2).

Relationship between early marine and late SW2 scale growth

We examined correlations between early marine scale (SW1 growth through the first eight circuli of SW2) and late SW2 growth (circuli 11 to annulus), corresponding with periods before and after the divergent scale growth pattern observed between odd- and even-numbered years. Negative correlations between early marine and late SW2 scale growth were observed among each stock and age group, before and after the 1977 regime shift, and among fish inhabiting the ocean during odd- or even-numbered years (Table 2). Only one of the 28 correlations (Egegik age-2.2, early period, odd SW2 year) was statistically insignificant. Thus, individual sockeye salmon that experienced somewhat low growth during early marine life tended to have somewhat high growth during later portions of their second year at sea, regardless of whether they competed with pink salmon. The strength of the

Table 2

Correlation between early marine scale growth (SW1 through SW2, circuli 1–8) and SW2 scale growth after growth difference in odd and even numbered years (SW2, circuli 11 to annulus). Measurements based on individual fish (n). Correlation coefficient and statistical significance are shown for each age group and stock during early (pre-1977) and recent (post-1976) periods for odd- and even-numbered years at sea. SW2=2 years in saltwater.

Age	Stock	Period	SW2 year	r	n	F-value	P-value
1.2	Kvichak	Early	Even	−0.11	408	5.18	<0.025
		Early	Odd	−0.20	429	18.20	<0.001
		Recent	Even	−0.22	550	27.84	<0.001
		Recent	Odd	−0.24	596	36.07	<0.001
2.2	Kvichak	Early	Even	−0.14	592	12.17	<0.001
		Early	Odd	−0.14	523	10.16	<0.002
		Recent	Even	−0.31	549	56.23	<0.001
		Recent	Odd	−0.17	568	16.78	<0.001
2.2	Egegik	Early	Even	−0.14	428	8.61	<0.004
		Early	Odd	−0.06	441	1.33	0.249
		Recent	Even	−0.14	551	10.21	<0.002
		Recent	Odd	−0.09	599	4.81	<0.030
1.3	Kvichak	Early	Even	−0.15	270	6.53	<0.020
		Early	Odd	−0.15	333	7.50	<0.010
		Recent	Even	−0.35	517	71.18	<0.001
		Recent	Odd	−0.20	504	21.89	<0.001
1.3	Egigik	Early	Even	−0.15	191	4.32	<0.040
		Early	Odd	−0.22	210	10.51	<0.002
		Recent	Even	−0.23	453	24.67	<0.001
		Recent	Odd	−0.27	479	38.60	<0.001
2.3	Kvichak	Early	Even	−0.15	347	7.78	<0.010
		Early	Odd	−0.16	376	10.12	<0.002
		Recent	Even	−0.24	438	25.86	<0.001
		Recent	Odd	−0.18	407	13.38	<0.001
2.3	Egegik	Early	Even	−0.16	460	12.35	<0.001
		Early	Odd	−0.23	416	23.94	<0.001
		Recent	Even	−0.18	546	17.94	<0.001
		Recent	Odd	−0.17	543	16.11	<0.001

correlations was low, but the consistent pattern among stocks, age groups, and time periods indicates that the negative correlations were not spurious.

Discussion

Previous research documented reduced annual scale growth of Nushagak Bay (Bristol Bay) sockeye salmon during odd-numbered years of their second and third years at sea (Ruggerone et al., 2003). The primary finding of our investigation was that salmon scale growth reduction during odd-numbered years did not occur throughout the second and third years at sea. During the second year at sea, scale growth reduction began three to five circuli after peak scale growth. During the third year at sea, scale growth reduction began immediately after peak growth. This finding was consistent among all age groups of both Kvichak and Egegik sockeye salmon prior to and after the mid-1970s regime shift that led to greater sockeye salmon abundance. Comparison of seasonal scale growth patterns before and after the regime shift indicated that the recent period of high sockeye salmon abundance was associated with relatively high growth 1) immediately after entry to Bristol Bay, 2) after peak scale growth during the first growing season, 3) during the middle of the second growing season, and 4) during the third spring but followed by below average growth during the remaining summer and fall.

Timing of peak scale growth and differences in scale growth between odd- and even-numbered years

The approximate time period of peak scale growth can be estimated from previous studies of salmon circuli formation at sea and timing of peak prey production. Bilton

and Ludwig (1966) reported that sockeye salmon in the Gulf of Alaska tended to form annuli during December and January, whereas salmon sampled farther west in the relatively cold waters below the Aleutian Islands appeared to form annuli during March (Birman, 1960). For example, sockeye salmon collected from the eastern range of Bristol Bay sockeye salmon in the Gulf of Alaska (e.g., 152–160°W) averaged 1.2 circuli beyond the winter annulus during January and 3.6 circuli in April. We observed peak circuli growth of Kvichak and Egegik sockeye salmon to occur near circuli 5 to 6 (all ages), indicating that peak scale growth occurred from approximately early May to mid-June. This finding is consistent with scale growth in the year of homeward migration when Bristol Bay sockeye salmon averaged approximately 1 to 2 circuli after peak circuli growth before reaching Bristol Bay, on average, during the first week in July. The estimated date of peak scale growth is also consistent with observations of peak biomass of zooplankton in the Gulf of Alaska and Bering Sea, which typically occurs during May or June (Brodeur et al., 1996; Coyle et al., 1996; Mackas et al., 1998; Mackas and Tsuda, 1999). However, Ishida et al. (1998) reported that salmon growth was greatest between June and July, a period apparently later than peak scale growth and peak zooplankton biomass. Furthermore, scale growth may lag behind body growth (Bilton, 1975). Based on these observations, the observed divergence in scale growth between odd- and even-numbered years likely began after zooplankton biomass declined and during a period of high potential body growth of salmon.

Differences in SW2 scale growth between odd- and even-numbered years at sea began three to five circuli after peak growth, rather than immediately after the peak as shown among fish during their third year at sea (SW3). Because younger salmon begin circuli formation earlier in winter than do older salmon (Bilton and Ludwig, 1966; Martinson and Helle, 2000), it is likely that the differences in time of SW2 scale growth was only slightly later than that scale growth during SW3. The reason for the somewhat later differences between odd and even years of younger sockeye salmon might relate to the degree of diet overlap with pink salmon. In the central North Pacific Ocean and Bering Sea, pink salmon in their second growing season have greater diet overlap with larger sockeye salmon (Davis, 2003), such as sockeye salmon in their third season at sea. Thus, competition for prey may be greatest between pink salmon and the larger, older sockeye salmon, leading to earlier growth differences between the SW3 than the SW2 growth period. Alternatively, this pattern may reflect differences in the distribution of age-2 and age-3 sockeye salmon: age-3 salmon maybe distributed farther west where overlap with Asian pink salmon is greater.

Interactions with pink salmon and prey

Spatial and temporal overlap between Asian pink salmon and Bristol Bay sockeye salmon are important factors that affect the degree of competition. Little or no overlap occurs between these stocks during the first growing season (SW1) and there are typically small numbers of pink salmon originating from Bristol Bay (Rogers[1]). Little sampling has occurred during winter (Myers[6]), but data collected during fall and spring indicate that some overlap between Asian pink salmon and Bristol Bay sockeye begins in the central North Pacific Ocean during winter (French et al., 1976; Takagi et al., 1981; Myers et al.[3]). The degree of overlap likely increases into spring when both species reach their southernmost distribution, which is somewhat farther south for pink salmon. As the temperature begins to increase, both species migrate northwest—pink salmon leading the migration. Both species enter the Bering Sea but many Bristol Bay salmon and some Asian pink salmon remain in the North Pacific Ocean. In June, some Asian pink salmon leave the high seas for coastal areas, whereas others remain offshore through July (Myers et al.[3]; Azumaya and Ishida, 2000). During odd-numbered years, pink salmon are more broadly distributed on the high seas and catch per effort in the Bering Sea remains high through at least mid-July (up to 400 fish per 30 tans (1.5 km) of gill net) compared with that during even-numbered years (Azumaya and Ishida, 2000). Catch per effort of pink salmon during July is somewhat lower in the central North Pacific Ocean. Most pink salmon in the Bering Sea likely originate from the eastern Kamchatka Peninsula, which supports a major Asian population that is dominated by odd-year pink salmon. Thus, the period of overlap between Asian pink salmon and Bristol Bay sockeye salmon is from approximately winter through July and greatest overlap likely occurs during late spring through at least mid-July.

The relatively slow growth of sockeye salmon scales during odd-numbered years at sea began in the period of overlap with pink salmon and continued for months after pink salmon left the high seas. This finding indicates that prey availability was reduced for months after most pink salmon left the high seas. Sugimoto and Tadokoro (1997) examined zooplankton biomass during June and July, 1950–81 and concluded that Asian pink salmon caused the observed alternating pattern of zooplankton biomass in the central North Pacific Ocean and the eastern Bering Sea. Shiomoto et al. (1997) examined macrozooplankton biomass in the central North Pacific Ocean during 1985–94 and also concluded that Asian pink salmon, especially those from the eastern Kamchatka Peninsula, reduced the biomass of macrozooplankton. Shiomoto et al. (1997) noted that lower zooplankton biomass was still apparent in the central North Pacific Ocean after many pink salmon had migrated into the Bering Sea. These findings support the hypothesis that predation by pink salmon altered zooplankton biomass from spring through at least July.

[6] Myers, K. 1996. Survey on overwintering salmonids in the North Pacific Ocean: Kaiyo Maru, 5 January–29 January 1996. Report FRI-UW-9607, 54 p. Univ. Washington, Seattle, WA.

Timing of peak zooplankton biomass occurs later in the year in northern regions, but zooplankton biomass typically declines during summer and fall (Batten et al., 2003). Declining zooplankton biomass in epipelagic waters is related, in part, to the ontogenetic migration to deep waters of some major zooplankton species, such as *Neocalanus* spp. (Mackas and Tsuda, 1999). Declining zooplankton biomass during summer likely enhanced the effect of competition exerted by pink salmon during odd-numbered years. July through at least September is a period of high potential salmon growth (Ishida et al., 1998); therefore sockeye salmon may be especially influenced by prey reduction during this period. During early spring, when scale growth of sockeye salmon was great and did not differ between odd- and even-numbered years, prey availability was apparently sufficient to minimize the effects of competition. Walker et al. (1998) reported that density-dependent growth of Asian pink salmon occurred after late June—a finding that is consistent with our study.

The transition from foraging on zooplankton to foraging on squid for both pink and sockeye salmon may also contribute to the alternating-year pattern of sockeye salmon growth. Aydin (2000) suggested that pink and sockeye salmon may begin to feed intensively on micronekton squid after reaching sufficient size during their second growing season. Pink salmon reportedly begin feeding on squid during spring, whereas sockeye salmon may not begin to feed on squid until summer because sockeye salmon are smaller. During odd-numbered years, pink salmon may have reduced the availability of squid to sockeye salmon and influenced the observed differences in scale growth after spring. In support of this hypothesis, sampling of sockeye and pink salmon during a recent 10-year period in the Bering Sea (June and July) indicated a 58% reduction among sockeye salmon and 32% reduction among pink salmon in the weight of squid consumed during odd- compared to even-numbered years (Davis, 2003). Few annual estimates of squid abundance are available, but Sobolevsky (1996) estimated that epipelagic squid biomass in the western Bering Sea was approximately five times greater in an even-year (1990) than in an odd-year (1989). Population dynamics and life history of squid are not well known (Nesis, 1997; Brodeur et al., 1999), but their apparent one- or two-year life history, in conjunction with predation by pink salmon, may lead to an alternating-year pattern of squid abundance that re-enforces the alternating-year pattern of sockeye salmon growth.

Ruggerone et al. (2003) reported that Bristol Bay sockeye salmon that inhabited the ocean in odd-numbered years of their second year at sea experienced lower smolt-to-adult survival compared with sockeye salmon that were present during even-numbered years. Lower survival was believed to be related to competition with Asian pink salmon. Our findings suggest that this mortality was likely related to reduced growth during late spring through fall, rather than during the first winter. We hypothesize that reduced sockeye salmon growth during the second year at sea led to lower energy reserves and to greater mortality during the second winter, but predation on smaller salmon may also be an important factor (Nagasawa, 1998). Bioenergetic modeling of salmon by Aydin (2000) indicated the greatest difference between the need for prey and prey availability is during winter. Nagasawa (2000) reported exceptionally low prey availability and corresponding low lipid content for salmon in the North Pacific Ocean during winter. Ishida et al. (1998) examined salmon on the high seas and determined that condition factor of all salmon species was lowest during late winter. Beamish and Mahnken (2001) provided evidence that relatively low growth of salmon during summer and fall can lead to significant growth-related mortality during the first winter at sea. Growth-related mortality appears to occur among Bristol Bay sockeye salmon in response to competition with pink salmon, but this competition-related mortality primarily occurs during the second winter at sea.

Bristol Bay sockeye salmon are broadly distributed across the North Pacific Ocean and Bering Sea. They occur in several oceanographic regions in which dominant prey may vary (e.g., the Bering Sea [euphausiids, squid, fish], subarctic current [squid], ridge domain [small zooplankton], the Alaska stream [small zooplankton, squid, fish], and the coastal domain [fish, euphausiids]) (Pearcy et al., 1988; Aydin, 2000). The alternating-year pattern of scale growth was persistent among adult Kvichak and Egegik sockeye salmon of all age groups returning to Bristol Bay even though many of these fish likely inhabited different ocean habitats. Thus, the observed scale growth pattern is either highly persistent in most of these ocean habitats or it is especially important in certain key regions inhabited by Bristol Bay sockeye salmon.

Salmon growth in relation to the regime shift of the mid-1970s

Several studies indicate that a significant change in the species assemblage of the North Pacific Ocean began near 1977 and concurrent with a dramatic shift in physical oceanic regimes (Francis et al., 1998; Anderson and Piatt, 1999). Pacific salmon abundance, including Bristol Bay sockeye salmon, more than doubled after this period (Rogers[1]). Zooplankton and squid biomass have appeared to increase substantially, especially in coastal regions, since the mid-1970s (Brodeur and Ware, 1992; Brodeur et al., 1996). Furthermore, Mackas et al. (1998) reported that the period of maximum zooplankton biomass shifted one or two months earlier after the mid-1970s. In comparison, seasonal scale growth of Kvichak and Egegik sockeye salmon during the first and second years at sea tended to be high after the regime shift. This pattern was also observed in annual scale measurements of sockeye salmon (Ruggerone et al., 2002). Spring scale growth of sockeye salmon after the regime shift was relatively high immediately after entry of sockeye salmon into Bristol Bay and during

their third year at sea, but spring growth was relatively low during the second year. Growth during the second year was relatively high during summer, a pattern that was different from SW1 and SW3 growth. Seasonal scale growth patterns of sockeye salmon indicate that the response of salmon to the 1977 ocean regime shift varied with age and season but that the greater growth during early marine life was associated with greater adult returns. The shift in seasonal growth patterns of sockeye salmon likely reflected their opportunistic forging behavior and the changes in prey species abundances caused by climate change (Kaeriyama et al, 2004).

Greater growth of sockeye salmon when they initially entered the Bering Sea after the 1977 ocean regime shift may reflect differences in seaward migration patterns. Prior to the 1977 regime shift, juvenile sockeye salmon were observed in a narrow band that extended from the shore along the Alaska Peninsula to as far as 50 km offshore (Straty, 1981; Hartt and Dell, 1986). However, recent survey results indicate that juvenile sockeye salmon are broadly distributed in the eastern Bering Sea from the Alaska Peninsula to north of 58°N and that the highest catch rates occur beyond 50 km offshore (Farley et al.[7]). Zooplankton are more abundant in offshore, deeper waters of Bristol Bay than within near shore waters (Straty, 1981; Napp et al., 2002), indicating that the recent northerly seaward migration patterns of juvenile sockeye salmon may place them in areas of higher prey densities and lead to higher early marine growth rates.

Sockeye salmon scale growth during the third year of growth (SW3) was relatively low after 1977, indicating that density-dependent growth was most apparent during this late life stage when mortality is likely relatively low (Ruggerone et al., 2002). Our study indicated the reduced SW3 growth after the 1977 regime shift occurred after peak spring growth, indicating that interspecific competition was most apparent during summer and fall. During the spring homeward migration (SWPL) period, scale growth was above average after 1977. Age-specific size of adult sockeye salmon returning to Bristol Bay was density dependent, but size at a given density was greater after 1977 (Rogers and Ruggerone, 1993; Ruggerone et al., 2003).

Salmon survival and scale growth

Biologists have suggested that rapid growth early in life can lead to greater growth in subsequent periods because larger animals have a greater variety of prey and prey size available to them (Pearcy et al., 1999). Aydin (2000) hypothesized that rapidly growing salmon in their first year at sea would more quickly reach a threshold size for feeding on abundant, energy-rich micronekton squid, leading to even greater growth in their second year. However, comparison of early marine scale growth (SW1 through SW2, circuli 8) with late season SW2 growth of individual Kvichak and Egegik sockeye salmon indicated a negative rather than positive relationship. Individual salmon having relatively great early marine scale growth tended to experience reduced scale growth during the later portion of their second year when sockeye salmon reach the size needed to readily consume larger prey such as squid. This finding reflects the growth of sockeye salmon survivors and not those that died at sea. Thus, we interpret this counterintuitive finding as an indication that slow growing sockeye salmon during late SW2 survived primarily when their early marine growth was relatively high. Salmon that experienced both low early marine growth and low SW2 growth apparently did not survive and were not represented in the scale collection. These observations do not necessarily reject the hypothesis that high early marine growth leads to high subsequent growth. In fact, other analyses of sockeye scales indicate spring growth is positively correlated with fall growth within a given year (G. Ruggerone, unpubl. data).

Effect of freshwater age on seasonal scale growth

Scale growth during the first year at sea was different among salmon spending one versus two winters in freshwater. Early SW1 scale growth of sockeye salmon spending two winters in freshwater (age-2.) was significantly greater than that of salmon spending only one winter in freshwater. This trend might reflect differences in migration timing or size (or both) of age-2 versus age-1 smolts. Age-2 smolts are approximately 17 mm longer than age-1 smolts and most age-2 smolts enter marine waters before age-1 smolts (Crawford and West[8]). After peak growth in spring, scale growth of age-1. smolts exceeded that of age-2. smolts. The different early marine growth patterns of age-1. and age-2. smolts did not appear to significantly affect the size of the fish at the end of the growing season. For example, during 1958–72, age-2.1 sockeye salmon sampled immediately south of the Aleutian Islands were 25 mm longer than age-1.1 sockeye salmon (French et al., 1976). The size difference between age-2. and age-1. smolts declined to 8 mm during the second growing season.

[7] Farley, E. V., Jr., R. E. Haight, C. M. Guthrie, and J. E. Pohl. 2000. Eastern Bering Sea (Bristol Bay) coastal research on juvenile salmon, August 2000. Doc. 499, 18 p. North Pacific Anadromous Fish Commission, 889 Pender Street, Vancouver, Canada.

Farley, E.V., Jr., C.M. Guthrie, S. Katakura, and M. Koval. 2001. Eastern Bering Sea (Bristol Bay) coastal research on juvenile salmon, August 2001. Doc. 560, 19 p. NPAFC, 889 Pender Street, Vancouver, Canada.

Farley, E.V., Jr., B.W. Wing, A. Middleton, J. Pohl, L. Hulbert, M. Trudel, J. Moss, T. Hamilton, E. Parks, C. Lagoudakis, and D. McCallum. 2002. Eastern Bering Sea (BASIS) Coastal Research (August–2002) on Juvenile Salmon. Doc. 678, 27 p. NPAFC, 889 Pender Street, Vancouver, Canada.

[8] Crawford, D. L., and F. W. West. 2001. Bristol Bay sockeye salmon smolt studies for 2000. Reg. Info. Rept. 2A01-12, 164 p. Alaska Dept. Fish Game, 333 Raspberry Road, Anchorage, AK.

Difference in growth by ocean age

Barber and Walker (1988) reported that peak SW2 scale growth for Bristol Bay sockeye salmon (Ugashik stock) was less than peak growth during SW1 and SW3. They suggested that this trend reflected lower prey availability for sockeye salmon in the North Pacific Ocean than in the Bering Sea (Mackas and Tsuda, 1999). But Bristol Bay sockeye salmon also develop in the Bering Sea during their second growing season (French et al., 1976; Myers et al.[3]). Kvichak and Egegik sockeye salmon scales, 1955–2000, exhibited relatively low growth throughout SW2 year compared to SW1 and SW3 years. We suggest that low SW2 growth may also be related to the inability of sockeye salmon to efficiently capture large prey (Aydin, 2000) and to a lower bioenergetic efficiency when consuming smaller prey. Salmon in their third year at sea may experience greater prey availability and capture efficiency because they are larger.

Late season growth of ocean age-2 sockeye salmon during SW2 was significantly greater than that of ocean age-3 sockeye salmon. This finding indicates that the greater size-at-age of ocean age-2 sockeye salmon compared to ocean age-3 sockeye salmon at the end of the second growing season (French et al., 1976) may be largely related to increased growth during the later portion of the second growing season at sea.

Conclusions

Seasonal scale growth patterns of Kvichak and Egegik sockeye salmon exhibited significant differences in SW2 and SW3 scale growth during odd- versus even-numbered years. Differences in scale growth did not begin until after peak scale growth and difference began somewhat later for younger SW2 sockeye salmon. The persistence of this pattern over the past 45 years may be caused by pink salmon, especially those from eastern Kamchatka that are highly abundant during odd-numbered years. During odd-numbered years, pink salmon reduced prey abundance prior to migrating to coastal areas in June and July (Shiomoto et al., 1997; Sugimoto and Tadokoro, 1997). This prey reduction, coupled with declining abundance and ontogenetic vertical migrations of some zooplankton (Mackas and Tsuda, 1999), appears to have influenced (reduced) growth of sockeye salmon from early summer through fall of odd-numbered years. We hypothesize that the alternating odd- and even-year growth pattern of sockeye salmon may be reenforced by the one- or two-year life cycle of prey, such as squid, whose abundance may be out-of-phase with the two-year cycle of pink salmon. These data, coupled with previous findings of reduced smolt-to-adult survival of sockeye salmon that interacted with odd-year pink salmon during the second year at sea (Ruggerone et al., 2003), indicate that reduced growth of salmon during the second year at sea can lead to measurable salmon mortality. Sockeye mortality associated with pink salmon likely occurs during winter when demand for prey by salmon exceeds the low availability of prey (Aydin, 2000), but it may also occur in response to size-selective predation. Our study indicates that salmon growth and survival are influenced by complex food web interactions, which are likely to significantly shift under various scenarios of climate change that affect temperature, CO_2, and phytoplankton community structure of the Bering Sea (Hare et al.[9]).

Acknowledgments

We appreciate the efforts of biologists and technicians of the Alaska Department of Fish and Game who collected salmon scales and associated data, and B. Agler and D. Oxman who helped compile the data. S. Goodman assisted with graphics. The manuscript benefited from comments provided by N. Davis, G. Duker, and two anonymous reviewers. This study was funded by the Global Change Program, Biological Resources Division, U.S. Geological Survey.

Literature cited

Anderson, P. J., and J. F. Piatt.
1999. Community reorganization in the Gulf of Alaska following ocean climate regime shift. Mar. Ecol. Progr. Ser. 189:117–123.

Aydin, K. Y.
2000. Trophic feedback and carrying capacity of Pacific salmon (*Oncorhynchus spp.*) on the high seas of the Gulf of Alaska. Ph.D. diss., 396 p. Univ. Washington, Seattle, WA.

Azumaya, T., and Y. Ishida.
2000. Density interactions between pink salmon (*Oncorhynchus gorbuscha*) and chum salmon (*O. keta*) and their possible effects on distribution and growth in the North Pacific Ocean and Bering Sea. North Pacific Anadr. Fish Comm. Bull. 2:165–174.

Barber, W. E., and R. J. Walker.
1988. Circuli spacing and annulus formation: is there more than meets the eye? The case for sockeye salmon, *Oncorhynchus nerka*. J. Fish Biol. 32:237–245.

Batten, S. D., D. W. Welch, and T. Jonas.
2003. Latitudinal differences in duration of development of *Neocalanus plumchrus* copepodites. Fish. Oceanogr. 12:201–208.

Beamish, R. J., and D. R. Bouillon.
1993. Pacific salmon production trends in relation to climate. Can. J. Fish Aquat. Sci. 50:1002–1016.

Beamish, R. J., and C. Mahnken.
2001. A critical size and period hypothesis to explain natural regulation of salmon abundance and linkage to climate and climate change. Progr. Oceanogr. 49: 423–437.

[9] Hare, C. E., G. R. DiTullio, P. D. Torell, R. M. Kudela, Y. Zhang, K. Leblanc, S. F. Riseman, and D. A. Hutchins. 2004. Experimental determination of climate change effects on Bering Sea biogeochemistry and phytoplankton community structure. Am. Soc. of Limnology and Oceanography and The Oceanography Society Ocean Research 2004 Conference; 15–20 February 2004, Honolulu, HI, 1 p.

Bigler, B. S., D. W. Welch, and J. H. Helle.
1996. A review of size trends among North Pacific salmon (*Oncorhynchus* spp.). Can. J. Fish. Aquat. Sci. 53: 445–465.

Bilton, H. T.
1975. Factors affecting the formation of scales. Int. North Pacific Fish. Comm. Bull. 32:102–108.

Bilton, H. T., and S. A. M. Ludwig.
1966. Times of annulus formation on scales of sockeye, pink, and chum salmon in the Gulf of Alaska. J. Fish. Res. Board Can. 23:1403–1410.

Birman, I. B.
1960. Times of formation of annuli on the scales of Pacific salmon, and the rate of growth of pink salmon. (Doklady Akad. Nauk SSSR 132:1187–1190). Transl. Fish Res. Board Can. No. 327.

Brodeur, R. D., B. W. Frost, S. R. Hare, R. C. Francis, and W. J. Ingraham Jr.
1996. Interannual variations in zooplankton biomass in the Gulf of Alaska, and covariation with California current zooplankton biomass. Calif. Coop. Oceanic Invest. Rep. 37:80–99.

Brodeur, R., S. McKinnell, K. Nagasawa, W. Pearcy, V. Radchencko, and S. Takagi.
1999. Epipelagic nekton of the North Pacific subarctic and transition zones. Progr. Oceanogr. 43:365–397.

Brodeur, R. D., and D. M. Ware.
1992. Long-term variability in zooplankton biomass in the subarctic Pacific Ocean. Fish. Oceanogr. 1:32–38.

Clutter, R. I., and L. E. Whitesel.
1956. Collection and interpretation of sockeye salmon scales. Bull. Int. Pac. Salmon Fish. Comm. 9, 159 p.

Coyle, K. O., V. G. Chavtur, and A. I. Pinchuk.
1996. Zooplankton of the Bering Sea: a review of Russian-language literature. *In* Ecology of the Bering Sea: a review of Russian literature (O. A. Mathisen, K. O. Coyle, eds.), p. 97–133. Alaska Sea Grant, Fairbanks, AK.

Davis, N. D.
2003. Feeding ecology of Pacific salmon (*Oncorhynchus* spp.) in the central North Pacific Ocean and central Bering Sea, 1991–2000. Ph.D. diss., 190 p. Hokkaido Univ., Hakodate, Japan.

Davis, N. D., K. Y. Aydin, and Y. Ishida.
2000. Diel catches and food habits of sockeye, pink, and chum salmon in the central Bering Sea in summer. North Pacific Anadr. Fish Comm. Bull. 2:99–109.

Davis, N., K. W. Myers, R. V. Walker, and C. K. Harris.
1990. The Fisheries Research Institute's high seas salmonid tagging program and methodology for scale pattern analysis. Am. Fish. Soc. Symp. 7:863–879.

Francis, R. C., S. R. Hare, A. B. Hollowed, and W. S. Wooster.
1998. Effects of interdecadal climate variability on the oceanic ecosystems of the NE Pacific. Fish. Oceanogr. 7:1–21.

French, R., H. Bilton, M. Osako, and A. Hartt.
1976. Distributions and origin of sockeye salmon (*Oncorhynchus nerka*) in offshore waters of the North Pacific Ocean. Int. North Pacific Fish. Comm. Bull. 34:1–113.

Fukuwaka, M.
1998. Scale and otolith patterns prove history of Pacific salmon. North Pacific Anadr. Fish Comm. Bull. 1: 190–198.

Fukuwaka, M., and M. Kaeriyama.
1997. Scale analyses to estimate somatic growth in sockeye salmon, *Oncorhynchus nerka*. Can. J. Fish Aquat. Sci. 54:631–636.

Groot, C., and L. Margolis.
1991. Pacific salmon life histories, 564 p. UBC Press, Vancouver, British Columbia, Canada.

Hartt, A. C., and M. B. Dell.
1986. Early oceanic migrations and growth of juvenile Pacific salmon and steelhead trout. Int. North Pacific Fish. Comm. Bull. 46:1–105.

Ishida, Y., S. Ito, Y. Ueno, and J. Sakai.
1998. Seasonal growth patterns of Pacific salmon (*Oncorhynchus* spp.) in offshore waters of the North Pacific Ocean. North Pacific Anadr. Fish Comm. Bull. 1:66–80.

Juanes, F.
1994. What determines prey size selectivity in piscivorous fishes? *In* Theory and application in fish feeding ecology (D. J. Stouder, K. L. Fresh, and R. J. Feller, eds.), p. 79–100. Univ. South Carolina Press, Columbia, SC.

Kaeriyama, M., M. Nakamura, R. Edpalina, J. R. Bower, M. Yamaguchi, R. V. Walker, and K. W. Myers.
2004. Change in the feeding ecology and trophic dynamics of Pacific salmon (*Oncorhynchus* spp.) in the central Gulf of Alaska in relation to climate events. Fish. Oceanogr. 13:197–207.

Koo, T. S. Y.
1962. Age and growth studies of red salmon scales by graphical means. *In* Studies of Alaska red salmon (T.S.Y. Koo, ed.), p. 49–121. Publ. Fish., New Series 1, University of Washington , Seattle.

Mackas, D. L., R. Goldblatt, and A. G. Lewis.
1998. Interdecadal variation in developmental timing of *Neocalanus plumchrus* populations at Ocean Station P in the subarctic North Pacific. Can. J. Fish. Aquat. Sci. 55:1878–1893.

Mackas, D. L., and A. Tsuda.
1999. Mesozooplankton in the eastern and western subarctic Pacific: community structure, seasonal life histories, and interannual variability. Progr. Oceanogr. 43:335–363.

Martinson, E. C., and J. H. Helle.
2000. Time of annulus formation of chum salmon in the North Pacific Ocean in 1998 and 1999. North Pacific Anadr. Fish Comm. Bull. 2:13–144.

Nagasawa, K.
1998. Predation by salmon sharks (*Lamna ditropis*) on Pacific salmon (*Oncorhynchus* spp.) in the North Pacific Ocean. North Pacific Anadr. Fish Comm. Bull. 1:419–433.
2000. Winter zooplankton biomass in the Subarctic North Pacific, with a discussion on overwintering survival strategy of Pacific salmon (*Oncorhynchus* spp.). North Pacific Anadr. Fish Comm. Bull. 2:21–32.

Napp, J. M., C. T. Baier, R. D. Brodeur, K. O. Coyle, N. Shiga, and K. Mier.
2002. Interannual and decadal variability in zooplankton communities of the southeastern Bering Sea shelf. Deep-Sea Res. Series II 49: 5991–6008.

Nesis, K. N.
1997. Gonatid squids in the subarctic North Pacific: ecology, biogeography, niche diversity and role in the ecosystem. Adv. Mar. Ecol. 32: 245–324.

Pearcy, W. G., K.Y. Aydin, and R. D. Brodeur.
1999. What is the carrying capacity of the North Pacific Ocean for salmonids. PICES Press 7:17–23.

Pearcy, W. G., R. D. Brodeur, J. Shenker, W. Smoker, and Y. Endo.
1988. Food habits of Pacific salmon and steelhead trout, midwater trawl catches, and oceanographic conditions in the Gulf of Alaska, 1980–1985. Bull. Ocean. Res. Inst. 26:29–78.

Peterman, R. M.
1984. Density-dependent growth in early ocean life of sockeye salmon (*Oncorhynchus nerka*). Can. J. Fish Aquat. Sci. 41:1825–1829.

Rogers, D. E.
1984. Trends in abundance of Northeastern Pacific stocks of salmon. *In* The influence of ocean conditions on the production of salmonids in the North Pacific (W. G. Pearcy, ed.), p. 100–127. Oregon State Univ., Corvallis, OR.
1987. The regulation of age at maturity in Wood River sockeye salmon *(Oncorhynchus nerka)*. Can. Spec. Publ. Fish. Aquat. Sci. 96:78–89.

Rogers, D. E., and G. T. Ruggerone.
1993. Factors affecting the marine growth of Bristol Bay sockeye salmon. Fish. Res. 18:89–103.

Ruggerone, G. T., J. Nielsen, E. Farley, S. Ignell, P. Hagen, B. Agler, D. Rogers, J. Bumgarner.
2002. Long-term trends in annual Bristol Bay sockeye salmon scale growth at sea in relation to sockeye abundance and environmental trends, 1955–2000. *In* Technical report 4: Joint meeting on causes of marine mortality of salmon in the North Pacific and North Atlantic oceans and in the Baltic Sea (IBSFC, NASCO, NPAFC, PICES, eds.), p. 56–58. NPAFC, Vancouver, B.C.

Ruggerone, G. T., M. Zimmermann, K. W. Myers, J. L. Nielsen, and D. E. Rogers.
2003. Competition between Asian pink salmon (*Oncorhynchus gorbuscha*) and Alaskan sockeye salmon (*O. nerka*) in the North Pacific Ocean. Fish. Oceanogr. 12:209–219.

Shiomoto, A., K. Tadokoro, K. Nagasawa, and Y. Ishida.
1997. Trophic relations in the subarctic North Pacific ecosystem: possible feeding effect from pink salmon. Mar. Ecol. Progr. Ser. 150:75–85.

Sinyakov, S. A.
1998. Stock conditions of Pacific salmon in Kamchatka and its fisheries management. Nat. Res. Inst. Far Seas Fish., Salmon Report Series 45:281–293.

Sobolevsky, Y. I.
1996. Species composition and distribution of squids in the western Bering Sea. *In* Ecology of the Bering Sea: a review of Russian literature (O. A. Mathisen and K. O. Coyle, eds.), p. 135–141. Alaska Sea Grant, Fairbanks, AK.

Straty, R. R.
1981. Trans-shelf movements of Pacific salmon. *In* The Eastern Bering Sea shelf: oceanography and resources (D. W. Hood and J. A. Calder, eds.), p. 575–610. NOAA, Dept. Commerce, Washington D.C.

Sugimoto, T., and K. Tadokoro.
1997. Interannual-interdecadal variations in zooplankton biomass, chlorophyll concentration and physical environment in the subarctic Pacific and Bering Sea. Fish. Oceanogr. 6:74–93.

Takagi, K., K. V. Aro, A. C. Hartt, and M. B. Dell.
1981. Distributions and origin of pink salmon (*Oncorhynchus gorbuscha*) in offshore waters of the North Pacific Ocean. Int. North Pacific Fish. Comm. Bull. 40:1–195.

Walker, R. V., K. W. Myers, and S. Ito.
1998. Growth studies from 1956–95 collections of pink and chum salmon scales in the central North Pacific Ocean. North Pacific Anadr. Fish Comm. Bull. 1:54–65.

Welch, D. W., and T. R. Parsons.
1993. ^{13}C-^{15}N values as indicators of trophic position and competitive overlap for Pacific salmon (*Oncorhynchus* spp.). Fish Oceanogr. 2:11–23.

Distribution, feeding condition, and growth of Japanese Spanish mackerel (*Scomberomorus niphonius*) larvae in the Seto Inland Sea

Jun Shoji

Masaru Tanaka

Laboratory of Estuarine Ecology
Field Science Education and Research Center
Kyoto University
Kita-shirakawa, Sakyo, Kyoto 606-8502, Japan
E-mail address (for J. Shoji): shog@kais.kyoto-u.ac.jp

Abstract—Distribution of eggs and larvae and feeding and growth of larvae of Japanese Spanish mackerel (*Scomberomorus niphonius*) were investigated in relation to their prey in the Sea of Hiuchi, the Seto Inland Sea, Japan, in 1995 and 1996. The abundance of *S. niphonius* eggs and larvae peaked in late May, corresponding with that of clupeid larvae, the major prey organisms of *S. niphonius* larvae. The eggs were abundant in the northwestern waters and the larvae were abundant in the southern waters in late May in both years, indicating a southward drift during egg and yolksac stages by residual flow in the central part of the Sea of Hiuchi. Abundance of clupeid larvae in southern waters, where *S. niphonius* larvae were abundant, may indicate a spawning strategy on the part of first-feeding *S. niphonius* larvae to encounter the spatial and temporal peak in ichthyoplankton prey abundance in the Seto Inland Sea. Abundance of the clupeid larvae was higher in 1995 than in 1996. Feeding incidence (percentage of stomachs with food; 85.3% in 1995 and 67.7% in 1996) and mean growth rate estimated from otolith daily increments (1.05 mm/d in 1995 and 0.85 mm/d in 1996) of *S. niphonius* larvae in late May were significantly higher in 1995. Young-of-the-year *S. niphonius* abundance and catch per unit of fishing effort of 1-year-old *S. niphonius* in the Sea of Hiuchi was higher in 1995, indicating a more successful recruitment in this year. Spatial and temporal correspondence with high ichthyoplankton prey concentration was considered one of the important determinants for the feeding success, growth, and survival of *S. niphonius* larvae.

Manuscript submitted 12 February 2004 to the Scientific Editor's Office.

Manuscript approved for publication 28 December 2004 by the Scientific Editor.

Fish. Bull. 103:371–379 (2005).

Scombrid fishes are considered to have adopted a survival strategy characterized by fast growth and the ability to consume large prey at an early age (Hunter, 1981). Their larvae have morphological features such as large eyes and mouths, with which piscivory and fast growth can be achieved in early life stages. Among scombrids, extremely early piscivory and fast growth have been observed in the early life stages of Spanish mackerels (*Scomberomorus* fishes). Fish larvae were dominant in stomachs of *Scomberomorus* larvae in three regions: 1) *S. semifasciatus*, *S. queenslandicus*, and *S. commerson*, in Australian waters (Jenkins et al., 1984), 2) Spanish mackerel (*S. maculatus*) and king mackerel (*S. cavalla*) in the southeastern United States (Finucane et al., 1990), and 3) Japanese Spanish mackerel (*S. niphonius*) in the Seto Inland Sea, Japan (Shoji et al., 1997). Larval growth rate was reported to be approximately 1.0 mm/d in king and Spanish mackerels (DeVries et al., 1990; Peters and Schmidt, 1997) and *S. niphonius* (Shoji et al., 2001). Tanaka et al. (1996) demonstrated precocious development of an adult-type digestive system (with a functional stomach and pyloric caecum) occurred in first feeding *S. niphonius* larvae. They suggested that *Scomberomorus* fish have adopted a specialized feeding strategy, namely piscivory and fast growth from the time of first feeding, which reduces the duration of the larval stage, the period of greatest vulnerability to predation (Houde, 1987).

Ichthyoplankton prey seem to be indispensable for growth and survival during larval period of *Scomberomorus* fish. Under laboratory conditions, Fukunaga et al. (1982) reported that *S. niphonius* larvae preferred fish larvae to invertebrate plankton prey (rotifer and *Artemia* nauplii). Shoji and Tanaka (2001) demonstrated that *S. niphonius* larvae began to cannibalize siblings when they were supplied with only invertebrate plankton prey. *Scomberomorus* larvae would need to exert greater searching effort and to swim fast to capture ichthyoplankton prey because they are larger and much less abundant in water than invertebrate plankton prey (Sheldon et al., 1972). *Scomberomorus* larvae with a high swimming performance have been shown to have high levels of larval mortality due to starvation. Margulies (1993) demonstrated by histological analysis that Pacific sierra (*S. sierra*) larvae could not survive beyond 48 hours without feeding in the Panama Bight. Shoji et al. (2002) observed that the point-of-no-return for *S. niphonius* larvae was one day after first feeding in laboratory experiments. *Scomberomorus niphonius* larvae fed after 1- or 2-days starvation showed significantly retarded growth during the following period

of adequate feeding compared to fish that had been fed from the time of first feeding. These observations suggest that ichthyoplankton prey availability can strongly influence growth and survival of *S. niphonius* larvae.

Scomberomorus niphonius is distributed in the coastal waters of Japan and supports important commercial fisheries in the Seto Inland Sea. The total catch exceeded 6000 metric tons (t) in the middle 1980s but decreased to less than 1000 t in the late 1990s in the Seto Inland Sea. Spawning migration of *S. niphonius* into the Seto Inland Sea occurs in May (Kishida and Aida, 1989) and the larvae are distributed in May and June in the Sea of Hiuchi, the central Seto Inland Sea (Kishida, 1988). In order to ensure that catches remain at stable levels and to establish more efficient fisheries management, it is necessary to accumulate biological information to elucidate the recruitment process of the species.

The objective of the present study is 1) to investigate spatial and temporal distribution of *S. niphonius* larvae and their prey and 2) to compare feeding conditions and growth of *S. niphonius* larvae for two consecutive years with contrasting levels of recruitment, 1995 and 1996, in the Seto Inland Sea, Japan. The catch-per-unit-of-fishing-effort (CPUE: no. of fish/boat/day) of 1-year-old *S. niphonius* (Fig. 1) fished by drift gill net in May, the major fishing season for the species, at the Kawarazu Fisherman's Association (Fig. 2) has been used as a recruitment index in the Sea of Hiuchi (Kishida, 1991). The CPUE fluctuated tenfold in the 1990s (Ehime Prefecture Chuyo Fisheries Experimental Station Toyo Branch[1]) and indicated recruitment in 1995 was more successful. Egg, larval, and larval prey distributions, larval feeding incidence and growth, and young-of-the-year (YOY) fish abundance were investigated in 1995 and 1996 in the Sea of Hiuchi.

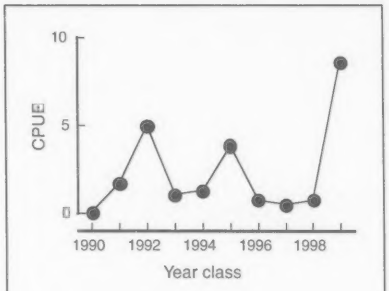

Figure 1

Catch per unit of fishing effort (CPUE: no. of fish/boat/day) of 1-year-old *Scomberomorus niphonius* in the 1990–99 year classes at the Kawarazu Fisherman's Association in the central Seto Inland Sea. Data were obtained from drift gill-net catches in May, the major fishing season for *S. niphonius*.

Materials and methods

Ichthyoplankton sampling

Three research cruises were carried out in 1995 (11–16 April, 24–28 May, and 20–23 June) and in 1996 (10–13 May, 27–30 May, and 18–21 June) in the Sea of Hiuchi (Fig. 2). Ichthyoplankton sampling and hydrographic survey were conducted from the RV *Shirafuji* (138 t) of the National Research Institute of Fisheries and Environment of Inland Sea (NRIFEIS). Double oblique tows from the surface to 5 m above the bottom were made by using a bongo net (0.7-m diameter, 0.315-mm mesh) at 80 stations during the cruises in 1995 and at 50 stations in 1996. Average depth of the Sea of Hiuchi is approximately 17.8 m (Montani, 1996). *Scomberomorus niphonius* larvae were quickly sorted from the samples and were preserved in 95% ethanol. Other ichthyoplankton were fixed in 10% formalin seawater for sorting in the laboratory. Flow meters were mounted in the mouth of the net to determine the filtered volume. Each tow followed a salinity-temperature-depth sensor cast to measure the water temperature and salinity profiles at each station.

YOY fish abundance

YOY *S. niphonius* have been reported to occur in the southern part of the Sea of Hiuchi from late June to early July (Watanabe, 1994). To detect a potential difference in *S. niphonius* recruitment abundance between 1995 and 1996, YOY fish abundance was assessed in the southern part of the Sea of Hiuchi. YOY *S. niphonius* were collected from catches by a seine fishery in the southern part of the Sea of Hiuchi (Fig. 2). The seine fishery primarily targets young and adult Japanese anchovy (*Engraulis japonicus*). The codend of the net has a 2-mm mesh aperture and was towed by two boats for about 1 hour at a ship velocity of 3 to 4 knots. Two to 10 kg of the catch by the seine fishery was sampled weekly (five times each year) from mid June to late July in 1995 and 1996. YOY abundance was expressed as the number of *S. niphonius* per 10 kg of the catch.

Laboratory procedures

Larval SL was measured to the nearest 0.1 mm, and stomach contents were identified under a dissecting microscope. After removal of *S. niphonius* larvae, the bongo-net samples were processed to estimate concentrations (no./100 m^2) of *S. niphonius* eggs. Larvae of two

[1] Ehime Prefecture Chuyo Fisheries Experimental Station Toyo Branch. 2000. Unpubl. data. Kawarazu, Toyo, Ehime 799-1303, Japan.

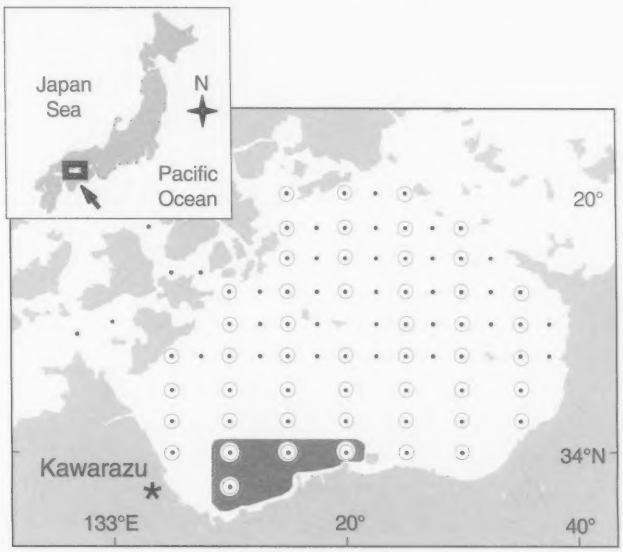

Figure 2

Map of the Sea of Hiuchi, central Seto Inland Sea, showing the sampling stations where ichthyoplankton were collected with a bongo net during the three cruises in 1995 (closed small circles) and in 1996 (large open circles). Catch data for 1-year-old *S. niphonius* were obtained at Kawarazu Fisherman's Association (asterisk). Young-of-the-year Japanese Spanish mackerel were collected by the seine fishery in the southern waters indicated by the shaded area.

clupeid species, gizzard shad (*Konosirus punctatus*) and Japanese sardine (*Sardinops melanostictus*), that were the major prey organisms of the post-first-feeding *S. niphonius* larvae (see "Results" section) were counted to estimate prey concentrations.

Scomberomorus niphonius larvae were aged by counting daily increments on otoliths. Right-side sagittal otoliths were removed under a dissecting microscope and the number of increments on the otolith were counted using an image-analysis system (ARP, version 4.21, Ratoc System Engineering Co., Ltd., Tokyo, Japan) connected to a compound light microscope at 400 to 1000× magnification. Daily increments begin to be deposited on the sagittal otoliths of *S. niphonius* larvae at first feeding (Shoji and Tanaka, 2004). *Scomberomorus niphonius* larvae initiate feeding on day 5 under 19.0°C (Shoji et al., 2001). Larval age was therefore estimated by adding five to the increment count because the water temperature in the southern part of the Sea of Hiuchi where *S. niphonius* larvae were abundant ranged between 18° and 20°C (see "Results" section) in late May. Data from cruises in late May only (the second cruise in both years) were included in the feeding and growth analyses because no *S. niphonius* larvae were collected during the first cruise and too few were collected during the third cruise in both years.

Results

Physical environment

The surface water temperature was higher in the southeastern area and lower in the northwestern area in all cruises. Mean surface temperatures (±SD) were 12.3° (±0.4), 18.6° (±1.2), and 20.5° (±0.6)°C in 11–16 April, 24–28 May, and 20–23 June, 1995, and were 14.3° (±0.6), 19.0° (±1.3), and 19.4° (±1.0)°C in 10–13 May, 27–30 May, and 18–21 June 1996, respectively (Fig. 3). Salinity ranged between 32.5 and 34.3 ppt and was lower in the southeastern area in all cruises. In late May, during the seasonal peak in abundance of *S. niphonius* larvae, the mean surface temperature was slightly higher in 1996 although there was no significant difference between the two years (ANOVA: $F=3.14$, $P=0.08$).

Scomberomorus niphonius eggs and larvae

A total of 1018 eggs and 272 larvae of *S. niphonius* were collected during the cruises. No eggs and larvae of *S. niphonius* were collected during the first cruise in both years. The egg and larval abundance peaked in late May and decreased thereafter in both years (Fig. 4, A and B). The eggs were abundant in the northwestern waters in

late May where the surface temperature was between 17° and 19°C (Fig. 5). The larvae were abundant in the middle to southern waters, where the surface temperature was between 18° and 20°C in late May (Fig. 6). There was no significant difference in egg and larval abundance in late May between the two years (ANOVA: F=0.03, P=0.87 for eggs; F=0.02, P=0.89 for larvae).

Clupeid larvae

Of the 107,252 larvae collected throughout the cruises, clupeid larvae were most dominant, accounting for 57.2% in number. Gizzard shad and Japanese sardine larvae accounted for 76.4% and 23.6% of clupeid larvae, respectively. A seasonal change in abundance of clupeid larvae and a peak in abundance in late May in both years were evident (Fig. 4C). Maximum abundance (no./m^2) was more than 400 in late May in 1995 in the southern waters and there was no station where the abundance exceeded 300/m^2 in 1996 (Fig. 7). The difference in abundance of clupeid larvae in late May between the two years was significant (ANOVA: F=8.12, P=0.005).

Feeding

Clupeid larvae (gizzard shad, Japanese sardine, and unidentified clupeid larvae) were the most dominant items in the stomachs of *S. niphonius* larvae (Table 1). Feeding incidence (percentage of stomachs with food) was significantly higher in 1995 than in 1996 (chi square test; df=1, chi-square=8.538, P=0.0035).

Growth

Age of *S. niphonius* larvae collected in late May in 1995 and 1996 was estimated to be between 5 and 14 days

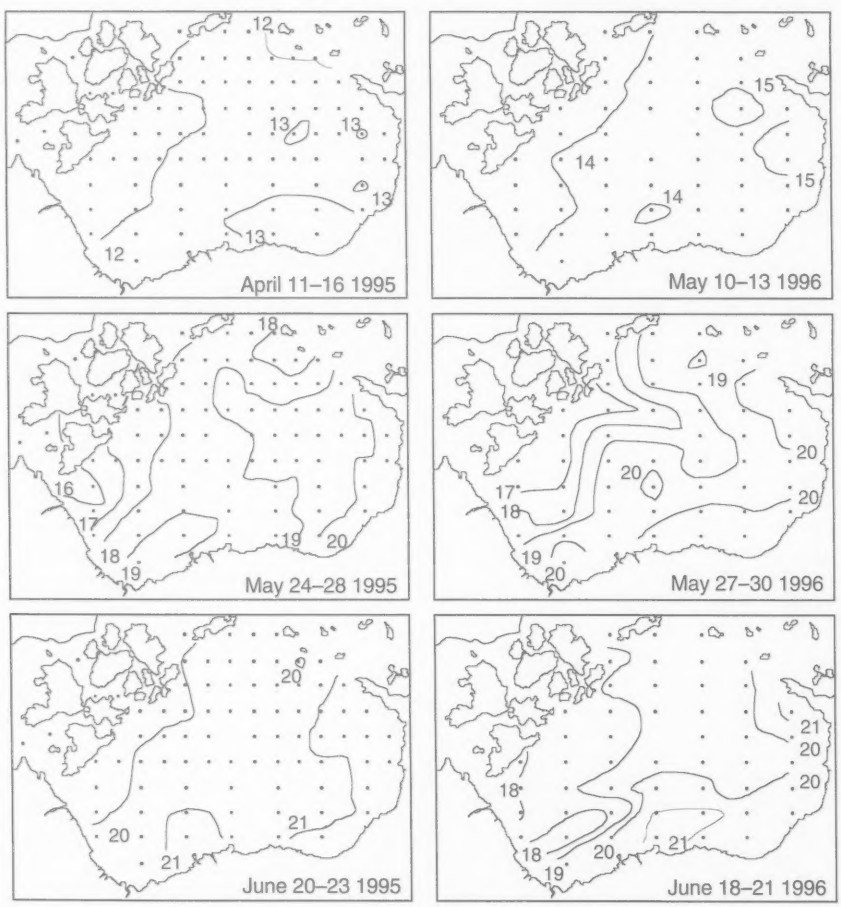

Figure 3

Contour plots of the surface water temperature (°C) of the Sea of Hiuchi during the three cruises in 1995 and 1996.

after hatching. Relationships between larval age (A) and SL (L, mm) were best described by a linear regression for each year (Fig. 8):

1995: $L = 1.05A - 1.39$ (n=102, r^2=0.87, P<0.0001)
1996: $L = 0.85A - 0.15$ (n=93, r^2=0.80, P<0.0001).

The slope of the equation for 1995 was significantly higher than that for 1996 (ANCOVA; df=1, F=11.01, P=0.001).

YOY *S. niphonius* abundance

YOY *S. niphonius* (14.6–122.8 mm in TL) were collected by the seine fishery in the Sea of Hiuchi from late June through late July in 1995 and 1996. Mean (±SE) abundance of YOY *S. niphonius* in 1995 (7.7 [±2.1] individuals/m^2) was significantly higher than that in 1996 (0.6 [±0.4] individuals/m^2; Mann-Whitney U-test; P=0.006, Fig. 9).

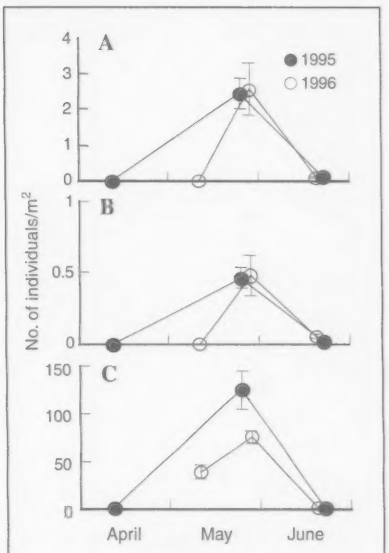

Figure 4

Seasonal change in abundance (no./m^2) of *S. niphonius* eggs (**A**), larvae (**B**) and clupeid prey larvae (**C**) in the Sea of Hiuchi in 1995 and 1996. Bars indicate standard error.

Discussion

Spawning strategy

Abundance of *S. niphonius* eggs and larvae peaked in late May in 1995 and 1996. A similar pattern was observed in the abundance of clupeid larvae, indicating that spawning of *S. niphonius* was synchronized with

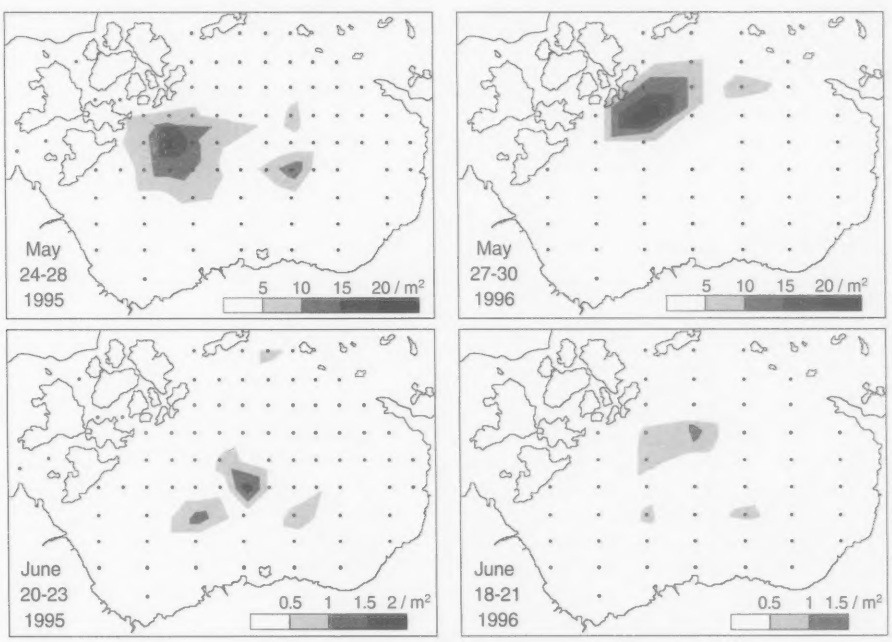

Figure 5

Horizontal distribution of *S. niphonius* eggs in the Sea of Hiuchi in 1995 and 1996.

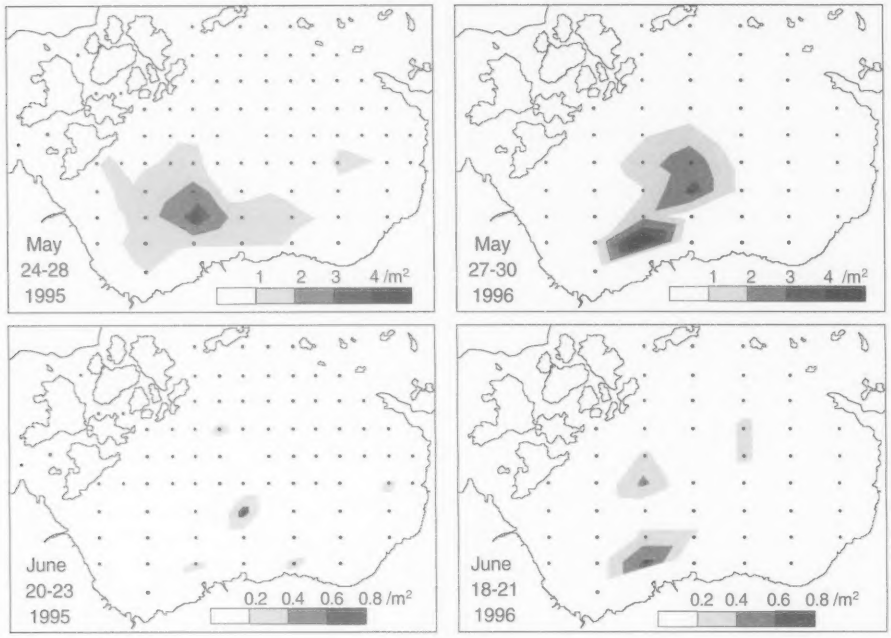

Figure 6

Horizontal distribution of *S. niphonius* larvae in the Sea of Hiuchi in 1995 and 1996.

that of clupeid fishes in the central Seto Inland Sea. Piscivorous fishes tend to spawn earlier than other fishes in freshwater ecosystems so that they attain sufficient size to enable consumption of other young fishes by the onset of piscivory (Keast, 1985). Because *S. niphonius* larvae are piscivorous from the first feeding stage, spawning that is synchronized with the seasonal peak in abundance of clupeid larvae would be advantageous for survival of *S. niphonius* larvae.

Larvae of *S. niphonius* were abundant in the southern part of the Sea of Hiuchi in late May 1995 and 1996 while eggs were abundant in the northwestern waters during the same season. This difference in horizontal distribution patterns of eggs and larvae seems to be associated with the drift by a residual flow (current) from northern to southern waters. In the central part of the Sea of Hiuchi, a residual flow in the middle (5–15 m) layers proceeds southward at a speed of about 5 cm/s (=4.32 km/d; Yanagi et al., 1995). Yolksac larvae of *S. niphonius* are abundant in the 5- to 10-m layers in the Sea of Hiuchi (Kishida, 1988) and do not exhibit diel vertical migration (Shoji et al., 1999). The horizontal distance between the stations with the highest egg and larval abundance in late May was approximately 15 km in 1995 and 20 km in 1996. Given that the yolksac stage is five days for mackerel larvae under 19°C (Shoji et al., 2001), drift distance while larvae are entrained in the southward residual flow during the yolksac stage would be estimated to be approximately 20 km. The estimate for the drift distance during the yolksac stage approximates the horizontal distance between the stations of egg and larval highest abundance. It is therefore plausible that the larvae were transported by the southward residual flow to the southern part of the Sea

Table 1

Feeding incidence (percentage of stomachs with prey) and stomach contents of *S. niphonius* larvae collected in late May of 1995 and 1996 in the Sea of Hiuchi.

	1995	1996
No. of larvae examined	102	93
No. of larvae feeding	87	63
Feeding incidence (%)	85.3	67.7
Size range (SL, mm)	4.2–13.8	4.5–14.2
Stomach contents	*n*	*n*
Sardinops melanostictus	4	2
Konosirus punctatus	21	14
Unidentified clupeids	19	11
Engraulis japonicus	2	4
Unidentified Clupeiformes	34	22
Mugiliidae	3	2
Gobiidae	13	9
Total	96	64

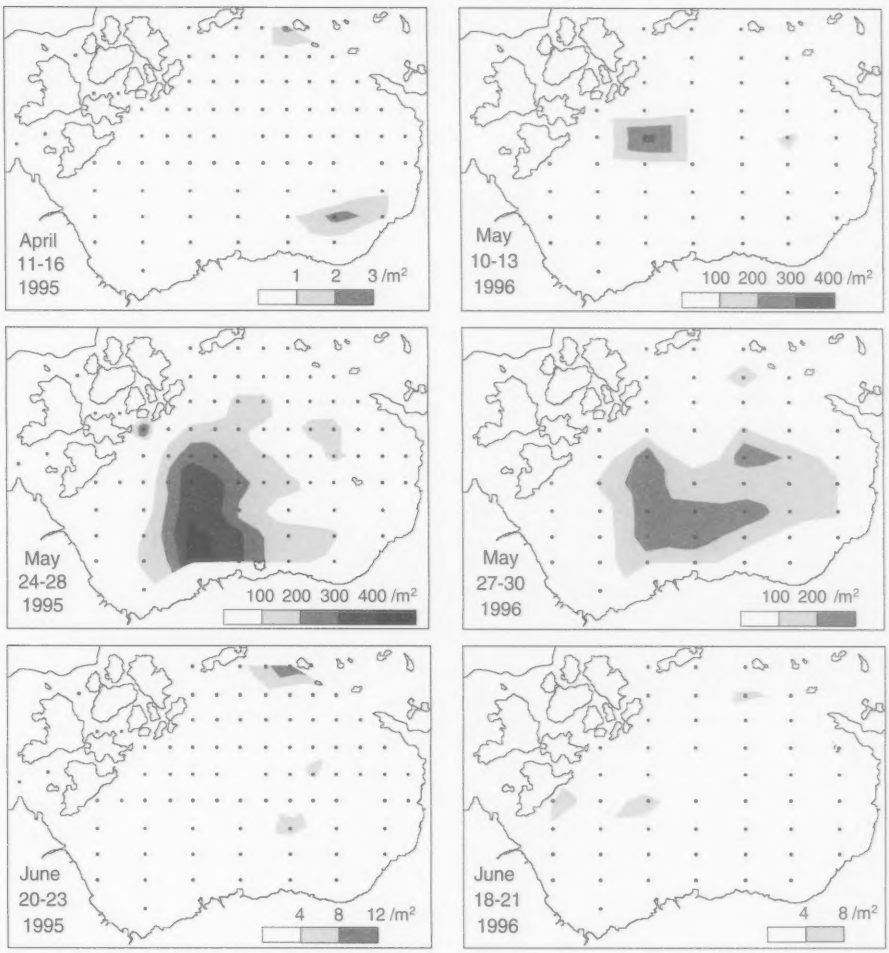

Figure 7

Horizontal distribution of clupeid larvae in the Sea of Hiuchi during the three cruises in 1995 and in 1996.

of Hiuchi where clupeid larva concentration was high in late May. We suggest that spawning of *S. niphonius* in the northern part of the Sea of Hiuchi would enable their first-feeding larvae to meet high prey abundance in the southern part.

Significance of high ichthyoplankton prey

Water temperature and prey concentration would be possible factors that can influence growth rates of *S. niphonius* larvae. In aquaria, the mean absolute growth rate of *S. niphonius* larvae fluctuated between 0.87 and 1.28 mm/d depending on temperature between 18.2° and 22.6°C (Fukunaga et al., 1982; Shoji et al., 2001). In the present study, the mean surface temperature of the Sea of Hiuchi in late May was slightly higher in 1996, although the difference was not significant.

The higher abundance of clupeid larvae in 1995 would better explain the higher larval growth rate in 1995. The mean larval growth rate in late May 1995, 1.05 mm/d, approximates those reported in aquaria at the same temperature (1.03 mm/d at 20.8°C; Fukunaga et al., 1982) where *S. niphonius* larvae were provided with an excess of prey, indicating that the prey concentration in late May 1995 met larval requirements. It is likely that the lower growth rate in late May 1996 resulted from lower prey concentration. This conclusion is supported by results of the stomach content analysis: the larval feeding incidence was significantly lower in May 1996. We conclude that clupeid larvae concentration had a significant effect on growth of the *S. niphonius* larvae.

In the Sea of Hiuchi, clupeid larvae abundance greatly increased from April to May. We suggest that the prey

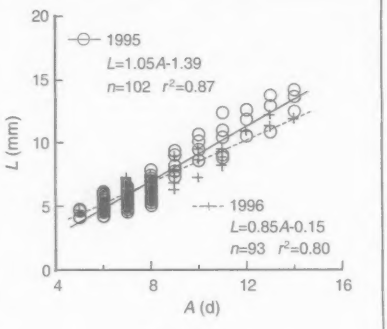

Figure 8

Relationships between standard length (L, mm) and otolith-estimated age (A, d) of *S. niphonius* larvae collected during the cruises in late May of 1995 and 1996 in the Sea of Hiuchi.

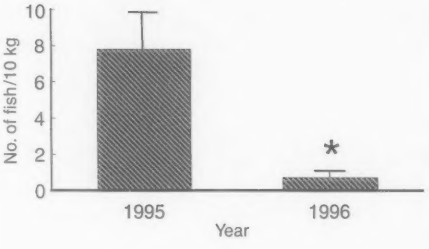

Figure 9

Mean (SE) young-of-the-year *S. niphonius* abundance collected by the seine fishery in 1995 and 1996 in the Sea of Hiuchi. Asterisk indicates a significant difference between the years (Mann-Whitney U-test, $P<0.01$).

availability for *S. niphonius* larvae fluctuated depending for the most part on seasonal change in abundance of gizzard shad larvae that were dominant in the Sea of Hiuchi. The difference in clupeid larval abundance in late May between 1995 and 1996 may be explained by between-year difference in gizzard shad spawning stock biomass. The total catch of gizzard shad in the southern Sea of Hiuchi (coastal waters of Ehime Prefecture) in 1995 (372 t) was higher than that in 1996 (217 t: Ehime Prefecture Agriculture, Forestry and Fisheries Statistics Association, 1998).

Implications for recruitment

Variability in larval growth rate can influence survival during the larval period by affecting the length of the early life stages because total mortality is positively correlated with the length of these early life stages (Houde, 1987). Campana (1996) demonstrated a significant correlation between growth to the end of the pelagic juvenile stage (90 d) and the year-class strength of Atlantic cod on the Georges Bank and suggested that the adult cohort strength could be predicted from growth during early life stages. In the present study, egg and larval *S. niphopius* abundance during their peak-occurrence period did not differ between 1995 and 1996, whereas YOY and 1-year-old *S. niphonius* were more abundant in 1995. These results indicate more successful recruitment and higher larval growth rate in 1995 although there are no data available for years other than 1995 and 1996. Larvae of *S. niphonius* initiate feeding at 5.59 mm SL at 18.5°C (Shoji et al., 2002). Given the mean larval growth rate in 1995 (1.05 mm/d) and 1996 (0.88 mm/d), the critical period (from first feeding to the onset of schooling at the early juvenile stage, 19.6 mm SL; Masuda et al., 2003) is estimated as 13.3 days in 1995 and 16.5 days in 1996. For *S. niphonius*, even a slight increase in larval stage duration due to retarded growth can greatly reduce larval survival because the larval daily mortality coefficient is expected to be extremely high (>0.6: Grimes and Kingsford, 1996). The lower recruitment of *S. niphonius* in 1996 may be partly explained by the prolonged larval period (3.2 d) which could have led to lower survival (1/6.82, assuming the daily mortality coefficient is 0.6) during the larval period of that year.

Acknowledgments

We thank M. Fukuda, N. Suzuki, N. Kohno, and the crew of RV *Shirafuji* of NRIFEIS and staff of Asagi-Suisan Co. Ltd. for their assistance with field sampling. We also thank T. Maehara and N. Murata, Ehime Prefecture Chuyo Fisheries Experimental Station Toyo Branch, and Y. Maki, Kawarazu Fisherman's Association, for their help in collecting young-of-the-year Japanese Spanish mackerel and data on the catch of 1-year-old fish. Two anonymous reviewers and M. Takahashi, National Research Institute of Fisheries Science, provided valuable comments on the manuscript.

Literature cited

Campana, S. E.
1996. Year-class strength and growth rate in young Atlantic cod *Gadus morhua*. Mar. Ecol. Prog. Ser. 135: 21–26.

DeVries, D., C. Grimes, K. Lang, and B. White.
1990. Age and growth of king and Spanish mackerel larvae and juveniles from the Gulf of Mexico and U.S. South Atlantic Bight. Environ. Biol. Fish. 29:135–143.

Ehime Prefecture Agriculture and Forestry Statistics Association.
1998. Agriculture, forestry and fisheries statistics of Ehime Prefecture, fiscal 1996, 278 p. Ehime Prefec-

ture Agriculture and Forestry Statistics Association, Matsuyama, Japan.

Finucane, J. H., C. B. Grimes,, S. P. Naughton.
1990. Diets of young king and Spanish mackerel off the southeast United States. Northeast Gulf Sci. 11: 145–153.

Fukunaga, T., N. Ishibashi, and N. Mitsuhashi.
1982. Artificial fertilization and seedling propagation of Spanish mackerel. Saibai-giken 11:29–48.

Grimes, C. B., and M. J. Kingsford.
1996. How do riverine plumes of different sizes influence fish larvae: do they enhance recruitment? Mar. Freshw. Res. 47:191–208.

Houde, E. D.
1987. Fish early life dynamics and recruitment variability. Am. Fish. Soc. Symp. 2:17–29.

Hunter, J. R.
1981. Feeding ecology and predation of marine fish larvae. *In* Marine fish larvae (R. Lasker, ed.), p. 33–77. Univ. Washington Press, Seattle, WA.

Jenkins, G. P., N. E. Milward, and R. F. Harwick.
1984. Food of larvae of Spanish mackerels, genus *Scomberomorus* (Telostei: Scombridae), in shelf waters of the Great Barrier Reef. Aust. J. Mar. Freshw. Res. 35, 477–482.

Keast, A.
1985. The piscivore guild of fishes in small freshwater ecosystems. Environ. Biol. Fish. 12:119–129.

Kishida, T.
1988. Vertical and horizontal distribution of eggs and larvae of Japanese Spanish mackerel in the central waters of the Seto Inland Sea. Bull. Jap. Soc. Sci. Fish. 54:1–8.
1991. Fluctuations in year-class strength of Japanese Spanish mackerel in the central Seto Inland Sea. Bull. Jap. Soc. Sci. Fish. 57:1103–1109.

Kishida, T., and K. Aida.
1989. Maturation and spawning of Japanese Spanish mackerel in the central and western waters of the Seto Inland Sea. Bull. Jap. Soc. Sci. Fish. 55:2065–2074.

Margulies, D.
1993. Assessment of the nutritional condition of larval and early juvenile tuna and Spanish mackerel (Pisces: Scombridae) in the Panama Bight. Mar. Biol. 115:317–330.

Masuda, R., J. Shoji, S. Nakayama, and M. Tanaka.
2003. Development of schooling behavior in Spanish mackerel *Scomberomorus niphonius* during early ontogeny. Fisheries Sci. 69:772–776.

Montani, S.
1996. Relationships between environment and fisheries in the Seto Inland Sea. *In* Resource and environment of the Seto Inland Sea (T. Okaichi, S. Komori, and H. Konishi, eds.), p. 1–37. Koseisha Koseikaku, Tokyo, Japan.

Peters, J. S., and D. J. Schmidt.
1997. Daily age and growth of larval and early juvenile Spanish mackerel, *Scomberomorus maculatus*, from the South Atlantic Bight. Fish. Bull. 95:530–539.

Sheldon, R. W., A. Prakash, and W. H. Sutcliffe Jr.
1972. The size distribution of particles in the ocean. Limnol. Oceanogr. 17:327–340.

Shoji, J., M. Aoyama, H. Fujimoto, A. Iwamoto, and M. Tanaka.
2002. Susceptibility to starvation by piscivorous Japanese Spanish mackerel *Scomberomorus niphonius* (Scombridae) larvae at first feeding. Fisheries Sci. 68:59–64.

Shoji, J., T. Maehara, M. Aoyama, H. Fujimoto, A. Iwamoto, and M. Tanaka.
2001. Daily ration of Japanese Spanish mackerel *Scomberomorus niphonius* larvae. Fish. Sci. 67: 238–245.

Shoji, J., T. Maehara, and M. Tanaka.
1999. Diel vertical movement and feeding rhythm of Japanese Spanish mackerel larvae in the central Seto Inland Sea. Fish. Sci. 65:726–730.

Shoji, J., and M. Tanaka.
2001. Strong piscivory of Japanese Spanish mackerel larvae from their first feeding. J. Fish Biol. 59: 1682–1685.
2004. Effect of prey concentration on growth of piscivorous Japanese Spanish mackerel *Scomberomorus niphonius* larvae in the Seto Inland Sea, Japan. J. Appl. Ichthyol. 20:271–275.

Tanaka, M., T. Kaji, Y. Nakamura, and Y. Takahashi.
1996. Developmental strategy of scombrid larvae: High growth potential related to food habits and precocious digestive system development. *In* Survival strategies in early life stages of marine resources (Y. Watanabe, Y. Yamashita, and Y. Oozeki, eds.), p. 125–139. A. A. Balkema, Rotterdam.

Watanabe, A.
1994. Fish caught by seine fisheries in the Sea of Hiuchi. Proceed. the Sea of Hiuchi Res. Meet. 2:4–9. Ehime Prefecture Chuyo Fisheries Experimental Station, Matsuyama, Ehime, Japan.

Yanagi, T., H. Tsukamoto, S. Igawa, and K. Shiota.
1995. Recruitment strategy of swimming crab, *Portunus trituberculatus*, in Hiuchi-nada, Japan. Fish. Oceanogr. 4:217–229.

Maximum likelihood estimation of mortality and growth with individual variability from multiple length-frequency data

You-Gan Wang
CSIRO Mathematical and Information Sciences
65 Brockway Road
Floreat Park
Western Australia 6014, Australia
E-mail address: You-Gan.Wang@csiro.au

Nick Ellis
CSIRO Marine Research
P.O. Box 120
Cleveland, Queensland 4163, Australia

Abstract—We consider estimation of mortality rates and growth parameters from length-frequency data of a fish stock and derive the underlying length distribution of the population and the catch when there is individual variability in the von Bertalanffy growth parameter L_∞. The model is flexible enough to accommodate 1) any recruitment pattern as a function of both time and length, 2) length-specific selectivity, and 3) varying fishing effort over time. The maximum likelihood method gives consistent estimates, provided the underlying distribution for individual variation in growth is correctly specified. Simulation results indicate that our method is reasonably robust to violations in the assumptions. The method is applied to tiger prawn data (*Penaeus semisulcatus*) to obtain estimates of natural and fishing mortality.

Estimation of growth and mortality is fundamental in fisheries because stock assessment and management rely on these population parameters. Length-frequency–based methods become important when aging techniques are either not possible or very expensive. Existing methods such as that of Beverton and Holt (1956) assume that recruitment is continuous and constant throughout the year, which leads to a population with an exponentially distributed age structure. Existing modifications to Beverton and Holt's method comprise some simple recruitment patterns or distributions (Ssentongo and Larkin 1973; Ebert 1980; Hoenig 1987; Wetherall et al. 1987). As pointed out by Vetter (1988), the existing methods for estimating mortality in the literature have strong limitations and disadvantages. In particular, they require the following assumptions:

1) each individual follows the same von Bertalanffy growth curve;
2) the recruitment is either continuous and constant throughout the year (as in Beverton and Holt [1956] and Wetherall et al. [1987]) or is a pulse function (as in Hoenig [1987]);
3) the total instantaneous mortality rate, z, is constant.

As pointed out by Sainsbury (1980), it is more realistic to allow individual variability in growth. For example, using tag-recapture data, Wang et al. (1995) found substantial individual variability for the tiger prawn species *P. semisulcatus*.

Estimation of mortality relies on the distribution of the lengths, which is determined by the age distribution, mortality rates, and the individual variability in growth rates. If individual variability in growth is ignored, an inappropriate length distribution will be generated, leading to biases in parameter estimates. It is also biologically interesting to quantify the individual variability in growth, which has important implications in fisheries management. Although it is well understood that variability leads to increased uncertainty in estimates, it is less well recognized (among the fisheries community) that variability can also lead to bias. Wang and Ellis (1998) analyzed the effect of ignoring individual variability in a simplified context of constant recruitment and a single length-frequency record. They found that, in the presence of individual variability, existing methods gave positively biased parameter estimates. More details about the background can be found in Ebert (1973), Askland (1994), and Wang and Ellis

Manuscript submitted 5 March 2004 to the Scientific Editor's Office.
Manuscript approved for publication 9 November 2004 by the Scientific Editor.
Fish. Bull. 103:380–391 (2005).

(1998). See DeLong et al. (2001) for alternative approaches to length-frequency data where individual variability is taken into account.

In our study, we develop a new framework for analyzing length-frequency data. In particular, we incorporate 1) individual variability in growth parameters; and 2) an arbitrary recruitment function. The model is flexible enough to incorporate various sizes at recruitment and a fishing selectivity function. However, we did not use these aspects in the analysis of tiger prawn data. Some analytical expressions are derived for these generalizations. A maximum likelihood approach is developed for estimation of mortality and growth parameters. Separation of fishing mortality from natural mortality is possible only when there is substantial contrast in the effort pattern. We also require a known recruitment pattern, and sampling times are spread out so that the length-frequency data will contain information on growth and mortality. Simulation studies are carried out to determine the performance of the method. The simulated data are generated from the recruitment pattern of the brown tiger prawn (*Penaeus esculentus*) in the northern prawn fishery of Australia. Finally we apply the maximum likelihood method to length-frequency data from grooved tiger prawn data (*P. semisulcatus*) in the northern prawn fishery of Australia.

Materials and methods

The model

We assume that the growth of individuals follow a von Bertalanffy curve so that the length at age a (relative to some origin t_0) is given by

$$L(a) = L_\infty(1-e^{-ka}). \tag{1}$$

In this study, age is always defined to be relative to t_0, i.e. t_0 is absorbed into a for the purpose of identifiability. We will consider estimation of (k, l_∞) only because t_0 is not estimable from length-frequency data with aging data. Note that this does not mean t_0 is assumed to be 0. To provide a general treatment we relax each of the assumptions mentioned in the introduction. First we relax assumption 1 by letting the maximum length, L_∞, vary within the population. We denote the density function of L_∞ as $p(x)$, which has a mean of l_∞ and a variance of σ^2. It is possible that recruits to the fishery have a range of sizes. To allow for this range we let the size at recruitment, L_0, be a random variable with density function $u(s)$. In practice, one may be able to use information from other studies (such as subadult abundance) to arrive at an approximate parametric form for $u(s)$.

If $f_t(l)$ is the probability density function of L at time t, then

$$f_t(l) = \int_0^\infty\int_l^\infty p(x|L_0=s)f_t(l|L_\infty=x, L_0=s)u(s)dxds, \tag{2}$$

where $f_t(l|L_\infty=x, L_0=s)$ is the conditional probability density function of L at time t when L_∞ is known to be x and the size at recruitment is s. Note the lower limit of the inner integral is l because L_∞ cannot be less than an individual's length.

Let the age (again, relative to t_0) at recruitment of an individual be A_0. From Equation 1, we have age a at length l is $a=-k^{-1}\log(1-l/L_\infty)$ and hence the conditional distribution, $f_t(l/L_\infty=x, L_0=s)$, which may be written as $f_t(l|x, s)$ for brevity, can be expressed by using the conditional distribution of age $\mathrm{ht}(a|L_\infty=x, A_0=a_0)$ (see Wang et al., 1995), as

$$f_t(l|x,s) = \frac{1}{k(x-1)}h_t\left(-k^{-1}\log(1-l/x)|x,a_0\right). \tag{3}$$

We now generalize assumptions 2 and 3 by introducing the intensity function of recruitment, $r(t)$, and the total instantaneous mortality, $z(t)$, which are arbitrary functions of time t. The total mortality would depend on time through the fishing mortality component F, where $z(t)=M+F(t)$ and M is the constant natural mortality.

The age distribution satisfies

$$h_t(a|L_\infty=x, A_0-a_0) \propto \exp\{-\int_{a_0}^{a} z(t-a+y)dy\}r(t-a+a_0). \tag{4}$$

This equation states that the density of individuals of age a is proportional to the intensity of recruitment at the time when these individuals were recruited, namely $t-a+a_0$, multiplied by a reduction factor due to mortality over the intervening period. We therefore have

$$\begin{aligned} h_t(a|x,s) &= h_t\left(a\middle|L_\infty=x, A_0=-k^{-1}\log(1-s/x)\right) \\ &\propto \exp\left(-\int_{-k^{-1}\log(1-s/x)}^{a} z(t-a+y)dy\right)r\left(t-a-k^{-1}\log(1-s/x)\right) \end{aligned} \tag{5}$$

and Equation 3 becomes (after substituting for a and shifting the dummy variable y)

$$\begin{aligned} &f_t(l|x,s) \\ &\propto \frac{1}{x-1}\exp\left(-\int_{t-k^{-1}\log\left(\frac{x-s}{x-1}\right)}^{t} z(y)dy\right)r\left(t-k^{-1}\log\left(\frac{x-s}{x-1}\right)\right). \end{aligned} \tag{6}$$

Let us consider the case of fixed recruitment length, i.e., $L_0=l_0$, and define a parameter vector, β, consisting of (k, l_∞, s), and other parameters quantifying mortality and catchability. Equation 2 then reduces to a single integral over x,

$$\begin{aligned} &f_t(l|\beta) \propto \int_l^\infty p(x)\exp \\ &\left(-\int_{t-k^{-1}\log\left(\frac{x-l_0}{x-1}\right)}^{t} z(y)dy\right)r\left(t-k^{-1}\log\left(\frac{x-l_0}{x-1}\right)\right)\frac{dx}{x-1}. \end{aligned} \tag{7}$$

A more convenient form for computation arises after changing the integration variable from the asymptotic length x to time since recruitment, $t-a+a_0$,

$$\tau = k^{-k}\log\left(\frac{x-l_0}{x-1}\right). \quad (8)$$

The expression (Eq. 7) then becomes

$$f_t(l|\beta) \propto \int_l^\infty p(x(\tau))\exp\left(-\int_{t-\tau}^{t} z(y)dy\right) r(t-\tau)\frac{d\tau}{1-e^{-k\tau}}. \quad (9)$$

In the special case of constant recruitment, i.e., $r(t)=1$, and constant mortality, $z(t)=z$, $f_t(l|\beta)$ becomes independent of time as first obtained by Powell (1979).

Maximum likelihood estimation

Let $p_{ij}(\beta)$ be the expected proportion of individuals in the i^{th} length class (l_{i-1}, l) on the j^{th} occasion, where $i=1, 2, \cdots, N$; and let n_{ij} be the corresponding observed numbers. The value of $p_{ij}(\beta)$ can be obtained from the density function $f_t(l;\beta)$ given by Equation 2. Thus

$$p_{ij}(\beta) = \frac{\int_{l_{i-1}}^{l_i} f_j(l;\beta)dl}{\int_{l_0}^{l_N} f_j(l;\beta)dl}, \quad (10)$$

in which $f_j(l;\beta)$ is the (unnormalized) density function on the j^{th} occasion. Under a multinomial model, estimation of the parameter vector β relies on the procedure

$$\text{maximize} \sum_{i,j} n_{ij}\log p_{ij}(\beta) \text{ with respect to } \beta. \quad (11)$$

The sum is the log-likelihood function up to a constant independent of the parameters. The probability, p_{ij}, can be approximated as $f_j(l_{i+1/2})/\Sigma_i f_j(l_{i+1/2})$, which is the normalized value of the density function for the j^{th} occasion at the midpoint of the i^{th} length class.

If sampling effort is known and expected catch is assumed to be a known function of effort and population abundance, the log-likelihood function in Equation 11 can be easily modified to incorporate effort information. For example, if the total number of individuals on each occasion, $n_j=\Sigma_i n_{ij}$, is assumed to follow a Poisson model with overdispersion parameter v, the log-likelihood function becomes

$$\sum_{i,j} n_{ij}\log p_{ij}(\beta) + v\sum_j \left\{n_j \log \lambda_j(\beta) - \lambda_j(\beta)\right\}, \quad (12)$$

where $\lambda_j(\beta)$ is the expected total number in the sample on the j-th occasion and depends on effort. One way to model this dependence is $\lambda_j(\beta)=\phi p_j(\beta)e_j$, where e_j is the sampling effort, ϕ is the total abundance index over all occasions; and p_j is the expected proportion of individuals on the j^{th} occasion (i.e., the relative abundance), so that ϕp_j is the expected catch per unit of effort. In this case we can obtain the maximum likelihood estimate of ϕ as $\Sigma_j n_j/\Sigma_j e_j p_j$. The probability, p_j, can be approximated as $\Sigma_i f_j(l_{i+1/2})/\Sigma_{i,j} f_j(l_{i+1/2})$. Here v is introduced to allow for overdispersion in the Poisson model. It plays a weighting role for the two terms in Equation 12, and the second summation can be regarded as auxiliary information. If n_j is assumed to follow a Poisson distribution exactly, we have $v=1$.

In our simulation and tiger prawn studies we specify a case of fixed, known recruitment length, l_0, and $f_j(l;\beta)$ is obtained from Equation 7 or 9. For definiteness we set the constant of proportionality implicit in these equations to one.

The integrals in Equations 7 and 9 present some subtleties for their evaluation, so that some details of the numerical implementation might be of interest. For the simulation study we used Equation 7. The integral was performed on an l-dependent grid of 41 and 81 quantiles of the L_∞ distribution $p(x)$ and then improved upon by using the Richardson extrapolation. Note that there is an apparent singularity at $x=1$. However, by decomposing the mortality into a mean and deviation term, $z(y)=\bar{z}+z(y)-\bar{z}$, we find that the factor involving mortality is proportional to $(x-l)^{\bar{z}/k}$. Hence the integrand is proportional to $(x-l)^{\bar{z}/k}$, and, because $\bar{z}/k-1>-1$, the singularity is integrable (i.e., the integral is finite). We used a quadrature scheme designed for integrands of the form $(x-l)^{\xi}f(x), \xi>-1$, to perform the integral in the neighborhood of $x=1$.

For the tiger-prawn study we used Equation 9. The integral was performed on uniform grids of 41 and 81 points over the interval $\tau\in(0,1.5)$ years and, as before, was improved by using the Richardson extrapolation. We used our knowledge that tiger prawns live for about 18 months to determine the upper limit of integration. Note that despite appearances, this integral contains no singularity because $x(\tau)\to\infty$ as $\tau\to 0$), and therefore the factor $p(x(\tau))/(1-e^{-k\tau})\to 0$. The effort integral within the integrand was computed by linear interpolation between cumulative totals of the weekly effort.

The prototype implementation of our maximum likelihood method was written in S-plus software (Lucent Technologies) by using the optimizer "nlminb." However, to improve the performance for a large number of simulations, the program was recoded in C by using Powell's optimization routine with numerical derivatives (Press et al., 1992). The C code and some relevant reports are available on request.

Results

Simulation studies

We simulated length-frequency data based on the recruitment pattern of tiger prawns *P. esculentus* in

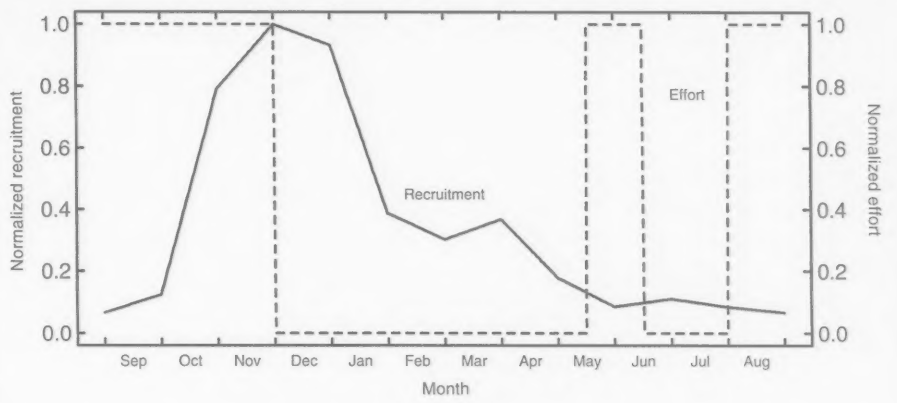

Figure 1

The empirical recruitment pattern (solid line) of the tiger prawn *Penaeus esculetus* in the northern prawn fishery of Australia and the fishing effort pattern (dashed line).

the northern prawn fishery of Australia. This pattern has been derived from experimental trawls in which the number of individuals in the lowest length class are counted (Wang and Die, 1996). We assume the recruitment and effort patterns are the same in each year (Fig. 1). The effort pattern (dashed line) consists of two constant-fishing periods: 15 May to 15 June, and 1 August to 1 December. The unit of effort, E, depends on the unit of catchability, q, because the fishing mortality $F=qE$ must have unit yr^{-1}: therefore we let $E=1$ during the fishing season. Note that the proportion of the year that is fished is $\int E(t)dt=5/12$.

The growth component of our models has $l_\infty=40$ mm and $k=3yr^{-1}$; the instantaneous natural mortality is $M=2yr^{-1}$; and the instantaneous fishing mortality, F, during the fishing season is $4yr^{-1}$ (i.e., $q=4$, because in our units, $F=q$). The resulting annual mortality, $Z=\int z(t)dt=M+q\int E(t)dt=2+4\times5/12=11/3$. The values for mortality come from Somers and Wang (1996). We assume that all recruits have length 19.5 mm. The L_∞ distribution is normal (standard deviation 4 mm) but is truncated at 19.5 mm. The truncated normal distribution at l_0 is simply a conditional normal distribution conditional on being greater than l_0.

We generate twelve length-frequency data sets, one for the beginning of each month. We choose a monthly time interval because the data from our case study in the next section were sampled at roughly monthly intervals. In addtion, because the recruitment pattern is periodic it is sufficient to analyze one year of data.

We obtain each monthly length-frequency data set by taking a sample of size 1000 from the theoretical length distribution $f_t(l)$ given by Equation 6, which depends on the recruitment pattern, the effort pattern, and the distribution of L_∞. That is, for each of the 12 time points t, we evaluate numerically the right-hand side of Equation 6 over a set of finely spaced l values (i.e., every 0.25 mm), aggregate the $f_t(l)$ to 1-mm intervals and finally normalize the function by dividing by the sum of $f_t(l)$. This results in an array of probabilities for an individual's length in each 1-mm interval. It is then straightforward to sample from the corresponding multinomial distribution.

We then obtain parameter estimates from the twelve months of simulated data. The process is repeated 100 times to provide a reasonable estimate of the sampling variance of the parameters. In practice, (k, l_∞) can often be estimated from a different study. We therefore consider two models. In model 1, we assume all five parameters are unknown, and, in model 2, we assume that l_∞ and k are known and we estimate M, F, and σ. It is also common practice (e.g., Sullivan, 1992) to assume that M is known and to estimate the remaining parameters; this is the case in our model 3.

The results are summarized in Table 1. All the parameters are quite well estimated, even for model 1. Estimates of both natural mortality and fishing mortality are quite reliable when growth parameters are assumed known. There is also a modest reduction in the standard deviation when (k, l_∞) are assumed known.

We have also tested for robustness by performing the estimation process on data generated from a log-normal distribution. The results are shown in Table 1. For model 1 the estimates of M and F have a larger and opposite bias, whereas the absolute bias for Z is somewhat smaller. Model 2 improves the estimates dramatically, despite the fact that an incorrect distribution (the truncated normal) is being used in the model. Note that the variation in the estimates of total annual mortality, Z, is somewhat less than that for F and M; this is because F and M are highly negatively correlated (typically 94%). In model 3 the estimate of

Table 1

Mean parameter estimates and standard deviations (in parentheses) for simulated tiger prawn (*Penaeus esculentus*) data. The model assumes an underlying truncated normal L_∞ distribution. The data are generated from two underlying L_∞ distributions: the truncated normal and the lognormal. With model 1 all parameters are unassumed to be unknown; with model 2 (k, l_∞) are assumed to be known; with model 3 M is assumed to be known.

Model	k	l_∞	σ	Z	M	F
Underlying truncated normal distribution						
True	3	40	4	3.67	2	4
1	2.99 (0.05)	40.00 (0.19)	4.02 (0.08)	3.65 (0.05)	1.98 (0.15)	3.99 (0.34)
2	3	40	4.01 (0.07)	3.65 (0.04)	2.00 (.11)	3.95 (0.28)
3	2.99 (0.05)	40.02 (0.15)	4.01 (0.07)	3.65 (0.05)	2	3.95 (0.12)
Underlying lognormal distribution						
True	3	40	4	3.67	2	4
1	3.02 (0.07)	39.53 (0.22)	4.28 (0.08)	3.53 (0.05)	1.51 (0.16)	4.84 (0.35)
2	3	40	4.14 (0.07)	3.62 (0.04)	1.93 (0.11)	4.05 (0.28)
3	2.96 (0.06)	39.92 (0.17)	4.16 (0.07)	3.57 (0.05)	2	3.76 (0.11)

F is negatively biased, but once again the standard deviation is reduced.

Application to tiger prawns (*P. semisulcatus*)

The data for this application consist of a six-year sequence of experimental length-frequency data from the trawling region around Albatross Bay in the eastern Gulf of Carpentaria, Australia. The data consist of catches of tiger prawns from 11 mm to 59 mm (carapace length) for each of 69 times ranging from March 1986 to March 1992. The catches from several stations covering the trawling region at each time (over a few consecutive days) are aggregated. Sampling was done roughly every lunar month.

We use the catch data for the smaller size classes to obtain two types of recruitment patterns: the *aperiodic* pattern and the *quasiperiodic* pattern. The aperiodic pattern is constructed by summing over all individuals with length 21 mm or less for each occasion. The resulting sequence of plotted time points is then joined up by straight lines. The quasiperiodic pattern is generated from the aperiodic pattern by averaging corresponding points across years to give a single annual pattern. The pattern for all six years is generated from the annual pattern by applying, for each biological year, a scale factor that is found by averaging the catch over all size classes within the year. The start of the biological year is defined as the time when the annual pattern reaches its minimum (see Fig. 2).

The effort pattern comes from commercial log books collected from fishermen for the period from 1986 to 1992 in the area. Effort is measured in boat-days (see Fig. 2). There is substantial contrast in the effort both within years (due to seasonal closures) and across years. This contrast may allow us to separate fishing mortality from natural mortality.

The instantaneous fishing mortality $F(t)$ is assumed to be $qE(t)$. The mean total mortality $Z=M+q\bar{E}$, where $\bar{E}$ is the mean effort over the study period. Given the results of the simulation study, we expect the parameter Z may be more reliably estimated than either M or q, whose estimates are negatively correlated.

We further assume that the L_∞ distribution is a truncated normal distribution. This choice is based on the shape of the observed length distribution from July to September, the period when this distribution should approximate the asymptotic length distribution. The truncated normal distributions are then reparameterized in terms of the mean $l_{\infty *}$ and variance σ_*^2 of this underlying normal distribution. It is more convenient to use these parameters than the mean l_∞ and variance σ^2 of the truncated normal distribution. Note that l_∞ is always larger than l_∞ and σ is always less than σ_*. However, in this application the two sets of parameters are nearly interchangeable because over the range of estimated values l_∞ exceeds $l_{\infty *}$ by at most 0.5 mm and σ_* exceeds σ by at most 0.6 mm (see Table 2).

We define a recruit to be an individual with length l_0, which can be chosen at discretion. We examine a range of candidate values of l_0 between 19.5 mm and 27.5 mm, to find out which values provide the most suitable definition of recruitment for this data set, i.e., that which leads to the least violation of model assumptions.

In our application the recruitment pattern was derived from size classes 21 mm or less. If we use this pattern at say 23.5 mm then we need to shift the pattern slightly to later times. It is not apparent to what degree we should shift the pattern; therefore we shall estimate the degree of shift. We call this parameter the *lag*. We expect the lag to increase with l_0. Also note that the derived recruitment pattern is an average over different size classes and hence it is an average over different times. The absolute timing of the pattern is

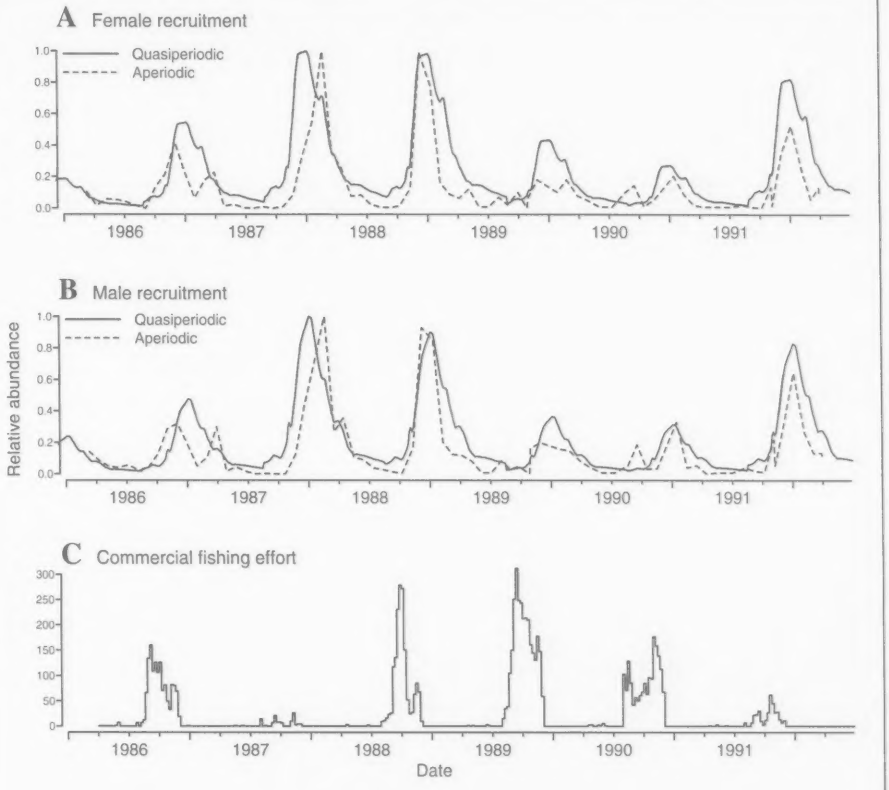

Figure 2

(**A**) Quasiperiodic (solid line) and aperiodic (dashed line) recruitment patterns for female tiger prawns (*Penaeus esculetus*) in the study area; (**B**) quasiperiodic and aperiodic recruitment patterns for female tiger prawns in the study area; (**C**) the weekly fishing effort pattern in the study area.

therefore uncertain and so the lag parameter adopts the role of estimating this uncertainty.

We do have sampling effort information, so that it would be reasonable to consider incorporating into the likelihood the Poisson term for the total catch as mentioned in section 3. Information on total catch per occasion would improve estimates of mortality. However, preliminary analysis found that there was a mismatch of the expected total catch with the observed total catch. Therefore, it appears to be unrealistic to assume that the catch is proportional to the sampling effort. In the subsequent data analysis we use the form of the log-likelihood in Equation 11, which uses the shape of the observed distribution and takes the total catch as given.

We have estimated all the parameters k, l_{∞}, σ_s, M, q, and the lag simultaneously (model 1). To achieve a better understanding of the data, we also estimate parameters for a range of fixed values of M (model 3). This is common practice in the fisheries literature (e.g. Sullivan, 1992). Estimates of q for corresponding values of M can be useful in some contexts where the outcome of an analysis is insensitive to the joint pairs (M, q) (Somers and Wang, 1996). Taking the rough values of Somers and Wang (1996) and Wang and Die (1996) as a guide, we choose the values M=1, 2, and 3yr^{-1}. The utility of considering a range of values of M applies equally to considering a range of values for (k, l_{∞}). Somers and Kirkwood (1991), Wang et al. (1995) and Wang (1998) have all reported estimates of (k, l_{∞}) for this species, and we would like to incorporate this information. However, it is well known that estimates of the growth parameters are strongly correlated. We therefore considered a range of feasible pairs (k, l_{∞}), and estimated the remaining parameters under model 2. The fixed values we used were, for males, (2, 39.3), (3, 37.7), and (4, 36.1), and for females, (2, 53.1), (3, 47.4), and (4, 41.7). These values were obtained by a

Table 2

Parameter estimates for tiger prawn (*Penaeus semisulcatus*) data. F_{89} is the estimated fishing mortality in 1989. cor(M, F_{89}) is the jackknifed correlation between M and F_{89}. The last column is the objective value per unit of effort. With model 1 all parameters are assumed to be unknown; with model 2 (k, l_∞) are assumed to be known; with model 3 M is assumed to be known.

Model	M	F_{89}	Z	k	l_∞	σ^*	cor(M, F_{89})	−2log
Males: quasiperiodic recruitment								
1	4.1	2.3	5.2	9.3	33.4	4.5	−0.82	72.96
2	2.9	0.3	3.1	2	39.3	5.1	−0.78	74.43
2	3.7	0.6	3.9	3	37.7	4.3	−0.35	73.99
2	3.4	2.1	4.4	4	36.1	4.3	−0.25	73.60
3	1	2.2	2.0	5.3	32.3	4.8	—	73.05
3	2	1.9	2.9	6.7	32.5	4.8	—	73.03
3	3	0.0	3.0	7.6	32.3	4.8	—	73.15
Males: aperiodic recruitment								
1	1.3	1.6	2.0	5.0	32.6	4.8	−0.67	72.91
2	2.8	0.4	3.0	2	39.3	5.8	−0.79	74.65
2	3.7	0.1	3.7	3	37.7	4.7	−0.81	74.31
2	3.5	0.5	3.7	4	36.1	4.5	−0.64	73.84
3	1	1.8	1.8	4.9	32.4	4.8	—	72.93
3	2	1.0	2.5	5.9	32.5	4.8	—	72.93
3	3	0.0	3.0	7.0	32.5	4.8	—	73.01
Females: quasiperiodic recruitment								
1	4.2	1.7	5.0	5.6	42.2	7.1	−0.65	86.83
2	3.9	0.3	4.1	2	53.1	8.3	−0.83	87.94
2	4.0	0.7	4.3	3	47.4	6.9	−0.66	87.31
2	2.7	1.3	3.3	4	41.7	7.7	−0.71	86.91
3	1	2.6	2.2	4.1	38.8	8.3	—	87.10
3	2	1.8	2.8	4.4	39.9	7.9	—	86.92
3	3	1.6	3.7	5.1	40.7	7.5	—	86.87
Females: aperiodic recruitment								
1	2.6	0.9	3.0	4.9	39.2	8.2	−0.67	86.90
2	3.9	0.1	4.0	2	53.1	13.5	−0.80	88.43
2	4.3	0.1	4.4	3	47.4	9.7	−0.70	87.88
2	3.0	0.8	3.4	4	41.7	8.1	−0.71	87.04
3	1	2.1	2.0	3.6	39.3	8.4	—	87.07
3	2	0.8	2.4	2.8	41.5	8.5	—	86.94
3	3	0.6	3.3	5.0	39.4	8.1	—	86.91

simple linear fit to the estimates in the three papers mentioned above.

The estimates of M from model 1 appear more reasonable for the aperiodic recruitment pattern. The correlations between M and F_{89} (the fishing mortality in 1989) are not as strong as in the simulation example. This is encouraging and indicates that there may be enough contrast in the effort pattern to separate fishing mortality from natural mortality.

The estimates of l_∞ and σ_* for model 3 are not sensitive to M. However k and M are quite strongly related. In the case of constant recruitment $r(t)$ and mortality $z(t)=Z$, it is well known that k and Z are perfectly correlated, and only their ratio Z/k is able to be estimated. The separation of M and k therefore relies on there being adequate contrast in recruitment and effort.

For model 2 there is little difference between the two recruitment models. The estimates of M show moderate dependence on (k, l_∞), but without trend. These estimates are generally somewhat higher than we expect from prior studies. But for the natural mortality rate, this is the first time we have obtained estimates of M, which is larger than what we have assumed in previous stock assessments, around 2.3 per year (Wang and Die, 1996). Estimates of F_{89} are too variable to be relied upon. All models agree reasonably on the σ_* parameter.

Our model assumes recruitment at a fixed length, l_0, which has to be chosen. In Figure 3 the parameter estimates for fixed (k, $l_{\infty *}$) are plotted against l_0 for the quasiperiodic recruitment model. Parameter estimates are consistent for given l_0 provided that all model assumptions are satisfied. However, when l_0 is too small

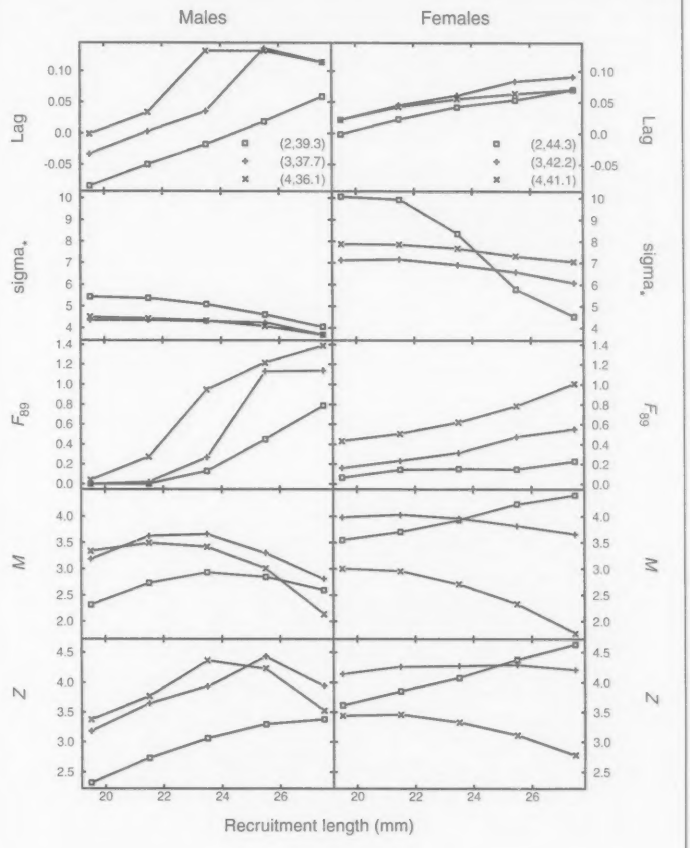

Figure 3

Parameter estimates against recruitment length l_0 for real tiger prawn (*Penaeus esculetus*) data using quasiperiodic recruitment under model 2. The mean annual total mortality Z is equal to $M+0.46F_{89}$, where F_{89} is the fishing mortality in 1989.

or too large, there is bound to be a violation of those assumptions, leading to high sensitivity of the estimates to changes in l_0. Therefore, we say the most reasonable value for l_0 is that for which the estimates are most slowly varying in the immediate neighborhood of l_0. On the basis of σ_*, M and Z for males, l_0=23.5 would be a reasonable choice. We exclude q from consideration because its standard deviation is comparable to its magnitude (see Table 2). In addition we exclude the lag because we expect it to increase approximately monotonically with l_0, as indeed it does. There is no clear choice for females; therefore we choose l_0=23.5, the same as for males. This choice is consistent with the consideration that l_0 should be somewhere between 20 mm and 30 mm, but in the lower half of the range so that more data can be included in the estimation (because lengths must exceed l_0).

Also shown in Table 2 are jackknife estimates of the standard deviations. The jackknifing is done by dropping the length-frequency record from each occasion in turn and re-estimating the parameters. From the over-all estimate $\hat{\theta}$ and the jackknife estimate $\hat{\theta}_i$ from dropping the i^{th} occasion we obtain a pseudovalue $\hat{\theta}-(n-1)\hat{\theta}_i/n$, where in our case n=69. The jackknifed standard deviation is simply the standard deviation of these pseudovalues. We also show the jackknifed correlation between M and q, which is simply the correlation between the corresponding pseudovalues. In most cases there is a large negative correlation.

The fishing mortality in 1989 (the year of peak effort), F_{89}, is simply proportional to q with constant of proportionality 2865, the number of boat-days of effort in that year. The mean total annual mortality Z is $M+0.46F_{89}$ because the mean annual effort was

1320 boat-days. The mostly high negative correlations between M and F_{89} (equivalently, q) may explain why Z tends to have a smaller standard deviation than either M or F_{89}. The results of Figure 3 can be regarded as a sensitivity study on the effect of changing l_0. The purpose of this sensitivity study is not to estimate l_0 but rather to check that the model assumptions have not been violated for the given l_0.

The results are fairly similar for the two recruitment models although there are differences: the quasiperiodic recruitment model gives larger F_{89} estimates and smaller σ_* estimates. Our method assumes that the recruitment pattern is known without error; therefore the preferred recruitment pattern should be the one with less error. Let us suppose that the true recruitment pattern consists of a periodic pattern with random variation both within years and between years. If the within-year variation is sufficiently large in comparison with the between-year variation, then the quasiperiodic pattern should be used. On the other hand, if the between-year variation is large, then the aperiodic pattern is preferred. Based on the objective values (−2log) in Table 2, model 2 with quasiperiodic recruitment pattern and fixed k at $4yr^{-1}$ appears to be the best model for both males and females.

Figure 4 shows the 40 length-frequency records for females with the largest total catch. Overlaid is the expected catch (given the total catch) from the model with (k, $l_{\infty *}$) fixed at (3, 47.4) for quasiperiodic recruitment (solid line) and for aperiodic recruitment (dashed line). Because the integral for the expected length distribution is singular in the neighbourhood of l_0, the first few size classes are omitted from the estimation; only data with length above l_0+2 are used in the estimation. The fit is quite reasonable for most records. It is interesting to compare the performance of the two recruitment models. In early 1988, when recruitment occurred later than usual (see Fig. 2), the aperiodic model tracks the data more closely than the quasiperiodic model, especially in March. On the other hand, the quasiperiodic model fits better in October 1990, whereas the aperiodic model predicts higher abundance of small females because of a recuitment "blip" in September, which was perhaps due to sampling variation.

Discussion

Methods such as McDonald and Pitcher's (1979), ELEFAN (Pauly et al., 1981), and Sparre's (1987) operate on multiple length-frequency data and attempt to identify cohorts in the frequency pattern. Essentially they estimate the growth parameters by tracing cohorts in time; then they estimate mortality by measuring the evolution in abundance of a cohort. For mortality estimation these methods need catch-per-unit-of-effort data. Sparre's method bears some similarity to ours because it attempts to fit the length distribution of a cohort to a normal distribution whose variance is a parameter to be estimated. Our method does not require separation of cohorts because samples are assumed to come from a length distribution which may be multimodal. Another advantage of our method is that it is not necessary to have information about sampling effort and thus may greatly reduce the complexity of sampling. However, our approach needs a known recruitment pattern.

In our application, recruitment was assumed to occur at a fixed length, l_0, which had to be chosen. We used prior information to constrain l_0 to lie somewhere between 20 mm and 30 mm. We then found the sensitivity of the estimates to changes in l_0 and chose a value that reduced this sensitivity. This choice could be further refined if more accurate constraints were available from other sources. Alternatively, Wang and Somers (1996), who also used l_0 to account for continuous recruitment in estimating growth parameters, have provided guidelines for choosing l_0.

Deriso and Parma (1988) and Sullivan et al. (1990) reported methods based on stochastic growth. Sullivan (1992) also applied the Kalman filter approach for estimating population parameters. Their models differ from ours in the way random variation is incorporated in the growth model. In their models the length increment from one time step to the next follows a distribution whose mean is given by a fixed growth model. As Wang and Thomas (1995) have demonstrated, this is equivalent to assuming that the growth rate changes randomly from time to time. In our model each individual follows a deterministic growth curve whose L_∞ parameter is chosen from a random distribution. An individual with larger than average growth at one time step will have above-average growth at subsequent time steps. Perhaps further modeling effort could be directed into combining these approaches.

DeLong et al. (2001) have reported a method for estimating density-dependent natural mortality and the growth rate from length-frequency data for juvenile winter flounder not subject to fishing mortality. Other growth parameters (l_∞ and the variability of k) were fixed by using information from other sources. Because their data were recorded in the latter half of the year, when recruitment was nearly complete, recruitment was not a complicated issue. In contrast, we had the challenge of a species that recruits all year round. The degree of fit in DeLong et al.'s Figure 5 is comparable to that in our Figure 4.

Our methods are based on distributional assumptions that must be tested for robustness, because, in practice, the l_∞ distribution of real prawn populations will not equal any of our mathematical distributions. We have found that, even for our ideal model, akin to any other existing model, biases occur for moderate to large coefficients of variation when violation of distributional assumptions occurs.

Our model is motivated by the trawl data from the tiger prawn fishery and relies on 1) known recruitment pattern, 2) contrast in commercial fishing effort for estimation of M and F simultaneously, and 3) contrast in sampling times. Requirement 3 is to spread sampling effort so that growth and mortality information

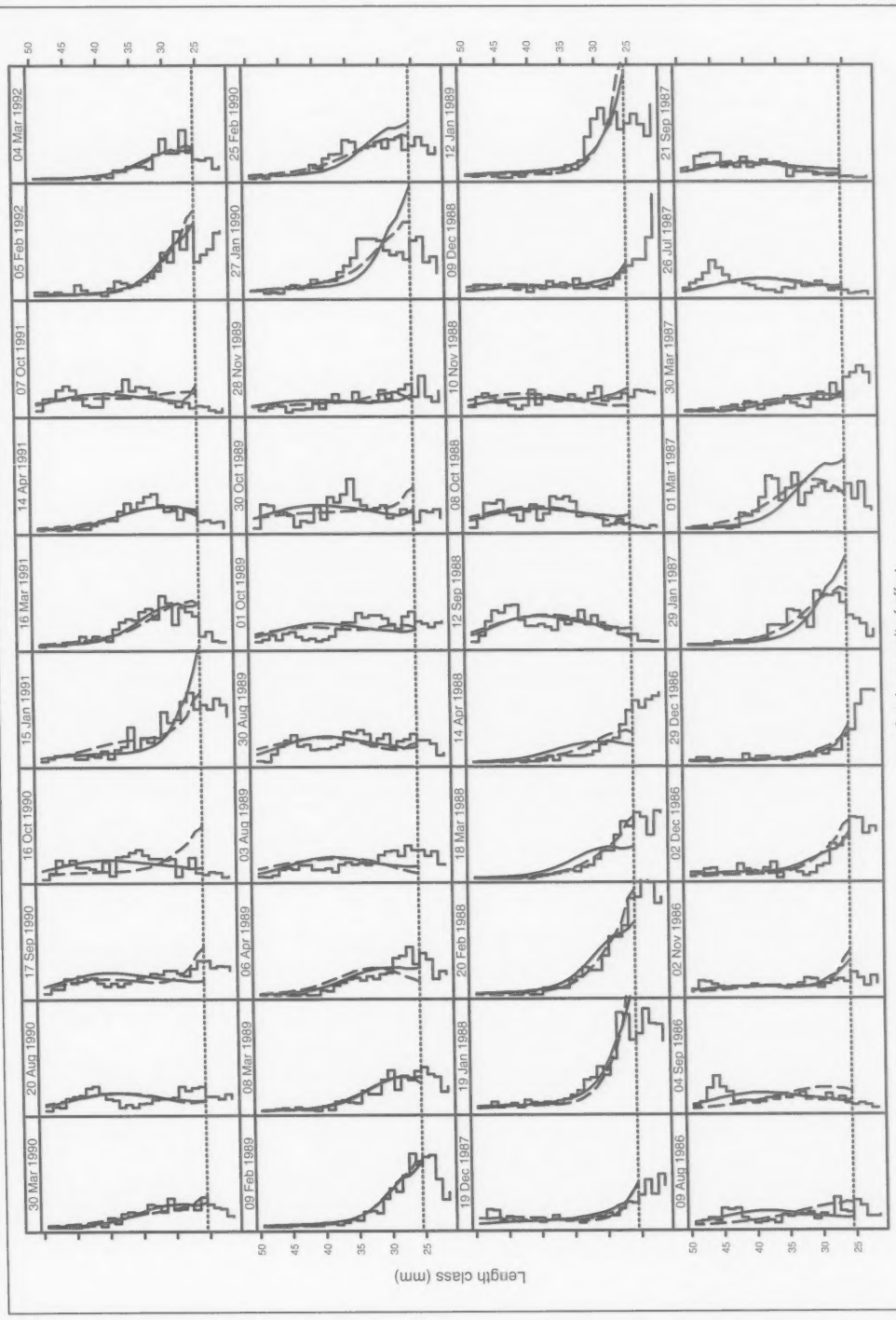

Figure 4

Female length-frequency records for the 40 occasions with the largest total catch of tiger prawns (*Penaeus esculetus*) (stepped line). The smooth solid curve is the expected catch (given the total catch) from model 2 with (k, l_{∞}) fixed at (3, 47.4) and quasiperiodic recruitment at length 23.5 mm. The dashed curve is the expected catch for the aperiodic recruitment model. Only data above the dotted line are included in the fit. The temporal sequence of the panels is from left to right, then from bottom to top.

are in the data. We fitted a variety of different models. The objective function –2log(likelihood) values in Table 2 should be used only as guidelines and should not drive the analysis or be used for model selection. Tiger prawns are subject to very high total mortality and hence are short-lived species. Our method is also applicable to longer-lived species. However, for application to other fisheries, some modification of the model may be necessary to incorporate relevant information in the model. Simulation studies may have to be carried out to see how reliable the modified version is for parameter estimation because many factors, such as growth rate and commercial effort patterns, will determine if parameter estimates can be found or how reliable they are if they can be found.

We aim to obtain growth and mortality parameter estimates simultaneously. However, this may be too ambitious, especially for short-lived species unless other information can be incorporated to assist estimation. For instance, Ebert (1973) found estimation of even two parameters (natural and fishing mortality) unreliable and had to assume one of them. This is perhaps why natural mortality is assumed to be known in traditional cohort analysis. Also Askland's method (1994), one of the most recent cohort-analysis methods, requires a known M. Nevertheless, in practice, (k, l_∞) may be estimated from different types of data. The results based on model 2 (assuming (k, l_∞) are known) indicate that both M and F can then be estimated more reliably when there is substantial contrast in the effort pattern. Another assumption is that catchability does not change over time. This may not be necessarily true when new technology is introduced into the fishery (Bishop et al., 2000). The assumption that growth parameters are known greatly reduces the complexity of estimating the remaining unknown parameters and improves the performance of the proposed methods.

We have chosen to allow only l_∞ to be random because, unlike tag-recapture data, the length-frequency data do not have multiple measures from each individual. Each individual is measured only once. Therefore, it might be problematic to allow random K and correlation between K and L_∞. Such an attempt using length-frequency data may lead to misleading conclusions because the conclusion will be model-driven instead of data-driven. Parameter estimates obtained by fixing M as a constant are deemed more reliable.

We provided a framework for length-frequency data analysis that incorporates continuous recruitment, selectivity, and time-dependent fishing mortality. We have also provided guidelines for how to compute the likelihood function, which depends on rather delicate integrals. Such a model would be very useful for many fisheries because such unified models are not available in the literature. Our work provides a sensible case study. Application of our method may require incorporation of specific information in a fishery. We believe our model, which generalizes the traditional model and is somewhat complicated, has provided us with some useful results for future stock assessment and evaluation of management strategies.

Acknowledgments

This research project was partly supported by the Fisheries Research and Development Corporation of Australia. We gratefully acknowledge the helpful suggestions and comments of David Die, André Punt, Neil Loneragan, and two anonymous referees.

Literature cited

Askland, M.
1994. A general cohort analysis method. Biometrics 50:917–932.

Beverton, R. J. H., and S. J. Holt.
1956. A review of methods for estimating mortality rates of fish in exploited fish populations, with special reference to sources of bias in catch sampling. Rapp. P.-V. Réun., Cons. Int. Explor. Mer 140: 67–83.

Bishop, J., D. Die, and Y.-G. Wang.
2000. A generalized estimating equations approach for analysis of fishing power in the Australian Northern Prawn Fishery. Aust. N. Z. J. Stat. 42:159–177.

DeLong, A. K., J. S. Collie, C. J. Meise, and J. C. Powell.
2001. Estimating growth and mortality of juvenile winter flounder, *Pseudopleuronectes americanus*, with a length-based model. Can. J. Fish. Aquat. Sci. 58:2233–2246.

Deriso, R. B., and A. M. Parma.
1988. Dynamics of age and size for a stochastic population model. Can. J. Fish. Aquat. Sci. 45:1054–1068.

Ebert, T. A.
1973. Estimating growth and mortality rates from size data. Oecologia 11:281–298.
1980. Estimating mortality from growth parameters and a size distribution when recruitment is periodic. Limnol. Oceanogr. 26:764–769.

Hoenig, J. M.
1987. Estimation of growth and mortality parameters for use in length-structure stock production models. *In* Length-based methods in fisheries research (D. Pauly and G. R. Morgan, eds.), p. 121–128. ICLARM Conf. Proc. 13.

McDonald, P. D., and T. J. Pitcher.
1979. Age groups from size-frequency data: a versatile and efficient method of analyzing distribution mixtures. J. Fish. Res. Board Can. 36:987–1001.

Pauly, D., J. Ingles, and T. Neal.
1981. Application to shrimp stocks of objective methods for the estimation of growth, mortality and recruitment-related parameters from length-frequency data (ELEFAN I and II). *In* Penaeid shrimps: their biology and management (J. A. Gulland and B. J. Rothschild, eds.), p.220–234. Fishing News Books Ltd., Farnham, England.

Powell, D. G.
1979. Estimation of mortality and growth parameters from the length frequency of a catch. Rapp. P.-V. Réun., Cons. Int. Explor. Mer 175:167–169.

Press, W. H., S. A. Teukolsky, W. T. Vetterling, and B. P. Flannery.
1992. Numerical recipes in C; the art of scientific computing (2nd ed.). Cambridge Univ. Press, Cambridge, England.

Sainsbury, K. J.
1980. Effect of individual variability on the von Bertalanffy growth equation. Can. J. Fish. Aquat. Sci. 37:241–247.

Somers I. F., and G. P. Kirkwood.
1991. Population ecology of the grooved tiger prawn, *P. semisulcatus*, in the North-western Gulf of Carpentaria, Australia: growth, movement, age structure and infestation by the bobyrid parasite *Epipenaeon ingens*. Aust. J. Mar. Freshw. Res. 42:349–367.

Somers, I. F., and Y.-G. Wang.
1996. A bioeconomic analysis of seasonal closures in Australia's multispecies Northern Prawn Fishery. N. Am. J. Fish. Manag. 17:114–130.

Sparre, P.
1987. A method for estimating growth, mortality and gear selection/recruitment parameters from length-frequency samples weighted by catch per effort. *In* Length-based methods in fisheries research. ICLARM Conf. Proc. 13 (D. Pauly and G. R. Morgan, eds.), p. 75–102.

Ssentongo, G. W., and P. A. Larkin.
1973. Some simple methods of estimating mortality rates of exploited fish populations. J. Fish. Res. Board Can. 30:695–698.

Sullivan, P. J.
1992. A Kalman filter approach to catch-length analysis. Biometrics 48:237–257.

Sullivan, P. J, H. L. Lai, and V. F. Gallucci.
1990. A catch-at-length analysis that incorporates a stochastic model of growth. Can. J. Fish. Aquat. Sci. 47:184–198.

Vetter, E. F.
1988. Estimation of natural mortality in fish stocks: a review. Fish. Bull. 86:25–43.

Wang, Y.-G.
1998. An improved Fabens method for estimation of growth parameters in the von Bertalanffy model with individual asymptotes. Can. J. Fish. Aquat. Sci. 55:397–400.

Wang, Y.-G., and D. Die.
1996. Stock-recruitment relationship of the tiger prawns (*Penaeus esculentus* and *Penaeus semisulcatus*) in the Australian Northern Prawn Fishery. Aust. J. Mar. Freshw. Res. 47:87–95.

Wang, Y.-G., and N. Ellis.
1998. Effect of individual variability on estimation of population parameters from length-frequency data. Can. J. Fish. Aquat. Sci. 55:2393–2401.

Wang, Y.-G., and I. F. Somers.
1996. A simple method for estimating growth parameters from multiple length-frequency data in presence of continuous recruitment. Fish. Res. 28:45–56.

Wang, Y.-G., and M. R. Thomas.
1995. Accounting for the individual variability in the von Bertalanffy growth model. Can. J. Fish. Aquat. Sci. 52:1368–1375.

Wang, Y.-G., M. R. Thomas, and I. F. Somers.
1995. A maximum likelihood approach for estimating growth parameters from tag-recapture data. Can. J. Fish. Aquat. Sci. 52:252–259.

Wetherall, J. A., J. J. Polovina, and S. Ralston.
1987. Estimating growth and mortality in steady-state fish stocks from length-frequency data. *In* Length-based methods in fisheries research (D. Pauly, and G. R. Morgan, eds.), p. 53–75. ICLARM Conf. Proc. 13.

Effects of fishing on growth traits: a simulation analysis

Erik H. Williams
Kyle W. Shertzer
Center for Coastal Fisheries and Habitat Research
101 Pivers Island Road
Beaufort, North Carolina 28516
E-mail address: Erik.Williams@noaa.gov

Abstract—Fisheries often target individuals based on size. Size-selective fishing can create selection differentials on life-history traits and, when those traits have a genetic basis, may cause evolution. The evolution of life-history traits affects potential yield and sustainability of fishing, and it is therefore an issue for fishery management. Yet fishery managers usually disregard the possibility of evolution, because little guidance is available to predict evolutionary consequences of management strategies. We attempt to provide some generic guidance. We develop an individual-based model of a population with overlapping generations and continuous reproduction. We simulate model populations under size-selective fishing to generate and quantify selection differentials on growth. The analysis comprises a variety of common life-history and fishery characteristics: variability in growth, correlation between von Bertalanffy growth parameters (K and L_∞), maturity rate, natural mortality rate (M), M/K ratio, duration of spawning season, fishing mortality rate (F), maximum size limit, slope of selectivity curve, age at 50% selectivity, and duration of fishing season. We found that each characteristic affected the magnitude of selection differentials. The most vulnerable stocks were those with a short spawning or fishing season. Under almost all life-history and fishery characteristics examined, selection differentials created by realistic fishing mortality rates are considerable.

Manscript submitted 16 April 2004
to the Scientific Editor's Office.
Manuscript approved for publication
20 December 2004 by the Scientific Editor.
Fish. Bull. 103:392–403 (2005).

Fishing is typically size selective. It almost always targets the larger individuals of a population and can thus shift the spawning stock towards smaller, slower-growing individuals. If somatic growth has some genetic basis, size-selective fishing may cause evolution toward a smaller size-at-age.

Changes in somatic growth are well documented in field data, and several studies implicate fishing (Ricker, 1981; Harris and McGovern, 1997; Haugen and Vøllestad, 2001; Sinclair et al., 2002). However, with typical field data, it is difficult to rule out other explanations. Changes in growth could result from fluctuations in population density or the environment. Furthermore, they may not be evolutionary, but instead expressions of phenotypic variability. Because of such possibilities, the idea that fishing can cause evolution has often been accepted because of compelling theoretical arguments, rather than on empirical support. However, the laboratory experiments of Conover and Munch (2002) demonstrated that size selection can cause evolution of growth traits. More and more, fishing-induced evolution is considered not just possible, but prevalent (Law, 2000; Stockwell et al., 2003).

The evolution of growth traits, despite wide acknowledgement of the potential for evolution of these traits, is usually a low priority in fishery management. However, it raises at least four management concerns. First, any reduction in growth rate or maximum size can decrease recreational and economic value (Miller and Kapuscinski, 1994). Second, size selection could reduce genetic variability (Falconer and Mackay, 1996), unpredictably altering correlated traits and population fitness. Third, evolution may not easily be reversed, even with after-the-fact management. Fourth, the evolution of growth and other life-history traits can modify population dynamics (Bronikowski et al., 2002; Shertzer and Ellner, 2002) and therefore potential yield (Edley and Law, 1988; Heino 1998). Evolution in fishes can be rapid (Reznick et al., 1997; Hendry et al., 2000; Quinn et al., 2001), so that evolutionary, population, and fishery dynamics occur on similar time-scales (Sinervo et al., 2000; Shertzer et al., 2002; Yoshida et al., 2003). These dynamics imply that evolution matters for fishery management on the time-scale of years or decades.

For fishing to cause evolution, two conditions must be met. There must be a selection differential on a phenotypic trait and a genetic basis must exist for the trait's expression (i.e., the trait must be heritable). Selection differential is defined as the difference in the mean phenotypic trait value of parents before and after selection (e.g., size-selective fishing). Stokes and Law (2000) argued that, under exploitation levels in many of today's fisheries, "selection differentials on body size should be substantial and measurable." Even so, attempts to estimate selection differentials of actual fish stocks have been rare (but see Law and Rowell, 1993; Miller and Kapuscinski, 1994). This lack of estimates is surprising, given that the data needed are often available, as noted by Law (2001).

The second necessary condition, heritability, is defined as the proportion of phenotypic variability in offspring

that is due to the genotypes of the parents. It can range from zero to one, with a higher value potentially speeding the evolutionary response to selection. Field estimates of heritability in fish size are uncommon because in nature it is difficult (although not impossible; McAllister et al., 1992) to separate genetic and environmental effects on phenotypes. Almost all estimates come from laboratory experiments (e.g., Hadley et al., 1991; Conover and Munch, 2002; Vandeputte et al., 2002), mostly on populations from aquaculture breeding programs (e.g., Gjedrem, 1983; Jarayabhand and Thavornyutikarn, 1995; Henryon et al., 2002). One might expect laboratory experiments to over-estimate natural heritabilities, because experiments tend to reduce environmental effects on total phenotypic variance, but estimates from the laboratory have been similar to those from the field (Weigensberg and Roff, 1996). The laboratory experiments indicate that heritabilities in fish growth traits may vary widely among populations but are high enough to allow rapid evolution, given a large enough selection differential.

Models of evolutionary response to selective harvest have usually taken one of two approaches: quantitative genetics (e.g., Law, 1991; Ratner and Lande, 2001) or life-history optimization (e.g., Blythe and Stokes, 1999). In the present study, we take a different approach. Rather than attempt to predict evolution explicitly, we focus on selection differentials, a necessary (but not sufficient) condition for an evolutionary response.

We use simulation analyses to compute selection differentials caused by fishing. The simulation model is one common in fisheries. It consists of an age-structured population following von Bertalanffy growth, with fishing and reproduction modeled as continuous processes.

Our goal is to compare selection differentials across a variety of life-history and fishery characteristics. We quantify selection differentials on growth parameters and body size. If growth traits are heritable, those life-history and fishery characteristics with the largest selection differentials are most likely to generate an evolutionary response. Armed with such knowledge, fishery managers can weigh potential evolutionary effects when choosing a fishing strategy.

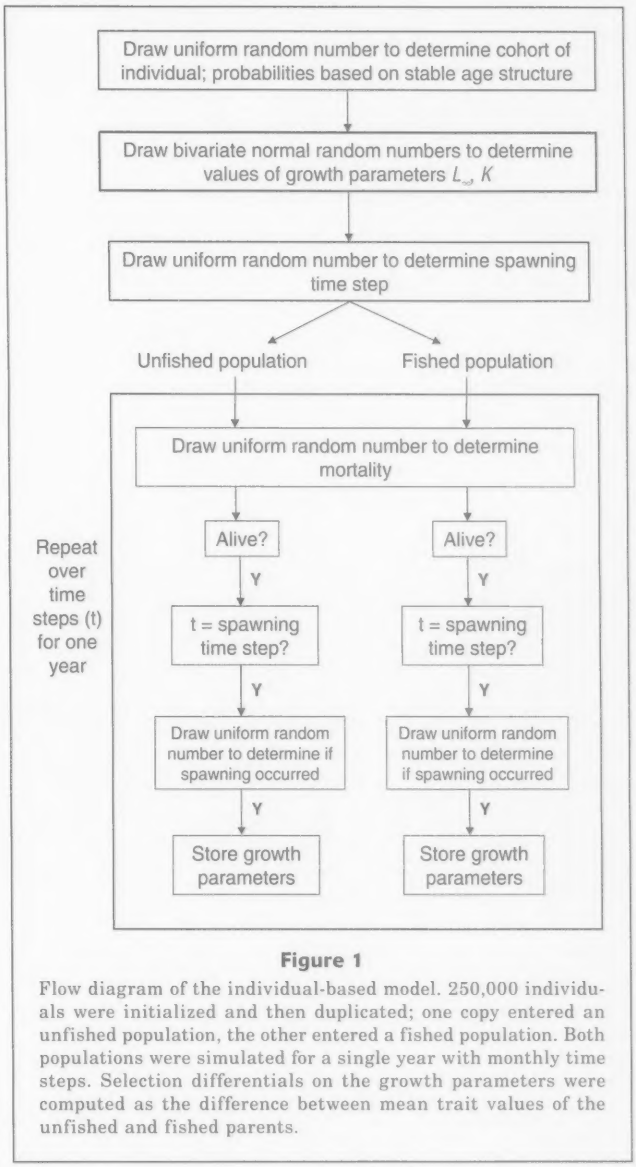
Draw uniform random number to determine cohort of individual; probabilities based on stable age structure
Draw bivariate normal random numbers to determine values of growth parameters L_∞, K
Draw uniform random number to determine spawning time step
Unfished population
Fished population
Draw uniform random number to determine mortality
Repeat over time steps (t) for one year
Alive?
Y
t = spawning time step?
Y
Draw uniform random number to determine if spawning occurred
Y
Store growth parameters
Alive?
Y
t = spawning time step?
Y
Draw uniform random number to determine if spawning occurred
Y
Store growth parameters

Figure 1

Flow diagram of the individual-based model. 250,000 individuals were initialized and then duplicated; one copy entered an unfished population, the other entered a fished population. Both populations were simulated for a single year with monthly time steps. Selection differentials on the growth parameters were computed as the difference between mean trait values of the unfished and fished parents.

Materials and methods

To compute selection differentials caused by size-selective fishing we used an individual-based model (Fig. 1). To initialize the model, 250,000 individual phenotypes were generated. Each was assigned a set of life-history parameters and then duplicated. One copy entered an unfished population that experienced only natural mortality; the other copy entered a fished population that experienced both natural and fishing mortality. Growth, survival, and reproductive success of individuals were simulated with monthly time steps for a single year. At the end of the simulation, selection differentials on growth parameters were computed as the percent change between the mean values of spawners in the two populations.

Model structure

The model comprised three basic life-history functions: growth, survival, and reproduction. For each individual,

size was assumed a function of age (a) and followed the von Bertalanffy model,

$$l(a) = L_\infty[1 - e^{-K(a-t_0)}], \quad (1)$$

where $l(a)$ = the length-at-age of an individual;
L_∞ = the theoretical maximum length;
K = the growth rate, and
t_0 = the theoretical age when size would have been zero.

In our study, each individual's age and size were updated at each monthly time step.

Survival was computed differently for the two populations. In the unfished population, individuals survived with a probability depending only on the natural mortality rate (M/yr). In the fished population, individuals survived with a probability depending on both the natural mortality rate and the size-specific fishing mortality rate. Size selectivity [$s(l)$] by the fishery increased with length according to the logistic equation

$$s(l) = \frac{1}{1 + e^{-\beta_s(l - L_s)}}, \quad (2)$$

where β_s = the slope of the selectivity curve; and
L_s = the length at 50% selectivity.

The function $s(l)$ describes the proportion of the fully-selected fishing mortality rate (F) experienced by individuals of length l. The size-specific fishing mortality rate, therefore, is $s(l)F$ per year. Fishing was applied over a fishing season of duration D_F.

The probability of reproduction was assumed equal to the probability of maturity [$m(a)$]. In the model, maturity increases with age and is independent of length. Although maturity likely relates to length through bioenergetics, the relationship was not modeled here because it is, in general, poorly understood. Like selectivity (Eq. 2), $m(a)$ was modeled by a logistic equation, but with a slope parameter, β_m, and age at 50% maturity, A_m.

In nature, values of life-history parameters K and A_m are related to a stock's natural mortality rate. A higher natural mortality rate reduces the expected lifespan and consequently tends to be associated with a higher growth rate (K) and a younger age at maturity (A_m). In the simulation, K and A_m were related to natural mortality by life-history invariants (detailed later). Life-history invariants have a strong theoretical and empirical basis (Roff, 1984; Beverton, 1992; Charnov, 1993) and have been valuable in other fishery applications (Mangel, 1996; Charnov and Skuladottir, 2000; Frisk et al., 2001; Williams and Shertzer, 2003).

Simulation

To initialize the simulation, individuals were assigned at random to a cohort. The number of cohorts was determined as the age at which approximately 1% of the population would be expected to remain under natural mortality [$-\ln(0.01)/M$, rounded to the nearest integer]. Probabilities of cohort membership decayed exponentially with age according to M; the probability of the oldest cohort was adjusted to include the remaining fraction of fish (i.e., a plus group). The probabilities were scaled to sum to one, and a uniform random number was drawn to determine an individual's cohort.

Next, individuals were assigned parameter values for von Bertalanffy growth. The value of t_0 was fixed at 0.5 yr. Values of L_∞ and K were chosen uniquely for each individual. Following Xiao (1994), L_∞ and K were assumed to follow a bivariate normal distribution with standard deviations σ_L and σ_K, respectively, and correlation ρ.

Finally, individuals were assigned a time step (month) within the year to attempt spawning. The time step was chosen from months distributed uniformly over a spawning season of duration, D_s.

Once assigned parameter values, each individual was duplicated. One copy entered the unfished population, the other the fished population. The populations were simulated in parallel over a single model year.

The simulation iterated each individual through monthly time steps. At each step, the simulation computed growth and checked for survival and reproduction. In the unfished population, the monthly probability of survival was $\exp(-M/12)$. In the fished population, the monthly probability of survival during the fishing season depended on natural mortality and on the size-specific fishing mortality. For simplicity, we assumed size within a month was fixed so that that the probability of survival was $\exp[(-M/12 - s(l_0)F)/D_F]$, where l_0 was an individual's size at the beginning of the month. Outside the fishing season, only natural mortality applied. To check for survival, a uniform random number was drawn and compared to the survival probability appropriate for the population.

Each individual surviving to its assigned spawning time had the opportunity to reproduce. In that case, a uniform random number was drawn and compared to the probability of reproduction. If reproduction was successful, the individual's growth parameters went into a pool of parents used to compute selection differentials.

Growth parameters L_∞ and K jointly determine size-at-age, and it is on these parameters that we describe selection differentials. At the end of the simulation year, we computed a selection differential on each growth parameter as the percent difference between mean trait values (L_∞ or K) of the unfished and fished parents. Based on the differences in L_∞ and K, we also computed upper and lower bounds of selection differentials on size-at-age. The bounds occur where age approaches t_0 or ∞. Because each population consisted of the same set of individuals at the beginning of the year, any difference in growth traits between parents at the end of the year could be attributed solely to fishing.

Base model and variations

We began with a base model built on parameter values chosen or computed to represent common life-history and

Table 1

Parameter values used in the base model. Formulas for the growth rate (K) and the age at 50% maturity (A_m) are life-history invariant relationships from Charnov (1993) and Beverton (1992), respectively. The formula for L_s is the length at age A_m according to von Bertalanffy growth. A value of ∞ for slope parameters corresponds to a knife-edge curve.

Parameter	Description	Formula	Value
M	Natural mortality rate (per year)	Fixed	0.2
F	Fishing mortality rate (per year)	Fixed	0 to 10
$\bar{L}_\infty$	Mean asymptotic size in growth function	Fixed	1000
$\bar{K}$	Mean growth rate in growth function	M/1.65	0.12
t_0	Location parameter in growth function	Fixed	−0.5
CV_L	Coefficient of variation in L_∞	Fixed	20%
CV_K	Coefficient of variation in K	Fixed	20%
ρ	Correlation between L_∞ and K	Fixed	0
β_s	Slope of the size selectivity curve	Fixed	∞
β_m	Slope of the maturity curve	Fixed	∞
A_m	Age at 50% maturity	$\log\left[(3\bar{K}+M)/M\right]/\bar{K}$	8.55
L_s	Length at 50% selectivity	$\bar{L}_\infty\left[1-\exp\left(-\bar{K}[A_m-t_0]\right)\right]$	666
D_S	Duration of spawning season (yr)	Fixed	1
D_F	Duration of fishing season (yr)	Fixed	1

fishery characteristics (Table 1). We then conducted a variety of sensitivity analyses.

In the base model, the natural mortality rate (M) was set at 0.2/yr, a value common for many fish species. Sensitivity analyses used M = 0.1, 0.4, or 0.8. The value of M affects the values of K, A_m, and L_s, according to the life-history invariant relationships (Table 1). The relationship between M and K is often referred to as the M/K ratio. Charnov (1993) suggested a central value for fishes of M/K=1.65, which we used in the base model. Beverton (1992) examined the M/K ratio for fishes and found a range of 0.5 to 2.5. We used this range in our sensitivity analyses to examine the effect of the M/K ratio on selection differentials (Table 2).

The base model treated L_∞ and K as independent variables (ρ=0, Table 1). Often these parameters are correlated. A meta-analysis by He and Stewart (2001) of 235 fish populations indicated a correlation value of −0.28. The negative correlation could be expected from a trade-off between growth rate (represented by K) and maximum size (represented by L_∞), as has been suggested in studies of bioenergetics (Stearns, 1992; Hutchings, 1993; Mangel, 1996). Our sensitivity analyses considered negative values of correlation that range from −0.25 to −1.

With the base model, selectivity and maturity were assumed to be "knife-edge," a functional form often used in fisheries for convenience. Also, in the base model the size at 50% selectivity (L_s) was assumed to occur at an age equal to the age at 50% maturity (A_m). Although these fishery characteristics are common, selectivity and maturity may not be knife-edge or coincide. In sensitivity analyses, we examined different shapes of selectivity and maturity curves (Fig. 2). We also examined the affect of shifting the age at 50% selectivity from −2 to 2, in relation to the base case. This shift corresponds to a range in L_s values from 574 to 738. For simplicity, we held F constant for these sensitivity analyses, implying constant effort but resulting in different amounts of removals.

Under logistic selectivity, the oldest, largest fish receive the highest rate of exploitation. Yet often the largest fish are unavailable to a fishery because of migration patterns or regulations (e.g., a maximum size limit). Thus our sensitivity analyses included a cap on susceptible sizes. The cap was set at 70, 80, or 90% of L_∞.

Using the base model, we examined the effects of annual fishing mortality rate over values that range from F=0 to F=10/yr, which is 0 to 50 times the natural mortality rate. Fishing mortality was applied continuously throughout the year (i.e., D_F=1). In sensitivity analyses, we examined shorter fishing seasons ranging from one to six months. The F was still an annual rate but was applied over fewer months and adjusted so that the number of fish removed was the same as when D_F=1. For seasons shorter than a full year, fishing was assumed to occur at the beginning of the year.

Like the fishing season, the duration of the spawning season was a full year in the base model (D_S=1).

Table 2

Percent selection differential on the von Bertalanffy growth coefficient (K) at fishing mortality = 0.8/yr. Columns correspond to the levels of the coefficient of variation (CV=0%, 10%, 20%) in K and in the asymptotic length (L_∞). Any combination with 0% CV in K is not presented because it results in zero selection differential. The first row corresponds to the base model and subsequent rows correspond to changes in the base model: correlation between L_∞ and K (ρ), slope of maturity curve (β_m), natural mortality (M), M/K ratio, duration of annual spawning season (D_S), maximum size limit (L_u), slope of selectivity curve (β_s), change in age at 50% selectivity (A_s) in relation to the base case, and duration of annual fishing season (D_F).

	Parameter values					
	L_∞: 0%CV K: 10%CV	L_∞: 10%CV K: 10%CV	L_∞: 20%CV K: 10%CV	L_∞: 0%CV K: 20%CV	L_∞:10%CV K: 20%CV	L_∞: 20%CV K: 20%CV
Base	0.7	0.5	0.3	2.1	1.7	1.2
$\rho = -1$	0.7	−0.7	−1.3	2.1	0.2	−2.3
$\rho = -0.75$	0.7	−0.3	−0.8	2.1	0.8	−0.9
$\rho = -0.5$	0.7	0.0	−0.4	2.1	1.1	0.1
$\rho = -0.25$	0.7	0.3	0.0	2.1	1.4	0.6
$\beta_m = 0.25$	0.2	0.2	0.1	0.7	0.7	0.6
$\beta_m = 0.5$	0.3	0.3	0.2	1.1	1.1	0.9
$\beta_m = 1$	0.5	0.4	0.3	1.7	1.4	1.1
$M = 0.1$	0.4	0.4	0.3	1.6	1.5	1.2
$M = 0.4$	0.7	0.4	0.3	2.0	1.5	1.0
$M = 0.8$	0.6	0.3	0.2	1.6	1.1	0.7
$M/K = 0.5$	0.6	0.3	0.1	1.9	1.0	0.6
$M/K = 1$	0.4	0.3	0.2	1.5	1.3	0.8
$M/K = 2$	0.5	0.4	0.3	1.9	1.6	1.2
$M/K = 2.5$	0.8	0.6	0.4	2.4	2.1	1.5
$D_S = 1/12$	1.6	1.0	0.6	4.5	3.6	2.3
$D_S = 3/12$	1.4	0.9	0.5	4.1	3.3	2.2
$D_S = 6/12$	1.1	0.8	0.5	3.3	2.7	1.8
$L_u = 700$	0.0	0.0	0.0	−0.1	−0.1	0.0
$L_u = 800$	0.2	0.0	0.0	0.3	0.2	0.0
$L_u = 900$	0.4	0.2	0.1	1.1	0.8	0.3
$\beta_s = 0.01$	0.3	0.2	0.2	1.1	1.0	0.8
$\beta_s = 0.05$	0.6	0.4	0.3	1.9	1.6	1.2
$\beta_s = 0.1$	0.6	0.5	0.3	2.0	1.7	1.2
$A_s = -2$	0.1	0.2	0.2	1.1	1.2	1.0
$A_s = -1$	0.4	0.4	0.3	1.7	1.6	1.1
$A_s = 1$	0.6	0.5	0.3	2.1	1.7	1.2
$A_s = 2$	0.5	0.4	0.3	1.9	1.6	1.1
$D_F = 1/12$	1.5	1.0	0.6	4.3	3.5	2.3
$D_F = 3/12$	1.3	0.9	0.6	3.9	3.1	2.1
$D_F = 6/12$	1.2	0.7	0.5	3.3	2.6	1.8

In sensitivity analyses, the spawning season ranged from one to six months and was assumed to occur at the end of the year.

A selection differential cannot exist without phenotypic variation. The base model assumed a coefficient of variation (CV) of 20% in both L_∞ and K. For sensitivity analyses, combinations of 0%, 10%, and 20% CV in L_∞ and K were examined for the influence of growth variability on selection differentials of L_∞ and K.

Results

Changes in growth parameters L_∞ and K affect size-at-age jointly, resulting in non-uniform selection differentials across ages (Fig. 3). The selection differentials on size are bounded by the differentials at the extreme ages, t_0 and ∞. At the youngest age, the selection differential on size is limited by the sum of the selection differentials on L_∞ and K plus their product. (At age t_0, the selection differential on size is undefined.) As age

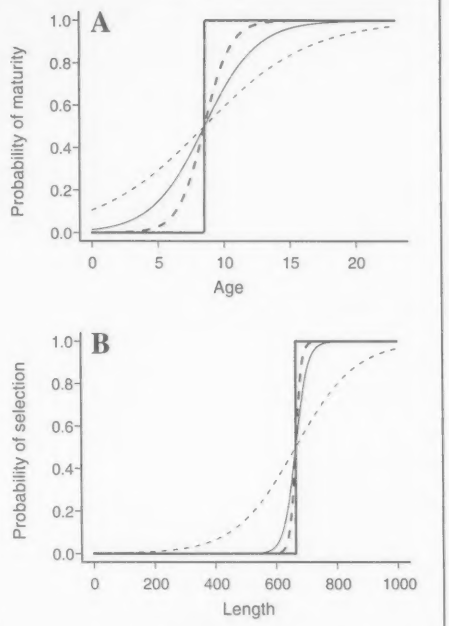

Figure 2

Effect of the slope parameter on (**A**) the probability of maturity and (**B**) the probability of selection. (A) Maturity slope parameter β_m=0.25 (light dash), β_m=0.5 (light solid), β_m=1.0 (heavy dash), and β_m=∞ (heavy solid). (B) Selectivity slope parameter β_s=0.01 (light dash), β_s=0.05 (light solid), β_s=0.1 (heavy dash), and β_s=∞ (heavy solid).

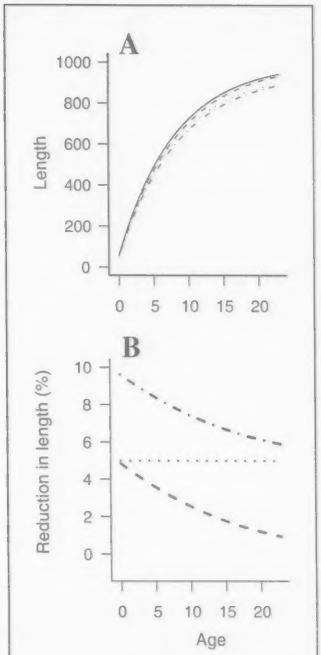

Figure 3

Hypothetical changes in length, given changes in growth parameters. (**A**) Growth trajectories in the base model (solid), a 5% decrease in growth parameter K (dash), a 5% decrease in growth parameter L_∞ (dot), and 5% decrease in both parameters (dash-dot). (**B**) The corresponding reductions in length are relative to the base model.

increases, the selection differential on size increases or decreases monotonically toward an asymptote, the selection differential on L_∞. Thus selection differentials on size across all ages are bounded by those at $L_\infty + K + L_\infty K$ and L_∞. The selection differential on the smallest fish (age approaching t_0) is an upper bound when the selection differential on K is positive, and a lower bound when negative. These properties are important for interpreting how selection differentials on size-at-age correspond to differentials on L_∞ and K.

Using the base model, we computed selection differentials on L_∞ and K as functions of fishing mortality, over the range F=0 to F=10/yr. The selection differentials increased with F nonlinearly, resulting in a concave relationship (Fig. 4). However for F<2.0, the relationship is nearly linear.

The alternative models also revealed linear relationships between selection differentials and F, for F<2.0 (figures not shown). In addition, those relationships have a zero intercept (by definition, no fishing, no selection differential). Because the relationships are (nearly) linear and have a common intercept, the rank of selection differentials among models does not change across values of F. A model that bears the highest selection differential at F=0.2 does so at F=2.0. We therefore present results of sensitivity analyses for a single value of F (F=0.8/yr), with the understanding that for other values of F (up to 2.0), magnitudes of selection differentials can be inferred and ranks among models are maintained.

Increased variation in L_∞ and K tended to increase the selection differentials, and interaction between the two growth parameters (Tables 2 and 3). Selection differentials on L_∞ were generally larger than those on K. In the base model, the largest selection differential on each growth parameter occurred when variation in the focal parameter was highest and variation in the other parameter was zero. The selection differentials on size-at-age were largest when variation in both parameters was highest (20% CV for both L_∞ and K).

Life-history parameters

The correlation (ρ) between L_∞ and K was assumed to be zero in the base model and negative in sensitivity analyses. The effect of correlation depended on variation in the growth parameters. When the CV was zero for either parameter, correlation had no effect on selection differentials (Tables 2 and 3). When the CV was positive for both, a negative correlation decreased selection differentials in relation to those from the base model (Tables 2 and 3). For decreased values of the correlation coefficient (i.e., stronger negative correlation), the percent selection differentials on K decreased, whereas the percent selection differentials on L_∞ either decreased or remained constant. The percent selection differentials on the size near age t_0 ranged from 3.7% to −0.1% for values of ρ from 0 to −1. The percent selection differentials on L_∞ remained relatively constant, ranging from 2.1% to 2.5%, with the highest at ρ=0 (Fig. 5).

Knife-edge maturity (β_m=∞) resulted in larger selection differentials than did other maturity curves (Tables 2 and 3). As the slope of the maturity curve became more gradual, the selection differentials decreased. For β_m values greater than 1, the selection differentials on size were similar to those of the knife-edge case (Fig. 5).

The effect of M on selection differentials was relatively small (Tables 2 and 3). Changes in M from 0.1 to 0.8 led to small changes in selection differentials (Fig. 5). The largest selection differentials tended to occur near intermediate values of M (Tables 2 and 3, Fig. 5). This nonlinear response in the selection differentials is not surprising because changes in M affected the values of K, A_m, and maximum age nonlinearly (Table 1).

Changes in the M/K ratio did not reveal a clear trend (Tables 2 and 3, Fig. 5). As with M, the M/K ratio affects other parameters; therefore changes in M/K could be expected to produce a nonlinear response in the selection differentials. The percent selection differential on L_∞ was lowest at an intermediate value of M/K=2 (Table 3). The percent selection differentials on K showed no consistent trend (Table 2). For M/K values from 0.5 to 2.5, the selection differentials on size across ages ranged from 2.3% to 4.0% (Fig. 5).

Decreases in the spawning season duration (D_s) caused a near linear increase in the selection differentials (Tables 2 and 3, Fig. 5). A compressed spawning duration of one month resulted in a range of 5.0% to 7.4% selection differential on size across ages (Fig. 5). Of all the life-history parameters examined in this analysis, spawning duration had the greatest effect.

Fishery parameters

A limit (L_u) on sizes susceptible to the fishery decreased the selection differentials (Tables 2 and 3, Fig. 5). The percent selection differential at all ages was zero for L_u = 800 and −0.1% for L_u = 700 (Fig. 5). In these analyses, F was held constant. Consequently, smaller values of L_u correspond to fewer fish removed. An alternative approach would have been to maintain constant catch by increasing F, which would have led to selection differentials larger than those in Tables 2 and 3.

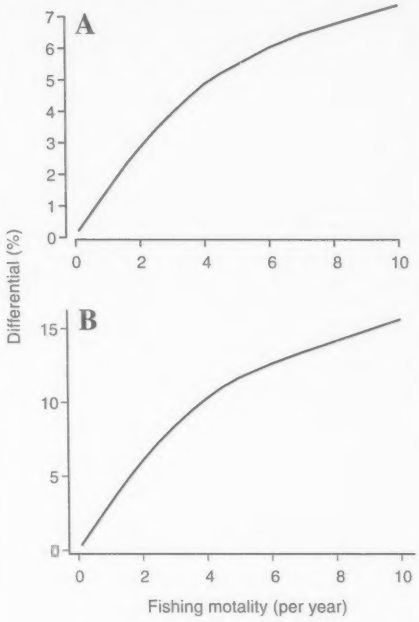

Figure 4

Selection differentials on growth parameters (A) K and (B) L_∞, computed as functions of fishing mortality. Parameter values are the same as those in the base model.

Knife-edge selectivity (β_s=∞) caused larger selection differentials than did selectivity curves with more gradual slopes (Tables 2 and 3). For β_s greater than 0.1, the selection differential rapidly converged to that of the knife-edge case (Fig. 5). As with L_u, F was held constant across β_s sensitivity analyses.

A change in the ages of fishery selectivity had little effect on selection differentials (Tables 2 and 3, Fig. 5). When selectivity was set to a larger age or size, the selection differential decreased slightly. In this case, selectivity was occurring after maturity, allowing more fish to reproduce before reaching sizes selected by the fishery. However if harvest had been held constant instead of F, the selection differentials would have been larger. When selectivity was set to a smaller age or size, the selection differential decreased slightly or remained constant. This result is due to a reduction in the time exposed to differential fishing mortality. Differential fishing mortality occurs only on the sizes where selectivity is less than one; otherwise fishing mortality is constant for all individuals. Under von Bertalanffy growth, younger fish grow more quickly. A decrease in the age or size of selectivity shifts the fishing pressure to ages with quicker growth, reducing the time

Table 3

Percent selection differential on the von Bertalanffy asymptotic length (L_∞) at fishing mortality = 0.8/yr. Columns correspond to the levels of the coefficient of variation (CV=0%, 10%, 20%) in L_∞ and in the growth coefficient (K). Any combination with 0% CV in L_∞ is not presented because it results in zero selection differential. The first row corresponds to the base model and subsequent rows correspond to changes in the base model: correlation between L_∞ and K (ρ), slope of maturity curve (β_m), natural mortality (M), M/K ratio, duration of annual spawning season (D_S), maximum size limit (L_u), slope of selectivity curve (β_s), change in age at 50% selectivity (A_s) in relation to the base case, and duration of annual fishing season (D_F).

	Parameter values					
	L_∞: 0%CV K: 10%CV	L_∞: 10%CV K: 10%CV	L_∞: 20%CV K: 10%CV	L_∞: 0%CV K: 20%CV	L_∞:10%CV K: 20%CV	L_∞: 20%CV K: 20%CV
Base	1.0	2.7	0.9	2.7	0.8	2.5
$\rho = -1$	1.0	2.8	0.7	2.7	−0.1	2.3
$\rho = -0.75$	1.0	2.7	0.7	2.6	0.2	2.2
$\rho = -0.5$	1.0	2.8	0.8	2.7	0.4	2.3
$\rho = -0.25$	1.0	2.8	0.9	2.7	0.6	2.4
$\beta_m = 0.25$	0.3	1.2	0.3	1.1	0.3	1.1
$\beta_m = 0.5$	0.5	1.8	0.5	1.8	0.5	1.7
$\beta_m = 1$	0.8	2.4	0.7	2.4	0.7	2.2
$M = 0.1$	0.8	2.6	0.7	2.5	0.7	2.4
$M = 0.4$	1.0	2.8	1.0	2.7	0.8	2.6
$M = 0.8$	1.0	2.6	1.0	2.6	0.8	2.4
$M/K = 0.5$	1.4	3.2	1.4	3.2	1.3	3.1
$M/K = 1$	0.9	2.7	0.9	2.7	0.8	2.5
$M/K = 2$	0.9	2.5	0.8	2.5	0.7	2.3
$M/K = 2.5$	1.1	2.8	1.0	2.7	0.8	2.5
$D_S = 1/12$	2.2	5.6	2.0	5.5	1.7	5.0
$D_S = 3/12$	2.0	5.1	1.8	5.0	1.5	4.6
$D_S = 6/12$	1.6	4.4	1.5	4.3	1.3	3.9
$L_u = 700$	−0.1	−0.1	−0.1	−0.1	−0.1	−0.1
$L_u = 800$	0.0	−0.1	0.0	−0.1	−0.1	−0.1
$L_u = 900$	0.3	0.5	0.2	0.5	0.1	0.4
$\beta_s = 0.01$	0.5	1.9	0.5	1.9	0.5	1.8
$\beta_s = 0.05$	0.9	2.7	0.9	2.6	0.8	2.5
$\beta_s = 0.1$	1.0	2.7	0.9	2.7	0.8	2.5
$A_s = -2$	0.4	2.1	0.4	2.1	0.4	2.1
$A_s = -1$	0.7	2.5	0.7	2.5	0.7	2.4
$A_s = 1$	1.0	2.8	1.0	2.7	0.9	2.5
$A_s = 2$	1.0	2.7	0.9	2.6	0.8	2.4
$D_F = 1/12$	2.2	5.5	2.0	5.3	1.6	4.8
$D_F = 3/12$	1.9	4.9	1.7	4.8	1.5	4.4
$D_F = 6/12$	1.6	4.2	1.5	4.1	1.2	3.7

individuals experience differential fishing pressure and therefore the potential for selection differentials. If harvest had been held constant instead of F, the selection differentials would have been larger.

The fishing season duration (D_F) affected selection differentials in ways similar to the spawning season duration (Tables 2 and 3, Fig. 5). A fishing season of one month resulted in an upper bound of selection differentials that ranged from 4.8% to 7.3% over all ages (Fig. 5). Of all the fishery parameters examined in this analysis, a concentrated fishing season resulted in the largest selection differentials.

Discussion

The individual-based simulation approach used here simplifies computation of selection differentials and

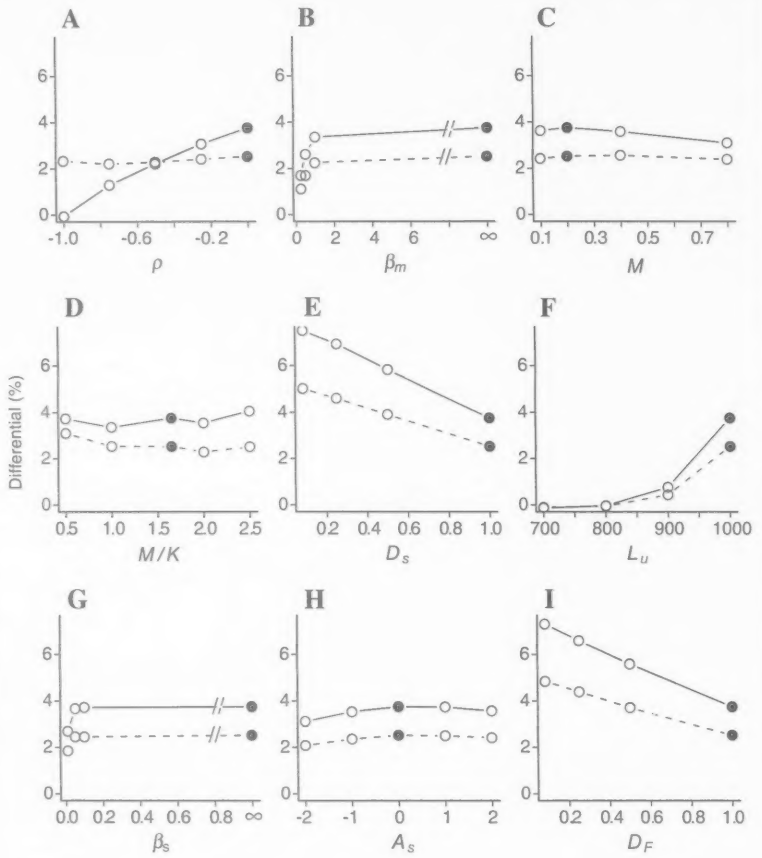

Figure 5

Upper and lower bounds of selection differentials on size across all ages. Solid line represents selection differential on the size near age t_0; dashed line represents selection differential on L_∞. (**A**) correlation between L_∞ and K (ρ); (**B**) slope of maturity curve (β_m); (**C**) natural mortality (M); (**D**) M/K ratio; (**E**) duration of annual spawning season (D_S); (**F**) maximum size limit (L_u); (**G**) slope of selectivity curve (β_s); (**H**) change in age at 50% selectivity (A_s) relative to the base case, and (**I**) duration of annual fishing season (D_F). In all panels, CV's in K and L_∞ are 20%. Filled circles refer to the base model.

isolates the cause—fishing. Yet with any simulation analysis, one must interpret results in light of model assumptions. With our model maturity was assumed to be a function of age, and the computation of selection differentials were consequently focused to those on growth traits and size. If maturity were considered a function of size, it too would have been subject to a selection differential. Changes in size or age at maturity have been considered in other studies (Stokes and Blythe, 1993; Haugen and Vøllestad, 2001; Olsen et al., 2004) and are likely connected to growth parameters through bioenergetic constraints.

A central assumption is that somatic growth follows the von Bertalanffy model. That model was chosen because of its successful track record (Chen et al., 1992; Quinn and Deriso, 1999). Life-history characteristics other than growth are assumed to follow life-history invariant relationships. The invariants constrain biological parameters to values that represent an "average stock." Of course, no stock is truly average, and therefore our sensitivity analyses incorporate considerable deviation from life-history invariants.

In our simulation, the largest selection differentials occurred when the spawning or fishing seasons were

compressed. We modeled fishing seasons at the beginning of the year and spawning seasons at the end of the year, and in a single-year simulation, the annual timing of the fishing and spawning seasons will affect selection differentials. For example, if the one-month fishing season had been modeled at the end of the year, the selection differential would be smaller because of the 11 months of spawning prior to fishing mortality. Over multiple years, however, the annual timing of the fishing and spawning seasons is less important than their duration and overlap.

Our model simulated selection differentials at the onset of a fishery. As a fishery progresses, selection differentials should decrease as life-history parameters shift in the direction of selection. A multiyear simulation of evolution would require knowledge or assumptions about heritability and trait distributions, both of which are likely to be dynamic. Even so, a short-term simulation, where selection differentials and heritability are assumed to be static, may be an informative approximation.

We simulated evolution of the base-model population, assuming a static heritability of 0.2 and selection differentials of 2.5% for L_∞ and 1.2% for K (values from Tables 2 and 3 with 20% CV's in both parameters). Two simulations were conducted with different values for fishing mortality. With $F = 4M$, five years of evolution led to a 9.0% decrease in the capacity of spawning biomass. With $F = M$, five years led to a 2.3% decrease.

With real fishery data it is often impossible to document conclusively that fishing causes a genetic change in growth. Any such change may be hard to measure, fall within the range of statistical variability due to sampling, or be masked by strong year classes. Selection for reduced growth may be compensated by density-dependent effects (for example, lower abundance leaving more resources for survivors to allocate towards growth). Even when a change can be demonstrated, fishing is just one potential explanation. Alternative explanations include environmentally driven evolution and reaction norms (i.e., phenotypic expressions of a genotype-environment interaction).

Nonetheless, size-selective fishing is widespread and often accompanies changes in somatic growth rates (Ricker, 1981; Harris and McGovern, 1997; Haugen and Vøllestad, 2001; Sinclair et al., 2002). Until recently, the question was whether fishing can cause changes in growth that are evolutionary, and the answer was "yes ... probably." The laboratory experiments of Conover and Munch (2002) removed any doubt. However, those experiments represented an extreme fishery in terms of its potential to inflict a selection differential: high F compressed in time (90% of population removed in one day), knife-edge selectivity, non-overlapping generations, and a population where all individuals are susceptible.

The goal of our study was to shed light on selection differentials created by fishing under realistic ranges of life-history and fishery characteristics. Understanding how life-history characteristics affect selection differentials is important for identifying which stocks are most susceptible to evolution of growth traits. For example, susceptibility increases with compression of the spawning season. Fish species with compressed spawning seasons, such as many anadromous species, may be at higher risk of evolution from size-selective fisheries.

Understanding how fishery patterns affect selection differentials has direct management implications because it is the fishery parameters that can be controlled. For example, our results indicate that size-selective fisheries compressed in time are apt to cause high selection differentials. Managers should avoid "derby" style harvests, such as the annual Pacific herring sac-roe fisheries, which are completed in only a few days. Other management strategies could reduce selection differentials, such as slot limits, reduction in the slope of selectivity curves, and partial selectivity after the age at maturity. However, because no size-selective fishing pattern can preclude some directional selection on growth, management by area closures may be the best option for avoiding fishery-induced evolution of growth traits.

As fishing technology improves, so does the ability to fully and rapidly exploit fish populations, and thus increase the potential for evolutionary responses. Still, when overfishing depletes a stock, low abundance is usually the paramount concern. With appropriate management, stock abundance may recover, but pre-fishing growth capacity may recover more slowly or not at all if genetic variation is lost. Given plausible heritabilities of growth traits, this analysis shows that under a wide variety of life-history and fishery characteristics, selection differentials are large enough to allow for rapid evolution.

Acknowledgments

We thank R. Muñoz, M. Prager, and D. Vaughan for comments on the manuscript. This work was supported by the National Marine Fisheries Service through its Southeast Fisheries Science Center.

Literature cited

Beverton, R. J. H.
1992. Patterns of reproductive strategy parameters in some marine teleost fishes. J. Fish. Biol. 41(suppl. B):137–160.

Blythe, S. P., and T. K. Stokes.
1993. Size-selective haresting and at-at-maturity. I: Some theoretical implications for management of evolving resources. *In* The exploitation of evolving resources (T. M. Stokes, J. M. McGlade, and R. Law, eds.), p. 232–247. Lecture Notes in Biomathematics 99. Springer-Verlag, Berlin.

Bronikowski, A. M., M. E. Clark, F. H. Rodd, and D. N. Reznick.
2002. Population-dynamic consequences of predator-induced life history variation in the guppy (*Poecilia reticulata*). Ecology 83:2194–2204.

Charnov, E. L.
1993. Life history invariants: some explorations of symmetry in evolutionary ecology, 159 p. Oxford Univ. Press, Oxford, England.
Charnov, E. L., and U. Skuladottir.
2000. Dimensionless invariants for the optimal size (age) of sex change. Evol. Ecol. Res. 2:1067–1071.
Chen, Y., D. A. Jackson, and H. H. Harvey.
1992. A comparison of von Bertalanffy and polynomial functions in modeling fish growth data. Can. J. Fish. Aquat. Sci. 49:1228–1235.
Conover, D. O., and S. B. Munch.
2002. Sustaining fisheries yields over evolutionary time scales. Science 297:94–6.
Edley, M. T., and R. Law.
1988. Evolution of life histories and yields in experimental populations of *Daphnia magna*. Biol. J. Linn. Soc. 34:309–326.
Falconer, D. S., and T. F. C. Mackay.
1996. An introduction to quantitative genetics, 4th ed., 245 p. Longman Group Ltd., Harlow, Essex, England.
Frisk, M. G., T. J. Miller, and M. J. Fogarty.
2001. Estimation and analysis of biological parameters in elasmobranch fishes: a comparative life history study. Can. J. Fish. Aquat. Sci. 58:969–981.
Gjedrem, T.
1983. Genetic variation in quantitative traits and selective breeding in fish and shellfish. Aquaculture 33:51–72.
Hadley, N. H., R. T. Dillon, and J. J. Manzi.
1991. Realized heritability of growth rate in the hard clam *Mercenaria mercenaria*. Aquaculture 93:109–119.
Harris, P. J., and J. C. McGovern.
1997. Changes in the life history of red porgy, *Pagrus pagrus*, from the southeastern United States, 1972–1994. Fish. Bull. 95:732–747.
Haugen, T. O., and L. A. Vøllestad.
2001. A century of life-history evolution in grayling. Genetica 112–113 and 475–491.
He, J. X., and D. J. Stewart.
2001. Age and size at first reproduction of fishes: predictive models based only on growth trajectories. Ecology 82:784–791.
Heino, M.
1998. Management of evolving fish stocks. Can. J. Fish. Aquat. Sci. 55:1971–1982.
Henryon, M., A. Jokumsen, P. Berg, I. Lund, P. B. Pederson, N. J. Olesen, W. J. Slierendrecht.
2002. Genetic variation for growth rate, feed conversion efficiency, and disease resistance exists within a farmed population of rainbow trout. Aquaculture 209: 59–76.
Hendry, A. P., J. K Wenburg, P. Bentzen, E. C. Volk, T. P. Quinn.
2000. Rapid evolution of reproductive isolation in the wild: evidence from introduced salmon. Science 290: 516–518.
Hutchings, J. A.
1993. Adaptive life histories effected by age-specific survival and growth rate. Ecology 74:673–684.
Jarayabhand, P., and M. Thavornyutikarn.
1995. Realized heritability estimation on growth rate of oyster, *Saccostrea cucullata* Born, 1778. Aquaculture 138:111–118.
Law, R.
1991. On the quantitative genetics of correlated characters under directional selection in age-structured populations. Phil. Trans. R. Soc. Lond. B 331:213–223.
2000. Fishing, selection, and phenotypic evolution. ICES J. Mar. Sci. 57:659–668.
2001. Phenotypic and genetic changes due to selective exploitation. *In* Conservation of exploited species (J. D. Reynolds, G. M. Mace, K. H. Redford, and J. G. Robinson, eds.), p. 323–342. Cambridge Univ. Press, Cambridge, England.
Law, R., and C. A. Rowell.
1993. Cohort-structured populations, selection responses, and exploitation of the North Sea cod. *In* The exploitation of evolving resources (T. K. Stokes, J. M. McGlade, and R. Law, eds.), p. 155–173. Lecture Notes in Biomathematics 99. Springer-Verlag, Berlin, Germany.
Mangel, M.
1996. Life history invariants, age at maturity and the ferox trout. Evol. Ecol. 10:249–263.
McAllister, M. K., R. M. Peterman, and D. M. Gillis.
1992. Statistical evaluation of a large-scale fishing experiment designed to test for a genetic effect of size-selective fishing on the British Columbia pink salmon (*Oncorhynchus gorbuscha*). Can. J. Fish. Sci. 49:1294–1304.
Miller, L. M., and A. R. Kapuscinski.
1994. Estimation of selection differentials from fish scales: a step towards evaluating genetic alteration of fish size in exploited populations. Can. J. Fish. Sci. 51:774–783.
Olsen, E. M., M. Heino, G. R. Lilly, M. J. Morgan, J. Brattey, B. Ernande, and U. Dieckmann.
2004. Maturation trends indicative of rapid evolution preceded the collapse of northern cod. Nature 428: 932–935.
Quinn, T. J., II, and R. B. Deriso.
1999. Quantitative fish dynamics, 542 p. Oxford Univ. Press, New York, NY.
Quinn, T. P., M. T. Kinnison, and M. J. Unwin.
2001. Evolution of Chinook salmon (*Oncorhynchus tshawytscha*) populations in New Zealand: pattern, rate, and process. Genetica 112–113:493–513.
Ratner, S., and R. Lande.
2001. Demographic and evolutionary responses to selective harvesting in populations with discrete generations. Ecology 82:3093–3104.
Reznick, D. N., F. H. Shaw, F. H. Rodd, and R. G. Shaw.
1997. Evaluation of the rate of evolution in natural populations of guppies (*Poecilia reticulata*). Science 275:1934–1937.
Ricker, W. E.
1981. Changes in the average size and average age of Pacific salmon. Can. J. Fish. Aquat. Sci 38: 1636–1656.
Roff, D. A.
1984. The evolution of life-history parameters in teleosts. Can. J. Fish. Aquat. Sci. 41:984–1000.
Shertzer, K. W., and S. P. Ellner.
2002. Energy storage and the evolution of population dynamics. J. Theor. Biol. 215:183–200.
Shertzer, K. W., S. P. Ellner, G. F. Fussmann, and N. G. Hairston Jr.
2002. Predator-prey cycles in an aquatic microcosm: testing hypotheses of mechanism. J. Anim. Ecol. 71:802–815.
Sinclair, A. F., D. P. Swain, and J. M. Hanson.
2002. Disentangling the effects of size-selective mortal-

ity, density, and temperature on length-at-age. Can. J. Fish. Aquat. Sci. 59:372–382.

Sinervo, B., E. Svensson, and T. Comendant.
2000. Density cycles and an offspring quantity and quality game driven by natural selection. Nature 406:985–988.

Stearns, S. C.
1992. The evolution of life histories, 379 p. Oxford Univ. Press, Oxford, England.

Stockwell, C. A., A. P. Hendry, and M. T. Kinnison.
2003. Contemporary evolution meets conservation biology. Trends Ecol. Evol. 18:94–101.

Stokes, T. K., and S. P. Blythe.
1993. Size-selective haresting and at-at-maturity. II: Real populations and management options. *In* The exploitation of evolving resources (T. K. Stokes, J. M. McGlade, and R. Law (eds.), p. 232–237. Lecture Notes in Biomathematics 99, Springer-Verlag, Berlin.

Stokes, K., and R. Law.
2000. Fishing as an evolutionary force. Mar. Ecol. Prog. Ser. 208:307–309.

Vandeputte, M., E. Quillet, and B. Chevassus.
2002. Early development and survival in brown trout (*Salmo trutta fario* L.): indirect effects of selection for growth rate and estimation of genetic parameters. Aquaculture 204:435–445.

Weigensberg, I., and D. A. Roff.
1996. Natural heritabilities: can they be reliably estimated in the laboratory. Evolution 50:2149–2157.

Williams, E. H., and K. W. Shertzer.
2003. Implications of life-history invariants for biological reference points used in fishery management. Can. J. Fish. Aquat. Sci. 60:710–720.

Yoshida, T., L. E. Jones, S. P. Ellner, G. F. Fussmann, and N. G. Hairson Jr.
2003. Rapid evolution drives ecological dynamics in a predator-prey system. Nature 424:303–306.

Xiao, Y.
1994. Von Bertalanffy growth models with variability in, and correlation between, K and L_∞. Can. J. Fish. Aquat. Sci. 51:1585–1590.

Preliminary evidence of increased spawning aggregations of mutton snapper (*Lutjanus analis*) at Riley's Hump two years after establishment of the Tortugas South Ecological Reserve

Michael L. Burton
Kenneth J. Brennan
Roldan C. Muñoz
Richard. O. Parker Jr.
Center for Coastal Fisheries and Habitat Research
National Marine Fisheries Service
National Oceanic and Atmospheric Administration
101 Pivers Island Rd.
Beaufort, North Carolina 28516-9722
E-mail address: Michael.Burton@noaa.gov

In this note we describe the re-formation of a spawning aggregation of mutton snapper (*Lutjanus analis*). A review of four consecutive years of survey data indicates that the aggregation may be increasing in size. Mutton snapper are distributed in the temperate and tropical waters of the western Atlantic Ocean from Florida to southeastern Brazil (Burton, 2002). Juveniles and subadults are found in a variety of habitats such as vegetated sand bottoms, bays, and mangrove estuaries (Allen, 1985). Adults are found offshore on coral reefs and other complex hardbottom habitat. They are solitary and wary fish, rarely found in groups or schools except during spawning aggregations (Domeier et al., 1996). Spawning occurs from May through July at Riley's Hump (Domeier et al., 1996) and peaks in June, as indicated by gonadosomatic indices (M. Burton, unpubl. data). Mutton snapper are highly prized by Florida fishermen for their size and fighting ability, and the majority of landings occur from Cape Canaveral, , through the Florida Keys, including the Dry Tortugas (Burton, 2002).

Reports of spawning aggregations of tropical reef fishes are abundant in the fisheries literature. Most documented aggregations of commercially important fishes are attributed to members of the grouper family, Serranidae, including observations of spawning Nassau grouper (*Epinephelus striatus*), red hind (*E. guttatus*), and tiger grouper (*Mycteroperca tigris*) in the Caribbean (see review in Domeier and Colin, 1997, and references therein). Eklund et al. (2000) observed black grouper (*M. bonaci*) aggregating during their spawning season just outside no-take zones along the Florida Keys reef tract. Samoilys and Squire (1994) and Samoilys (1997) documented spawning aggregations of coral trout (*Plectropomus leopardus*) from the Great Barrier Reef, and Johannes (1988) described the aggregating behavior of squaretail coralgrouper (*P. areolatus*) from the Solomon Islands. Most recently, Sala et al. (2003) observed aggregating behavior in two species of serranids—the sawtail grouper (*M. prionura*) and the leopard grouper (*M. rosacea*) from the Gulf of California.

There are fewer descriptions of spawning aggregations of the commercially important snappers (Lutjanidae) in the literature. Wicklund (1969) described spawning behavior of lane snapper (*Lutjanus synagris*) from southeast Florida, Carter and Perrine (1994) described a spawning aggregation of dog snapper (*L. jocu*) from Belize, and Sala et al. (2003) described spawning behavior in two lutjanids from the Gulf of California (yellow snapper, *L. argentiventris*; Pacific dog snapper, *L. novemfasciatus*). Mutton snapper (*L. analis*) are perhaps the best known snapper to form spawning aggregations. Craig (1966) observed concentrated commercial fishing on an apparent "spawning run" of mutton snapper in August at Long Cay, Belize. Domeier and Colin (1997) described an aggregation of *L. analis* in the Turks and Caicos Islands in April 1992, and Domeier et al (1996) identified a spawning aggregation at Riley's Hump.

Because of their predictable nature with respect to location and time, spawning aggregations become extremely vulnerable to heavy exploitation once discovered by fishermen. The majority of annual catches of Nassau grouper in some areas comes from annual spawning aggregations (Colin, 1992; Aguilar-Perera and Aguilar-Dávila, 1996), whereas other aggregations have been completely extirpated (Olsen and LaPlace, 1978; Sadovy and Eklund, 1999; Heyman, 2003). Russ (1991) observed that uncontrolled fishing on spawning aggregations could lead to recruitment overfishing. During a May 1991 survey of Riley's Hump, a site of a known mutton snapper spawning aggregation in the Dry Tortugas, Florida, Domeier and Colin (1997) noted that fish were more scattered and far less abundant than they were at the Turks and Caicos site. The authors suggested that this difference was attributable to heavy commercial fishing pressure at Riley's Hump during the several years prior to 1991.

Although recent literature indicates that fishing pressure on Riley's Hump has been intensive for several years prior to 1991 (Domeier and Colin, 1997), anecdotal information indicates otherwise. According to a commercial hook-and-line fisherman who fished on Riley's Hump from 1978 through 2001, the first known

Mansucript submitted 20 December 2003 to the Scientific Editor's Office.
Manuscript approved for publication 29 December 2004 by the Scientific Editor.
Fish. Bull. 103:404–410 (2005).

instance of commercial fishing on this area occurred in 1968 by a fisherman named Riley.[1] However, the navigation device in common use in 1968 was LORAN (long range navigation) A; thus, the likelihood of a fisherman finding the exact spot where he fished previously was much less likely than with today's global positioning system (GPS) receivers. Large-scale commercial fishing of Riley's Hump began in 1976, with the introduction of the improved LORAN C navigation system.

Commercial fishermen began fishing the area with longline gear in 1979, and fish traps were introduced there in 1984. This was the period of the most intensive fishing; longliners harvested between 10 and 21 metric tons per trip and fish trappers typically landed an average of 11.5 metric tons (Gladding[1]). It is necessary to rely on knowledgeable fishermen for anecdotal data such as this because the National Marine Fisheries Service (NMFS) did not separate out individual species in their data sets prior to 1986, instead consolidating all snappers into an unclassified snapper category. After 1986, landings from the Dry Tortugas were included with the rest of the Florida Keys in a Monroe County total; therefore it is virtually impossible to obtain an exact magnitude of the landings from the Dry Tortugas for this time frame without information from knowledgeable fishermen who were involved in the fishery at the time. In addition to the commercial effort, a small fleet of headboats ran multiday fishing trips to Riley's Hump and other areas in the Dry Tortugas (Dixon[2]).

Fishermen began to realize declining catches in the mid-1980s and brought this to the attention of the fishery management councils. The Gulf of Mexico Fishery Management Council (GMFMC) enacted a spawning-season closure in 1992, prohibiting fishing on Riley's Hump in May and June (Gulf of Mexico Fishery Management Council, 1992). An analysis of pre- and postclosure commercial landing data revealed that, as a result of the closure, there was a shift in effort to the months on either side of the period of closure, and landings during the two-month closure decreased in only one of the months while annual landings increased (Burton, 1997). After further urging by fishermen and an effort by the Tortugas Working Group (a group of stakeholders appointed by the Florida Keys National Marine Sanctuary [FKNMS] Advisory Council), the Tortugas South Ecological Reserve (TSER) was created in July 2001 specifically to protect the spawning aggregation and habitat of mutton snapper. Current regulations prohibit all uses of the reserve, except continuous transit through the reserve, for any vessels without a FKNMS research permit. The authors initiated data collection on Riley's Hump in July 2001 to document the effect of the newly designated ecological reserve on abundance of snappers and groupers.

[1] Gladding, P. 2003. Personal commun. 27A 12th Avenue, Stock Island, FL 33040.

[2] Dixon, R. 2003. Personal commun. CCFHR, NMFS, NOAA, 101 Pivers Island Rd., Beaufort, NC 28516-9722.

Materials and Methods

Study area

Riley's Hump is a carbonate bank of Holocene origin located 20 km southwest of the Dry Tortugas National Park (DTNP) island of Garden Key (Ft. Jefferson). Riley's Hump sits in the northeast corner of the TSER within the FKNMS (Fig. 1). The area has a predominantly low-relief hardbottom and patchy hard coral and scattered gorgonian sponge-soft coral communities. Rising to within 30 m of the surface, Riley's Hump covers an area of approximately 10 km^2. Habitat mapping efforts by Franklin et al. (2000), who used a nine-tier habitat classification scheme, and visual observations from SCUBA dives revealed that Riley's Hump consisted mostly of areas of rocky outcropping and some patchy hard bottom in sand. More detailed multibeam mapping showed that the top of the bank is relatively flat and has an escarpment on the south side of the bank dropping from 30 m to well over 50 m deep (Fig. 2) (Mallinson et al., 2003).

Sampling

Initial sampling stations were selected in 2001 by dividing the top of Riley's Hump into a grid consisting of 0.40-km^2 sections and by conducting a census with the ship's depth sounder in order to identify (within as many grids as possible) reef habitat that could be reached by dives. Ten initial stations were selected according to this procedure. Five more stations were added in 2002 at the recommendation of our vessel captain, Peter Gladding (Fig. 2). Two-man dive teams conducted several 30-m visual census strip transects (Brock, 1954) at each station during the summer months of each year, enumerating all species of snappers and groupers observed.

Results

We summarize our observations of mutton snapper abundance and behavior on Riley's Hump in Table 1, along with the observation's relation in time to the lunar calendar. The initial sighting of an unusually large group of mutton snapper occurred on 17 July 2001. A group of 10 fish was observed by the senior author at station 2 (Fig. 2). The fish were swimming 0.5–1 m apart in a group approximately 1.5 m above the seafloor. The next year, on 27 May 2002, we observed a larger group of approximately 75–100 mutton snapper on the same site, station 2 (Fig. 2). These fish were exhibiting similar behavior to that observed the preceding year. The group remained schooled while the dive team completed one 30-m visual transect and then slowly dispersed as the divers returned to the aggregation location. On 15 June 2003, a team of divers discovered an aggregation of over 200 individual mutton snapper at station 12 (Fig 2). The fish repeatedly swam up to the diver doing the census transects and then slowly turned and swam

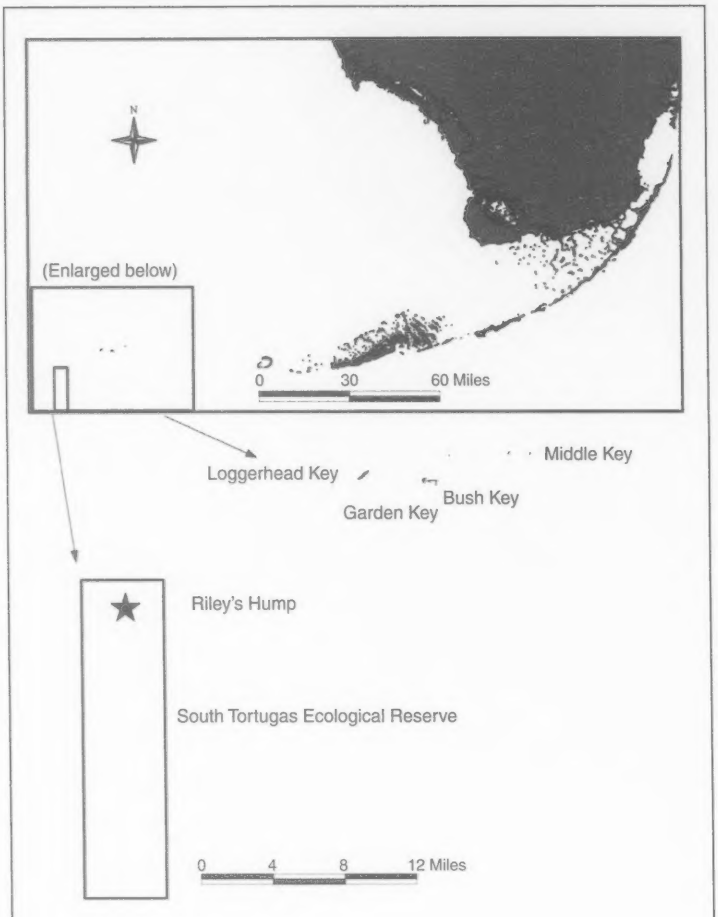

Figure 1

Location of Riley's Hump, Tortugas South Ecological Reserve, Florida Keys National Marine Sanctuary.

away. The aggregation was spread out over a wide area, was not as dense as in the previous two sightings, and exhibited the milling behavior similar to that described by Thresher (1984) for several other species of lutjanids. This aggregation remained at the site throughout the entire 20-minute census dive. Later that day, divers recording their observations at nearby station 2 reported a group of approximately 100 mutton snapper. These fish were more widely dispersed and maintained a distance of 3–5 m from divers. Finally, on 4 July 2004, the senior author and another diver encountered a large school of approximately 300 mutton snapper at station 12, exhibiting behavior similar to that observed during the preceding year.

Discussion

We believe that the large groups of fish encountered at station 12 in June 2003 and again in July 2004 were spawning aggregations based on their behavior and on the timing and location of the aggregation. First, behavior of the snappers themselves was not typical of nonspawning individuals. Although Humann (1997) described them as being very curious, mutton snapper are typically described as solitary animals (Domeier and Colin, 1997), cautious of divers, and not allowing close approach. Many large reef fishes exhibit similar solitary behavior, such as Nassau grouper (Smith, 1972) and black grouper (Eklund et al., 2000). The

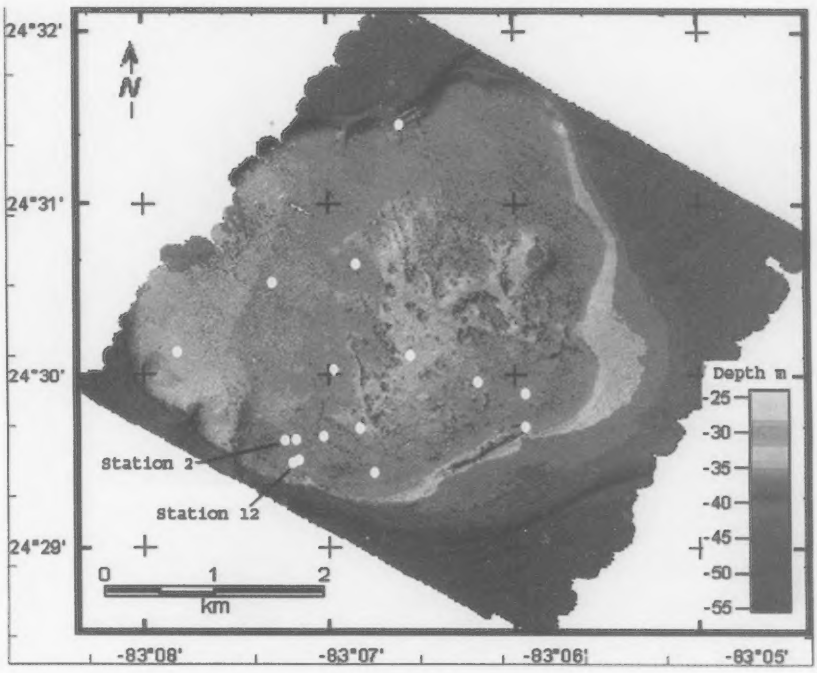

Figure 2

Multibeam bathymetric image of the top of Riley's Hump showing locations of visual census stations (white circles) and mutton snapper aggregation sightings (stations 2 and 12). Bathymetric image was provided courtesy of D. Naar and B. Donahue, Univ. S. Florida, from Mallinson et al., 2003.

Table 1

Observations on mutton snapper (*Lutjanus analis*) on Riley's Hump and their behavior as noted by the authors.

Date and station	Numbers observed	Behavior	Moon phase
28 May–1 June 1999	Solitary *L. analis* observed on 3 of 11 dives	Slowly swimming, diver avoidance	Full moon May 30
31 July–3 Aug 2000	Solitary *L. analis* observed on 5 of 6 dives	Slowly swimming, diver avoidance	New moon July 30
17 Jul 2001			
Station 2	10	Swimming in a tightly packed group, 1.5 m off bottom	3 days before new moon
27 May 2002			
Station 2	75–100	Swimming in tightly packed group, 1.5 m off bottom	1 day after full moon
15 June 2003			
Station 2	75–100	Widely dispersed, diver avoidance	1 day after full moon
Station 12	200+	Widespread aggregation, actively swimming, did not avoid divers	
4 July 2004			
Station 12	300	Widespread aggregation, actively swimming, did not avoid divers	2 days after full moon

senior author completed over 115 dives on Riley's Hump from 1995 through 2004, and the typical mutton snapper sighting during dives made outside the spawning season (February, 5 dives; August, 5 dives; October, 7 dives) was a single fish. In these instances, the closest approach allowed by the fish was 3 m, and when an attempt was made to approach, the fish would swim away, maintaining separation. The only exceptions to this behavior were the four sightings in which groups of fish were apparently unconcerned with the presence of divers (Table 1). Johannes (1981) described a condition he termed "spawning stupor" in *P. areolatus* from Palau. He took this term from the Palauan fishermen's description of the fish as "stupid." We do not believe that "stupid" in this context means unaware, but more closely approximates Johannes et al.'s (1999) modified description of spawning stupor as more of a lack of concern about divers. Mutton snapper in the spawning aggregation we observed seemed aware of our presence because they approached and retreated from the divers many times. Domeier and Colin (1997) asserted that spawning or courtship behavior is easily broken off by a diver's close approach or SCUBA exhalation, although Johannes et al. (1999) offered evidence showing that this is not always the case. We conducted our dive operations primarily in the day and thus did not witness spawning, which is thought to occur at dusk or later (Domeier and Colin, 1997). Courtship behavior has not been described for mutton snapper except by Domeier and Colin (1997) who observed that fish in the Turks and Caicos aggregation "milled in a dense school from the bottom to within a few meters of the surface." The mutton snapper we observed exhibited this milling behavior and did not change it because of our presence.

Consistent timing of spawning with respect to a specific lunar phase has long been thought to be a characteristic of many spawning aggregations. Johannes (1978) noted that the majority of fishes with known lunar-associated spawning rhythms spawned near the full or new moon. However, the published literature does not provide strong support for a correlation between spawning of most lutjanid species and any single lunar phase. The lane snapper aggregation observed by Wicklund (1969) occurred just after the new moon but has not been corroborated since this single observation. Spawning of dog snapper in Belize was variable, however, occurring three days after the new moon on Cay Glory (Carter and Perrine, 1994) and just after the full moon on English Cay (Domeier and Colin, 1997). Spawning peaks for gray snapper off Key West, Florida, were also variable, occurring on the new and full moons of June–August, although the strongest spawning peak was associated with the last quarter moon of August, half way between the new and full moons (Domeier et al., 1996). Back-calculated spawning dates of gray snapper collected in ichthyoplankton samples near Beaufort Inlet, North Carolina, have indicated that spawning takes place primarily at the time of the new moon and secondarily at the time of the full moon (Tzeng et al., 2003).

Evidence of mutton snapper spawning tends to support the argument that the species spawns during a full moon, in contrast to the examples of other lutjanids above. Mutton snapper aggregations off Gladden Spit, Belize, peaked during the April and May full moons and were heavily exploited by fishermen (Heyman et al., 2001). Domeier and Colin's (1997) observation of a mutton snapper aggregation off West Caicos occurred on the April 1992 full moon, and Domeier collected specimens with hydrated oocytes from the Riley's Hump location within one day of the full moon in May 1991 (Domeier and Colin, 1997). Our observation of a small group of about 10 mutton snapper at Riley's Hump in July 2001 occurred three days before the new moon. Our observations of groups of approximately 100, 200, and 300 fish, however, occurred one day after the full moons of May 2002 and June 2003, and two days after the full moon of July 2004, respectively. In contrast, the back-calculated spawning dates of mutton snapper collected in icthyoplankton samples near Beaufort Inlet, NC, indicated that spawning occurred from two days after the full moon to three days before the new moon and that peak spawning occurred between the full moon and last quarter moon phase (Hare[3]). These data are not inconsistent, however, with our observations of fish beginning to aggregate on or around the full moon for spawning. Our sightings of such large groups of mutton snapper around the full moon indicate activity associated with a spawning aggregation.

Finally, many species of reef fishes consistently aggregate to spawn at specific locations at regular intervals (e.g., daily, annually). The two main hypotheses as to why reef fishes do this are to offer increased chances of 1) immediate survival of eggs and larvae, and 2) entrainment of larvae in favorable currents for transport to suitable nursery habitat (Johannes, 1978; Lobel, 1978; Gladstone, 1994), although the former hypothesis currently has more support (Hensley et al., 1994; Peterson and Warner, 2002). Without invoking the hypothesis of local adaptation to the aggregation sites on Riley's Hump, several studies have indicated that the physical oceanography of the region is favorable for transporting larvae spawned at Riley's Hump up the Florida Keys reef tract (Lee et al., 1994; Lee and Williams, 1999) and even as far north as Vero Beach, Florida (Domeier, 2004), presumably to suitable habitat. We believe that the specific location on Riley's Hump where we observed aggregations supports our conclusion that these were spawning aggregations.

In describing lutjanid behavior Thresher (1984) said, "A key feature of reproduction ... is an extensive spawning migration to select areas along the outer reef." Observations in the literature of reef fish spawning aggregations occurring on the outer reef edge, on seaward extensions or promontories, near the shelf-edge

[3] Hare, J. 2002. Personal commun. Center for Coastal Fisheries and Habitat Research, National Ocean Service, NOAA, 101 Pivers Island Rd., Beaufort, NC 28516-9722.

break, on the reef slope or near drop-offs are numerous (Randall and Randall, 1963; Smith, 1972; Munro, 1974; Colin, 1992; Shapiro et al., 1993; Sadovy et al., 1994a, 1994b; Samoilys and Squire, 1994; Sala et al., 2003, and others). Heyman (2003) described a single promontory on a Belize reef that harbored spawning aggregations of 26 different species throughout the year. The mutton snapper aggregation from West Caicos (Domeier and Colin, 1997) occurred on a reef near a drop-off into deep water. The south end of Riley's Hump drops quickly from 35 m to well over 50 m. The two sites where we have observed unusually large numbers of mutton snapper are in the vicinity of this drop-off. Station 2, where we observed aggregations of various sizes in all four years, is approximately 300 m inshore of the edge, whereas station 12, where we observed the largest aggregation in June 2003 and July 2004, is within 150 m of the edge (Fig. 2).

We conclude from behavior, timing, and location that we are observing spawning aggregations of mutton snapper beginning to re-form on Riley's Hump following more than two decades of intensive exploitation. Although the numbers we observed are not close to anecdotal descriptions of the numbers of fish caught during the height of the commercial fishery at this location, it is encouraging to note that we have seen an increasing number of fish for each successive year that we have surveyed these stations. It is too early to say definitively whether the fish are actually becoming more abundant, but preliminary indications are that one effect of the TSER has been to increase numbers of mutton snapper. Current research plans include continued annual monitoring of transects and increased exploration for additional spawning sites, as well as an expansion of our surveys to the last quarter and new-moon phases in order to continue to try to document the exact timing of spawning.

Acknowledgments

We gratefully acknowledge and dedicate this paper to Peter Gladding, master of the FV *Alexis M*, for his superb boat handling skills and knowledge of Riley's Hump; Peter recently lost his battle with cancer and we will greatly miss his guidance and company on our trips. We acknowledge the contributions of Richard Stoker, first mate of the *Alexis M* for his repeated suggestions and help that improved our research efforts; Don Field, Don Demaria, Bill Gordon, and Ian Workman for their assistance at various times with diving efforts; Lisa Wood for her help with the figures; Jon Hare, Erik Williams, Michael Prager, and three anonymous reviewers for constructive reviews of the manuscript that greatly improved it.

Literature cited

Aguilar-Perera, A., and W. Aguilar-Dávila.
1996. A spawning aggregation of Nassau grouper *Epinephelus striatus* (Pisces: Serranidae) in the Mexican Caribbean. Environ. Biol. Fish. 45:351–361.

Allen, G. R.
1985. Snappers of the world. An annotated and illustrated catalogue of lutjanid species known to date. FAO Fish. Synop. 125:1–208.

Brock, V. E.
1954. A preliminary report on a method of estimating reef fish populations. J. Wildl. Manage. 18:297–308.

Burton, M. L.
1997. The effect of spawning season closures on landings of two reef associated species. Proc. Gulf. Caribb. Fish. Inst. 50:896–918.
2002. Age, growth and mortality of mutton snapper, *Lutjanus analis*, from the east coast of Florida, with a brief discussion of management implications. Fish. Res. 59:31–41.

Carter, J., and D. Perrine.
1994. A spawning aggregation of dog snapper, *Lutjanus jocu* (Pisces: Lutjanidae) in Belize, Central America. Bull. Mar. Sci. 55:228–234.

Colin, P.
1992. Reproduction of the Nassau, grouper, *Epinephelus striatus* (Pisces: Serranidae) and its relationship to environmental conditions. Environ. Biol. Fish. 34: 357–377.

Craig, A. K.
1966. Geography of fishing in British Honduras and adjacent coastal waters. Tech. Rep. Coastal Studies Lab. No. 28, Louisiana State Univ., Baton Rouge, LA.

Domeier, M. L.
2004. A potential larval recruitment pathway originating from a Florida marine protected area. Fish. Oceanogr. 13:287–294.

Domeier, M. L., and P. L. Colin.
1997. Tropical reef fish spawning aggregations: defined and reviewed. Bull. Mar. Sci. 60:698–726.

Domeier, M. L., C. Koenig, and F. Coleman.
1996. Reproductive biology of gray snapper (*Lutjanus griseus*) with notes on spawning for other western Atlantic snappers (Lutjanidae). *In* Biology and culture of tropical groupers and snappers (F. Arreguin-Sanchez, J. L. Munro, M. C. Balgos, and D. Pauly, eds.), p. 189–201. International Center for Living Aquatic Resources Management Conference Proceedings 48, ICLARM, Makati City, Phillipines.

Eklund, A. M., D. B. McClellan, and D. E. Harper.
2000. Black grouper aggregations in relation to protected areas within the Florida Keys National Marine Sanctuary. Bull. Mar. Sci. 66:721–728.

Franklin, E. C., J. S. Ault, S. G. Smith, J. Luo, G. A Meester, G. A. Diaz, M. Chiappone, D. W. Swanson, S. L. Miller, and J. A. Bohnsack.
2000. Benthic habitat mapping in the Tortugas region, Florida. Mar. Geodesy 26:19–34.

Gladstone, W.
1994. Lek-like spawning, parental care and mating periodicity of the triggerfish *Pseudobalistes flavimarginatus* (Balistidae). Environ. Biol. Fish. 39:249–257.

Gulf of Mexico Fishery Management Council.
1992. Help proposed for mutton snapper. Gulf Fishery News 12(4):2.

Hensley, D. A., R. S. Appledoorn, D. Y. Shapiro, M. Ray, and R. G. Turingan.
1994. Egg dispersal in a Caribbean coral reef fish,

Thalossoma bifasciatum. I. Dispersal off the reef platform. Bull. Mar. Sci. 54:256–270.

Heyman, W.
2003. Session introduction: conservation of multi-species reef fish spawning aggregations. Proc. Gulf Caribb. Fish. Inst. 54:650–651.

Heyman, W. D, R. T. Graham, B. Kjerfve, and R. E. Johannes.
2001. Whale sharks *Rhincodon typus* aggregate to feed on fish spawn in Belize. Mar. Ecol. Prog. Ser. 215:275–282.

Humann, P.
1997. Reef fish identification: Florida, Caribbean, Bahamas, 2nd ed., 396 p. New World Publications, Inc. Jacksonville, FL.

Johannes, R. E.
1978. Reproductive strategies of coastal marine fishes in the tropics. Environ. Biol. Fish. 3: 65–84.
1981. Words of the lagoon: fishing and marine lore in the Palau district of Micronesia, 245 p. Univ. California Press, Berkeley, CA.
1988. Spawning aggregation of the grouper *Plectropomus aerolatus* (Rüppel) in the Solomon Islands. *In* Proceedings of the 6th international coral reef symposium, Townsville, Australia, 1988 (J. H. Choat, D. Barnes, M. A. Borowitzka, J. C. Coll, P. J. Davies, P. Flood, B. G. Hatcher, D. Hopley, P. A. Hutchings, D. Kinsey, G. R Orme, M. Pichon, P. F. Sale, P. Sammarco, C. C. Wallace, C. Wilkinson, E. Wolanski, and O. Bellwood, eds.), p. 751–755. Sixth International Coral Reef Symposium Executive Committee, Townsville, Australia.

Johannes, R. E., L. Squire, T. Graham, Y. Sadovy, and H. Renguul.
1999. Spawning aggregations of groupers (Serranidae) in Palau. Mar. Conserv. Res. Ser. Publ. 1, 144 p. The Nature Conservancy, Arlington, VA.

Lee, T. N., M. E. Clarke, E. Williams, A. F. Szmant, and T. Berger.
1994. Evolution of the Tortugas Gyre and its influence on recruitment in the Florida Keys. Bull. Mar. Sci. 54:621–646.

Lee, T. N., and E. Williams.
1999. Mean distribution and seasonal variability of coastal currents and temperature in the Florida Keys with implications for larval recruitment. Bull. Mar. Sci. 64:35–56.

Lobel, P.
1978. Diel, lunar and seasonal periodicity in the reproductive behavior of the pomacanthid fish, *Centropyge potteri*, and some other reef fishes in Hawaii. Pac. Sci. 32:193–207.

Mallinson, D., A. Hine, P. Hallock, S. Locker, E. Shinn, D. Naar, B. Donahue, and D. Weaver.
2003. Development of small carbonate banks on the south Florida platform margin: response to sea level and climate change. Mar. Geol. 199:45–63.

Munro, J. L.
1974. The biology, ecology and bionomics of Caribbean reef fishes. Mullidae (goatfishes). Res. Rept. 3, 44 p. Zool. Dept., Univ. West Indies, Kingston, Jamaica.

Olsen, D. A., and J. A. LaPlace.
1978. A study of a Virgin Islands grouper fishery based on a breeding aggregation. Proc. Gulf Caribb. Fish. Inst. 31:130–144.

Peterson, C. W., and R. R. Warner
2002. The ecological context of reproductive behavior. *In* Coral reef fishes: dynamics and diversity in a complex ecosystem (P. F. Sale, ed.), p. 103–118. Academic Press, New York, NY.

Randall, J. E., and H. A. Randall.
1963. The spawning and early development of the Atlantic parrotfish, *Sparisoma rubripinne*, with notes on other scarid and labrid fishes. Zoologica 48:49–60.

Russ, G. R.
1991. Coral reef fisheries: effects and yields. *In* The ecology of fishes on coral reefs (P. F. Sale, ed.), p. 601–635. Academic Press, New York, NY.

Sadovy, Y., P. L. Colin, and M. L. Domeier.
1994a. Aggregation and spawning in the tiger grouper, *Mycteroperca tigris* (Pisces: Serranidae). Copeia 1994:511–516.

Sadovy, Y., and A. M. Eklund.
1999. Synopsis of biological data on the Nassau grouper, *Epinephelus striatus* (Bloch, 1972) and the jewfish, *E. itajara* (Lichtenstein, 1822). NOAA Tech. Rep. NMFS 146, 68 p.

Sadovy, Y., A. Rosario, and A. Román.
1994b. Reproduction in an aggregating grouper, the red hind, *Epinephelus guttatus*. Environ. Biol. Fish. 41:269–286.

Sala, E., O. Aburto-Orapeza, G. Paredes, and G. Thompson.
2003. Spawning aggregations and reproductive behavior of reef fishes in the Gulf of California. Bull. Mar. Sci. 72:103–121.

Samoilys, M.
1997. Periodicity of spawning aggregations of coral trout *Plectropomus leopardus* (Pisces:Serranidae) on the northern Great Barrier Reef. Mar. Ecol. Prog. Ser. 160:149–159.

Samoilys, M., and L. Squire.
1994. Preliminary observations on the spawning behavior of coral trout, *Plectropomus leopardus* (Pisces: Serranidae) on the Great Barrier Reef. Bull. Mar. Sci. 54:332–342.

Shapiro, D. Y., Y. Sadovy, and M. A. McGehee.
1993. Size, composition and spatial structure of the annual spawning aggregation of the red hind, *Epinephelus guttatus* (Pisces: Serranidae). Copeia 1993:399–406.

Smith, C. L.
1972. A spawning aggregation of Nassau grouper, *Epinephelus striatus* (Bloch). Trans. Am. Fish. Soc. 101:257–261.

Thresher, R. E.
1984. Reproduction in reef fishes, 399 p. T.F.H. Publications, Neptune City, NJ.

Tzeng, M. W., J. A. Hare, and D. G. Lindquist.
2003. Ingress of transformation stage gray snapper, *Lutjanus griseus* (Pisces: Lutjanidae) through Beaufort Inlet, North Carolina. Bull. Mar. Sci. 72:891–908.

Wicklund, R.
1969. Observations on spawning of lane snapper. Underw. Nat. 6:40.

Feeding habits of European hake (*Merluccius merluccius*) in the central Mediterranean Sea

Paolo Carpentieri
Francesco Colloca
Department of Animal and Human Biology
University "La Sapienza"
Viale dell'Università 32
00185 Rome, Italy
E-mail address (for P. Carpentieri): paolo.carpentieri@uniroma1.it

Massimiliano Cardinale
Institute of Marine Research
National Board of Fisheries
P.O. Box 4
45 332, Lysekil, Sweden

Andrea Belluscio
Giandomenico D. Ardizzone
Department of Animal and Human Biology
University "La Sapienza"
Viale dell'Università 32
00185 Rome, Italy

European hake (*Merluccius merluccius*) is an important predator of deeper shelf-upper slope Mediterranean communities. It is a nectobenthic species distributed over a wide depth range (20–1000 m) throughout the Mediterranean Sea and the north east Atlantic region (Fisher et al., 1987). Notwithstanding the ecological and economic importance (Oliver and Massutí, 1995) of hake in the Mediterranean, many aspects of its biology (e.g., recruitment and reproduction), due to multiple spawning (Sarano, 1986) and the current state of exploitation, are poorly understood (Arneri and Morales-Nin, 2000).

Recent studies on hake feeding habits in the Mediterranean (Papacostantinou and Caragitsou, 1987; Bouaziz et al., 1990; Oliver and Massutí, 1995) have focused on 0–3 age groups using data from trawl catches (Recasens et al., 1998; Colloca et al., 2000). For this reason, trophic habits of older individuals (Bozzano et al., 1997) and possible ontogenesis-related diet changes are almost unknown. Therefore, in this study we combined samples from trawl and gillnet fisheries collected in the same fishing ground (Colloca et al., 2000) to address these issues.

Materials and methods

The study area is located off the central western coasts of Italy, covering 13,404 km^2 between 20 and 700 meters depth (outer boundaries: latitude 40°52′64, longitude 13°23′13; latitude 42°20′30, longitude 11°16′32).

Monthly size-stratified samples were obtained from spring 1997 to winter 1998 both from bottom-trawls, gillnet commercial-vessels, and from commercial landings. Trawlers catch mainly 0–2 year-old juveniles; they rarely capture adults (Aldebert et al., 1993; Abella et al., 1997; Ardizzone and Corsi, 1997). The gillnet fishery exploits mainly adults of the species (>25 cm TL).

Caught fish were kept on ice, subsequently frozen to prevent digestion of their stomach contents, taken to the laboratory, measured (total length: TL) to the nearest 1 mm, and weighed to the nearest 0.01 g. Sex and maturity stage were also recorded. Maturity state was determined by macroscopic analysis of the gonads by using the maturity scale for partial spawners (Holden and Raitt, 1974).

Stomachs were removed and their contents weighed to the nearest 0.001 g. Prey items were identified and sorted into taxonomic groups to the species level whenever possible. When the state of digestion was more advanced, prey were checked and grouped into unidentified fish, cephalopods, or crustaceans. The degree of digestion of the prey was not considered in the analysis. Empty stomachs and those with partially everted or unidentified contents were excluded from the total sample.

With the exception of the largest individuals (grouped into two heterogeneous length classes), all remaining hakes in the sample were grouped into 5-cm length classes. The study of size-related diet variations was based on these groups. The contribution of each food item to the diet of these fish length groups was evaluated by using the index of relative importance (IRI, Pinkas et al., 1971) as modified by Hacunda (1981): $IRI = F(N + W)$.

This index, expressed as

$$IRI\% = IRI \cdot {}^{\Sigma IRI} \times 100,$$

incorporates the percentage by number (N%), wet weight (W%), and frequency of occurrence (F%) (Hyslop, 1980). Hierarchical cluster analysis and nonmetric multidimensional scaling (NMDS), based on Bray-Curtis similarity and on the IRI%, were used for classification and ordination of hake size classes (Clarke and Warwick, 1994).

Manuscript submitted 27 April 2003 to the Scientific Editor's Office.
Manuscript approved for publication 13 December 2004.
Fish. Bull. 103:411–416 (2005).

Results

A total of 2761 hakes between 5 and 90 cm TL were collected (Table 1). The total number of prey was about 1700, divided into 46 different species. Cluster and NMDS analysis (stress=0.02) based on the IRI allowed the identification of four groups below 50% similarity that were separated along a size gradient (Fig. 1).

Euphausiids (*Nictiphanes couchi*, IRI=76%) and mysids (*Lophogaster typicus*, IRI=22%) dominated the diet of group A (hake between 5 and 10.9 cm TL), and decapods were the secondary prey.

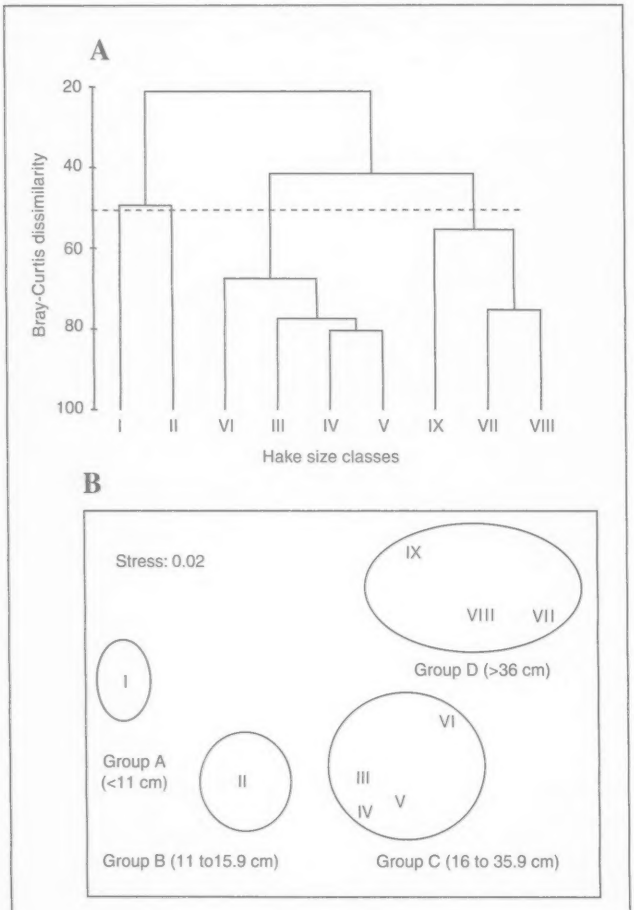

Figure 1

Dendrogram and NMDS (nonmetric multidimensional scaling) plot, based on IRI% values, of the nine hake (*Merluccius merluccius*) size classes using group-average clustering from Bray-Curtis similarity on diet data. (**A**) The four groups defined at arbitrary similarity level of 50% are indicated (dotted line); (**B**) NMDS showing the ordination of hake into four size classes with similar diets (the details of each size class are explained in the text).

Group B (hake from 11 to 15.9 cm TL) showed a more heterogeneous diet characterized by a high occurrence of euphausiids but also with a considerable number of decapods (IRI=18%). Decapods were represented by a wide variety of species, such as *Chlorotocus crassicornis*, *Alpheus glaber*, *Plesionika heterocarpus*, *Pasiphaea sivado*, and *Solenocera membranacea*. Pisces and mysids showed lower percentages (IRI=15% and 4%, respectively). Sepiolidae (IRI=0.9%), *Sepietta oweniana* and *Alloteuthis media*, dominated among cephalopods.

The data suggest a gradual change towards a fully piscivorous diet (Fig. 2) which begins around 16 cm TL and is completed when sexual maturity is attained (TL=32 cm for males and TL=38.5 cm for females; Colloca et al., 2002).

The importance of teleosts strongly increased in group C (hake from 16 to 35.9 cm TL), where they accounted for 91% of hake diet. The main prey were Clupeiformes (IRI=61 %), *Sardina pilchardus* and *Engraulis encrasicolus*. Fish (IRI=96%) represented almost the entire diet of group D (>36 cm TL). In this group a shift towards Centracanthidae (*Spicara flexuosa*, *Centracanthus cirrus*) and a simultaneous decline in consumption of Clupeiformes was observed. Among decapods (IRI=4%), two species occurred most frequently: *Processa* spp. and *S. membranacea*. Euphausiids, mysids, and cephalopods were absent in the diet of hakes larger than 36 cm TL.

Cannibalism of hake juveniles also accounted for some of the diet and increased with predator size. In hake between 36 and 40 cm TL cannibalism represented 12% of IRI, reaching the highest values (IRI=17%) among larger individuals (TL >51 cm).

Discussion

Hake is a top predator that occupies different trophic levels during its ontogenetic development. Hake size classes are differentiated along food niche dimensions according to different prey sizes or different prey taxa. Hake diet shifted from euphausiids, consumed by the smaller hakes (<16 cm TL), to fishes consumed by larger hakes. Before the transition to the complete icthyophagous phase, hake showed more generalized feeding habits where decapods, benthic (Gobiidae, *Callionymus* spp., *Arnoglossus* spp.) and nectonic fish (*S. pilchardus*, *E. encrasicolus*) dominated the diet, and cephalopods had a lower incidence. Specific size-related differences in prey spectrum seem to be associated with different spatial distributions or genetic needs (or with both) (Flamigni, 1984; Jukic and Arneri, 1984; Velasco and Olaso, 1998).

The patterns observed in the present study indicated a strong partitioning among hake

Table 1

Number of hakes and values of IRI (index of relative importance) (%) for the nine size classes. The four groups identified from the cluster analysis are indicated.

	A	B	C				D		
Size group	I	II	III	IV	V	VI	VII	VIII	IX
Length (cm)	5.0–10.9	11.0–15.9	16.0–20.9	21.0–25.9	26.0–30.9	31.0–35.9	36.0–40.9	41.0–50.9	51.0–90.0
Number of hakes	202	430	564	454	555	224	139	107	75
Stomach contents	93	215	239	173	170	78	45	35	26
Prey									
Cephalopoda									
Alloteuthis media		0.22	0.02	0.01					
Sepietta oweniana		0.02	0.02	0.01					
Unid. Sepiolidae		0.35	0.30	0.03					
Unid. Cephalopoda		0.42	0.10	0.01	0.02				
Crustacea									
Alpheus glaber		0.02	0.33	0.05	0.22	0.05	0.81	1.54	
Aristeidae			0.01	0.02					
Aristeus antennatus		0.02							
Chlorotocus crassicornis		1.61	1.83	1.09	1.10	0.48			
Crangonidae			0.01	0.01					
Pandalidae		0.03		0.01					
Parapenaeus longirostris				0.01					
Pasiphaea multidentata		0.02		0.01					
Pasiphaea sivado		0.20	0.04	0.05	0.02	0.05			0.33
Plesionika heterocarpus		0.11	0.01						
Plesionika sp.		0.62	0.07	0.01	0.04	0.05			
Pontocaris lacazei		0.01	0.02	0.01			0.20		
Pontophilus spinosus		0.01	0.01	0.03	0.05	0.20			
Processa sp.		0.25	0.06	0.06	0.15	1.77	0.83	1.54	
Solenocera membranaca		0.04	0.02	0.05	0.34	0.58	3.27	3.53	
Squilla sp.					0.05				
Unid. Decapoda	3.05	19.91	6.19	2.84	2.73	1.45		1.58	1.32
Lophogaster typicus	28.77	4.34	0.16			0.01			
Nictiphanes couchi	54.10	31.83	0.37						
Unid. Euphasiacea	13.99	3.43	0.11						
Unid. Isopoda	0.07	0.02	0.01						
Pisces									
Argentina sphyraena				0.08	0.41	1.06	4.04	3.29	2.34
Arnoglossus laterna			0.01	0.01					
Arnoglossus sp.			0.01	0.01	0.01				
Callionymus sp.			0.01	0.01	0.01	0.06			
Centracanthidae				0.03	0.11	2.60	2.43	11.23	53.97
Centracanthus cirrus						1.93	26.54	4.62	3.80
Clorophthalmus agassizi			0.01						
Conger conger							0.34	0.85	
Echiodon dentatus					0.05				
Engraulis encrasicolus		1.95	11.61	1.28	4.45	9.91	0.87	1.27	1.86
Gadiculus argenteus					0.08	0.65	0.31	0.58	
Gobiidae		0.04	0.02	0.01	0.01	0.05			
Gobius quadrimaculatus			0.02	0.02	0.01				
Lepidotrigla dieuzedei				0.01	0.01				0.78
Lesuerigobius friesii			0.01	0.02	0.03				
Merluccius merluccius					0.07	0.18	12.00	4.10	17.95

continued

Table 1 (continued)

	A	B	C				D		
Size group	I	II	III	IV	V	VI	VII	VIII	IX
Pisces (continued)									
Mullus barbatus						0.12	0.44		0.49
Myctophidae		0.30	0.28	0.03	0.15				
Nettastoma melanurum		0.02		0.01	0.01				
Sardina pilchardus		0.05	45.23	72.55	46.19	62.0	5.20	12.77	10.31
Sphyraena sphyraena							0.60	4.98	
Spicara flexuosa				0.02	0.10	1.33	12.63	21.83	0.01
Spicara sp.						0.37	4.57	0.54	1.69
Trachurus trachurus					0.09	0.13	1.60	1.93	
Trisopterus m. capelanus			0.02	0.01	0.01	0.05			
Unid. Osteichthyes	0.04	34.19	33.14	21.61	43.44	15.01	23.09	22.90	4.25
Raja sp.								0.50	

size classes. Two main thresholds associated with ontogenesis-related diet changes have been identified. The first one was observed around 16 cm TL and corresponded to a significant change in depth distribution. The second, around 36 cm TL, corresponded to the attainment of sexual maturity (Colloca et al., 2002).

Although hakes are demersal fishes, they feed typically upon fast-moving pelagic prey that are ambushed in the water column (Alheit and Pitcher, 1995). There is evidence that hakes feed in mid-water or near the surface at night, undertaking daily vertical migrations (Hickling, 1927; Papacostantinou and Caragitsou, 1987; Orsi-Relini et al., 1989) which are more frequent for juveniles. Small hakes feed daily on small Euphausiacea (*Nictiphanes couchi*). This school-forming planktonic crustacean carries out vertical migrations at night (Casanova, 1970; Franqueville, 1971; Vallet and Dauvin, 2001). They rise to near the surface at night to feed on phytoplankton and sink during daylight between 50 and 800 m depth (Buchholz et al., 1995). Juveniles of *M. merluccius* may follow such migrations, moving from near the bottom, 100–200 m depth, to midwater at night (Froglia 1973; Papaconstantinou and Caragitsou, 1987; Orsi-Relini et al., 1989). Nocturnal vertical migration behavior has been described for gadoids such as hake and cod and is considered responsible for the reduction of trawl catches of these fish at night (Beamish, 1966; Bowman and Bowman, 1980).

Considerable diet changes have been observed after the first year of life (>16 cm TL) when juveniles move from nursery areas on the shelf-break and upper slope to the middle shelf (Andaloro et al., 1985; Ardizzone and Corsi, 1997). The data indicate that such migration is induced by a change in trophic requirements. In this size class, diet changed to fish prey (Clupeiformes), and the importance of the small epiplanktonic crustaceans (Euphausiacea) strongly decreased. Clupeiforms *S. pilchardus* and *E. encrasicolus* are distributed largely on the continental coastal shelf forming schools usually deeper than 25 m (Fisher et al., 1987).

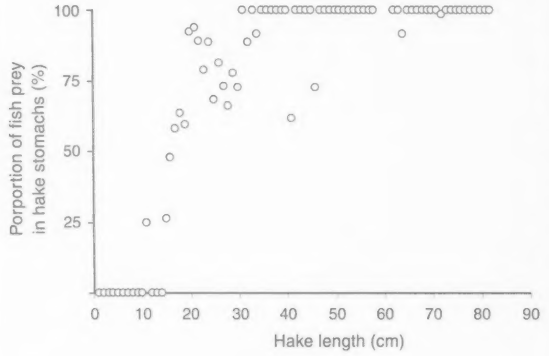

Figure 2

Proportion (%) of fish prey occurring in the diet of hake (*Merluccius merluccius*) during its growth.

The size-depth distribution pattern of hake was confirmed by experimental trawl surveys carried out in the Mediterranean (Relini and Piccinetti, 1996; Relini et al., 1999). Juveniles (modal length of 10 cm TL) are found mostly between 100 and 200 m depth. Intermediate hakes reach the highest abundance mainly on the shelf (<100 m). Large hakes (>36 cm) are found in a wide depth range but concentrate on the shelf break during the spawning period (Recasens et al., 1998; Colloca et al., 2000; Alvarez et al., 2001).

Growth induces a continuous qualitative and quantitative change in diet that is reflected in the increasing

mean weight of prey and decreasing mean number of prey items per stomach. The shift towards large fish prey (i.e., Centracanthidae) usually occurs slightly before maturity—the life history stage with much higher energetic demands due to gonad development (Ross, 1978). A similar pattern was observed for Atlantic cod (*Gadus morhua*) where sexual maturation and spawning are also associated with an ontogenetic change in diet (Paz et al., 1993). Thus, increased energy demands related to sexual requirements, gonad development, and breeding activity appear to be the critical factors driving the changes in feeding strategy of *M. merluccius*.

In large hakes (>36 cm), cannibalism played an important role and should be carefully considered in stock-recruitment analyses. Studies carried out in the Mediterranean (Macpherson, 1977; Bozzano et al., 1997) and in the Atlantic (Guichet, 1995; Link and Garrison, 2002) showed that cannibalism has some importance for hake. In silver hake (*M. bilinearis*), cannibalism notably increased with ontogeny (Link and Garrison, 2002). In the large cape hakes, *M. capensis*, hake is the dominant food item (50% of the diet) for individuals larger than 60 cm (Roel and Macpherson, 1988). Conversely, a low cannibalism rate was observed for *M. paradoxus* in the same area (Payne et al., 1987). This could be a response to the greater accessibility of conspecifics compared to other species. As Payne et al. (1987) pointed out, small hake are not found in the vicinity of adults of the species. This is supported by the observed size segregation by depth, which is more pronounced in *M. paradoxus* than in *M. capensis* (Gordoa and Duarte, 1991). Density-dependent cannibalism may be an important source of natural mortality that can stabilize fish populations (Smith and Reay, 1991), and for *M. capensis*, cannibalism has even been considered the main cause of natural mortality (Lleonart et al., 1985; Payne and Punt, 1985).

Our results on the trophic ecology of hake are of primary importance for future management of fish assemblages where this species plays an important predatory role. Multispecies management requires quantitative data on fish diet to elucidate the relationships between species and, consequently, to forecast temporal biomass fluctuations, under specific fishing regimes, in an integrated manner.

Literature cited

Abella, A., J. F. Caddy, and F. Serena.
1997. Do natural mortality and availability decline with age? An alternative yield paradigm for juvenile fisheries, illustrated by the hake *Merluccius merluccius* fishery in the Mediterranean. Aquat. Living. Resour. 10:1–14.

Aldebert, Y., L. Recasens, and J. Lleonart.
1993. Analysis of gear interaction in a hake fishery: the case of the Gulf of Lions (NW Mediterranean). Sci. Mar. 57:207–217.

Alheit, J., and T. J. Pitcher (eds.).
1995. Hake: fisheries, ecology and markets, 478 p. Chapman and Hall, London.

Alvarez, P., L. Motos, A. Uriarte, and J. Egana.
2001. Spatial and temporal distribution of European hake, *Merluccius merluccius* (L.), eggs and larvae in relation to hydro-biological conditions in the Bay of Biscay. Fish. Res. 50:11–128.

Andaloro, F., P. Arena, and S. Prestipino Giarritta.
1985. Contribution to the knowledge of the age, growth and feeding of hake *Merluccius merluccius* (L. 1758) in the Sicilian channel. FAO Fish Rep. 336:93–97.

Ardizzone, G. D., and F. Corsi.
1997. Atlas of Italian demersal fishery resources. Biol. Mar. Medit. 4(2), 568 p.

Arneri, E., and B. Morales-Nin.
2000. Aspects of the early life history of European hake from the central Adriatic. J. Fish. Biol. 53:1155–1168.

Beamish, F. W. H.
1966. Vertical migration of demersal fish in the northwest Atlantic. J. Fish. Res. Board Can. 23: 109–139.

Bouaziz, A., F. Djabali, and C. Maurin.
1990. Régime alimentaire du merlu (*Merluccius merluccius*, L., 1758) en baie de Bou Ismaïl. Rapp. Comm. int. Mer Médit. 32(1) :273.

Bowman, R. E., and E. W. Bowman.
1980. Diurnal variation in the feeding intensity and catchability of the silver hake (*Merluccius bilinearis*). Can. J. Fish. Aquat. Sci. 37:1562–1572.

Bozzano, A., L. Recasens, and P. Sartor.
1997. Diet of the European hake *Merluccius merluccius* (Pisces: Merlucciidae) in the Western Mediterranean (Gulf of Lions). Mar. Sci. 61(1):1–8.

Buchholz, F, C. Buchholz, J. Reppin, and J. Fischer.
1995. Diel vertical migration of *Meganyctiphanes norvegica* in the Kattegat: comparison of net catches and measurements with acoustic Doppler current profilers. Helgol. Wiss. Meeresunters 49:849–866.

Casanova, B.
1970. Répartition bathymétrique des euphausiacés dans le bassin occidental de la Méditerranée. Rev. Trav. Inst. Pêches Marit. 34(2):205–219.

Clarke, K. R., and R. M. Warwick.
1994. Change in marine communities: an approach to statistical analysis and interpretation, 144 p. Natural Environment Research Council, UK.

Colloca, F., A. Belluscio, and G. D. Ardizzone.
2000. Sforzo di pesca, cattura e gestione dello stock di nasello (*Meluccius merluccius*) in un'area del tirreno centrale. Biol. Mar. Medit. 7(1):117–129.

Colloca, F., P. Gentiloni, A. Belluscio, P. Carpentieri, and G. D. Ardizzone.
2002. Estimating growth parameters of the European hake (*Merluccius merluccius*) through the analysis and validation of annual increments in otoliths. Arch. Fish. Mar. Res. 50 (2):174–179.

Fisher, W., W. M. Bauchot, and M. Schneider.
1987. Fiches FAO d'identification pour les besoins de la pêche révision 1. Méditerranée et mer Noire. Zone de pêche 37, vol. 2: Vertèbres, p. 761–1530. FAO, Rome.

Flamigni, C.
1984. Preliminary utilization of trawl survey data for hake (*Merluccius merluccius*, L.) population dynamics in the Adriatic Sea. FAO Fish. Rep. 290:109–115.

Franqueville, C.
1971. Macroplancton profond (invertébrés) de la Méditerranée nord-occidentale. Tethys 3(1):11–56.

Froglia, C.
1973. Osservazioni sull'alimentazione del merluzzo (*Merluccius merluccius* L.) del Medio Adriatico. *In* Atti V Congresso Naz. Soc. It. Biol. Mar. (N. Salentina, ed.), p. 327–341.

Gordoa, A., and C. M. Duarte.
1991. Internal school density of Cape hake (*Merluccius capensis*). Can. J. Fish. aquat. Sci. 48:2095–2099.

Guichet, R.
1995. The diet of European hake (*Merluccius merluccius*) in the northern part of the Bay of Biscay. ICES J. Mar. Sci. 52:21–31.

Hacunda, J. S.
1981. Trophic relationships among demersal fishes in a coastal area of the Gulf of Maine. Fish. Bull. 79: 775–788.

Hickling, C. F.
1927. The natural history of the hake. Parts I and II. Fish. Invest. Serv. II, 10 (2), 112 p.

Holden, M. J., and D. F. S. Raitt.
1974. Manual of fisheries science. Part 2: Methods of resources investigation and their application. FAO Fish. Tech. Paper 115, 214 p. FAO, Rome.

Hyslop, E. J.
1980. Stomach content analysis: a review of methods and their application. J. Fish Biol. 17:411–429.

Jukic, S., and E. Arneri.
1984. Distribution of hake (*Merluccius merluccius,* L.) striped mullet (*Mullus barbatus,* L.) and pandora (*Pagellus erythrinus,* L.) in the Adriatic Sea. FAO Fish. Rep. 290:85–91.

Lleonart, J., J. Salat, and E. Macpherson.
1985. CVPA, an expanded VPA with cannibalism. Application to a hake population. Fish. Res. 12:119–146.

Link, J. S., and L. P. Garrison.
2002. Changes in piscivory associated with fishing induced changes to the finfish community on Georges Bank. Fish. Res. 55:71–86.

Macpherson, E.
1977. Estudio sobre relaciones troficas en peces bentonicos de la costa catalana. Ph.D. diss., 369 p. Universitat de Barcelona, Barcelona.

Oliver, P., and E. Massutí.
1995. Biology and fisheries of western Mediterranean hake (*M. merluccius*). *In* Fish and fisheries series 15, hake, fisheries, ecology and markets (J. Alheit and T. J. Pitcher), p. 181–202. Chapman and Hall, London.

Orsi Relini, L., F. Fiorentino, and A. Zamboni.
1989. Spatial-temporal distribution and growth of *Merluccius merluccius* recruits in the Ligurian Sea. Observations on the O group. Cybium (13):263–270.

Papaconstantinou, C., and E. Caragitsou.
1987. The food of hake (*Merluccius merluccius*) in Greek Seas. Vie Milieu 37:77–83.

Payne, A. I. L., B. Rose, and R. W. Leslie.
1987. Feeding of hake and a first attempt at determining their trophic role in the South African west coast marine environment, in The Benguela and comparable ecosystem (A. I. L. Payne, J. A. Gulland and K. H. Brink, eds.). S. Afr. J. Mar. Sci. 5:471–501.

Payne, A. I. L., and A. E. Punt.
1985. Biology and fisheries of South African cape hakes (*M. capensis* and *M. paradoxus*). Hake—fisheries, ecology and markets. Chapman and Hall, London.

Paz, J., J. M. Casas, and G. Perez-Gandaras.
1993. The feeding of cod (*Gadus morhua*) on Flemish Cap, 1989–90. NAFO Scientific Council Studies 19, p. 41–50.

Pinkas, L., M. S. Oliphant, and I. L. K. Iverson.
1971. Food habits of albacore, bluefin tuna and bonito in California waters. Calif. Dep. Fish Game Fish. Bull. 152:1–150.

Recasens, L., A. Lombarte, B. Morales-Nin, and G. J. Torres.
1998. Spatiotemporal variation in the population structure of the European hake in the NW Mediterranean. J. Fish. Biol., 53:387–401.

Relini, G., and C. Piccinetti.
1996. Ten years of trawl surveys in Italian seas (1985–1995). FAO Fish. Rep. 533:21–41.

Relini, G., J. Bertrand, and A. Zamboni.
1999. Synthesis of the knowledge on bottom fishery resources in central Mediterranean (Italy and Corsica). Biol. Mar. Medit. 6, 868 p.

Roel, B., and E. Macpherson.
1988. Feeding of *Merluccius capensis* and *M. paradoxus* off Namibia. S. Afr. J. Mar. Sci. 6:227–643.

Ross, S. T.
1978. Trophic ontogeny of the leopard searobins, *Prionotus scitulus* (Pisces: Triglidae). Fish. Bull. 76:225–234.

Sarano, F.
1986. Cycle ovarien du Merlu, *Merluccius merluccius*, poisson a ponte fractionnee. 2ev. Trav. Inst. Peches Marit. 48:65–67.

Smith, C., and P. Reay.
1991. Cannibalism in teleost fish. Rev. Fish Biol. Fish 1:41–64.

Vallet, C., and J. C. Dauvin.
2001. Biomass changes and bentho-pelagic transfers throughout the Benthic Boundary Layer in the English Channel. J. Plankton Research, vol. 23(9):903–922.

Velasco, F., and I. Olaso.
1998. European hake *Merluccius merluccius* (L., 1758) feeding in the Cantabrian Sea: seasonal, bathymetric and length variations. Fish. Res. 38:33–44.

Biology of queen snapper (*Etelis oculatus*: Lutjanidae) in the Caribbean

Bertrand Gobert
Institut de Recherche pour le Développement (IRD)
Technopôle Brest-Iroise
BP 70
29280 Plouzané, France
E-mail address: gobert@ird.fr

Alain Guillou
Institut Français de Recherche pour l'Exploitation de la Mer (Ifremer)
Boulevard Jean Monnet
BP 171
34203 Sète Cedex, France

Peter Murray
Organization of Eastern Caribbean States (OECS)
Environment and Sustainable Development Unit
The Morne
PO Box 1383
Castries, Saint Lucia

Patrick Berthou
Institut Français de Recherche pour l'Exploitation de la Mer (Ifremer)
BP 70
29280 Plouzané, France

Maria D. Oqueli Turcios
38, rue Desaix
75015 Paris, France

Ester Lopez
Département Halieutique
Ecole Nationale Supérieure Agronomique de Rennes
65, rue de Saint-Brieuc
CS 84215
35042 Rennes Cedex, France

Pascal Lorance

Jérôme Huet
Institut Français de Recherche pour l'Exploitation de la Mer (Ifremer)
BP 70
29280 Plouzané, France

Nicolas Diaz
Boyer
97129 Lamentin
Guadeloupe, French West Indies

Paul Gervain
Rue Authe 2
Petit Paris
97100 Basse Terre
Guadeloupe, French West Indies

The queen snapper (*Etelis oculatus*) is among the deepest dwelling species of the family Lutjanidae, and the only Atlantic species of *Etelis*. Its distribution covers the tropical western Atlantic Ocean, from North Carolina to the eastern tip of Brazil, at depths of 130 to 450 m (Allen, 1985).

Although it reaches a large size and presents no risk of ciguatoxicity (Lorance[1]), the species is exploited by only a few fisheries in the Caribbean. Most often it is only a minor part of the catch of line fisheries that focus on the whole community of deep snappers, or on more abundant species such as vermilion snapper (*Rhomboplites aurorubens*) or silk snapper (*Lutjanus vivanus*) (e.g., in Venezuela: Mendoza and Larez, 1996). In a few cases, however, *E. oculatus* is specifically sought by fishermen; for example, in Saint-Lucia within a traditional fishery operating during the months when migratory pelagics are not fished (Murray et al., 1992), or in Bermuda where it has been caught irregularly (pulse fishery) since the ban on potfishing (Luckhurst, 1996). Commercial exploitation is only beginning in the French West Indies, but is much more developed in Barbados (Prescod et al., 1996) and Puerto Rico (Matos-Caraballo, 2000). Exploitation of the queen snapper is poorly documented, and very few detailed catch statistics are available; in all cases, the amounts landed in each country are small (probably not exceeding a few tens of tons per year), but the potential production of these resources has never been estimated.

Owing to the depth of its habitat and to the relatively small economic importance of the fisheries for queen snapper on the local scale, very little is known about the biology of *E. oculatus*. It is generally cited in species checklists or in general descriptions of deepwater fisheries. Very few studies actually have focused on the species itself (Murray, 1989; Murray and Charles, 1991; Murray et al., 1992; Murray and Moore, 1992; Murray and Neilson, 2002).

The objective of this study is to present new information about the biology of *E. oculatus*, obtained from fishing experiments undertaken since the 1980s in the French West Indies (Martinique, Guadeloupe, Saint-Barthélemy, and the French part of Saint-Martin), Dominica and Saint-Lucia, and from a study conducted in the late 1990s on the artisanal and semi-industrial fisheries off the Caribbean coast of Honduras.

Material and methods

Areas studied

The data were collected from various research projects (Fig. 1 and Table 1):

[1] Lorance, P. 1988. La ciguatoxicité des poissons sur les bancs de Saint-Barthélémy, Saint-Martin et Anguilla. Doc. Sci. Pôle Caraïbe 15, 31 p. [Available from Ifremer, Pointe Fort, 97231 Le Robert, France.]

Manuscript submitted 16 September 2003 to the Scientific Editor's Office.
Manuscript approved for publication 20 October 2004 by the Scientific Editor.
Fish. Bull. 103:417–425 (2005).

Figure 1

Study area and locations sampled for queen snapper (*Etelis oculatus*) by Caribbean fisheries 1982–2001.

1) On the French parts of the wide shelf shared by St-Martin, St Barthémely, and Anguilla (abbreviated as SMSBA shelf in the text), exploratory fishing experiments were conducted to assess the fishing potential and the risk of ciguatoxicity (Lorance[2]). The deep slopes of the bank (200–300 m) were fished in 1986–87, using bottom longlines, trammel nets, and secondarily bottom gill nets.
2) In Martinique, exploratory fishing experiments were conducted in 1986–87 on various parts of the shelf slope (100–300 m), and some observations were made in 1982 and 1988–91, mainly with gill nets and trammel nets (Guillou[3]).
3) In Saint-Lucia, observations were made in 1987 on the commercial fishery, and fishing experiments were conducted in 1992 with longlines (Guillou[4]).
4) In Dominica, fishing experiments were conducted in 1992 with longlines and gill nets.
5) In Guadeloupe, experiments were conducted in 2001 with gill nets in the range 200–400 m (Diaz et al., in press); some small *Etelis* were also caught with 10-mm-mesh traps used for a survey of deep crustacean resources.
6) In the Bay Islands, off the Caribbean coast of Honduras, a fisheries survey was conducted in 1999–2000 as part of a coastal zone management project (Berthou et al.[5]). This artisanal fishery uses mainly handlines to catch snappers and groupers on the shelf, but a fraction of the fishing effort is directed towards the deepwater snappers on the shelf slopes.
7) In Honduras, the landings of the semi-industrial fishing fleet based in Roatán (Bay Islands) were studied, through catch statistics of the export firms and by sampling in the collecting centers (de Rodellec[6]). These fleets target snappers and groupers over the entire Caribbean shelf of Honduras, and fish with handlines.

---

[2] Lorance, P. 1989. Ressources demersales et descriptions des pêcheries des bancs de St-Martin et St Barthelemy. Rapp. Int. Dir. Ressources Vivantes Ifremer, DRV-89.039-RH/Martinique, 75 p. [Available from Ifremer, Pointe Fort, 97231 Le Robert, France.]

[3] Guillou, A. 1989. Ressources démersales du talus insulaire de la Martinique. Rapp. int. Dir. Ressources Vivantes Ifremer DRV-89.037-RH/Martinique, 121 p. [Available from Ifremer, Pointe Fort, 97231 Le Robert, France.]

[4] Guillou A., A. Lagin, and P. Murray. 1996. Observations réalisées sur la biologie et la pêche du «gros yeux» *Etelis oculatus* Val. aux Petites Antilles de 1982 à 1992. Doc. Sci. Pôle Caraïbe 33, 137 p. [Available from Ifremer, Pointe Fort, 97231 Le Robert, France.]

[5] Berthou P., M. D. Oqueli, E. Lopez, B. Gobert, C. Macabiau, and P. Lespagnol. 2001. Diagnostico de la pesca artesanal de la Islas de la Bahía, Honduras. Proyecto Manejo Ambiental de las Islas de la Bahía (PMAIB), Informe Tecnico PES-06, vol 1, 194 p. [Available from PMAIB, Roatán, Islas de la Bahía, Honduras.]

[6] de Rodellec, A. 2001. Les débarquements de poissons destinés à l'exportation dans l'île d'Utila (Iles de la Bahía, Honduras). Unpubl. report, IRD-Brest, 51 p. [Available from IRD, BP 70, 29280 Plouzané, France.]

Table 1

Summary of sample sizes and depth ranges of queen snapper (*Etelis oculatus*) by area and fishing gear, in exploratory or commercial fishing operations (SMSBA=Saint Martin-Saint Barthélémy-Anguilla).

Area	Trammel nets (exploratory)	Gill nets (exploratory)	Lines (exploratory)	Lines (commercial)	Depth range (m)
Martinique	300	209	6		140–300
SMSBA shelf	249		406		230–430
Saint-Lucia			34	394	210–290
Dominica		191	20		180–300
Guadeloupe		1133			195–410
Bay Islands				794	unknown
Honduran shelf				3948	unknown

Fishing gears used

In all islands but Guadeloupe, gill nets had mesh sizes of 65 mm (knot to knot) and a stretched height of 6.4 m. In Guadeloupe, mesh was 60 mm and height was 4 m; in addition, the nets were given more slack than in Martinique to increase their efficiency, and thus caught a wider size range of fish.

Trammel nets had mesh sizes of 40 mm (knot to knot) on the central panel and 200 mm on the outer panels, and were 2 m high. All nets (trammel nets and gill nets) were set overnight (15 to 20 hours of fishing time) in units of 200 or 300 m.

Three types of longlines were used in the fishing experiments. Vertical longlines were derived from those used by fishermen in the Lesser Antilles and had about 20 hooks on 40 cm-long secondary lines. Pole longlines were adapted from a technique used in Florida and Puerto-Rico: poles about 2 m long are fastened to the main line lying on the bottom, each having 12 to 25 hooks on very short secondary lines (20 to 30 cm). Reinforced longlines are horizontal longlines whose main line is heavier, in order to fish on very rough grounds. All longlines were hauled after 30 to 45 minutes fishing. For the analysis, no distinction was made between samples of these three types of longlines. Various kinds of longlines are used in the small-scale queen snapper fishery in Saint-Lucia. Handlines used in the artisanal and semi-industrial Honduran fisheries are either mono- or multifilament, and bear one or several hooks. No detailed observations were made on the size of hooks or on the bait used in the commercial queen snapper fisheries.

Data collected

None of these studies was specifically designed for the study of *E. oculatus*, and therefore the nature and amount of available information (sampling coverage though time, space, and depth) for this species were variable. Species identification (Allen, 1985; Anderson, 1987) could be done reliably in the field for adults and juveniles, but had to be confirmed under the microscope for the smallest individuals (less than 10 cm). Fish length was the only information recordable from professional landings (St-Lucia, Honduras); fishing experiments yielded more detailed data, by order of decreasing frequency: length (fork length FL, total length TL, or both; unless specified, all lengths mentioned in the text are fork lengths), weight, and sexual stage, and occasionally a few additional observations (such as unusual number or length of fin rays). Sexual stages were identified by using the macroscopic scale defined by Barnabé (1973) and were coded as follows: 1 (immature, without identifiable sex), 2 (immature, of identifiable sex), 3 (mature), 4 (prespawning), 5 (spawning), 6 (postspawning), and 7 (resting). Depth was recorded only in the fishing experiments; for gillnet and trammel-net stations, it was measured at each end of the net, and the depth used in the analysis was the average of these two values.

Length-frequency analysis

In most cases, length-frequency analysis was strongly hindered by gear selectivity and sample sizes. We attempted to estimate L_∞ and Z/K with the method of Wetherall et al. (1987) applied to the sample of the semi-industrial Honduran fishery. All other samples were unsuitable for length-frequency analysis because of severe violations of one or several assumptions, principally regarding constant catchability above the full selection length, which was obviously not the case for the three gears used in the fishing experiments.

Results

Depth distribution

During the fishing experiments, *E. oculatus* of marketable size (i.e., larger than about 20 cm) were caught

between 140 and 430 m. In Martinique, the trammel nets were set between 100 and 300 m but did not catch any *E. oculatus* in the shallowest part of this range. In Guadeloupe, gill nets were set down to 410 m, but the deepest catch of queen snapper was 340 m. No *E. oculatus* were caught in shallower (<80 m) fishing experiments with any of the gears used (traps, gill nets, trammel nets, and longlines) on the SMSBA shelf. According to some local fishermen, however, queen snappers can be caught from about 100 m down to 550 m (Lorance[2]).

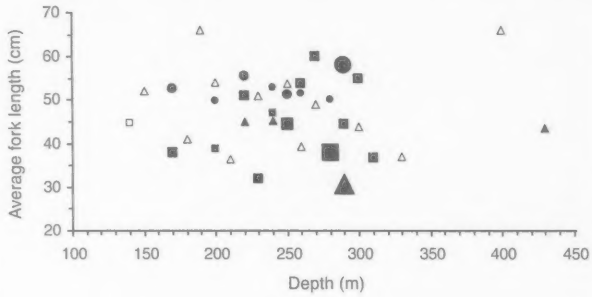

Figure 2

Average fork length of queen snapper (*Etelis oculatus*) by depth (m) strata in the fishing experiments with gill nets (circles), trammel nets (squares), and lines (triangles). Sample sizes are indicated by size of the symbols: empty symbol (n<10), filled symbol by increasing size (n=11–20, 21–50, 51–100, >100).

Depth-size relationship

No clear relationship between depth and average size of fish was found in the fishing experiments (Fig. 2). This is not unexpected given the selectivity of some gears (gill nets) and the small sample sizes in most depth strata outside the main fishing range (250–300 m); 70% of the 456 fish caught by longlines were in the 290 m depth stratum, and five or fewer fish were caught in most of the other strata.

A different picture emerges from the analysis of the professional fisheries of Honduras. Multivariate analysis (principal component analysis followed by hierarchical classification) applied to the landings by species revealed the two different categories of fish caught by the two types of semi-industrial vessels operating from Roatán (de Rodellec[6]), the shelf-operating fleet and the slope-operating fleet. The first category of fish were dominated by shallow species such as *Ocyurus chrysurus* (59.8%), *Lutjanus analis* (7.8%), and several grunts (Haemulidae), whereas *E. oculatus* accounted for only 2.2%. On the other hand, the second category comprised mainly deep snappers: *L. vivanus* (39.6%), *E. oculatus* (22.4%), *R. aurorubens* (6.9%) or *L. buccanella* (1.9%). The two divisions of the fleet independently exploit the continental shelf and the deep slope. Although actual depth of fishing operations is unknown, the shelf-operating fleet probably catches *E. oculatus* in the deepest part of its working area (i.e., at the shallowest part of the species' bathymetric range), whereas the slope-operating fleet exploits the main habitat of the deepwater snappers. The size structures of *Etelis* catches (Fig. 3, A and B) strongly indicate that only the fish up to 45–50 cm live on the shelf or its edge, whereas individuals of all sizes, and particularly the largest ones, inhabit the shelf slope.

A similar observation was made for the island of Roatán, where the artisanal fleet is the least developed of the archipelago: fishermen using small (<6 m) and often (57%) nonpowered canoes fish quite close to the shore and catch a large diversity of coastal reef fishes, a large proportion of which are juveniles. *Etelis oculatus* is rarely caught by these small-scale fishermen but is so only as individuals smaller than 50 cm, sometimes as small as 16 cm (Fig. 3C).

Habitat of early juveniles

Some observations were made on very small (smaller than 10 cm) individuals of *E. oculatus*. Off Guadeloupe, a few of them were entangled in gill nets at 300 m depth (Fig. 3D); on the same island, previous exploratory fishing operations with small-mesh traps caught six juveniles ranging from 5.5 to 7 cm FL at 490 m depth; off Dominica, one small individual (8.5 cm TL) was found in the stomach of a predator caught at a depth greater than 200 m (see below). In spite of the general tendency of increasing size with depth found for the larger individuals, these observations show that the habitat of early postsettlement juveniles is not restricted to the shallowest part of the species depth range.

Morphometric relationships

The main morphometric relations were computed from the fish sampled in commercial or scientific fishing operations in the Lesser Antilles (Martinique, Saint-Lucia, SMSBA shelf). Because the differences between relations for males and females were insignificant, only global equations are given (Table 2).

Maximum size and weight

The largest individual caught was 90 cm FL in the Lesser Antilles (Guadeloupe) and 86 cm in Honduras, and the maximum weight recorded was 6280 g, in the Lesser Antilles; fish were not weighed individually in Honduras.

Sex-related length differences

When sex was recorded, the largest fish were always female, and no male was found above 70 cm. The difference between size-structure of male and female catches

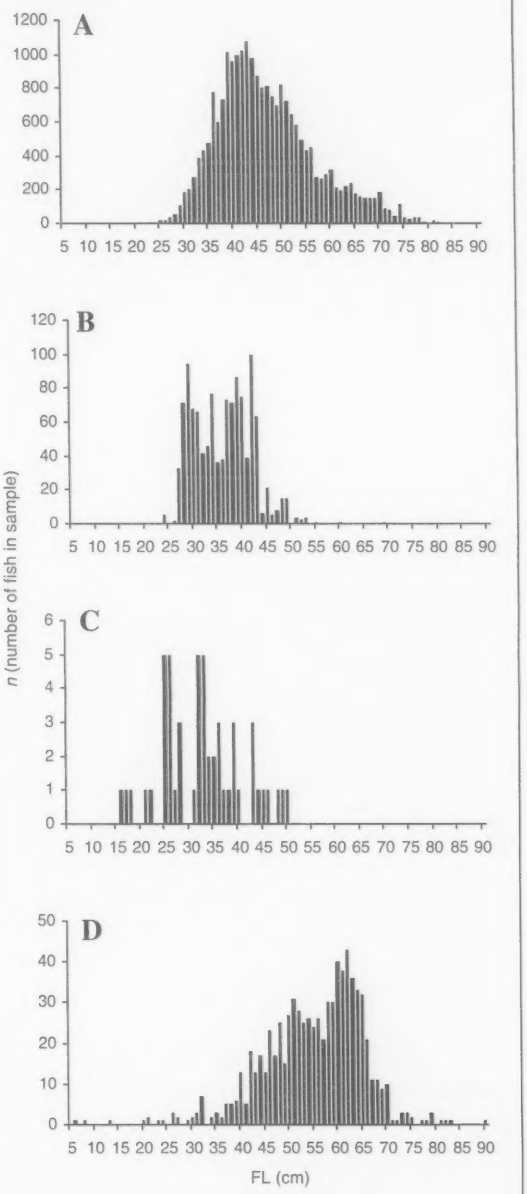

Figure 3

Length-frequency distributions for queen snapper (*Etelis oculatus*) catches. (**A**) Semi-industrial deepwater Hondurian line fishery (n=3415). (**B**) Semi-industrial shallow-water Hondurian line fishery (n=387). (**C**) Artisanal line fishery of Roatán (Honduras) (n=52). (**D**) Gillnet exploratory fishing in Guadeloupe (n=779). (**E**) Trammel-net exploratory fishing in all areas: males (n=231). (**F**) Trammel-net exploratory fishing in all areas: females (n=227).

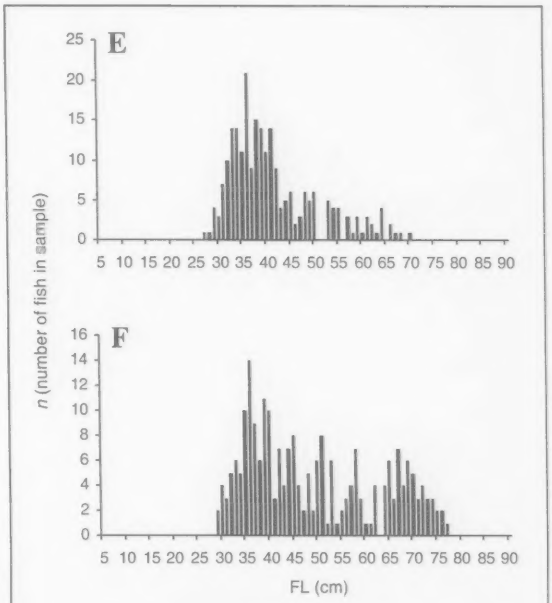

Figure 3 (continued)

was particulary clear for trammel nets (Fig. 3, E and F): the mode corresponding to fish gilled in the small-mesh central panel had similar characteristics for both sexes (range 25–45 cm and peak at 36 cm), as opposed to the diffuse mode for fish >45 or 50 cm (predominantly females) entangled in the large-mesh outer panels. With many fewer fish (n=23 for both sexes), the longline samples showed a similar difference between sizes of males (maximum 55 cm, mean 43.8 cm) and females (maximum 71 cm, mean 51.8 cm). In Guadeloupe, the sex of fish was not determined, but the existence of two modes in the overall size structure of gillnet catches (Fig. 3D) could possibly be related to this sex-related length difference.

Growth and mortality

The data collected in the various surveys did not allow any reliable analysis of the growth of *E. oculatus*. Because growth may be different for males and females, the length-frequency distributions of the large samples (where sex was not determined) from Honduras could not be processed rigorously to estimate life-history population parameters. However, in order to provide preliminary information on such a little known species, the regression method of Wetherall et al. (1987) was used in the modified version of FiSAT (Gayanilo et al., 1996) to estimate L_∞ and Z/K. With a satisfactory fit of the regression line (r=0.986), the estimates were L_∞ = 90.57 cm and Z/K = 3.73. For the reason mentioned above (together with other weaknesses related to possible violations of the hypotheses underlying the regression

Table 2
Morphometric relationships established for queen snapper (*Etelis oculatus*).

Parameters	Equation	Sample size	r
FL (cm) – TL (cm)	$TL = 2.7458 + 1.1644 \times FL$	842	0.987
TL (cm) – FL (cm)	$FL = -1.0028 + 0.8368 \times TL$	842	0.987
FL (cm) – W (g)	$W = 0.02748 \times FL^{2.8348}$	499	0.990
TL (cm) – W (g)	$W = 0.03006 \times FL^{2.8147}$	487	0.990

method), these estimates have to be seen only as indications that the asymptotic length of *E. oculatus* is quite large and that the Hondurian population is moderately exploited (if $M \approx 2K$, as suggested by Ralston (1987) for snappers, then $Z/K = 3.73$ and $E = F/Z \approx 0.46$).

Reproduction

Macroscopic observations of gonads were recorded for 309 fish whose sex could be identified (118 males and 191 females); all stages of the reproductive cycle were observed, but only 20 individuals were in the prespawning to postspawning stages, and a single one was found to be in the process of spawning.

The smallest fish with developing gonads was 36 cm for females and 29 cm for males (Fig. 4). Although only part of the length range of males was adequately sampled (100 out of the 118 fish were smaller than 44 cm), it appears that the progressive build-up of the reproductive male population occurs between about 30 cm and 45 cm. The picture is clearer for females, whose sample size was larger and more evenly spread over the length range: above 54 cm, all females were found to be in a reproductive cycle. The maturing process therefore occurs at clearly lower sizes for males (30–45 cm) than for females (35–55 cm). Females in advanced reproductive stages (postspawning and resting stages) were observed across the length range, including the smallest adult sizes, those below 45 cm (Fig. 4).

A full analysis of the seasonality of reproduction is not possible because data were collected in only seven months, out of which only four (May, June, November, and December) yielded samples large enough for the analysis (21 to 72 females per month). No females were found to be spawning, but most of the pre- and postspawning stages (14 out of 17) were observed in November and December, and half of maturing females were fished during the last quarter of the year (Fig. 5). However, 74% of females at sexual rest (resting stage) were caught in May and June. Additional pieces of information confirm this pattern: the only spawning individual, a male, was observed in November (Dominica); females gonads in advanced stage of vitellogenesis were observed in September (Guadeloupe); no mature individual was found in Honduras in April–June. These observations show that an active spawning period occurs at the end of the year (even if all fish caught at this period were not close to the spawning phase), as opposed to late spring which is a period of sexual inactivity.

Such limited results leave open the overall interpretation of the annual reproductive cycle of *E. oculatus*. In particular, according to the fishermen working on the SMSBA shelf, the species could have an extended spawning season, lasting from November to April or May.

Predators and prey

No systematic observations were made on the trophic relationships of *E. oculatus*, but a few occasional recordings were made of its predators and prey. The only record of a predator was that of a beardfish (*Polymixia lowei*: Polymixiidae) measuring 40 cm TL containing a very small queen snapper (8.5 cm TL) and which was caught deeper than 200 m. This is the first record of such a food item for this beryciform fish whose diet had so far been reported to comprise cephalopods (Cervigon, 1991). The stomachs of *E. oculatus* that could be observed were most often empty; on a few occasions, unidentified squids were the only items present. This was the case for three fish (58 to 62 cm) caught at 430 m depth.

Discussion

Etelis oculatus was found on the upper part of the continental and insular slopes, from about 150 to 450 m; this observed range confirms previous indications (Allen, 1985), but the bathymetric distribution of the species could possibly extend beyond the maximum depth fished in these surveys. The presence of *E. oculatus* in shallower waters of the shelf seems possible, according to a statement that juveniles can be found in less than 30 m (Appeldoorn et al., 1987) and to the reported catch of one fish (size not recorded) at 59 m depth by a trawl survey off southeastern United States (Cuellar et al., 1996). However the present data, other fishery-independent surveys focusing on snappers (i.e., Marcano et al., 1996, down to 128 m), and most studies on Caribbean coastal fisheries strongly indicate that the species is very rare on the shelf itself.

Within the observed depth range, there is a tendency for the largest fish to be found in the deeper areas, as observed in the closely related Pacific species

E. carbunculus and *E. coruscans* (Brouard and Grandperrin[7]), other deepwater lutjanids (Boardman and Weiler, 1980; Cuellar et al., 1996), and many reef fish species. The maximum size recorded for large samples (90 cm FL) is much greater than the 60 cm TL indicated by Allen (1985) but is consistent with other field observations, such as 94 cm TL in Saint-Lucia (Murray, 1989) or 100 cm TL in Venezuela (Cervigon, 1991).

No reliable growth estimate could be obtained because males and females showed very different size structures, and the only data suitable for length-frequency analysis were data for which the sexes had not been determined.

Important differences were found between sexes in terms of size structure and maturation size. Male *E. oculatus* attain a smaller length than females, and are much rarer above 45 cm. Sex-ratios skewed in favor of females in large size classes were observed in the most complete studies of snapper populations (Grimes, 1987), including Pacific deepwater snappers (Brouard and Grandperrin[7]), and probably result from a difference in growth and mortality between the sexes; in Cuba, for instance, females of most snapper species have been found to grow faster than males (Claro and Garcia-Arteaga, 2001). In the present study, sex-specific growth and mortality estimates were not available, but our interpretation seems likely because other possible causes could be ruled out, such as selectivity of nets (morphometric relationships are identical for both sexes) and fish behavior in relation to fishing gear (differences between sexes, however, were observed in trammel nets and lines whose catch mechanism is completely different). Different habitat preferences, which can lead to sex-related size structures in reef species (Garcia-Cagide et al., 2001), seem unlikely in our study because the deep slopes have fewer habitat gradients than the shallower reef environments and because no relation was found between depth and sex-ratio. A similar difference between males and females was found for reproductive size. Male snappers generally mature at a slightly smaller size than females, but sex does not appear as a significant factor of variation for relative length at first reproduction, as opposed to depth or continental or insular habitat (Grimes, 1987).

In the Lesser Antilles, *E. oculatus* spawns at the end of the year and has a period of sexual rest during from late spring through early summer. These results are not sufficient to establish the entire annual reproductive pattern, and even these partial findings cannot be applied to other parts of the Caribbean because snapper populations of continental and insular shelves generally show different seasonal patterns of reproduction (Grimes, 1987). This indication of a spawning period for *E. oculatus* in the cold season contrasts with the two eteline species (*Aprion virescens* and *E. coruscans*) studied in Hawaii, which have a protracted spawning period extending through the summer (May or June through October or November) (Everson et al., 1989).

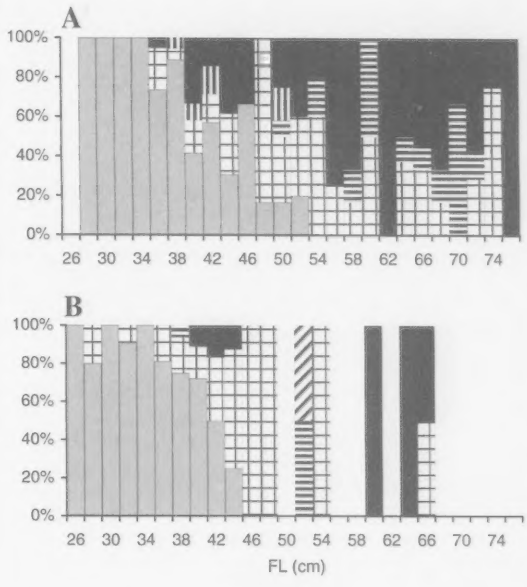

Figure 4

Proportion of sexual stages by 2-cm length classes for (**A**) female (n=191) and (**B**) male (n=118) queen snapper (*Etelis oculatus*): immature fish (gray), maturing fish (large squares), prespawning (horizontal bars), spawning (oblique bars), postspawning (vertical bars), sexual rest (black). Empty areas indicate the absence of data for the length class.

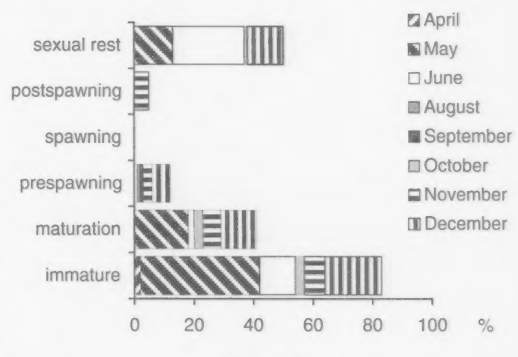

Figure 5

Distribution of sexual stages of queen snapper (*Etelis oculatus*) by month.

[7] Brouard, F., and R. Grandperrin. 1985. Les poissons profonds de la pente récifale externe à Vanuatu. South Pacific Commission, 17ème conférence technique régionale des pêches, Nouméa (Nouvelle Calédonie) 5–9 August 1985. SPC/Fisheries 17/WP.12 , 131 p. [Available from SPC, BP D5, 98848 Noumea Cedex, New-Caledonia, France.]

The data collected in these studies did not allow the analysis of the aggregation pattern of *E. oculatus*. In the Pacific, *E. coruscans* was found to form feeding aggregations near underwater promontories and these aggregations had important consequences for catchability (Ralston et al., 1986). For the deeper living alfonsinos (*Beryx* spp.) and orange roughy (*Hoplostethus atlanticus*), fisheries have shown their ability to quickly fish down aggregations once they are discovered (Lorance and Dupouy, 2001). Added to "K-selected" life-history strategies (high longevity, slow growth, late reproduction) and irregular recruitment, this aggregating behavior reinforces the vulnerability of deepwater species to overfishing (Koslow et al., 2000).

Recently gained knowledge about the exploitation of seamount and deep bank fish resources (Clark, 2001) cannot be applied directly to *E. oculatus* and the other slope-dwelling snappers which, although they are the deepest dwelling species of the family, are much closer in terms of demographic strategy to their shallow relatives (longevity 10–20 years; Manooch, 1987) than to these truly deep species (longevity 50 to more than 100 years; Koslow et al., 2000). However, less extreme life history traits do not protect deep snappers against overfishing, as shown by the example of *E. coruscans* and *E. carbunculus* in Hawaii (Simonds, 1995). The limited fishery data available on *E. oculatus* in the Caribbean do not seem to show evidence of a similar situation so far, but the stocks are being increasingly fished without much scientific basis (i.e., catch statistics) for management (Mahon, 1990; FAO, 1993). Regulation measures continue to be defined (Diaz et al., in press), but so far they are based only on conservative rules of thumb because of a lack of reliable biological information. To address this lack of information, future research on *E. oculatus* therefore should address, in particular, sex-specific growth, reproductive biology, and fine-scale distribution patterns.

Acknowledgments

The data presented here were collected and processed with the help of many people; the authors particularly wish to thank E. Burgos, T. and J. Chapelle, P. Galera, J. Grelot, A. Lagin, P. Lespagnol, L. Reynal, J. Robin, B. Séret, and the Chief Fisheries Officers of Dominica and Saint-Lucia.

Literature cited

Allen, G. R.
1985. FAO species catalogue. Vol. 6. Snappers of the world. An annotated and illustrated catalogue of lutjanid species known to date. FAO Fish. Synop. 125, vol. 6:1–208.

Anderson, W. D.
1987. Systematics of fishes of the family Lutjanidae (Perciformes: Percoidei), the snappers. *In* Tropical snappers and groupers. biology and fisheries management (J. J. Polovina and S. R. Ralston, eds), p. 1–31. Westview Press, Boulder, CO.

Appeldoorn, R., G. D. Dennis, and O. Monterrosa Lopez.
1987. Review of shared demersal resources of Puerto-Rico and the Lesser Antilles region. FAO Fish. Rep. 383:36–106.

Barnabé, G.
1973. Contribution à la connaissance de la croissance et de la sexualité du Loup (*Dicentrarchus labrax* L.) de la region de Sète. Ann. Inst. Oceanogr. Paris (nouv. ser.) 49:49–75.

Boardman C., and D. Weiler.
1980. Aspects of the life history of three deepwater snappers around Puerto Rico. Proc. Gulf Carib. Fish. Inst. 32:158–172.

Cervigón, F.
1991. Los peces marinos de Venezuela, 951 p. Fundación Científica Los Roques, Caracas, Venezuela.

Claro, R., and J. P. García-Arteaga
2001. Growth patterns of fishes of the Cuban shelf. *In* Ecology of the marine fishes of Cuba (R. Claro, K. C. Lindeman, and L. R. Parenti, eds.), p. 149–178. Smithsonian Institution Press, Washington and London.

Clark, M.
2001. Are deepwater fisheries sustainable ? The example of orange roughy (*Hoplostethus atlanticus*) in New Zealand. Fish. Res. 51:123–135.

Cuellar, N., G. R. Sedberry, D. J. Machowski, and M. R. Collins.
1996. Species composition, distribution and trends in abundance of snappers of the southeastern USA, based on fishery-independent sampling. ICLARM Conf. Proc. 48:59–73.

Diaz, N., P. Gervain, and V. Druault-Aubin.
In press. Queen snapper (*Etelis oculatus*) experimental deep-sea gillnet fishery in Guadeloupe (F.W.I.). Proc. Gulf Carib. Fish. Inst. 55.

Everson A. R., H. A. Williams, and B. M. Ito.
1989. Maturation and reproduction in two Hawaiian eteline snappers, uku, *Aprion virescens*, and onaga, *Etelis coruscans*. Fish. Bull. 87:877–888.

FAO (Food and Agricultural Organization of the United Nations).
1993. Marine fishery resources of the Antilles. FAO Fish. Tech. Paper 326:1–235.

García-Cagide A., R. Claro, and B. V. Koshelev.
2001. Reproductive patterns of fishes of the Cuban shelf. *In* Ecology of the marine fishes of Cuba (R. Claro, K. C. Lindeman, and L.R. Parenti, eds.), p. 73–114. Smithsonian Institution Press, Washington and London.

Gayanilo F., P. Sparre, and D. Pauly.
1996. FAO-ICLARM stock assessment tools. User's manual. FAO Comput. Inform. Ser. Fisheries 8:1–126.

Grimes C. B.
1987. Reproductive biology of the Lutjanidae: a review. *In* Tropical snappers and groupers: biology and fisheries management (J. J. Polovina and S. R. Ralston, eds.), p. 239–294. Westview Press, Boulder, CO.

Koslow J. A., G. Boehlert, J. D. M. Gordon, R. L. Haedrich, P. Lorance, and N. Parin.
2000. Continental slope and deep-sea fisheries: implications for a fragile ecosystem. ICES J. Mar. Sci. 57:548–557.

Lorance P., and H. Dupouy.
2001. CPUE abundance indices of the main target species of the French deep-water fishery in ICES sub-areas V–VII. Fish. Res. 51:137–149.
Luckhurst B. E.
1996. Trends in commercial fishery landings of groupers and snappers in Bermuda from 1975 to 1992 and associated fishery management issues. ICLARM Conf. Proc. 48:277–288.
Mahon, R.
1990. Fishery management options for Lesser Antilles countries. FAO Fish. Tech. Paper 313:1–126.
Manooch, C. S.
1987. Age and growth of snappers and groupers. *In* Tropical snappers and groupers: biology and fisheries management (J. J. Polovina and S. R. Ralston, eds.), p. 329–373. Westview Press, Boulder, CO.
Marcano, L. A., R. Guzman, and G. J. Gomez.
1996. Exploratory fishing with traps in oceanic islands off eastern Venezuela during 1992. ICLARM Conf. Proc. 48:331–336.
Matos-Caraballo, D.
2000. Overview of Puerto Rico's small-scale fisheries statistics: 1994–1997. Proc. Gulf Carib. Fish. Inst. 51:215–231.
Mendoza, J. J., and A. Larez,
1996. Abundance and distribution of snappers and groupers targeted by the artisanal medium range fishery off northeastern Venezuela (1981–1992). ICLARM Conf. Proc. 48:266–276.
Murray, P. A.
1989. A comparative study of methods for determining mean length-at-age and von Bertalanffy growth parameters for two fish species. M. Phil. thesis, 222 p. Univ. West Indies, Cave Hill, Barbados.
Murray, P. A., and A. V. Charles.
1991. Some considerations for increasing landings of the queen snapper, *Etelis oculatus* Val., in the Saint Lucian fishery. FAO Fish. Rep. 431 (suppl):75–77.
Murray P. A., L. E. Chinnery, and E. A. Moore.
1992. The recruitment of the queen snapper, *Etelis oculatus* Val., into the St Lucian fishery: recruitment of fish and recruitment of fisherman. Proc. Gulf Carib. Fish. Inst. 41:297–303.
Murray, P. A., and E. A. Moore.
1992. Some morphometric relationships in *Etelis oculatus* Valenciennes (Queen snapper), landed in St Lucia, W.I. Proc. Gulf Carib. Fish. Inst. 41:416–421
Murray, P. A., and J. D. Neilson.
2002. A method for the estimation of the von Bertalanffy growth rate parameter by direct examination of otolith microstructure. Proc. Gulf Carib. Fish. Inst. 53:516–525.
Prescod, S. D., H. A. Oxenford, and C. Taylor.
1996. The snapper fishery of Barbados: present status and a preliminary assessment of the potential for expansion. Proc. Gulf Carib. Fish. Inst. 44:159–179.
Ralston, S.
1987. Mortality rates of snappers and groupers. *In* Tropical snappers and groupers: biology and fisheries management (J. J. Polovina and S. R. Ralston, eds.), p. 375–404. Westview Press, Boulder, CO.
Ralston, S., R. M. Gooding, and G. M. Ludwig.
1986. An ecological survey and comparison of bottom fish resource assessments (submersible versus handline fishing) at Johnston atoll. Fish. Bull. 84:141–155.
Simonds, K.
1995. Federal state cooperation in managing deepwater bottom fish in Hawaii. South Pacific Commission workshop on the management of South Pacific inshore fisheries, Noumea (New Caledonia), 26 Jun–7 Jul 1995. South Pac. Comm. Tech. Doc. Intergr. Coast. Fish. Manag. Proj. 12:299–309.
Wetherall, J. A., J. J. Polovina, and S. Ralston.
1987. Estimating growth and mortality in steady state fish stocks from length-frequency data. ICLARM Conf. Proc. 13:53–74.

Courtship and spawning behaviors of carangid species in Belize

Rachel T. Graham
Wildlife Conservation Society
P.O. Box 37
Punta Gorda, Belize
E-mail address: rgraham@wcs.org

Daniel W. Castellanos
Monkey River Village
Toledo District, Belize

Many species of reef fish aggregate seasonally in large numbers to spawn at predictable times and sites (Johannes, 1978; Sadovy, 1996; Domeier and Colin, 1997). Although spawning behavior has been observed for many reef fish in the wild (Wicklund, 1969; Smith, 1972; Johannes, 1978; Sadovy et al., 1994; Aguilar Perera and Aguilar Davila, 1996), few records exist of observations on the courtship or natural spawning for the commercially important family Carangidae (jacks) (von Westernhagen, 1974; Johannes, 1981; Sala et al., 2003). In this study, we present the first observations on the natural spawning behavior of the economically-valuable permit (*Trachinotus falcatus*) (Linnaeus, 1758) from the full to new moon period at reef promontories in Belize, with notes on the spawning of the yellow jack (*Carangoides bartholomaei*) (Cuvier, 1833), and the courtship of five other carangid species.

Permit belong to the family Carangidae and are broadly distributed in the western Atlantic Ocean from Massachusetts to southeastern Brazil, including the Caribbean Sea and Gulf of Mexico (Smith, 1997). Considered an inshore pelagic species (Valdez Muñoz and Mochek, 2001) that spawns offshore, permit utilize a range of habitats that include coastal mangroves and seagrass beds, reef flats, and fore-reef areas during their life-cycle (Crabtree et al., 2002). Permit are reported to feed during the day and may show similar feeding characteristics to the closely related *T. carolinus* that displays a clear circadian rhythm entrained to the light phase during its feeding period (Heilman and Spieler, 1999). According to otolith analysis of fish caught in Florida, permit live to at least 23 years and reach a maximum published fork length of 110 cm and a weight of 23 kg (Crabtree et al., 2002).[1,2] Permit are gonochoristic and Crabtree et al. (2002) recorded 50% sexual maturity for females at 547 mm FL or 3.1 years and males at 486 mm FL and 2.3 years. Permit exhibit a protracted spawning season from March to September in Cuba (García-Cagide et al., 2001) and from March to July in Florida (Crabtree et al., 2002). High gonadosomatic indices recorded for March and maturation of oocytes noted in late June–July (Crabtree et al., 2002) support the observations by García-Cagide et al. (2001) that permit are batch spawners and have an asynchronous cycle of vitellogenesis. Spawning cued by the full moon has been recorded in many species of reef and inshore fish (Johannes, 1978, 1981; Moyer et al., 1983; Crabtree, 1995; Hoque et al., 1999). Macroscopic gonadal analysis and observations on the timing of courtship and spawning in several carangid species in the wild (Johannes, 1981; Sala et al., 2003), coupled with gonadal sampling observations on the captive spawning behavior of the related bluefin trevally (*Caranx melampygus*) (Moriwake et al., 2001), further indicate that permit and other carangids display circa lunar periodicity when spawning naturally.

Permit represent a valuable resource for recreational fishermen throughout their range. In Florida, recreational fisheries land more than 100,000 fish per year, but declines in landings from 1991 to date prompted regulation (Crabtree et al., 2002) and a move towards catch-and-release of fish. As such, Belize is rapidly becoming known as a world-class flyfishing location due to its abundance of permit. The fishery is highly lucrative: flyfishers pay up to US$500 per day in Belize to catch and release a permit. This niche tourism industry has also become an economic alternative for local fishermen (Heyman and Graham[3]). Consequently, information on the timing and behavior of reproduction of permit can underpin conservation efforts that focus on a vulnerable stage in their life cycle.

[1] The IGFA (International Game Fishing Association) notes a record length for permit of 122 cm FL. 2001. Database of IGFA angling records until 2001. IGFA, Dania Beach, Florida, 33004.

[2] The United Nations notes a maximum weight of 36 kg for a permit. (Cervigón, F., R. Cipriani, W. Fischer, L. Garibaldi, M. Hendrickx, A.J. Lemus, R. Márquez, J. M. Poutiers, G. Robaina and B. Rodriguez. 1992. Fichas FAO de identificación de especies para los fines de la pesca. Guía de campo de las especies comerciales marinas y de aquas salobres de la costa septentrional de Sur América, 513 p. FAO, Rome.

[3] Heyman W. D., and R. T. Graham. 2000. The voice of the fishermen of Southern Belize, 44 p. TIDE (Toledo Institute for Environment and Development), P.O. Box 150, Punta Gorda, Belize.

Manuscript submitted 9 December 2003 to the Scientific Editor's Office.

Manuscript approved for publication 9 November 2004 by the Scientific Editor.

Fish. Bull. 103:426–432 (2005).

Materials and methods

Turneffe Elbow (17°09′N, 87°54′W) and Gladden Spit (16°35′N, 88°00′W) are two sites located on the Belize Barrier Reef that were monitored for abundance and behavior of many species of spawning reef fish between 1999 and 2002. Both sites are promontories with a sloping reef shelf that drops off steeply at a depth of 35–45 m to over 1000 m into the southern tip of the Cayman Trench. According to the spawning aggregation criteria developed by Domeier and Colin (1997), Turneffe Elbow and Gladden Spit attract, respectively, an estimated 13 and 27 species of reef fish that aggregate seasonally to spawn (Graham, 2003).

We logged over 270 hours of underwater monitoring of reef fish spawning aggregations at Turneffe Elbow and Gladden Spit, primarily from the full-moon to the new-moon from March to July from 2000 through 2002. Additional dives took place variously over the course of 3–5 days during the same lunar period from 1999 to 2002. Most dives for monitoring spawning aggregations took place between 0830 and 1100 hours, at midday, and between 1600 to 1730 hours of each diving day. Dives began 150–250 m north of both spawning aggregation sites and proceeded to the south along the reef platform edge. Dive depth usually began at about 30 m and decreased to 15 m as the dive progressed because of SCUBA decompression constraints. Dives normally lasted between 35 and 50 minutes. Horizontal and vertical visibility rarely dropped below 20–25 m.

Results and discussion

During 10 dive surveys (15 diving hours) at Turneffe Elbow, we observed a large school of 250 to 500 permit aggregating on the reef promontory (Table 1). The aggregated fish slowly swam into the south current along the south-facing sloping fore-reef shelf at 5–15 m depth and the steep drop-off located at ~30–35 m. The school streamed down to the spur and groove formations at about 20 m depth on the reef shelf and rose up into the upper water column again. Permit were loosely grouped and displayed little fear of divers, a behavior commonly observed among a range of other fish species that aggregate to spawn (Graham, 2003). Several individuals displayed a dark patch located above and behind the pectoral fin on both flanks. Permit displayed this same behavior coloration change during each encounter.

On 22 August 2000, 7 days after the full moon, at ~1730 (41 minutes before sunset at 1811 hours local time) we conducted our standard north to south fish census dive at a depth of ~20–30 m along the fore-reef drop off. During all dives horizontal and vertical visibility was at least 20 m and often over 40 m. We observed a school of ~300 permit descend from 5–15 m depth above the fore-reef drop-off to 25 m directly on the shelf edge. At ~1745 hours (26 min before sunset) within-group activity increased as permit schooled densely on the edge of the reef drop-off. At ~1750 hours, a subgroup of eight permit left the dense school and ascended in the water column to ~18 m depth. The lead individual initiating the ascent was ~100 cm FL and was pursued by seven fish ranging from ~55 to 75 cm FL. The pursuing fish nuzzled the larger fish's vent as it rose in the water column. All fish displayed a dark flank patch behind their pectoral fins. The lead permit then ceased its ascent at ~15 m, tilted its head down slightly and convulsed rapidly, releasing a puff of gametes. Pursuing permit tried to position their vents as closely as possible to the lead individual's while releasing their gametes. The resulting gamete cloud was less than 50 cm in diameter and dispersed within seconds (Fig. 1). Following gamete release, all fish descended quickly to the main school still located ~25 m below. Within moments this behavior was repeated and observed in two smaller groups of permit before all observations ceased because of a lack of light.

At Gladden Spit, we observed slightly different permit spawning behavior. On 7 April 2002 (10 days after the full moon), the aggregation remained in a restricted area ~100 m north of where we previously witnessed the spawning of several species of fish and ~30 m east of where we have also observed groupers *Epinephelus striatus*, *Mycteroperca tigris*, *M. venenosa*, and *M. bonaci* aggregate to spawn (Graham, 2003). Ambient water temperature was 27.7°C as measured by a temperature logger (Onset Corp. Tidbit data logger) moored at the spawning site at 30 m depth.

At least 300 permit—many of them large individuals (~70–90 cm FL)—schooled densely into a ball at ~1700 hours (66 minutes before sunset local time) near the reef shelf drop-off at a depth of ~40–48 m. Subgroups comprised five to nine fish, and the lead fish was much larger than the pursuers. Subgroups rapidly rose up on the periphery of the school, spawned at the apex of the aggregation, and descended towards the bottom of the school again. Spawning was more frenetic than that observed at Turneffe Elbow. Permit subgroups behaved in the same manner as that observed at Turneffe during spawning, and all spawning individuals displayed a large dark flank patch behind the pectoral fins.

Based on our observations of courtship and spawning behavior, our estimate of spawning season for permit in Belize may stretch from February to the end of October, beyond the period of March to September as suggested by García-Cagide et al. (2001) and Crabtree et al. (2002). Permit may also reach larger sizes than published by Crabtree et al. (2002); we estimated the largest individual permit observed at Turneffe Elbow in Belize to be ~120 cm FL, which may indicate that permit exceed a lifespan of 23 years.

We could not determine if the lead permit was female and the pursuing permit were males because no individuals were caught for gonadal analysis. However, carangids are gonochoristic and it is highly likely that the lead fish in the spawning rush was female. García-Cagide et al. (2001) noted that spawning females are often larger than mature males in several species of

Figure 1

Subgroup of eight permit (*Trachinotus falcatus*) immediately following spawning at Truneffe Elbow, Belize. The subgroup detached itself from the main aggregation to spawn in midwater at ~15 m. The larger fish led the ascent to 15 m; all fish in the subgroup hovered at that depth, released gametes, and returned to the main school at a depth of ~25 m. The arrow indicates the dark patch behind the pectoral fin that each fish sports during spawning.

reef fish. This is also supported by our observations of gonochoristic spawners such as the cubera snapper (*Lutjanus cyanopterus*) and the dog snapper (*L. jocu*) that display a pattern of group, broadcast spawning where larger females are swollen with roe and lead the subgroup spawning ascents (Graham, 2003).

Group spawning behavior in the yellow jack (*C. bartholomaei*) closely resembled that of permit. We recorded yellow jacks schooling at Gladden Spit on only two occasions (Table 1). On 7 April 2002, we observed that the yellow jacks spawned at ~1705 hours (61 minutes before sunset local time) at Gladden Spit, less than 50 m south of the school of spawning permit. The jacks schooled densely at ~40–45 m and subgroups of 5 to 8 fish detached themselves from within the school, ascending rapidly to ~35 m, releasing gametes at the apex, and descending into the school again. Observations ceased shortly thereafter because of depth constraints and decreasing light.

Not all species of carangids are group spawners. Pair spawning has been observed in species such as *C. ignobilis* and *Alectis indicus* in the Pacific (von Westernhagen, 1974) and *C. sexfasciatus* in the Gulf of California (Sala et al., 2003). We have also observed on numerous occasions pair courtship in crevalle jack (*C. hippos*), horse-eye jack (*C. latus*), and bar jack (*Carangoides ruber*) in schools exceeding 1000 fish, in rainbow runner (*Elagatis bipinnulata*) in schools of up to ~300 fish, and occasionally greater amberjack (*Seriola dumerili*) in schools numbering ~120 individuals, primarily following during the full-moon and waning moon periods between February and October (Table 1). These five species displayed extended pair courtship within and outside a large aggregation of conspecific fish as they swam along the edge of the reef drop-off. All courting pairs observed showed similar behavior. The chasing fish nuzzled the gonopore of the lead fish (whose head and upper body half had turned black but whose fins were lighter, Fig. 2, A and B) during prolonged chases, often swimming close to and at a perpendicular angle to the lead fish. *Seriola dumerili* also displayed dichromatism; the pursuing fish turned a vivid electric blue and exhibited a scrawled pattern on its upper flanks, similar to that displayed by the scrawled filefish (*Aluterus scriptus*). Occasionally, 1–10 individuals that did not display coloration changes followed the courting pairs. These five species may also pair spawn because their courtship behavior parallels that of *C. sexfasciatus*, observed by Sala et al. (2003) to spawn in pairs from the full moon to waning crescent periods from July to September. However, we did not observe any release of gametes during all pair courtship behavior.

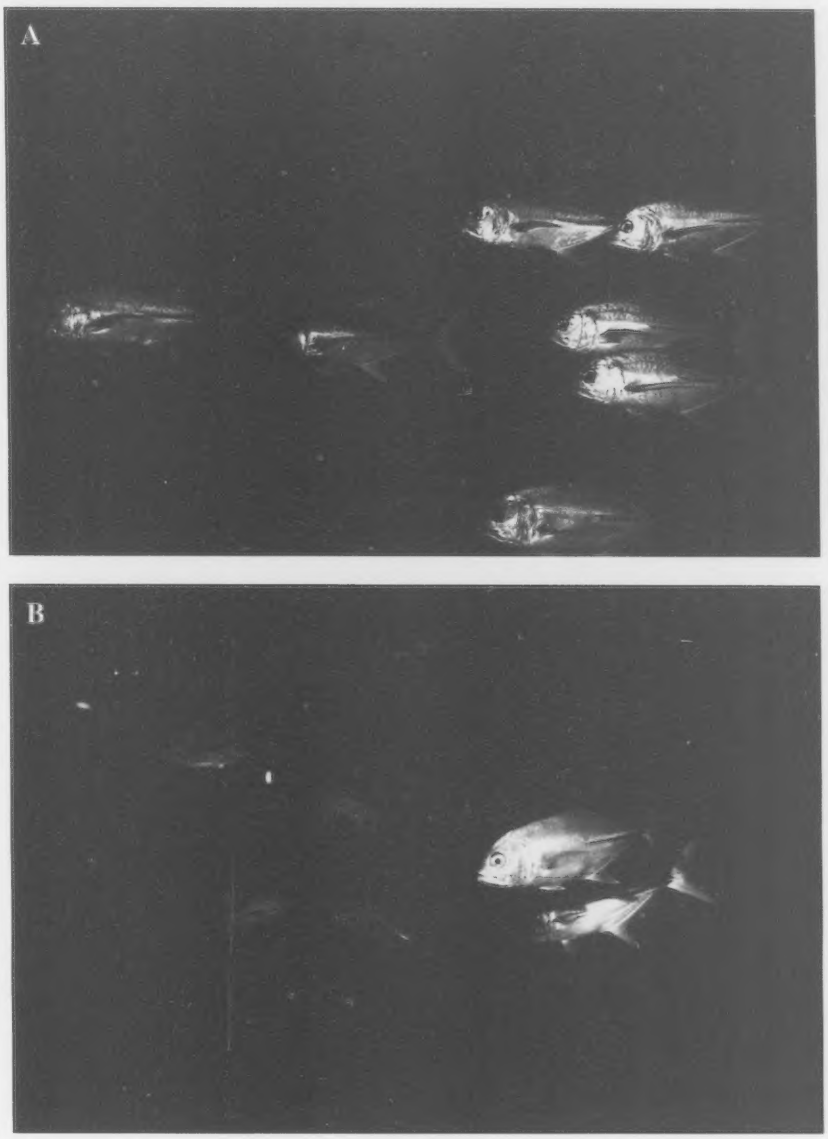

Figure 2

Pair courtship behavior in the horse-eye jack (*Caranx latus*) at Gladden Spit, Belize. The pursuing fish often swims slightly behind the lead and their flanks touch. The lead fish (**A**) remains silver colored, and the pursuing fish (**B**) takes on a very dark coloration around the head and upper flank during courtship.

Conclusions

Our observations confirm that permit spawn offshore at reef promontories that support other reef fish spawning aggregations. Permit demonstrate group broadcast spawning behavior and spawning events take place close to sunset. Further observations indicate that other species of carangids, such as yellow jack are also group broadcast spawners, occupying the same spatiotemporal spawning niche as permit. If observed courtship behav-

Table 1

Timing and lunar phase of observations on the schooling, courtship, and spawning of seven carangids at two reef promontories in Belize from April 1999 to July 2002. fm = full moon; dafm = days after full moon; dbfm = days before full moon. Sch = schooling; C = courting and color change; Spawn = spawning observed.

Date	Dive start time	Moon phase	Location	Species	Behavior
2 Apr 1999	12:04	2 dafm	Gladden	Yellow jack	Sch
3 Apr 1999	10:25	3 dafm	Gladden	Crevalle	Sch
5 Apr 1999	16:40	5 dafm	Gladden	Crevalle, horse-eye, rainbow runner	Sch
2 May 1999	16:50	2 dafm	Gladden	Bar jack, crevalle	Sch
5 May 1999	5:40	5 dafm	Gladden	Horse-eye, crevalle	Sch, C
30 May 1999	12:45	fm	Gladden	Amberjack, bar jack	Sch, C
3 Jun 1999	9:10	4 dafm	Gladden	Horse-eye, bar jack	Sch
4 Jun 1999	15:30	5 dafm	Gladden	Crevalle	Sch
30 Jun 1999	12:00	2 dafm	Gladden	Bar jack, horse-eye	Sch
27 Sep 1999	16:30	2 dafm	Gladden	Crevalle, amberjack	Sch, C
28 Sep 1999	10:50	3 dafm	Gladden	Crevalle, bar jack, horse-eye	Sch
	16:30	3 dafm	Gladden	Horse-eye, amberjack	Sch, C
24 Mar 2000	17:15	4 dafm	Gladden	Horse-eye	Sch, C
17 Apr 2000	16:25	1 dbfm	Gladden	Horse-eye, crevalle	Sch, C
18 Apr 2000	16:25	fm	Gladden	Bar jack, rainbow runner	Sch
19 Apr 2000	17:10	1 dafm	Gladden	Horse-eye	Sch, C
20 May 2000	17:00	2 dafm	Gladden	Crevalle	Sch, C
23 May 2000	16:45	5 dafm	Gladden	Amberjack	Sch, C
24 May 2000	16:21	6 dafm	Gladden	Bar jack	Sch
25 May 2000	~16:30	7 dafm	Gladden	Crevalle	Sch
26 May 2000	16:00	8 dafm	Gladden	Horse-eye, crevalle	Sch, C
23 Jun 2000	17:30	7 dafm	Gladden	Bar jack	Sch, C
18 Aug 2000	15:36	3 dafm	Gladden	Bar jack	Sch
	15:36	3 dafm	Gladden	Horse-eye, rainbow runner	Sch, C
19 Aug 2000	~12:00	4 dafm	Gladden	Bar jack, crevalle	Sch
20 Aug 2000	15:00	5 dafm	Turneffe	Horse-eye	C
	15:00	5 dafm	Turneffe	Permit	Sch
20 Aug 2000	17:00	5 dafm	Turneffe	Permit	Sch, C
	17:00	5 dafm	Turneffe	Amberjack, bar jack	Sch, C
21 Aug 2000	15:00	6 dafm	Turneffe	Crevalle, horse-eye	Sch, C
	15:00	6 dafm	Turneffe	Permit	Sch
22 Aug 2000	17:30	7 dafm	Turneffe	Horse-eye	C
	17:30	7 dafm	Turneffe	Permit	Spawn
14 Oct 2000	17:30	1 dafm	Gladden	Horse-eye, crevalle	C
15 Oct 2000	17:30	2 dafm	Gladden	Rainbow runner	C
17 Oct 2000	16:30	4 dafm	Turneffe	Horse-eye, crevalle	C
	16:30	4 dafm	Turneffe	Permit, amberjack	Sch
18 Oct 2000	16:30	5 dafm	Turneffe	Horse-eye, crevalle, amberjack, permit	C
13 Dec 2000	16:30	2 dafm	Gladden	Horse-eye	Sch
9 Apr 2001	16:00	1 dafm	Gladden	Horse-eye	C
8 May 2001	11:15	1 dafm	Gladden	Crevalle	C
9 May 2001	~10:30	2 dafm	Gladden	Crevalle	Sch
7 Jun 2001	17:00	1 dafm	Gladden	Crevalle, bar jack, horse-eye	Sch

continued

Table 1 (continued)

Date	Dive start time	Moon phase	Location	Species	Behavior
8 Jun 2001	17:00	2 dafm	Gladden	Amberjack, crevalle, horse-eye	Sch, C
9 Jun 2001	11:00	3 dafm	Gladden	Crevalle, horse-eye	Sch
10 Jun 2001	17:50	4 dafm	Gladden	Crevalle, horse-eye	Sch, C
3 Oct 2001	~17:00	1 dafm	Turneffe	Horse-eye	C
6 Feb 2002	16:00	9 dafm	Turneffe	Horse-eye, permit	Sch
7 Feb 2002	8:30	10 dafm	Turneffe	Horse-eye, permit	C
	16:30	10 dafm	Gladden	Horse-eye, crevalle, bar jack	Sch
28 Mar 2002	16:48	fm	Gladden	Crevalle, permit	Sch
	16:48	fm	Gladden	Horse-eye	C
29 Mar 2002	16:30	1 dafm	Gladden	Crevalle, bar jack, horse-eye	Sch
30 Mar 2002	16:45	2 dafm	Gladden	Crevalle, horse-eye	Sch
31 Mar 2002	16:40	3 dafm	Gladden	Horse-eye	Sch
1 Apr 2002	16:35	4 dafm	Gladden	Bar jack, horse-eye	Sch
3 Apr 2002	9:40	5 dafm	Gladden	Bar jack, horse-eye	Sch
7 Apr 2002	10:30	9 dafm	Gladden	Bar jack	Sch
	16:30	9 dafm	Gladden	Permit, yellow jack	Spawn
	16:30	9 dafm	Gladden	Bar jack	Sch
6 May 2002	9:40	9 dafm	Gladden	Horse	Sch
27 May 2002	12:18	1 dafm	Gladden	Horse-eye	C
30 May 2002	11:07	4 dafm	Gladden	Horse-eye	Sch
31 May 2002	16:20	5 dafm	Gladden	Crevalle	Sch
1 Jun 2002	16:15	6 dafm	Gladden	Bar jack, rainbow runner	Sch
2 Jun 2002	16:15	7 dafm	Gladden	Bar jack, horse-eye	Sch
29 Jun 2002	12:00	5 dafm	Turneffe	Permit, horse-eye	Sch
1 Jul 2002	15:00	7 dafm	Gladden	Bar jack, crevalle, horse-eye	Sch

ior is included, the spawning season for permit and horse-eye jacks is protracted from February through October, and the five other carangid species described in the present study spawned within this period. Protection of permit stocks throughout their life cycle, and particularly during their spawning season, underpins the associated rapidly growing and economically lucrative flyfishing tourism. Future directions of study should include a study of permit movement patterns between feeding and spawning grounds and mortality rates of catch-and-release fishing.

Acknowledgments

We would like to thank two anonymous reviewers who provided helpful suggestions for the improvement of this paper. The fieldwork and observations were supported by grants from the UK Darwin Initiative and the UK's Natural Environment Research Council. We worked under permits provided by the Belize Department of Fisheries.

Literature cited

Aguilar Perera, A., and W. Aguilar Davila.
1996. A spawning aggregation of Nassau grouper *Epinephelus striatus* (Pisces: Serranidae) in the Mexican Caribbean. Environ. Biol. Fishes 45:351–361.

Crabtree, R. E.
1995. Relationship between lunar phase and spawning activity of tarpon, *Megalops atlanticus*, with notes on the distribution of larvae. Bull. Mar. Sci. 56:895–899.

Crabtree, R. E., P. B. Hood, and D. Snodgrass.
2002. Age, growth and reproduction of permit (*Trachinotus falcatus*) in Florida waters. Fish. Bull. 100:26–34.

Domeier, M. L., and P. L. Colin.
1997. Tropical reef fish spawning aggregations: defined and reviewed. Bull. Mar. Sci. 60:698–726.

García-Cagide, A., R. Claro, and B. V. Koshelev.
2001. Reproductive patterns of fishes of the Cuban shelf. *In* Ecology of the marine fishes of Cuba (R. Claro, K. C. Lindeman and L. R. Parenti, eds.), p. 73–114. Smithsonian Institution Press, Washington DC.

Graham, R. T.
2003. Behavior and conservation of whale sharks on the

Belize Barrier Reef. Ph.D. diss., 408 p. Environment Department, Univ. York, York, UK.

Heilman, M. J., and R. W. Spieler.
1999. The daily feeding rhythm to demand feeders and the effects of timed meal-feeding on the growth of juvenile Florida pompano, *Trachinotus carolinus*. Aquaculture 180:53–64.

Hoque, M. M., A. Takemura, M. Matsuyama, S. Matsuura, and K. Takano.
1999. Lunar spawning in *Siganus canaliculatus*. J. Fish Biol. 55:1213–1222.

Johannes, R. E.
1978. Reproductive strategies of coastal marine fishes in the tropics. Environ. Biol. Fishes 3: 65–84.

Johannes, R. E.
1981. Words of the lagoon: fishing and marine lore in the Palau, District of Micronesia, p. 245. Univ. California Press, Berkeley, CA.

Moriwake, A. M., V. N. Moriwake, A. C. Ostrowski, and C. S. Lee.
2001. Natural spawning of the bluefin trevally *Caranx melampygus* in captivity. Aquaculture 203(1–2): 159–164.

Moyer, J. T., R. E. Thresher, and P. L. Colin.
1983. Courtship, spawning and inferred social organization of American angelfishes (Genera *Pomacanthus, Holacanthus* and *Centropyge; Pomacanthidae)*. Environ. Biol. Fishes 9:25–39.

Sadovy, Y.
1996. Reproduction of reef fishery species. *In* Reef fisheries (N. V. C. Polunin and C. M. Roberts, eds.), p. 15–59. Chapman and Hall, London.

Sadovy, Y., P. L. Colin, and M. L. Domeier.
1994. Aggregation and spawning in the tiger grouper, *Mycteroperca tigris* (Pisces: Serranidae). Copeia 1994:511–516.

Sala, E., O. Aburto-Oropereza, G. Paredes, and G. Thompson.
2003. Spawning aggregations and reproductive behavior of reef fishes in the Gulf of California. Bull. Mar. Sci. 72(1):103–121.

Smith, C. L.
1972. A spawning aggregation of Nassau grouper, *Epinephelus striatus* (Bloch). Trans. Am. Fish. Soc. 101:257–261.
1997. National Audubon Society field guide to tropical marine fishes of the Caribbean, the Gulf of Mexico, Florida, the Bahamas, and Bermuda, 718 p. Alfred A. Knopf, Inc., New York, NY.

Valdez Muñoz, E., and A. D. Mochek.
2001. Behavior of marine fishes of the Cuban shelf. *In* Ecology of the marine fishes of Cuba (R. Claro, K. C. Lindeman and L. R. Parenti, eds.), p. 53–72. Smithsonian Institution Press, Washington DC.

von Westernhagen, H.
1974. Observation on the natural spawning of *Alectis indicus* (Ruppell) and *Caranx ignobilis* (Forsk.) (Carangidae). J. Fish Biol. 6:513–516.

Wicklund, R.
1969. Observations on spawning of the lane snapper. Underwater Naturalist 6:40.

Comparison of two approaches for estimating natural mortality based on longevity*

David A. Hewitt
John M. Hoenig
Virginia Institute of Marine Science
The College of William and Mary
P.O. Box 1346
Gloucester Point, Virginia 23062
E-mail address (for D. A. Hewitt): dhewitt@vims.edu

Vetter (1988) noted that her review of the estimation of the instantaneous natural mortality rate (M) was initiated by a discussion among colleagues that identified M as the single most important but least well-estimated parameter in fishery models. Although much has been accomplished in the intervening years, M remains one of the most difficult parameters to estimate in fishery stock assessments. A number of novel approaches using tagging and telemetry data provide promise for making reliable direct estimates of M for a given stock (Hearn et al., 1998; Frusher and Hoenig, 2001; Hightower et al., 2001; Latour et al., 2003; Pollock et al., 2004). However, such methods are often impracticable and fishery scientists must approximate M by using estimates made for other stocks of the same or similar species or by predicting M from features of the species' life history (Beverton and Holt, 1959; Beverton, 1963; Alverson and Carney, 1975; Pauly, 1980; Hoenig, 1983; Peterson and Wroblewski, 1984; Roff, 1984; Gunderson and Dygert, 1988; Chen and Watanabe, 1989; Charnov, 1993; Jensen, 1996; Lorenzen, 1996).

We are concerned with two approaches for predicting M based solely on the longevity of the members of a stock—an approach that can be used when data are not available to make direct estimates of the parameter. One is a linear regression model (Hoenig, 1983) and the other is a simple rule-of-thumb approach. Hoenig (1983) found that M was inversely correlated with longevity across a wide variety of taxa and recommended use of the following predictive equation relating the maximum age observed in the stock (t_{max}) to M:

$$\ln(\hat{M}) = 1.44 - 0.982 \times \ln(t_{\max}). \quad (1)$$

The rule-of-thumb approach consists of determining the value of M such that $100(P)\%$ of the animals in the stock survive to the age t_{max}; thus,

$$\hat{M} = \frac{-\ln(P)}{t_{\max}}. \quad (2)$$

The challenge in this approach is determining an appropriate value for the proportion P.

The rule-of-thumb approach has the potential to be used widely because it is presented in Quinn and Deriso (1999) and stock assessment manuals of the Food and Agriculture Organization of the United Nations (FAO; Sparre and Venema, 1998; Cadima, 2003). The approach has recently been used extensively, in the specific form $M \approx 3/t_{max}$, in work related to stock assessments for blue crab (*Callinectes sapidus*). In this note, we 1) show that the regression model and the rule-of-thumb approach can be compared directly; 2) illustrate the difference in the estimates of M generated by the two approaches; 3) discuss the origins and current use of the rule-of-thumb approach; and 4) recommend that the regression model be used instead of the rule-of-thumb approach.

Methods

With the rule-of-thumb approach, the fraction of a population that survives to a given age is used to estimate M. This approach is equivalent to a quantile estimator (Bury, 1975). Suppose the fraction surviving to age t is described by the negative exponential function

$$\frac{N_t}{N_0} = e^{-Zt}, \quad (3)$$

where Z is the total instantaneous mortality rate. The quantile estimator is of the form

$$P = e^{-Z\tau_P}, \quad (4)$$

where τ_P is the age at which $100(P)\%$ of the population remains. In the case where $P = 0.05$, the estimator, based on data from a sample of the population, is

$$0.05 = e^{-\hat{Z}t_{0.05}}, \quad (5)$$

where 5% of the animals in the sample are older than age $t_{0.05}$.

To estimate M, an empirical approach is usually taken where $t_{0.05}$ is replaced with $t_{\max}$:

$$0.05 = e^{-\hat{M}t_{\max}}, \quad (6)$$

where $t_{\max}$ is either the oldest age observed in the stock or the oldest age found in the literature for the species of interest. When age composition data are used from an exploited stock, Equation 6 will provide an estimate of M only if fishing mortality is reasonably close to zero ($M \approx Z$) or if there is a refuge where older animals can accumulate. If exploitation affects all

* Contribution 2637 of the Virginia Institute of Marine Science, The College of William and Mary, Gloucester Point, VA 23062.

Manuscript submitted 25 March 2004 to the Scientific Editor's Office.
Manuscript approved for publication 12 October 2004 by the Scientific Editor.
Fish. Bull. 103:433–437 (2005).

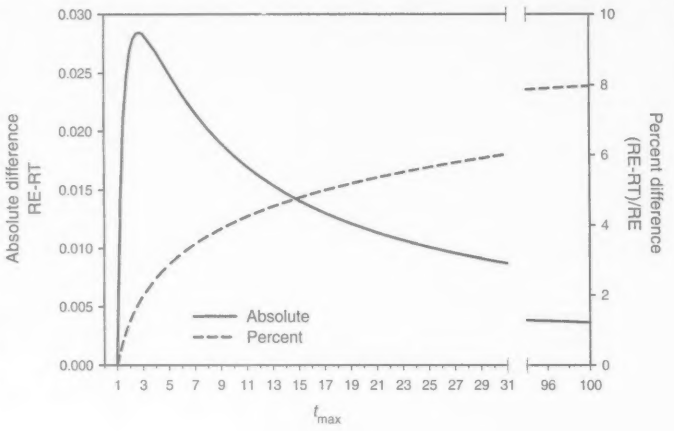

Figure 1

The absolute and percent difference between estimates of M from the regression estimator (RE) and the approximate rule of thumb, $4.22/t_{max}$ (RT).

animals in the stock, Equation 6 is unlikely to provide a reliable estimate of M.

The rule of thumb for approximating M follows directly from Equation 6:

$$-\ln(0.05) = \hat{M} \times t_{max}$$
$$\hat{M} = \frac{2.996}{t_{max}} \approx \frac{3}{t_{max}}. \quad (7)$$

Most importantly, note that the use of 0.05 or any other proportion in the equations is arbitrary because we have no reason to believe that t_{max} pertains to any particular quantile.

We show in the present study that this arbitrary rule of thumb for approximating M is unnecessary, as an empirical method (Hoenig, 1983) provides an analogous estimate based on a substantial data set. Equation 1 is based on the same model as that in Equation 3 and was developed from a regression of $\ln(M)$ on $\ln(t_{max})$ from data on 134 stocks of 79 species of fish, mollusks, and cetaceans. It can be shown to be of the same form as the rule-of-thumb approach as follows:

$$e^{\ln(\hat{M})} = e^{1.44 - 0.982 \times \ln(t_{max})}$$
$$\hat{M} = \frac{e^{1.44}}{e^{0.982 \times \ln(t_{max})}}$$
$$= \frac{4.22}{(t_{max})^{0.982}} \quad (8)$$
$$\approx \frac{4.22}{t_{max}}$$

Results

We substituted 1.0 for 0.982 in Equation 8 to allow the development of a simple, approximate rule of thumb for direct comparison with $3/t_{max}$. As a result, this rule of thumb strictly applies only to the case where $t_{max} = 1$. Estimates from the regression estimator in Equation 1 are always greater than estimates from Equation 8 for $t_{max}>1$, although the difference is usually small (Fig. 1).

Estimates from the regression estimator are typically 40–50% greater than estimates from $3/t_{max}$ (Fig. 2). For example, if a maximum age of eight years is used for blue crab in Chesapeake Bay (Rugolo et al., 1998), $3/t_{max}$ gives an estimate for M of 0.375/yr and the regression estimator gives 0.548/yr.

Perhaps the most significant result is the finding that rearrangement of the regression model yields an estimate of an appropriate value for P in Equation 2. The value of 4.22 in Equation 8 approximately corresponds to $-\ln(0.015)$, indicating that the average longevity for stocks in the data set used by Hoenig (1983) is the age at which about 1.5% of the stock remains alive (versus 5% in $3/t_{max}$).

Discussion

Development of the rule-of-thumb approach

The rule-of-thumb approach appears to have arisen independently in four different places. Cadima (2003) supported the approach by citing the early work of Tanaka (1960). Sparre and Venema (1998) based their presen-

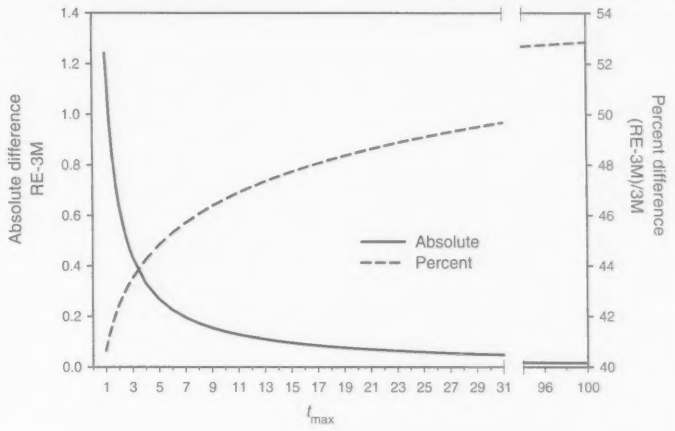

Figure 2

The absolute and percent difference between estimates of M from the regression estimator (RE) and $3/t_{max}$ (3M).

tation on the work of Alagaraja (1984), who provided the mathematics of a method that Sekharan (1975) used without description. Interestingly, Shepherd and Breen (1992) rearranged Equation 3 to obtain the rule of thumb based on the results of Hoenig (1983). This latter presentation is provided in Quinn and Deriso (1999). In all of these cases, the proportion of animals surviving to t_{max} is assumed to be some arbitrarily small value, typically 1% or 5%.

The development and use of the specific form $3/t_{max}$ in blue crab work occurred altogether separately. Its use began with an assessment for the Chesapeake Bay stock, in which Rugolo et al. (1998) used an estimate of M based on "the ICES [International Council for the Exploration of the Sea] convention; that is, 5% survivorship at maximum age following negative exponential depletion." The approach is more explicitly defined in their original document (Rugolo et al.[1]) as $M = (3/maximum\ age)$. The report also states that "this convention ... is widely used for many east coast finfish stocks (NMFS [National Marine Fisheries Service]/NEFSC [Northeast Fisheries Science Center], ASMFC [Atlantic States Marine Fisheries Commission])." Following its introduction by Rugolo et al. (Rugolo et al.[1]; Rugolo et al., 1998), the $3/t_{max}$ approach has been used in nearly all blue crab stock assessment work conducted on the east coast of the United States (Miller and Houde[2]; Miller, 2001; Murphy et al.[3]; Helser et al., 2002; Kahn[4]).

The references used by Rugolo et al. (1998) in support of what they termed the "ICES convention" (Anthony[5]; Vetter, 1988) do not mention the $3/t_{max}$ approach. Rather than advocating a method for determining M, Anthony[5] called for standardization of the range of ages to include in the calculation of yield-per-recruit for a stock; this range of ages was termed the stock's "fishable life span." He proposed that the fishable life span should be defined such that the oldest age would be that

[1] Rugolo, L., K. Knotts, A. Lange, V. Crecco, M. Terceiro, C. Bonzek, C. Stagg, R. O'Reilly, and D. Vaughan. 1997. Stock assessment of Chesapeake Bay blue crab (*Callinectes sapidus*), 267 p. Report of the Technical Subcommittee of the Chesapeake Bay Stock Assessment Committee of the National Marine Fisheries Service, NOAA (National Oceanic and Atmospheric Administration). NOAA Chesapeake Bay Office, 410 Severn Avenue, Suite 107, Annapolis, MD 21403.

[2] Miller, T. J., and E. D. Houde. 1999. Blue crab target setting, 167 p. Final report to the Living Resources Subcommittee of the Chesapeake Bay Program. University of Maryland Center for Environmental Science (UMCES) Technical Series No. TS-177-99. Chesapeake Bay Program, U.S. EPA (Environmental Protection Agency), 410 Severn Avenue, Annapolis, MD 21403.

[3] Murphy, M. D., C. A. Meyer, and A. L. McMillen-Jackson. 2001. A stock assessment for blue crab, *Callinectes sapidus*, in Florida waters, 56 p. FMRI (Florida Marine Research Institute) Inhouse Report Series IHR 2001-008. Florida Fish and Wildlife Conservation Commission, FMRI, 100 Eighth Avenue SE, St. Petersburg, FL 33701.

[4] Kahn, D. M. 2003. Stock assessment of Delaware Bay blue crab (*Callinectes sapidus*) for 2003, 52 p. Delaware Department of Natural Resources and Environmental Control, Division of Fish and Wildlife, P.O. Box 330, Little Creek, DE 19961.

[5] Anthony, V. C. 1982. The calculation of $F_{0.1}$: a plea for standardization, 16 p. Northwest Atlantic Fisheries Organization (NAFO) Serial Document N557, SCR 82/VI/64. NAFO Secretariat, P.O. Box 638, Dartmouth, Nova Scotia B2Y 3Y9, Canada.

at which 5% or less of the initial recruits survived. The use of Anthony's standard to approximate M makes the assumption that the fishable life span of an exploited stock is the same as the longevity of the members of the stock in an unexploited condition. It is unlikely that this assumption will be met unless the fishery is at an early stage in its development because fishing may alter the age structure of the stock (Hilborn and Walters, 1992). We note that although a limited number of scientists involved with ICES have used $3/t_{max}$ in a general way, the method has not been adopted as a convention within ICES (O'Brien[6]). Furthermore, we did not find evidence that the approach is currently in common use in stock assessments on the east coast of the United States, with the exception of those for blue crab. Nonetheless, the rule-of-thumb approach certainly has the potential to be used widely, given its repeated presentation in fishery literature and its accumulated momentum in blue crab work.

Recommendations

The power of empirical relationships for predicting natural mortality can be rather limited (Vetter, 1988; Pascual and Iribarne, 1993), and the uncertainty associated with parameter estimates should be taken into account whenever possible (Patterson et al., 2001). Furthermore, methods for directly estimating M are likely to be preferable to making predictions based on life history features. Nonetheless, such estimates may be needed when available data are inadequate for making a direct estimate. Given the results of our comparison, we recommend that the regression estimator be used instead of the rule-of-thumb approach when longevity is used to predict M. The regression estimator is based on a least squares fit to an extensive data set and thus matches experience better than a rule-of-thumb approach based on an arbitrary constant.

We recommend that use of the $3/t_{max}$ rule of thumb be abandoned, despite it being entrenched in blue crab literature. For a species like blue crab, for which t_{max} is less than 10 years, the differences in the estimates of M from the regression estimator and $3/t_{max}$ are not trivial (~45%). Although the regression estimator was based on data for fish, mollusks, and cetaceans (Hoenig, 1983) and may not be applicable to other exploited taxa, such as crustaceans, the model had a good fit to the data across widely disparate taxa. Finally, estimates of M for blue crab based on longevity are controversial because of continued difficulty in determining an appropriate t_{max}. In the absence of data to directly estimate M for this species, we suggest that the most prudent course of action is a review and comparison of other methods for predicting M.

[6] O'Brien, C. M. 2004. Personal commun. Chair of ICES Working Group on Methods of Fish Stock Assessments and ICES Resource Management Committee. CEFAS (Centre for Environment, Fisheries and Aquaculture Science) Lowestoft Laboratory, Pakefield Road, Lowestoft, Suffolk NR33 0HT, England.

Acknowledgments

We thank Doug Vaughan for helping investigate the use of the rule-of-thumb approach, and Russell Burke, Romuald Lipcius, Jacques van Montfrans, and three anonymous reviewers for helpful comments on the manuscript. D.A.H. gratefully acknowledges the support of the Willard A. Van Engel (WAVE) Fellowship for Crustacean Research. This work was supported by funding from the NOAA Chesapeake Bay Office, award no. NA03NMF4570376.

Literature cited

Alagaraja, K.
1984. Simple methods for estimation of parameters for assessing exploited fish stocks. Indian J. Fish. 31:177–208.

Alverson, D. L., and M. J. Carney.
1975. A graphic review of the growth and decay of population cohorts. J. Cons. Int. Explor. Mer 36:133–143.

Beverton, R. J. H.
1963. Maturation, growth and mortality of clupeid and engraulid stocks in relation to fishing. Rapp. P.-V. Réun. Cons. Int. Explor. Mer 154:44–67.

Beverton, R. J. H., and S. J. Holt.
1959. A review of the lifespans and mortality rates of fish in nature, and their relation to growth and other physiological characteristics. *In* The lifespan of animals, CIBA Foundation colloquia on ageing, vol. 5 (G. E. W. Westenholme and M. O'Connor, eds.), p. 142–177. Little, Brown and Company, Boston, MA.

Bury, K. V.
1975. Statistical models in applied science, 625 p. John Wiley and Sons, New York, NY.

Cadima, E. L.
2003. Fish stock assessment manual. FAO Fish. Tech. Pap. 393, 161 p. FAO, Rome.

Charnov, E. L.
1993. Life history invariants: some explorations of symmetry in evolutionary ecology. Oxford Univ. Press, New York, NY.

Chen, S., and S. Watanabe.
1989. Age dependence of natural mortality coefficient in fish population dynamics. Nippon Suisan Gakkaishi 55:205–208.

Frusher, S. D., and J. M. Hoenig.
2001. Estimating natural and fishing mortality and tag reporting rate of southern rock lobster (*Jasus edwardsii*) from a multiyear tagging model. Can. J. Fish. Aquat. Sci. 58:2490–2501.

Gunderson, D. R., and P. H. Dygert.
1988. Reproductive effort as a predictor of natural mortality rate. J. Cons. Int. Explor. Mer 44:200–209.

Hearn, W. S., K. H. Pollock, and E. N. Brooks.
1998. Pre- and post-season tagging models: estimation of reporting rate and fishing and natural mortality rates. Can. J. Fish. Aquat. Sci. 55:199–205.

Helser, T. E., A. Sharov, and D. M. Kahn.
2002. A stochastic decision-based approach to assessing the status of the Delaware Bay blue crab stock. *In* Incorporating uncertainty into fishery models (J. M. Berkson, L. L. Kline, and D. J. Orth, eds.), p. 63–82. Am. Fish. Soc., Symposium 27, Bethesda, MD.
Hightower, J. E., J. R. Jackson, and K. H. Pollock.
2001. Use of telemetry methods to estimate natural and fishing mortality of striped bass in Lake Gaston, North Carolina. Trans. Am. Fish. Soc. 130:557–567.
Hilborn, R., and C. J. Walters.
1992. Quantitative fisheries stock assessment: choice, dynamics and uncertainty, 570 p. Chapman and Hall, New York, NY.
Hoenig, J. M.
1983. Empirical use of longevity data to estimate mortality rates. Fish. Bull. 82:898–903.
Jensen, A. L.
1996. Beverton and Holt life history invariants result from optimal trade-off of reproduction and survival. Can. J. Fish. Aquat. Sci. 53:820–822.
Latour, R. J., J. M. Hoenig, D. A. Hepworth, and S. D. Frusher.
2003. A novel tag-recovery model with two size classes for estimating fishing and natural mortality, with implications for the southern rock lobster (*Jasus edwardsii*) in Tasmania, Australia. ICES J. Mar. Sci. 60:1075–1085.
Lorenzen, K.
1996. The relationship between body weight and natural mortality in juvenile and adult fish: a comparison of natural ecosystems and aquaculture. J. Fish Biol. 49:627–647.
Miller, T. J.
2001. Matrix-based modeling of blue crab population dynamics with applications to the Chesapeake Bay. Estuaries 24:535–544.
Pascual, M. A., and O. O. Iribarne.
1993. How good are empirical predictions of natural mortality? Fish. Res. 16:17–24.
Patterson, K., R. Cook, C. Darby, S. Gavaris, L. Kell, P. Lewy, B. Mesnil, A. Punt, V. Restrepo, D. W. Skagen, and G. Stefansson.
2001. Estimating uncertainty in fish stock assessment and forecasting. Fish and Fisheries 2:125–157.
Pauly, D.
1980. On the interrelationships between natural mortality, growth parameters, and mean environmental temperature in 175 fish stocks. J. Cons. Int. Explor. Mer 39:175–192.
Peterson, I., and J. S. Wroblewski.
1984. Mortality rate of fishes in the pelagic ecosystem. Can. J. Fish. Aquat. Sci. 41:1117–1120.
Pollock, K. H., H. Jiang, and J. E. Hightower.
2004. Combining telemetry and fisheries tagging models to estimate fishing and natural mortality rates. Trans. Am. Fish. Soc. 133:639–648.
Quinn, T. J. II, and R. B. Deriso.
1999. Quantitative fish dynamics, 542 p. Oxford Univ. Press, New York, NY.
Roff, D. A.
1984. The evolution of life history parameters in teleosts. Can. J. Fish. Aquat. Sci. 41:989–1000.
Rugolo, L. J., K. S. Knotts, A. M. Lange, and V. A. Crecco.
1998. Stock assessment of Chesapeake Bay blue crab (*Callinectes sapidus* Rathbun). J. Shellfish Res. 17: 493–517.
Sekharan, K. V.
1975. Estimates of the stocks of oil sardine and mackerel in the present fishing grounds off the west coast of India. Indian J. Fish. 21:177–182.
Shepherd, S. A., and P. A. Breen.
1992. Mortality in abalone: its estimation, variability and causes. *In* Abalone of the world: biology, fisheries and culture (S. A. Shepherd, M. J. Tegner, and S. A. Guzman del Proo, eds.), p. 276–304. Fishing News Books, Cambridge, UK.
Sparre, P., and S. C. Venema.
1998. Introduction to tropical fish stock assessment, Part 1: manual. FAO Fish. Tech. Pap. 306/1, rev. 2, 407 p. FAO, Rome.
Tanaka, S.
1960. Studies on the dynamics and the management of fish populations. Bull. Tokai Reg. Fish. Res. Lab. 28:1–200.
Vetter, E. F.
1988. Estimation of natural mortality in fish stocks: a review. Fish. Bull. 86:25–43.

Effects of current speed and turbidity on stationary light-trap catches of larval and juvenile fishes

David C. Lindquist
Richard F. Shaw
Coastal Fisheries Institute
School of the Coast and Environment
Louisiana State University
Baton Rouge, Louisiana 70803
E-mail address (for D. C. Lindquist): dlindq1@lsu.edu

Light traps are one of a number of different gears used to sample pelagic larval and juvenile fishes. In contrast to conventional towed nets, light traps primarily collect larger size classes, including settlement-size larvae (Choat et al., 1993; Hickford and Schiel, 1999; Hernandez and Shaw, 2003), and, therefore, have become important tools for discerning recruitment dynamics (Sponaugle and Cowen, 1996; Wilson, 2001). The relative ease with which multiple synoptic light trap samples can be taken means that larval distribution patterns can be mapped with greater spatial resolution (Doherty, 1987). Light traps are also useful for sampling shallow or structurally complex habitats where towed nets are ineffective or prohibited (Gregory and Powles, 1985; Brogan, 1994; Hernandez and Shaw, 2003).

As with any sampling gear, there are concerns about light trap sampling biases and efficiency. Light traps are taxon-selective because they target fishes that are photopositive and able to swim to and enter the trap (Thorrold, 1992; Choat et al. 1993; Hernandez and Shaw, 2003), and size-selective because both phototactic behavior and swimming abilities change during ontogeny (Stearns et al., 1994; Fisher et al., 2000). Unlike conventional towed nets, it is difficult, if not impossible, to quantify the volume of water sampled by light traps. This is largely due to external, environmental factors such as lunar phases, current speed or water clarity, which may have a large impact on catch rates (Doherty, 1987; Meekan et al, 2000).

Few studies have attempted to address the effects of environmental factors on light trap performance. Catches have been found to be lower during full moons as compared to new moons, either because of the greater ambient illumination interfering with light trap efficiency (Gregory and Powles, 1985; Hickford and Schiel, 1999) or because of higher abundances of presettlement fish during the darker lunar phases (Johannes, 1978; Robertson et al., 1988). Thorrold (1992) showed that catches were greater for light traps drifting with the current as compared to traps anchored in the current flow. Anderson et al. (2002) found that anchored light traps were less efficient at a high-current sampling site as compared with a low-current sampling site. The latter two studies, however, did not provide any information on catch rates with variation in current speed. The purpose of this study was to assess the relationships between catch rates from stationary (anchored or tethered) light traps at offshore petroleum platforms and concurrent measurements of current speed and turbidity.

Materials and methods

Study sites

Larval and juvenile fishes were collected at five oil and gas platforms (platforms) in the north-central Gulf of Mexico. These platforms included: Mobil's Green Canyon 18 (27°56′37″N, 91°0′45″W; sampled from July 1995–June 1996); Mobil's Grand Isle 94B (28°30′57″N, 90°07′23″W; April–August 1996); Exxon's South Timbalier 54G (28°50′01″N, 90°25′00″W; April–September 1997); Santa Fe-Snyder's Main Pass 259A (29°19′32″N, 88°01′12″W; May–September 1999); and Murphy Oil's Viosca Knoll 203 (29°46′53″N, 88°19′59″W; May–October 2000). All platforms had similar underwater structural complexity, and had well-developed biofouling communities when sampled.

Sampling procedures

Sampling procedures have been described in detail elsewhere (Hernandez and Shaw, 2003) and will be briefly described here. Fish collections were made by using a modified quatrefoil light trap with a Brinkman Starfire II halogen light (250,000 candlepower) powered through an umbilical by a 12-volt marine battery. Light traps were deployed in surface waters within the platform structure along a stainless-steel guidewire (within-platform light trap), and tethered and floated in surface waters to a distance of 20 m from the down-current side of the platform (off-platform light trap). Light traps were deployed with their lights off, fished with lights on for 10–15 min, and retrieved with lights off.

Sampling was undertaken generally twice monthly coincident with new and full moon phases. During each trip, light traps were fished during four to six sets per night, starting at least one hour after sunset and ending at least one hour before sunrise, over two to three consecutive nights. Each sample set consisted of a within-platform light trap collec-

Manuscript submitted 4 February 2004 to the Scientific Editor's Office.
Manuscript approved for publication 1 December 2004 by the Scientific Editor.
Fish. Bull. 103:438–444 (2005).

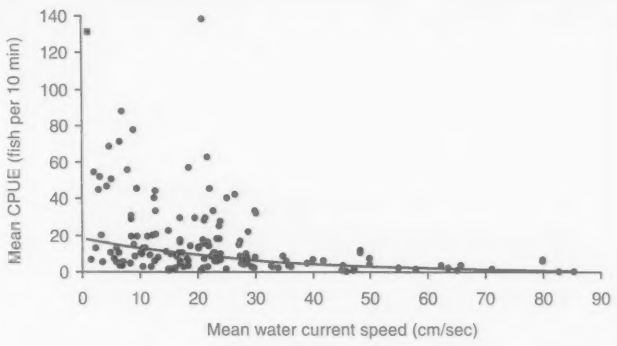

Figure 1

Mean total CPUE per sampling set (from within- and off-platform light traps) in relation to the mean current speed per sampling set. Data from all platforms were combined. Line calculated from the regression equation: $\log_{10}(y+1) = -0.013x + 1.302$, $r^2=0.23$.

tion and an off-platform light trap collection in random order. During sampling, turbidity (Nephelometric turbidity unit: NTU) was measured every 5 sec by using a Hydrolab DataSonde3 suspended in surface waters within the platform structure. Current speed and direction were measured every 10 min with an InterOcean S4 Current Meter suspended 1–2 m below the surface on the up-current side of the platform. Because the platform structure undoubtedly reduced current speeds (Forristall, 1996), current data taken from this location should be considered as relative estimates for the light trap collections.

Samples were preserved in 10% buffered formalin and transferred to ethanol within 12 hours. Fish were enumerated and identified to the lowest possible taxonomic level. Preflexion larvae were measured to notochord length, and postflexion and juvenile fish were measured to standard length. Data from light trap catches were standardized to a catch per unit of effort (CPUE) of number of fish per 10 minutes.

Data analyses

We assumed that there were no inter-location differences in the relationship between light trap CPUE and current speed or turbidity; therefore, data from all platforms for the months May to September were combined. The relationship between total light trap CPUE and current speed or turbidity was analyzed by using regression analysis. Current speed and turbidity were analyzed separately, rather than in a multiple regression analysis, because there was a limited number of sampling sets where we had data for light trap CPUE, current speed and turbidity together (n=60, or 31% and 37% of the available turbidity and current data, respectively). There were no significant differences in the regression coefficients of CPUE vs. current speed or turbidity between within- and off-platform light traps (P>0.15); therefore, the CPUEs from both light traps were averaged for each sampling set. Mean total CPUEs were log-transformed ($\log_{10}(y+1)$) and analyzed with the mean current speed or turbidity from each respective sampling set. Mean CPUEs were also calculated for the dominant families collected; however, regression analyses could not be performed because variances remained heterogeneous after transformation.

To investigate how fish size (i.e., locomotive ability) influenced light trap catches with increasing current speed, length-frequency distributions of all fishes collected at different current speed intervals (0–9, 10–19, 20–29, 30–39, 40–49 and >49 cm/sec) were compared by using Kolmogorov-Smirnov tests (α=0.05). The length-frequency figures were subdivided by three ecological groupings: clupeiforms (Clupeidae and Engraulidae); demersal taxa (predominantly Synodontidae and Blenniidae); and scombrids and carangids, to further assess whether any changes in the size of fish collected over the current intervals were due to a particular group. All statistics were performed with SAS version 6.12 (SAS Institute, Cary, NC).

Results

Current speed

Mean total CPUEs generally decreased with increasing current speed (Fig. 1). At current speeds ≤30 cm/sec, light trap catches were highly variable (CPUEs ranged from 0 to 138 fish per 10 min); however, CPUEs >20 fish per 10 min occurred only at these lower speeds. Although there were fewer samples at speeds >30 cm/sec,

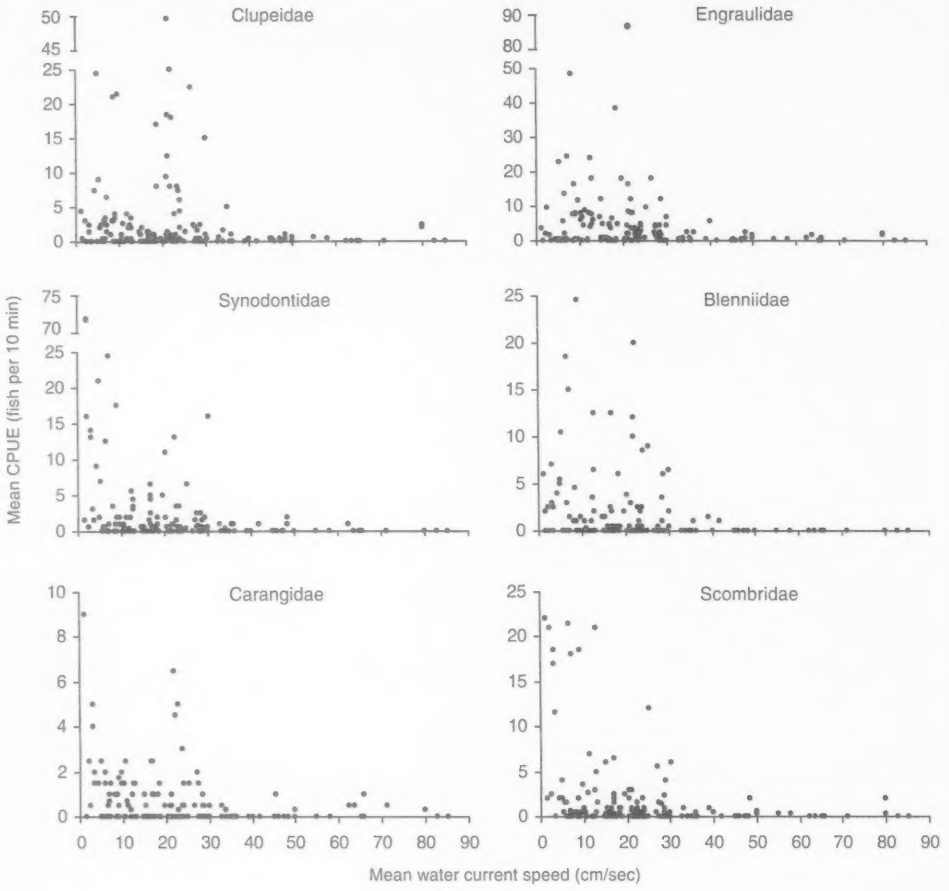

Figure 2

Mean CPUE per sampling set (from within- and off-platform light traps) in relation to the mean current speed per sampling set for each of the dominant families collected. Data from all platforms were combined. Note changes in the scale of the *y*-axis.

CPUEs were mostly <5 fish per 10 min at these speeds. There was a significant linear relationship between log-transformed mean total CPUE data and mean current speed ($\log_{10}(y+1) = -0.013x + 1.302$, $r^2=0.23$; $F=49.61$, $P<0.0001$).

Each of the dominant families collected by light traps showed a similar pattern of highest mean CPUEs at current speeds <30 cm/sec and relatively low mean CPUEs at higher current speeds (Fig. 2). Clupeidae, Engraulidae, and Blenniidae showed a slight trend of highest CPUEs at intermediate current speeds (10–30 cm/sec), whereas the other families generally had highest CPUEs at the lowest speeds (<10 cm/sec). Synodontidae and Blenniidae were rarely collected at current speeds >40 cm/sec, and small numbers of Clupeidae, Engraulidae, Carangidae, and Scombridae were collected at speeds up to 80 cm/sec.

As current speeds increased, light trap collections became limited to smaller size classes of fish (Fig. 3). For the first three current intervals, i.e., 0–9, 10–19, and 20–29 cm/sec, a broad range of sizes were collected and the distributions had median lengths of 15–19 mm. However, beginning at the fourth current interval, 30–39 cm/sec, the size distributions shifted toward an increasingly greater proportion of the catch <10 mm in length. This trend was most pronounced at the two highest current intervals, 40–49 and >49 cm/sec, both of which had distributions with median lengths of 5 mm. The size distributions from the two highest current intervals were the only distributions that were not

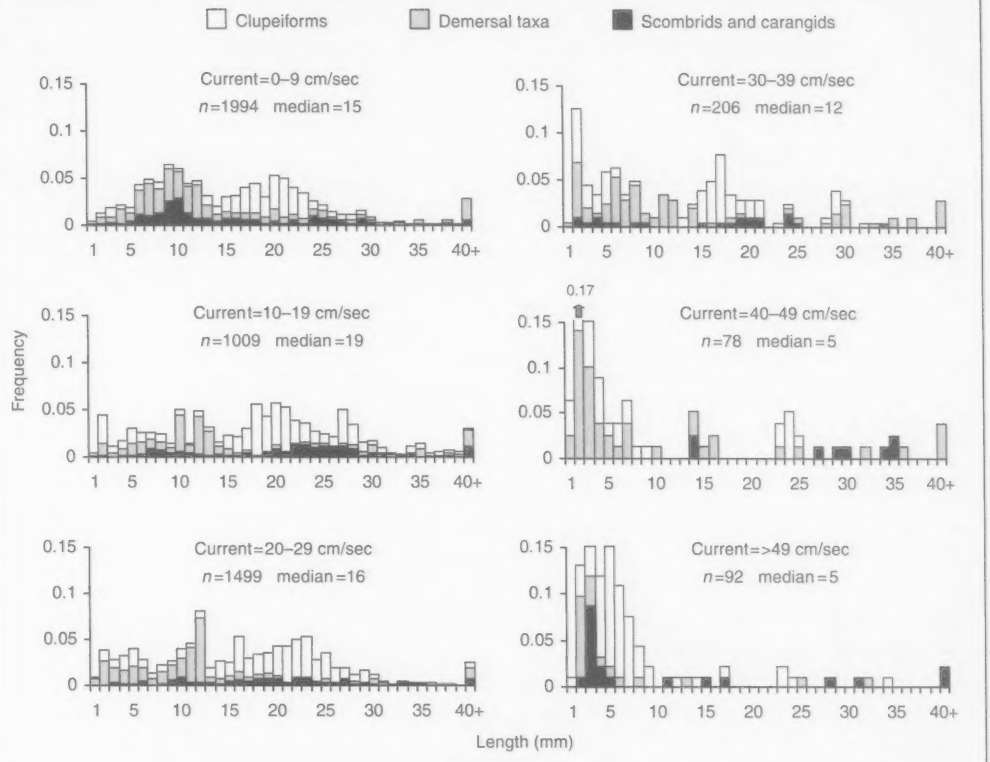

Figure 3

Size distributions of fishes collected by light traps from all platforms at different current speed intervals. The total number of fish collected (n) and the median length (mm) over each interval are included. Size distributions are further subdivided by three general ecological groupings: clupeiforms (Clupeidae and Engraulidae), demersal taxa (i.e., more substrate-oriented fishes such as synodontids and blenniids), and scombrids and carangids.

significantly different from each other (P=0.11). The decrease in the frequency of fishes larger than 10 mm at the higher current intervals was not limited to any particular ecological grouping, i.e., pelagic fishes such as clupeiforms, scombrids, and carangids were as rare as demersal taxa.

Turbidity

Mean total CPUEs generally decreased with increasing turbidity (Fig. 4). Highest catches (CPUEs >50 fish per 10 min) predominantly occurred at turbidities below 1.0 NTU, whereas at higher turbidities catches were generally lower. There was a significant linear relationship between log-transformed mean total CPUE data and mean turbidity ($\log_{10}(y+1)=-0.25x + 1.48$, $r^2=0.08$; F=11.86, P=0.0007).

The majority of the dominant families showed a similar pattern of highest mean CPUEs at turbidities <1.0 NTU, and relatively low mean CPUEs at higher turbidities (Fig. 5). Clupeidae, however, showed a pattern of high CPUEs at turbidities <0.5 NTU and between 1.0 and 2.0 NTU.

Discussion

Light trap catches of larval and juvenile fishes appeared to be negatively affected by increasing current speeds at platforms. This was expected because stronger currents may interfere with a fish's ability to swim to and enter a light trap (Doherty, 1987; Thorrold, 1992; Anderson et al., 2002). Doherty (1987) predicted that, for stationary (anchored or tethered) light traps, catches should increase initially with current speed as more water is sampled, but then decrease as current speed interferes with catchability. Although mean total CPUEs clearly decreased with increasing current speed, they

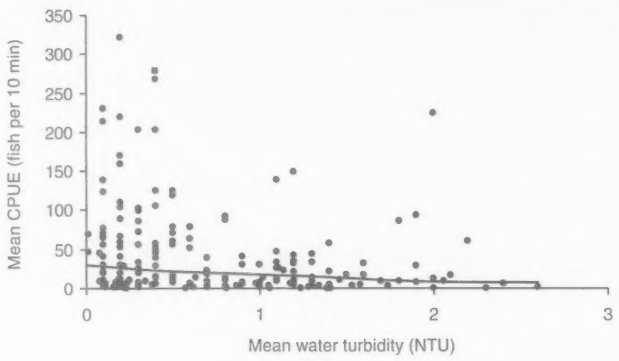

Figure 4

Mean total CPUE per sampling set (from within- and off-platform light traps) in relation to the mean turbidity per sampling set. Data from all platforms were combined. The line was calculated from the regression equation: $\log_{10}(y+1) = -0.25x + 1.48$, $r^2=0.08$. Included in the analysis, but not shown in the plot, were three points from 583 to 878 CPUE between 0.2 to 0.5 NTU.

did not appear to peak at some intermediate current level. These results, however, represented the total catch of all fishes, and the relationship between current speed and light trap catches may be more taxon specific (Doherty, 1987). When analyzed at the family level, a bell-shaped relationship may have occurred for Clupeidae, Engraulidae, and Blenniidae; however, the pattern was indistinct and there was generally little difference among families.

The lack of any strong differences in the relationship between light trap CPUEs and current speed among the dominant families was unexpected, considering the potential differences in swimming abilities. Because larvae and juveniles of demersal fishes are generally believed to have lower swimming speeds (Blaxter, 1986), it was anticipated that catches of synodontids and blenniids would have been more negatively affected by increasing current speed than relatively stronger-swimming pelagic taxa (e.g., scombrids and carangids). Perhaps larvae of demersal taxa have greater swimming capabilities than previously considered, as has been recently found for certain settlement-stage larval reef fishes (sustained swimming speeds of 20–60 cm/sec; Stobutzki and Bellwood, 1994; Leis and Carson-Ewart, 1997). However, despite possible strong swimming abilities, few larval and juvenile demersal or pelagic fishes were collected at current speeds >40 cm/sec, and of these the majority were preflexion larvae that were undoubtedly passively entrained in the light trap. It is possible that the larvae and juveniles of taxa collected at platforms were unable to maintain the metabolic power required to swim against the stronger currents over extended distances from the light trap (Fisher and Bellwood, 2002).

Currents may have interfered with the functioning of the light traps. Assuming that larval and juvenile fishes were able to swim against the stronger currents, their ingress into the light trap may have been impeded by turbulence created by the current flow around the trap. If turbulence occurred after some critical current speed, then this may explain the lower CPUEs beginning at around 30 cm/sec observed for each of the dominant families.

Higher turbidity also appeared to have a negative effect on light trap catches at platforms. Light trap catch efficiency should be greatly impaired by highly turbid waters because greater light attenuation would reduce the effective sampling radius of the trap. In addition, the phototactic response of larval and juvenile fishes may be lower at lower light intensities (Gehrke, 1994; Stearns et al., 1994). However, it is uncertain whether the relatively small range of turbidities (0.1–2.6 NTU) sampled during this study would result in a significant decrease in light trap catch efficiency, particularly given the intensity of the light source used (250,000 candlepower). The observed patterns may have been a reflection of intrusions of turbid coastal and Mississippi River plume water at the platforms, during which light trap catches comprised large numbers of coastal clupeids and relatively few other taxa (Fig. 5).

Although they were treated separately for the purposes of this study, the effects of current speed and turbidity also may have been interrelated. A positive relationship between turbidity and current speed was found for a limited data set where both variables were available ($r^2=0.28$, $P<0.0001$). It is unlikely that this relationship was caused by the resuspension of benthic sediments, given the water depth at the platforms (20–230 m), but

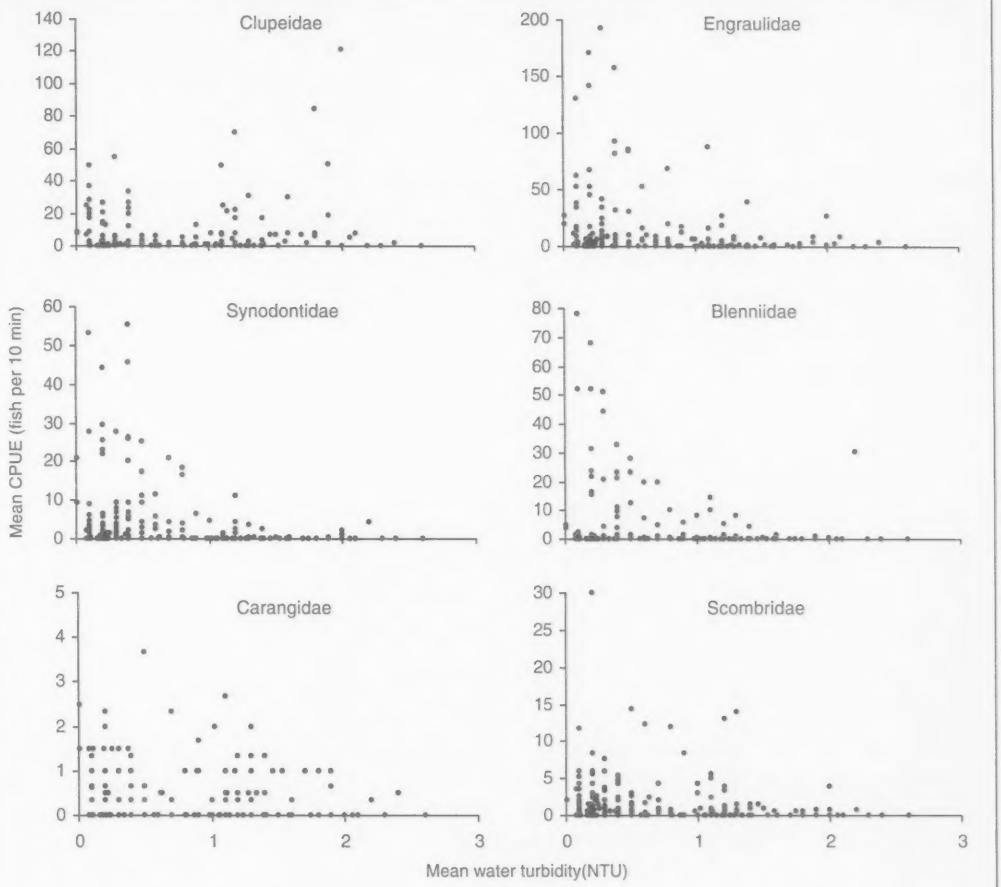

Figure 5

Mean CPUE per sampling set (from within- and off-platform light traps) in relation to the mean turbidity per sampling set for each of the dominant families collected. Data from all platforms were combined. Note changes in the scale of the *y*-axis. Not shown in the Engraulidae plot were three points from 551 to 606 CPUE between 0.2 and 0.5 NTU.

particles may have been flushed from the platforms and their associated biofouling communities by currents. In a comparison of light trap catches between adjacent beach and rocky shore habitats, Hickford and Schiel (1999) attributed lower catches at the beach to lower water clarity caused by sediment resuspension by wave action. Therefore, high current speeds at platforms may have indirectly affected light trap catch efficiency by reducing water clarity.

Results from this study have clear implications for future studies with light traps. At platforms, light trap CPUEs began to decline noticeably at current speeds of 30 cm/sec, and by 40 cm/sec catches of active swimming larval stages (i.e., all but preflexion stages) were rare. This finding suggests that, for comparison studies, estimates of relative abundance from light traps may be biased where there is considerable variation in current flow (Doherty, 1987; Anderson et al., 2002). Drifting traps may be used to avoid the confounding effect of differential water flow (Thorrold, 1992); however such a deployment method may not be applicable when habitats of interest are fixed (e.g., platforms, coral reefs). In such cases, the best course may be to not consider light trap samples at high current speeds (≥40 cm/sec). For turbidity, study results were not as clear; however, temporal or spatial variation in turbidity also would undoubtedly bias light trap results. Short of using light traps at times or locations of similar water clarity, an adjustable light source may be incorporated into light trap design so that equivalent light intensities, and

therefore sampling fields, can be maintained across a variety of water conditions. The alternative would be to standardize the volumes of water sampled by light traps; however, considering the suite of external factors that affect light trap efficiency, such attempts may be fruitless (Meekan et al., 2000).

Acknowledgments

We would like to thank A. Scarborough-Bull, C. Wilson, D. Stanley, J. Ditty, F. Hernandez Jr., J. Cope, J. Plunket, T. Farooqi, and all of those who assisted in the field and laboratory for their assistance and efforts during this research. We also thank Exxon USA, Inc., Mobil USA Exploration and Production, Inc., Santa Fe-Snyder Oil Corp., and Murphy Oil Corp. for access to their oil and gas platforms and logistical support, the crews of GC 18, GI 94B, ST 54G, MP 259A and VK 203 for their assistance and hospitality, and two anonymous reviewers for their helpful comments on this manuscript. This research was funded by the Minerals Management Service-Louisiana State University-Coastal Marine Institute (contract no. 14-35-0001-30660-19961).

Literature cited

Anderson, T. W., C. T. Bartels, M. A. Hixon, E. Bartels, M. H. Carr, and J. M. Shenker.
2002. Current velocity and catch efficiency in sampling settlement-stage larvae of coral reef fishes. Fish. Bull. 100:404–413.

Blaxter, J. H. S.
1986. Development of sense organs and behaviour of teleost larvae with special reference to feeding and predator avoidance. Trans. Am. Fish. Soc. 115:98–114.

Brogan, M. W.
1994. Distribution and retention of larval fishes near reefs in the Gulf of California. Mar. Ecol. Prog. Ser. 115:1–13.

Choat, J. H., P. J. Doherty, B. A. Kerrigan, and J. M. Leis.
1993. A comparison of towed nets, purse seine, and light-aggregation devices for sampling larvae and pelagic juveniles of coral reef fishes. Fish. Bull. 91:195–209.

Doherty, P. J.
1987. Light-traps: selective but useful devices for quantifying the distributions and abundances of larval fishes. Bull. Mar. Sci. 41:423–431.

Fisher, R., and D. R. Bellwood.
2002. The influence of swimming speed on sustained swimming performance of late-stage reef fish larvae. Mar. Biol. 140:801–807.

Fisher, R., D. R. Bellwood, and S. D. Job.
2000. Development of swimming abilities in reef fish larvae. Mar. Ecol. Prog. Ser. 202:163–173.

Forristall, G. Z.
1996. Measurements of current blockage by the Bullwinkle platform. J. Atmos. Ocean. Technol. 13:1247–1266.

Gehrke, P. C.
1994. Influence of light intensity and wavelength on phototactic behaviour of larval silver perch *Bidyanus bidyanus* and golden perch *Macquaria ambigua* and the effectiveness of light traps. J. Fish Biol. 44:741–751.

Gregory, R. S., and P. M. Powles.
1985. Chronology, distribution, and sizes of larval fish sampled by light traps in macrophytic Chemung Lake. Can. J. Zool. 63:2569–2577.

Hernandez, F. J., Jr., and R. F. Shaw.
2003. Comparison of plankton net and light trap methodologies for sampling larval and juvenile fishes at offshore petroleum platforms and a coastal jetty off Louisiana. *In* Fisheries, reefs and offshore development (D. R. Stanley and A. Scarborough-Bull, eds.), p. 15–38. Am. Fish. Soc. Symp. 36.

Hickford, M. J. H., and D. R. Schiel.
1999. Evaluation of the performance of light traps for sampling fish larvae in inshore temperate waters. Mar. Ecol. Prog. Ser. 186:293–302.

Johannes, R. E.
1978. Reproductive strategies of coastal marine fishes in the tropics. Environ. Biol. Fish. 3:65–84.

Leis, J. M., and B. M. Carson-Ewart.
1997. *In situ* swimming speeds of the late pelagic larvae of some Indo-Pacific coral reef fishes. Mar. Ecol. Prog. Ser. 159:165–174.

Meekan, M. G., P. J. Doherty, and L. White Jr.
2000. Recapture experiments show the low sampling efficiency of light traps. Bull. Mar. Sci. 67:875–885.

Robertson, D. R., D. G. Green, and B. C. Victor.
1988. Temporal coupling of production and recruitment of larvae of a Caribbean reef fish. Ecology 69:370–381.

Sponaugle, S., and R. K. Cowen.
1996. Nearshore patterns of coral reef fish larval supply to Barbados, West Indies. Mar. Ecol. Prog. Ser. 133:13–28.

Stearns, D. E., G. J. Holt, R. B. Forward, and P. L. Pickering.
1994. Ontogeny of phototactic behavior in red drum larvae (Sciaenidae, *Sciaenops ocellatus*). Mar. Ecol. Prog. Ser. 104:1–11.

Stobutzki, I. C., and D. R. Bellwood.
1994. An analysis of the sustained swimming abilities of presettlement and postsettlement coral-reef fishes. J. Exp. Mar. Biol. Ecol. 175:275–286.

Thorrold, S. R.
1992. Evaluating the performance of light traps for sampling small fish and squid in open waters of the central Great Barrier Reef lagoon. Mar. Ecol. Prog. Ser. 89:277–285.

Wilson, D. T.
2001. Patterns of replenishment of coral-reef fishes in the nearshore waters of the San Blas Archipelago, Caribbean Panama. Mar. Biol. 139:735–753.

Can a change in the spawning pattern of Argentine hake (*Merluccius hubbsi*) affect its recruitment?*

Gustavo J. Macchi

Consejo Nacional de Investigaciones Científicas y Técnicas (CONICET)
Rivadavia 1917
1033 Buenos Aires, Argentina
Present address: Instituto Nacional de Investigación y Desarrollo Pesquero (INIDEP)
Paseo Victoria Ocampo N° 1. CC. 175
Mar del Plata, 7600, Argentina
E-mail address gmacchi@inidep.edu.ar

Marcelo Pájaro

Adrián Madirolas

Instituto Nacional de Investigación y Desarrollo Pesquero (INIDEP)
Paseo Victoria Ocampo N° 1 CC. 175
Mar del Plata, 7600, Argentina

Argentine hake (*Merluccius hubbsi*) inhabit waters of the Southwest Atlantic Ocean between 22° and 55°S, at depths ranging from 50 to 500 m (Cousseau and Perrota, 1998). This species has historically been among the more abundant fish resources in the Argentine Sea, where its biomass has ranged between one and two million metric tons annually since 1986 (Aubone et al., 2000). In this area, there are two identified fishing stocks, limited by the 41°S parallel. The southern group (Patagonian stock) is the more important with an abundance of about 85% of the total biomass estimated for this species in 1999 (Aubone et al., 2000). During the late 1990s, the spawning biomass of both stocks and their recruitment indices declined drastically, both of which were attributed to an increase in exploitation (Aubone et al., 2000).

The Patagonian stock of Argentine hake spawns from November through March and peak spawning occurs in January (Macchi et al., 2004). This species is a batch spawner and has indeterminate annual fecundity, which is to say that unyolked oocytes continuously mature and are spawned throughout the reproductive season (Macchi and Pájaro, 2003). Thus, to estimate total fecundity, it is necessary to determinate the number of eggs released at one spawning (batch fecundity) and to estimate the number of batches spawned in a reproductive season (spawning frequency). Macchi et al. (2004) estimated these parameters for the southern stock of *M. hubbsi*. They analyzed total egg production during the reproductive season and determined that the size composition of the spawning fraction influences the reproductive potential of the stock.

Reproductive activity of the Patagonian hake historically has taken place mainly in coastal waters off the Chubut province at depths near 50 m, in the area known as Isla Escondida (43°30′–44°S) (Ciechomski et al., 1983). Since 1997–98, a movement of reproductive hake to deeper waters and a decrease in fish density have been observed (Ehrlich et al.[1]). These changes, mainly in the location of the spawning area, may have affected the reproductive potential of this species, reducing the survival of eggs and larvae. If so, we would expect a negative effect on the number of juveniles recruited after this period.

In this note, we hypothesize that a change in spawning site for Patagonian hake can affect species recruitment. We studied temporal changes in the location and density of spawning aggregations, egg production, and recruitment of this stock in different years between 1988 and 2001.

Materials and methods

Samples of *M. hubbsi* were collected from the area where the Patagonian stock is known to reproduce during four acoustic surveys in December 1988, 1993, 1996, and 2000 and during six trawl cruises carried out in January between the years 1996 and 2001.

Acoustic surveys covered the Isla Escondida area between 43° and 45°S (Fig. 1). A SIMRAD EK400/QD echointegrator was used for the 1988 survey and a SIMRAD EK500 echosounder and BI500 postprocessing program were employed for subsequent surveys. To avoid possible biases due to the presence of fish in the near-bottom, acoustic transects were carried out at night when hake assume a more pelagic behavior. Trawl catches were carried out during the day, when fish are concentrated close to the bottom, and immediately after each acoustic transect. Because trawls were intentionally biased to those areas of higher fish density, their positions were different between 1988 and 2000. Nevertheless, the study area, transect design, and sampling effort were similar for all cruises covering the main spawning shoals.

In January, information was collected from trawl surveys to assess the Patagonian stock of juvenile hake between 1996 and 2001. These cruises covered a wide area between 43° and 47°S that included a section

* Contribution 1357 from the Instituto Nacional de Investigación y Desarrollo Pesquero, Mar del Plata, Argentina.

[1] Ehrlich, M. D., P. Martos, A. Madirolas, and R. P. Sánchez. 2000. Causes of spawning pattern variability of anchovy and hake on the Patagonian shelf. ICES CM 2000/N:06.

Manuscript submitted 2 July 2003
to the Scientific Editor's Office.

Manuscript approved for publication
20 December 2004 by the Scientific Editor.

Fish. Bull. 103:445–452 (2005).

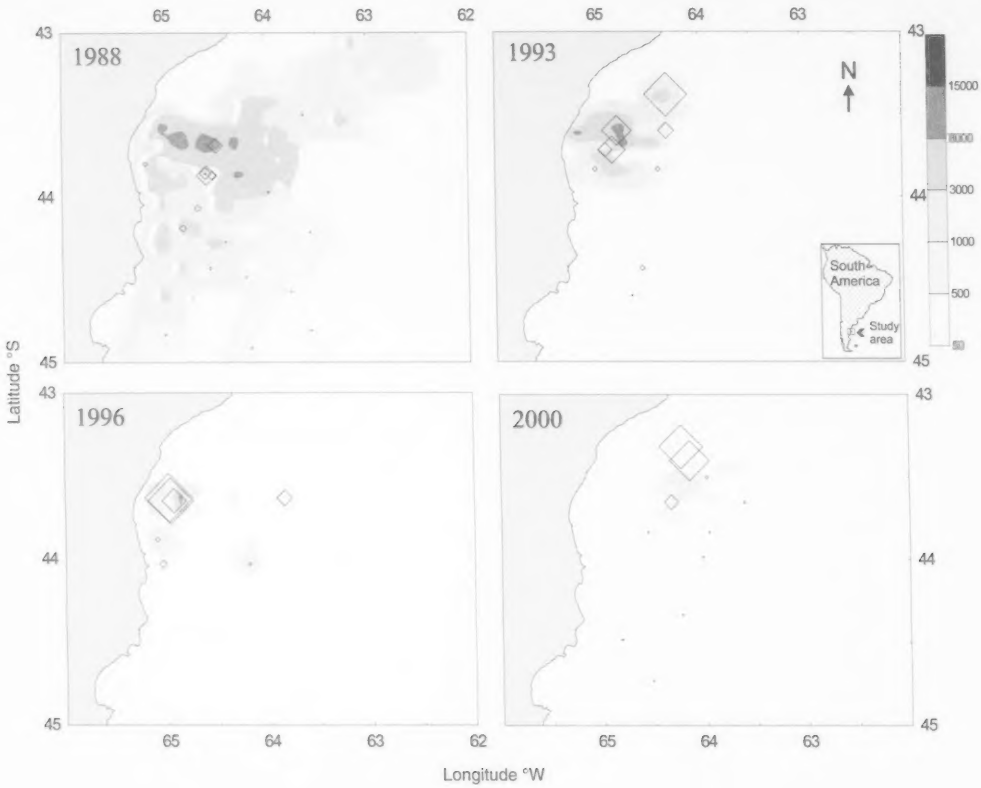

Figure 1

Distribution and density (s_A) of Argentine hake (*Merluccius hubbsi*) estimated from acoustic surveys carried out during December (1988, 1993, 1996, and 2000) in the Isla Escondida area. The size of the symbols is proportional to the percentage of spawning females (with hydrated oocytes). Vertical shaded scale represents scattering coefficient values (sA), where 7.14 s_A units = 1 t/nautical mile^2.

of the main spawning ground of hake. Thus, to analyze spawning individuals we used only data from 33 fish stations located offshore within the spawning area between 43°30′ and 46°S (Fig. 2). Trawl station sites were the same during all cruises. In January of 1996 and 2001 additional information from catches obtained inshore near Isla Escondida was analyzed (Fig. 2).

Argentine hake were collected with a bottom net with a mouth width of about 20 m, a height of about 4 m, and with 20-mm mesh at the inner cover of the codend. Total length (TL) in cm, total weight (TW) in g, and sex were recorded for each fish sampled; for females a subsample was randomly selected from different trawl stations (Table 1) and the maturity stage was determined for each individual. A macroscopic maturity key of five stages designed for biological studies was employed: 1) immature; 2) developing and partially spent; 3) spawning (gravid and running); 4) spent; and 5) resting (Macchi and Pájaro, 2003). This scale was validated by the histological analysis of ovaries collected during December 2000 and January 2001 (Macchi et al., 2004). Females were classified as reproductively active or inactive, according to the presence of yolked oocytes and atresia stages following the criteria of Hunter et al. (1992). When we consider the codes used in the visual assessment of maturity, stages 2 and 3 corresponded to active females, which were capable of spawning at the time of capture or in the near future (Hunter et al., 1992).

Abundance of active females was estimated from data collected during each survey. Information obtained from sampling the trawl catch was expanded to obtain estimates of the number of individuals per length class, following the method described by Macchi et al. (2004).

During December, information from acoustic surveys was used to assign a different weight to each trawl station, based on the relative density and size of the school targeted by the trawl. The transect segment that contained a given trawl was determined and the average value of the water column scattering coefficient

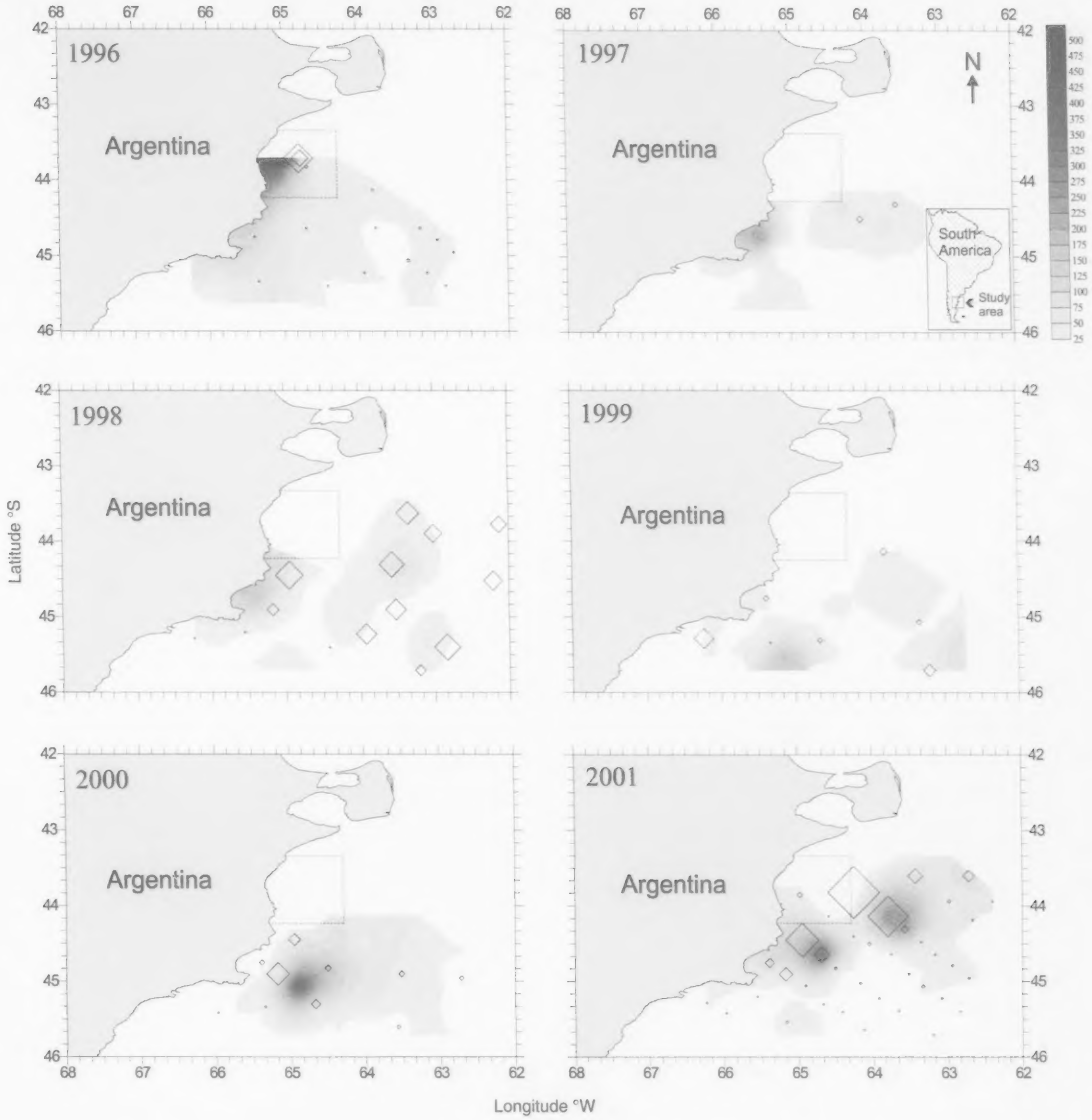

Figure 2

Distribution and density of Argentine hake (*Merluccius hubbsi*) estimated from trawl surveys carried out during January (1996–2001) in the offshore area. The size of the symbols is proportional to the percentage of spawning females (with hydrated oocytes). The square shows the Isla Escondida area. Vertical shaded scale represent biomass in t/nautical mile^2.

(sA) was calculated and weighed by the corresponding number of acoustic observations.

The number of active females for each survey was estimated by multiplying the number of hake within each length class by the proportion of females and the proportion of active females for that length class obtained for that survey (Marshall et al., 1998). The sum of values estimated across the size range was an index of the number of reproductive females in the sampled area during that survey.

Egg production of the Patagonian hake in December during the period 1988–2000 and in January from 1996 to 2001 was based on estimates of three variables: the abundance of active females per length class, the

Table 1

Number of Argentine hake (*Merluccius hubbsi*) sampled during research surveys carried out in the north Patagonian area in December and January, between 1988 and 2001.

Period	Number of trawls	Number of individuals sampled	Number of females subsampled
December			
1988	18	9527	2054
1993	6	2156	1060
1996	9	1563	690
2000	12	4390	708
January			
1996	38	17,715	1509
1997	33	12,687	842
1998	33	15,804	1092
1999	33	14,987	817
2000	33	14,389	958
2001	37	17,944	856

batch-fecundity–size relationship, and spawning frequency. The batch fecundity–total-length relationship and the spawning frequency values used for December (1988–2000) and for January (1996–2001) were those estimated in December 2000 and January 2001, respectively (Macchi et al., 2004). We assumed that these values were applicable to all previous years, because in general, annual differences of these variables were not significant for hake females of the same length range (Macchi et al., 2004).

Egg production by length for each month was estimated by multiplying the number of active females in each length class by the batch fecundity corresponding to that length class and by the number of spawnings estimated for each month. The sum of the egg production values estimated across the size range was the total number of eggs produced in the sampled area during each month (December or January) in different years.

To analyze the relationship between egg production and recruitment, estimates of the relative abundance at age 1 (number of individuals per trawl hour) of Argentine hake were used as a recruitment index. These data were obtained from samples to assess hake juveniles collected from the whole area covered during the cruises carried out in January 1997–2001. In 2002, this index was estimated with samples collected in the same area, but in a different month (March) (GEM, unpubl. data[2]). The number of age-1 individuals in year t+1 was the recruitment index corresponding to the year t.

Results

Abundance of hake and location of spawning females

Figure 1 shows the acoustic densities estimated for Argentine hake and the distribution of spawning females (with hydrated oocytes) in the Isla Escondida area during December 1988, 1993, 1996, and 2000. A decline in hake abundance from 1988 to 2000 was observed—in particular, a drastic decrease in 2000, when the mean density value (14.6 t/nautical mile^2) was thirty times less than that estimated in 1988 (469.2 t/nautical mile^2). During December 1988–96, spawning females were mainly located in the northern area (between 43° and 44°S) inshore at depths lower than 50 m. In 2000 reproductive activity was concentrated at the same latitude as in previous years, but offshore (Fig. 1).

In January 1996 the highest densities of *M. hubbsi* and the spawning females of this species were located in the Isla Escondida area (Fig. 2). Between 1997 and 2000 we did not obtain data from this zone, but the increase in the proportion of spawning hake in deep waters observed since 1998 indicates a spatial change in the reproductive area. During January 2000 and 2001, in addition to the increase of reproductive females offshore, the abundance of hake was higher than that estimated previously for the same area (Fig. 2). In January 2001, trawl stations located near Isla Escondida showed very low values of hake density, in contrast to that observed offshore. This contrast could be attributed to the movement of individuals from the traditional spawning area near the coast to deeper water.

Egg production

Egg production estimated for December in the Isla Escondida area showed a considerable decrease from 1988 to 2000 (Fig. 3). The number of eggs produced

[2] GEM (Grupo de Evaluación Merluza). 2002. Evaluación del estado del recurso merluza (*Merluccius hubbsi*) al sur de 41° S, año 2002. Unpubl report. INIDEP, CC. 175, Mar del Plata (7600), Argentina.

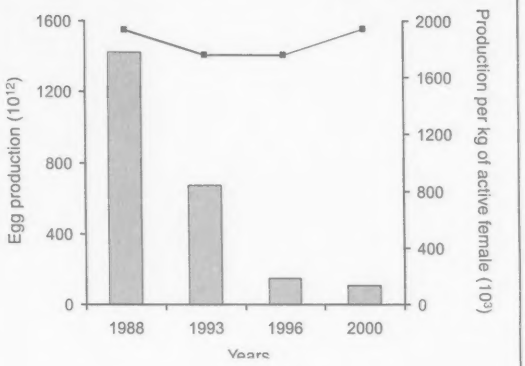

Figure 3

Egg production of Argentine hake (*Merluccius. hubbsi*) estimated for December (1988, 1993, 1996, and 2000) in the Isla Escondida area (bars), and production by unit-weight of reproductively active female (line) for the same month.

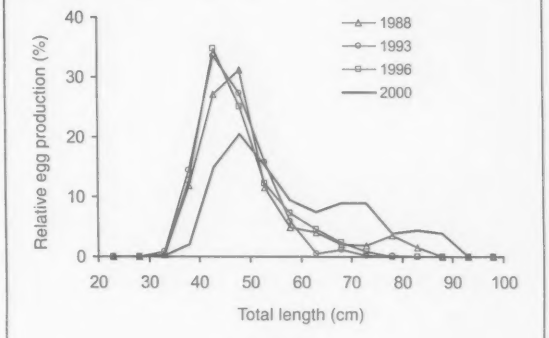

Figure 4

Relative egg production (%) by length class estimated for Argentine hake (*Merluccius hubbsi*) from December 1988, 1993, 1996, and 2000.

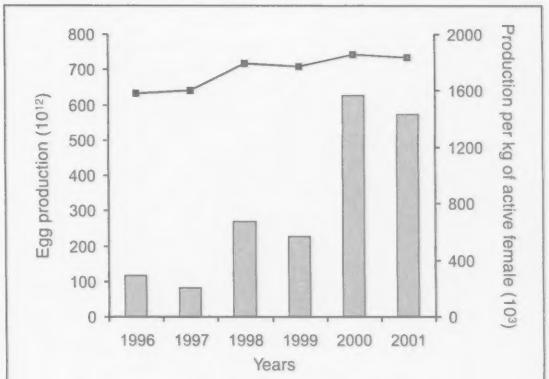

Figure 5

Egg production of Argentine hake (*Merluccius hubbsi*) estimated for January (1996–2001) in the offshore area (bars), and production by unit-weight of reproductively active female (line) for the same month.

per unit of weight (kg of active females) declined from 1988 to 1996, and to a value of around 1700 eggs/kg in the last year (Fig. 3). During December 2000, however, relative egg production increased to 2000 eggs/kg, which can be attributed to the effect of a higher proportion of larger females in reproductive activity. In fact, when the percentage of eggs produced by length class was analyzed, the distribution obtained for December 2000 was different from that for 1988, 1993, and 1996 (Fig. 4). During the earlier years, production mainly depended on young females (<50 cm TL), whereas in December 2000 most of the eggs produced (about 70%) where spawned by females larger than 50 cm TL.

Egg production estimated for the offshore area in January increased from 1996 to 2001 (Fig. 5), in contrast to that observed during December in shallow water near Isla Escondida. The number of eggs produced per unit of weight of active females was similar in 1996 and 1997 (about 1600 eggs/kg), but increased in 1998–2001 to about 1800 eggs/kg. This increase was similar to that observed for December 2000, which was attributed to the higher proportion of larger females within the spawning fraction of hake. In fact, percentage-distribution of eggs produced by length class showed a change beginning in 1998 (Fig. 6). In 1996 and 1997, 70% of the eggs were produced by young females (<50 cm TL), but subsequent production of old females increased to 60% in 1998–99 and to 70% in 2000–01.

Recruitment

Relative abundance data for hake at age 1 (year t+1) in the north Patagonian area were contrasted with the egg production obtained in January from the previous year (t). To estimate egg production, only information from the offshore area was used; thus, the number of eggs estimated was a fraction of that produced by all spawning females in January. However, the increase in egg production observed offshore for the parental stock in 2000 and 2001 was coincident with higher values of age-1 recruitment estimated one year later during 2001 and 2002, respectively (Table 2).

Discussion

The spatial pattern of *M. hubbsi* spawning aggregations inshore and offshore of the north Patagonian area between 1988 and 2001 has changed since 1998. This

Table 2

Egg production estimates for Argentine hake (*Merluccius hubbsi*) for January cruises (1996–2001) taken offshore of the north Patagonian area, and indices of abundance at age 1 corresponding to these annual classes.

Year	Egg production (10^{12})	Index of age-1 hakes (individuals per trawl hour)
1996	116.625	
1997	81.774	347
1998	270. 512	438
1999	228.020	133
2000	627.484	250
2001	572.485	1367
2002		2444

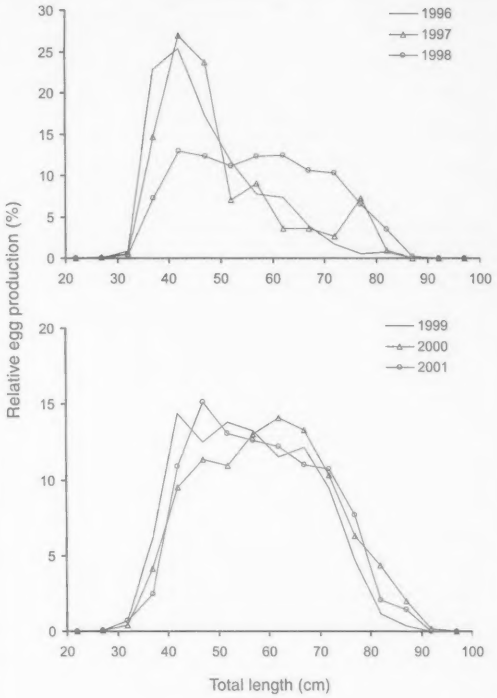

Figure 6

Relative egg production (%) by length class estimated for Argentine hake (*Merluccius hubbsi*) in January from 1996 to 2001.

change was characterized by a decrease in density on shoals and a movement of spawning females to deeper water, withand a more scattered distribution than in the early 1990s. Our results confirm previous observations reported by Ehrlich et al.[1], who analyzed ichtyoplankton samples collected from 1973 to 1999, in the traditional spawning area of Isla Escondida. These authors did not observe significant environmental anomalies that might have affected the spawning of hake and associated the change with the high levels in fishing exploitation in the 1990s. These shifts in the pattern of reproduction led to the following question: "How does the movement of the center of spawning affect the recruitment of Patagonian hake?"—given that different environmental conditions could be present in the new spawning area.

Our analyses show that the abundance of active females offshore of the north Patagonian area increased from 1998 to 2001, coinciding with a significant decrease in hake biomass in the shallow waters of Isla Escondida. During these years, demographic changes in the offshore area were characterized by an increase of larger females (>50 cm TL) compared to previous years. The increase in proportion of older individuals in spawning condition may result in a greater contribution to egg production because of the higher fecundity produced by larger females (Mairteinsdottir and Thorarinsson, 1998). In fact, egg production estimated for the offshore Patagonian hake during January showed an increase since 1998, with the highest values in 2000 and 2001 (400% more than those estimated in 1996–97). A high proportion (70%) of these eggs were spawned by females larger than 50 cm TL (≥5-year old, Otero et al., 1986), whereas in January 1996 and 1997 eggs were mainly produced by young females.

Because of the displacement of active females to deep water, the offshore north Patagonian area from 43°30′ to 45°S and between 50 m and 100 m depths was considered an important section of the spawning ground for Patagonian hake after 1998. The comparison between the January 1996 and 2001 surveys, in which inshore and offshore samples of the north Patagonian area were collected, demonstrated this change. In January 1996, spawning of Patagonian hake was concentrated inshore (Isla Escondida), whereas in January 2001 reproduction of this stock took place mainly offshore (Fig. 2). For this reason, the offshore egg production value obtained after 1998 was considered a representative index of the spawning area.

Relative abundance of hake at age 1 (number of individuals/hour) in the north-Patagonian area, showed a decline from 1996 to 2000 and an increase in 2001 and 2002, reaching the highest values of the study period. The recruitment index obtained for 2002 (2444 individuals/h) was about twice that estimated for 2001 (1367 individuals/h). According to Santos et al.,[3] it is possible that this value has been overestimated, because it was determined

[3] Santos, B. A., E. B. Louge, and R. Castrucci. 2003. Estudio de las variaciones conjuntas de la temperatura y de la salinidad del área de cría de la merluza con los índices de abundancia de los grupos de edad 0, 1 y 2. (enero 1995–enero 2002). Tech. Rep. 10/03, 6 p. INIDEP, CC. 175, Mar del Plata (7600), Argentina.

from samples collected two months later (March) than those during 1996–2001. These authors suggested that the spatial distribution or catchability of juvenile hake could have changed from January to March, resulting in a greater abundance index during 2002.

The higher recruitment levels observed for Patagonian hake during 2001 and 2002 were coincident with higher indices of egg production estimated offshore in January during the two previous years (2000 and 2001). Therefore, in principle we concluded that the change in spatial location of spawners in the Patagonian stock did not appear to negatively affect the recruitment of this species. The next question to be answered is: "Why were recruitment indices in the early 2000s higher than in previous years?"

Several authors have analyzed the spawner-recruit relationship in different species and have concluded that recruitment is often positively correlated with spawner biomass estimated from virtual population analysis (VPA) (Myers and Barrowman, 1996). In the case of Patagonian hake, the increase in abundance at age 1 observed in 2001 and 2002 was not associated with higher values of the VPA-based spawner biomass in previous years (GEM, unpubl. data[2]). Thus, environmental and ecological factors affecting prerecruit mortality should be considered, mainly in association with a no-fishing area implemented in 1997. Moreover, the demographic composition and the nutritional state of spawning females (maternal effect) are other factors that have been related to recruitment levels (Trippel et al., 1997; Kjesbu et al., 1998; Cardinale and Arrhenius, 2000).

Analysis of hydrographic characteristics from the north-Patagonian waters in the 1980s and 1990s indicated that the Patagonian shelf, including the Isla Escondida area, is a relatively stable environment (Erhlich et al.[2]). On the other hand, analysis of temperature and salinity data collected from 1995 to 2002 in the nursery area of the Patagonian stock (San Jorge Gulf), showed that higher values of salinity and temperature during the time of hatching were associated with higher indices of abundance at age 1, one year later (Santos et al.[3]).

The high proportion of larger females in the offshore area mainly in 2000 and 2001 may have affected the quality as well as the quantity of hake progeny. In general, older females produce larger eggs and larger larvae with higher rates of survival, in combination with more egg batches over a longer spawning season (Kjesbu et al., 1996; Trippel, 1998). Previous reports showed that *M. hubbsi* older than 5-years have a longer spawning season (Macchi et al., 2004) and produce heavier eggs than young females do (Pájaro et al.[4]). Thus, an increase in the proportion of older spawning females in the stock may result in improved recruitment, as has been reported for other species (Mairteinsdottir and Thorarinsson, 1998).

The fishing regulation for Patagonian hake implemented in the late 1990s mainly affected bottom trawlers and the factory freezer fleet, which applied greater fishing effort in the north Patagonian area during the 1990s. It is possible that this decline in harvesting pressure by trawlers on Patagonian hake after 1997 influenced the reproductive success of this species. Stress can have a negative impact on fish reproduction (Campbell et al, 1994; Clearwater and Pankhurst, 1997). The potential effects of trawl avoidance can affect the reproductive physiology and behavior during spawning, which could lead to the production of fewer viable juveniles (Morgan et al., 1999).

Finally, other factors, such as predation and feeding conditions within the new spawning ground of Patagonian hake, can affect survival of the early life stages. In addition, future studies should include a comparison between the inshore and offshore waters of the north-Patagonian area with respect to the abundance of jellyfish (i.e., Medusae and Ctenophora), which are known to be major predators of fish eggs and larvae (Bailey, 1984; Fancett, 1988).

[4] Pájaro, M, E. Louge, G. J. Macchi, N. Radovani, and L. Rivas. 2002. Calidad de los ovocitos de la población patagónica de merluza (*Merluccius hubbsi*) durante la época de puesta estival. Tech. Rep. 55/02, 13 p. INIDEP, CC. 175, Mar del Plata (7600), Argentina.

Acknowledgments

We thank Jorge Hansen for assistance with the method used to estimate fish abundance. We would also like to thank Hector Cordo for reading and making suggestions to improve the manuscript.

Literature cited

Aubone, A., S. Bezzi, R. Castrucci, C. Dato, P. Ibañez, G. Irusta, M. Pérez, M. Renzi, B. Santos, N. Scarlato, M. Simonazzi, L. Tringali, and F. Villarino.
2000. Merluza (*Merluccius hubbsi*). *In* Síntesis del estado de las pesquerías marítimas argentinas y de la Cuenca del Plata. Años 1997–1998, con una actualización de 1999 (S. Bezzi, R. Akselman and E. Boschi, eds.), p. 29–40. INIDEP, Mar del Plata, Argentina.

Bailey, K. M.
1984. Comparison of laboratory rates of predation on five species of marine fish larvae by three planktonic invertebrates. Effects of larval size on vulnerability. Mar. Biol. 79:303–309

Campbell, P. M., T. G. Pottinger, and J. P. Sumpter.
1994. Preliminary evidence that chronic confinement stress reduces the quality of gametes produced by brown and rainbow trout. Aquaculture 120:151–169.

Cardinale, M., and F. Arrhenius.
2000. The influence of stock structure and environmental conditions on the recruitment process of Baltic cod estimated using a generalized additive model. Can. J. Fish. Aquat. Sci. 57: 2402–2409.

Ciechomski, J. D., R. P. Sánchez, C. A. Lasta, and M. D. Ehrlich.
1983. Distribución de huevos y larvas de anchoíta (*En-*

graulis anchoita) y de merluza (*Merluccius hubbsi*), evaluación de sus efectivos desovantes y análisis de los métodos empleados. Contrib. Inst. Nac. Invest. Desarr. Pesq. (Mar del Plata) 432:3–37.

Clearwater, S. J., and N. W. Pankhurst.
1997. The response to capture and confinement stress of plasma cortisol, plasma sex steroids and vitellogenic oocytes in the marine teleost, red gurnard. J. Fish Biol. 50:429–441.

Cousseau, M. B., and R. G. Perrota.
1998. Peces marinos de Argentina. Biología distribución y pesca, 163 p. INIDEP, Mar del Plata, Argentina.

Fancett, M. S.
1988. Diet and prey selectivity of scyphomedusae from Port Phillip Bay, Australia. Mar. Biol. 98:503–509.

Hunter, J. R., B. J. Macewicz, N. C. H. Lo, and C. A. Kimbrell.
1992. Fecundity, spawning, and maturity of female Dover sole *Microstomus* 13 *pacificus*, with an evaluation of assumptions and precision. Fish. Bull. 90:101–128.

Kjesbu, O. S., P. Solemdal, P. Bratlan, and M. Fonn.
1996. Variation in annual egg production in individual captive Atlantic cod (*Gadus morhua*). Can. J. Fish. Aquat. Sci. 53:610–620.

Kjesbu, O. S., P. R. Witthames , P. Solemdal, and M. Greer Walker.
1998. Temporal variations in the fecundity of Arcto-Norwegian cod (*Gadus morhua*) in response to natural changes in food and temperature. J. Sea Res. 40:303–321.

Macchi G. J., and M. Pájaro.
2003. Comparative reproductive biology of some commercial marine fishes from Argentina. Fisken Og Havet 12:69–77.

Macchi, G. J., M. Pájaro, and M. Ehrlich.
2004. Seasonal egg production pattern of the Patagonian stock of Argentine hake (*Merluccius hubbsi*). Fish. Res. 67:25–38.

Mairteinsdottir, G., and K. Thorarinsson.
1998. Improving the stock-recruitment relationship in Icelandic cod (*Gadus morhua* L.) by including age diversity of spawners. Can. J. Fish. Aquat. Sci. 55:1372–1377.

Marshall, T., O. S. Kjesbu, N. A. Yaragina, P. Solemdal, and O. Ulltang.
1998. Is spawner biomass a sensitive measure of the reproductive and recruitment potential of Northeast Arctic cod? Can. J. Fish. Aquat. Sci. 55:1766–1783.

Morgan, M. J., C. E. Wilson, and L. W. Crim.
1999. The effect of stress on reproduction in Atlantic cod. J. Fish Biol. 54 (3):477–488.

Myers, R. A., and N. J. Barrowman.
1996. Is fish recruitment related to spawner abundance? Fish. Bull. 94:707–724.

Otero, H. O., M. S. Giangiobe, and M. A. Renzi.
1986. Aspectos de la estructura de población de la merluza (*Merluccius hubbsi*). II Distribución de tallas y edades. Estadios sexuales. Variaciones estacionales. Publ. Com. Téc. Mix. Fr. Mar. 1 (1):147–179.

Trippel, E. A.
1998. Egg size and viability and seasonal offspring production of young Atlantic cod. Trans. Am. Fish. Soc. 127:339–359.

Trippel, E. A., O. S. Kjesbu, and P. Solemdal.
1997. Effects of adult age and size structure on reproductive output in marine fishes. *In* Early life history and recruitment in fish populations (R. C. Chambers and E. A. Trippel, eds.), p. 31–62. Chapman & Hall, New York, NY.

Feeding habits of the dwarf weakfish (*Cynoscion nannus*) off the coasts of Jalisco and Colima, Mexico

Alma R. Raymundo-Huizar
Centro Universitario de la Costa, Departamento de Ciencias
Universidad de Guadalajara
Av. Universidad 203
Puerto Vallarta, Jalisco, CP 48280 México

Horacio Pérez-España
Centro de Ecología y Pesquerías
Universidad Veracruzana
Dr. Castelazo s/n. Xalapa
Veracruz, CP 91190 México

Maite Mascaró
Laboratorio de Ecología y Conducta
Unidad Académica Sisal
Universidad Nacional Autónoma de México
Sisal, Yucatán, CP 97355 México

Xavier Chiappa-Carrara
Unidad de Investigación en Ecología Marina, FES–Z
México, DF, CP 09230 México
Present address: Unidad Académica Sisal
Universidad Nacional Autónoma de México
Sisal, Yucatán, CP 97355 México
E-mail address (for X. Chiappa-Carrara, contact author): chiappa@servidor.unam.mx

Sciaenids from the Pacific coast of Mexico are used as a second-class fish species for human consumption (Aguilar-Palomino et al., 1996). The dwarf weakfish (*Cynoscion nannus*) (Castro-Aguirre and Arvizu-Martínez, 1976) is often caught as bycatch in the shrimp fishery but, because of its small size (<27 cm TL, total length), it is not considered a valuable resource. This species can be found in great numbers in waters between 100 and 812 m (Allen and Robertson, 1994; Fischer et al., 1995) associated with the soft-bottom regions off the coast of Jalisco and Colima (González-Sansón et al., 1997).

Previous studies of the trophic biology of the Sciaenidae (Chao and Musik, 1977; Campos and Corrales, 1986; Chao, 1995; Peláez-Rodríguez, 1996; Cruz-Escalona, 1998; Lucena et al., 2000) have shown that they feed on a variety of small fish and benthic invertebrates (Allen and Robertson, 1994). However, there are few studies concerning the feeding habits of *C. nannus*, and its dietary preferences are not known. Considering its abundance, *C. nannus* must play an important role in the trophic relationships of soft-bottom ecosystems in this region.

Most studies describing the feeding habits of fish have used the normalized version of the breadth niche index proposed by Levins (1968). This index is based both on the number of food resources and on the proportion of prey used by a species. The appropriate distribution function for this index ensures sample independence among prey found in any particular stomach. Distribution functions based either on the number or the relative biomass or volume of dietary items do not ensure such independence, given that all items found in any particular stomach are statistically associated (Hurlbert, 1984). Therefore, neither the number nor the relative biomass or volume of dietary items should be used to calculate the Levins index. The only distribution function that ensures statistical independence is that which is based on the proportion of stomachs in which a certain food resource is found (Krebs, 1999).

Considering the ecological importance of studying the feeding habits of this abundant fish species, we examined trophic breadth variations (temporally and ontogenetically) of *C. nannus*. When attempting to correctly apply the Levins index, we used the distribution function of prey that ensures statistical independence among sampling units.

Materials and methods

The sampling area was located in the central region of the continental shelf off the Pacific coast of Mexico, where the mouth of the river Cuitzmala, in Punta Farallón, Jalisco (19°22′N, 105°01′W), is the northern limit, and Cuyutlán, Colima (18°55′N, 104°08′W), is the southern limit. Samples of *C. nannus* were collected on a monthly basis from January to December 1996 (except February, August, and September) on the research vessel *BIP V*, equipped with a trawl net with a pair of codends. Sampling was carried out over seven transects perpendicular to the coast, each comprising four bathymetric strata: 20, 40, 60, and 80 m mean depth.

Fish were individually identified, measured (TL, ±1 mm), and the total weight of each fish was recorded to the nearest 0.1 g. The stomachs of individual fish were dissected and preserved in 10% neutralized formalin. Stomach contents were analyzed

Manuscript submitted 16 May 2003
to the Scientific Editor's Office.
Manuscript approved for publication
20 December 2004 by the Scientific Editor.
Fish. Bull. 103:453–460 (2005).

with a stereoscopic microscope and dietary items were identified to the lowest taxonomic level possible by using specialized keys. Garth (1958), Rodríguez de la Cruz (1987), Hendrickx and Salgado-Barragán (1991), and Hendrickx (1996), were consulted for crustacean identification, whereas Jordan and Evermann (1896–1900), Castro-Aguirre (1978), Allen and Robertson (1994), Thomson et al. (2000), and FAO guides were used for fish identification (Fischer et al., 1995).

Both the number of individuals and weight of each dietary category were quantified, and mean proportions in terms of number ($\%N_{\bar{x}}$) and biomass ($\%W_{\bar{x}}$) were calculated according to Tirasin and Jørgensen (1999):

$$\%\bar{X}_i = \frac{\sum_{j=1}^{n_j} X_{ij}}{\sum_{i=1}^{k}\sum_{j=1}^{n_j} X_{ij}} \times 100,$$

where X_{ij} = the number or weight of each taxa i in the j^{th} stomach; and
k = the number of dietary components found in all stomachs analyzed, n_j.

The percent frequency of occurrence of each component was also obtained ($\%F$). Finally, the index of relative importance for each dietary category was calculated (*IRI*, Pinkas et al., 1971; Rosecchi and Nouaze, 1987):

$$IRI_i = (\%N_i + \%P_i) \times \%F_i.$$

Relative importance index values were expressed as a percentage of the total items analyzed (Cortés, 1997) and results were graphically represented as a rectangle of base $\%F$ and height $\%N + \%W$.

Variance analysis was applied on transformed $W' = \sin^{-1}(\sqrt{W})$] gravimetric proportions of the dietary components (Zar, 1999) to evaluate both monthly and ontogenetic variations in the feeding habits of *C. nannus*. The number [$q=1+3.322(\mathrm{Log}_{10}n)$] and width of size classes ($w=R_{TL}/q$) were considered for analysis, where n is the sample size and $R_{TL}=TL_{max}-TL_{min}$.

For the analysis of trophic niche breadth, the normalized version of the index proposed by Levins (1968) was used. This index combines both the number of prey resources used (k) (i.e., the trophic spectrum) and the relative frequency with which each prey resource is consumed (j). This represents the distribution function of prey proportions in diet (Hespenheide 1975; Hurlbert, 1978):

$$Ba = \frac{\left(\sum_{j=1}^{n_j} p_j^2\right)^{-1} - 1}{k-1}.$$

Because the ensemble of prey found in any given stomach does not constitute independent samples (Hurlbert, 1984), p_j was calculated as the proportion of individual fish (N^*) that consumed a certain food resource in relation to the number of resources used by the total number of fish:

$$P_j = \frac{N_j^*}{\sum_i \sum_j N_j^*} \text{ so that } \sum p_j = 1.$$

Ba values range between 0 and 1. Zero values indicate that fish feed on only one prey type, representing the minimum diet breadth and high feeding specialization. Unity values, on the other hand, indicate that the species consumed all k food resources in the same proportion ($p_j=1/k$), representing no selection among prey types and the widest possible trophic niche (Gibson and Ezzi, 1987; Labropoulou and Eleftheriou, 1997). *Ba* values were calculated on the basis of matrix resources (Colwell and Futuyma, 1971) both for each month and for each size class. The percentage similarity measure (R) between size classes q' and q'' (Renkonen, 1938; Schoener, 1970; Hurlbert, 1978) was calculated as

$$R_{q'q''} = 1 - \frac{1}{2}\left[\sum_{j=1}^{k} \left| p_{jq'} - p_{jq''} \right|\right],$$

where p_{jq} is the proportion of individual fish in each size class that consumed a certain food resource, calculated over the total number of stomachs per size class.

Confidence intervals ($\mathrm{CI}_{95\%}$) of *Ba* were obtained by means of the bootstrap method (Mueller and Altenberg, 1985; Efron and Tibshirani, 1986) by considering two thousand resamplings of the data (Hamilton, 1991).

Results

The 311 *Cynoscion nannus* examined ranged from 7.5 to 20.6 cm TL. Food was found in 287 (92%, ranging from 85% to 98% among size classes) stomachs. The trophic spectrum of *C. nannus* is composed of 29 dietary items (Table 1), which were classified into four general categories: penaeid shrimp, fish, stomatopods, and cephalopods.

Penaeid shrimp constituted the principal dietary category of *C. nannus* ($N_{\bar{x}}$=82.5%, $W_{\bar{x}}$=35.4%; $F_{\bar{x}}$=43.9%, $IRI_{\bar{x}}$=74.6%; Fig. 1), of which juvenile stages were the most frequent ($F_{\bar{x}}$=23.4%). Fish were the second most important category ($N_{\bar{x}}$=6.5%, $W_{\bar{x}}$=36.5%, $F_{\bar{x}}$=37.7%, $IRI_{\bar{x}}$=14.5%), followed by stomatopods of the *Squilla* genus ($N_{\bar{x}}$=5.8%, $W_{\bar{x}}$=8.6%, $F_{\bar{x}}$=25.5%, $IRI_{\bar{x}}$=6.6%). The cephalopod *Loliopsis diomedae* was the last category in order of importance ($N_{\bar{x}}$=1.0%, $W_{\bar{x}}$=12.4%, $F_{\bar{x}}$=4.2%, $IRI_{\bar{x}}$=1.8%).

Overall, significant differences in diet were found between individuals of different size classes (F=1.03; $P<0.05$). Values of the percentage similarity of diet (R) between size classes were, in general, <50% (Table 2). R-values were relatively high only among size classes 2

Table 1

Composition of the trophic spectrum of *Cynoscion nannus* (7.5 cm ≤TL ≤20.6 cm; n=287) from the coast of Jalisco and Colima (mean percentage by weight [g; *%W*], frequency of occurrence [*%F*], number [*%N*], and index of relative importance [*%IRI*] of prey).

Dietary categories		*%W*	*%F*	*%N*	*%IRI*
Cephalopods	*Loliopsis diomedae*	12.4	4.2	1.0	1.8
	Remains	0.1	0.4	0.1	0.0
Stomatopods	*Squilla* sp.	5.9	19.7	4.0	6.4
	S. panamensis	1.5	1.7	0.8	0.1
	S. hancocki	0.5	1.7	0.4	0.0
	S. mantoidea	0.7	2.5	0.7	0.1
Penaeid shrimps	*Solenocera* sp.	7.6	10.9	4.3	4.2
	S. florea	2.2	1.3	0.6	0.1
	S. mutator	3.8	2.9	4.6	0.8
	Trachypenaeus brevisuturae	3.5	5.4	2.3	1.0
	Juvenile shrimps	18.2	23.4	70.8	68.4
Other crustaceans	Carideans	1.3	4.2	0.9	0.3
	Panulirus sp. larvae	0.1	0.4	0.1	0.0
	Other crustacean larvae	0.1	0.4	0.3	0.0
	Euphausiids	0.5	1.3	2.3	0.1
	Microcrustaceans	0.2	0.4	0.1	0.0
	Unidentified remains	4.2	13.8	—	1.9
Fish	*Cynoscion nannus*	2.1	0.8	0.4	0.1
	Cherublemma emmelas	1.3	1.7	1.0	0.1
	Polydactylus opercularis	1.6	1.3	0.4	0.1
	Ophidium sp.	0.7	0.4	0.8	0.0
	Monolene sp.	0.9	0.4	0.1	0.0
	Symphurus sp.	0.1	0.4	0.1	0.0
	Bregmaceros bathymaster	1.6	2.5	0.7	0.2
	Anguilliformes	1.2	2.1	0.5	0.1
	Leptocephalus larvae	8.9	4.2	1.1	1.4
	Other fish larvae	1.4	1.7	1.0	0.1
	Unidentified remains	16.6	22.2	0.3	12.3
Anelids	Polychaeta	0.62	1.26	0.38	0.0

Table 2

Percentage similarity values (R) of the diet between size classes (cm, TL) of *Cynoscion nannus* (n=287) from the coast of Jalisco and Colima.

	Size class (cm)					
	7.0–8.9	9.0–10.9	11.0–12.9	13.0–14.9	15.0–16.9	17.0–18.9
Size class (cm)						
9.0–10.9	37.0					
11.0–12.9	44.2	54.2				
13.0–14.9	33.5	65.1	51.1			
15.0–16.9	31.0	47.6	51.4	64.1		
17.0–18.9	12.5	31.6	39.6	38.0	40.4	
19.0–20.9	29.3	45.8	44.3	47.9	40.1	21.6

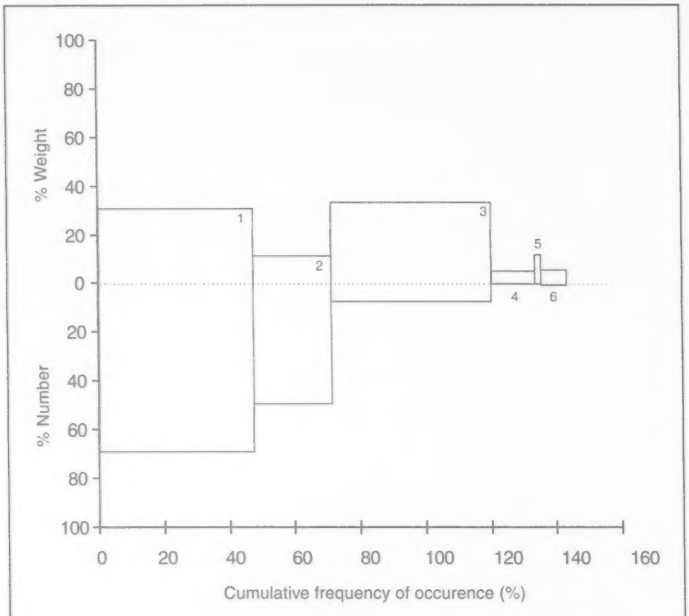

Figure 1

Graphical representation of the percentage values of the index of relative importance (*IRI*) of the main dietary components found in the stomachs of *Cynoscion nannus* (n=287). 1: penaeid shrimps; 2: stomatopods; 3: fish; 4: crustacean remains; 5: cephalopods; 6: other crustaceans.

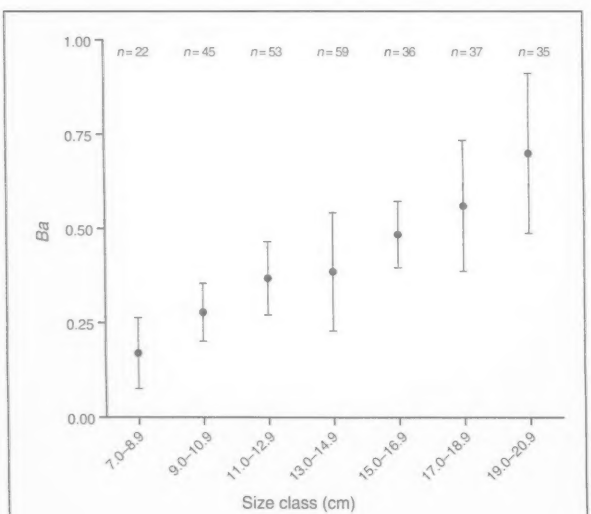

Figure 2

Ontogenetic variations of the diet diversity index ($Ba \pm CI_{95\%}$) of *Cynoscion nannus* (n is the number of stomachs containing food).

through 5 (51.1%–65.1%). The trophic spectrum of the smallest *C. nannus* (7 cm ≤TL ≤10.9 cm, n=67) was composed by crustaceans ($W_{\bar{x}}$=68%), mostly carideans and stomatopods ($W_{\bar{x}}$=20%). The diet of intermediate individuals (11 cm ≤TL ≤16.9 cm; n=148) was composed by penaeid shrimp, fish, and stomatopods. Only fish of the size classes grouped in this range showed percentages of diet similarity >50%. Among *C. nannus* between 17 and 18.9 cm TL (n=37), the value of consumed fish biomass attained 69%, whereas that of penaeid shrimp reached 20%. Only among the larger individuals (19 cm ≤TL ≤20.9 cm; n=35) did cephalopods attain high gravimetric values ($W_{\bar{x}}$=45%) followed by penaeid shrimp ($W_{\bar{x}}$=38%).

Values of trophic niche breadth for each size class indicated ontogenetic variation in the diet (Fig. 2). The smallest individuals fed on a smaller number of prey species and showed a trend towards higher trophic specialization. Larger individuals, however, had a wider trophic spectrum and fed on a greater number of different prey species.

Temporal variations in the dietary composition of *C. nannus* were significant (F=3.58; P<0.05). During the first months of the year, *C. nannus* consumed a higher percentage of fish ($W_{\bar{x}}$=37.2%),

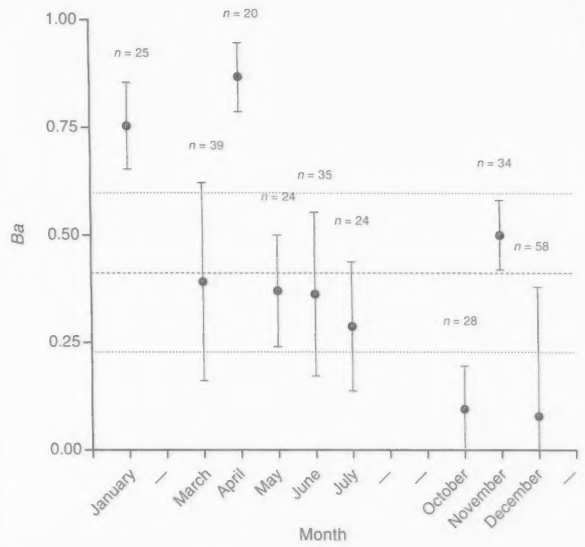

Figure 3

Monthly mean values of the diet diversity index ($Ba \pm CI_{95\%}$) of *Cynoscion nannus*. The overall mean value of the index (Ba; - - -) and its confidence intervals ($CI_{95\%}$; ....) are shown (n is the number of stomachs containing food).

whereas towards the end of the year, penaeid shrimp were eaten in higher proportions ($W_{\bar{x}}$=50.6%). During May, stomatopods and carideans were found with higher biomass values than during the rest of the year ($W_{\bar{x}}$ =68.2% and 20%, respectively). Cephalopods were found in most months with biomass values ranging from 4% to 34% of consumed biomass.

The mean value of diet diversity was 0.41 (±0.18 $CI_{95\%}$). Although the number of dietary categories for *C. nannus* that were identified was high (29 prey types), there were a few items with significant importance. Monthly variations in *Ba* ranged from 0.1 to 0.8 (Fig. 3). During most of the period analyzed, *Ba* values were not significantly different from each other as shown by the lack of overlap between $CI_{95\%}$. The only exceptions were January and April, when $CI_{95\%}$ was above the mean $Ba \pm CI_{95\%}$ value, and October when $CI_{95\%}$ was below the mean *Ba*.

Discussion

Cynoscion nannus is a carnivorous fish that feeds on at least 29 different prey types. Although cannibalistic behavior has been reported for several fish species in a variety of habitats and life-history strategies (Smith and Reay, 1991), *C. nannus* as a prey type was found in only 0.8% (two individuals >15.0 cm TL) of all stomachs analyzed. According to the IRI values, crustaceans—specifically juvenile shrimp and stomatopods of the genus *Squilla*—appear to be the most important items in the diet. The type of substrate can influence the feeding habits of these fish. For example, Minello and Zimmerman (1984) observed that under experimental conditions, the feeding preferences of *C. nebulosus* (16 cm≤TL≤21 cm) for *Farfantepenaeus aztecus* varied depending on the substrate. These authors suggested that substrate characteristics determine the burrowing capacity of *F. aztecus* and thus predator avoidance. In the study area, juvenile shrimp and stomatopods of the genus *Squilla* can be abundantly found in soft-bottom habitats (González-Sansón et al., 1997). Both the cephalopod (*Loliopsis diomedae*) and the fish species found in the stomach contents of *C. nannus* are pelagic or demersal species, indicating that the feeding activities of *C. nannus* are not exclusively limited to the benthos, and that this species can forage throughout the water column. Results in the present study provide evidence that fish feeding at different water depths have access to a broader variety of prey types. This has been shown both for other Sciaenidae (Chao and Musik, 1977; Campos and Corrales, 1986; Chao, 1995; Peláez-Rodríguez, 1996; Cruz-Escalona, 1998), and other species of demersal fish (Lucena et al., 2000).

It should be noted that graphic representations of the IRI values are more accurate in describing the diet of fish species (Cortés, 1997). Our results (Fig. 1) demonstrate that the three indices representing the relative importance of each food item highlight the influence that the percentages of occurrence, by number and by weight, have on the overall IRI values.

The temporal analysis of the tropic spectrum of *C. nannus* showed that during October, November, and December this species fed mainly on penaeid shrimps. Fish prey were abundant in stomachs collected only during March, April, June, and November. Stomatopods were present all year round, but only abundant during May. Low *Ba* values in October were due to the prevailing consumption of *Solenocera* spp. Monthly differences in the diet of *C. nannus* were most probably in accordance with the seasonal variations in prey species abundance, which in turn determined their availability. Lucena et al. (2000) found that temporal variations in the diet of *C. guatucupa* from southern Brazil are related to seasonal production cycles of prey, mainly fish and crustaceans, thus supporting the view that sciaenids can generally be considered opportunistic species.

Results of this study showed ontogenetic variations in the trophic spectrum of *C. nannus*. The smallest individuals (7 cm ≤TL ≤10.9 cm) feed mainly on stomatopods, whereas larger individuals (≥11 cm TL), consume less stomatopods and more penaeid shrimp and fish. Merriner (1975) also found ontogenetic variations in the diet of *C. regalis*, where the smallest individuals (age group "0") fed on crustaceans and small fish. The relative importance of shrimp, however, decreased as *C. regalis* increased in size, and individuals of age group "2" generally consumed different species of clupeids, depending on the local abundance of each prey species. The measure of percentage similarity among size classes (Table 2) shows that *C. nannus* share a limited number of resources. Only fish belonging to intermediate lengths feed on the same prey types in percentages greater than 50% for the total number of food resources used.

Ontogenetic changes in the diet of *C. nannus* observed in the present study are due to differences in diet composition and proportions of consumed prey. These results suggest that food types are ingested unequally as fish grow and that morphological and physiological changes take place. As fish grow, the size of their mouth increases proportionally, their swimming capacity is modified, and their energetic requirements vary. Thus, larger fish have different feeding requirements than smaller ones and will attempt to satisfy them by consuming a larger variety of prey types. As *C. nannus* grow, *Ba* values increase and the trophic spectrum of the species grows wider (Fig. 2). Our results indicate that there is a pattern of differential use of food resources throughout the different size classes of *C. nannus*, and suggest a possible ecological strategy to reduce intraspecific competition for food in the population (Schoener, 1974; Werner, 1979).

The increasing variety of food resources used as predators increase in size is a common pattern among marine organisms, including invertebrates (Rangeley and Thomas, 1987; Mascaró and Seed, 2001). These ontogenetic variations in food preferences can be explained by changes in foraging behavior where predators of certain size classes actively select their prey (Jubb et al., 1983; Allan et al., 1987). Alternatively, they can be the result of passive mechanisms that do not involve individual decisions associated with age or life stages, such as differences in the predator's mouth structures, changes in movement velocity of both prey and predator, and spatial or temporal variations in habitat as predators increase in size (Hughes, 1979; Rodrigues et al., 1987).

To show that *Ba* values are affected by the type of prey distribution function used, we calculated the mean diet diversity index using 1) the proportion of the number of prey (N; Ba=0.03), 2) the percent frequency of occurrence of prey (F; Ba=0.16), and 3) the proportion of prey biomass (W; Ba=0.32). The values obtained were then compared to those calculated by considering the proportion of individuals (N^*; Ba=0.41) that use a certain food resource for the total number of stomachs analyzed. *Ba* values calculated by using N, F, and W are markedly lower than the *Ba* value obtained by using N^*. These differences serve to underline the importance of complying strictly with the property of statistic independence of sampling units when the feeding habits of a species are being studied.

Given the numerical importance of *C. nannus* as part of demersal assemblages, observations on the trophic spectrum of this and other species can help to generate a conceptual model of the trophic webs and dynamics of the feeding relations among communities found on the continental shelf of Jalisco and Colima, an area that has received little attention in the past.

Acknowledgments

J. Arciniega, R. García de Quevedo, and V. Landa-Jaime kindly verified the taxonomic status of prey. We also thank L. E. Hidalgo-Arcos for his technical support and S. Bowers who edited the text.

Literature cited

Aguilar-Palomino, B., J. Mariscal-Romero, G. González-Sansón, and L. E. Rodríguez-Ibarra.
1996. Ictiofauna demersal de fondos blandos de la plataforma continental de Jalisco y Colima, México, en la Primavera de 1995. Cienc. Mar. 22:469–481.

Allan, J. D., A. S. Flecker, and N. L. McClintock.
1987. Prey preference of stoneflies: sedentary vs. mobile. Oikos 49:323–331.

Allen, G. R., and R. Robertson.
1994. Fishes of the tropical Eastern Pacific, 380 p. Univ. Hawaii Press, Honolulu, HI.

Campos, J., and A. Corrales.
1986. Preliminary results on the trophic dynamics of the Gulf of Nicoya, Costa Rica. An. Inst. Cienc. Mar y Limnol. Univ. Nal. Autón. México 13:329–334.
Castro-Aguirre, J. L.
1978. Catálogo sistemático de los peces marinos que penetran a las aguas continentales de México, con aspectos zoogeográficos y ecológicos. Dep. Pesca, Inst. Nal. Pesca (México), Ser. Cient. 19, 298 p
Castro-Aguirre, J. L., and J. Arvizu-Martínez.
1976. Una nueva especie de *Cynoscion*, del Pacífico de México (Pisces: Sciaenidae: Otholitinae). Rev. Soc. Mex. Hist. Nat. 37:323–329
Chao, L. N.
1995. Familia Sciaenidae. *In* Guía FAO para la identificación de especies para los fines de la pesca. Pacífico Centro–oriental. Vertebrados, parte 1 (W. Fischer, F. Krupp, W. Schneider, C. Sommer, K. E. Carpenter, and V. H. Niem, eds.), p. 647–1200. FAO, Rome.
Chao, L. N., and J. A. Musick.
1977. Life history, feeding habits and functional morphology of juvenile sciaenid fishes from the York River estuary, Virginia. Fish. Bull. 75:675–702.
Colwell, R. K., and D. J. Futuyma.
1971. On the measurement of niche breadth and overlap. Ecology 52:567–576.
Cortés, E.
1997. A critical review of methods of studying fish feeding based on analysis of stomach contents: application to elasmobranch fishes. Can. J. Fish. Aquat. Sci. 54:726–738.
Cruz-Escalona, V. H.
1998. Análisis trófico de la ictiofauna de la laguna de San Ignacio, B.C.S. M.Sc. thesis, 128 p. Instituto Politécnico Nacional, México.
Efron, B., and R. Tibshirami.
1991. Statistical analysis in computer age. Science 253:390–395.
Fischer, W., F. Krupp, C. Sommer, C. E. Carpenter, and V. H. Niem.
1995. Guía FAO para la identificación de especies para los fines de pesca. Pacífico centro–oriental. FAO II–III:647–1200.
Garth, J. S.
1958. Brachyura of the Pacific coast of America; Oxyrhyncha: Majidae. Allan Hancock Pacific Expeditions 21(1–2):1–854.
Gibson, R. N., and I. A. Ezzi.
1987. Feeding relationships of a demersal fish assemblage on the west coast of Scotland. J. Fish Biol. 31: 55–69.
González-Sansón, G., B. Aguilar-Palomino, J. Arciniega-Flores, R. García de Quevedo-Machain, E. Godínez-Domínguez, V. Landa-Jaime, J. Mariscal-Romero, J. E. Michel-Morfín, and M. Saucedo-Lozano.
1997. Variación espacial de la abundancia de la fauna de fondos blandos en la plataforma continental de Jalisco y Colima, México (Primavera 1995). Cienc. Mar. 23:93–110.
Hamilton, L. C.
1991. Bootstrap programming. Stata Tech. Bull. 4:18–27.
Hendrickx, M. E.
1996. Los camarones Penaeoidea bentónicos (Crustacea: Decapoda: Dendrobranchiata) del Pacífico mexicano, 147 p. CONABIO–Instituto de Ciencias del Mar y Limnología, Universidad Nacional Autónoma de México.
Hendrickx, M. E., and J. Salgado-Barragán.
1991. Los estomatópodos (Crustacea: Hoplocarida) del Pacífico mexicano. An. Inst. Cienc. Mar y Limnol. Univ. Nal. Autón. México, Publ. Esp. 10, 200 p
Hespenheide, H. A.
1975. Prey characteristics and predator niche width. *In* Ecology and evolution of communities (M. L. Cody and J. M. Diamond, eds.), p. 158–180. Harvard Univ. Press., Boston, MA.
Hughes, R. N.
1979. Optimal diets under the energy maximization premise: the effects of recognition time and learning. Am. Nat. 113:209–221.
Hurlbert, S. H.
1978. The measurement of niche overlap and some relatives. Ecology 59:67–77.
1984. Pseudoreplication and the design of ecological field experiments. Ecol. Monogr. 54:187–211.
Jordan, D. S., and B. W. Evermann.
1896–1900. The fishes of North and Middle America: a descriptive catalogue of the species of fish-like vertebrates found in the waters of North America, North of the Isthmus of Panama. Bull. U.S. Nat. Mus. 47(1–4):1–3313.
Jubb, R. N., R. N. Hughes, and T. ap Rheinallt.
1983. Behavioral mechanisms of size–selection by crabs *Carcinus maenas* feeding on the mussels *Mytilus edulis*. J. Exp. Mar. Biol. Ecol. 66:81–87.
Krebs, C. J.
1999. Ecological methodology, 620 p. Benjamin/Cummings, Mendo Park, CA.
Labropoulou, M., and A. Eleftheriou.
1997. The foraging ecology of two pairs of congeneric demersal fish species: importance of morphological characteristics in prey selection. J. Fish Biol. 50:324–340.
Levins, R.
1968. Evolution in changing environments: some theoretical explorations, 120 p. Princeton Univ. Press, Princeton, NJ.
Lucena, F. M., T. Vaske Jr., J. R. Ellis, and C. M. O'Brien.
2000. Seasonal variation in the diets of bluefish, *Pomatomus saltatrix* (Pomatomidae) and striped weakfish, *Cynoscion guatucupa* (Sciaenidae) in southern Brazil: implications of food partitioning. Environ. Biol. Fish. 57:423–434.
Mascaró, M., and R. Seed.
2001. Foraging behaviour of juvenile *Carcinus maenas* (L.) and *Cancer pagurus* L. Mar. Biol. 139:1135–1145.
Merriner, J. V.
1975. Food habits of the weakfish, *Cynoscion regalis*, in North Carolina waters. Chesapeake Sci. 16:74–76.
Minello, T. J., and R. J. Zimmerman.
1984. Selection for brown shrimp, *Penaeus aztecus*, as prey by the spotted seatrout, *Cynoscion nebulosus*. Contrib. Mar. Sci. 27:159–167.
Mueller, L. D., and L. Altenberg.
1985. Statistical inference on measures of niche overlap. Ecology 66:1204–1210.
Peláez-Rodríguez, E.
1996. Relaciones ecológicas de los peces ictiófagos demersales de la zona de pesca comercial de Alvarado, Veracruz. B.Sc. thesis, 84 p. Universidad Nacional Autónoma de México, México.
Pinkas, L., M. S. Oliphant, and I. L. K. Iverson.
1971. Food habits of albacore, bluefin tuna and bonito in

California waters. Calif. Dep. Fish Game, Fish Bull. 152:1–105.

Rangeley, R. W., and M. L. H. Thomas.
1987. Predatory behavior of juvenile shore crab *Carcinus maenas*. J. Exp. Mar. Biol. Ecol. 108:191–197.

Renkonen, O.
1938. Statistisch-ökologische Untersuchungen über die terrestische Käferwelt der finnischen Bruchmoore. Ann. Zool. Soc. Zool-Bot. Fenn. Vanamo 6:1–231.

Rodrigues, C. L., S. Nojima, and T. Kikuchi.
1987. Mechanics of prey size preference in the gastropod *Neverita didyma* preying on the bivalve *Ruditapes philippinarium*. Mar. Ecol. Prog. Ser. 40:87–93.

Rodríguez de la Cruz, M. C.
1987. Crustáceos Decápodos del Golfo de California. Secretaría de Pesca, México 2:145–306

Rosecchi, E., and Y. Nouaze.
1987. Comparaison de cinq indices alimentaires utilisés dans l'analyse des contenus stomacaux. Rev. Trav. Inst. Pêches Mar. Nantes 49:111–123.

Schoener, T. W.
1970. Nonsynchronous spatial overlap of lizards in patchy habitats. Ecology 51:408–418.
1974. Resource partitioning in ecological communities. Science 185:27–39.

Smith, C., and P. Reay.
1991. Cannibalism in teleost fish. Rev. Fish Biol. Fish. 1:41–64.

Thomson, D. A., L. T. Findley, and A. N. Kerstitch.
2000. Reef fishes of the Sea of Cortez, 407 p. Univ. Texas Press, Austin, TX

Tirasin, E. M., and T. Jørgensen.
1999. An evaluation of the precision of diet description. Mar. Ecol. Prog. Ser. 182:243–252.

Werner, E. E.
1979. Niche partitioning by food size in fish communities. *In* Predator-prey systems in fisheries management (R. H. Stroud and H. Clepper, eds.), p 311–322. Sport Fishing Institute, Washington, DC.

Zar, J. H.
1999. Biostatistical analysis, 663 p. Prentice Hall, Englewood Cliffs, NJ.

Using bone measurements to estimate the original sizes of bluefish (*Pomatomus saltatrix*) from digested remains

Anthony D. Wood

Box 200
Graduate School of Oceanography
University of Rhode Island Bay Campus
South Ferry Rd.
Narragansett, Rhode Island 02882
E-mail address: awood@gso.uri.edu

The ability to estimate the original size of an ingested prey item is an important step in understanding the community and population structure of piscivorous predators (Scharf et al., 1998). More specifically, knowledge of original prey size is essential for deriving important biological information, such as predator consumption rates, biomass of the prey consumed, and selectivity of a predator towards a specific size class of prey (Hansel et al., 1988; Scharf et al., 1997; Radke et al., 2000). To accurately assess the overall "top-down" pressure a predator may exert on prey community structure, prey size is crucial. However, such information is often difficult to collect in the field (Trippel and Beamish, 1987). Stomach-content analyses are the most common methods for examining the diets of piscivorous fish, but the prey items found are often thoroughly digested and sometimes unidentifiable. As a result, obtaining a direct measurement of prey items is frequently impossible.

Because of the problems of reconstructing original prey size directly from prey remains, numerous methods involving correlations between measurements of specific morphological features of the prey and prey size (length) have been devised. External body measures such as eye diameter, and caudal peduncle depth (Crane et. al., 1987; Serafy et. al., 1996; Scharf, et. al., 1997), as well as numerous internal measures such as pharyngeal arch length (Fickling and Lee, 1981; McIntyre and Ward, 1986; Radke et. al., 2000), vertebral diameter (Pikhu and Pikhu, 1970; Feltham and Marquiss, 1989), and a variety of skeletal bones (Newsome, 1977; Hansel et. al., 1988; Scharf et. al., 1998) have been used to generate models for predicting original prey size.

The bluefish (*Pomatomus saltatrix*) is a voracious piscivore and is among the top predatory fish species in the western North Atlantic Ocean (Buckel et. al., 1999). Bluefish are an important fish both commercially and recreationally, and over the past two decades stocks off the eastern coast of the United States have experienced a dramatic decline. From 1978 through 1996, the commercial landings and spawning stock biomass of bluefish declined by over 60% (Fahay et. al.[1]). A variety of mechanisms have been proposed to explain this dramatic decline, including intense predation by large apex predators. It is known that bluefish act as an important prey species for a number of apex predators in the North Atlantic, most notably the shortfin mako (*Isurus oxyrinchus*). Stillwell and Kohler (1982) sampled 399 makos from 1972–79 and found that bluefish made up 85% of the diet by volume. The mako diet has recently been reviewed and it appears that the incidence of bluefish in the diet has increased (assume 1 mL=1 g for flesh) to 94% of their diet by weight (Wood et al.[2]). Bluefish have also been found to be important in the diet of bluefin tuna (*Thunnus thynnus*) (Chase, 2002), swordfish (*Xiphias gladius*) (Stillwell and Kolhler, 1985), blue shark (*Prionace glauca*) (Kohler, 1989), and the thresher shark (*Alopias vulpinis*) (Kohler[3]).

The motivation for this study came from field sampling shortfin mako (*Isurus oxyrinchus*) stomach contents where it was observed that bluefish jaw bones and various other skull bones were often intact, even if the rest of the prey fish was digested. To generate accurate estimates of the original prey size a series of predictive equations was generated by regressing bluefish skull bone measurements with the fork length (FL) and total length (TL) of the fish. Five skull bones were chosen to obtain measurements for the relationships: the dentary, maxilla, premaxilla, opercle, and cleithrum (Fig. 1). These five bones were chosen because they are strong bones (with the exception of the opercle), covered by extensive musculature, and assumed to be resilient to digestion.

Materials and methods

During June–September of 2000 and 2001, bluefish were collected by rod and reel and by otter trawl in Narragansett Bay, RI, and at bluefish fishing tournaments along the northeast coast of the United States from Ocean

[1] Fahay, M. P., P. L. Berrien, D. L. Johnson, and W. W. Morse. 1999. Essential fish habitat source document: Bluefish, *Pomatomus saltatrix*, life history and habitat characteristics. NOAA Tech. Memo. NMFS-NE-144, 68 p. U.S. Department of Commerce, NOAA, NMFS-NEFSC, Woods Hole, MA.

[2] Wood, A. D., B. Wetherbee, N. E. Kohler, F. Juanes and C. Wilga. 2004. In prep. Predator prey interaction between the shortfin mako (*Isurus oxyrinchus*) and bluefish (*Pomatomus saltatrix*).

[3] Kohler, N. E. 2001. Personal commun. NMFS Narragansett lab, 28 Tarzwell Drive, Narragansett, RI 02882.

Manuscript submitted 4 February 2004 to the Scientific Editor's Office.

Manuscript approved for publication 21 December 2004 by the Scientific Editor.

Fish. Bull. 103:461–466 (2005).

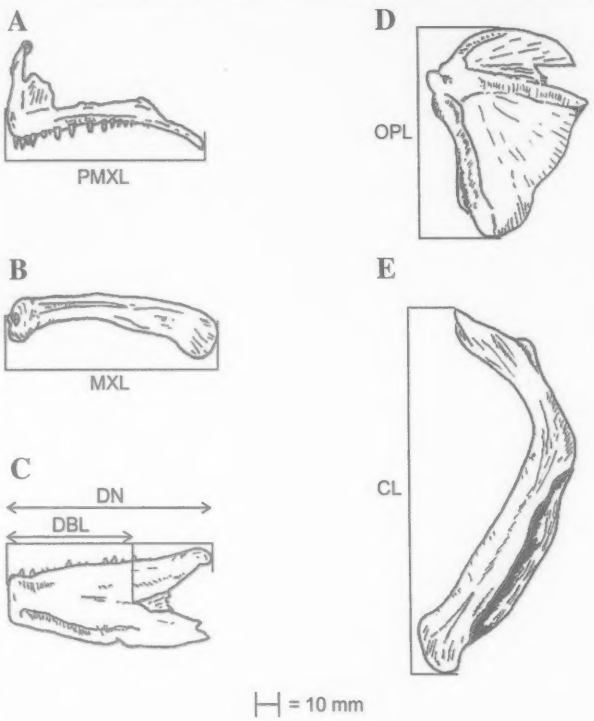

Figure 1

Diagrams of the five bluefish (*Pomatomus saltatrix*) skull bones used in this study: (**A**) premaxilla; (**B**) maxilla; (**C**) dentary; (**D**) opercle; and (**E**) cleithrum. Bones came from a 701-mm (FL) fish and are drawn to scale with respect to each other. The scale bar represents 10 mm. Measurements for each bone were taken along the longest axis and were given the following abbreviations: PMXL (premaxilla length), MXL (maxilla length), DN (dentary length), DBL (dentary body length), OPL (opercle length), CL (cleithrum length).

City, MD, north to Bayshore, NY. Upon retrieval, the fork length (FL) and total length (TL) of each fish were measured to the closest mm. The heads of the bluefish were then removed by cutting approximately 5 cm behind the pectoral girdle, and all heads were immediately placed on ice. Samples were returned to the laboratory and kept in a cool room on ice until the selected bones could be extracted and measured (within 24 hours). Bones were extracted by immersing the bluefish heads in boiling water for a short period of time (between 30 and 180 seconds, depending on the size of the fish and on the amount of musculature around the bones). The dentary, maxilla, premaxilla, opercle, and cleithrum were dissected from the left side of each fish and measured to the nearest 0.1 mm by using 0–150 mm dial calipers. Measurements were taken linearly along the longest axis of each bone and the following abbreviations were used to indicate lengths: DBL (dentary body length), DN (dentary length), OPL (opercle length), CL (cleithrum length), MXL (maxilla length), and PMXL (premaxilla length) (Fig. 1). In cases where left bones were damaged, or it was determined that an accurate measurement could not be retrieved, right-side bones were measured in place of the damaged bones.

Least squares regression analyses, which reveal the relationship of each of the bone measurements to FL and TL, were then conducted to generate predictive equations. The strength of each of the correlations was judged by both the r^2 values and by calculating the mean percent prediction error for each model, where the percent prediction error for a model (Sharf et. al., 1997) is calculated by the following equation:

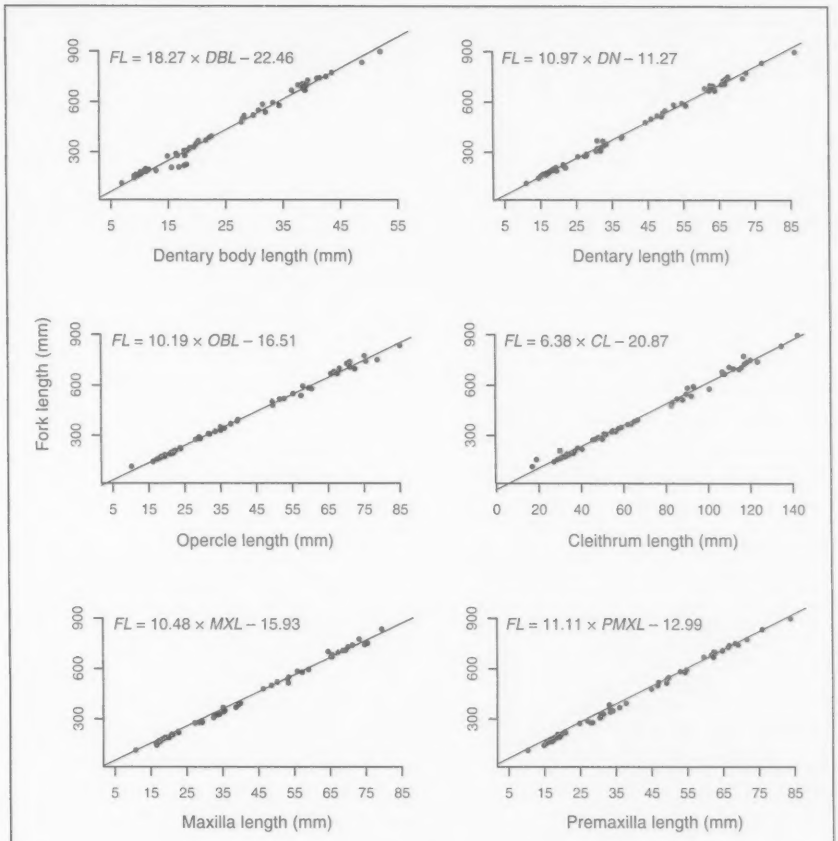
FL = 18.27 × DBL – 22.46
Dentary body length (mm)
FL = 10.97 × DN – 11.27
Dentary length (mm)
Fork length (mm)
FL = 10.19 × OBL – 16.51
Opercle length (mm)
FL = 6.38 × CL – 20.87
Cleithrum length (mm)
FL = 10.48 × MXL – 15.93
Maxilla length (mm)
FL = 11.11 × PMXL – 12.99
Premaxilla length (mm)

Figure 2

Fork length (mm) in relation to six skull bone measurements (mm) in bluefish (*Pomatomus saltatrix*). Resulting linear regression models and trendlines are shown.

$$\frac{(Observed - Predicted)}{(Predicted)} \times 100.$$

To determine if any one bone or set of bones provided the best predictor equation, comprehensive models involving sets of bones were fitted in a stepwise linear algorithm by using the Akaike information criterion (AIC) as the criterion for model selection. Models were generated in both a forwards and backwards manner in order to confirm that the same model was returned in all cases.

Results

Fork length (FL) and total length (TL) measurements were taken from 58 bluefish ranging from 110 mm to 900 mm FL. The resulting regression equations correlating skull bone measurements to FL (Fig. 2) were highly significant (P=0.005 for the dentary correlation and P<0.001 for the rest of the models). The r^2 values for the FL predictive equations ranged from 0.988 to 0.997, and the mean percent predictive errors ranged from −0.03 to 1.19 (Table 1). Similarly, all of the resulting models correlating the bone measurements to total length (Fig. 3) were highly significant (P<0.001, r^2 values ranging from 0.987 to 0.996, and mean percent predictive errors ranging from −0.11 to 1.07 [Table 1]).

Bones were ranked from best predictor to worst predictor for both the FL and TL models by using the Akaike information criterion (AIC). In both cases the premaxilla was ranked the best predictor bone, followed by the maxilla, the opercle, the dentary, the cleithrum, and finally dentary body length. The bone measurements included in the stepwise multiple regression model for predicting fork length were PMXL, OPL, and DN (Table 2). In the best predictor model for total length, PMXL, OPL, DN and CL were included (Table 2).

Table 1

Resulting predictive equations of fork and total length in relation to several skull bone measures with corresopnding coefficient of determination (r^2) and *P*-values, and mean percent predictive errors (%PE) for each model.

Bone	Fork length	r^2	*P*-value	%PE
Dentary body length (DBL)	$FL = 18.27(DBL) - 22.46$	0.988	<0.001	0.54
Dentary (DN)	$FL = 10.97(DN) - 11.27$	0.996	0.005	−0.03
Opercle (OPL)	$FL = 10.19(OPL) - 16.51$	0.997	<0.001	0.28
Cleithrum (CL)	$FL = 6.38(CL) - 20.87$	0.993	<0.001	1.19
Maxilla (MXL)	$FL = 10.48(MXL) - 15.93$	0.997	<0.001	0.31
Premaxilla (PMXL)	$FL = 11.11(PMXL) - 12.99$	0.997	<0.001	0.26
Bone	Total length	r^2	*P*-value	%PE
Dentary body length (DBL)	$TL = 20.20(DBL) - 27.69$	0.987	<0.001	0.46
Dentary (DN)	$TL = 12.13(DN) - 15.42$	0.996	<0.001	−0.11
Opercle (OPL)	$TL = 11.27(OPL) - 21.13$	0.996	<0.001	0.15
Cleithrum (CL)	$TL = 7.05(CL) - 26.13$	0.994	<0.001	1.07
Maxilla (MXL)	$TL = 11.59(MXL) - 20.43$	0.996	<0.001	0.19
Premaxilla (PMXL)	$TL = 12.28(PMXL) - 17.20$	0.996	<0.001	0.14

Table 2

Independent variables included in the stepwise linear regression models used to estimate original bluefish fork length and total length.

	Variables included in forward stepwise regression model	Variables included in backward stepwise regression model
Fork length	PMXL, OPL, DN	PMXL, OPL, DN
Total length	PMXL, OPL, DN, CL	PMXL, OPL, DN, CL

Discussion

This study revealed that measurements of five skull bones can be used as accurate predictors of original fork length and total length of bluefish. Although the methods of other studies were incorporated in this study, the information is the first of its kind for bluefish and may serve as a tool for the future study of this species in the North Atlantic.

In recent years there has been growing concern over the stability of the bluefish stock and an increased effort to gather information on the possible mechanisms affecting bluefish abundance and distribution in the western North Atlantic.[4] One of the proposed mechanisms that could be adversely influencing the recovery of bluefish is top-down pressure by a number of apex predators in the North Atlantic. Although indiscriminant predation on bluefish may not be a significant pressure on the stock, size selective predation can dramatically alter the structure of the prey community (McIntyre and Ward, 1986; Trippel and Beamish, 1987; Sharf et. al., 1997).

In order to study the consumption rates of key predators in an ecosystem it is necessary to gather information on the sizes of the prey being consumed (Elliot and Persson, 1978; Sharf et. al., 1998). However, it is often difficult to estimate the original size of a prey item from stomach content data because of the complications caused by digestion. Erosion of the prey bones from digestive juices can lead to measurement error or bias when prey sizes are back-calculated from digested parts (Sharf et al., 1998). Although bias from digestion is a concern that should be addressed in studies, internal bones and hard parts of fishes have been shown to be excellent predictors of original prey size (Trippel and

[4] In 1997 Rutgers University and the NMFS organized a workshop to study the factors that could be contributing to the depressed state of the bluefish stock. A similar concern was expressed by Congress at this time, and the Rutgers and NMFS workshop led to a request for proposals for bluefish-related research in 1998, 1999, and 2000.

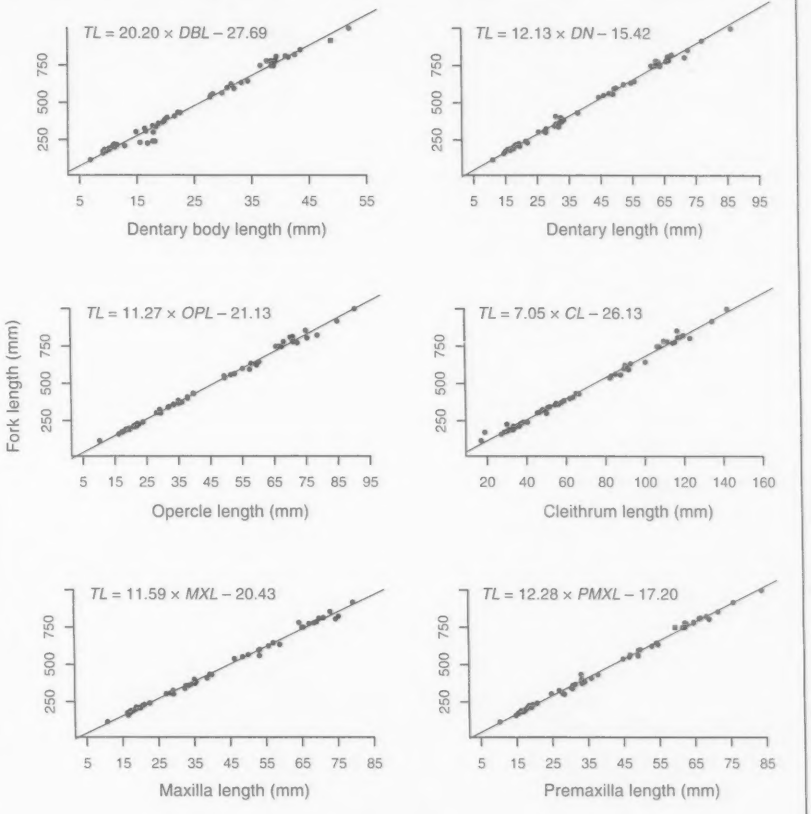
TL = 20.20 × DBL – 27.69
Dentary body length (mm)
TL = 12.13 × DN – 15.42
Dentary length (mm)
TL = 11.27 × OPL – 21.13
Fork length (mm)
Opercle length (mm)
TL = 7.05 × CL – 26.13
Cleithrum length (mm)
TL = 11.59 × MXL – 20.43
Maxilla length (mm)
TL = 12.28 × PMXL – 17.20
Premaxilla length (mm)

Figure 3

Total length (mm) in relation to six skull bone measurements (mm) in bluefish (*Pomatomus saltatrix*). Resulting linear regression models and trendlines are shown.

Beamish, 1987; Hansel, 1988, Sharf et al., 1998). In addition, the bones used in the present study are strong bones (with the exception of the opercle), that are liable to resist digestive erosion.

All the relationships generated in the present study yielded very accurate predictions of original prey size, but the jaw bones are of special interest. Bluefish can be classified as predators that exhibit a biting behavior during predation. Fish that show this type of predation behavior have very heavy, robust jaw bones (Norton, 1995). The jaw bones (maxilla, premaxilla, and dentary) of bluefish are both easily identifiable and likely resistant to digestion, and when combined with the adequacy with which original size can be determined from these bones (based on AIC rankings and %PE), they are the best option for researchers interested in back-calculating original bluefish sizes.

The results of this study provide a means to further analyze the stomach contents of bluefish predators beyond identifying, and quantifying prey items. The usefulness of this type of data has been shown repeatedly for a number of species (McIntyre and Ward, 1986; Feltham and Marquiss, 1989; Serafy et. al., 1996; Sharf et. al., 1997; Sharf et. al., 1998). The ability to back-calculate the original size of a prey leads to the enhancement of diet studies and allows for more accurate estimates of predator consumption rates. The lack of this kind of data and correlations for many key prey species in the Atlantic and elsewhere is surprising.

Acknowledgments

Funding for this study was provided by the Bluefish-Striped Bass Dynamics Research Program at Rutgers University in cooperation with the National Marine Fisheries Service (grant NA97FE0363). I am indebted to the numerous fishing tournament directors, as well as the fishermen at the tournaments for allowing me to collect many of the bluefish needed for this study. I am

also especially grateful to Abby McLean for her help with the exhausting task of measuring bones. Finally, I wish to thank Francis Juanes for encouraging me to pursue and publish this study and Jeremy Collie and two anonymous reviewers for comments that helped to improve this manuscript.

Literature cited

Buckel, J. A., M. J. Fogarty, and D. O. Conover.
1999. Foraging habits of bluefish, *Pomatomus saltatrix*, on the U.S. east coast continental shelf. Fish. Bull. 97:758–775.

Chase, B. C.
2002. Differences in diet of Atlantic bluefin tuna (*Thunnus thynnus*) at five seasonal feeding grounds on the New England continental shelf. Fish. Bull. 100:168–180.

Crane, S. A., J. M. Fenaughty, and R. W. Gauldie.
1987. The relationship between eye diameter and fork length in the spiny oreo dory, *Allocyttus sp.* N.Z.J. Mar. Freshw. Res. 21:641–642.

Elliott, J. M., and L. Persson.
1978. The estimation of daily rates of food consumption for fish. J. Anim. Ecol. 47:977–991.

Feltham, M. J., and M. Marquiss.
1989. The use of first vertebrae in separating, and estimating the size of, trout (*Salmo trutta*) and salmon (*Salmo salar*) in bone remains. J. Zool. 219:113–122.

Fickling, N. J., and R. L. G. Lee.
1981. Further aids to the reconstruction of digested prey lengths. Fish Manage. 12:107–110.

Hansel, H. C., S. D. Duke, P. T. Lofy, and G. A. Gray.
1988. Use of diagnostic bones to identify and estimate original lengths of ingested prey fishes. Trans. Am. Fish. Soc. 117:55–62.

Kohler, N.E.
1989. Aspects of the feeding ecology of the blue shark, Prionace glauca, in the western North Atlantic. Diss. Abst. Int. Pt. B-Sci. & Eng. 49:1–179.

McIntyre, D. B., and F. J. Ward.
1986. Estimating fork lengths of fathead minnows, *Pimephales promelas*, from measurement of pharyngeal arches. Can. J. Fish. Aquat. Sci. 43:1294–1297.

Newsome, G. E.
1977. Use of opercular bones to identify and estimate lengths of prey consumed by piscivores. Can. J. Zool. 55: 733–736.

Norton, S. F.
1995. A functional approach to ecomorphological patterns of feeding in cottid fishes. Environ. Biol. Fishes 44:61–78.

Pikhu, E. Kh., and E. R. Pikhu.
1970. Reconstruction of the size of fishes swallowed by predators from fragments of their vertebral column. J. Ichthyol. (USSR), vol. 10:706–709.

Radke, R. J., T. Petzoldt, and C. Wolter.
2000. Suitability of pharyngeal bone measures commonly used for reconstruction of prey fish length. J. Fish Biol. 57:961–967.

Scharf, F. S., J. A. Buckel, F. Juanes, and D. O. O'Connor.
1997. Estimating piscine prey size from partial remains: Testing for shifts in foraging mode by juvenile bluefish. Environ. Biol. Fishes 49:377–388.

Scharf, F. S., R. M. Yetter, A. P. Summers, and F. Juanes.
1998. Enhancing diet analyses of piscivorous fishes in the northwest Atlantic through identification and reconstruction of original prey sizes from ingested remains. Fish. Bull. 96:575–588.

Serafy, J. E., C. M. Schmitz, T. R. Capo, M. E. Clarke, and J. S. Ault.
1996. Total length estimation of red drum from head dimensions. Prog. Fish-Cult. 58:289–290.

Stillwell, C. E., and N. E. Kohler.
1982. Food, Feeding Habits, and Estimates of Daily Ration of the Shortfin Mako (*Isurus oxyrinchus*) in the Northwest Atlantic. Can. J. Fish. Aquat. Sci. 39: 407–414.
1985. Food and feeding ecology of the swordfish *Xiphas gladias* in the western North Atlantic Ocean with estimates of daily ration. Mar. Ecol. Prog. Ser. 22: 239–247.

Trippel, E. A., and F. W. H. Beamish.
1987. Characterizing piscivory from ingested remains. Trans. Am. Fish. Soc. 116:773–776.

☆ U.S. GOVERNMENT PRINTING OFFICE: 2005 — 791-119 / R7356 Region No. 10

Superintendent of Documents **Publications** Order Form

*5178

☐ YES, please send me the following publications:

____ Subscriptions to *Fishery Bulletin*
for $55.00 per year ($68.75 foreign)

The total cost of my order is $ _____ . Prices include regular domestic postage and handling and are subject to change.

_____
(Company or Personal Name) (Please type or print)

_____
(Additional address/attention line)

_____
(Street address)

_____
(City, State, ZIP Code)

_____
(Daytime phone including area code)

_____
(Purchase Order No.)

Charge your order.
IT'S EASY!

VISA

MasterCard

Please Choose Method of Payment:

☐ Check Payable to the Superintendent of Documents
☐ GPO Deposit Account ☐☐☐☐☐☐☐–☐
☐ VISA or MasterCard Account
☐☐☐☐☐☐☐☐☐☐☐☐☐☐☐☐
☐☐☐☐ (Credit card expiration date)

To fax your orders (202) 512-2250

_____
(Authorizing Signature)

Mail To: Superintendent of Documents
P.O. Box 371954, Pittsburgh, PA 15250-7954

Thank you for your order!

Fishery Bulletin

Guidelines for contributors

Content of papers

Articles

Articles are reports of 10 to 30 pages (double spaced) that describe original research in one or a combination of the following fields of marine science: taxonomy, biology, genetics, mathematics (including modeling), statistics, engineering, economics, and ecology.

Notes

Notes are reports of 5 to 10 pages without an abstract that describe methods and results not supported by a large body of data. Although all contributions are subject to peer review, responsibility for the contents of articles and notes rests upon the authors and not upon the editor or the publisher. It is therefore important that authors consider the contents of their manuscripts carefully. Submission of an article is un-derstood to imply that the article is original and is not being considered for publication elsewhere. Manuscripts must be written in English. Authors whose native language is not English are strongly advised to have their manuscripts checked for fluency by English-speaking colleagues prior to submission.

Preparation of papers

Text

Title page should include authors' full names and mailing addresses (street address required) and the senior author's telephone, fax number, e-mail address, as well as a list of key words to describe the contents of the manuscript. **Abstract** must be less than one typed page (double spaced) and must not contain any citations. It should state the main scope of the research but emphasize the author's conclusions and relevant findings. Because abstracts are circulated by abstracting agencies, it is important that they represent the research clearly and concisely. **General text** must be typed in double-spaced format. A brief introduction should state the broad significance of the paper; the remainder of the paper should be divided into the following sections: Materials and methods, Results, Discussion (or Conclusions), and Acknowledgments. Headings within each section must be short, reflect a logical sequence, and follow the rules of multiple subdivision (i.e. there can be no subdivision without at least two subheadings). The entire text should be intelligible to interdisciplinary readers; therefore, all acronyms and abbreviations should be written out and all lesser-known technical terms should be defined the first time they are mentioned. The scientific names of species must be written out the first time they are mentioned; subsequent mention of scientific names may be abbreviated. Follow *Scientific style and format: CBE manual for authors, editors, and publishers* (6th ed.) for editorial style and the most current issue of the *American Fisheries Society's common and scientific names of fishes from the United States and Canada* for fish nomenclature. Dates should be written as follows: 11 November 1991. Measurements should be expressed in metric units, e.g. metric tons (t). The numeral one (1) should be typed as a one, not as a lower-case el (l).

Footnotes

Use footnotes to add editorial comments regarding claims made in the text and to document unpublished works or works with local circulation. Footnotes should be numbered with Arabic numerals and inserted in 10-point font at the bottom of the first page on which they are cited. Footnotes should be formatted in the same manner as citations. If a manuscript is unpublished, in the process of review, or if the information provided in the footnote has been conveyed verbally, please state this information as "unpubl. data," "manuscript in review," and "personal commun.," respectively. Authors are advised wherever possible to avoid references to nonstandard literature (unpublished literature that is difficult to obtain, such as internal reports, processed reports, administrative reports, ICES council minutes, IWC minutes or working papers, any "research" or "working" documents, laboratory reports, contract reports, and manuscripts in review). If these references are used, please indicate whether they are available from NTIS (National Technical Information Service) or from some other public depository. Footnote format: author (last name, followed by first-name initials); year; title of report or manuscript; type of report and its administrative or serial number; name and address of agency or institution where the report is filed.

Literature cited

The literature cited section comprises works that have been published and those accepted for publication (works in press) in peer-reviewed journals and books. Follow the name and year system for citation format. In the text, write "Smith and Jones (1977) reported" but if the citation takes the form of parenthetical matter, write "(Smith and Jones, 1977)." In the literature cited section, list citations alphabetically by last name of senior author: For example, Alston, 1952; Mannly, 1988; Smith, 1932; Smith, 1947; Stalinsky and Jones, 1985. Abbreviations of journals should conform to the abbreviations given in the *Serial sources for the BIOSIS previews database*. Authors are responsible for the accuracy and completeness of all citations. Literature citation format: author (last name, followed by first-name initials); year; title of report or article; abbreviated title of the journal in which the article was published, volume number, page numbers. For books, please provide publisher, city, and state.

Tables

Tables should not be excessive in size and must be cited in numerical order in the text. Headings in tables should be short but ample enough to allow the table to be intelligible on its own. All unusual symbols must be explained in the table legend. Other incidental comments may be footnoted (use italic arabic numerals for footnote markers). Use asterisks only to indicate probability in statistical data. Place table legends on the same page as the table data. We accept tables saved in most spreadsheet software programs (e.g. Microsoft Excel). Please note the following:

- Use a comma in numbers of five digits or more (e.g. 13,000 but 3000).
- Use zeros before all decimal points for values less than one (e.g. 0.31).

Figures

Figures include line illustrations, computer-generated line graphs, and photographs (or slides). They must be cited in numerical order in the text. Line illustrations are best submitted as original drawings. Computer-generated line graphs should be printed on laser-quality paper. Photographs should be submitted on glossy paper with good contrast. All figures are to be labeled with senior author's name and the number of the figure (e.g. Smith, Fig. 4). Use Helvetica or Arial font to label anatomical parts (line drawings) or variables (graphs) within figures; use Times Roman bold font to label the different sections of a figure (e.g. **A**, **B**, **C**). Figure legends should explain all symbols and abbreviations seen within the figure and should be typed in double-spaced format on a separate page at the end of the manuscript. We advise authors to peruse a recent issue of *Fishery Bulletin* for standard formats. Please note the following:

- Capitalize the first letter of the first word of axis labels.
- Do not use overly large font sizes to label axes or parts within figures.
- Do not use boldface fonts within figures.
- Do not create outline rules around graphs.
- Do not use horizontal lines through graphs.
- Do not use large font sizes to label degrees of longitude and latitude on maps.
- Indicate direction of degrees longitude and latitude on maps (e.g. 170°E).
- Avoid placing labels on a vertical plane (except on *y* axis).
- Avoid odd (nonstandard) patterns to mark sections of bar graphs and pie charts.

Copyright law

Fishery Bulletin, a U.S. government publication, is not subject to copyright law. If an author wishes to reproduce any part of *Fishery Bulletin* in his or her work, he or she is obliged, however, to acknowledge the source of the extracted literature.

Submission of papers

Send four printed copies (one original plus three copies)—clipped, *not stapled*—to the Scientific Editor, at the address shown below. Send photocopies of figures with initial submission of manuscript. Original figures will be requested later when the manuscript has been accepted for publication. Do not send your manuscript on diskette until requested to do so.

Dr. Norman Bartoo
National Marine Fisheries Service, NOAA
8604 La Jolla Shores Drive
La Jolla, CA 92037

Once the manuscript has been accepted for publication, you will be asked to submit a software copy of your manuscript. The software copy should be submitted in WordPerfect or Word format (in Word, save as Rich Text Format). Please note that we do not accept ASCII text files. Color figures must be CMYK files.

Reprints
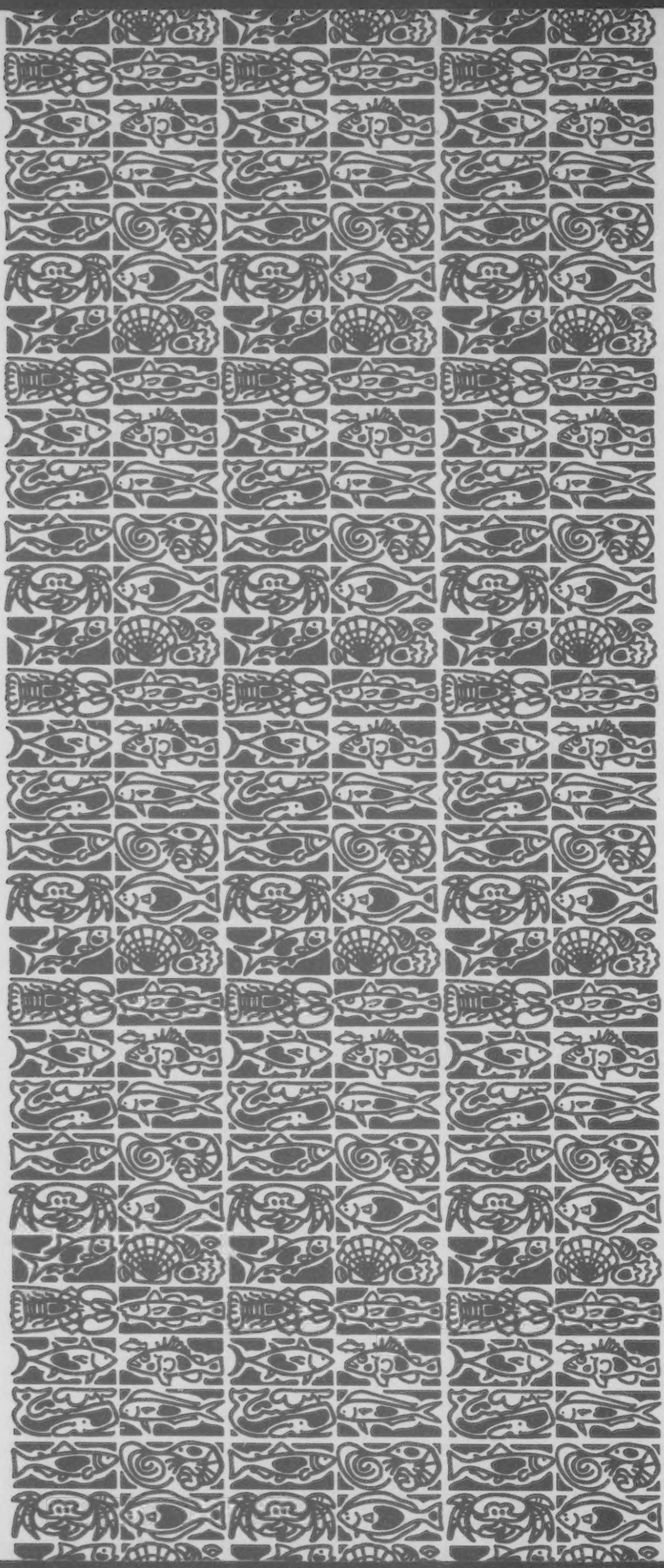
Copies of published articles and notes are available free of charge to the senior author (50 copies) and to his or her laboratory (50 copies). Additional copies may be purchased in lots of 100 when the author receives page proofs.